Contemporary Cardiology
Series Editor: Peter P. Toth

Arman T. Askari
Adrian W. Messerli
Editors

Cardiovascular Hemodynamics

An Introductory Guide

Second Edition

Humana Press

Contemporary Cardiology

Series Editor:

Peter P. Toth
Ciccarone Center for the Prevention of Cardiovascular Disease
Johns Hopkins University School of Medicine
Baltimore, Maryland
USA

For more than a decade, cardiologists have relied on the Contemporary Cardiology series to provide them with forefront medical references on all aspects of cardiology. Each title is carefully crafted by world-renown cardiologists who comprehensively cover the most important topics in this rapidly advancing field. With more than 75 titles in print covering everything from diabetes and cardiovascular disease to the management of acute coronary syndromes, the Contemporary Cardiology series has become the leading reference source for the practice of cardiac care.

More information about this series at http://www.springer.com/series/7677

Arman T. Askari • Adrian W. Messerli
Editors

Cardiovascular Hemodynamics

An Introductory Guide

Second Edition

Humana Press

Editors
Arman T. Askari
Premier Health Advocates
Beachwood, OH
USA

Adrian W. Messerli
Gill Heart and Vascular Institute
University of Kentucky HealthCare
Lexington, KY
USA

ISSN 2196-8969 ISSN 2196-8977 (electronic)
Contemporary Cardiology
ISBN 978-3-030-19130-6 ISBN 978-3-030-19131-3 (eBook)
https://doi.org/10.1007/978-3-030-19131-3

This Humana imprint is published by the registered company Springer Nature Switzerland AG.
The registered company address is: Gewerbestrasse 11, 6330 Cham, Switzerland

To our families for their unwavering support.

Preface to the Second Edition

For any cardiovascular care provider, an understanding of physiology is absolutely essential for delivering patient care. Whether sitting in the echocardiography reading room, performing procedures in the catheterization laboratory, or rounding in the coronary care unit, such an understanding is equally vital. While the underpinnings of cardiovascular physiology from a systems perspective have changed little in recent time, there have been substantial advances in the ability to apply these concepts to newer technologies.

Our primary goal for this second edition of *Cardiovascular Hemodynamics: An Introductory Guide* is not only to expound on the fundamental education of cardiovascular physiology but also to focus additionally on the clinical application of these hemodynamic principles. In order to achieve this, we have updated all of the first edition chapters and have added a new section, "Effects of Selected Interventions on Cardiovascular Hemodynamics."

Born out of the huge economic burden of heart failure is an increased pressure on the healthcare system to decrease the often-avoidable readmissions for those patients with heart failure. We believe that a solid knowledge of heart failure physiology will arm those charged with the care of these patients with the tools necessary to decrease these costly readmissions. In addition, we have added another chapter, "Objective Evaluation of Hemodynamics in the Outpatient," that aims to familiarize the reader with the recent advancements (medical and technological) that have proven helpful with regard to optimizing patient care.

Of course, an emphasis on the basic tenets of cardiovascular physiology remains our central focus, and we use numerous figures, hemodynamic tracings, tables, board style review questions, and hemodynamic "pearls" in order guide our readers. We believe this manual will be of immense value and interest to every student and practitioner of cardiovascular medicine who wishes to fully learn the hemodynamic foundation of cardiovascular medicine.

Beachwood, OH, USA — Arman T. Askari, MD
Lexington, KY, USA — Adrian W. Messerli, MD

Acknowledgment

We would like to acknowledge the authors, who, in many cases, were also mentors.

Contents

Contributors

Ahmed Abdel-Latif VA Medical Center, Lexington, KY, USA

Saha Cardiovascular Research Center, University of Kentucky, Lexington, KY, USA

Olcay Aksoy David Geffen School of Medicine, UCLA Medical Center, Los Angeles, CA, USA

Paul Anaya Gill Heart Institute, University of Kentucky, Lexington, KY, USA

Jordan D. Awerbach Division of Cardiovascular Medicine, Duke University Health System, Durham, NC, USA

Chirag Bavishi Department of Cardiology, Lifespan Cardiovascular Institute, Rhode Island Hospital, Warren Alpert Medical School of Brown University, Providence, RI, USA

David C. Booth The Gill Heart and Vascular Institute, University of Kentucky Medical Center, Lexington, KY, USA

Michael P. Brunner Spectrum Health Medical Group, Grand Rapids, MI, USA

Justin M. Dunn Interventional Cardiology, Summa Health, Akron, OH, USA

Stephen G. Ellis Cleveland Clinic, Cleveland, OH, USA

Michael D. Faulx Cleveland Clinic, Cleveland, OH, USA

Sachin S. Goel Prairie Heart Institute, St John's Hospital, Springfield, IL, USA

Andrew D. M. Grant Libin Cardiovascular Institute, Calgary, AB, Canada

Brian P. Griffin Cardiovascular Imaging, Cleveland Clinic, Cleveland, OH, USA

Richard A. Grimm Cleveland Clinic, Cleveland, OH, USA

Ehud Grossman The Chaim Sheba Medical Center, The Sackler Faculty of Medicine, Tel-Aviv University, Tel Aviv, Israel

Mazen A. Hanna Cleveland Clinic, Cleveland, OH, USA

Michael A. Hanna Cleveland Clinic, Cleveland, OH, USA

James E. Harvey York Hospital, WellSpan Health System, York, PA, USA

Frederick Heupler Cleveland Clinic, Cleveland, OH, USA

Daniel H. Katz Beth Israel Deaconess Medical Center, Boston, MA, USA

Allan Klein The Miller Family Heart and Vascular Institute, Cleveland Clinic, Cleveland, OH, USA

Richard A. Krasuski Division of Cardiovascular Medicine, Duke University Health System, Durham, NC, USA

Amar Krishnaswamy Interventional Cardiology, Cleveland Clinic, Cleveland, OH, USA

Tracy E. Macaulay Gill Heart Institute, University of Kentucky, Lexington, KY, USA

Franz H. Messerli Department of Cardiology, University of Bern, Bern, Switzerland

Alexandra-Maria Neagoe Department of Cardiology, University Hospital Bern, Bern, Switzerland

Gbolahan Ogunbayo Gill Heart Institute and Division of Cardiovascular Medicine, University of Kentucky, Lexington, KY, USA

VA Medical Center, Lexington, KY, USA

Alper Ozkan Acibadem University, Istanbul, Turkey

Navin Rajagopalan Heart Failure/Cardiac Transplant Program, The Gill Heart and Vascular Institute, Lexington, KY, USA

Roberto Ramirez Department of Cardiology, Mount Sinai St. Luke's Hospital, New York, NY, USA

Emrush Rexhaj Department of Cardiology, University Hospital Bern, Bern, Switzerland

Department for Biomedical Research, University of Bern, Bern, Switzerland

Leonardo Rodriguez Cleveland Clinic, Cleveland, OH, USA

Marwa A. Sabe Beth Israel Deaconess Medical Center, Boston, MA, USA

Harvard Medical School, Boston, MA, USA

Begum Sezer UCLA Medical Center, Los Angeles, CA, USA

William J. Stewart Department of Cardiovascular Medicine, Cleveland Clinic, Cleveland, OH, USA

Jose Mariano T. Tan Spectrum Health Medical Group, Grand Rapids, MI, USA

Jordan S. Thomas Advanced Heart Failure/Transplant Cardiology, Ohio State University, Columbus, OH, USA

E. Murat Tuzcu Heart and Vascular Institute, Cleveland Clinic, Cleveland, OH, USA

Amanda R. Vest Division of Cardiology, Tufts Medical Center, Boston, MA, USA

Chun Pong Wong Department of Cardiology, Khoo Teck Puat Hospital, National Healthcare Group, Singapore, Singapore

Omeed Zardkoohi Northwestern Medicine, Chicago, IL, USA

Khaled M. Ziada Gill Heart and Vascular Institute, University of Kentucky, Lexington, KY, USA

Andrew O. Zurick III St. Thomas Heart, Nashville, TN, USA

List of Figures

List of Tables

Part I

Components of Myocardial Performance

Preload

1

Amanda R. Vest

Understanding the Concept

The four major determinants of cardiac output are cardiac preload, myocardial contractility, heart rate, and afterload. Of these four elements, preload is the primary determinant. Cardiac preload is a semiquantitative composite assessment that is variously described in different cardiovascular physiology texts and articles as end-diastolic myocardial fiber tension, end-diastolic myocardial fiber length, ventricular end-diastolic volume, and ventricular end-diastolic filling pressure [1]. There is a general recognition that preload is not synonymous with any one of these measurable parameters, but is rather a physiological concept that encompasses all of the factors that contribute to passive ventricular wall stress at the end of diastole.

Cardiac preload may be expressed as a mathematical concept based upon the Law of LaPlace. This law states that, for a thin-walled spherical structure, $T = PR/2$, where T is wall tension, P is chamber pressure, and R is chamber radius. In the case of a thick-walled structure such as the left ventricle, the relationship is better described by $\sigma = PR/2w$, where σ is wall stress, and w is wall thickness, and where $T = \sigma w$. From the structure of the LaPlace's equation, the preload for the ventricle can be described as the left ventricular σ, whereby $\sigma\text{LV} = (\text{EDPLV})(\text{EDRLV})/2w\text{LV}$, with EDPLV representing the left ventricular end-diastolic pressure and EDR as the left ventricular end-diastolic radius. Thus, the parameters of pressure, radius (a surrogate for volume), and wall thickness are all demonstrated to contribute to this mathematical definition.

Clinically, a more tangible and measurable representation of preload has been sought from invasive hemodynamic monitoring. A measurement of end-diastolic pressure – the ventricular pressure measured after atrial contraction just before the onset of systole – is the most relevant representation of preload to many clinicians. Noninvasive assessments of end-diastolic chamber volume are also possible, but volume assessments rely on geometric assumptions that can be undermined by arrhythmias, changes in heart rate, localized wall motion abnormalities, and the chronic ventricular dilatation that occurs in many forms of heart failure. The passive pressure–volume relationship within a chamber, which is a reflection of the passive length–tension curve in isolated myocardium, is exponential and not linear. This fact poses one of the greatest limitations to the use of pressure as a surrogate for preload, with the ratio of change in chamber pressure to

A. R. Vest (✉)
Division of Cardiology, Tufts Medical Center, Boston, MA, USA
e-mail: avest@tuftsmedicalcenter.org

A. T. Askari, A. W. Messerli (eds.), *Cardiovascular Hemodynamics*, Contemporary Cardiology,
https://doi.org/10.1007/978-3-030-19131-3_1

volume being greater at higher volumes compared to lower volumes. In addition, the relationship between pressure and volume will also be distorted by various cardiac pathologies, such as the presence of pericardial constriction. Overall, it should be remembered that preload as a physiological concept encompasses more than just a single value on a pressure tracing (Fig. 1.1).

The concept of preload can be applied to either the atria or the ventricles. In the structurally normal heart, the preload experienced by the right atrium will determine the subsequent preloads in the right ventricle and ultimately the left side of the heart. The other determinants of cardiac output will be addressed in later chapters of this section.

Preload Physiology and Theory

Chamber Anatomy and Function

Cardiac preload will increase with a rise in total circulating volume or greater venous return, which increases myocardial wall stress and the pressure within a chamber at the end of its diastolic phase. Conversely, hypovolemia or decreased venous return will result in decreased chamber filling and wall stress and hence a decreased end-diastolic pressure. The chamber most easily and frequently accessed for invasive monitoring of cardiac preload is the right atrium. A central venous catheter, commonly employed in intensive care settings, can contribute useful

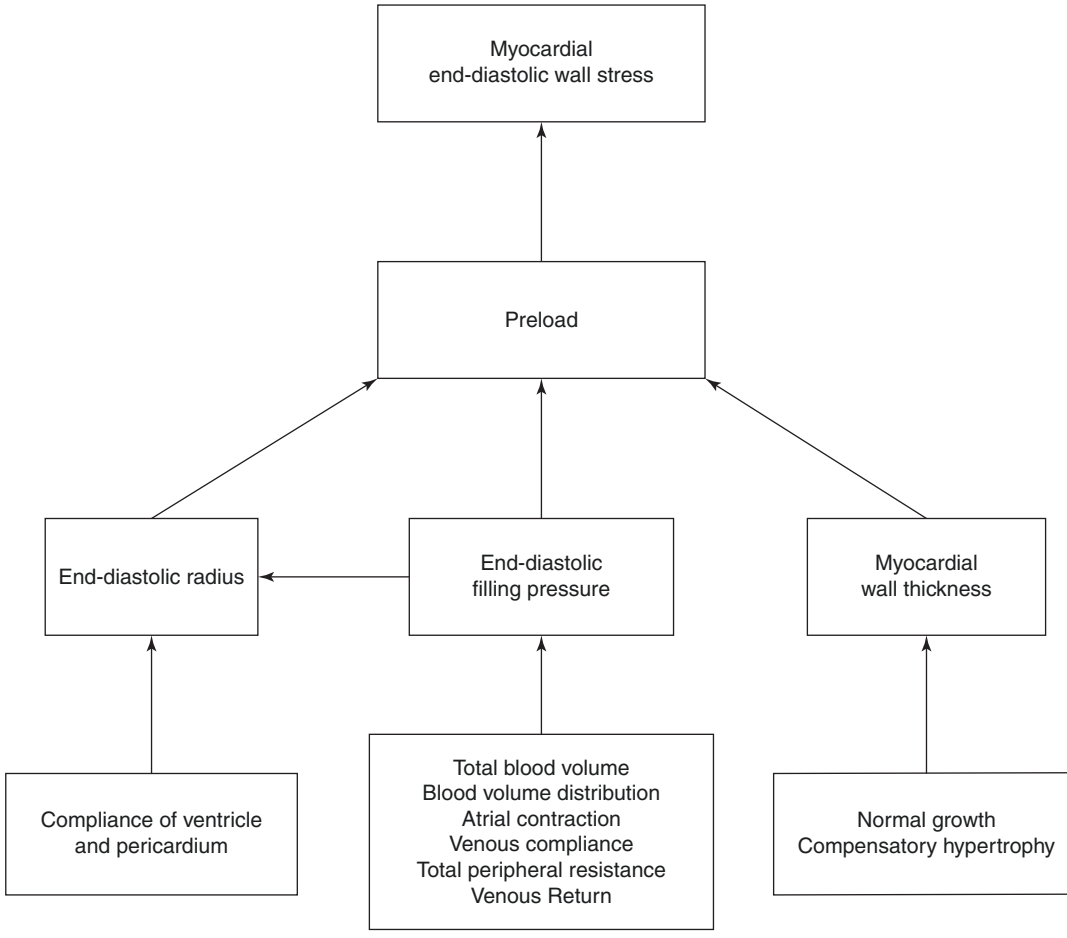

Fig. 1.1 Factors determining preload. (From Norton [1])

information for the clinician when assessing the patient's preload status.

The cardiac cycle comprises diastolic ventricular filling, augmentation by atrial systole to achieve the end-diastolic volume, isovolumic contraction, and then aortic (and pulmonary) valve opening, and stroke volume ejection. Meanwhile, atrial pressure progressively increases during ventricular systole as blood continues to enter the atrium while the atrioventricular valves are closed. Once the ventricle reaches its end-systolic volume, there is a period of isovolumic relaxation, which brings about mitral and tricuspid opening and diastolic filling from the atrium into the ventricle to begin the next cycle. Throughout the diastolic ventricular filling period, the pressure gradient between the atrium and ventricle is minimal. This is because a normal open mitral or tricuspid valve offers little resistance to flow; there is also significant passive filling of both the atrium and ventricle as blood returns from the systemic or pulmonary venous system. At a normal resting heart rate, diastole occupies approximately two-thirds of the cardiac cycle. With increased heart rate, both systolic and diastolic intervals will shorten (Fig. 1.2) [2].

The main difference between the left and right pumping systems is the pressure magnitude. In the normal heart, the pressures developed in the right heart are significantly lower than those on the left side, because resistance across the pulmonary vasculature is far less than the resistance to flow offered by the systemic vascular system. Normal pulmonary artery systolic and diastolic pressures typically do not exceed 30 mmHg and 15 mmHg respectively; the maximal right atrial pressure is generally 8 mmHg (Fig. 1.3).

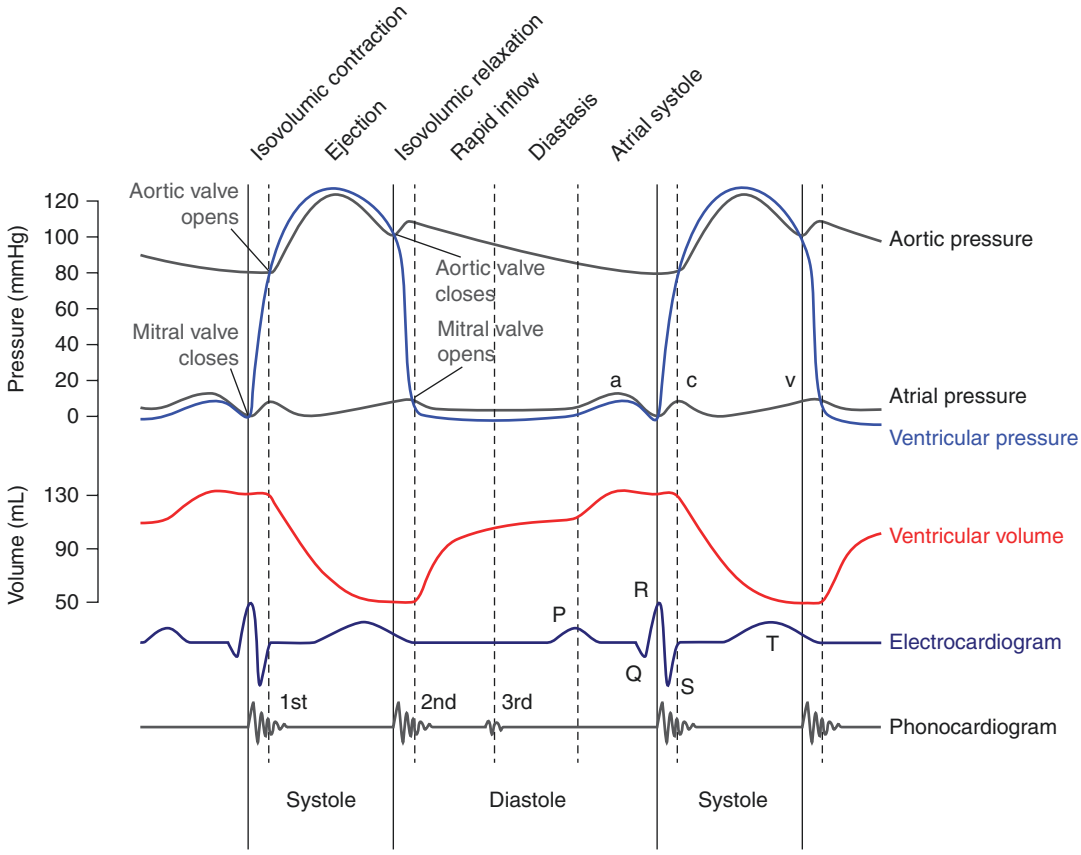

Fig. 1.2 The cardiac cycle. (From Wikipedia: DanielChangMD revised original work of DestinyQx; Redrawn as Xavax)

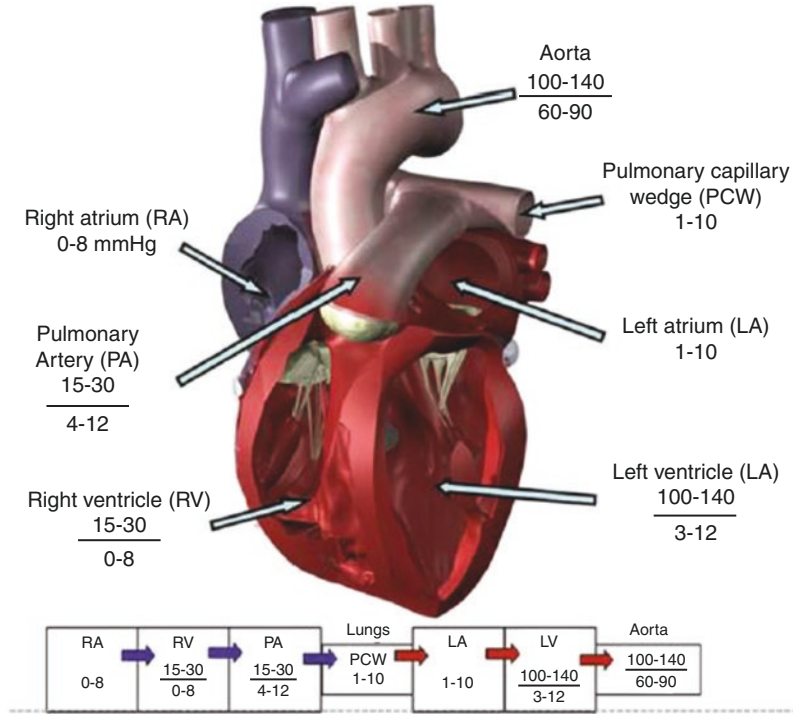

Fig. 1.3 Average pressures within the chambers and great vessels of the heart. (From Iaizzo [48])

The Right Atrial Pressure Waveform

A central venous catheter is correctly placed when its tip is situated in the distal superior vena cava [3]; at this position it approximates pressures within the right atrium. As illustrated above, right atrial pressure also approximates the right ventricular end-diastolic pressure, because minimal pressure gradient exists across the normal tricuspid valve. In turn, the right ventricular end-diastolic pressure reflects the right ventricular end-diastolic volume and, due to the conservation of volume passing through the right and left ventricles, will also mirror left ventricular end-diastolic pressure (LVEDP) and volume. Hence, the right atrial pressure alone can serve as a useful surrogate for cardiac preload while requiring slightly less invasive catheter insertion than pulmonary artery catheterization. However, it is also evident that abnormalities of cardiac structure and function will interfere with the assumptions by which central venous pressure monitoring can approximate left ventricular preload. Therefore, the central venous pressure has a greater role in preload assessment in the medical and surgical intensive care units for patients with structurally normal hearts, than in critically ill cardiac patients. The right atrial pressure waveform demonstrates pressure elevations concurrent with atrial contraction (the *a* wave), reflection of ventricular systole as transmitted by the tricuspid valve (the *c* wave), and venous filling of the right atrium against a closed tricuspid valve (the *v* wave). The *x* descent probably arises from right ventricular contraction pulling the tricuspid annulus downward, whereas the *y* descent corresponds to blood emptying from the right atrium into the ventricle [4] (Fig. 1.4).

As illustrated, there is generally an electromechanical delay of approximately 80 ms between the atrial depolarization of the P wave and the pressure deflection of atrial systole represented by the *a* wave. The degree of delay is dependent upon the length of tubing used for pressure transduction.

The normal right atrial pressure, or central venous pressure, ranges from 0 to 8 mmHg (approximately 0–10 cmH_2O if measured with a water manometer). The atrial pressure is usually taken to be the mean of the *a* waves on the pressure

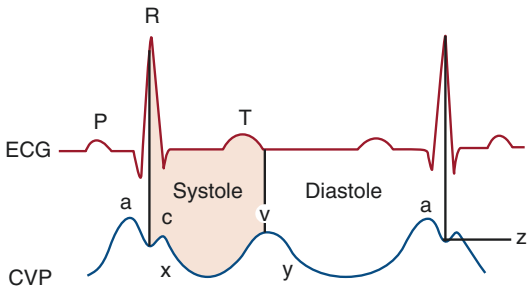

Fig. 1.4 Example of a typical central venous pressure waveform. (From Atchabahian and Gupta [49]). The base of the "c" wave represents the onset of right ventricular contraction and is therefore the best estimate of the final right ventricular filling pressure and preload.

Table 1.1 Variations of the right atrial waveform and their implications

Finding	Implication
Absence of the *a* wave	Atrial fibrillation or atrial standstill
Cannon waves	Atrioventricular dissociation – atrial contraction against a closed tricuspid valve
Elevation of all chamber pressures, with prominent *x* descent	Cardiac tamponade
Elevation of all chamber pressures, with steep *y* descent	Constrictive pericarditis
Large systolic wave	Tricuspid regurgitation

tracing. When the atrial wave is not present (due to atrial fibrillation or atrial standstill), the pressure tracing correlating with the R wave that occurs just before the *c* wave, referred to as the *z* point, is the most appropriate point for central venous pressure measurement. Because the central veins lie within the thorax, the waveform obtained will be influenced by intrathoracic pressure changes during inspiration and expiration. Inspiration is achieved by creating a negative intrathoracic pressure (by expansion of the thoracic cavity) which will be reflected by a downward shift of the central venous tracing. Exaggerated spontaneous inspirations may magnify this deviation. Therefore, it is customary to read the mean pressure at end-expiration, just before the inspiratory drop. The relationship is reversed in patients who are mechanically ventilated because inspiration is typically achieved by applying positive pressure and hence, the pressure at end-expiration is often at the low point of the respiratory nadir. The electronic transducer should always be leveled and zeroed in line with the right atrium, with the fourth intercostal space in the mid-axillary line often used as the anatomical landmark for leveling.

Other variations of the waveform that should be taken into account are listed in Table 1.1. Of particular relevance is the large systolic wave seen in tricuspid regurgitation. In the setting of significant tricuspid regurgitation, the *c* wave and *x* descent will be replaced by a prominent upward deflection (the systolic wave) occurring just before the *v* wave would be expected. This wave represents the regurgitant flow of blood back into the atrium with ventricular contraction.

Assessing Preload from the Right Atrial Pressure

The mean right atrial pressure, or central venous pressure, is primarily a reflection of venous return to the heart and thus the volume status of the patient. Lower pressures will be seen in the hypovolemic patient, as well as those in vasodilatory shock, e.g., due to sepsis or anaphylaxis. Elevated right atrial pressures are seen in cases of right ventricular failure (such as right ventricular infarction, pulmonary embolus), pulmonary hypertension (currently defined as mean pulmonary artery pressure at rest ≥25 mmHg [5]), tricuspid stenosis or regurgitation, cardiac tamponade, pericardial constriction, and hypervolemia (during anuric renal failure for example). The right atrial pressure may also be elevated in chronic or acutely decompensated left ventricular failure with either systolic or diastolic failure mechanisms.

Preload Reserve and the Venous System

In one of the early studies of preload dependence on human subjects, individuals with both normal

hearts and diseased hearts were observed to sustain a reduction in LVEDP and a reduction in cardiac index upon inflation of an occlusive balloon in the inferior vena cava, just caudal to the liver [6]. Conversely, it has been demonstrated in various settings that passive leg raising (PLR) from the horizontal plane in the supine subject increases the volume of blood returning to the right heart and, for a heart that is under filled and demonstrates preload reserve, this additional volume will boost left ventricular stroke volume. The venous system contains the major portion of circulating volume – up to 75% in some situations – because of the greater capacitance of veins than arteries. Therefore, venoconstriction has the potential to displace significant quantities of blood from the peripheral vasculature to the central circulation.

Venous return is the rate of blood flow from the periphery to the right atrium and depends upon the pressure gradient and the resistance to venous return. If blood were removed from a subject's circulating volume until there was no pressure within the venous system (i.e., no outward luminal force distending blood vessel walls), the volume of blood still contained within the system would be called the unstressed volume. The unstressed volume can be modulated by altering the contractile state of the venous smooth muscle. Venoconstriction decreases unstressed volume and, all other parameters being equal, will increase venous return and right atrial pressure. Venodilation increases unstressed volume and decreases right atrial pressure. In experiments using hexamethonium chloride, the unstressed volume has been seen to increase by almost 18 mL/kg, demonstrating the range of reflex compensation available [7]. During exercise, such as running, reflex venoconstriction of vascular beds in the spleen and skin, in combination with the action of the skeletal muscle pump, all help to increase venous return to the higher output heart and hence maintain sufficient pressure in the right atrium to support ventricular filling. In response to a sudden reduction in cardiac output, passive recoil of the veins will redistribute blood to the heart and act to restore adequate stroke volume. Conversely, sequential reductions in cardiac pump output lead to consequent decreases in arterial pressure and increases in venous pressure [8].

Movement of a volume of blood from the arterial system to the venous system will lower arterial pressure and raise venous pressure. However, due to the differing capacitances in these two systems, the arterial pressure change will be 19 times greater than that in the veins [9]. If cardiac output were to fall suddenly, the drop in pressure in the arterial system would far exceed the small rise in pressure in the venous system. Likewise, a large rise in arterial pressure will cause only a small reciprocal fall in venous pressure. All other factors being equal, the relationship venous pressure and cardiac output is reciprocal. Therefore, a constant interplay occurs between the heart and venous system to accommodate changes in posture and volume status. An equilibrium state can be reached at a right atrial pressure where venous return equals cardiac output. The reflex control of venous tone, and the signals governing this primary reservoir for cardiovascular homeostasis, are still incompletely understood.

Preload and the Respiratory Cycle

During inspiration, the negative intrathoracic cavity pressure is transmitted to the thoracic structures resulting in a decrease in the observed intravascular and intracardiac pressures. As previously described, right atrial and pulmonary wedge pressure tracings will be seen to fall. Inspiration will be followed by an increase in right atrial filling as an increased venous blood volume moves down the pressure gradient toward the heart. This leads to increased right ventricular volume and end-diastolic pressure in relation to the pleural pressure, although overall the expansion of the thoracic cavity causes the absolute right ventricular end-diastolic pressure to fall. Increased right-sided flow results in a slight increase in transmural pulmonary pressure during spontaneous inspiration. Events on the left side of the heart are inconsistent, as they are influenced by potentially contradictory changes in several parameters. However, the augmented blood volume moving through the right ventricle has been shown in closed-chest animal models to transiently decrease left ventricular stroke volume, likely due to deviation of the intraventricu-

lar septum into the left ventricular cavity which decreases its end-diastolic volume [10]. The respiratory relationship is reversed in patients who are mechanically ventilated with positive pressure during inspiration and calculation of the transmural pressure, by subtraction of the pleural pressure from the measured hemodynamic pressure, would show a more complex sequence of changes during the respiratory cycle. Intrapleural pressures can be measured with esophageal catheters, or roughly estimated based on the pressure settings of a patient's mechanical ventilation mode.

The Pulmonary Capillary Wedge Pressure Waveform

A key tenet of using the central venous pressure to assess cardiac preload is the relationship of right ventricular end-diastolic pressure to the left ventricular end-diastolic pressure. Experience has shown that there are many situations in which this pressure relationship does not hold true [11]. Pulmonary artery catheterization was previously a procedure limited to the research laboratory, but it made the transition to the bedside in the 1970s following the advent of the Swan-Ganz catheter. This is a multiple lumen catheter that permits pulmonary artery pressure measurement at the distal injection port and right atrial pressure at the proximal injection port. The balloon inflation port is used to inflate and deflate a small air-filled balloon at the distal catheter tip, which is introduced into a pulmonary artery branch. When the balloon is inflated and advanced within a pulmonary arterial branch, a column of static blood will exist between the left atrium and the catheter tip, enabling measurement of the downstream pressure in the left atrium (Figs. 1.5 and 1.6).

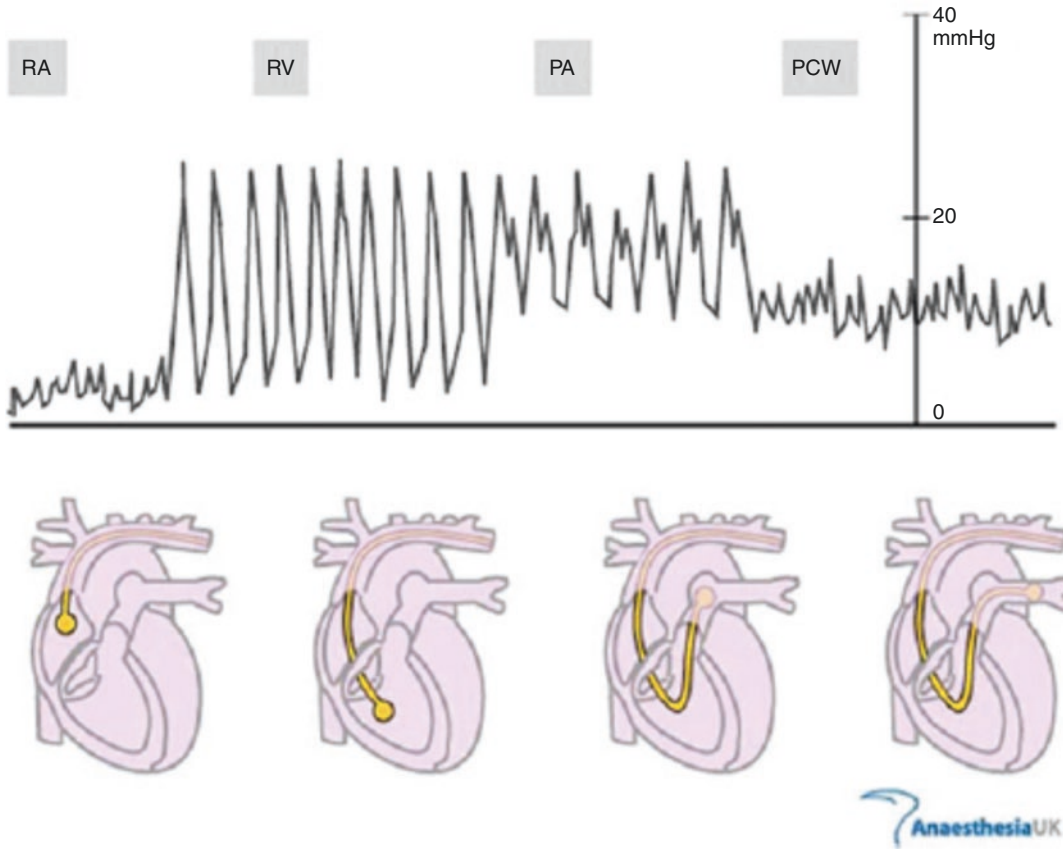

Fig. 1.5 Characteristic intracardiac pressure waveforms derived from the pulmonary artery catheter. (From Anesthesia UK, frca.co.uk)

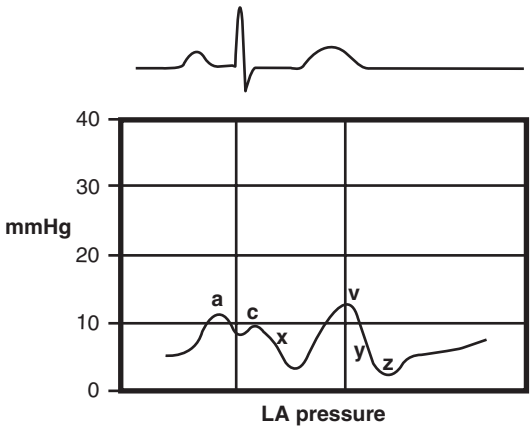

Fig. 1.6 Example of a typical pulmonary capillary wedge pressure waveform. (From The ABCs of A to V: Right Atrial/Left Atrial (PCW) Pressures, CathLabDigest.com). Note the occurrence of the "*a*" wave of left atrial contraction shortly after the electrocardiographic "*P*" wave and the occurrence of the "*v*" wave after the electrocardiographic "*T*" wave. The "*v*" wave falling after the "*T*" wave can be of help when distinguishing a prominent "*v*" wave in pulmonary capillary wedge profile from the systolic deflection of a pulmonary artery waveform, which occurs before the "*T*" wave and means the catheter is not in the wedge position

The waveform obtained at balloon inflation is a reflection of the left atrial pressure and therefore it will show a similar contour as the right atrial tracing with *a*, *c*, and *v* waves produced by the corresponding left-sided physiological events, although the wedge pressure is normally higher than the right atrial pressure. The pulmonary capillary wedge pressure (PCWP) is the key parameter in the clinical assessment of preload in heart failure patients, because in the absence of mitral stenosis, it will approximate left ventricular end-diastolic pressure (LVEDP), and therefore correct measurement technique is essential. The *a* wave will occur near the end of, or just after, the QRS complex, and the *v* wave follows the T wave. The PCWP pressure is measured as the mean amplitude of the *a* wave, or alternatively at the *z* point near the end of the QRS complex if an atrial contraction is not present. If a large systolic wave (*v* wave) is present, suggesting mitral regurgitation, a ventricular septal defect or diastolic dysfunction with impaired atrial compliance, the amplitude should also be recorded. If there is any uncertainty as to whether a true PCWP waveform has been attained, it should be ensured that the v wave falls after the T wave; in the catheterization laboratory, a blood sample can be withdrawn from the distal catheter port in the wedge position and should be the same as the arterial saturation is a true PCWP position has been attained. The PCWP should be measured at end-expiration if the waveform has respiratory variation.

The total electromechanical time delay is greater for the wedge waveform than for the right atrium as the changes in left atrial pressure have to be transmitted back through the pulmonary vasculature to the catheter tip. A balloon-tipped pulmonary artery catheter typically shows a mechanical time delay of 150–160 ms. A pressure gradient should exist between the mean pulmonary artery and the PCWP, with a gradual drop in PCWP occurring as the balloon is inflated. Indeed, there is usually a gradient of approximately 1–4 mmHg between the pulmonary artery diastolic (PAD) pressure and the mean PCWP to ensure forward movement of blood through the pulmonary vasculature, although sometimes the PAD and PCWP can be measured as almost equal [12]. However, a wedge pressure that exceeds PAD suggests an error in measurement, such as misidentification of a dampened PA tracing in place of a PCWP waveform or balloon inflation into a very small branch vessel, called overwedging. The difference between PAD and PCWP will be greater in the setting of pulmonary arterial hypertension, where elevated pulmonary artery pressures are seen without a concurrent PCWP elevation.

Assessing Preload from the Pulmonary Capillary Wedge Pressure

The value in the PCWP lies in its ability to represent (a) the volume status of the patient and (b) the adequacy of left ventricular function. If correctly obtained, the PCWP measures the capillary hydrostatic pressure that will tend to force movement of fluid out of the capillaries and into the pulmonary interstitium. This force is normally 6–12 mmHg

and is opposed by the capillary plasma colloid oncotic pressure at approximately 20–25 mmHg and acts to retain fluid in the vessel [13]. An imbalance of these opposing forces, or a change in the filtration coefficient, can promote the movement of fluid into the interstitium resulting in pulmonary edema. When the only altered parameter is hydrostatic pressure, there is a useful correlation between PCWP and the chest X-ray. From 18 mmHg, features of pulmonary edema may be seen; once hydrostatic pressure exceeds oncotic pressure around 25 mmHg, frank pulmonary edema would be expected. Therefore, a PCWP cut-off of 18 mmHg is often used as the hemodynamic numeric correlate of pulmonary edema [14]. A normal PCWP is usually quoted as 8–12 mmHg [12].

The gold standard invasive clinical assessment of cardiac preload is the left ventricular end-diastolic pressure (LVEDP), which is measured with a catheter retrogradely via the arterial system by crossing the aortic valve into the left ventricle. The correlation of PCWP with the left ventricular end-diastolic pressure, but not pulmonary artery pressures, has previously been demonstrated in settings such as acute myocardial infarction [15]. Although the PCWP is a good surrogate of left ventricular preload, one study showed that LVEDP was >5 mmHg higher than the PCWP in approximately 30% of heart disease patients [16].

It is important to understand situations in which the PCWP will not accurately assess preload. As previously mentioned, there is an exponential relationship between left ventricular end-diastolic pressure and volume. Therefore, the same volume change will cause a small pressure change at a low ventricular volume and a large pressure change in a more distended ventricle. The relationship between left ventricular volume and pressure may also be skewed in pericardial tamponade or constriction. Other scenarios where the PCWP can potentially misrepresent the LVEDP are outlined in Table 1.2. Mitral regurgitation causes a systolic regurgitant wave with onset just before the *v* wave, with similar morphology to that seen in tricuspid regurgitation in the central venous waveform. In pure mitral stenosis, the *a* wave will be prominent and elevated due to the resistance to blood flow through the narrowed valve orifice during atrial systole. The *y* descent is usually prolonged, indicative of the increased resistance to passive left ventricular filling. It is also important to remember that PCWP measured in the resting state may not adequately represent the hemodynamic etiology of dyspnea on exertion. Right heart catheterization during bicycle exercise is increasingly utilized when evaluating patients with potential heart failure with preserved ejection fraction, in whom the left atrial pressure may only rise to abnormal levels during exertion [17].

Table 1.2 Situations where pulmonary capillary wedge pressure (PCWP) may inaccurately represent left ventricular end-diastolic pressure (LVEDP)

PCWP lower than LVEDP	PCWP higher than LVEDP
Aortic regurgitation	Positive pressure ventilation
Highly compliant left atrial chamber	Mitral stenosis
	Mitral regurgitation
	Pulmonary venous obstruction between pulmonary capillary and left atrium
	Left atrial myxoma

Another recent advance in clinical heart failure management is the ability to measure ambulatory pulmonary artery pressures and attain a daily assessment of cardiac preload that guides outpatient therapies. The CHAMPION trial led to the approval of the CardioMEMS device (Abbott, St. Paul, Minnesota, USA) for which a pressure sensor is implanted into the pulmonary artery and wirelessly transmit PA systolic and diastolic measurements to their care providers. The CHAMPION trial showed a 30% reduction in heart failure hospitalizations in the 6 months following randomization to the monitoring strategy versus control, although the single-blind design of the trial and the lack of a comprehensive heart failure disease management comparator arm have left questions about the clinical impact of this approach [18]. However, the ability to assess ambulatory cardiac preload from a PA diastolic surrogate and identify an uptrend in volume status prior to clinical congestion manifestation is clearly a technological advance in the application of hemodynamic principles to clinical care.

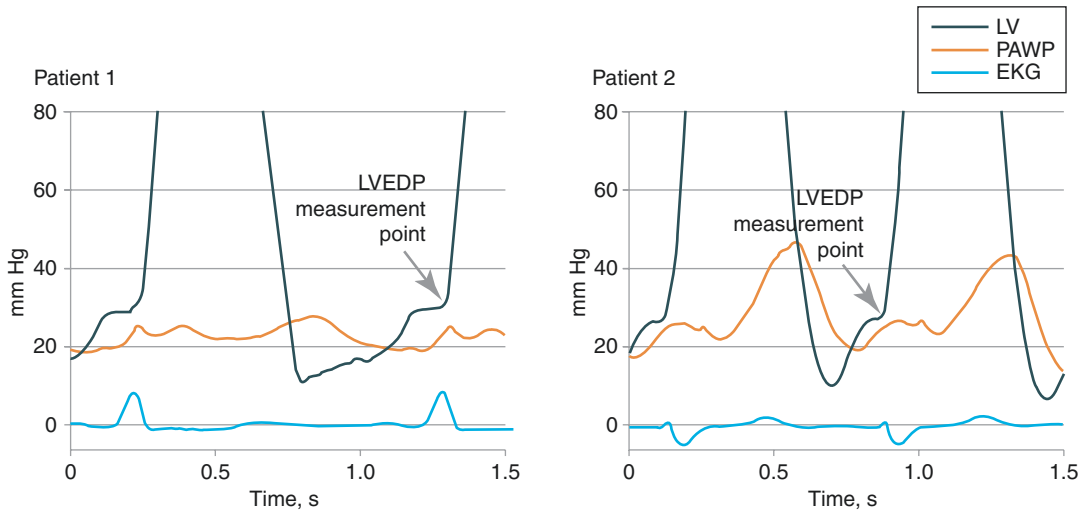

Fig. 1.7 Examples of two patients with similar left ventricular end-diastolic pressures, but differing pulmonary capillary wedge pressures, with patient 1 showing better left atrial compensation for the elevated LVEDP. (From Reddy et al. [50])

In the absence of any of these complicating factors, the wedge pressure should reflect the end-diastolic filling pressure in the left ventricle. The LVEDP is considered the gold standard single parameter in quantifying cardiac preload with the caveat that, as defined above, preload is a composite of several elements that contribute to passive ventricular wall stress at the end of diastole. In situations where it is essential to know the left ventricular preload precisely, such as in the evaluation of pulmonary hypertension etiologies, a left ventricular catheter for direct LVEDP measurement may be necessary. The downside is that the LVEDP requires arterial cannulation and retrograde passage of the catheter across the aortic valve into the left ventricle. This procedure is associated with risks and is usually performed only as a component of a more extensive left heart catheterization procedure. In addition, as the catheter enters the left ventricle for only a matter of minutes, usually only a single measurement of LVEDP is obtained during a patient's hospitalization. This is in contrast to the Swan-Ganz catheter which may remain in place for many days, with many critically ill patients having serial PCWP measurements throughout their intensive care admission. It should, however, be remembered that the LVEDP only reflects the LV operating compliance and can be higher than the PCWP if the left atrium is highly compliant and able to compensate for a chronically elevated LVEDP (Fig. 1.7).

A normal LVEDP is often quoted as 8–12 mmHg, with 16 or 18 mmHg usually being used as the threshold for significant elevation in clinical trials [19]. As illustrated in Fig. 1.3, chamber pressures on the left side of the heart are normally higher than those in the low-pressure system on the right.

Preload Dependency and Pressure–Volume Loops

Having successfully obtained an accurate hemodynamic estimate of preload, the next challenge is to interpret the impact of that parameter on overall cardiac function. The first concept is the preload dependency of ventricular performance. Carl Ludwig is reported as being the first to describe the dependence of cardiac work on diastolic filling, when he wrote in 1856 "… a strong heart that is filled with blood empties itself more or less completely, in other words, [filling of the heart with blood] changes the extent of contractile power" [20]. This relationship of preload to

performance was described in detail by Ernest Henry Starling, who published this relationship in a series of papers between 1912 and 1914 and in his 1915 Linacre Lecture at Cambridge University [21]. The relationship between ventricular pressure and volume during the cardiac cycle can be illustrated by pressure–volume loops, as depicted in Fig. 1.8. End-diastole is located at the lower right corner of the loop. The subsequent upstroke (the vertical line on the right of the graph) is isovolumic contraction. This is followed by ejection, with end-systole located in the upper left corner, and then the downstroke of isovolumic relaxation. As illustrated, increases in preload will result in a greater volume of blood ejection during systole – at least up until a point. Controversy exists as to whether the nondiseased human heart reaches a point of preload at which further end-diastolic stretch will result in decreasing blood ejection [22]. The so-called descending limb of the Frank–Starling curve is better described in the failing heart and will be discussed elsewhere in this book (Fig. 1.8).

At this point, it is valuable to reflect on the myocardial cellular mechanics that underlie the preload concept. The term preload originally arose from the isolated myofiber studies where myocytes were physically loaded with defined forces in the form of a weight applied to one end of a quiescent muscle sample, such as papillary muscle. The other end remains tethered and the force applied prior to contraction is the preload. By varying preload, the relationship between initial length and shortening (isotonic contraction), or developed force (isometric contraction), can be recorded. The maximal force developed at any sarcomere length is determined by the degree of overlap of thick and thin filaments and therefore the number of available actin-myosin cross bridges. Forces increase linearly until a sarcomere length with maximal overload (approx. 2.2 μm) is achieved [23]. Structural proteins constitute a strong parallel elastic component within the myocardium and prevent an increase in developed force beyond this maximal degree of preload. The ascending limb of the myofiber length–tension relationship, which is analogous to the increase in stroke volume with increasing preload in the whole heart, is also modulated by length-dependent increases in myofilament calcium sensitivity [24]. Proposed mechanisms include enhanced calcium binding to troponin C, narrower interfilament gaps at longer sarcomere length, and increased sarcoplasmic reticulum calcium release and uptake at longer sarcomere lengths.

Returning to the whole heart, the major determinants of the left ventricular pressure–volume relationship are the initial ventricular volume, chamber geometry, wall thickness, and myocardial stiffness. Pressure–volume loops highlight the nonlinear pressure and volume relationship during diastolic filling. The instantaneous slope of the curve in the filling phase (i.e., change in pressure/

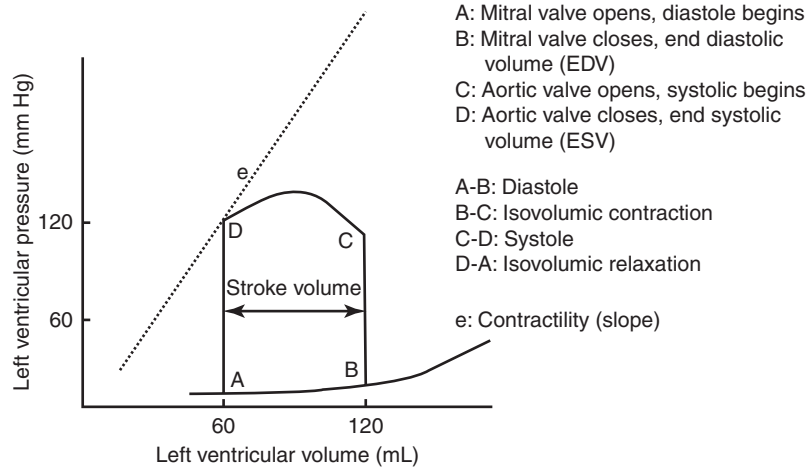

Fig. 1.8 Pressure–volume loop for a single cardiac cycle. (From Loushin et al. [51])

change in volume) represents diastolic stiffness. This parameter is correctly termed as elastance and can be conceptualized by the ventricle behaving as a spring with a stiffness (the inverse of compliance) that increases during contraction and decreases during relaxation. Elastance can be calculated at any point during the ventricle's diastole by calculating the gradient of the curve. Beyond a volume of approximately 140 mL (the exact volume will depend on individual heart dimensions), the chamber becomes progressively more difficult to fill, requiring a greater pressure increase to effect volume changes than earlier in diastole. A thicker, stiffer ventricle, for example in an individual with left ventricular hypertrophy, will show a steeper gradient to the diastolic curve, and hence a greater elastance. The mathematical inverse of elastance (i.e., change in volume/change in pressure) is compliance. The thicker, stiffer ventricle would be described as having reduced compliance. It should be remembered that diastole is an active process that consumes energy; ATP is hydrolyzed to break the actin-myosin crosslink and permit sarcomere lengthening. Therefore ventricular compliance also often falls during ischemia. In the setting of low compliance, a high LVEDP may actually reflect a relatively small LVEDV. Conversely in the normal left ventricle, compliance is high within the typical physiological range, because the chamber operates on the flatter region of the curve where reasonably small pressure rises give significant volume increases, promoting optimal stroke volume.

The importance of the physiological pressure–volume relationship is its role in modulating ventricular performance by the changes in preload. This heterometric regulation occurs on a beat-by-beat basis and ensures matching of the right and left ventricular output with changes in respiration and body posture [25]. In response to myocardial pathology, rises in end-diastolic pressure and volume can also provide a longer term compensatory increase in stroke volume due to increased myocardial fiber length in the remaining functional myocardium. However, the scope of this compensation is limited, as the dilated failing heart will also develop fibrosis, adverse remodeling, and unfavorable metabolic status. This explains the disparity between acute increases in end-diastolic volume resulting in augmented stroke volume, vs. the chronically dilated heart generating a poorer stroke volume.

These considerations illuminate the inherent difficulties in judging preload adequacy. The level of preload at which the heart will show its optimal stroke volume will be dependent on not only the intravascular volume status but also the ventricular compliance and geometry unique to the individual heart. Clinical experience has shown that some dilated, failing ventricles perform optimally at a higher wedge and LVEDP than would be judged normal. However, this cannot be assumed to be the case, as many heart failure patients show improved symptom status and cardiac output following aggressive diuresis and return of their wedge pressure to a value that would be considered to lie in the normal range (Fig. 1.9).

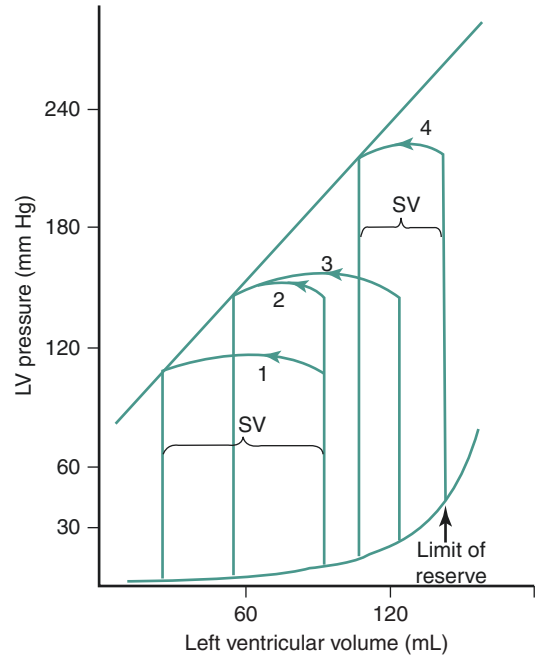

Fig. 1.9 Effects of acutely increasing preload on the pressure–volume loop, to the point of maximal preload reserve. (From Ross [52] and Kaplan [53]). When the ventricle reaches the limit of preload reserve, it is unable to distend any further and the preload is fixed; at this point (loop 4), any further increases in afterload will lead to a reduction in stroke volume

Preload in Clinical Practice

Invasive Hemodynamics

Assessment of preload reserve and preload adequacy is of particular relevance to the management of hypovolemic or septic shock patients. The use of invasive hemodynamic monitoring, with either a central venous catheter or pulmonary artery catheter, is generally the standard technique in the intensive care unit or operating room. Fluid resuscitation is titrated to right atrial or pulmonary wedge pressure, or to the central or mixed venous saturation which serves as a reflection of tissue oxygenation adequacy. Various goal-directed algorithms have been developed in the research setting and have demonstrated the value of early effective volume resuscitation in trauma, surgical, or sepsis patients [26]. However, since its introduction to clinical care almost 40 years ago, the limitations of the pulmonary artery catheter in actual clinical practice have been well documented. As described earlier, for the pulmonary wedge pressure to accurately reflect LVEDP, the following criteria must be met: (a) the catheter is correctly positioned with a valid and accurate wedge tracing obtained, (b) the wedge pressure is correctly interpreted, (c) the wedge pressure is an accurate reflection of LVEDP, and (d) there is a linear and predictable relationship between left ventricular end-diastolic pressure and volume. In an assessment of the technical adequacy of 2711 pulmonary wedge recordings, the authors reported that 31% of these recordings were technically inadequate [27]. Even if a valid waveform is obtained, it is estimated that in approximately a third of cases, data will be incorrectly interpreted by the physician making management decisions [28]. These issues, and the added difficulties brought by positive pressure ventilation, changes in myocardial compliance, and ventricular interdependence, can severely impact on the utility of the pulmonary capillary wedge pressure in accurately reflecting cardiac preload. Such factors may partially explain why randomized controlled trials have, to date, not shown improved outcomes with pulmonary artery catheterization in critically ill patients.

Noninvasive Preload Assessment Techniques

Alternative techniques for assessment of preload adequacy, and responsiveness of the stroke volume to further preload delivery, have also been trialed over recent years (Table 1.3). Various transthoracic and transesophageal echocardiographic measurements have been experimented with. One simple strategy is assessment of venal caval collapse during positive pressure ventilation, with the goal being to identify those patients with a RA pressure less than 10 mmHg who would benefit from further intravenous volume before being subjected to positive pressure ventilation [29]. Another related technique is passive leg raising (PLR) which has gained interest as a maneuver for assessing functional hemodynamic status and assessing potential fluid responsiveness. As described above, passive leg raising from the horizontal position effects a transient increase in preload and acts as an endogenous fluid challenge. Radiolabeled erythrocyte studies to determine venous blood volume in the lower extremities have demonstrated a reduction of approximately 150 mL in each leg when this maneuver is performed [30]. If the right ventricle is preload responsive, the 300 mL increase in venous return will augment right ventricular output and hence left ventricular filling. A small number of studies have proven increases in pulmonary wedge pressure and LVED dimensions with PLR, supporting the theory that the transfer of this volume of blood into the right atrium does significantly contribute to cardiac preload. However, in situations where the preload reserve of the heart is limited, meaning that further diastolic filling will not raise left ventricular stroke volume, the increased venous return will not result in greater cardiac output. The transient increase in cardiac output seen in the preload responsive heart has been observed to be greater after withdrawal of 500 mL blood [31], suggesting that the effect of this maneuver is dependent upon the volume status of the individual. The clinical utility of this observation was highlighted in a study of mechanically ventilated patients judged to be requiring volume expansion, with recording of aortic blood flow after PLR and then a 500 mL intravenous fluid

Table 1.3 Techniques for clinical assessment of cardiac preload

Technique	Pros	Cons
Pulmonary capillary wedge pressure (PCWP) [15]	Multiple right heart and pulmonary pressures, cardiac output, and index all measurable	Invasive, inaccurate with some structural diseases, requires interpretation
Left ventricular end-diastolic pressure (LVEDP) [15]	Gold standard for preload measurement	Requires arterial cannulation, traversing the aortic valve
Ambulatory pulmonary artery diastolic pressure sensor [18]	Enables ambulatory monitoring to detect preload increases	Relies on PA diastolic, further clinical validation required
Vena caval ultrasound assessment	Noninvasive and simple to perform	Sensitivity may be poor
Passive leg raising (PLR) [7]	Noninvasive and simple to perform	Requires bed that performs appropriate movements
Right ventricular end-diastolic volume index (RVEDVI) [33]	Predicts change in stroke volume in response to fluids	Requires a rapid response thermistor and PA catheterization
Left ventricular end-diastolic area (EDA) [36]	No vascular access required	Requires a transesophageal echocardiogram study
Intrathoracic blood volume assessment (ITBV) [38]	Stronger predictor of preload than PCWP or CVP	Requires femoral artery cannulation
Esophageal Doppler [41]	Esophageal probe is minimally invasive	Role in medical intensive care is still to be defined
Deuterium oxide and sodium bromide dilution techniques	Accurate estimation of total body water and extracellular water, respectively	Requires isotope ingestion or injection and blood or urine collections
Radioisotope blood volume analysis (red cell mass and plasma volume measurement) [44]	Measures intravascular volume	Requires isotope injection and blood collections
Bioimpedance spectroscopy [45]	Noninvasive	Does not differentiate intravascular fluid from total body water
Thoracic impedance measurement [46]	Noninvasive	Imperfect representation of invasive hemodynamics

challenge. The PLR was achieved by taking the patient from a semirecumbent position with 45 ° head elevation, through a negative 45 ° tilt of the bed, so that the upper body lay parallel to the horizontal with the lower extremities elevated at a 45 ° angle. An increase in aortic blood flow of at least 10% by PLR predicted a volume expansion-induced increase in aortic blood flow of at least 15% with a sensitivity of 97% and specificity of 94% [32]. Thus, an initial trial of PLR appears to offer a potentially useful noninvasive clinical tool for assessing which critically ill patients will be preload responsive and should receive further volume expansion.

Additional Invasive Preload Assessment Techniques

The use of a pulmonary artery catheter with a rapid response thermistor and an ECG electrode allows computation of the right ventricular ejection fraction, from which right ventricular end-diastolic and end-systolic volumes can be calculated. Right ventricular end-diastolic volume index (RVEDVI) is by dividing right ventricular end-diastolic volume by body surface area, and has been evaluated in surgical critical care settings in mechanically ventilated patients. One such study aimed to determine preload status in acute respiratory failure patients. The degree of positive end-expiratory pressure (PEEP) was titrated and corresponding serial measurement of RVEDVI, wedge pressure, and cardiac index were recorded. They found that, at all levels of PEEP, cardiac index correlated significantly better with RVEDVI than with wedge pressure – at high levels of PEEP, cardiac index inversely correlated with wedge pressure, but remained positively correlated with the RVEDVI [33]. The value of RVEDVI is its ability to predict the change in stroke volume in response to a

fluid challenge, and has been demonstrated to be a superior predictor of recruitable cardiac output than wedge pressure [34]. Of note, though, some authors suggest that the RVEDVI overestimates the preload in comparison to echocardiographic techniques [35].

Left ventricular dimensions have also been employed in the assessment of preload adequacy (Table 1.3). Transesophageal echocardiography is also increasingly used to assess left ventricular filling, with the LV end-diastolic area (EDA) in the transgastric mid-papillary short axis view proving to be a useful parameter that correlated with cardiac preload. In a cohort of heterogeneous medical intensive care unit patients, the left ventricular EDA was significantly lower in those patients who showed a good response to volume challenge [36]. However, the utility of EDA assessment was felt to be lower in this study than in several others evaluating EDA and preload in cardiac surgery patients. Nonetheless, at least one intensive care center has had such success with left ventricular echocardiographic assessment of preload reserve that it has become the primary method for hemodynamic [37].

Another technique that features in the anesthesiology and surgical literature is transpulmonary thermal-dye indicator dilution, which enables bedside measurement of intrathoracic blood volume (ITBV). ITBV has been shown to be a stronger predictor of preload than PCWP and CVP [38]. Transpulmonary double indicator dilution measurements of cardiac output and ITBV can be performed using a catheter positioned in the descending aorta (via the femoral artery) that simultaneously measures thermodilution and dye-dilution. The two indicators are the freely diffusible cold saline and a plasma bound indicator such as indocyanine green (ICG). When injected simultaneously, the cold indicator will equilibrate with the interstitium whereas the ICG will remain in the intravascular space. Based upon the conservation of mass, intrathoracic blood volume (ITBV) can then be calculated from cardiac output and the mean transit time of the dye tracer between the site of injection – the right atrium – and the site of detection. A study in 10 anesthetized patients observed significant decreases in ITBV after a standardized change from supine to sitting body position, which correlated with changes in the stroke volume index. This study found ITBV and EDV to be equivalent indices of cardiac preload in their small sample of anesthetized patients [39]. Another group that compared preload variables in the early phase of hemodynamic stabilization of 57 critical care patients found ITBV to be a more reliable indicator of preload than CVP or PCWP [40]. However, femoral artery catheterization is required for this technique.

An invasive technique for assessing preload adequacy that may be appropriate in high-risk surgical patients is esophageal Doppler. This is a minimally invasive method of measuring real-time descending aortic blood flow that employs the Doppler shift phenomenon as a marker for blood cell velocity. A probe situated in the esophagus is in close proximity to the descending aorta and provides an excellent window for obtaining Doppler flow signal from which cardiac output can be calculated. The left ventricular ejection time (or flow time) corrected for heart rate correlates well with left ventricular preload. In general, a corrected flow time of less than 0.35 s suggests a potential to respond to volume expansion, whereas reading above 0.45 s suggests that volume expansion will not stimulate further increases in cardiac output [41]. Esophageal Doppler has been demonstrated to be effective in guiding nurse-led, protocolized resuscitation in the early postoperative hours, resulting in reduced complications and shorter hospital stays for cardiac surgery patients [42]. Its promise has also been recognized in the medical intensive care setting, where the continuous real-time monitoring could be of use in gaining instantaneous feedback on interventions. Probe insertion takes only minutes, requires minimal technical skill, and is not associated with any major complications [43]. However, the calculations that generate measurements of aortic blood flow do depend upon aortic geometric assumptions.

Finally, a range of techniques for ambulatory assessment of blood volume, as a surrogate for cardiac preload, have been developed to inform the clinically management of heart failure patients

who are at risk of developing congestion years (Table 1.3). Techniques range from the research-only use of deuterium oxide and sodium bromide, to measure the total body water and extracellular volumes, respectively, to the radioisotope measurement of red cell mass and plasma volume in a blood volume analysis test [44]. The relationship between elevated preload and increased tissue edema is harnessed for the techniques of bioimpedance spectroscopy, which involves the placement of voltage and current electrodes at landmarks on the body [45], and for thoracic impedance measurements either via implantable pacemaker-defibrillator devices or from measurement on the chest wall [46]. There is much current interest in the potential for left ventricular assist device (LVAD) flow waveforms to offer a noninvasive assessment of preload for mechanically supported end-stage heart failure patients, with a recent publication showing correlation between the PCWP and the ventricular filling phase slope of the Heartware LVAD flow waveform [47].

Bullet Point Summary

- Preload is a composite assessment of cardiac filling that represents the primary determinant of cardiac output.
- End-diastolic left ventricular pressure and volume are common surrogates for preload.
- However, the passive myocardial length–tension relationship is exponential rather than linear, limiting the role of pressures as a direct surrogate for preload.
- Preload increases with greater circulating volume, venoconstriction, exercise, arteriovenous fistulae, increased ventricular compliance, increased ventricular filling time, left ventricular systolic failure.
- Preload decreases with volume depletion, decreased venous return, impaired atrial contraction, tricuspid or mitral stenosis, less compliant ventricles.
- The atrial pressure waveform comprises *a*, *c*, and *v* waves, with *x* and *y* descents.
- Atrial pressure is usually measured as the mean of the *a* waves.
- Inspiration normally decreases all intracardiac pressures.
- Inflation of the Swan-Ganz catheter balloon within a pulmonary artery branch enables measurement of downstream pressure in the left atrium.
- Pressure–volume loops are orientated with end-diastole located at the lower right corner of the loop.
- The instantaneous slope of the pressure–volume curve in the filling phase elastance.
- Invasive methods of assessing left ventricular preload adequacy include: central venous pressure, pulmonary artery diastolic pressure, and pulmonary capillary wedge pressure. Left ventricular end-diastolic pressure is considered the gold standard.
- Noninvasive methods of assessing left ventricular preload adequacy include vena caval collapse, right ventricular end-diastolic volume index, left ventricular end-diastolic area, esophageal Doppler evaluation of left ventricular inflow, and intrathoracic blood volume.

Review Questions

1. Which of the following has *not* been used as surrogate parameter for cardiac preload?
   (a) Left ventricular end-systolic pressure
   (b) Pulmonary capillary wedge pressure
   (c) Intrathoracic blood volume
   (d) End-diastolic myocardial fiber tension
   (e) Degree of venal caval collapse
   Answer is (a). However, left ventricular end-*diastolic* pressure is a commonly used clinical surrogate for cardiac preload.
2. Which one of the following statements is true regarding central venous pressure monitoring?
   (a) The normal central venous pressure in a healthy adult ranges from 5 to 12 mmHg
   (b) The central venous pressure should be taken to be the lowest point between the *a* and v waves as measured during inspiration
   (c) Central venous pressure rises during deep inspiration
   (d) The *x* descent is absent in cardiac tamponade

(e) Significant tricuspid regurgitation will cause a prominent upward deflection just before the *v* wave would be expected

Answer is (e). The normal central venous pressure is 0–8 mmHg, although a higher rage may well be an appropriate target for a critically ill individual in whom maintenance of preload is important. The pressure is usually read as the mean peak of the *a* waves, ideally at the end of expiration, just before the inspiratory fall in central venous pressure. Cardiac tamponade causes absence of the *y d*escent, and often results in a prominent *x d*escent.

3. Which of the following does *not* generally cause the pulmonary capillary wedge pressure to be unrepresentative of the left atrial pressure?
   (a) Pulmonary venous hypertension
   (b) Balloon inflation in a very small branch vessel
   (c) Aortic stenosis
   (d) Mitral regurgitation

   Answer is (c). Pulmonary venous hypertension, overwedging of the Swan-Ganz balloon and an atrial myxoma can all cause the pulmonary capillary wedge pressure to read higher than the actual left atrial pressure. Severe mitral regurgitation causes a large systolic regurgitant wave with onset just before the *v* wave, and so care must be taken to correctly interpret the pressure waveform and estimate the pressure as the peak of the a waves, because inclusion of the regurgitant upward deflection will cause overestimation of the true pressure. The presence of mitral stenosis and aortic regurgitation can also cause the pulmonary capillary wedge pressure to misrepresent the left ventricular end-diastolic pressure.
4. Which one of the following statements is true regarding ventricular "elastance"?
   (a) This is an expression of the ease of diastolic stretching of the myocardium.
   (b) Can be a calculated as the change in pressure divided by change in volume, which is the instantaneous slope of the pressure–volume curve in the filling phase.
   (c) Beyond a volume of 40 mL in the adult heart, the left ventricle becomes more difficult to fill, and shows lower elastance.
   (d) A heart with left ventricular hypertrophy shows lower elastance than normal.
   (e) In the setting of low elastance, a high LVEDP may actually reflect a relatively small LVEDV.

   Answer is (b). Elastance is a measure of the diastolic stiffness of the myocardium, and is the inverse of compliance. Elastance is decreased above approximately 140 mL in the adult left ventricle. Left ventricular hypertrophy results in higher elastance and lower compliance than normal. It is a higher elastance ventricle in which a high LVEDP may actually reflect a relatively small LVEDV.
5. A 74-year-old female with long-standing hypertension and diabetes presents with confusion, fever and hypotension, with a blood pressure of 88/48. She is diagnosed with urosepsis and admitted to an intensive care unit. A prior outpatient echocardiogram showed severe left ventricular hypertrophy, most marked in the upper septal region, with a left ventricular ejection fraction of 65%. Are the following statements true or false?
   (a) The concentric hypertrophy confers greater elastance, compared to a normal left ventricle.
   (b) Preload is increased in a stiffer left ventricle.
   (c) This individual may be particularly sensitive to volume depletion.
   (d) After recovery from sepsis, beta-blockers and nitrates should be included in this individual's outpatient medication regimen.
      (a) True. A stiffer ventricle has greater elastance, and lesser compliance – these two parameters are inversely related.
      (b) False. As a ventricle becomes less compliant, the preload will decrease as the end-diastolic volume achieved with the same degree of venous return and filling time will be less.

(c) True. Due to the decreasing end-diastolic volume with worsening left ventricular hypertrophy, this heart becomes more "preload dependent," meaning that the same reduction in preload will cause a greater fall in stroke volume compared to a structurally normal heart. An individual such as the one described can show significantly reduced stroke volumes in the setting of volume depletion or distributive shock, due to the development left ventricular outflow tract obstruction, with or without systolic anterior motion of the mitral valve. This patient's blood pressure will likely improve markedly when the preload is augmented, for example, by intravenous volume resuscitation.

(d) False. Beta-blockers are often indicated in patients with significant left ventricular hypertrophy, or hypertrophic cardiomyopathy. By reducing heart rate, the diastolic ventricular filling period is increased, so improving the preload. Conversely, nitrates cause venodilatation and a reduction in preload, and hence may decrease this patient's preload and induce a left ventricular outflow tract gradient.

6. A 60-year-old male with coronary artery disease, hypertension, and active tobacco use presents with chest pain and inferior ST elevations. He was also noted to be in complete heart block with a heart rate of 48 bpm. At emergent cardiac catheterization, there was an acute right coronary occlusion, which was successfully intervened upon. However, the peak troponin T was 28 ng/mL, signifying a significant inferior myocardial infarction. On arrival in the coronary intensive care unit, the blood pressure was 90/72, with a right atrial pressure of 21, PA pressure 27/17, pulmonary capillary wedge pressure 14, cardiac index 1.8 l/min/m^2. Are the following statements true or false?

(a) Passive leg raising could be used as a measure of preload dependence.

(b) Positive end-expiratory pressure will not affect the cardiac index as the pulmonary capillary wedge pressure is normal.

(c) Atrioventricular pacing would be expected to improve the cardiac index.

(d) Use of dobutamine in this setting will increase the preload.

(a) True. Passive leg raising provides an "endogenous fluid challenge" and temporarily enhanced venous return and therefore preload. If the blood pressure and/or cardiac index improves immediately after this maneuver, it suggests that the patient will be responsive to volume resuscitation. The scenario described is consistent with a right ventricular infarction. In this setting, the blood pressure and cardiac index often improve with judicious use of small fluid boluses, as the patient is highly preload dependent.

(b) False. Mechanical ventilation with positive end-expiratory pressure will hinder venous return to the thorax during inspiration and hence may decrease stroke volume, especially in the heart with inadequate preload.

(c) True. The loss of atrial contraction, which usually supplies approximately 20% of ventricular filling, may be particularly detrimental for the preload-dependent right ventricle in this individual. Restoration of atrioventricular coordination with temporary pacing wires can significantly augment ventricular performance.

(d) False. Use of dobutamine in this setting would be expected to enhance contractility and decrease the right ventricular afterload by inducing some vasodilatation in the pulmonary vasculature. The preload may be slightly decreased by systemic peripheral vasculature dilatation.

References

1. Norton JM. Towards consistent definitions for preload and afterload. Adv Physiol Educ. 2001;25:53–61.
2. Mohrman DE, Lois JH. Cardiovascular physiology, Lange physiology series. 5th ed. London: McGraw Hill; 2003.
3. Schuster M, Nave H, Piepenbrock S, Pabst R, Panning B. The carina as a landmark in central venous catheter placement. Br J Anaesth. 2000;85:192–4.
4. Daily EK, Schoroeder JS. Techniques in bedside hemodynamic monitoring. 2nd ed. St. Louis: Mosby; 1994.
5. Badesch DB, Champion HC, Sanchez MA, Hoeper MM, Loyd JE, Manes A, McGoon M, Naeije R, Olschewski H, Oudiz RJ, Torbicki A. Diagnosis and assessment of pulmonary arterial hypertension. J Am Coll Cardiol. 2009;54(1 Suppl):S55–66.
6. Ross J Jr, Braunwald E. Studies on Starling's Law of the Heart: IX. The effect of impeding venous return on performance of the normal and failing human left ventricle. Circulation. 1964;30:719–27.
7. Rothe CF. Physiology of venous return. An unappreciated boost to the heart. Arch Intern Med. 1986;146(5):977–82.
8. Tyberg JV. Venous modulation of ventricular preload. Am Heart J. 1992;123(4. Pt 1):1098–104.
9. Johnson LR. Essential medical physiology. 3rd ed. San Diego: Academic; 2003.
10. Peters J, Fraser C, Stuart RS, Baumgartner W, Robotham JL. Negative intrathoracic pressure decreases independently left ventricular filling and emptying. Am J Phys. 1989;257(1 Pt 2):H120–31.
11. Forrester JS, Diamond G, McHugh TJ, Swan HJ. Filling pressures in the right and left sides of the heart in acute myocardial infarction. A reappraisal of central-venous-pressure monitoring. N Engl J Med. 1971;285(4):190–3.
12. Ahrens TS, Taylor LA. Hemodynamic waveform analysis. Philadelphia: WB Saunders; 1992.
13. Warren SE, Dennish G. Vasodilator treatment for acute and chronic heart failure. Br Heart J. 1978;40:1059–60.
14. Yamamuro A, Yoshida K, Hozumi T, Akasaka T, Takagi T, Kaji S, Kawamoto T, Yoshikawa J. Noninvasive evaluation of pulmonary capillary wedge pressure in patients with acute myocardial infarction by deceleration time of pulmonary venous flow velocity in diastole. J Am Coll Cardiol. 1999;34:90–4.
15. Rahimtoola SH, Loeb HS, Ehsani A, Sinno MZ, Chuquimia R, Lal R, Rosen KM, Gunnar RM. Relationship of pulmonary artery to left ventricular diastolic pressures in acute myocardial infarction. Circulation. 1972;46:283–90.
16. Flores ED, Lange RA, Hills LD. Relation of mean pulmonary arterial wedge pressure and left ventricular end-diastolic pressure. Am J Cardiol. 1990;66:1532–3.
17. Borlaug BA, Nishimura RA, Sorajja P, Lam CSP, Redfield MM. Exercise hemodynamics enhance diagnosis of early heart failure with preserved ejection fraction. Circ Heart Fail. 2010;3:588–95.
18. Abraham WT, Adamson PB, Bourge RC, Aaron MF, Costanzo MR, Stevenson LW, Strickland W, Neelagaru S, Raval N, Krueger S, Weiner S, Shavelle D, Jeffries B, Yadav JS, CHAMPION Trial Study Group. Wireless pulmonary artery haemodynamic monitoring in chronic heart failure: a randomised controlled trial. Lancet. 2011;377:658–66.
19. Zile MR, Gaasch WH, Carroll JD, Feldman MD, Aurigemma GP, Schaer GL, Ghali JK, Liebson PR. Heart failure with a normal ejection fraction: is measurement of diastolic function necessary to make the diagnosis of diastolic heart failure? Circulation. 2001;104:779–82.
20. Katz AM. Ernest Henry Starling, his predecessors, and the "law of the heart". Circulation. 2002;106:2986–92.
21. Starling EH. The Linacre lecture on the law of the heart. In: Chapman CB, Mitchell JH, editors. Starling on the heart. London: Dawsons of Pall Mall; 1965. p. 119–47.
22. Ross J Jr, Franklin D, Sasayama S. Preload, afterload, and the role of afterload mismatch in the descending limb of cardiac function. Eur J Cardiol. 1976;4(Suppl):77–86.
23. Julian FJ, Morgan DL. The effect on tension of non-uniform distribution of length changes applied to frog muscle fibres. J Physiol. 1979;293:379–92.
24. Fuchs F, Smith SH. Calcium, cross-bridges, and the Frank-Starling relationship. News Physiol Sci. 2001;16:5–10.
25. Fuster V, Walsh R. Hurst's the heart, vol. 1. 13th ed. Harrington: McGraw Hill; 2011.
26. Plnsky PR. Hemodynamic evaluation and monitoring in the ICU. Chest. 2007;132:2020–9.
27. Morris AH, Chapman RH, Gardner RM. Frequency of technical problems encountered in the measurement of pulmonary artery wedge pressure. Crit Care Med. 1984;12:164–70.
28. Iberti TJ, Fischer EP, Leibowitz AB, Panacek EA, Silverstein JH, Albertson TE. A multicenter study of physicians' knowledge of the pulmonary artery catheter. Pulmonary Artery Catheter Study Group. JAMA. 1990;264:2928–32.
29. Jellinek H, Krafft P, Fitzgerald RD, Schwarz S, Pinsky MR. Right atrial pressure predicts hemodynamic response to apneic positive airway pressure. Crit Care Med. 2000;28(3):672–8.
30. Pinsky MR, Brochard L, Mancebo J. Applied physiology in intensive care medicine. Berlin: Springer; 2006.
31. Wong DH, O'Connor D, Tremper KK, Zaccari J, Thompson P, Hill D. Changes in cardiac output after acute blood loss and position change in man. Crit Care Med. 1989;17:979–83.
32. Monnet X, Rienzo M, Osman D, Anguel N, Richard C, Pinsky MR, Teboul JL. Passive leg raising predicts

fluid responsiveness in the critically ill. Crit Care Med. 2006;34(5):1402–7.
33. Cheatham ML, Nelson LD, Chang MC, Safcsak K. Right ventricular end-diastolic volume index as a predictor of preload status in patients on positive end-expiratory pressure. Crit Care Med. 1998;26(11):1801–6.
34. Diebel L, Wilson RF, Heins J, Larky H, Warsow K, Wilson S. End-diastolic volume versus pulmonary artery wedge pressure in evaluating cardiac preload in trauma patients. J Trauma. 1994;37(6):950–5.
35. Kraut EJ, Owings JT, Anderson JT, Hanowell L, Moore P. Right ventricular volumes overestimate left ventricular preload in critically ill patients. J Trauma. 1997;42(5):839–46.
36. Tousignant CP, Walsh F, Mazer CD. TEE and preload assessment in critically ill patients. Anesthesiol Analg. 2000;90:351–5.
37. Loubieres Y, Vieillard-Baron A, Beauchet A, Fourme T, Page B, Jardin F. Echocardiographic evaluation of left ventricular function in critically ill patients: dynamic loading challenge using medical antishock trousers. Chest. 2000;118:1718–23.
38. Hoeft A, Schorn B, Weyland A, Scholz M, Buhre W, Stepanek E, Allen SJ, Sonntag H. Bedside assessment of intravascular volume status in patients undergoing coronary bypass surgery. Anesthesiology. 1994;81:76–86.
39. Buhre W, Buhre K, Kazmaier S, Sonntag H, Weylandà A. Assessment of cardiac preload by indicator dilution and transoesophageal echocardiography. Eur J Anaesthesiol. 2001;18:662–7.
40. Sakka SG, Meier-Hellmann A. Evaluation of cardiac output and cardiac preload. In: Vincent JL, editor. Yearbook of intensive care and emergency medicine. Berlin: Springer; 2000. p. 671–9.
41. Barash PG, Cullen BF, Stoelting RK, editors. Clinical anesthesia. Philadelphia: Lippincott Williams & Wilkins; 2009.
42. McKendry M, McGloin H, Saberi D, Caudwell L, Brady AR, Singer M. Randomised controlled trial assessing the impact of a nurse delivered, flow monitored protocol for optimisation of circulatory status after cardiac surgery. BMJ. 2004;329:258–61.
43. Marik ME. Pulmonary artery catheterization and esophageal Doppler monitoring in the ICU. Chest. 1999;116:1085–91.
44. Manzone TA, Dam HQ, Soltis D, Sagar VV. Blood volume analysis: a new technique and new clinical interest reinvigorate a classic study. J Nucl Med Technol. 2007;35:55–63.
45. Weyer S, Zink MD, Wartzek T, Leicht L, Mischke K, Vollmer T, Leonhardt S. Bioelectrical impedance spectroscopy as a fluid management system in heart failure. Physiol Meas. 2014;35:917–30.
46. Zile MR, Sharma V, Johnson JW, Warman EN, Baicu CF, Bennett TD. Prediction of all-cause mortality based on the direct measurement of intrathoracic impedance. Circ Heart Fail. 2016;9:e002761.
47. Grinstein J, Rodgers D, Kalantari S, Sayer G, Kim GH, Sarswat N, Adatya S, Ota T, Jeevanandam V, Burkhoff D, Uriel N. HVAD waveform analysis as a noninvasive marker of pulmonary capillary wedge pressure: a first step toward the development of a smart left ventricular assist device pump. ASAIO J. 2018;64:10–5.
48. Iaizzo PA, editor. Handbook of cardiac anatomy, physiology, and devices. 2nd ed. New York: Springer; 2009.
49. Atchabahian A, Gupta R. The Anesthesia Guide. New York: McGraw-Hill Medical, 2013.
50. Reddy YNV, El-Sabbagh A, Nishimura RA. Comparing pulmonary arterial wedge pressure and left ventricular end diastolic pressure for assessment of left-sided filling pressures. JAMA Cardiol. 2018;3:453–4.
51. Loushin MK, Quill JL, Iaizzo PA. Mechanical aspects of cardiac performance. In: Iaizzo PA, editor. Handbook of cardiac anatomy, physiology, and devices. 2nd ed. New York: Springer; 2009. p. 271–96.
52. Ross J. Afterload mismatch in aortic and mitral valve disease: implications for surgical therapy. J Am Coll Cardiol. 1985;5:811.
53. Kaplan JL. Kaplan's cardiac anesthesia. 7th ed. Amsterdam: Elsevier; 2016.

Suggested Reading

Ahrens TS, Taylor LA. Hemodynamic waveform analysis. Philadelphia: WB Saunders; 1992. Chapters 2 and 3.
Daily EK, Schoroeder JS. Techniques in bedside hemodynamic monitoring. 5th ed. St. Louis: Mosby; 1994.
Fuster V, Walsh R. Hurst's the heart, vol. 1. 13th ed. McGraw Hill: Harrington; 2011. Part 2, Chapters 5.

Afterload

2

Amanda R. Vest

Understanding the Concept

As discussed in Chap. 1 regarding preload, cardiac afterload is also a semiquantitative composite assessment of a determinant of cardiac output. The four major determinants of cardiac output are cardiac preload, myocardial contractility, heart rate, and afterload. Afterload is the force against which the heart pumps to expel blood into the vasculature. In isolated myofiber experiments, myocytes are physically loaded with defined forces in the form of a weight, to the lower end of a vertically mounted quiescent muscle sample. The opposing end of the myofiber remains tethered. The muscle is then electrically stimulated to contract and lift the additional weight. Once stimulated, the muscle develops tension, or force, until it meets and then overcomes the opposing force of the applied load, which is termed the afterload. Once the afterload is exceeded, the weight will be physically lifted and fiber shortening occurs. The degree and velocity of myofiber shortening is inversely related to the afterload applied. If both ends of the muscle sample are tethered and immobilized, or if the afterload applied is in excess of the myofiber's maximal force generation, the resulting contraction will remain isometric, meaning that the fiber length will be unchanged when tension is generated during contraction [1].

An alternate expression of the afterload is as a stress (defined as unit force per cross-sectional area) enabling comparison of differently sized samples of myofiber. It also permits transfer of the concept to the intact ventricle. Afterload in the whole heart can be understood as the stress encountered by left ventricular myofibers as they contract against the end-diastolic volume. Ventricular wall forces are difficult to directly measure, but the wall tension can be described by LaPlace's equation through $\sigma = PR/2w$, where σ is wall stress, P is pressure, R is ventricular radius, and w is wall thickness. This equation applies to a spherical chamber, whereas the equation is modified toward $\sigma = PR/w$ for a cylindrical vessel. More complex mathematical calculations can also be used to quantify end-systolic wall stress that take into account variations on chamber geometry. It can be seen from the law of LaPlace that, at a given intraventricular

A. R. Vest (✉)
Division of Cardiology, Tufts Medical Center, Boston, MA, USA
e-mail: avest@tuftsmedicalcenter.org

A. T. Askari, A. W. Messerli (eds.), *Cardiovascular Hemodynamics*, Contemporary Cardiology,
https://doi.org/10.1007/978-3-030-19131-3_2

pressure, a dilated left ventricle (increased ventricular radius) will have to develop a greater inward force than a smaller heart to generate the same systolic pressure. This makes the ventricle vulnerable to an "afterload-contractility mismatch" and explains why stroke volume may be augmented by reducing the afterload of a dilated left ventricle. Conversely, a hypertrophied left ventricular wall will achieve a lower wall stress and more easily generate a systolic pressure that overcomes ventricular afterload.

Another concept for defining afterload is in terms of the impedance to blood flow entering the aorta, known as arterial input impedance. This parameter quantifies the ratio of change in pressure to change in flow. It can be calculated using values for arterial pressure, elasticity, vessel dimension, and blood viscosity, and it requires invasive instantaneous aortic pressure and flow measurements which render it a research tool only. With the two principal determinants of ventricular afterload being systolic pressure and ventricular radius, and because the ventricular dimensions are assumed to remain relatively consistent, the systolic arterial pressure is the parameter most commonly used as a surrogate for afterload in clinical practice. In the absence of aortic or pulmonic stenosis, the maximum systolic pressure beyond the valve reflects the maximum pressure generated by the corresponding ventricle. Hence, the peak aortic pressure and peak pulmonary pressure can be measured to estimate the left and right ventricular afterloads, respectively.

An inverse relationship exists between stroke volume and the afterload [2]. As above, this is a consequence of the fact that muscle cannot shorten in excess of the length determined by the total load acting upon it. When this load is increased, sarcomere shortening will stop at a greater length, and so the extent of thick-thin filament overlap and cross-bridge formation will be diminished compared to a lower afterload (Fig. 2.1).

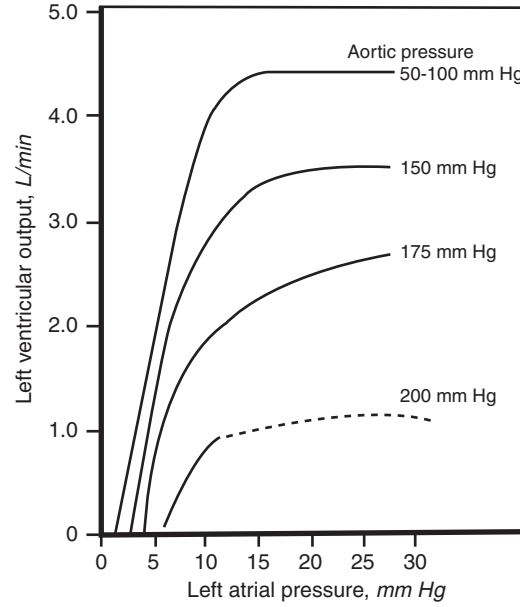

Fig. 2.1 The inverse relationship between afterload and cardiac performance. (Adapted from Sagawa [31])

Afterload Physiology and Theory

Afterload and Arterial Vasculature

The forces that oppose ventricular shortening are a summation of factors encountered throughout the arterial tree and can be referred to as arterial impedance. The total systolic load includes not only the impedance to flow from the large arteries but also the impedance provided by the medium peripheral arteries and smaller arterioles. Stephen Hales (1677–1761) suggested a simplistic model for the function of the arterial system, with the functions of cushion, conduit, and resistance being fulfilled by the proximal elastic arteries, medium-sized muscular arteries, and peripheral arterioles, respectively [3]. This classic model is useful in defining the differing properties of vessels along the arterial tree and in highlighting the peripheral arterioles as the site of the majority of peripheral resistance.

The three major determinants of arterial impedance are resistance, inertia, and compliance.

Resistance in a vessel is described by the Poiseuille equation $R = 8 \times \eta \times l/\pi r^4$, where R is resistance, η represents the viscosity of blood, l is vessel length, and r is vessel radius. Thus, it can be seen that elevated viscosity, such as in polycythemia, will increase resistance to flow. Importantly, resistance is inversely proportional to the fourth power of the radius, enabling small changes in arteriolar diameter to have profound changes on total peripheral resistance [4]. Total peripheral resistance can be expressed with regard to the ascending aorta as $R = P_o/\mathrm{CO}$, where P_o represents the mean arterial pressure, CO is the cardiac output, and R is the total peripheral vascular resistance. This can be re-arranged to $P_o = (\mathrm{CO})R = (\mathrm{SV})(\mathrm{HR})R$ by inputting the equation for cardiac output. This expression allows appreciation that the mean aortic pressure is directly related to both the cardiac output and the peripheral resistance. Inertia, which is related to the mass of the blood column, opposes acceleration of blood flow and is dependent upon the heart rate. Compliance is a property of the vascular walls, with highly compliant vessels being more distensible. Elastance is the reciprocal of compliance. Compliance is also heart rate dependent; the rate dependence of both inertia and compliance leads to phase shifts between instantaneous pressure and flow within the pulsatile arterial system [1]. The arterial pulse waveform begins with the upstroke imposed by ventricular systole, with a rapid increase in aortic pressure in early systole. The peak proximal aortic flow velocity slightly precedes the peak pressure. The aorta and large arteries expand during systole to accommodate some of the pressure fluctuation. This intermittent input into the proximal system is translated to an almost constant flow into the distal capillary bed, fulfilling the cushion function of the Hales model. This is achieved by absorption of stroke volume by the large elastic vessels, with conversion of the energy of systole into stretch of the arterial walls. The walls recoil as pressure within the vessel falls, and the stored energy is returned during diastole to maintain the blood pressure and distal blood flow during this period of the cardiac cycle. This is termed the Windkessel effect and is dependent both upon the capacitance of the aorta and large arteries, and the resistance to flow in the smaller vessels that do not show systolic expansion. However, this now considered an overly simplistic model and contemporary modeling incorporates elements of wave propagation and reflection.

Reflected Pressure Waves

An additional potential contributor to the afterload, not accounted for in the Hales model, is the phenomenon of retrogradely reflected pressure waves traveling from the periphery back toward the ventricle. The speed of propagation, known as the pulse wave velocity, is high enough for the reflected wave to arrive in the proximal aorta within the same cardiac cycle and so the reflection overlays the incident wave with both contributing to the arterial waveform. A reflected wave occurring during systole will increase the afterload; a reflected wave arriving in the proximal aorta during diastole is more advantageous as it will augment coronary blood flow. Major sites of reflection are arterial branch points, particularly the renal artery branches off the abdominal aorta, and the iliac bifurcation. The degree of wave reflection can change the pressure and flow waveforms seen in older subjects and in hypertensive individuals. Aging in industrialized societies is accompanied by increased systolic pressure and decreased arterial compliance; diastolic pressures tend to fall slightly. Intima-media thickening occurs, which causes progressive stiffening of the aging larger elastic arteries, resulting in elevation of aortic systolic and pulse pressures due to a combination of a rise in the forward incident wave and early return of the reflected wave [5] (Fig. 2.2).

A Framingham substudy documented the increases in arterial stiffness (elastance, the inverse of compliance) with advancing age [6]. The result is increased velocity of both the incident and retrograde reflection waves, with an

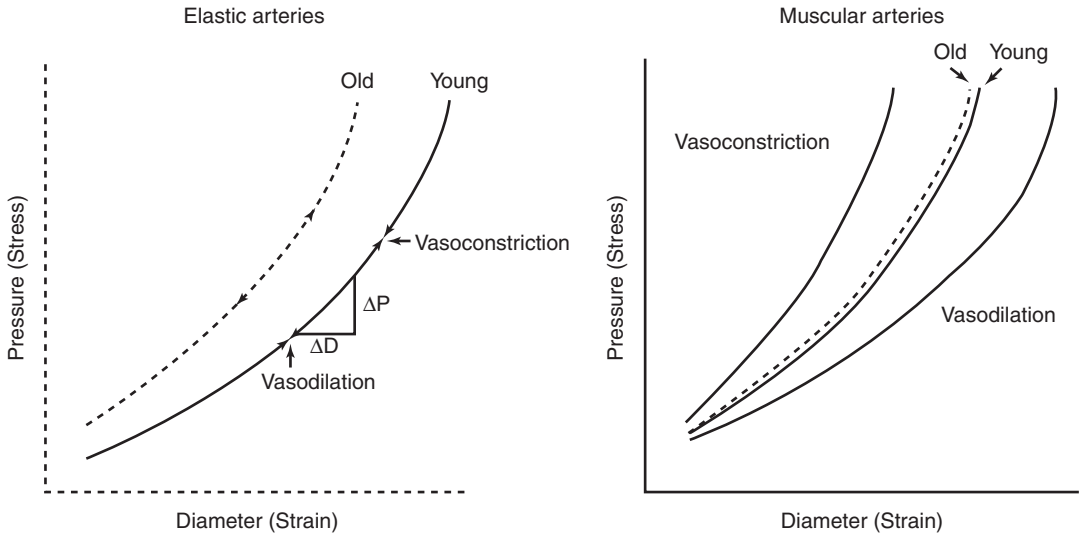

Fig. 2.2 Pressure-diameter relations for elastic and muscular arteries. (From Nichols and Edwards [5])

increase in systolic and pulse pressures. The enhanced incident wave raises myocardial oxygen demand, which can induce ventricular hypertrophy over time. In addition, the early return of reflected pressure waves adds to the afterload by augmenting late systolic pressure and removes the diastolic support of coronary blood flow; hence, the favorable ventriculo-arterial coupling is progressively lost [7]. It is the large central arteries, rather than the peripheral vasculature, that undergo the greatest capacitance changes with age. These changes in reflected waves contribute toward diastolic dysfunction, decreased exercise capacity, and an increased long-term risk of heart failure onset, especially heart failure with preserved ejection fraction (HFpEF) [8]. Large artery stiffness, as measured by carotid-femoral pulse wave velocity, predicts cardiovascular events and mortality, even after accounting for other established cardiovascular risk factors [9].

Decreased compliance in the large arteries may also induce macrovascular damage in organs such as the kidneys and the brain once the cushion effect that absorbs systolic pulsations is lost, causing the microvasculature to be subjected to pulsatile flow. The microvasculature is generally considered to include the small arteries of less than 400 μm diameter, arterioles of less than 100 μm diameter, and the capillaries with their single layer of endothelial cells. It is hypothesized that a more pulsatile microvasculature flow induced by age-related decline in the Windkessel effect is a contributor to end-organ damage [10].

Input Impedance and Characteristic Impedance

Parallels have been suggested between the flow of blood in the arterial system and the flow of current within an alternating current (AC) electrical circuit [11]. An analogous electrical circuit would contain capacitors and resistors, with the alternating storage and discharge of the capacitor separating peak pressure and flow. Impedance is a vector consisting of two components: the magnitude (modulus) and the phase angle, representing the number of degrees by which the sinusoidal pressure is separated from the sinusoidal flow. Electrical impedance occurs as current and voltage fluctuate with AC cycles and can be conceptionally translated into arterial impedance (Z_{in}). However, it should be remembered that blood does not behave sinusoidally, and so biological pressure and flow values must be converted into a fundamental sine wave and a series of harmonic waves using Fourier analysis. A value for impedance is derived from each pair of sine waves of pressure and flow (i.e., harmonics) at their specific phase angle. To validly apply Ohm's law in

this setting, the system should be in the steady state (vasomotor tone should be constant), time invariant (free of beat-to-beat changes in resistance), and linear. The nonlinearity of the ventricle during contraction does somewhat limit this technique, with the variations in elastance of the chamber during contraction being unaccounted for. Therefore, it would not be accurate to derive input impedance from invasive values for the left ventricular pressure and aortic flow, because the intervening aortic valve adds significant nonlinearity. However, when considering the arterial tree, the variations in pressure and flow are minor enough to enable systemic and pulmonary arterial input impendence to be considered valid mathematical descriptions of the systemic and pulmonary arterial trees, respectively.

When using the impedance concept in a compliant vascular system, the flow will be advanced with respect to the pressure sine wave. This is depicted as −90 ° in the phase angle. With inertance the flow is delayed, giving a +90 ° phase angle. The modulus of impedance will decrease with increasing frequency. In a large elastic artery, the compliance and inertia effects interact to keep pressure and flow sine waves in phase. This gives a pulsatile, or characteristic, impedance with a phase angle of 0. In this setting, the modulus will be constant and independent of changes in frequency. If the system were without reflection waves, the input impendence would equal the characteristic impedance. However, the reflected waves moving retrogradely toward the proximal aorta result in a significant difference between arterial input impedance and the characteristic impedance, which incorporates the reflected waves. This difference is more apparent at lower frequencies, where reflected waves return out of phase. Conversely, at high frequencies, the wavelengths are less than the arterial system length and so reflected waves are out of phase and cancel each other out. Therefore, at high frequencies, input impedance is almost equal to characteristic impendence [12]. The aortic input impedance spectrum gives information in the frequency domain about the arterial elastance, pulse wave reflectance, and the peripheral resistance. The clinical relevance is that increases in the pulsatile components – the elastance and reflectance – will lead to ventriculo-arterial mismatch and are, therefore, detrimental to cardiac efficiency (Fig. 2.3).

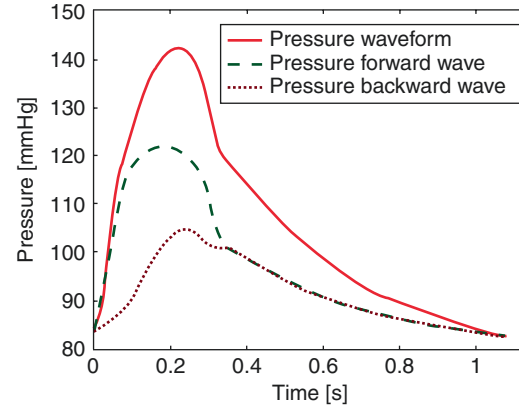

Fig. 2.3 The effects of wave reflection on the systolic pressure profile. (From Chirinos and Sweitzer [32]). Wave separation analysis showing the contributions of the forward (green dashed line) and backward (red dotted line) pressure waves to the systolic pressure profile

Assessing Afterload from Invasive Hemodynamics

Efforts to apply the impedance concept as a clinically measurable tool have been hampered by the complexity of the many advanced analytic functions required to derive values, and hence, the much simpler mean aortic pressure or mean systolic pressure remains the more commonly used surrogate of afterload. Clinically, the invasive measurement of cardiac afterload is usually achieved with a pressure tracing from a fluid-filled catheter with its tip lying just above the aortic valve in the ascending aorta. One phenomenon that the clinician must bear in mind in this setting is the possibility of pressure recovery. This describes the increase in pressure downstream from a stenosis caused by reconversion of kinetic energy to potential energy and can be a source of discrepancy between catheter and Doppler valvular pressure gradients. Bernoulli's theorem, from which Doppler evaluations of flow across a stenosis can be derived, requires that the sum of the pressure head, potential energy, and kinetic energy must be equivalent throughout all parts of the flow system. Therefore, in the setting of aortic

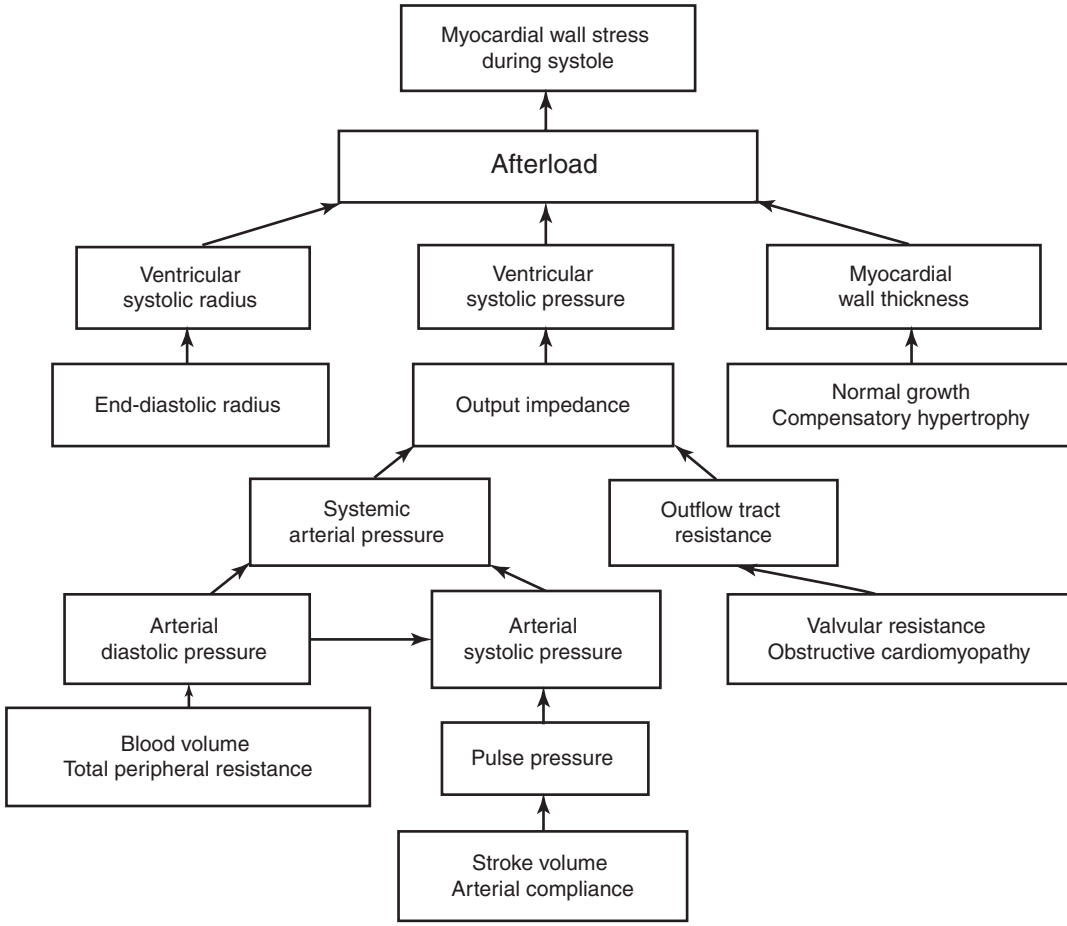

Fig. 2.4 Factors determining afterload. (From Norton [33])

stenosis, the lowest pressure is found where the velocity is highest and hence where the valve orifice is the smallest. Beyond the stenosis, velocity decreases and so pressure will increase, with the total amount of pressure increase (pressure recovery) being dependent upon the dissipation of kinetic energy due to flow separation and vortex formation across the valve. The consequence is that when Doppler gradients are measured at the point of minimal diameter of the stream of blood flow (the vena contracta), they will be higher than the invasive catheter measurements obtained in the proximal aorta, where pressure has been recovered. It has been noted that in milder aortic stenosis, the cusps of the valve form a funnel-shaped orifice and cause greater pressure recovery than in a more severely stenosed valve [13]. The extent of the phenomena is also dependent on the relationship between the dimensions of the valve orifice and the ascending aorta. A smaller aorta will lead to a lesser pressure loss and hence increased pressure recovery, compared to a larger aorta with the same degree of aortic stenosis.

The complexity of the relationship between the contracting ventricle, the arterial system, and its blood flow is such that finding a single parameter to fully encompass the cardiac afterload is probably impossible (Fig. 2.4).

Ventricular Wall Stress Versus Arterial Input Impedance

As previously introduced, aortic input impedance is only one of two biophysical concepts available to define afterload; the other is ventricular wall

stress, defined by LaPlace as $PR/2w$. Wall stress also carries with it some clinical limitations, as the values for pressures and dimensions are instantaneous and cannot account for rapidly changing loads encountered during the cardiac cycle. The calculations are also highly dependent upon ventricular geometric assumptions. The two differing afterload approaches of input impedance and wall stress have been compared in their validity as indicators of ventricular performance. Ross et al. constructed an animal model protocol to elucidate the relative importance of wall stress and impedance in negatively impacting ventricular stroke volume. These early experiments concluded that the dominant factor in regulating ventricular performance, as demonstrated by reduced fractional shortening, was the level of wall stress, rather than input resistance or pulsatile impendence [14].

Afterload Mismatch

Allied to this observation is the recognition that when pulsatile impedance is greater, changes in mean resistance produce greater changes in wall stress. This is presumably the result of the large increase in ventricular volume when pulsatile resistance rises, again emphasizing the impact of ventricular geometry on the outcome of these maneuvers. This appreciation led to the concept of afterload mismatch in 1976, a framework for assessing the matching between the afterload and the inotropic state in the whole heart. Under normal physiologic circumstances, an increase in afterload is usually accompanied by increased venous return (due to movement of blood from the arterial to venous systems) and hence increased end-diastolic volume. This helps to maintain stroke volume in the face of an increased afterload. A mismatch can be induced acutely in a normal heart if end-diastolic volume is not allowed to compensate for the increase in afterload [15]. The result will be a fall in stroke volume, ejection fraction, and ventricular circumference. An example of mismatch creation could be a scenario with sudden infusion of vasopressor into a volume depleted vascular system. An afterload mismatch can also be induced in a normal left ventricle in the opposite hemodynamic situation of volume overload, when the limit of preload reserve has already been reached and the average sarcomere length exceeds 2.2 μm. Additional afterload applied to the ventricle already working at a maximal end-diastolic volume will cause a sharp drop in stroke volume, unless contractility is also enhanced by an inotrope. Thus, an applied afterload stress can serve as an indicator that a heart is operating near either the upper or lower limits of preload [16]. The concept that afterload mismatch can exist even in the basal state explains why therapeutic afterload reduction in conditions such as severe left ventricular dysfunction or mitral regurgitation can significantly improve cardiac output, so long as preload is maintained and the ventricle can achieve an increased end-diastolic volume.

In addition to the acute afterload response studies on the intact heart in unanesthetized large animal subjects, the longer term effects of a sustained increase in afterload have also been extensively studied in animal models. Ross et al. instrumented 12 dogs with ultrasound transducers placed across the left ventricle for measuring the extent and velocity of wall shortening and a micromanometer measuring left ventricular cavity pressure. Transaortic constriction was performed using an inflatable rubber cuff around the proximal aorta to maintain an average systolic blood pressure of 210 mmHg. Ventricular pressures and dimensions were recorded prior to constriction, immediately after constriction, at an early phase after constriction (average 9 days), and a later phase (average 2.5 weeks). Calculations of wall forces relied on a spherical model. Immediately after constriction, there was a decrease in ventricular wall thickness and a 55% increase in calculated peak wall stress above control. Percentage shortening fell by 24% acutely and mean circumferential shortening velocity (V_{CF}) decreased by 39% from control. In the acute phase (mean 9 days), the ventricles were seen to dilate with a 4% increase in end-systolic diameter and peak wall stress fell to 37% above control despite a constant peak systolic left ventricular pressure averaging 210 mmHg. Percentage shortening and

mean V_{CF} remained below control levels at −12% and −20%, respectively. By the later phase at mean 2.5 weeks, the left ventricular walls had significantly hypertrophied with a 15% increase in ventricular wall cross-sectional area above control, with the increased wall thickness successfully reducing peak wall stress to 22% above control. End-diastolic diameter and percent shortening returned to normal [16]. The ventricle was considered to have successfully compensated at this time point by resuming its baseline fractional shortening in the face of a marked sustained elevation in afterload. This study reinforces the concept that the initial afterload mismatch, which causes an acute reduction in stroke volume, can be overcome by the development of physiological hypertrophy with thickened walls once again generating baseline stroke volumes. However, the limited duration in this early proof of concept study does not permit observation of the rapidly hypertrophied heart as it continues to maintain the higher degree of pressure generation against an increased afterload over time. The technique of transaortic banding has been applied to many species of experimental animal models, most commonly mice, enabling investigators to study the development of physiological hypertrophy and subsequent progression to heart failure, so elucidating the myocardial signaling pathways that govern the hypertrophic response [17].

Ventriculo-Arterial Coupling and Pressure–Volume Loops

The relationship between the ventricle and its afterload is key to the concept of ventriculo-arterial coupling and can be illustrated by pressure–volume loops. The effective arterial elastance (E_a) describes the ability of the vessel to accommodate pulsatile flow. E_a can be calculated by dividing the end-systolic pressure by the stroke volume and is, therefore, the slope of the stress/strain or pressure/diameter graphs ($\Delta P/\Delta D$), also known as the end-diastolic pressure–volume relationship. Elastance is the reciprocal of compliance, compliance being the ease of distension. At lower levels of arterial pressure, the arterial wall is supported by compliant elastin fibers, whereas the stiffer collagen fibers predominate at higher pressures. Therefore, the slope of the curve will be greater at higher levels of arterial pressure. Collagen in the human aorta is at least 500 times stiffer than elastin, and the aortic wall collagen content more than doubles from age 20 to 70 years (Fig. 2.5).

During the left ventricular ejection phase of the cardiac cycle, as ventricular volume decreases, the potential for the ventricle to develop pressure also drops. The smallest volume reached is the end-systolic volume, which marks the point of full stroke volume ejection. The aortic valve subsequently closes and the diastolic phase begins. The end-systolic volume at a certain degree of contractility and preload will, therefore, be determined by the afterload. A rise in aortic pressure, all else being equal, will correlate with a decreased stroke volume and a lower aortic pressure with an increased stroke volume. For example, in an individual with aortic stenosis, the pressure–volume loop may show a higher peak pressure, a lesser stroke volume, and an increased end-systolic volume, so shifting the curve into a taller and narrower configuration. Over time, compensatory hypertrophy will mitigate the high wall stress and improve the ventricle's ability to overcome the high afterload and increase the stroke volume, thus causing the loop to increase in width. With a sudden increase in afterload, the stroke volume will be diminished, which causes the end-systolic volume to rise. Over the following few beats, the increase in end-systolic volume predominates over the increased end-diastolic volume (which usually augments ventricular function), with the net change being a decrease in stroke volume and hence a decrease in the width of the pressure–volume loop. With a reduced afterload, the left ventricle ejects blood with greater ease, so augmenting the stroke volume and decreasing end-systolic volume. With less blood remaining in the ventricle after the ejection phase, the ventricle will fill to a lesser end-diastolic volume compared to prior the afterload reduction. Despite this mild reduction in preload, stroke volume shows a net increase because the reduction in end-diastolic volume is less than the reduction in end-systolic volume.

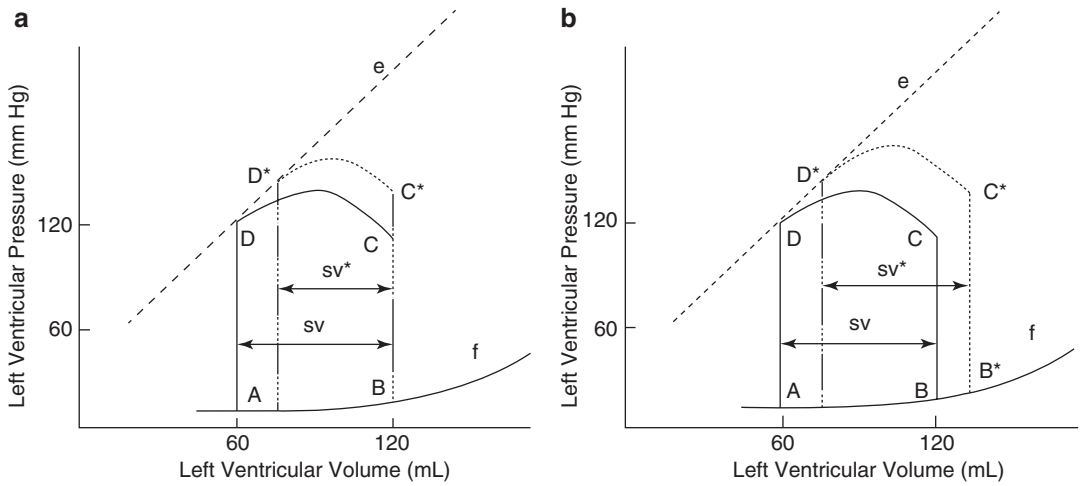

Fig. 2.5 Effects of acutely increasing afterload on the pressure–volume loop. . *A* mitral valve opens, *B* mitral valve closure, *C* aortic valve opens, *D* aortic valve closure, *e* end-systolic pressure–volume relationship, *f* end-diastolic pressure–volume relationship (or ventricular elastance). The dotted loop represents the effect of increasing afterload. Panel b demonstrates the impact of afterload plus (dotted loop) increased preload, increased end-diastolic volume, and therefore preservation of stroke volume. (From Iaizzo [19])

The ratio of the effective arterial elastance to the E_{es} (the slope of the ventricular end-systolic pressure–volume relationship) represents a measure of pump efficiency in expelling blood into the vasculature. This value can be used as a reflection of the ventriculo-arterial coupling and helps conceptualize the relationship between the pump and the vasculature. As E_a increases initially, the arteries accommodate greater blood flow, permitting a greater stroke work. If E_a were to continue to increase, the stroke work would reach a maximal plateau value where arterial and ventricular properties are equal, meaning that $E_a = E_{es}$. The E_a also increases with improvements in ventricular efficiency, which is defined by external stroke work/MVO_2/beat. Ventricular efficiency is maximal at $E_a = E_{es}/2$, meaning that the most favorable ventriculo-arterial coupling occurs when the E_a/E_{es} ratio lies in the range 0.5–1.0 [18] (Fig. 2.6).

Afterload and Cardiac Efficiency

The heart requires significant energy generation to perform its functions. Cardiac metabolism is predominantly aerobic, and hence, the work performed by the heart is typically gauged in terms of myocardial oxygen consumption (MVO_2). Myocytes are densely packed with mitochondria to generate sufficient ATP, predominantly from fatty acid breakdown, to fulfill the required cellular mechanics to sustain the cardiac cycle. The energy required for development and maintenance of systolic wall tension is a key factor in determining myocardial energy expenditure. One hallmark of the failing heart is its disordered and inefficient myocardial metabolism. The degree of afterload is also highly relevant in the ischemic heart, where reducing afterload and reducing heart rate are the major strategies in reducing myocardial oxygen consumption. A systolic pressure increase of only 20–30 mmHg can have a dramatic negative impact on function in a failing or ischemic left ventricle, both by inducing a lower stroke volume and by raising myocardial oxygen demands. Oxygen extraction in the capillary bed is near-maximal, and hence, the capacity to meet the oxygen demands of the myocardium may not be possible in the setting of a high afterload, especially if coronary blood flow can no longer be increased due to flow-limiting stenoses. The other determinants of myocardial oxygen demand are the heart rate, preload, and contractility. The MVO_2 in the rest-

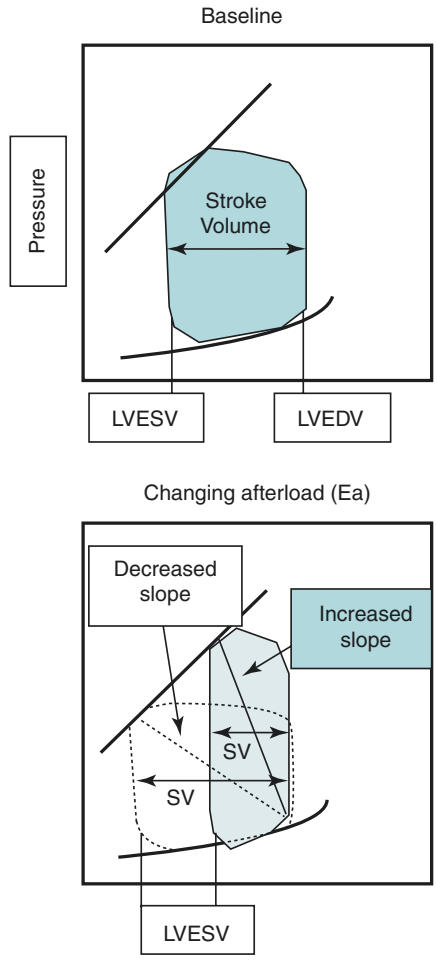

$$EF = \frac{SV}{LVEDV} = \frac{\text{Width of PV Loop}}{LVEDV}$$

Fig. 2.6 The pressure–volume relationship and elastance. Increased elastance, as illustrated by the steeper diagonal slope, leads to smaller stroke volume. (From Bashore [35])

ing heart is approximately 8 mL O_2/min per 100 g [19]. The instantaneous cardiac oxygen consumption can be measured in a human heart by employing the Fick principle; however, this does require catheterization of the coronary sinus to directly measure the venous oxygen saturation and coronary blood flow. Therefore, indirect assessments of the MVO_2 are necessary. Relative changes can be estimated by calculating the pressure-rate product. A simple method, described as early as 1912 using isolated cat and rabbit myocardium, is multiplication of the heart rate with the systolic blood pressure [20]. This noninvasive hemodynamic determinant of oxygen consumption has been validated by other investigators using the isolated dog heart, with the aortic pressure being shown to be the dominant influence in determining myocardial oxygen requirement. A 175% increase in work with afterload elevation was matched with a 178% increase in oxygen consumption as calculated by the product of coronary flow and coronary arteriovenous oxygen difference [21]. These investigators also established the use of the time-tension index/beat in mmHg seconds, derived from the area under the systolic portion of the aortic pressure curve, as an alternate metric of oxygen consumption. They also point out, by the Law of LaPlace, that the generation of the same intraventricular time-tension index will require greater myocardial fiber tension in a large radius heart compared to a smaller one. This fact highlights the inherent mechanical inefficiency of the dilated failing heart. Also of note is a study using healthy humans that demonstrated a corre-

lation of 0.88 between MVO_2 and heart rate alone and 0.90 using the rate–pressure product [22] although some authors have emphasized the limitations of these indirect indices of MVO_2 which do not capture all potentially important changes in myocardial contractility and ventricular dimensions, particularly in less healthy subjects [23].

The Law of LaPlace can also be used to explain why the pressure-overloaded left ventricle (such as that associated with aortic stenosis) will incur a higher myocardial oxygen demand than the volume-overloaded ventricle (as in aortic regurgitation). LaPlace stated that wall tension is proportional to $PR/2$, where P is chamber pressure and R is chamber radius. The pressure-overloaded ventricle shows a large increase in the pressure variable, which will equate to much higher wall tension, and hence MVO_2. Conversely, in the volume-overloaded ventricle, the radius will increase, but not as dramatically as the pressure in the pressure-overload model. Hence, the rise in wall stress in the volume-overload setting will be less substantial, and the corresponding MVO_2 less dramatically elevated.

Afterload in Clinical Practice

Afterload in the Pulmonary Vasculature

Afterload is most frequently discussed in reference to the left ventricle, but can also be applied to the right ventricle and the pulmonary vasculature into which this chamber pumps. It should be noted that significant differences exist in the manners in which the right and left ventricle handle increases in their afterloads. Normally, the resistance to flow in the pulmonary vascular system is much lower at about one-tenth of the resistance met by the left ventricle for the same stroke volume. The thicker walled left ventricle is able to generate much greater pressures and usually successfully generates unchanged stroke volumes in the face of afterload increases. The right ventricle operates much nearer to its full contractility capacity, because it has only a sixth of the muscle mass of the left ventricle and yet performs a quarter of the work. It succeeds in pumping the same cardiac output as the left ventricle due to the much lower resistance in the pulmonary vasculature than the systemic circulation. Operating within this closely matched ventriculo-arterial framework, the right ventricle is extremely sensitive to elevations in its afterload. Even a structurally normal right ventricle may decrease its stroke volume to small elevations in pulmonary vascular resistance. However, the right ventricle can also remodel and adapt to higher pulmonary pressures with time, with the maximal mean artery pressure normally accommodated without right ventricular failure being in the order of 40 mmHg. Severe right ventricular dilatation and dysfunction usually result from its attempts to compensate and maintain stroke volume as the pulmonary pressures rise beyond this [24].

- The pulmonary arterioles also serve as the site of major resistance to flow; however, the pulmonary arterioles receive a more pulsatile input of blood flow than their systemic counterparts. Within this much smaller vascular system, the roles of cushion, conduit, and resistance are not as clearly ascribed to certain generations of vessels as in the systemic circulation. Pulmonary hypertension is currently defined as a mean pulmonary artery pressure of greater than 25 mmHg, with a pulmonary capillary wedge pressure less than 15 mmHg indicating that the hypertension is not secondary to left-sided heart disease [25]. The various etiologies of pulmonary hypertension all tend to show common histopathology features, namely, initial fibrosis, medial thickening, and pulmonary arteriolar occlusion [26]. Right ventricular afterload reduction with pulmonary vasodilators is key to the management of pulmonary hypertension and right ventricular failure. Inhaled nitric oxide has a role during the invasive assessment of pulmonary vascular pressures to help determine the potential for pulmonary vasodilatation, and the use of continuous oxygen therapy can help reduce the degree of hypoxic vasoconstriction. Pulmonary hypertension therapeutics include calcium channel antagonists (nifedipine, amlodipine), prostacyclin analogs (epo-

prostenol, treprostinil, iloprost), endothelin receptor antagonists (bosentan, ambrisentan, macitentan), phosphdiesterase-5 inhibitors (sildenafil, tadalafil), and soluble guanylate cyclase simulators (riociguat) [27].

Afterload and the Respiratory Cycle

The potential for mechanical ventilation to affect invasive assessments of preload (such as the right atrial and pulmonary capillary wedge pressures) and possibly reduce preload by decreasing the pressure gradient into the thorax was discussed in Chap. 1. Positive pulmonary pressures during mechanical ventilation also affect afterload. The degree of pulmonary vascular resistance, and hence RV afterload, is proportional to the degree of airway pressure elevation. With significant RV afterload elevations, the right ventricle will dilate and induce intraventricular dependence, with shifting of the septum into the left ventricle, which reduces left ventricular filling and stroke volume. Conversely, the direct effect of positive airway pressure on the left ventricle is to increase stroke volume by increasing the intrathoracic aortic pressures relative to peripheral arterial pressure. Also worth mentioning in the consideration of valvular lesions and afterload is the effect of mitral regurgitation on the degree of cardiac afterload. Mitral regurgitation will decrease afterload because, during ventricular systole, a fraction of the left ventricular end-diastolic volume will take a retrograde route and flow back into the left atrium through the incompetent valve. Hence, the left ventricle will be working against a reduced afterload, as some blood ejection is into the lower-pressure atrium rather than the usual anterograde flow into the higher-pressure aorta.

Total Peripheral Resistance

The term "total peripheral resistance" (TPR) encompasses the sum of all regional resistances in the systemic circulation. It is sometimes used to infer the total afterload faced by the heart, although as we have already seen the resistance to flow, largely imposed by the arterioles, is actually only one component of the complete cardiac afterload. TPR can be approximated from Ohm's law. In the patient with Swan-Ganz calculations of cardiac output, values for systemic vascular resistance (SVR) and pulmonary vascular resistance (PVR) are routinely derived in Wood units from:

$$\text{SVR} = 80 \times \left(\text{mean arterial pressure} - \text{mean right atrial pressure}\right) / \text{cardiac output}$$

$$\text{PVR} = 80 \times \left(\text{mean pulmonary artery pressure} - \text{pulmonary capillary wedge pressure}\right) / \text{cardiac output}$$

These equations give values in dyn s cm^{-5}. Other units for measuring vascular resistance are pascal seconds per cubic meter (Pa s/m^3), or for convenience when using pressure in mmHg and cardiac output in l/min, resistance can be expressed in mmHg min/L. This equates to hybrid reference units (HRU), also known as Wood units, favored by pediatric cardiologists. Multiplying by a factor of 8 converts from Wood units to MPa s/m^3 or by a factor of 80 converts from Wood units to the international unit of dyn s cm^{-5}.

The resistances imposed by the arterial system are arranged in both serial and parallel orientations. In a circuit where resistances lie in series, the total resistance will be the sum of the individual resistive components. Conversely, a parallel circuit will have a total resistance equaling the sum of the reciprocals of the individual resistive components, thus creating a much lower overall resistance than in a series circuit. Therefore, most organ arterial supplies are configured in a parallel arrangement, so limiting the pressure generation required by the ventricle to perfuse all organs. A rise in resistance within one organ bed will have minimal impact on the other arterial beds.

The majority of the resistance component of arterial input impedance lies in the arterioles.

These vessels range 10–150 μm in diameter and are under constant vasoactivity regulation from the sympathetic nervous system and local mediators, thus controlling the flow of blood into specific capillary beds. Local vasodilators include platelet-derived substances, such as serotonin, and endothelium-derived mediators, such as nitric oxide.

Therapeutic Afterload Reduction

The concept of therapeutic afterload reduction was initially clinically applied in the form of intra-aortic balloon counterpulsion to support patients with cardiogenic shock post myocardial infarction. This technique was demonstrated to unload the left ventricle, enhance left ventricular ejection fraction, and improve coronary artery perfusion. Pharmacological afterload reduction strategies for unloading the left ventricle, principally the use of a sodium nitroprusside infusion, are useful tools in acute cardiac care. Nitroglycerin, which combines more venodilation with arteriolar vasodilation in comparison to nitroprusside, may also be used for afterload reduction. The angiotensin-converting enzyme (ACE) inhibitors, angiotensin receptor blockers, hydralazine, and dihydropyridine calcium channel blockers are additional options, and clevidipine, an intravenous dihydropyridine drug, is increasingly used in critical care settings.

Vasodilating drugs have minimal direct effect on the large elastic arteries, but can markedly reduce reflected wave amplitude from the periphery by decreasing elastance of the smaller muscular arteries. The decreased amplitude and velocity of the reflected wave decreases systolic arterial pressure and increases proximal aortic flow during the deceleration phase. The resulting afterload reduction can help to optimize cardiac output and clinical status in patients with cardiogenic shock, severe mitral or aortic regurgitation, or even aortic stenosis with decompensated left ventricular dysfunction [28], by correcting the afterload mismatch. The afterload tends to be high in decompensated heart failure due to activation of the renin–angiotensin–aldosterone system, as well as a higher effective blood velocity due to slow forward flow. Although the sympathetic activation causing vasoconstriction in heart failure is compensatory to maintain arterial blood pressure despite low output, these adaptations can be counterproductive and impose further afterload on the failing ventricle. Pharmacological afterload reduction can, therefore, achieve marked improvements in cardiac output and symptoms for patients with a dilated left ventricle and sufficient preload reserve (Fig. 2.7).

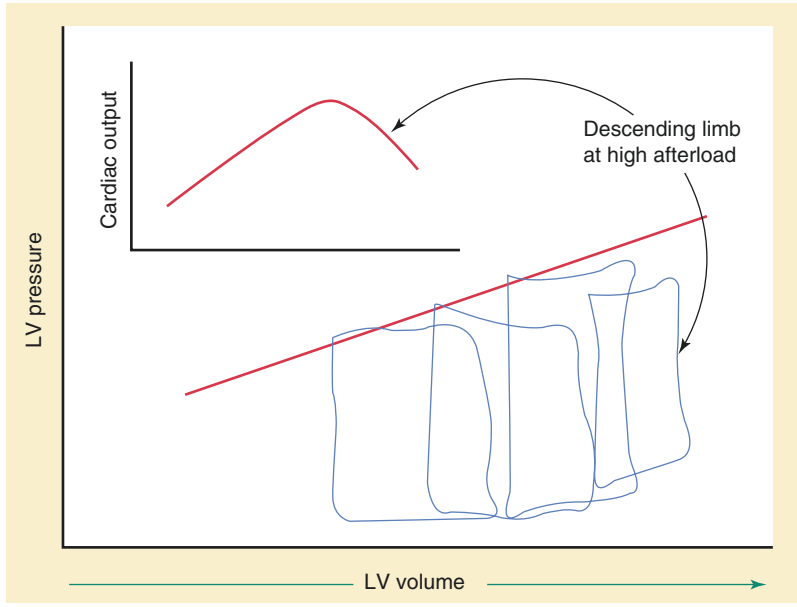

Fig. 2.7 Conditions for afterload mismatch in systolic heart failure. (From Ross [15]). The stroke volume is seen to decrease (decreased width of the pressure–volume loop) as afterload increases

The use of afterload reduction in patients with aortic stenosis may initially seem counterintuitive as the cardiac output across a stenotic aortic valve has traditionally been considered to be fixed with a risk of hypotension without improvements in output if the blood pressure is lowered. However, this scenario underlines the complexity of afterload, because the aortic stenosis in not actually the sole factor determining the force against which the ventricle must pump. Resistances in series are additive, and so the resistive component of aortic input impedance can still be lowered by reducing the most distal resistances in the arterioles despite the proximal resistance across the valve remaining constant. The reduction in total peripheral resistance and hence mean arterial pressure with nitroprusside can, therefore, successfully reduce the afterload mismatch of the dysfunctional ventricle pumping against a high afterload despite the presence of severe and fixed aortic stenosis. Conversely, the administration of nitroprusside to a relatively normal cardiovascular system, or to the heart with aortic stenosis but a preserved ejection fraction, would be expected to lower the cardiac output. This is due to some concurrent venodilation, which will reduce preload and actually induce an afterload mismatch. Another setting where pharmacological afterload reduction can precipitate a worsened clinical status is in the setting of a significant pulmonary shunt. Nitroprusside can inhibit the hypoxic vasoconstriction in a region of pulmonary vasculature, thus supplying blood flow to an area of the lung not receiving good oxygenation (e.g., due to lobar consolidation). This will exaggerate a perfusion–ventilation mismatch and potentially worsen the arterial oxygen saturation. The use of nitroprusside as a lone afterload reducer in the setting of ischemia should also be avoided. Nitroprusside has been shown to decrease myocardial perfusion in the setting of coronary stenoses, whereas nitroglycerin can enhance myocardial perfusion, largely through dilatation of coronary collateral vessels [28, 29].

Bullet Point Summary

- Afterload consists of the forces against which the heart pumps to expel blood into the vasculature.
- Afterload can be defined in terms of wall stress, using the law of LaPlace.
- Alternatively, afterload can be conceptualized as arterial input impedance, drawing parallels from electrical circuits.
- An inverse relationship exists between stroke volume and afterload.
- The aorta and proximal large arteries have a higher ratio of elastic to collagen and are, therefore, highly compliant.
- These elastic arterial walls absorb the systolic pulsations in blood flow, converting stored energy into recoil that maintains the pressure and flow during diastole – the Windkessel effect.
- The arterioles are the site of the majority of arterial resistance, with arteriolar tone being highly dependent on the sympathetic nervous system and local mediators.
- Reflected waves from bifurcations and arterial discontinuities can increase afterload when they return to the proximal aorta during systole.
- With aging, or pathological processes such as hypertension, afterload rises due to increased magnitude of the incident systolic wave and also early return of the reflected wave.
- Afterload mismatch is a scenario in which the ventricular performance is not well coupled to the afterload it encounters, which increases myocardial oxygen consumption and decreases cardiac energy efficiency.
- Over time, an afterload mismatch can induce ventricular hypertrophy.
- Intra-aortic balloon counterpulsion, and drugs such as nitroprusside, hydralazine, and ACE inhibitors, can decrease systemic afterload.
- Pulmonary vasodilators are the cornerstone of pulmonary hypertension management and decrease the afterload faced by the right ventricle.

Review Questions

1. The primary determinant of cardiac output is:
   (a) Preload
   (b) Myocardial contractility
   (c) Heart rate
   (d) Afterload
   Answer is (a).

2. Which one of the following statements regarding the vasculature is *false*?
   (a) With aging, changes in the media of the large elastic arteries cause them to stiffen.
   (b) Vascular compliance is heart rate dependent.
   (c) The small peripheral vessels show a prominent Windkessel effect.
   (d) Retrogradely reflected pressure waves usually arise from arterial branch points such as the iliac bifurcation.
   (e) A reflected wave falling during diastolic is more advantageous to the cardiovascular system,

   Answer is (c). It is the proximal elastic arteries that show the Windkessel effect. The smaller peripheral arteries and arterioles have the capacity to vasoconstrict substantially, but they are not exposed to highly pulsatile blood flow and do not have the elastic properties to permit significant recoil if the pressure within the vessel falls. A reflected wave falling within diastole can help to augment coronary blood flow.
3. Which one of the following statements is true regarding the concept of afterload mismatch?
   (a) Afterload mismatch can occur when the patient is vasodilated.
   (b) An increase in afterload is usually accompanied by a decrease in venous return, due to decreased availability of blood in the venous system.
   (c) Afterload mismatch may occur with sudden infusion of vasopressor in the setting of volume depletion.
   (d) Afterload mismatch can be induced in a normal left ventricle with high preload, when a sudden increase in both afterload and myocardial contractility occurs.
   (e) A chronic afterload mismatch does not result in structural myocardial changes.

   Answer is (c). Under normal physiologic circumstances, an increase in afterload is usually accompanied by increased venous return, due to movement of blood from the arterial to venous systems. A mismatch can be induced acutely in a normal heart if end-diastolic volume is not allowed to compensate for the increase in afterload. Alternatively, additional afterload applied to a ventricle already working at a maximal end-diastolic volume will cause a sharp drop in stroke volume, unless contractility is also enhanced.
4. Which one of the following statements is true regarding potential strategies to reduce afterload clinically?
   (a) The goal of intra-aortic balloon counterpulsion is to lower systolic blood pressure and hence reduce afterload.
   (b) In the setting of some pulmonary conditions, nitroprusside can cause hypoxia.
   (c) Afterload reduction is strictly contraindicated in the setting of a fixed obstructive lesion such as aortic stenosis.
   (d) The sympathetic activation causing vasoconstriction in heart failure is compensatory to maintain blood pressure despite low cardiac output, and hence, afterload reduction should be avoided.
   (e) Sildenafil is a selective pulmonary arterial vasodilator and has no effect on the systemic vasculature.

   The answer is (b). Nitroprusside can inhibit the hypoxic vasoconstriction in a region of pulmonary vasculature, thus supplying blood flow to an area of the lung not receiving good oxygenation (e.g., due to lobar consolidation). This will exaggerate a perfusion–ventilation mismatch and potentially worsen the arterial oxygen saturation. Intra-aortic balloon counterpulsion augments diastolic blood pressure, thus reducing left ventricular wall stress. Afterload reduction with an IABP or nitroprusside may be indicated in acutely ill patients with severe aortic stenosis and a reduced left ventricular ejection fraction. Vasodilation in the setting of decompensated systolic heart failure can correct an afterload mismatch and improve the cardiac output. Sildenafil does have some peripheral vasodilating affects, and hence, dosage may be limited by systemic hypotension.

5. A 70-year-old male with severe aortic stenosis (peak/mean pressures by echocardiography 68/42 mmHg, aortic valve area by continuity equation 0.6 cm^2) presents with worsening dyspnea, lower extremity edema, oliguria, and a 15-lb. weight gain. The blood pressure is 88/74. He is peripherally cool and mildly confused. The left ventricular ejection fraction on his most recent echo was 25%. Are the following statements true or false?
   (a) Due to the severity of the aortic valve stenosis, the only option for reducing afterload is valvuloplasty or valve replacement.
   (b) There is an afterload mismatch.
   (c) Pressure recovery may lead to overestimation of the valve gradient by Doppler measurements and is more likely to occur with smaller ascending aorta diameter.
   (d) The calculated SVR is likely to be elevated; a lower than expected SVR may suggest a septic component to the hypotension.
      (a) False. The total resistance presented by the arterial system is the sum of the many components arranged in series through the vasculature. The significant resistive contribution provided by the arterioles is additive to the resistance imposed by the stenotic valve. Therefore, the afterload can be reduced by vasodilatation of the arterioles.
      (b) True. Although we do not have invasive hemodynamics provided for this patient, the cool peripheries, delayed mentation, and oliguria strongly suggest a low cardiac output state. Therefore, the poor ventricular performance is not well matched to the high afterload imposed by the aortic stenosis plus peripheral vasoconstriction due to the activation of the renin–angiotensin system in cardiogenic shock. Better matching of the low stroke volume may be achieved through peripheral vasodilatation, if this can be tolerated by the low blood pressure. Aortic balloon counterpulsion and/or low doses of intravenous nitroprusside may be successful in improving the cardiac output and stabilizing the decompensated patient ahead of definitive aortic stenosis management.
      (c) True. Pressure recovery is a phenomenon arising from the decrease in velocity and increase in pressure in the proximal aorta, beyond the stenotic aortic valve. This can lead to overestimation of the valve gradient by Doppler measurements and is more likely to occur with smaller ascending aorta diameter.
      (d) True. As described above, the systemic vascular resistance would be expected to be at the higher end, or above, the normal range for SVR. A value in the range of 1200–2500 dyn s/cm^5 would be consistent with the scenario. If the calculated value lies much below this, consideration should be made of an additional distributive shock process, such as sepsis. Of note, a patient with cardiogenic shock and a poor cardiac output can sometimes be seen to have an encouraging rise in their mixed venous saturation, cardiac output, and a fall in the SVR, with the actual etiology being early sepsis causing peripheral vasodilatation.
6. A 55-year-old female with hypertension, diabetes, and chronic kidney disease presents acutely dyspneic. Her blood pressure is 210/110 mmHg, right atrial pressure 15 mmHg, and heart rate is 92 bpm. Her examination is consistent with pulmonary edema. A diagnosis of hypertensive emergency is made. Are the following statements true or false?
   (a) The decrease in arterial compliance associated with hypertension and diabetes is most pronounced in the arterioles.
   (b) Effective arterial elastance is calculated by dividing the stroke volume by end-systolic pressure.
   (c) If the mean arterial pressure is known to be 143 mmHg and the cardiac output

4.0 L/min, the systemic vascular resistance will calculate in the region of 2500 dyn s/cm5.

(d) If this patient receives an arteriovenous fistula in preparation for future hemodialysis, the afterload would be expected to fall and the preload increase.

(a) False. The arteriosclerosis associated with hypertension and diabetes is most prominent in the large elastic arteries. The enhanced incident wave increases afterload, as does the early return of reflected pressure waves.

(b) False. Effective arterial elastance is calculated by dividing the end-systolic pressure by the stroke volume. It is visualized as the slope on the stress/strain graph.

(c) True. MAP = (2 × diastolic pressure + systolic pressure)/3 = 143. SVR = 80 × (MAP − RA pressure)/cardiac output = 80 × (143 – 15)/4 = 2560.

(d) True. Creation of a shunt from the arterial to venous system would be expected to decrease the afterload by directing blood flow away from the high resistance arterioles into the lower resistance venous system, and so enhancing venous return to the heart. The decreased afterload has been shown to slightly reduce myocardial oxygen demand, but also negatively impacts the coronary blood flow [30].

References

1. Fuster V, Walsh R, Harrington R. Hurst's the heart, vol. 1. 13th ed. New York: McGraw Hill; 2011.
2. MacGregor DC, Covell JW, Mahler F, Dilley RB, Ross JJ. Relations between afterload, stroke volume, and descending limb of Starling's curve. Am J Physiol. 1974;227(4):884–90.
3. Hales S. Statistical essays: containing haemastaticks, History of medicine series. Library of New York Academy of Medicine. New York: Hafner; 1733. Reproduced in 1964, no. 22.
4. Poiseuille JLM. Recherches experimentales sur le mouvement des liquids dans les tubes de tres petits diametres. Mem Savant Etrangers. 1846;9:433–544.
5. Nichols WW, Edwards DG. Arterial elastance and wave reflection augmentation of systolic blood pressure: deleterious effects and implications for therapy. J Cardiovasc Pharmacol Ther. 2001;6:5.
6. Mitchell GF, Parise H, Benjamin EJ, Larson MG, Keyes MJ, Vita JA, Vasan RS, Levy D. Changes in arterial stiffness and wave reflection with advancing age in healthy men and women: the Framingham heart study. Hypertension. 2004;43:1239–45.
7. Hashimoto J, Ito S. Some mechanical aspects of arterial aging: physiological overview based on pulse wave analysis. Ther Adv Cardiovasc Dis. 2009;3:367.
8. Chirinos JA, Kips JG, Jacobs DR Jr, Brumback L, Duprez DA, Kronmal R, Bluemke D, Townsend RR, Vermeersch S, Segers P. Arterial wave reflections and incident cardiovascular events and heart failure. J Am Coll Cardiol. 2012;60:2170–7.
9. Ben-Shlomo Y, Spears M, Boustred C, May M, Anderson SG, Benjamin EJ, Boutouyrie P, Cameron J, Chen C-H, Cruickshank JK, Hwang S-J, Lakatta EG, Laurent S, Maldonado J, Mitchell GF, Najjar SS, Newman AB, Ohishi M, Pannier B, Pereira T, Vasan RS, Shokawa T, Sutton-Tyrell K, Verbeke F, Wang K-L, Webb DJ, Willum Hansen T, Zoungas S, McEniery CM, Cockcroft JR, Wilkinson IB. Aortic pulse wave velocity improves cardiovascular event prediction: an individual participant meta-analysis of prospective observational data from 17,635 subjects. J Am Coll Cardiol. 2014;63:636–46.
10. O'Rourke MF, Hashimoto J. Mechanical factors in arterial aging: a clinical perspective. J Am Coll Cardiol. 2007;50:1–13.
11. Little RC, Little WC. Cardiac preload, afterload, and heart failure. Arch Intern Med. 1982;142(4):819–22.
12. Westerhof N, Stergiopulos N, Noble MIM. Snapshots of hemodynamics: an aid for clinical research and graduate education. 2nd ed. New York: Springer; 2010.
13. Niederberger J, Schima H, Maurer G, Baumgartner H. Importance of pressure recovery for the assessment of aortic stenosis by Doppler ultrasound. Role of aortic size, aortic valve area, and direction of the stenotic jet in vitro. Circulation. 1996;94:1934–40.
14. Covell JW, Pouleur H, Ross J Jr. Left ventricular wall stress and aortic input impedance. Fed Proc. 1980;39(2):202–7.
15. Ross J Jr. Afterload mismatch and preload reserve: a conceptual framework for the analysis of ventricular function. Prog Cardiovasc Dis. 1976;18(4):255–64.
16. Ross J Jr, Franklin D, Sasayama S. Preload, afterload, and the role of afterload mismatch in the descending limb of cardiac function. Eur J Cardiol. 1976;4(Suppl):77–86.
17. Rockman HA, Ross RS, Harris AN, Knowlton KU, Steinhelper ME, Field LJ, Ross J Jr, Chien KR. Segregation of atrial-specific and inducible expression of an atrial natriuretic factor transgene in an *in vivo* murine model of cardiac hypertrophy. Proc Natl Acad Sci. 1991;88:8277–81.

18. Fuster V, Walsh R. Hurst's the heart, vol. 1. 13th ed. McGraw Hill: Harrington; 2011.
19. Iaizzo PA. Handbook of cardiac anatomy, physiology and devices. 2nd ed. New York: Springer; 2009. p. 271–96.
20. Rhode E, Ogawa S. Uber den einfluss der mechanischen bedingungen auf die totigkeit und den sauerstaffverback des warmbluterheizens. Arch Exp Path u Pharmakol. 1912;68:401–34.
21. Sarnoff SJ, Braunwald E, Welch GH Jr, Case RB, Stainsby WN, Macruz R. Hemodynamic determinants of oxygen consumption of the heart with specific reference to the tension time index. Am J Phys. 1958;192:148–56.
22. Kitamura K, Jorgensen CR, Gobel FL, Taylor HL, Wang Y. Hemodynamic correlates of myocardial oxygen consumption during upright exercise. J Appl Physiol. 1972;32:516–22.
23. Goldstein RE, Epstein SE. The use of indirect indices of myocardial oxygen consumption in evaluating angina pectoris. Chest. 1973;63(3):302–5.
24. Daily EK, Schroeder JS. Techniques in bedside hemodynamic monitoring. 5th ed. St. Louis: Mosby; 1994.
25. Badesch DB, Champion HC, Sanchez MA, Hoeper MM, Loyd JE, Manes A, McGoon M, Naeije R, Olschewski H, Oudiz RJ, Torbicki A. Diagnosis and assessment of pulmonary arterial hypertension. J Am Coll Cardiol. 2009;54:S55–66.
26. Farber HW, Loscalzo J. Pulmonary arterial hypertension. N Engl J Med. 2004;351:1655–65.
27. Hoeper MM, McLaughlin VV, Dalaan AM, Satoh T, Galie N. Treatment of pulmonary hypertension. Lancet Respir Med. 2016;4(4):323–36.
28. Khot UN, Novaro GM, Popović ZB, Mills RM, Thomas JD, Tuzcu EM, Hammer D, Nissen SE, Francis GS. Nitroprusside in critically ill patients with left ventricular dysfunction and aortic stenosis. N Engl J Med. 2003;348:1756–63.
29. Flaherty JT, Magee PA, Gardner TL, Potter A, MacAllister NP. Comparison of intravenous nitroglycerin and sodium nitroprusside for treatment of acute hypertension developing after coronary artery bypass surgery. Circulation. 1982;65:1072–7.
30. Bos WJ, Zietse R, Wesseling KH, Westerhof N. Effects of arteriovenous fistulas on cardiac oxygen supply and demand. Kidney Int. 1999;55(5):2049–53.
31. Sagawa K. Analysis of the ventricular pumping capacity as function of input and output pressure loads. In: Reeve EB, Guyton AC, editors. Physical bases of circulatory transport: regulation and exchange. Philadelphia: WB Saunders; 1967. p. 141–9.
32. Chirinos JA, Sweitzer N. Ventricular-Arterial coupling in chronic heart failure. Card Fail Rev. 2017;3:12–8.
33. Norton JM. Toward consistent definitions for preload and afterload. Adv Physiol Educ. 2001;25(1–4):53–61.
34. Loushin MK, Quill JL, Iaizzo PA. Mechanical aspects of cardiac performance. In: Iaizzo PA, editor. Handbook of cardiac anatomy, physiology, and devices. 2nd ed. New York: Springer; 2009. p. 271–96.
35. Bashore TM. Clinical hemodynamics in valvular heart disease. In: Wang A, Bashore TM, editors. Valvular heart disease. New York: Humana-Springer; 2009. p. 93–122.

Suggested Reading

Fuster V, Walsh R, Harrington R. Hurst's the heart, vol. 1. 1st ed. New York: McGraw Hill; 2011. (Part 2, Chapter 5 and Part 3, Chapter 14).

Nichols WW, Edwards DG. Arterial elastance and wave reflection augmentation of systolic blood pressure: deleterious effects and implications for therapy. J Cardiovasc Pharmacol Ther. 2001;6:5.

Ross J Jr. Afterload mismatch and preload reserve: a conceptual framework for the analysis of ventricular function. Prog Cardiovasc Dis. 1976;18(4):255–64.

Weber T, Chirinos JA. Pulsatile arterial haemodynamics in heart failure. Eur Heart J. 2018;37:2129.

Contractility

3

Jordan S. Thomas and Justin M. Dunn

Introduction

Myocardial contractility—often referred to as inotropy—is the inherent capacity of the myocardium to contract *independent* of loading conditions, that is, preload and afterload (discussed in Chaps. 1 and 2, respectively). Thus, for a given preload and afterload, contractility is a manifestation of all other factors that influence the interactions between contractile proteins. The incorporation of all these factors makes a simple definition of "contractility" difficult, and it is more easily understood through discussions of *changes* in contractility. Clinically, a change in left ventricular contractility can be defined as a change in the work performed per beat at a constant end-diastolic volume and aortic pressure.

Contractility is best understood by assessing the rate of rise of left ventricular pressure or dP/dt (Fig. 3.1). The contours of these left ventricular pressure curves provide a reasonable index of myocardial contractility. The slope of the ascending limb of each curve indicates the maximal rate of force development by the ventricle. The maximal rate of change in pressure over time, also referred to as the maximum dP/dt, is shown by the tangents to the steepest portion of the ascending limb of each curve. This slope is maximal during the isovolumic phase of early systole in the cardiac cycle, from closure of the mitral valve until opening of the aortic valve (Fig. 3.2).

Accurate clinical measurement of contractility is difficult. In the cardiac catheterization lab, the maximum rate of pressure development (dP/dt_{max}) can be measured during isovolumetric contraction by placing catheters directly in the ventricle. This measurement is often used as an index of contractility [3]. Decreases in left ventricular dP/dt_{max} below the normal value of 1200 mmHg/s suggest depressed myocardial contractility.

The ejection fraction (EF), defined as the ratio of stroke volume to end-diastolic volume, is widely used clinically as a noninvasive surrogate index of cardiac contractility [4]. In current practice, EF is most often measured noninvasively with echocardiography, but alternative methods including nuclear imaging and, more recently, cardiac MRI also exist with each having their own relative strengths and weaknesses. Normal ejection fraction reference values vary depending on gender and the imaging modality used. In clinical practice, however, a range of approximately 50–70% can be considered normal by the majority of imaging modalities, while an EF less than 50% suggests at least some degree of depressed myocardial contractility.

J. S. Thomas
Advanced Heart Failure/Transplant Cardiology, Ohio State University, Columbus, OH, USA
e-mail: Jordan.thomas@osumc.edu

J. M. Dunn (✉)
Interventional Cardiology, Summa Health, Akron, OH, USA
e-mail: dunnjus@summahealth.org

A. T. Askari, A. W. Messerli (eds.), *Cardiovascular Hemodynamics*, Contemporary Cardiology,
https://doi.org/10.1007/978-3-030-19131-3_3

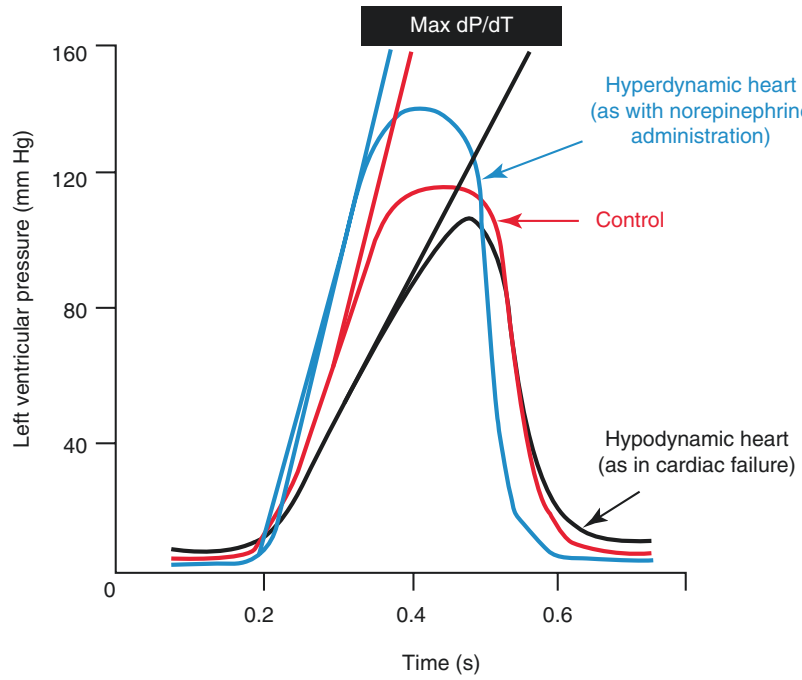

Fig. 3.1 Left ventricular pressure curves with tangents drawn to the steepest portions of the ascending limbs to indicate maximal dP/dt values. *Red*: Control. *Blue*: Hyperdynamic heart, as with norepinephrine administration. *Black*: Hypodynamic heart, as in cardiac failure. (Adapted from Berne and Levy [1], p. 313, Fig. 16.9)

With recent advancements in imaging techniques, 2D speckle tracking echocardiography (STE) with strain imaging has become a key noninvasive tool and is one of the most direct measurements of both global and segmental myocardial tissue deformation and underlying contractility. With its high sensitivity and reproducibility, strain echocardiography has been validated in multiple cardiovascular disease states and holds tremendous promise in both clinical and research settings [5].

Physiology of Contraction

Contraction of cardiac muscle begins when a wave of excitation spreads via gap junctions along the myocardial sarcolemma and into the cells via T tubules. During phase 2 of the action potential, calcium permeability in the sarcolemma increases, and calcium enters the cell via calcium channels in the sarcolemma/T tubules (invaginations in the sarcolemma). This extracellular calcium triggers the release of a much larger store of calcium from the sarcoplasmic reticulum within the cell. This calcium then binds to troponin C forming the calcium–troponin complex, which subsequently interacts with tropomyosin to unblock active sites between the thin actin and thick myosin filaments and allows cross-bridge cycling and thus contraction to occur.

To understand the concept of contractility, it is important to revisit the underlying mechanisms by which contractility changes, beginning at the cellular level. This discussion must begin with the fundamental role of calcium in cardiac contraction and relaxation. With each spontaneous wave of excitation in the myocardium, sodium channels in the sarcolemma are opened by an action potential. Sodium moves into the cytosol depolarizing the membrane. Depolarization opens voltage-gated L-type calcium channels in the sarcolemma/T tubules, allowing an influx of calcium from the extracellular space. Each calcium channel controls a number of calcium release channels which are composed of four ryanodine receptors in the membrane of the sarcoplasmic reticulum. The influx of calcium through the L-type calcium channels triggers a conformational change in the ryanodine receptors, which allows calcium to flow from the sarcoplasmic reticulum into the cytosol via the

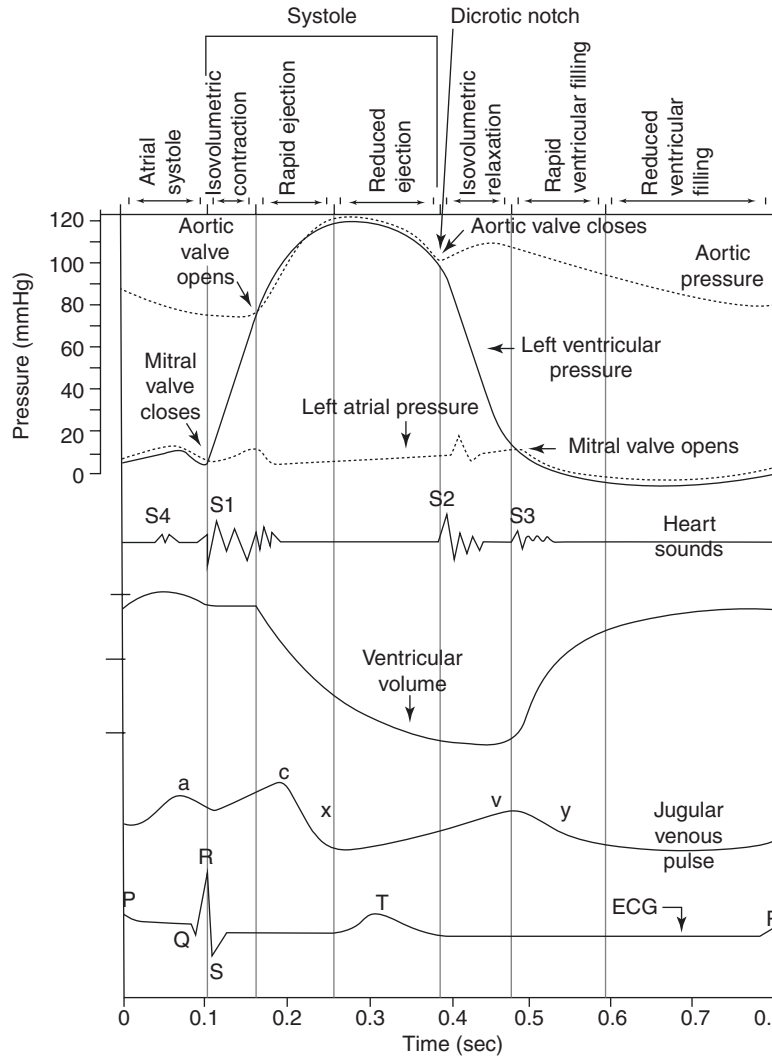

Fig. 3.2 Left atrial, aortic, and left ventricular pressure pulses correlated in time with aortic flow, ventricular volume, heart sounds, venous pulse, and the electrocardiogram for a complete cardiac cycle. (Adapted from Berne and Levy [2], p. 313, Fig. 16.10)

calcium release channels. The amount of calcium released from the sarcoplasmic reticulum is approximately 10 times the amount entering from the extracellular space (Fig. 3.3).

During systole, calcium in the cytosol binds to troponin C, initiating myocardial contraction by relieving the baseline inhibition of the contractile proteins (thin actin filament and thick myosin filament) by troponin I. When cytosolic calcium levels are low, the troponin complex (troponin C/I/T) holds tropomyosin in a position on the thin actin filament that prevents interaction between the cross-bridges on the thick myosin filament and the myosin-binding sites on the thin actin filament. When calcium binds to troponin C, a conformational change occurs, which weakens the bond between troponin I and actin. This conformational change moves the tropomyosin away from the myosin-binding sites and allows the myosin cross-bridges to interact with actin (Fig. 3.4).

At the end of systole, the calcium influx from the extracellular space ceases and the sarcoplasmic reticulum is no longer stimulated to release calcium. The sarcoplasmic reticulum then begins to avidly take up calcium via an ATP-dependent process. A cAMP-dependent protein kinase A (cAMP-PKA) phosphorylates phospholamban, which in turn stimulates the sarcoendoplasmic reticulum calcium ATPase (SERCA) pump in the membrane of the sarcoplasmic reticulum to take up calcium

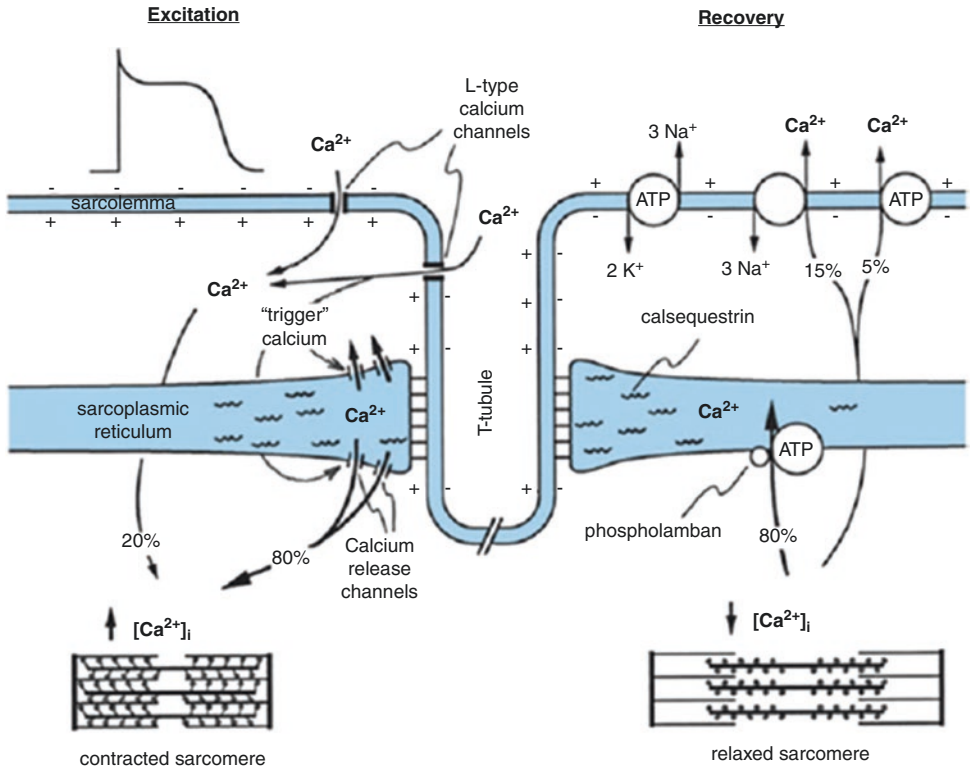

Fig. 3.3 Schematic diagram of the movements of calcium in excitation–contraction coupling in cardiac muscle. The influx of calcium (Ca^{2+}) from the interstitial fluid during excitation triggers the release of Ca^{2+} from the sarcoplasmic reticulum. The free cytosolic Ca^{2+} activates contraction of the myofilaments (systole). Relaxation (diastole) occurs as a result of uptake of Ca^{2+} by the sarcoplasmic reticulum, by extrusion of intracellular Ca^{2+} by Na^+–Ca^{2+} exchange, and to a limited degree by the Ca^{2+} pump. (Adapted from Berne and Levy [2], p. 365)

and facilitate relaxation. Phosphorylation of troponin I by cAMP-PKA also inhibits the calcium binding to troponin C, allowing tropomyosin to return to its resting inhibition of the myosin-binding sites and allowing diastole.

Cardiac contraction and relaxation are both enhanced by catecholamines, a physiologic phenomenon which has important clinical implications. Catecholamines (primarily endogenous norepinephrine, but also endogenous epinephrine) acting at the β receptor in the myocardial sarcolemma lead to the formation of cAMP from ATP and activation of PKA, which in turn increases the influx of extracellular calcium via increased opening of L-type calcium channels in the sarcolemma as discussed above. Catecholamines also enhance myocardial contractile force by increasing the rate of calcium release from the ryanodine receptor in response to calcium entry. The inotropic and lusitropic (relaxation) effects of catecholamine stimulation are mediated by the phosphorylation of phospholamban, accelerating calcium uptake into the sarcoplasmic reticulum by the SERCA receptors. Phosphorylation of phospholamban by cAMP-PKA removes its baseline inhibitory effect on SERCA receptors. While less physiologically significant, catecholamine stimulation of $\alpha 1$ receptors increases the formation of inositol 1,4,5-triphosphate (IP3) in the cytosol, which also stimulates some calcium release from the sarcoplasmic reticulum.

The parasympathetic nervous system has a much smaller effect on contractility as the vagus nerve fibers, mediated via acetylcholine at muscarinic (M2) receptors, are primarily distributed to the atria with very few to the ventricles. This explains the primary effect of parasympathetic stimulation on heart rate rather than contractility. However, under normal circumstances, there is a

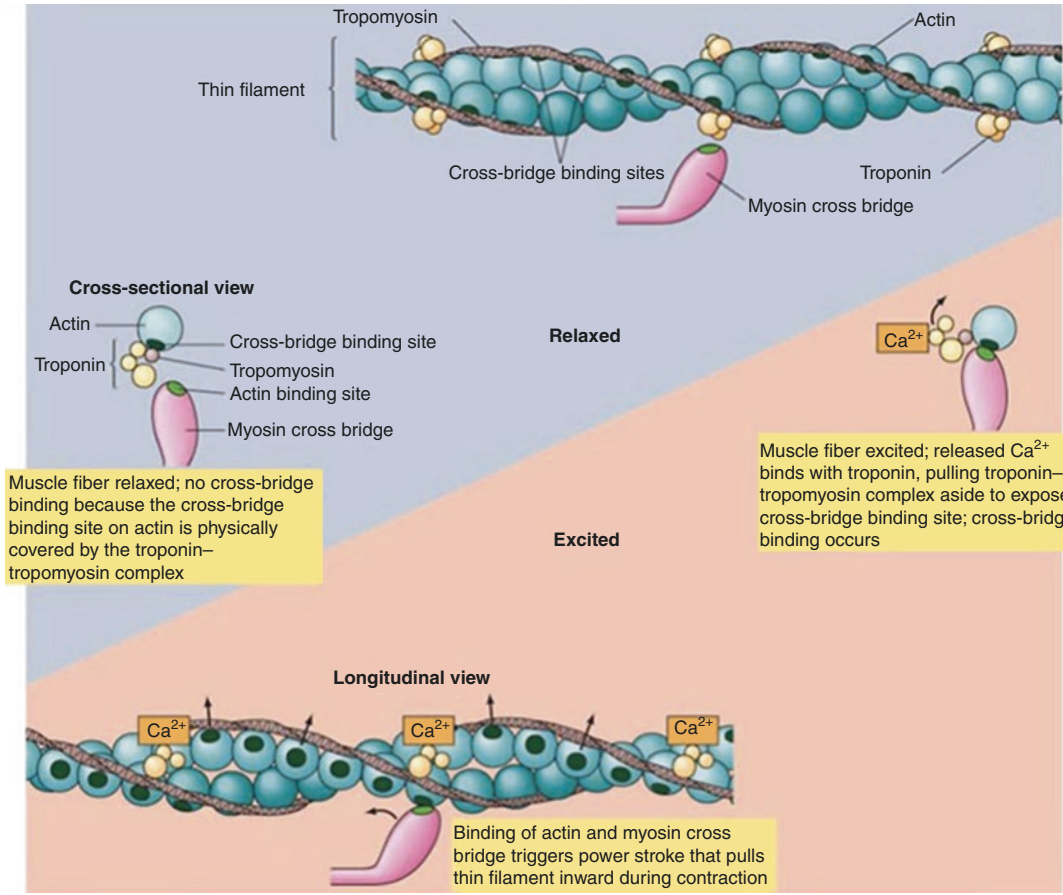

Fig. 3.4 Organization of the thin filament in both the relaxed and excited states. In the relaxed state, the myosin-binding site on actin is covered by the troponin–tropomyosin complex. In the presence of elevated calcium (Ca^{2+}), the troponin–tropomyosin complex is pulled away from the myosin-binding site when Ca^{2+} binds to troponin, allowing the myosin cross-bridge to interact with actin. Hydrolysis of ATP causes a conformational change in the myosin molecule, which pulls the actin filament toward the center of the sarcomere. A new ATP binds to myosin causing the release of the cross-bridge. If Ca^{2+} levels are still elevated, the cycle repeats. If Ca^{2+} are low, relaxation results

complex interplay between the sympathetic and parasympathetic nervous systems such that the sympathetic nerve fibers discharge continuously against tonic vagal inhibition.

There are two factors which affect inotropy that are worth mentioning despite the fact they are poorly understood: the Anrep effect and the Bowditch effect. The Anrep effect is the intrinsic ability of the heart to increase inotropy in response to abrupt increases in afterload [6]. This is seen in denervated hearts, suggesting it is an intrinsic mechanism. The other factor is the Bowditch or treppe effect, also called frequency-dependent activation. This is the ability of the heart to increase contractility slightly in the setting of an increase in heart rate [7]. This phenomenon is likely due to the inability of the Na/K-ATPase to keep up with the sodium influx at high heart rates, leading to an increase in intracellular calcium via the sodium–calcium exchanger.

Contractility in Cardiac Disease

Ischemia

Myocardial ischemia causes a decrease in contractility primarily by reducing ATP production in the mitochondria secondary to inadequate oxygen delivery [8]. This reduction in aerobic

ATP formation results in dysfunctional contractile shortening and reduced sarcoplasmic reticulum calcium pump function. Under these conditions, there is an increase in glycolysis, glucose uptake, and glycogen breakdown resulting in an increase in pyruvate [9]. Pyruvate is not readily oxidized in the mitochondria and is converted to lactate in the cytosol, resulting in a fall in intracellular pH [10]. When the intracellular pH falls, the sarcoplasmic calcium pump requires even more ATP to function properly [11]. In addition, the calcium concentration required for a given amount of myocyte force generation increases as the pH falls [12]. This leads to more ATP use in order to pump calcium back into the sarcoplasmic reticulum, leaving even less ATP to be used for contraction.

Heart Failure

At low inotropic states, the force-generating capabilities of ventricular muscle strips from normal and failing human hearts are similar [13]. As the inotropic demand increases, however, the ability of the failing heart to maintain its contractility reserve (the ability to increase contractility with heart rate or sympathetic stimulation) is severely depressed [14].

One of the major mechanisms of poor contractile reserve in heart failure is blunted adrenergic effects on myocyte contractility compared to normal myocardium [15]. Myocardium from heart failure patients shows significant reduction in beta-adrenergic receptor density, isoproterenol-mediated adenylyl cyclase stimulation, and contractile response to beta-adrenergic agonists [16]. The poor pump performance of the failing heart produces a reflex-mediated, sustained increase in sympathetic activity to maintain blood pressure [17]. It is this sustained sympathetic activity and an increased concentration of norepinephrine at the beta-adrenergic receptors that induce significant changes in beta-adrenergic signaling and downregulation of beta-adrenergic receptors [18]. In dilated cardiomyopathy, the $\beta 1$ receptor density is selectively reduced compared to the $\beta 2$ receptor which maintains its density but appears to be uncoupled from some downstream effector molecules. It is yet unclear whether adrenergic signaling abnormalities are adaptive or maladaptive in heart failure. By reducing LV contractility, desensitization may be detrimental; however, it may also be advantageous by reducing energy expenditure and protecting muscle from the effects of sustained adrenergic stimulation.

A second major mechanism contributing to altered contractility in the failing heart is abnormal calcium regulation within the myocyte. The sarcoplasmic reticulum is altered in heart failure such that the peak systolic cytosolic calcium level is decreased and the uptake of calcium into the sarcoplasmic reticulum is slowed. These abnormalities can explain features of systolic dysfunction including reduced force-generating capacity and slower rates of force decay [19] as well as diastolic dysfunction due to rate-dependent elevations in diastolic calcium levels [20]. There is some evidence to suggest that alterations in SERCA, L-type calcium channels, the ryanodine receptor, Na/K-ATPase, and the Na/Ca exchanger may all play some role in the initiation and progression of heart failure. Research continues in order to further elucidate the mechanisms of heart failure in the hope that targeted therapies may be developed.

Medications and Contractility [21, 22]

Dobutamine ($\beta 1 > \beta 2 > \alpha$)

Dobutamine is a synthetic sympathomimetic amine that approximates the hemodynamic profile of a pure $\beta 1$ agonist. The clinically available formulation is a racemic mixture of enantiomers. Both the (+) and (−) enantiomers stimulate $\beta 1$ receptors and, to a lesser degree, $\beta 2$ receptors. The (+) enantiomer, however, acts as an $\alpha 1$ antagonist, while the (−) enantiomer acts as an $\alpha 1$ agonist. Thus, the enantiomers essentially negate one another in their effect on the $\alpha 1$ receptor. The aggregate effect is that of an agonist at the $\beta 1$ receptor, leading to increased heart rate,

contractility, and diastolic relaxation. Dobutamine does have a modest agonist effect at peripheral β2 receptors causing mild peripheral vasodilation. Due to the increase in stroke volume secondary to its effects on contractility, however, blood pressure often does not change and can even increase despite the peripheral vasodilatory effects. Dobutamine is often used for short-term management of low output heart failure. Usual dosage: 2.5 μg/kg/min is initial dose, titrated to desired effect. Max dose is 20 μg/kg/min, though doses over 10 μg/kg/min are rarely needed. Onset of action is within 1–2 min, with a peak effect in 10 min. Drug effects cease very shortly after the drug infusion is discontinued. Tachycardia and ectopy are seen at higher doses, though these side effects are seen more frequently with dopamine.

Dopamine (D → β → α)

Dopamine is an endogenous sympathomimetic amine that functions as a neurotransmitter. It is a biosynthetic precursor of norepinephrine and epinephrine, and unlike dobutamine, it releases endogenous norepinephrine from stores in the nerve endings in the heart (this is overridden peripherally by prejunctional dopaminergic receptors which inhibit norepinephrine release). At low doses (<3 μg/kg/min), it has a peripheral vasodilatory effect by activating D1 receptors in the renal and mesenteric vascular beds. At intermediate doses (3–10 μg/kg/min), dopamine stimulates β1 and β2 receptors increasing heart rate, contractility, and peripheral vasodilation. At high doses (>10 μg/kg/min), dopamine begins to activate peripheral α1 receptors. This effect leads to a progressive increase in peripheral vasoconstriction with increasing doses. At these higher doses, the actions of dopamine become more like norepinephrine. Higher doses can also cause pulmonary vasoconstriction, and PCWP may be an unreliable estimate of LVEDP in the setting of a high-dose dopamine infusion. Dopamine is typically not recommended for patients with pulmonary edema because its venoconstrictor effects can increase venous return.

Onset of action is within 1–5 min and lasts for approximately 10 min. Tachycardia and ventricular arrhythmias are common at higher doses.

Norepinephrine (β1 > α > β2)

Norepinephrine (noradrenaline) is an endogenous neurotransmitter and is a potent β1 receptor agonist in the heart, with positive inotropic and chronotropic effects. It is also a potent peripheral α1 receptor agonist (more than epinephrine) and causes a dose-dependent increase in systemic vascular resistance. Due to these potent alpha effects, the resultant vasoconstriction limits the inotropic benefit of norepinephrine. It does have a small effect on β receptors. It is synthesized from dopamine and is precursor of epinephrine. Norepinephrine can be used in cardiogenic shock and is considered safer than epinephrine in ischemic disease, though it is still not a first-line choice.

Dosing: Typically start with 8–12 μg/min and titrate or wean to desired effect. Effects are seen within 1–2 min and duration is approximately 1–2 min.

Epinephrine (β1 = β2 > α)

Epinephrine (adrenaline) is an endogenous neurotransmitter synthesized from norepinephrine which is relatively nonselective at all receptors, but it primarily gives mixed β1 and β stimulation with some added α-mediated effects at higher doses. A low physiologic infusion rate (<0.01 μg/kg/min) increases contractility and speeds impulse generation via β activation, but often decreases peripheral resistance and blood pressure via β2 activation. Higher doses (>0.2 μg/kg/min) increase peripheral resistance when α-medicated constriction dominates over β2-mediated vasodilation. The positive inotropy, positive chronotropy, and vasoconstriction act together to raise blood pressure.

Epinephrine should typically be avoided in patients with cardiogenic shock due to myocardial ischemia because of the dramatic increases

in cardiac work and myocardial oxygen consumption. Usual dosing: for ACLS 1 mg IV (10 mL 1:10,000), for anaphylaxis 0.1 mg SQ/IM (0.1 mL 1:1000) or 0.1 mg IV (1 mL 1:10,000) over 5–10 min. The effects are seen within seconds of administration and last for 1–2 min.

Isoproterenol ($\beta 1 > \beta 2$)

Isoproterenol (isoprenaline) is a synthetic epinephrine analog. It is a pure β-agonist with almost no α effect. It has positive inotropic and chronotropic effects in the heart. In the peripheral vessels, $\beta 2$ stimulation leads to a decrease in peripheral resistance and often causes a drop in blood pressure. This drug causes a significant increase in myocardial work and oxygen consumption, so it is rarely used in patients with ischemic heart disease. Its use is typically limited to temporary treatment of bradyarrhythmias, refractory torsades de pointes, refractory bronchospasm, and in cardiac transplant patients to increase heart rate. Dosing: Initially 0.5 μg/min, with most patients responding to 2–20 μg/min. Onset is seen within 30–60 s and lasts anywhere from 8 to 50 min.

Milrinone (PDE-3 Inhibitor)

Milrinone exerts its positive inotropic actions by inhibiting phosphodiesterase in cardiac myocytes. This inhibition reduces the breakdown of intracellular cAMP, ultimately leading to enhanced calcium entry into the cell and increased force of contraction. It also causes some peripheral vasodilation. Milrinone, therefore, has inotropic, vasodilatory, and minimal chronotropic effects. It is used for short-term management of low output heart failure, similar to dobutamine. Dosing: Initial loading dose of 50 μg/kg over 10 min followed by 0.25–0.75 μg/kg/min. The effect is usually seen within 5–15 min. Milrinone is primarily excreted unchanged by the kidney, so dose adjustments may be necessary in patients with significant renal dysfunction.

Digoxin

It is theorized that digoxin (digitalis) improves contractility via inhibition of the sarcolemmal Na^+K^+-ATPase pump, normally responsible for maintaining transmembrane Na^+ and K^+ gradients. Inhibiting this pump causes intracellular Na^+ to rise, which then reduces Ca^{++} extrusion from the cell by the Na^+–Ca^{++} exchanger. This leads to more Ca^{++} being pumped into the sarcoplasmic reticulum with higher amounts of Ca^{++} being released into the myofilaments with each action potential. Increased Ca^{++} release from the sarcoplasmic reticulum enhances the force of contraction. The magnitude of the positive inotropic effect correlates with the degree of Na^+ K^+-ATPase inhibition.

Digoxin is a relatively weak inotropic agent and is used primarily for the treatment of chronic symptomatic systolic dysfunction, especially if accompanied by atrial arrhythmias.

Bullet Point Summary

- Contractility, or inotropy, is the inherent capacity of the myocardium to contract *independent* of preload and afterload.
- Contractility can be evaluated through assessing the rate of rise of left ventricular pressure, or dP/dt. With advancements in echocardiography, 2D speckle tracking with strain imaging now represents an effective method of noninvasive assessment of both global and segmental myocardial contractile function and has been well-validated in multiple cardiovascular disease states.
- In relation to a normal heart, a hypodynamic heart has an elevated end-diastolic pressure, a slowly rising ventricular pressure, and a prolonged ejection phase. A hyperdynamic heart has a reduced end-diastolic pressure, a fast-rising ventricular pressure, and a brief ejection phase.

- Contractility is primarily determined by the way calcium is processed and utilized in the cardiac myocyte.
- Ischemia causes reduced contractility primarily via a decrease in ATP production.
- The failing heart loses its contractile reserve via multiple mechanisms, including blunting of the response to adrenergic stimulus and abnormalities in the handling of calcium within the cardiac myocyte.
- Exogenous inotropic agents work to enhance cardiac contractility via several different mechanisms.

Review Questions

1. An influx of calcium into the cell triggers a conformational change in which receptors to allow calcium release from the sarcoplasmic reticulum?
   A. SERCA
   B. L-type
   C. Calcium release channels
   D. Na/Ca exchanger
   E. Ryanodine

   Answer: E. Depolarization of the myocyte membrane causes calcium inflow via voltage-gated L-type calcium channels. This calcium inflow then triggers a conformational change in ryanodine receptors in the sarcoplasmic reticulum membrane, which allows calcium to flow out into the cytosol via the calcium release channels.
2. The ability of the heart to increase inotropy in response to abrupt increases in afterload is known as the:
   A. Bowditch effect
   B. Lusitropic effect
   C. Anrep effect
   D. Chronotropic effect
   E. Treppe effect

   Answer: C. The Anrep effect is the intrinsic ability of the heart to increase contractility in response to an acute increase in afterload. This is even seen in denervated hearts. The Bowditch or treppe effect is the ability of the heart to increase contractility in the setting of an increasing heart rate.

Special thanks to Frederick Heupler Jr., MD, for his contributions to the previous version of this chapter.

References

1. Berne RM, Levy MN. Physiology. 5th ed. St. Louis: Mosby; 2004.
2. Berne RM, Levy MN. Physiology. 4th ed. St. Louis: Mosby; 1998.
3. Mohrman DE, Heller LJ. Cardiovascular physiology. 6th ed. London: McGraw-Hill; 2006.
4. Berne RM, Levy MN. Cardiovascular physiology. 8th ed. St. Louis: Mosby; 2001.
5. Gorcsan J III, Tanaka H. Echocardiographic assessment of myocardial strain. J Am Coll Cardiol. 2011;58:1401–13.
6. von Anrep G. On the part played by the suprarenals in the normal vascular reactions of the body. J Physiol. 1912;45:307.
7. Bowditch HP. Uber die Eigenthiimlichkeiten der Reizbarkeit, welche die Muskelfasern des Herzens zeigen. Ber Sachs Ges Wiss. 1871;23:652–89.
8. Leidtke AJ. Alterations of carbohydrate and lipid metabolism in the acutely ischemic heart. Prog Cardiovasc Dis. 1981;23:321–36.
9. Young LH, et al. Regulation of myocardial glucose uptake and transport during ischemia and energetic stress. Am J Cardiol. 1999;83:25H–30.
10. Stanley WC. Myocardial energy metabolism during ischemia and the mechanisms of metabolic therapies. J Cardiovasc Pharmacol Ther. 2004;9:S31–45.
11. Fabiato A, et al. Effects of pH on the myofilaments and the sarcoplasmic reticulum of skinned cells from cardiac and skeletal muscles. J Physiol. 1978;276:233–55.
12. Murphy E, et al. Amiloride delays the ischemia-induced rise in cytosolic free calcium. Circ Res. 1991;68:1250–8.
13. Hasenfuss G, et al. Calcium cycling in congestive heart failure. J Mol Cell Cardiol. 2002;34:951–69.
14. Houser SR, et al. Is depressed myocyte contractility centrally involved in heart failure? Circ Res. 2003;92:350–8.
15. Mann DL. Basic mechanisms of disease progression in the failing heart: the role of excessive adrenergic drive. Prog Cardiovasc Dis. 1998;41:1–8.
16. Bristow MR. Beta-adrenergic receptor blockade in chronic heart failure. Circulation. 2000;101:558.

17. Alpert NR, et al. The failing human heart. Cardiovasc Res. 2002;54:1–10.
18. Bristow MR. The adrenergic nervous system in heart failure. N Engl J Med. 1984;311:850–1.
19. Houser SR, et al. Functional properties of failing human ventricular myocytes. Trends Cardiovasc Med. 2000;10:101–7.
20. Beuckelmann DJ, et al. Altered diastolic [Ca2+] i handling in human ventricular myocytes from patients with terminal heart failure. Am Heart J. 1995;129:684–9.
21. Opie LH. Drugs for the heart. 7th ed. Philadelphia: Saunders Elsevier; 2009.
22. Marino PL. ICU book. 3rd ed. Philadelphia: Lippincott Williams & Wilkins; 2007.

Suggested Reading

Darovic GO. Hemodynamic monitoring: invasive and noninvasive clinical application. 3rd ed. Philadelphia: WB Saunders; 2002.
Kern MJ. Hemodynamic rounds: interpretation of cardiac pathophysiology from waveform analysis. 2nd ed. New York: Wiley-Liss; 1999.
Ragosta M. Textbook of clinical hemodynamics. Philadelphia: Saunders; 2008.

Cardiac Output

4

Daniel H. Katz, Frederick Heupler Jr.,
and Marwa A. Sabe

Definition and Determinants of Cardiac Output

Cardiac output is defined as the volume of blood ejected from the heart every minute. At rest the normal adult cardiac output is approximately 5–6 L/min [1] and the normal cardiac output indexed to body surface area is 2.6–3.2 L/min/m^2. Cardiac output is the product of stroke volume and heart rate [2]. The three major determinants of stroke volume, and thus cardiac output, are preload, afterload, and contractility, which are discussed in depth in the three preceding chapters. Preload and contractility are directly correlated to stroke volume, while afterload is inversely correlated [2]. Cardiac output can also be affected by structural abnormalities of the heart such as valvular regurgitation and intracardiac shunts, which reduce the volume of forward flow. These will be discussed in later chapters.

Preload contributes to cardiac output by its effects on stroke volume and heart rate (see Chap. 1). Preload is most directly associated with the ventricular end-diastolic pressure or simply the "filling pressure." The effect of preload on stroke volume is described by the Frank-Starling mechanism [3] (Fig. 4.1). As more volume fills the left ventricle, the pressure at end-diastole increases, and there is greater stretch of the left ventricular walls. The walls behave like a spring, so the greater the stretch of the walls, the more forceful their recoil, and thus the greater the amount of ejected blood [3]. However, as seen in isolated heart preparations, if the stretch on the myocardium exceeds a certain point, the opposite occurs, and stroke volume as well as cardiac output can decrease. Preload also affects heart rate. Although the common conception is that volume depletion leads to tachycardia due to a reduction in baroreceptor firing, an increase in the effective circulating volume may also lead to an increase in heart rate. With increased stretching in the right atrium, the heart pumps at a faster rate due to stretch of the sinus node. The stretching of the right atrium also causes the Bainbridge reflex, a sympathetic nervous system-mediated reflex that increases heart rate in response to this stretching [4].

Afterload is a force that opposes myocardial contraction (see Chap. 2). It is equal to the tension across the ventricular wall during systole.

D. H. Katz
Beth Israel Deaconess Medical Center,
Boston, MA, USA
e-mail: dkatz@bidmc.harvard.edu

F. Heupler Jr.
Cleveland Clinic, Cleveland, OH, USA
e-mail: heuplef@ccf.org

M. A. Sabe (✉)
Beth Israel Deaconess Medical Center,
Boston, MA, USA

Harvard Medical School, Boston, MA, USA
e-mail: msabe@bidmc.harvard.edu

A. T. Askari, A. W. Messerli (eds.), *Cardiovascular Hemodynamics*, Contemporary Cardiology,
https://doi.org/10.1007/978-3-030-19131-3_4

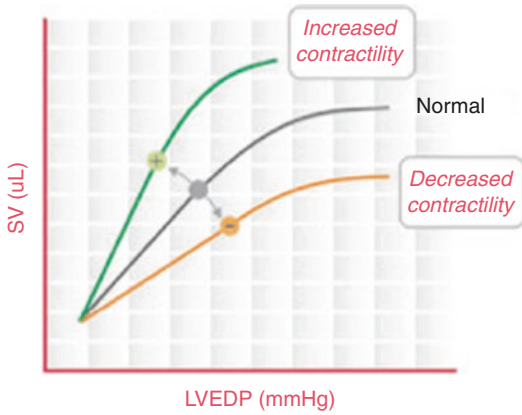

Fig. 4.1 Relationship between cardiac output, preload, and contractility. (*SV* stroke volume, *LVEDP* left ventricular end-diastolic pressure, a measure of preload). (Adapted from http://scisense.com/education/cv-application.html)

The Law of Laplace describes the relationship between the determinants of ventricular wall tension, or afterload, by the equation: $\sigma = (P \times r)/(2w)$, where σ is wall stress, P is chamber pressure, r is the radius of the chamber, and w is the wall thickness. In other words, wall stress (afterload) is directly proportional to ventricular pressure and size (radius) and indirectly related to wall thickness. Ventricular dilation increases afterload, and left ventricular hypertrophy (LVH) is a compensatory mechanism that attempts to decrease afterload [4]. A major component of afterload is captured by forces exerted on the ventricle by the vasculature, which is well estimated by vascular resistance.

Please refer to Chap. 3 for an in-depth discussion of the relationship between contractility and cardiac output. Increases in contractility increase the cardiac output for any given preload or afterload.

Circulatory Hemodynamics

The heart is at the center of two interrelated cardiovascular systems: the systemic, or peripheral, cardiovascular system and the pulmonary cardiovascular system. The flow through each of these systems is fundamentally described with the same equation that describes flow through any tube, wherein the pressure gradient across the tube is equal to the flow across the tube multiplied by the resistance of that tube.

$$\Delta P = Q \times R$$

The abovementioned equation is applied to the circulatory system by defining Q as the cardiac output, R as either the systemic vascular resistance (SVR) or the pulmonary vascular resistance (PVR), and ΔP as the change in pressure across either of the two circuits. In general terms, it is the difference between the average blood pressure before the circuit and the average blood pressure after the circuit. Specifically, the change in pressure across the pulmonary circulation is estimated as the mean pulmonary artery pressure minus the pulmonary capillary wedge pressure (mPAP – PCWP) while the change in pressure across the systemic circulation is estimated as the mean arterial pressure minus the right atrial pressure (MAP – RAP). Right atrial pressure is also referred to as the central venous pressure (CVP). Thus, systemic cardiac output is equal to (MAP – RAP)/SVR. As discussed previously, the noted pressures can easily be determined from a combination of a Swan-Ganz catheter and either invasive or noninvasive blood pressure monitoring [3].

Physiologically, it is useful to see Ohm's law expressed as written above because it reminds us that the pressure gradient across a vascular circuit is the *result* of flow and resistance. Clinically, this means that blood pressure depends both on cardiac output and vascular resistance. Perturbations in blood pressure, either from illness or medications, are the result of changes to one or both of these two factors. It also highlights that a normal blood pressure can occur in the setting of a low cardiac output with a compensatory increase in vascular resistance. Normal blood pressure does not mean that there is normal tissue perfusion!

Despite the fact that the pressure change is the result of changes in cardiac output and resistance, resistance is not measured directly. Instead, we measured the pressures and cardiac output using a variety of tools which will be discussed in detail in this chapter (but most commonly a Swan-Ganz catheter), and calculated the resistance from

Table 4.1 Hemodynamic parameters

Hemodynamic parameter	Formula	Normal range
CO	HR × SV	4–6 L/min
CI	CO/BSA	2.6–4.3 L/min/m^2
SVR	(MAP-CVP)/CO × 80	800–1400 dyn s/cm^5
SVRI	(MAP-CVP)/CI × 80	1500–2300 dyn s/cm^5/m^2
PVR	(PAP-PCWP)/CO × 80	140–250 dyn s/cm^5
PVRI	(PAP-PCWP)/CI × 80	240–450 dyn s/cm^5/m^2

CO cardiac output, *CI* cardiac index, *BSA* body surface area, *SVR* systemic vascular resistance, *SVRI* SVR index, *PVR* peripheral vascular resistance, *PVRI* PVR index

Ohm's law. Normal values for cardiac output, filling pressures, and vascular resistances are listed in Table 4.1.

Hemodynamic Disturbances: The Failing Heart and Shock

Heart failure is defined as either: (1) inadequate cardiac output to support normal organ function, or (2) maintenance of adequate cardiac output at elevated filling pressures. The majority of encountered clinical heart failure falls into the latter category. These patients often present with signs and symptoms of volume overload which are the result of such elevated filling pressures (see Chap. 10). The volume overloaded state can be managed with fluid removal either by diuresis or dialysis. However, a variety of insults can push a heart which functions adequately (either with normal or elevated filling pressures) into a state in which cardiac output is inadequate, assuming the body's demand is held constant. These insults must affect one or more of the four factors of cardiac output (Table 4.2).

Table 4.2 Selected hemodynamic insults to cardiac output

	Examples of insults that predominantly affect listed factor
Preload	Hemorrhage, cardiac tamponade, pulmonary embolism
Afterload	Increase in sympathetic tone, vasopressors
Contractility	Ischemia, systemic acidemia, negative inotropes (calcium channel blockers, beta-blockers)
Heart rate	Heart block, sinus, or AV nodal blocking agents

AV atrioventricular

Inadequate tissue perfusion is a clinical state known as circulatory shock. Human tissues require a constant supply of oxygen to maintain aerobic metabolism. When this supply is impaired, the body tissues slowly revert to anaerobic metabolism, producing toxic metabolic breakdown products, such as lactic acid. By this mechanism, shock leads to end organ dysfunction and eventual failure. Shock resulting from low cardiac output, as described above, is one possible cause of inadequate tissue perfusion. From a hemodynamic standpoint, the three major types of circulatory shock are cardiogenic, hypovolemic, and vasogenic (also known as distributive). Cardiogenic shock and hypovolemic shock are low cardiac output states, whereas vasogenic shock is a high output type of shock [5].

Differentiating these states can be achieved by determining the hemodynamic parameters already discussed. Cardiogenic shock and hypovolemic shock are both associated with low cardiac output and high SVR, but may be differentiated by PCWP, which is elevated in cardiogenic shock but decreased in the hypovolemic shock. Vasogenic shock is a low SVR state due to vasodilation, and with causes including sepsis, thyrotoxicosis, anemia, anaphylaxis, and AV fistulas [6]. Vasogenic shock is typically accompanied by a high cardiac output. Management of heart failure and shock will be discussed more extensively in Chaps. 19 and 21, respectively.

Methods of Determining Cardiac Output

In critically ill patients, differentiating the shock states described above is essential to management, especially when inadequate cardiac output may be related to increased morbidity and mortality [7]; therefore, it is essential to have reliable methods to measure cardiac output.

There are multiple bedside indicators that help estimate the adequacy of cardiac output and/or tissue perfusion. Mental status, specifically, patients falling asleep during their interviews, and decreased urine output are early indicators of inadequate perfusion of the brain and kidneys. Cool forearms and legs also signal low cardiac output as vascular resistance increases and blood is shunted away from the extremities in favor of internal organs [8]. The proportional pulse pressure is another useful bedside marker, and can be calculated as the difference between the systolic and diastolic blood pressures divided by the systolic blood pressure ((SBP-DBP)/SBP). A ratio of less than 25% suggests a cardiac index of less than 2.2 L/min/m^2 [9].

There are also several methods of actually measuring cardiac output. These include invasive methods such as thermodilution and Fick methods, which require the use of a Swan-Ganz pulmonary artery catheter, and noninvasive methods such as transpulmonary thermodilution [10]. Noninvasive clinical measures may help determine whether a patient is in a low output state; however, invasive methods of measuring cardiac output in the intensive care unit are mainstays for precise monitoring to guide therapeutic management.

Thermodilution

With the use of a pulmonary artery catheter, cardiac output may be measured directly by the thermodilution method (introduced in 1953 by Fegler) or indirectly by means of the Fick principle [1]. The thermodilution method of measuring cardiac output involves injection of cold fluid into the Swan-Ganz catheter positioned in the pulmonary artery. This injectate flows through the catheter and exits into the right ventricle where it mixes with blood, which is warmer than the injected fluid. This mixture of blood and indicator fluid then moves into the pulmonary artery, where a thermistor at the catheter tip senses temperature changes [6]. With each beat, the blood temperature rises as the cold fluid is washed out of the right side of the heart [1]. A time-temperature curve is electronically obtained, and the cardiac output is calculated using the Stewart-Hamilton Formula. The key components of this formula are cardiac output, amount of indicator, and the integral of the amount of indicator concentration over time. The cardiac output is inversely related to the area under the thermodilution curve as measured by the integral of the amount of indicator concentration over time [3, 6]. When cardiac output is low, it takes longer for the cold fluid to wash out of the right ventricle and thus for the temperature of the blood to return to baseline, producing a low amplitude, prolonged curve with a large area underneath it. On the other hand, the blood temperature returns to baseline quicker when the injection fluid moves at a faster rate through the heart, as it does with higher cardiac output [3]. This produces a higher amplitude, shorter curve with a smaller area Fig. 4.2. The advantage of this method is the use of computer calculations to give quick measurements as well as less need for blood draws. However, this method becomes less useful in patients with cardiac output less than 2.5 L/min as it tends to overestimate the cardiac output in these cases [3]. It also miscalculates cardiac output in patients with tricuspid regurgitation because the indicator fluid is recycled, thus producing a curve that is similar to the low cardiac output curve and thus underestimates cardiac output [5]. On the other hand, left-to-right shunts tend to overestimate the cardiac output as a portion of the injectate crosses through the shunt and thus the temperature change that is detected downstream occurs quickly as would occur in a true high cardiac output state [5].

Another thermal method of measuring cardiac output is the continuous cardiac output method. This method uses a warm indicator rather than a cold one in the standard thermal dilution [11]. A thermal filament on the right ventricular portion of the pulmonary artery catheter releases small amounts of heat, which is measured by the thermistor at the tip of the pulmonary artery catheter.

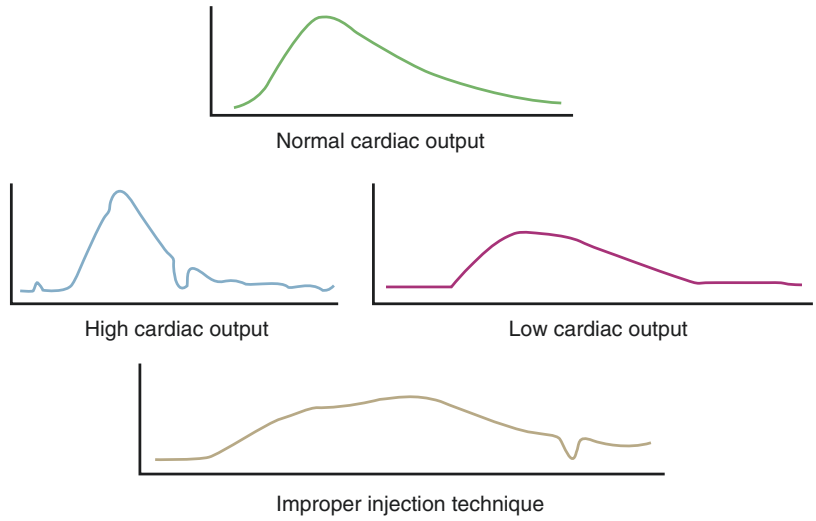

Fig. 4.2 Thermodilution cardiac output curves. (Adapted from Braunwald et al. [3])

The cardiac output is automatically calculated and updated every 30–60 s, giving an average cardiac output over 3–6 min. The major disadvantage of this method is that it does not respond quickly in unstable hemodynamic conditions, such as fluid resuscitation or hemorrhage [12].

The Fick Cardiac Output

The Fick principle is employed to provide an indirect measurement of cardiac output that is based on the oxygen saturation of blood samples obtained through a Swan-Ganz catheter. This method was developed by Eugene Fick in 1870, and is based on the principle that the rate of oxygen consumption by the peripheral tissues is equal to the cardiac output multiplied by the change in oxygen concentration between the arterial and venous system [1]. In other words, when blood volume arrives to tissues at a lower rate, tissues must extract a greater percentage of the available oxygen in each mL of blood to meet their rate of oxygen consumption. This principle is expressed:

$$\text{oxygen consumption} = \text{cardiac output} \times \text{arteriovenous oxygen difference}$$

To calculate the *exact* concentration of oxygen in either the arterial or venous blood, one must calculate the amount of oxygen carried by the red blood cells and the very small amount dissolved in the blood. The following equation is used:

$$\text{Oxygen content} = \text{Hgb}\left(\text{g/dl}\right) \times 1.34\left(\text{mL O}_2\text{/g of Hgb}\right) \times \text{SO}_2\left(\%\right) + 0.0032 \times \text{PO}_2$$

where Hgb is the hemoglobin concentration, SO_2 is the oxygen saturation, and PO_2 is the partial pressure of oxygen not bound to hemoglobin and freely dissolved in the blood. The freely dissolved oxygen is extremely small compared to oxygen bound to hemoglobin and is frequently ignored. Therefore, the arteriovenous oxygen difference can be expressed as:

$$\text{Arteriovenous oxygen difference} = \left(\text{SaO}_2 - \text{SvO}_2\right) \times 1.34 \times \text{Hgb}$$

where SaO_2 and SvO_2 are the arterial and venous oxygen saturations respectively. SaO_2 is measured from either an arterial line or a pulse oximeter with a reliable tracing. SvO_2 is measured as the oxygen saturation in the main pulmonary artery, and is also referred to as the mixed venous oxygen saturation. Together, the entire Fick equation can then be rewritten as:

$$\text{Cardiac output}\left(\text{L}/\text{min}\right) = \frac{\text{VO}_2\left(\text{mL}/\text{min}\right)}{\left(\text{SaO}_2 - \text{SvO}_2\right)\times 1.34 \times \text{Hgb}} \times 10$$

where VO_2 is oxygen consumption. Cardiac output is usually corrected for body size using this equation: cardiac index (CI) = CO/BSA where CI is the cardiac index and BSA is the body surface area. CI is commonly used in the ICU setting to monitor a patient's hemodynamic status and guide therapy. The normal CI is 2.6–4.3 L/min/m^2 [13], and it is normally lower in elderly persons. In healthy adults, the normal value for VO_2 is 200–300 mL/min, or 110–160 mL/min/m^2 when adjusting for body size [5].

The Fick method is more accurate when VO_2 is measured using a calorimeter rather than estimated, as is the usual practice, especially in hyperdynamic states such as sepsis [10]. However, in general practice, even if the calculated CI is not exactly precise, the trend in the estimated CI indicates clinical changes from therapies or insults. The disadvantages of the Fick method are similar to other invasive methods including risk of infection or pulmonary hemorrhage.

Other Methods of Assessing Cardiac Output

An alternate, but still invasive, method of measuring cardiac output is ventriculography [1]. This method requires placement of a catheter in the left ventricle and subsequent injection of contrast dye. The cardiac cycle is recorded in a cine loop, and the stroke volume is calculated by subtracting the end systolic volume from the end-diastolic volume. This method is particularly useful in the setting of valve stenosis or regurgitation. However, the CO may be miscalculated in patients with enlarged ventricles [1]. It is more invasive, requiring arterial access, and catheter placement in the left ventricle with associated risks of structural damage and arrhythmia.

A less invasive method of measuring CO is called the transpulmonary thermodilution technique, which is used by the PICCO monitor. There is no need for catheter placement into the heart using this method [10]. Instead, a central venous catheter is placed along with an arterial catheter with a thermistor at the tip. Indicator fluid is injected into the central line, and the arterial catheter thermistor senses the blood as it passes through the thorax, producing a similar thermodilution curve as the standard thermodilution method. The advantage of this method is that it is less invasive and less influenced by the respiratory cycle than the thermodilution technique, which employs a pulmonary artery catheter [14]. However, it may be inaccurate in patients with aortic stenosis, aortic aneurysm, and intracardiac shunts.

Other noninvasive or minimally invasive methods (See Chap. 13) of measuring CO include esophageal Doppler analysis of aortic blood flow, the indirect Fick method which uses partial carbon dioxide rebreathing, thoracic electrical bioimpedance, and pulse contour analysis of the arterial pressure waveform [6]. Each of these methods has disadvantages that make them less practical in the clinical setting. Esophageal Doppler analysis requires sufficient training to obtain accurate measurements. The indirect Fick method, which is applicable to intubated patients, is less accurate in severe lung injury or when there is variability in tidal volume (as is seen with spontaneous breathing) [6]. Thoracic electrical bioimpedance is less accurate in patients with peripheral edema or pleural effusions, and pulse contour analysis requires that another method of measuring CO be used in order to calibrate the pulse contour device [6].

Summary

- Cardiac output is defined as stroke volume multiplied by heart rate, and the determinants of stroke volume are afterload, preload, and contractility.
- Cardiogenic shock is a low cardiac output, high wedge pressure state that is often associated with hypotension. In cases of impending cardiogenic shock, blood pressure may be preserved. It is important to measure cardiac output in patients who are extremely hemodynamically unstable in order to guide therapy.
- Cardiac output is most commonly measured with a Swan-Ganz catheter using either the thermodilution or the Fick method.
- The Fick principle states that cardiac output is inversely proportional to the arteriovenous oxygen difference and directly proportional to oxygen consumption.

Equations

$$CO = SV \times HR$$

$$CI = CO / BSA$$

$$\text{Fick Principle}: CO = VO_2 / 1.34 \times 10 \times Hgb\left(SaO_2 - SvO_2\right)$$

$$CO = \left(MAP - CVP\right) / SVR$$

Review Questions

1. A 65-year-old male with a history of coronary artery disease status post CABG 5 years prior and known ischemic cardiomyopathy with an ejection fraction of 35% on his last echocardiogram, presents to the ER with palpitations and shortness of breath. His vital signs are blood pressure 120/95, heart rate 130 in sinus rhythm, and oxygen saturation 88% on room air. During his medical interview, he falls asleep between questions. On physical examination, his JVP is estimated to be 14 cm, he has an audible S3, bilateral crackles, and his extremities are cool to the touch. A Swan-Ganz catheter is placed. What is his most likely hemodynamic profile?
   (a) CI = 3.5, PCWP = 24, SVR = 400
   (b) CI = 1.8, PCWP = 30, SVR = 2500
   (c) CI = 2.5, PCWP = 10, SVR = 1800
   (d) CI = 2.0, PCWP = 10, SVR = 800
   - *Answer*: (b) This patient is cold and wet on physical exam and is in severe, decompensated HF.
2. Nitroprusside, a potent vasodilator, is administered to the abovementioned patient. What is the expected effect on blood pressure when it is given?
   (a) The blood pressure will increase
   (b) The blood pressure will decrease
   (c) The blood pressure will stay exactly the same
   (d) The change in blood pressure is uncertain
   - *Answer:* (d) While vascular resistance will drop, the reduction in afterload will increase cardiac output. The percent change in each of these factors will determine the direction and magnitude of blood pressure change, but this cannot be predicted beforehand. Administering a vasodilator to a patient in acute decompensated heart failure can make the blood pressure increase!
3. A 40-year-old female presents with shortness of breath 6 weeks after giving birth. A Swan-Ganz catheter is placed to calculate her cardiac output. Her SvO_2 is 40%, Hgb is 11, and SaO_2 is 98%. What is her cardiac output in L/min output using the Fick equation? Assume a VO_2 of 250 ml/min.
   (a) CO = 2.9 L/min
   (b) CO = 4.2 L/min
   (c) CO = 3.9 L/min
   (d) CO = 6.2 L/min
   - *Answer:* (a) *The Fick cardiac output is calculated as follows*:

$$CO = \left(VO_2\left(\text{assumed}\right) / 1.34 \times Hgb \times \left(SaO_2 - SvO_2\right)\right) \times 10.$$

4. In which of the following situations would the thermodilution method overestimate the cardiac output?
   (a) A 55-year-old woman with carcinoid syndrome associated with severe tricuspid regurgitation.
   (b) A 48-year-old male who presents with an acute inferior myocardial infarction associated with right ventricular failure.
   (c) A 40-year-old male who had an acute ST elevation myocardial infarction 1 week ago who now presents with acute cardiogenic shock due to ventricular septal rupture (VSR).
   (d) A 66-year-old female who presents with a type A dissection associated with severe aortic insufficiency.
   - *Answer:* (c) Shunts tend to overestimate CO when the thermodilution technique is used as a portion of the injectate crosses through the VSR and thus the temperature change that is sensed downstream occurs at a rate similar to a high CO state. Severe TR (choice a) tends to underestimate the cardiac output when using their modulation.
5. In which of the following situations is the estimated oxygen consumption (VO_2) (rather than a direct measurement) most likely to be inaccurate?
   (a) A 60-year-old female with right ventricular infarction.
   (b) An 80-year-old male with sepsis due to *Clostridium difficile* colitis.
   (c) A 48-year-old male with acute ischemic mitral regurgitation.
   (d) A 90-year-old male with severe aortic stenosis.
   - *Answer*: (b) The estimated VO_2 is inaccurate in hyperdynamic states such as sepsis.

References

1. Fuster R, O'Rourke R, Walsh R, Poole-Wilson P. Hurst's the heart. 12th ed. New York: The McGraw-Hill Companies, Inc; 2008.
2. Lilly L. Pathophysiology of heart disease. 3rd ed. Philadelphia: Lippincott Williams & Wilkins; 2003. p. 61, 213–4.
3. Braunwald E, Libby P, Bonow R, Mann D, Zipes D. Braunwald's heart disease. 18th ed. Philadelphia: Saunders; 2008. p. 452–5.
4. Boron W, Boulpaep E. Textbook of medical physiology. Philadelphia: Saunders; 2009.
5. Hall J, Schmidt G, Kress J. Principles of critical care. 4th ed. New York: McGraw-Hill; 2015.
6. Stevenson LW, Perloff JK. The limited reliability of physical signs for estimating hemodynamics in chronic heart failure. JAMA. 1989;261:884–8.
7. Marino P. The ICU book. 4th ed. Philadelphia: Wolters Kluwer Health/Lippincott Williams & Wilkins; 2014. p. 135–50, 239–262
8. Dupont H, Squara P. Cardiac output monitoring. Curr Opin Anaesthesiol. 1996;9:490–4.
9. Nohria A, Lewis E, Stevenson LW. Medical management of advanced heart failure. JAMA. 2002;287(5):628–40.
10. Mohammed I, Phillips C. Determining cardiac output in the intensive care unit. Crit Care Clin. 2010;26:355–64.
11. Miller R. Miller's anesthesia. 7th ed. New York: Churchill Livingstone; 2010.
12. Siegel LC, Hennessy MM, Pearl RG. Delayed time response of the continuous cardiac output pulmonary artery catheter. Anesth Analg. 1996;83:1173–7.
13. Longo DL, Fauc AS, Kasper DL, Hauser SL, Jameson JL, Loscalto J, editors. Harrijan's principles of internal medicine. 18th ed. New York: McGraw–Hill; 2012.
14. Sakka SG, Ruhl CC, Pfeiffer UJ, et al. Assessment of cardiac preload and extravascular lung water by single transpulmonary thermodilution. Intensive Care Med. 2000;26(2):180–7.

Suggested Reading

Zipes D, Libby P, Bonow R, Mann D, Tomaselli G, editors. Braunwald's heart disease: a textbook of cardiovascular medicine. 11th ed. Philadelphia: Elsevier; 2019. p. 418–61.

Vincent JL, Abraham E, Moore F, Kochanek P, Fink M. Textbook of critical care. 7th ed. Philadelphia: Elsevier; 2017. p. 617–36.

Hall J, Schmidt G, Kress J. Principles of critical care. 4th ed. New York: The McGraw-Hill Companies, Inc; 2015.

Part II

Effects of Selected Interventions on CV Hemodynamics

5 Renin–Angiotensin–Aldosterone Axis Modulators and Other Vasodilators

Chirag Bavishi, Roberto Ramirez, and Franz H. Messerli

Introduction

The renin–angiotensin–aldosterone system (RAAS) is a complex system that plays an important role in maintaining hemodynamic stability in the human body through regulation of arterial blood pressure, water and electrolyte balance, as well as cardiovascular hemodynamics. Both over- and under activation of the RAAS can result in loss of vital cardiac and vascular functions leading to pathological consequences. Blockade of the RAAS has been shown to be beneficial in patients with hypertension, acute myocardial infarction, and chronic systolic heart failure.

C. Bavishi
Department of Cardiology, Lifespan Cardiovascular Institute, Rhode Island Hospital, Warren Alpert Medical School of Brown University, Providence, RI, USA
e-mail: Cbavishi@lifespan.org

R. Ramirez
Department of Cardiology, Mount Sinai St. Luke's Hospital, New York, NY, USA
e-mail: Roberto.ramirez@mountsinai.org

F. H. Messerli (✉)
Department of Cardiology, University of Bern, Bern, Switzerland

Mechanism of Raas Inhibitors

The renin–angiotensin–aldosterone system (RAAS) plays an integral role in the homeostatic regulation of arterial pressure, tissue perfusion, and extracellular volume. This pathway is initiated by the secretion of renin synthesized by the juxtaglomerular cells in the afferent arteriole of the renal glomerulus. Renin secretion is modulated through interplay of pathways such as renal baroreceptor mechanism, changes in sodium and chloride delivery in distal tubule, sympathetic stimulation through beta-1 adrenergic receptors, and negative feedback by direct action of angiotensin II. Once activated, renin cleaves angiotensinogen to angiotensin-I, which is then hydrolyzed by the circulating and local angiotensin-converting enzyme (ACE) to the active angiotensin II. Angiotensin-converting enzyme also inactivates bradykinin with its nitric oxide and prostacyclin stimulating and vasodilatory activity. Angiotensin II acts mainly via angiotensin type 1 (AT-1) and angiotensin type 2 (AT-2) receptors. Angiotensin II also stimulates the release of aldosterone from the adrenal cortex. Aldosterone enhances the reabsorption of sodium and water in the distal tubules and collecting ducts and promotes potassium excretion. Like Angiotensin II, aldosterone is an effector hormone of the RAAS, principally involved in volume and blood pressure regulation. It also facilitates cardiovascular and renal inflammation, fibrosis, and remodeling.

A. T. Askari, A. W. Messerli (eds.), *Cardiovascular Hemodynamics*, Contemporary Cardiology,
https://doi.org/10.1007/978-3-030-19131-3_5

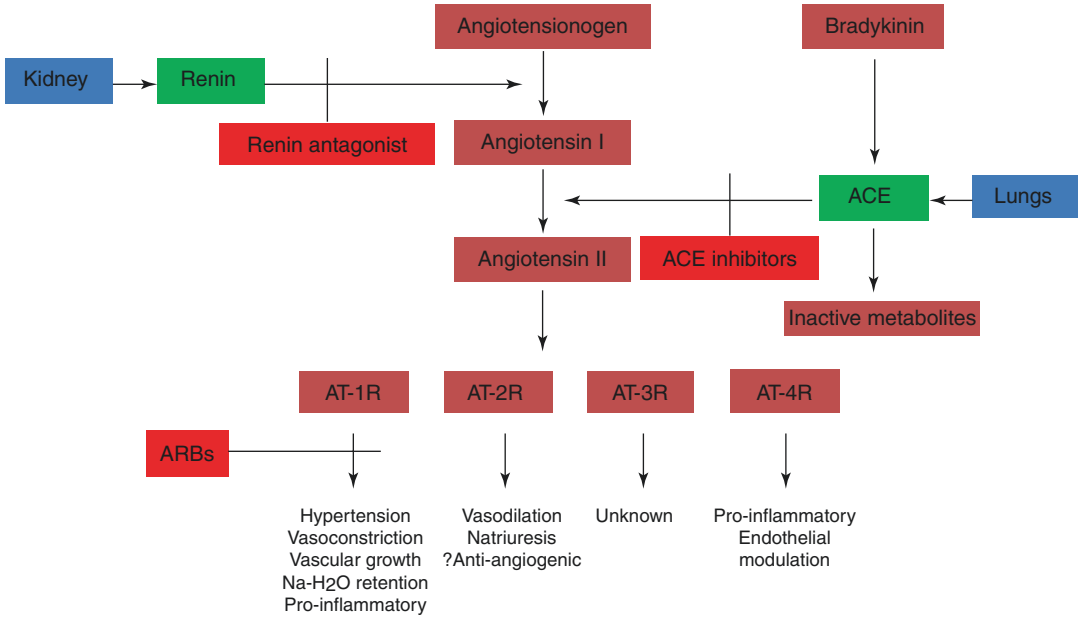

Fig. 5.1 The renin–angiotensin–aldosterone system. Mechanism of action of ACEIs, ARBs, and DRIs

ACE inhibitors (ACEIs) competitively inhibit the enzyme ACE, thereby preventing the conversion of angiotensin I into angiotensin II (Fig. 5.1) and blocking downstream activity of angiotensin II via both AT-1 and AT-2 receptors. They also reduce aldosterone, vasopressin, and plasminogen activator inhibitor-1. ACEIs increase the concentration of bradykinin which contributes to their vasodilatory action; however, this mechanism is also implicated in the occurrence of side effects such as cough and angioedema. Moreover, chronic ACEI use triggers ACE escape pathways; hence, angiotensin II is produced despite blockage of ACE. Angiotensin receptor blockers (ARBs) prevent the binding of angiotensin II to AT-1 receptors, leading to inhibition of all the deleterious effects modulated by angiotensin II, yet preserving the potential beneficial effect of angiotensin II via the AT-2 receptor pathway. Like ACEIs, ARBs reduce BP by decreasing systemic vascular resistance through selective AT-1 receptor blockade. Due to direct receptor blockade, ARBs do not demonstrate angiotensin II escape phenomenon and bradykinin-associated effects.

Table 5.1 Mechanistic differences between ARBs and ACEIs

Principle mechanism of action	ARBs	ACEIs
Plasma angiotensin II	↑	↓
Plasma renin activity	↑	↑
Bradykinin	–	↑
Prostaglandin E_2 and prostacyclin	–	↑
Nitric oxide release	–	↑
Uric acid levels	↓[a]	–
Cough	Not observed	Class specific

[a]Losartan potassium only. Table adapted from Messerli et al. Angiotensin II receptor inhibition. A new therapeutic principle. *Arch Intern Med*. 1996

However, stimulation of the AT2 receptor may result in some bradykinin release. Direct renin inhibitors, DRI (aliskiren), bind to renin with high affinity and prevent the conversion of angiotensinogen to angiotensin I, thereby blocking the synthesis of all angiotensin peptides downstream. These different modes of RAAS inhibition may explain some of the clinical differences between these agents (Table 5.1).

Cardiovascular Hemodynamics

Angiotensin-Converting Enzyme Inhibitors

The cardiovascular effects of ACEIs are evident immediately after the first dose. Single oral dose causes decrease in pulmonary capillary wedge pressure, mean arterial blood pressure, total systemic vascular resistance and increase in cardiac output [1]. Chronic oral dosing produces sustained beneficial hemodynamic effects translating into considerable improvement in LV function and symptoms in patients with systolic heart failure. In patients with systolic heart failure, ACEIs cause dose-dependent reduction in cardiac preload and afterload preventing progressive left ventricular dilatation and systolic dysfunction. These effects probably result from a combination of altered remodeling and sustained reduction in preload and afterload [1], causing leftward shift of the pressure-volume loop (Fig. 5.2). ACEIs also decrease renal vascular resistance, increase renal blood flow, and promote sodium and water excretion mainly though cellular effects in the kidney and alteration in glomerular hemodynamics. All these mechanisms underline the beneficial effects of these agents in heart failure.

ACEIs decrease Ang II and aldosterone formation and potentiate the vasodilatory effects of the kallikrein-kinin system, causing reduction in total peripheral vascular resistance without significant change in heart rate [2]. Moreover, improvement in stroke volume and cardiac output, seen in systolic heart failure patients, is also seen in patients with essential hypertension [3]. The hemodynamic effect of ACEIs in hypertension extends to the regional circulation. During acute or prolonged ACE inhibition, renal and coronary blood flow is increased in patients with heightened RAAS activity [4, 5]. Thus, ACEIs may augment myocardial perfusion both by preventing the vasoconstrictor effect of angiotensin II and by reducing coronary vasoconstriction induced by cardiac sympathetic activation. ACEI also affects arterial compliance and wave reflections in patients with hypertension [6] (Fig. 5.3). ACEIs reduce pulse wave velocity and augmentation index which are markers of arterial stiffness, and this effect is at least partly independent of changes in blood pressure [7]. ACEIs also cause regression of left ventricular hypertrophy, independent of their effects on blood pressure reduction [8]. Inhibitors of the RAAS permit regression of pathologic LVH more effectively than other antihypertensive agents. Table 5.2 summarizes key landmark trials of ACEI in patients with heart failure, hypertension, and myocardial infarction.

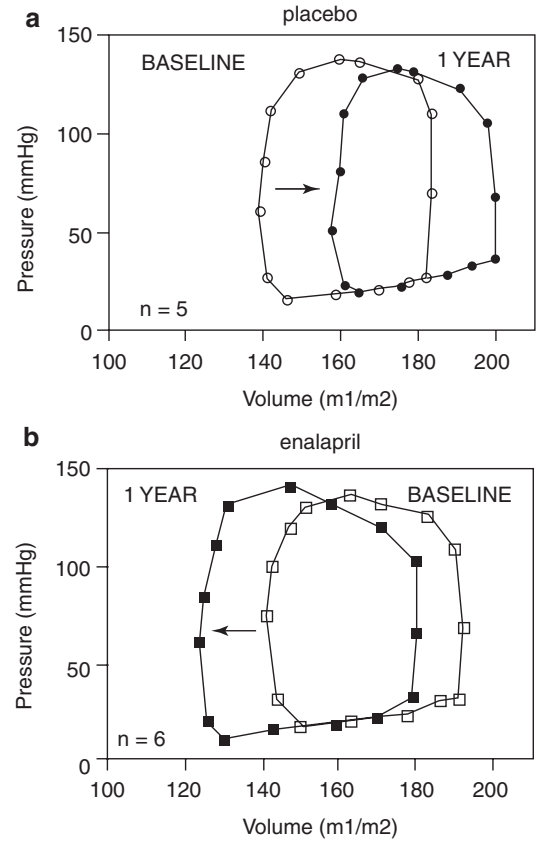

Fig. 5.2 Mean left ventricular pressure-volume loops at baseline and 1 year in patients randomized to placebo (panel A) and to enalapril (panel B) in SOLVD trial. At 1 year, there was a rightward shift in placebo group and leftward shift in enalapril group. (Reprinted from Konstam et al. with permission of the publisher)

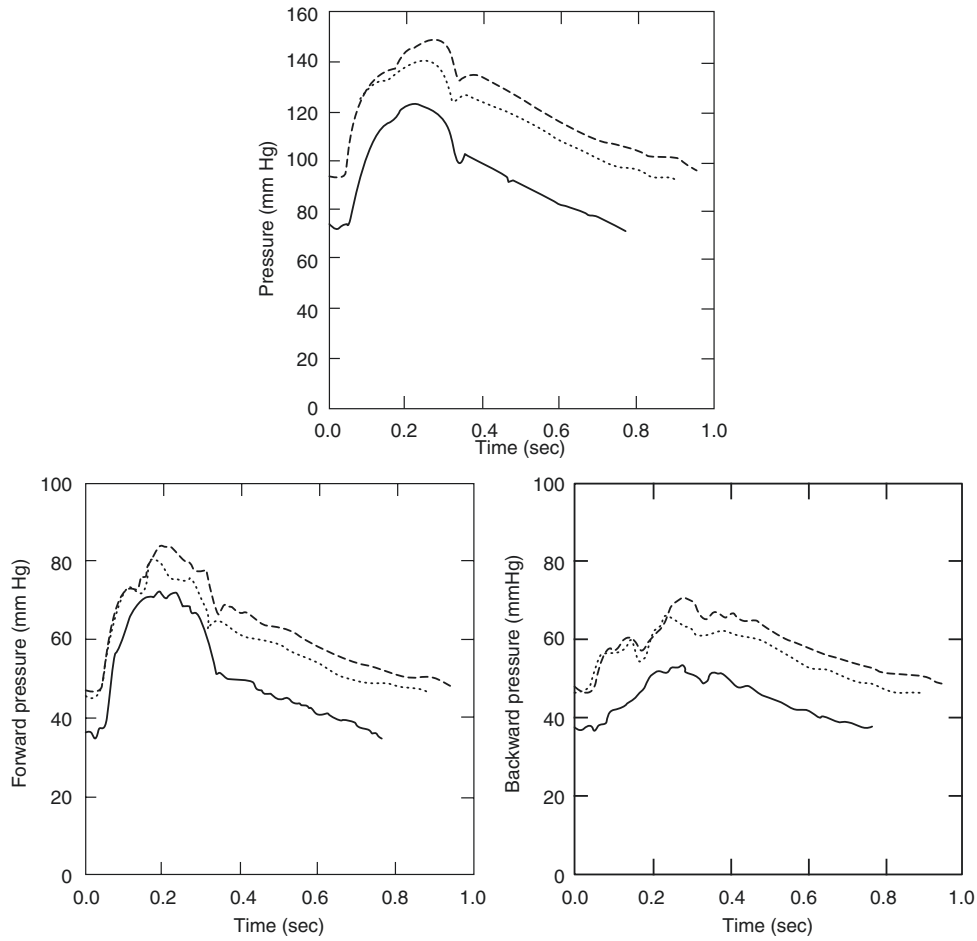

Fig. 5.3 Plots showing ascending aorta pressure waveforms (top) along with their forward (bottom left) and backward (bottom right) components in a representative normotensive (solid line) and hypertensive patient (dashed line). After captopril infusion (dotted line), attenuation of the higher backward wave and prominent late systolic peak in hypertensive patient was seen. (Reprinted from Ting et al. with permission of the publisher)

Angiotensin Receptor Blockers

The cardiovascular hemodynamic effects of ARBs are similar to ACEIs due to similarity in their mechanism of action. However, unlike ACE inhibitors, ARBs do not directly modulate the formation of bradykinin. Due to more downstream inhibition by ARBs and lack of angiotensin II escape phenomenon, they may exert more potent antihypertensive effects compared to ACEIs. Table 5.3 summarizes key landmark trials of ARBs in patients with heart failure, hypertension, and myocardial infarction. Although head-to-head trials comparing ACEIs and ARBs have shown equivocal results, ARB trials had lower rates of events in the placebo arm due to better use of contemporary medications (statins). Moreover, due to fewer adverse events with ARBs, the risk-to-benefit analysis should favor use of ARBs, particularly in patients with hypertension [9].

Aldosterone Antagonists

The pathophysiological effects of hyperaldosteronism on the cardiovascular hemodynamics extend beyond increased intravascular fluid reten-

Table 5.2 Key clinical outcome trials of ACEI in cardiovascular diseases

Trial and year	Active arm (N)	Comparator (N)	Patients	Primary outcome	Follow-up	Major findings
ALLHAT, 2002	Lisinopril (9054)	Chlortalidone (15,255), Amlodipine (9048)	Hypertension	Combined fatal coronary heart disease or nonfatal MI	4.9 years	No difference in primary outcomes
ANBP-2, 2003	Enalapril (3044)	HCTZ (3039)	Hypertension	All CV events or all-cause mortality	4.1 years	Enalapril showed 11% reduction in all CV events or mortality
Pilot HYVET, 2003	ACEI (usually Lisinopril) (431)	Diuretic (usually Bendroflumen-thiazide) (426), Placebo (426)	Hypertension	Stroke, all-cause mortality	1.12 years	No difference in all-cause mortality. Diuretic showed 69% reduction in stroke compared to placebo
SOLVD, 1991	Enalapril (1285)	Placebo (1284)	Chronic heart failure	All-cause mortality	3.5 years	Enalapril showed 16% reduction in all-cause mortality
CONSENSUS, 1987	Enalapril (127)	Placebo (126)	Chronic heart failure	All-cause mortality	6 months	Enalapril showed 40% reduction in mortality
CONSENSUS II, 1992	Enalapril (3044)	Placebo (3046)	MI	All-cause mortality	6 months	No difference in all-cause mortality
SAVE, 1992	Captopril (1115)	Placebo (1116)	MI and left ventricular dysfunction	All-cause mortality	1.8 years	Captopril decreased all-cause mortality by 19%
EUROPA, 2003	Perindopril (6110)	Placebo (6108)	Stable coronary artery disease	Composite of CV mortality, nonfatal MI, and cardiac arrest	4.2 years	Perindopril reduced composite primary end point by 20%
HOPE trial, 2000	Ramipril ($n = 4645$)	Placebo ($n = 4652$)	Multiple CV risk factors	Composite of MI, stroke, or CV death	5 years	Ramipril showed 22% reduction in primary end point

ACEI angiotensin-converting enzyme inhibitor, *CV* cardiovascular, *MI* myocardial infarction

tion and volume overload. Hyperaldosteronism alters fibrinolysis by increasing plasminogen activator inhibitor-1 expression and promotes tissue fibrosis and inflammation [10]. Increased aldosterone activity leads to endothelial dysfunction and arterial stiffness [11]. Moreover, aldosterone is intriguingly involved in sympathetic nervous system activation, decreased baroreceptor sensitivity, increased electrolyte excretion, and cardiomyocyte apoptosis. These effects exerted by aldosterone, one of the final mediators of the RAAS pathway, are only partially inhibited by ACEIs/ARBs. Thus, in addition to modulating volume status, some of the clinical benefits of aldosterone antagonists come from abrogating these adverse effects to limit target organ dysfunction.

Aldosterone antagonists improve LV structural remodeling and performance by increasing LV ejection fraction and decreasing LV end-diastolic and end-systolic volumes, particularly in patients with systolic heart failure and myocardial infarction. Experimental studies have shown that early use of aldosterone antagonist after myocardial infarction could improve myocardial healing as well as both electrical and structural remodeling [12, 13]. Table 5.4 summarizes key

Table 5.3 Key clinical outcome trials of ARBs in cardiovascular diseases

Trial and year	Active arm (N)	Comparator (N)	Patients	Primary outcome	Follow-up	Major findings
LIFE, 2002	Losartan (4605)	Atenolol (4588)	Hypertension	Death, MI, or stroke	4.8 years	Losartan caused 13% reduction in primary end point compared to atenolol
SCOPE, 2003	Candesartan (2477)	Placebo (2460)	Hypertension	CV death, nonfatal stroke, and nonfatal MI	3.7 years	No difference in primary end point, candesartan cause 28% reduction in nonfatal stroke
Val-HeFT, 2001	Valsartan ($n = 2511$)	Placebo ($n = 2499$)	Chronic heart failure	All-cause mortality; combined end point of all-cause mortality, cardiac arrest with resuscitation, heart failure hospitalization, IV inotropic or vasodilator drugs	1.9 years	No difference in all-cause mortality, valsartan showed 23% reduction of combined end point
VALIANT, 2003	Valsartan ($n = 4909$)	Valsartan + captopril ($n = 4885$); captopril ($n = 4909$)	MI	All-cause mortality	2.1 years	No difference in all-cause mortality among the three groups
OPTIMAAL, 2002	Losartan ($n = 2744$)	Captopril ($n = 2733$)	MI	All-cause mortality	2.7 years	No difference in all-cause mortality between the two groups

ARB angiotensin receptor blocker, *CV* cardiovascular, *IV* intravenous, *MI* myocardial infarction

Table 5.4 Key clinical outcome trials of aldosterone antagonists in cardiovascular diseases

Trial and year	Active arm (N)	Comparator (N)	Patients	Primary outcome	Follow-up	Major findings
RALES, 1999	Spironolactone (822)	Placebo (841)	Chronic systolic heart failure	All-cause mortality	2 years	Spironolactone showed 30% reduction in all-cause mortality
EMPHASIS-HF, 2011	Eplerenone (1364)	Placebo (1373)	Chronic systolic heart failure	CV mortality or heart failure hospitalization	1.8 years	Eplerenone showed 37% reduction in primary end point
TOPCAT, 2014	Spironolactone (1722)	Placebo (1723)	Chronic heart failure and ejection fraction ≥45%	CV mortality, aborted cardiac arrest or heart failure hospitalization	3.3 years	No difference in primary composite end point between the two groups
EPHESUS, 2003	Eplerenone (3313)	Placebo (3319)	MI	All-cause mortality and CV mortality or hospitalization or events	1.3 years	Eplerenone reduced all-cause mortality by 15% and CV mortality or hospitalization or CV events by 13%

CV cardiovascular, *MI* myocardial infarction

landmark trials of aldosterone antagonists in patients with heart failure and myocardial infarction.

Direct Renin Inhibitors

Direct renin inhibitor, Aliskiren, is a potent competitive renin inhibitor that binds strongly to renin, resulting in very low circulating levels of angiotensin II and other peptides, thereby rendering the RAAS quiescent. Aliskiren has been as effective as other RAAS inhibitors in reducing blood pressure and left ventricular remodeling [14, 15]. In patients with systolic heart failure, Aliskiren has a potent vasodilatory effect on the efferent arteriole in the glomerulus, leading to marked reduction in renal blood flow and a drop-in filtration fraction [16]. Overall, the lack of incremental benefit in reducing cardiovascular outcomes over ACEI/ARBs, coupled with the noteworthy incidence of adverse effects (diarrhea, hypotension, hyperkalemia, and renal dysfunction), has placed this drug out of favor.

Dual RAAS Blockade

In theory, combination of an ACEI and ARB should result in enhanced RAAS blockade. Conceivably, combination therapy has been shown to be more effective in reducing BP compared with monotherapy alone [17]. In spite of this, dual therapy of ACEI and ARBs were not found superior compared to individual therapy. Multiple studies have also documented increased risk of adverse events such as worsening renal function, hyperkalemia, symptomatic hypotension, and increased medication discontinuation due to adverse effects with combination therapy of ACEIs and ARBs. Based upon the clear evidence of possible harm, ACEIs should not be combined with ARBs. With the advent of the Aliskiren, dual RAAS blockade could now be achieved by combining an ACEI or an ARB with Aliskiren. However, such dual RAAS blockade also has not proven safe, and should be avoided. Table 5.5 summarizes key landmark trials of dual RAAS blocking agents in patients with heart failure and myocardial infarction.

Table 5.5 Key clinical outcome trials of dual RAAS blockade in cardiovascular diseases

Trial and year	Active arm (N)	Comparator (N)	Patients	Primary outcome	Follow-up	Major findings
ALOFT, 2008	Aliskiren + ACEI/ARB (156)	Placebo (146)	Chronic heart failure	Between treatment difference in N-terminal pro-BNP	3 months	Aliskiren added to ACEI/ARB decreased NT-proBNP by 25%
ATMOSPHERE, 2016	Enalapril +Aliskiren (2340)	Aliskiren (2340), Enalapril (2336)	Chronic heart failure	Composite end point of CV death or heart failure hospitalization	3.1 years	No difference in primary end point
CHARM-Added, 2003	Candesartan + ACEI (1276)	Placebo (1272)	Chronic heart failure	CV mortality or heart failure hospitalization	3.4 years	Candesartan added to ACEI showed 15% reduction in primary end point
ONTARGET, 2008	Ramipril + Telmisartan (8502)	Ramipril (8576), Telmisartan (8542)	CV disease	Composite end point of CV death, MI, stroke, or heart failure hospitalization	4.6 years	No difference in primary outcomes among the three groups
VALIANT, 2003	Valsartan + Captopril (4885)	Valsartan (4909), Captopril (4909)	MI	All-cause mortality	2.1 years	No difference in all-cause mortality among the three groups

ACEI angiotensin-converting enzyme inhibitor, *ARB* angiotensin receptor blocker, *BNP* brain natriuretic peptide, *CV* cardiovascular, *MI* myocardial infarction

Other Vasodilators

Several physiological studies demonstrated the dependence of cardiac function on vascular resistance, so vasodilator therapies that reduce systemic vascular resistance should improve cardiovascular hemodynamics. Vasodilators are broadly subclassified into venodilators (e.g., nitrates), which reduce left ventricular filling pressure and relieve pulmonary congestion; arteriolar dilators (e.g., hydralazine), which enhance cardiac output; and balanced vasodilators (e.g., nitroprusside, nitroglycerine), which dilate both resistance and capacitance vessels. Seminal work conducted by Franciosa et al. in the early 1970s showed that intravenous infusion of sodium nitroprusside produced a marked reduction in the elevated left ventricular filling pressure and systemic arterial pressure, resulting in a modest increase in cardiac output [18]. A subsequent study in patients with refractory heart failure revealed even more striking improvements in systemic vascular resistance and cardiac output, with reduced left ventricular filling pressure [19]. Similar effects of nitroprusside were seen in patients with myocardial infarction and depressed left ventricular ejection fraction [20]. Despite being a potent vasodilator, sodium nitroprusside is seldom used these days as prolonged infusion has been associated with thiocyanate toxicity, particularly in those with severe renal dysfunction and systemic hypotension. Currently, intravenous nitroglycerine is the preferred vasodilator in acute conditions. It has comparable hemodynamic effects compared to nitroprusside and likely has more beneficial effects on intercoronary collateral blood flow in the setting of regional ischemia [21]. Although vasodilators are effective in relieving congestion and improving symptoms in patients with acute heart failure, their role in improving cardiac indices has not been demonstrated consistently. The increase in stroke volume and cardiac output with intravenous vasodilators is modulated by several factors such arterial elastance, ventricular function, preload dependence, presence of mitral regurgitation etc. In patients with severely impaired ventricular function, isolated reduction in preload may not translate into higher stroke volume due to markedly reduced cardiac contractility [22] (Fig. 5.4). Combination therapy of dobutamine and nitroglycerin can result in greater overall hemodynamic improvement than either drug alone in such cases.

The hemodynamic benefits of intravenous vasodilators led to the evolution of various oral agents with vasodilatory properties. Combination

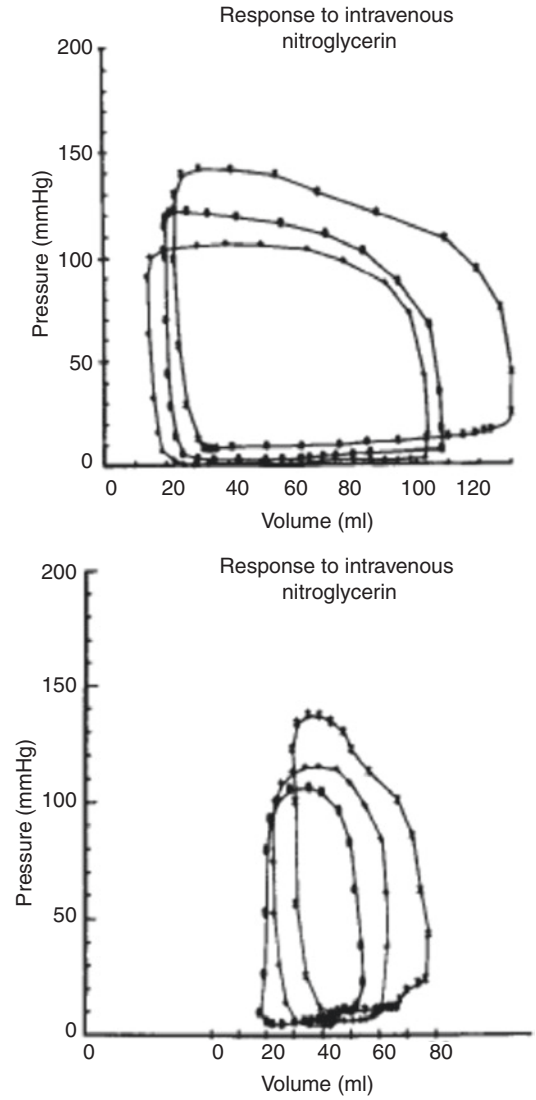

Fig. 5.4 Sequential left ventricular pressure-volume loops after administration of sodium nitroglycerine showing with leftward and downward shift due to changing loading conditions. (Reprinted from McKay et al. with permission of the publisher)

therapy of hydralazine and isosorbide dinitrate (H-ISDN) is one of the common agents used widely in management of chronic systolic heart failure. There is simultaneous reduction of preload with isosorbide dinitrate and afterload with hydralazine (Fig. 5.5). H-ISDN reduce left ventricular filling pressure and pulmonary capillary wedge pressure, increase cardiac index, and

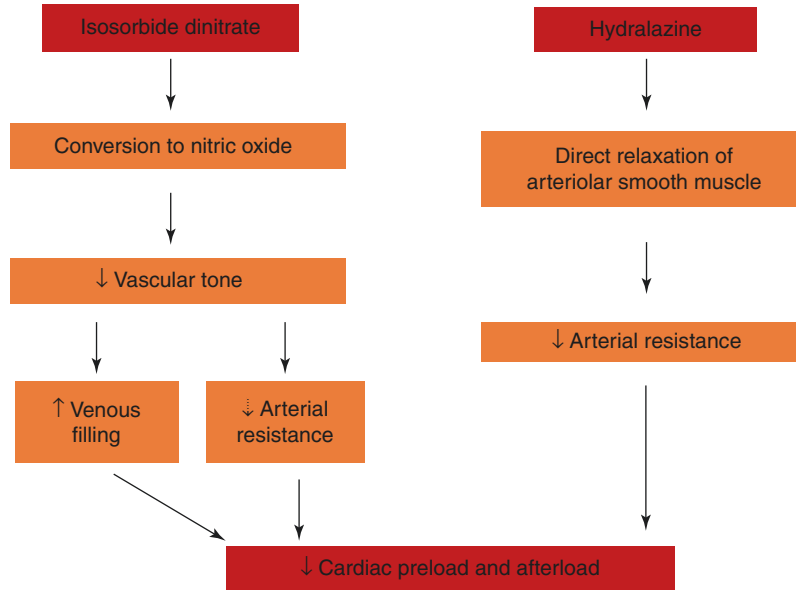

Fig. 5.5 Schematic diagram of mechanism of action of hydralazine and Isosorbide dinitrate

Table 5.6 Key clinical outcome trials of vasodilators in cardiovascular diseases

Trial and year	Active arm (N)	Comparator (N)	Patients	Primary outcome	Follow-up	Major findings
V-HeFT I, 1986	Hydralazine-Isosorbide dinitrate	Placebo	Chronic heart failure	All-cause mortality	2.3 years	Hydralazine-Isosorbide showed 36% reduction in all-cause mortality
A-HeFT, 2004	Hydralazine-Isosorbide dinitrate	Placebo	Chronic heart failure	Composite all-cause mortality, heart failure hospitalizations, and change in quality of life	10 months	Hydralazine-Isosorbide showed 43% reduction in all-cause mortality
WMAC, 2002	IV nesiritide (204), IV nitroglycerin (143)	Placebo (142)	Acute decompensated heart failure	Change in PCWP or dyspnea	3 h, 24 h	Nesiritide improved PCWP at 3 and 24 h than IV nitroglycerin or placebo. Nesiritide resulted in improvement in dyspnea compared with placebo but not IV nitroglycerin
ROSE, 2013	IV dopamine (122), IV nesiritide (119)	Placebo (119)	Acute decompensated heart failure	72-h cumulative urine volume, change in serum cystatin C	72 h	Low-dose dopamine or low-dose nesiritide showed no benefit when added to diuretic therapy

IV intravenous, *PCWP* pulmonary capillary wedge pressure

reduce systemic vascular resistance [23]. These properties make H-ISDN an effective therapy in patients with systolic heart failure. When compared to enalapril, H-ISDN resulted in greater improvements in ejection fraction, peak exercise oxygen consumption, and exercise tolerance [24]. Nesiritide, a synthetic natriuretic peptide, is an intravenous vasodilator with diuretic properties. In patients with heart failure, nesiritide produces dose-dependent balanced arterial and venous vasodilatation leading to reduction in pulmonary capillary wedge pressure, with minimal effect on cardiac contractility or output. Nesiritide also possesses anti-fibrotic, anti-hypertrophic, anti-inflammatory, and aldosterone-inhibiting properties, and may prevent adverse left ventricular remodeling. In a small study, low-dose nesiritide showed reduction of cardiac dilatation and improvement in ejection fraction in patients with acute myocardial infarction. The role of intravenous vasodilators is predominantly limited to management of acute decompensated heart failure. For oral agents, H-ISDN is a part of guideline-directed medical therapy for patients with chronic systolic heart failure. Hydralazine and long-acting nitrates are occasionally used in management of resistant hypertension. Table 5.6 summarizes key landmark trials of vasodilators in management of patients with acute and chronic systolic heart failure.

Review Questions

Question 1: Angiotensin-converting enzyme inhibitors:

A. Decrease preload
B. Decrease afterload
C. May cause hyperkalemia
D. Improve long-term outcome for patients with HFrEF
E. All of the above are correct

Answer 1: E. ACEIs are associated with all of the listed choices.

Question 2: 4. An elderly, nonverbal male is admitted to your facility after initial treatment for a heart attack. You notice that over the past 3 days, he has become lethargic. His appetite has decreased. His urine output has decreased. His blood pressure has been 190/100. His weight has increased 2 pounds. He has rales on his lung examination. His lower extremities are cold with trivial swelling.

Given the above scenario what would be the best way to improve his current state?

A. Decrease his afterload with an ACE inhibitor
B. Decrease his afterload with a beta-blocker
C. Decrease his afterload with a pure vasodilator
D. Decrease his preload with a diuretic
E. Both A and B
F. Both A and D

Answer 2: C. This patient is already exhibiting a decreased CO (cold extremities) and evidence of congestion at rest (rales on examination). A pure afterload-reducing agent would be optimal at this point. Any agent that may decrease this patient's preload will make an already low cardiac output worse. ACEI decrease preload and afterload. Beta-blockers do not decrease afterload but negatively impact contractility and heartrate. Giving a diuretic alone to this person will decrease an already low CO further through a decrease in preload.

Question 3: The mechanism(s) by which ACEIs decrease preload is:

A. Venodilation
B. Inhibition of bradykinin breakdown
C. A direct effect on sodium reabsorption
D. Both A and B
E. Both A and C

Answer 3: D. ACEI decreases both preload and afterload. The mechanism(s) by which these agents decrease preload are thought to be the following: Decrease breakdown of bradykinin and through its effect on decreasing angiotensin II levels. Bradykinin is a potent venodilator and the increase in bradykinin with ACEI use is a major contributor to the reduction in preload seen with these agents.

Question 4: A 68-year-old male presents with an acute anterior MI. After a successful PCI of the proximal LAD, he is started on statin, dual antiplatelet therapy, an ACEI, and beta-blocker. What would be an indication to initiate an aldosterone antagonist?

A. He is a nondiabetic with depressed ejection fraction and no heart failure

B. He is a diabetic with depressed ejection fraction and no heart failure
C. He is a nondiabetic with depressed ejection fraction, heart failure and a serum creatinine of 2.8
D. He is a diabetic with a depressed ejection fraction, heart failure and a serum potassium of 5.1 mmol/liter

Answer 4. B. In the Ephesus trial, patients with an acute MI and the presence of a reduced EF (≤40%) and heart failure (rales, pulmonary venous congestion, or an S3) were randomized to eplerenone or placebo. Diabetic patients could be randomized without any evidence of heart failure. Exclusion criteria included a potassium >5 mmol/liter and a serum creatinine >2.5 mg/dl.

Question 5: ARBs and ACEIs:

A. Both decrease angiotensin II levels
B. Both decrease plasma renin activity
C. Both increase levels of bradykinin
D. Both increase plasma renin activity

Answer: D. Both ACEI and ARB increase plasma renin activity. ACEI decrease angiotensin II levels while ARBs are associated with increased levels. ACEI block the breakdown of bradykinin while ARBs do not.

References

1. Konstam MA, Rousseau MF, Kronenberg MW, Udelson JE, Melin J, Stewart D, et al. Effects of the angiotensin converting enzyme inhibitor enalapril on the long-term progression of left ventricular dysfunction in patients with heart failure. SOLVD Investigators. Circulation. 1992;86(2):431–8.
2. Lund-Johansen P, Omvik P. Cardiac effects of ACE inhibition. J Cardiovasc Pharmacol. 1993;22(Suppl 1):S36–40.
3. Oren S, Messerli FH, Grossman E, Garavaglia GE, Frohlich ED. Immediate and short-term cardiovascular effects of fosinopril, a new angiotensin-converting enzyme inhibitor, in patients with essential hypertension. J Am Coll Cardiol. 1991;17(5):1183–7.
4. Paulson OB, Waldemar G, Andersen AR, Barry DI, Pedersen EV, Schmidt JF, et al. Role of angiotensin in autoregulation of cerebral blood flow. Circulation. 1988;77(6 Pt 2):I55–8.
5. Daly P, Rouleau JL, Cousineau D, Burgess JH. Acute effects of captopril on the coronary circulation of patients with hypertension and angina. Am J Med. 1984;76(5B):111–5.
6. Ting CT, Yang TM, Chen JW, Chang MS, Yin FC. Arterial hemodynamics in human hypertension. Effects of angiotensin converting enzyme inhibition. Hypertension. 1993;22(6):839–46.
7. Mallareddy M, Parikh CR, Peixoto AJ. Effect of angiotensin-converting enzyme inhibitors on arterial stiffness in hypertension: systematic review and meta-analysis. J Clin Hypertens (Greenwich). 2006;8(6):398–403.
8. Mathew J, Sleight P, Lonn E, Johnstone D, Pogue J, Yi Q, et al. Reduction of cardiovascular risk by regression of electrocardiographic markers of left ventricular hypertrophy by the angiotensin-converting enzyme inhibitor ramipril. Circulation. 2001;104(14):1615–21.
9. Messerli FH, Bangalore S, Bavishi C, Rimoldi SF. Angiotensin-converting enzyme inhibitors in hypertension: to use or not to use? J Am Coll Cardiol. 2018;71(13):1474–82.
10. Luther JM, Wang Z, Ma J, Makhanova N, Kim HS, Brown NJ. Endogenous aldosterone contributes to acute angiotensin II-stimulated plasminogen activator inhibitor-1 and preproendothelin-1 expression in heart but not aorta. Endocrinology. 2009;150(5):2229–36.
11. Mahmud A, Mahgoub M, Hall M, Feely J. Does aldosterone-to-renin ratio predict the antihypertensive effect of the aldosterone antagonist spironolactone? Am J Hypertens. 2005;18(12. Pt 1):1631–5.
12. Fraccarollo D, Galuppo P, Schraut S, Kneitz S, van Rooijen N, Ertl G, et al. Immediate mineralocorticoid receptor blockade improves myocardial infarct healing by modulation of the inflammatory response. Hypertension. 2008;51(4):905–14.
13. Perrier E, Kerfant BG, Lalevee N, Bideaux P, Rossier MF, Richard S, et al. Mineralocorticoid receptor antagonism prevents the electrical remodeling that precedes cellular hypertrophy after myocardial infarction. Circulation. 2004;110(7):776–83.
14. Chen Y, Meng L, Shao H, Yu F. Aliskiren vs. other antihypertensive drugs in the treatment of hypertension: a meta-analysis. Hypertens Res. 2013;36(3):252–61.
15. Solomon SD, Shin SH, Shah A, Skali H, Desai A, Kober L, et al. Effect of the direct renin inhibitor aliskiren on left ventricular remodelling following myocardial infarction with systolic dysfunction. Eur Heart J. 2011;32(10):1227–34.
16. Schroten NF, Damman K, Hemmelder MH, Voors AA, Navis G, Gaillard CA, et al. Effect of additive renin inhibition with aliskiren on renal blood flow in patients with Chronic Heart Failure and Renal Dysfunction (Additive Renin Inhibition with Aliskiren on renal blood flow and Neurohormonal Activation in patients with Chronic Heart Failure and Renal Dysfunction). Am Heart J. 2015;169(5):693–701 e3.
17. Doulton TW, He FJ, MacGregor GA. Systematic review of combined angiotensin-converting enzyme inhibition and angiotensin receptor blockade in hypertension. Hypertension. 2005;45(5):880–6.
18. Franciosa JA, Limas CJ, Guiha NH, Rodriguera E, Cohn JN. Improved left ventricular function during

nitroprusside infusion in acute myocardial infarction. Lancet. 1972;1(7752):650–4.
19. Guiha NH, Cohn JN, Mikulic E, Franciosa JA, Limas CJ. Treatment of refractory heart failure with infusion of nitroprusside. N Engl J Med. 1974;291(12):587–92.
20. Chatterjee K, Parmley WW, Ganz W, Forrester J, Walinsky P, Crexells C, et al. Hemodynamic and metabolic responses to vasodilator therapy in acute myocardial infarction. Circulation. 1973;48(6):1183–93.
21. Flaherty JT, Magee PA, Gardner TL, Potter A, MacAllister NP. Comparison of intravenous nitroglycerin and sodium nitroprusside for treatment of acute hypertension developing after coronary artery bypass surgery. Circulation. 1982;65(6):1072–7.
22. Haber HL, Simek CL, Bergin JD, Sadun A, Gimple LW, Powers ER, et al. Bolus intravenous nitroglycerin predominantly reduces afterload in patients with excessive arterial elastance. J Am Coll Cardiol. 1993;22(1):251–7.
23. Massie B, Chatterjee K, Werner J, Greenberg B, Hart R, Parmley WW. Hemodynamic advantage of combined administration of hydralazine orally and nitrates nonparenterally in the vasodilator therapy of chronic heart failure. Am J Cardiol. 1977;40(5):794–801.
24. Cohn JN, Johnson G, Ziesche S, Cobb F, Francis G, Tristani F, et al. A comparison of enalapril with hydralazine-isosorbide dinitrate in the treatment of chronic congestive heart failure. N Engl J Med. 1991;325(5):303–10.

6 Beta Blockers and Calcium Channel Blockers

Alexandra-Maria Neagoe, Emrush Rexhaj, Ehud Grossman, and Franz H. Messerli

Introduction

In this chapter, we present pharmacological characteristics and hemodynamic effects of beta blockers (BBs) and calcium channel blockers (CCBs) as well as their main therapeutic indications. These classes of medications are two of the most frequently used for the treatment of cardiovascular diseases such as arterial hypertension, arrhythmia, and heart failure. The main clinical studies will be summarized.

A.-M. Neagoe
Department of Cardiology, University Hospital Bern, Bern, Switzerland
e-mail: alexandra-maria.neagoe@zgks.ch

E. Rexhaj
Department of Cardiology, University Hospital Bern, Bern, Switzerland

Department for Biomedical Research, University of Bern, Bern, Switzerland
e-mail: emrush.rexhaj@insel.ch

E. Grossman
The Chaim Sheba Medical Center, The Sackler Faculty of Medicine, Tel-Aviv University, Tel Aviv, Israel
e-mail: grosse@tauex.tau.ac.il

F. H. Messerli (✉)
Department of Cardiology, University of Bern, Bern, Switzerland

Beta Blockers

Introduction

Propranolol was the first BB discovered in 1964 by Sir James Black while he was working on the effects of adrenalin on heart in patients with angina pectoris [1]. Ever since, BBs have been the most prescribed drug class in cardiovascular disorders, especially in patients after myocardial infarction. The term "cardioprotection" was extensively used to describe their benefits. As their name indicates, BBs block the action of adrenaline and noradrenaline at β-adrenergic receptors. Table 6.1 summarizes the distribution and the main responses of activation of β-adrenergic receptors. Depending on the selectivity of their actions, they are divided in two groups: cardioselective and non-cardioselective. The stimulation of β1-receptors increases heart rate (chronotropy) and myocardial contractility (inotropy) and speeds up atrioventricular node conduction (dromotropy), while the stimulation of β2-receptors induces vasodilation and bronchodilation and stimulates glycogenolysis in the liver. Thus, inhibition of β1-receptors by BBs results in decreased chronotropy, inotropy, and dromotropy and increased relaxation (lusitropy). At low doses β1-selective BBs act more selectively at a cardiac level, with insignificant effects on vascular and bronchial β-receptors,

A. T. Askari, A. W. Messerli (eds.), *Cardiovascular Hemodynamics*, Contemporary Cardiology,
https://doi.org/10.1007/978-3-030-19131-3_6

reducing in that way the risk of vasoconstriction and bronchospasm. These cardioselective effects are dose dependent and may disappear with high doses.

Table 6.1 Distribution of α- and β-receptors and mediated effects

Receptor subtype	Organ system	Effect
α	Blood vessel	↑ Constriction
	Uterus	↑ Contraction
	Pancreas	↓Insulin secretion
β1	Heart	↑ Heart rate
	Kidneys	↑ Contractility
	Adipose tissue	↑ Conduction
	Parathyroid glands	↑ Excitation
		↑ Automaticity
		↑ Renin secretion
		↑ Lipolysis
		↑ Secretion
β2	Heart	↑ Heart rate
	Blood vessels	↑ Contractility
	Skeletal muscle	↑ Conduction
	Liver	↑ Excitation
	Lungs	↑ Automaticity
	Pancreas	↑ Vasodilation
	Uterus	↑ Glycogenolysis
	Urinary bladder	↑ Contractility
	Gastrointestinal	↑ Potassium uptake
	Gall bladder and ducts	↑ Bronchodilation
	Nerve terminals	↑ Insulin and glucagon secretion
	Thyroid	↑ Relaxation
	Parathyroid glands	↑ Adrenaline release
		↑ T4-T3 conversion
		↑ Secretion

Pharmacological Characteristics of Beta Blockers

Some specific *pharmacological* properties of BBs distinguish one agent from another (Table 6.2): (1) cardioselectivity and relative affinity for the β1- and/or β2-receptors; (2) intrinsic sympathomimetic activity (slow heart rate less than other BBs by partially acting as β-agonist); (3) lipid solubility; (4) half-life elimination and the way of elimination; (5) additional effects of the drug such as vasodilation.

As Poirier et al. have pointed out in an excellent review [2], the following are of clinical significance:

1. Cardioselectivity

By definition, cardioselectivity represents the property of an agent to block β1-receptors, predominantly present in the heart and renal juxtaglomerular apparatus. Nebivolol and bisoprolol are the agents with the highest β1-selectivity. The β2-inhibition is also dose related, so agents with β1-inhibition can also inhibit β2-receptors at higher doses. Bronchial reactivity in asthma appears to be less enhanced with more cardioselective BBs and is a concern with nonselective agents.

2. Vasodilation

Some agents such as nebivolol and carvedilol exert their effects through vasodilatory properties. Nebivolol administration in healthy subjects

Table 6.2 Pharmacological properties of selected beta blockers

β-Blocker	β-Receptor activity	Membrane stabilizing activity	Intrinsic sympathomimetic activity	Vasodilatation	Elimination half-life (hours)	Route of elimination	Lipid solubility
Propranolol	No	Yes	No	No	3.5–6	Hepatic	High
Atenolol	β1	No	No	No	6–7	Renal	Low
Bisoprolol	β1	No	No	No	9–12	Renal	Low
Carvedilol	No	No	No	Yes	7–10	Hepatic	Moderate
Metoprolol	β1	At high levels	No	No	Tartrate 3–4 Succinate 3–7	Hepatic	Moderate
Nebivolol	β1	No	No	Yes	12	Hepatic	Low
Sotalol	No		No	No	12	Renal	Low

decreased systolic and diastolic blood pressure, and heart rate at rest and during submaximal and maximal exercise [3]. BBs with vasodilation effect (carvedilol via α1 blockade and nebivolol via stimulation of NO release) significantly decrease central blood pressure and wave reflection (augmentation index) as compared to atenolol [4]. Carvedilol and nebivolol have been shown to improve left ventricular systolic function in patients with nonischemic heart failure [5].

3. Lipophilicity/Hydrophilicity

Lipophilic agents such as propranolol, metoprolol, and nebivolol have the ability to cross the blood-brain barrier and have a shorter half-life. They are mainly eliminated through hepatic metabolism and are more susceptible to drug interaction. Due to crossing of blood-brain barrier, one of the most common side effects is vivid dreams and nightmares. Hydrophilic agents are eliminated mainly through renal metabolism, and their dosage needs to be adjusted in renal failure. Special attention needs to be given to sotalol in patients with renal failure since its accumulation might lead to torsade de pointes.

Hemodynamic Effects of Beta Blockers

Due to different properties, there is a difference in the cardiovascular hemodynamics of different BBs.

Intravenous administration of propranolol in anesthetized dogs decreased heart rate, myocardial contractile force, and cardiac output, whereas it increased LV end-diastolic pressure, left atrial pressure, and total and pulmonary peripheral resistances [6]. As shown by Nakano and Kusakari, acute administration of cumulative doses of propranolol results in a shift to the right of the left ventricular function curves, resulting in a reduction of cardiovascular performances. In a small study published in 1967 [7], it was showed the administration of propranolol to healthy subjects while exercising was associated with a reduction of cardiac output, mean arterial pressure, left ventricular minute work, and maximal O_2-uptake and increased the calculated arteriovenous O_2 difference and the central venous pressure. The administration of the same medication in patients with heart disease showed the same effect, although the cardiac outputs achieved during exercise were usually lower than in normal subjects. The cardiac output in patients under propranolol decreased 18%. At the same time, in all patients the heart rate as well as the pulmonary arterial O_2 saturation decreased. The reduction of cardiac output by only 18% with beta blockade suggests there are also other mechanisms through which the cardiac output is increasing during exercise, not only sympathetic stimulation.

The decrease of cardiac output with BBs was noted in another study [8]. Carvedilol, propranolol, bopindolol, and celiprol have each showed a decrease in cardiac output. The maximum decrease was induced by administrating propranolol, whereas the minimum through administrating celiprol. At the same time, in comparison to propranolol, improved coronary flow through coronary vasodilatation as well as reduced peripheral resistance has been demonstrated with carvedilol.

Nebivolol on the other hand has been proven to maintain the cardiac output while concomitantly reducing the arterial stiffness, vascular resistance, blood pressure, and heart rate and increasing the systolic function and stroke volume. Peripheral vasodilatation is caused by nitric oxide release [9].

To conclude, the non-vasodilating beta blockers increase the afterload through increase of the peripheral resistance, while the beta blockers with vasodilating properties cause a decrease of afterload through reducing the peripheral resistance and therefore reducing the blood pressure. At the same time all beta blockers cause bradycardia which consequently decreases the myocardial oxygen consumption and increases the duration of diastole, thereby increasing preload.

Effect on Central Pressure

Studies have shown the carotid and aortic blood pressure (BP) curves are a result of the summation of two different waves: a forward wave coming from the heart during ventricular ejection and a backward wave that has been reflected at the periphery back toward the heart. Normally, when there is physiological ventricular-vascular coupling, the reflected pulse wave returns to the left ventricle in diastole and serves to increase coronary perfusion. When resting heart rate (RHR) is slowed down by a negative chronotropic drug, the reflected pulse wave may return during ventricular systole. The resulting ventricular-vascular mismatch will augment central systolic pressure. To maintain cardiac output when RHR is low, the stroke volume has to increase in parallel with the fall in RHR. An elevated stroke volume will increase pulse pressure, which, in turn, is prone to increase systolic and decrease diastolic BP, particularly when aortic Windkessel function is impaired. For obvious reasons not all BBs are created equal; the vasodilating agents have little if any effect on central pressure [10].

The Therapeutic Indications of Beta Blockers

Hypertension

The mechanism of lowering BP is not clear; no single mechanism can explain the effect for all agents in this class of medication. One possibility is that lowering the cardiac output results in lower blood pressure and increased peripheral resistance [6]. Continuous therapy results in a decrease in peripheral resistance, but still above pretreatment levels and in consequence cannot be the only mechanism responsible for blood pressure lowering [11]. The second possibility is the decrease in sympathetic activity in the central nervous system results in a reduced sympathetic activity in the periphery. This is however only true for agents that cross the blood/brain barrier. Hydrophilic agents like practolol and sotalol do not decrease peripheral sympathetic activity while lowering blood pressure [12]. The reduction of renin secretion, and the consequent reduction of angiotensin II in plasma, is another possible mechanism [13–15]. The BBs with ISA such as pindolol have been shown to increase plasma renin levels while simultaneously reducing the blood pressure [11]. Blocking the β2-receptors diminishes the release of norepinephrine which consequently reduces the BP. This is obvious with nonselective agents such as propranolol, whereas β1 selective agents such as atenolol seemingly are good blood pressure lowering agents [16] However, as already described before, there is a pseudo-antihypertensive effect due to elevation (or lesser decrease) of the central aortic pressure. The slower the heart rate, the greater the pseudo-antihypertensive effect, and the less the reduction in morbidity and mortality [17].

The American, British, and most other formal hypertension guidelines no longer recommend the use of BBs as first-line therapy, except in some patients with ischemic heart disease or heart failure. In older patients, BBs have never been shown to reduce the risk of heart attack, stroke, and/or death [18].

The European guidelines for hypertension still consider the use of BBs as a class I indication for monotherapy or combined therapy. The preferred combination consists of thiazide diuretics, calcium antagonist, and ACE inhibitors/angiotensin receptor blockers with addition of BB in specific situations. Thus we should consider BBs in certain clinical conditions (e.g., aortic dilatation or patients who are symptomatic in case of excessive sympathetic activity). In the young, both atenolol and non-atenolol BBs have been proven to reduce the cardiovascular endpoints for hypertension without other indication. Atenolol is associated with an increased risk for stroke in the elderly, but whether this extends to other non-atenolol BBs is uncertain [19]. The availability of vasodilating BBs with both alpha and beta effect influences positively the cardiac output, heart rate, blood pressure, and systemic vascular resistance. Carvedilol may be superior to traditional BBs in several regards, it has a lower rate of new-

onset diabetes, it has a beneficial effect on lipid profile, and it increases plasma flow to the kidneys [20]. Due to well-documented adverse effects as well as different responses in different patient population, the use of BBs should be used selectively if at all in hypertension.

Arrhythmia

BBs have not only an antihypertensive effect but also an antiarrhythmic effect. They are considered to be class II agents in the Vaughan Williams classification. They act by blocking the effects of catecholamines at the site of β1-receptor, thereby decreasing the sympathetic activity in the heart.

The European guidelines for the management of patients with ventricular arrhythmias and the prevention of sudden cardiac death recommend BBs as a first-line therapy in the management of ventricular ectopic beats and ventricular tachycardia and the prevention of sudden cardiac death in patients with or without heart failure. Furthermore, the same guidelines recommend the use of BBs in patients with long QT-syndrome.

BBs are also used as rate control therapy in patients who have atrial fibrillation (AF). Importantly, a mortality benefit in patients with atrial fibrillation receiving BBs in comparison with placebo in patients with heart failure with reduced ejection fraction (HFrEF) has not been shown [21]. In general, BBs do not reduce the risk of AF or recurrent AF after ablation. However, in patients with HFrEF in sinus rhythm pretreated with ACE inhibitors/ARBs, BBs were shown to reduce the incidence of AF [21].

Sotalol is the only BB used as a rhythm control therapy in patients with atrial fibrillation and normal ventricular systolic function. However, there is a risk of torsades de pointes so the benefits and risks have to be taken into consideration when administrating sotalol.

Heart Failure

BBs are part of the standard therapy for HFrEF along with ACE inhibitors and diuretics since it has been proven to reduce the mortality and morbidity in such patients [22–28]. BBs should be started in stable patients and gradually up-titrated to the maximum tolerated dose. In patients admitted due to acute heart failure, BBs should be initiated under medical surveillance once the patient is stable.

Coronary Artery Disease

BBs have been shown to reduce the cardiovascular mortality after a myocardial infarction [29–31]. The reduction in mortality was shown to be smaller in Afro-Americans, patients 80 years old or older, and those with an ejection fraction below 20% or patients with renal insufficiency or diabetes. After a myocardial infarction, even in patients with relative contraindications such as pulmonary disease, BBs have shown a benefit [32]. The necessity as well as the duration of BBs after a non ST-elevation myocardial infarction in patients where the ejection fraction is normal or close to normal still needs to be assessed [33, 34].

Beta blockers are also used in stable coronary artery disease to treat patients with stable angina. The antianginal effect is explained through a reduction in myocardial oxygen demand.

Conclusion

After five decades of clinical experience, heart failure with reduced EF remains the only iron-clad indication for BBs in cardiovascular disease – the very indication that decades ago was considered to be the only contraindication for BB therapy. Many of so-called cardioprotective effects of BBs were mostly based on old studies and on hearsay and have never been documented in contemporary prospective randomized trials [35, 36].

Calcium Channel Blockers (CCBs)

Introduction

The observation made by Fleckenstein in 1967 that a reduction of calcium movement into cardiac myocytes determined a negative inotropic effect facilitated the development of calcium antagonist drugs, currently called calcium channel blockers (CCBs). CCBs were introduced for the treatment of hypertension in the 1980s. Their

use was subsequently expanded to disorders such as angina pectoris, paroxysmal supraventricular tachycardia, hypertrophic cardiomyopathy, coronary spasm, Raynaud phenomenon, pulmonary hypertension, esophageal spasms, migraine, and cerebral vasospasm. In this chapter, the main hemodynamic and cardiovascular effects of CCBs will be summarized.

Mechanism of Action

The mechanism of action is reducing the cytosolic free calcium concentration by blocking calcium entry into cells, acting on the L (long-lasting) subtype. There is a difference in selectivity for L-Type and T-Type channels, although all calcium blockers act on both subtypes. Mibefradil has showed the highest selectivity on the T-Type channels, whereas lacidipine was showed to have the highest selectivity on the L-Type channels [37].

Classification

According to their chemical structure, CCBs can be subdivided into dihydropyridines (nifedipine, amlodipine, nitrendipine) and non-dihydropyridines. The non-dihydropyridines are divided into two major groups: (1) phenylalkylamines (verapamil) and (2) benzothiazepines (diltiazem) (Table 6.3). CCBs act on different receptor sites on Ca channels due to their different molecular structure. Since their discovery, there has been an evolvement of different CCB generations. The first generation is characterized by a rapid onset of action and very short half-life, whereas the second and third generations provide a longer duration of action or extended-release mechanisms, poor activation of the sympathetic nervous system, and fewer side effects [38–40] (Fig. 6.1).

Cardiovascular Hemodynamics

CCBs vary in their effects on cardiovascular hemodynamics. Dihydropyridines such as amlodipine and nifedipine are potent arterial vasodilators, whereas non-dihydropyridines work primarily on the heart; phenylalkylamines (verapamil) have a negative chronotropic, dromotropic, and inotropic effect with a positive lusitropic effect, while benzothiazepines (diltiazem) have intermediate chronotropic, dromotropic, and inotropic effects (Table 6.4 and Fig. 6.2).

All CCBs lower arterial pressure when given over the short term and with prolonged administration [41–46]. Head-to-head comparisons of five different calcium antagonists reveal little, if any, difference in blood pressure lowering potency among the various agents, provided that adequate doses are given.

Table 6.3 CCB classification, recommended uses, and adverse effects

Calcium channel blockers	Amlodipine, clevidipine, nicardipine, nifedipine, nimodipine (dihydropyridines, act on vascular smooth muscle); diltiazem, verapamil (non-dihydropyridines, act on heart)
Mechanism	Block voltage-dependent L-type calcium channels of cardiac and smooth muscle → ↓ muscle contractility
	Vascular smooth muscle – amlodipine = nifedipine > diltiazem > verapamil
	Heart – verapamil > diltiazem > amlodipine = nifedipine (verapamil = ventricle)
Clinical use	Dihydropyridines (except nimodipine): hypertension, angina (including Prinzmetal), Raynaud phenomenon
	Nimodipine: subarachnoid hemorrhage (prevents cerebral vasospasm)
	Nicardipine, clevidipine: hypertensive urgency or emergency
	Non-dihydropyridines: hypertension, angina, atrial fibrillation/flutter
Adverse effects	Non-dihydropyridine: cardiac depression, AV block, hyperprolactinemia, constipation
	Dihydropyridine: peripheral edema, flushing, dizziness, gingival hyperplasia

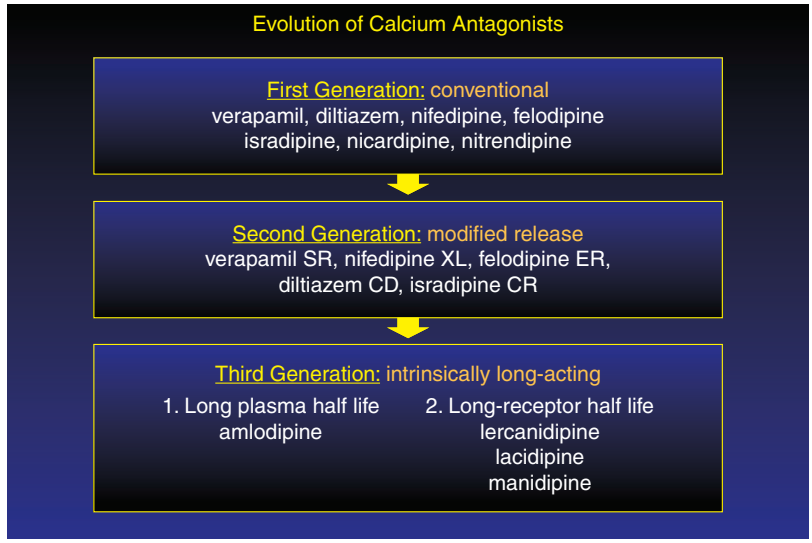

Fig. 6.1 Evolution of CCBs

Table 6.4 Effect of calcium channel blockers

	Dihydropyridines	Non-dihydropyridines	
		Benzothiazepines	Phenylalkylamines
	Amlodipine	Diltiazem	Verapamil
(−) Chronotropic effect	–	↓	↓
(−) Dromotropic effect	–	↓	↓
(−) Inotropic effect	↓/–	↓↓	↓↓
(+) Lusitropic effect	↑	↑↑	↑↑
Peripheral dilatation	↑↑	↑	↑
Coronary dilatation	↑	↑	↑
Cardiac output	–	↓	↓
Blood pressure	↓	↓	↓

(−) negative effect, ↑ increase, ↓ decrease, – no difference

Fig. 6.2 Effect of CCBs on hemodynamics

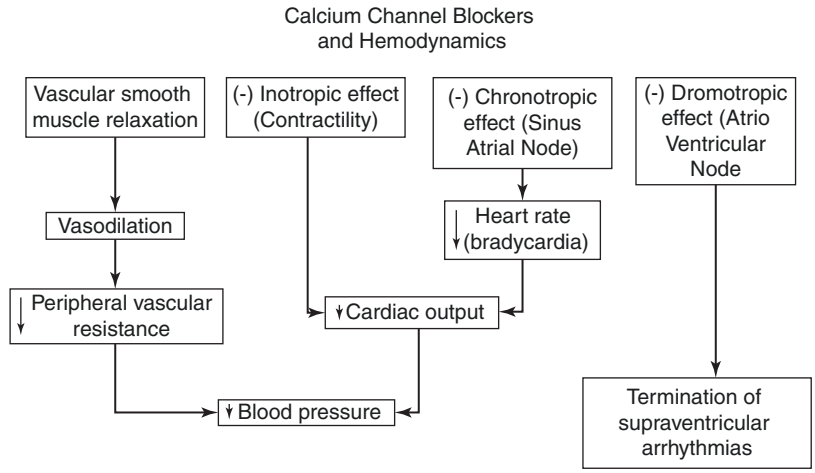

Left Ventricular Hypertrophy

Most CCBs tend to reduce left ventricular mass (LVM) when given for a sustained period [41–43, 45, 47–85]. In a meta-analysis of 80 randomized, double-blind trials, calcium antagonists decreased LVM by 11% compared with a 10% decrease by ACE inhibitors, 8% decrease by diuretics, 6% decrease by β-blockers, and 13% decrease by angiotensin receptor blockers [85]. The decrease in LVM documented with CCBs is associated with improved ventricular filling, diminished ventricular ectopy, and preserved LV contractility. Evidence from experimental studies indicates that nifedipine, nisoldipine, and amlodipine additionally lead to regression of interstitial and perivascular myocardial fibrosis, which may contribute to the improvement of diastolic function (see below) and coronary reserve.

Effects on Cardiac Contractility

By and large, CCBs are negative inotropic agents and, therefore, are likely to impair cardiac pump function to some extent [86–98]. The most profound negative inotropic effect is seen with verapamil and diltiazem. To some extent this effect is overridden by afterload reduction and reflexive sympathetic activity elicited predominantly by the dihydropyridine derivatives. Favorable hemodynamic responses such as a decrease in pulmonary wedge pressure and end-diastolic ventricular pressure were documented when isradipine, felodipine, and amlodipine were given over the short term. However, improvement of hemodynamics in patients with heart failure did not translate into an increased survival rate. In the Prospective Randomized Amlodipine Survival Evaluation (PRAISE I) [99] study, retrospective subgroup analysis suggested that amlodipine prolonged survival only in patients with nonischemic dilated cardiomyopathy; there was no beneficial effect on cardiovascular morbidity or mortality in patients with ischemic cardiomyopathy. A follow-up trial, PRAISE-2 was specifically crafted to test the hypothesis observed in the prespecified subgroup analysis of a secondary outcome in the original PRAISE study; that is, that amlodipine would reduce the rates of death from all causes in patients with heart failure. The results of PRAISE-2 did not validate the favorable association of amlodipine with improved survival for patients with nonischemic heart failure observed in the initial PRAISE-1 trial. Combined analysis of both trials suggests that amlodipine has no appreciable harmful or beneficial effect on mortality in patients with severe chronic heart failure. Similarly, in the Vasodilator-Heart Failure Trial (V-HeFT) III study, felodipine was safe but not clearly efficacious in patients with heart failure [100].

Left Ventricular Filling

In simplistic terms, left ventricular filling consists of an early diastolic active relaxation phase and a late diastolic passive distensibility phase. CCBs have been documented to have a favorable effect on both. This effect may be heart rate – dependent and appears to be most pronounced with verapamil, less pronounced with diltiazem, and even less so with the dihydropyridine CCBs. However, with prolonged administration of most CCBs, late diastolic passive distensibility is improved as well. The clinical significance of decreased left ventricular filling in patients with hypertension and of its improvement by CCBs is unclear. Certain patients with long-standing hypertension have been documented to have latent or overt heart failure, primarily as a result of impaired filling. In such patients, CCBs that lower heart rate may be helpful because they not only lower arterial pressure but also improve ventricular filling.

Endothelial and Anti-atheromatous Effects

Various experimental studies have documented that CCBs exert anti-atheromatous effects in certain animal models, such as cholesterol-fed rab-

bits. CCBs, particularly of the dihydropyridine class, can reverse endothelial dysfunction in various vascular beds, including subcutaneous, epicardial, and peripheral arteries and forearm circulation. In the Comparison of Amlodipine vs Enalapril to Limit Occurrences of Thrombosis (CAMELOT) trial [101], the slowest rate of progression of coronary atherosclerosis was observed in those patients whose BP fell within the "normal" JNC-7 category (i.e., systolic BP <120 mm Hg and diastolic BP <80 mm Hg). Administration of amlodipine (but not of enalapril) to patients with CAD and normal blood pressure resulted in reduced adverse cardiovascular events. Intravascular ultrasound imaging noted evidence of slowing of atherosclerosis progression in the amlodipine cohort.

Outcome Data

In a meta-analysis of 15 studies evaluating 47,694 patients with coronary heart disease, Bangalore et al. [102] showed that long-acting CCBs (either dihydropyridines or non-dihydropyridines) were associated with a reduction in the risk of stroke, angina pectoris, and heart failure, with similar outcomes for other cardiovascular events as the comparison group. When compared with placebo, CCBs resulted in a 28% reduction in the risk of heart failure (95% CI, 0.73–0.92). Similarly, in a recent Cochrane meta-analysis on first-line therapy in hypertension, first-line ACE inhibitors and CCBs were similarly effective as low-dose thiazides to reduce all morbidity and mortality outcomes in adult patients [103]. Of note, the Avoiding Cardiovascular events through Combination therapy in Patients Living with Systolic Hypertension (ACCOMPLISH) study showed that in combination therapy with benazepril, amlodipine was superior to hydrochlorothiazide in reducing morbidity and mortality [104]. Even in diabetes which was for years a primary indication for blockers of the renin-angiotensin system, a meta-analysis of 19 randomized controlled trials that enrolled 25,414 participants revealed no superiority of ACE inhibitors or ARBs compared to other drug classes such as CCBs in reducing the risk of hard cardiovascular and renal endpoints [105]. Finally, Wang et al. [106] looking at amlodipine specifically in head-to-head studies concluded that compared with other drug regimens, amlodipine-based antihypertensive regimen, as evidenced by the Antihypertensive and Lipid-Lowering Treatment to Prevent Heart Attack Trial (ALLHAT) [107] and Anglo Scandinavian Cardiac Outcomes Trial (ASCOT) [108], the two largest-ever trials in hypertension, might confer more outcome benefit, possibly by better lowering central systolic pressure or ambulatory pressure over 24 hours (Fig. 6.3).

Dihydropyridine CCBs

The most commonly used dihydropyridine CCBs are amlodipine and nifedipine. These drugs induce a selectively transmembrane influx of Ca++ into vascular smooth muscle and cardiac cells, thus causing vasodilation and decreasing the peripheral vascular resistance of coronary arteries and peripheral vasculature (Fig. 6.2). As a result of this effect, blood pressure will be reduced, while coronary blood flow and myocardial oxygen delivery will be increased [109]. The slow-onset, long-acting formulations such as amlodipine, lacidipine, and lercanidipine exert their hemodynamic effects over days and induce long-acting smooth and graded changes of blood pressure.

One of the primary indications for dihydropyridines is blood pressure reduction; many clinical trials have shown that this class of CCBs offers an equivalent reduction in blood pressure when compared to other antihypertensives, which translates into comparable cardiovascular events reduction. These studies include Syst Eur [110], Syst China, ASCOT, ALLHAT, Valsartan Antihypertensive Long-term Use Evaluation (VALUE), and ACCOMPLISH.

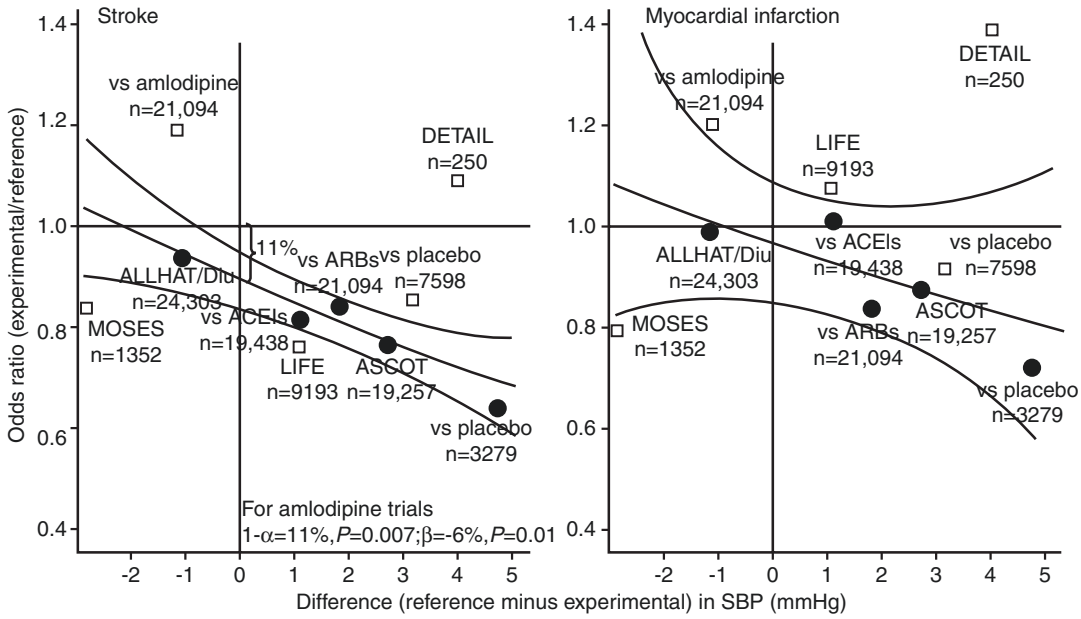

Fig. 6.3 Odds ratios for fatal and nonfatal stroke (left) and fatal and nonfatal myocardial infarction (right) in relation to corresponding differences in systolic blood pressure. Odds ratios were calculated for the amlodipine group vs placebo or other classes of antihypertensive drugs including ARBs (dots) or for the angiotensin receptor group vs placebo or other classes of antihypertensive drugs including amlodipine (squares). Blood pressure differences were obtained by subtracting the mean change in the amlodipine or ARB group from the corresponding mean change in the reference group. When a group of trials was pooled, the blood pressure difference was calculated by averaging the between-group blood pressure difference within each trial with the number of randomly assigned patients as weighting factor. Positive values indicate tighter blood pressure control in the experimental group. The regression line was drawn for trials involving an amlodipine group and weighted by the inverse of the variance of the individual odds ratios [105]

Non-dihydropyridine CCBs

1. *Phenylalkylamines*

The most commonly prescribed CCB in this subclass is verapamil; less commonly used are gallopamil and tiapamil. The systemic vasodilation is moderate and less strong in comparison to dihydropyridines. However, the negative inotropic and negative chronotropic effects induced by verapamil depress sinoatrial (SA) node and atrioventricular (AV) node conduction. As a result, there is commonly a decrease in heart rate. The cardiac output remains stable however due to the increase in stroke volume [111].

Verapamil is most commonly used for decreasing blood pressure and attenuation of angina pectoris. Moreover, verapamil offers similar efficacy as adenosine in reversing supraventricular tachycardia [112–115]. The effects of dihydropyridines and verapamil on atheromatous plaque have been studied in the Verapamil in Hypertension and Atherosclerosis Study (VHAS) trial [116]; in brief, no significant differences between verapamil and chlorthalidone on progression/regression of the atheromatous plaque were appreciated [117]. Studies such as the Controlled Onset Verapamil Investigation of Cardiovascular Endpoints (CONVINCE) [118] and the International Verapamil SR/Trandolapril Study (INVEST) ([119]) showed the reduction in cardiovascular events was not significantly different compared with drugs such as beta blockers or diuretics. Verapamil should be used with caution in combination with any beta blocker due to the additive negative inotropic and chronotropic effects [120].

2. *Benzothiazepines*

Diltiazem causes vasodilatation, especially in the coronary arteries [121, 122]. Overall, diltiazem has similar hemodynamic properties as verapamil. In atrial fibrillation or flutter without heart failure, diltiazem is preferred over digoxin for control of the heart rate [123]. Due to its moderate negative inotropic and chronotropic effect, the use of diltiazem is contraindicated in patients who have heart failure with reduced ejection fraction [124], sick sinus syndrome [125], and second-degree or third-degree atrioventricular block [126]. For the same reason, combination therapy with beta blockers is also relatively contraindicated.

In the Nordic Diltiazem (NORDIL) trial, the arm treated with diltiazem lowered the risk for stroke compared to the diuretics and β-blocker arm, despite the fact that the systolic pressure was higher in the group treated with diltiazem [127].

Questions

Question 1: A person presents with an anterior MI. Current vital signs are blood pressure 100/60 mmHg, heart rate of 120 beats per minute, rales are noted bilaterally. Extremities are cool with 1+ bilateral lower extremity edema.

Which of the following class of medications should not be initiated acutely?

A. ACEI
B. ARB
C. Beta blocker
D. Diuretic

Answer 1. C. Of all the agents listed, beta blockers would have the most acute deleterious effects. Given CO = HR ∗ SV. The HR in this person is what is maintaining the cardiac output.

Question 2: The optimal time to initiate beta blockers in the above person would be:

A. Immediately
B. Upon initiation of discharge planning
C. Once the person is stable
D. At the same time dobutamine (if required) is being administered
E. Not during this admission

Answer 2: C. Beta blockers should be initiated in patients once they are in a stable state.

Question 3: Beta blockers:

A. Increase contractility, increase heart rate, and decrease dromotropy
B. Increase contractility, decrease heart rate, and decrease dromotropy
C. Decrease contractility, increase heart rate, and increase dromotropy
D. Decrease contractility, decrease heart rate, and decrease dromotropy

Answer 3: D. Beta blockers affect hemodynamics in many ways including negative inotropy, negative chronotropy, and negative dromotropy. The result is decreased contractility, decreased heart rate, and decreased dromotropy.

Question 4: The Prospective Randomized Amlodipine Survival Evaluation (PRAISE 2) trial revealed the following about amlodipine in patients with chronic, severe heart failure:

A. A beneficial effect of amlodipine on mortality in ischemic cardiomyopathy patients
B. A reduction in mortality in nonischemic cardiomyopathy patients
C. No appreciable harmful or beneficial effect in patients with chronic severe heart failure
D. Both A and B

Answer 4: C. Analysis of trials suggests that amlodipine has no appreciable harmful or beneficial effect on mortality in patients with severe chronic heart failure.

Question 5: Arrange the following CCBs in order of their negative inotropic effects:

A. Diltiazem, verapamil, amlodipine
B. Amlodipine, verapamil, diltiazem
C. Verapamil, diltiazem, amlodipine
D. Amlodipine, diltiazem, verapamil

Answer 5: C

Parts of this chapter are modified and updated from Grossman E and Messerli F, Calcium Antagonists, Progress in Cardiovascular Diseases [40].

References

Beta Blockers

1. James Black (pharmacologist). Wikipedia.
2. Poirier L, Tobe SW. Contemporary use of b-blockers: clinical relevance of subclassification. Can J Cardiol. 2014;30(5 Suppl):S9–S15.
3. Predel HG, et al. Integrated effects of the vasodilating beta-blocker nebivolol on exercise performance, energy metabolism, cardiovascular and neurohormonal parameters in physically active patients with arterial hypertension. J Hum Hypertens. 2001;15(10):715–21.
4. Polónia J, et al. Different patterns of peripheral versus central blood pressure in hypertensive patients treated with β-blockers either with or without vasodilator properties or with angiotensin receptor blockers. Blood Press Monit. 2010;15(5):235–9.
5. Karabacak M, Doğan A, Tayyar Ş, Özaydın M, Erdoğan D. Carvedilol and nebivolol improve left ventricular systolic functions in patients with non-ischemic heart failure. Anatol J Cardiol. 2015;15(4):271–6.
6. Epstein SE, Braunwald E. Clinical and hemodynamic appraisal of beta adrenergic blocking drugs. Ann N Y Acad Sci. 1967;139(3):952–67.
7. Nakano A, Kusakari T. Effect of beta adrenergic blockade on the cardiovascular dynamics. Am J Phys. 1966;210(4):833–7.
8. Takahashi H, et al. Effect of vasodilatory B-adrenoceptor blockers on cardiovascular haemodynamics in anaesthetized rats. Clin Exp Pharmacol Physiol. 2002;29:198–203.
9. Kamp O, Metra M, Bugatti S, Bettari L, Dei Cas A, Petrini N, Dei Cas L. Nebivolol: haemodynamic effects and clinical significance of combined beta-blockade and nitric oxide release. Drugs. 2010;70(1):41–56.
10. Messerli FH, Rimoldi SF, Bangalore S, Bavishi C, Laurent S. When an increase in central systolic pressure overrides the benefits of heart rate lowering. J Am Coll Cardiol. 2016;68(7):754–62.
11. Man In't Veld AJ, Schalekamp MA. Effects of 10 different beta-adrenoceptor antagonists on hemodynamics, plasma renin activity, and plasma norepinephrine in hypertension: the key role of vascular resistance changes in relation to partial agonist activity. J Cardiovasc Pharmacol. 1983;5(1):S30–45.
12. Cruickshank JM. Beta blockers in clinical practice. 2nd ed. Edinburgh: Churchill-Livingstone; 1994. p. 1–1204.
13. Buhler FR, Laragh JH, Baer L, et al. Propranolol inhibition of renin secretion: a specific approach to diagnosis and treatment of renin-dependent hypertensive diseases. N Engl J Med. 1972;287(24):1209–14.
14. Castenfors J, Johnsson H, Oro L. Effect of alprenolol on blood pressure and plasma renin activity in hypertensive patients. Acta Med Scand. 1973;193(3):189–95.
15. Hansson L. Beta-adrenergic blockade in essential hypertension: effects of propranolol on hemodynamic parameters and plasma renin activity. Acta Med Scand Suppl. 1973;550:1–40.
16. Vincent HH, Man In't Veld AJ, Boomsma F, et al. Elevated plasma noradrenaline in response to beta-adrenoceptor stimulation in man. Br J Clin Pharmacol. 1982;13(5):717–21.
17. Bangalore S, Sawhney S, Messerli FH. Relation of beta-blocker-induced heart rate lowering and cardioprotection in hypertension. J Am Coll Cardiol. 2008;52(18):1482.
18. Messerli FH, Grossman E, Goldbourt U. Are beta-blockers efficacious as first-line therapy for hypertension in the elderly? A systematic review. JAMA. 1998;279(23):1903–7.
19. Kuyper LM, Khan NA. Atenolol vs nonatenolol β-blockers for the treatment of hypertension: a meta-analysis. Can J Cardiol. 2014;30(5 Suppl):S47–53.
20. Messerli FH, Grossman E. Beta blockers in hypertension: is carvedilol different? Am J Cardiol. 2004;93(9A):7B–12B.
21. Kotecha D, Holmes J, Krum H, Altman DG, Manzano L, Cleland JG, Lip GY, Coats AJ, Andersson B, Kirchhof P, von Lueder TG, Wedel H, Rosano G, Shibata MC, Rigby A, Flather MD. Beta-blockers in heart failure collaborative group. Efficacy of beta blockers in patients with heart failure plus atrial fibrillation: an individual-patient data meta-analysis. Lancet. 2014;384:2235–43.
22. Hjalmarson A, Goldstein S, Fagerberg B, Wedel H, Waagstein F, Kjekshus J, Wikstrand J, ElAllaf D, Vı ´t J, Aldershvile J, Halinen M, Dietz R, Neuhaus KL, Ja ´n A, Thorgeirsson G, Dunselman PH, Gullestad L, Kuch J, Herlitz J, Rickenbacher P, Ball S, Gottlieb S, Deedwania P. MERIT-HF Study Group. Effects of controlled-release metoprolol on total mortality, hospitalizations, and wellbeing in patients with heart failure: the MetoprololCR/XL randomized intervention trial in congestive heart failure (MERIT-HF). JAMA. 2000;283:1295–130.
23. Packer M, Coats AJ, Fowler MB, Katus HA, Krum H, Mohacsi P, Rouleau JL, Tendera M, Castaigne A, Roecker EB, Schultz MK, DeMets DL. Effect of carvedilol on survival in severe chronic heart failure. N Engl J Med. 2001;344:1651–8.
24. Packer M, Bristow MR, Cohn JN, Colucci WS, Fowler MB, Gilbert EM, Shusterman NH. The effect of carvedilol on morbidity and mortality in patients with chronic heart failure. N Engl J Med. 1996;334:1349–55.
25. Hjalmarson A, et al. Effect of metoprolol CR/XL in chronic heart failure: metoprolol CR/XL randomised intervention trial in congestive heart failure (MERIT-HF). Lancet. 1999;353:2001–7.
26. Packer M. Effect of carvedilol on the morbidity of patients with severe chronic heart failure: results of the carvedilol prospective randomized cumulative survival (COPERNICUS) study. Circulation. 2002;106:2194–9.

27. CIBIS-IIInvestigatorsandCommittees. The cardiac insufficiency bisoprolol study II (CIBIS-II): a randomised trial. Lancet. 1999;353:9–13.
28. Flather MD, Shibata MC, Coats AJS, Van Veldhuisen DJ, Parkhomenko A, Borbola J, Cohen-Solal A, Dumitrascu D, Ferrari R, Lechat P, Soler-Soler J, Tavazzi L, Spinarova L, Toman J, Bo¨hm M, Anker SD, Thompson SG, Poole-Wilson PA, SENIORS Investigators. Randomized trial to determine the effect of nebivolol on mortality and cardiovascular hospital admission in elderly patients with heart failure (SENIORS). Eur Heart J. 2005;26:215–25.
29. Hjalmarson A, et al. The beta blocker heart attack trial: beta blocker heart attack study group. JAMA. 1981;246(18):2073–4.
30. Pedersen TR. The Norwegian multicenter study of Timolol after myocardial infarction. Circulation. 1983;67(6/2):I49–53.
31. Dargie HJ. Effect of carvedilol on outcome after myocardial infarction in patients with left-ventricular dysfunction: the CAPRICORN randomised trial. Lancet. 2001;357(9266):1385–90.
32. Gottlieb SS, McCarter RJ, Vogel RA. Effect of beta-blockade on mortality among high-risk and low-risk patients after myocardial infarction. N Engl J Med. 1998;339(8):489–97.
33. Bangalore S, Makani H, Radford M, Thakur K, Toklu B, Katz SD, DiNicolantonio JJ, Devereaux PJ, Alexander KP, Wetterslev J, Messerli FH. Clinical outcomes with β-blockers for myocardial infarction: a meta-analysis of randomized trials. Am J Med. 2014;127(10):939–53.
34. Bangalore S, Steg G, Deedwania P, Crowley K, Eagle KA, Goto S, Ohman EM, Cannon CP, Smith SC, Zeymer U, Hoffman EB, Messerli FH, Bhatt DL, REACH Registry Investigators. β-Blocker use and clinical outcomes in stable outpatients with and without coronary artery disease. JAMA. 2012;308(13):1340–9. https://doi.org/10.1001/jama.2012.12559.
35. Messerli FH, Bangalore S, Yao SS, Steinberg JS. Cardioprotection with beta-blockers: myths, facts and Pascal's wager. J Intern Med. 2009;266(3):232–41.
36. Messerli FH, Suter T, Bangalore S. What ever happened to cardioprotection with β-blockers? Mayo Clin Proc. 2018;93(4):401–3.

CCBs

37. De Paoli P, Cerbai E, Koidl B, Kirchengast M, Sartiani L, Mugelli A. Selectivity of different calcium antagonists on T- and L-type calcium currents in guinea-pig ventricular myocytes. Pharmacol Res. 2002;46(6):491–7.
38. Ruzicka M, Leenen FH. Relevance of 24 H blood pressure profile and sympathetic activity for outcome on short- versus long-acting 1,4-dihydropyridines. Am J Hypertens. 1996;9(1):86–94.
39. Leenen FH. Clinical relevance of 24 h blood pressure control by 1,4-dihydropyridines. Am J Hypertens. 1996;9(10 Pt 2):97S–104S; discussion 8S–9S.
40. Grossman E, Messerli FH. Calcium antagonists. Prog Cardiovasc Dis. 2004;47(1):34–57.
41. Amodeo C, Kobrin I, Ventura HO, et al. Immediate and short-term hemodynamic effects of diltiazem in patients. With hypertension. Circulation. 1986;73:108–13.
42. Grossman E, Oren S, Garavaglia GE, et al. Systemic and regional hemodynamic and humoral effects of nitrendipine in essential hypertension. Circulation. 1988;78:1394–400.
43. Grossman E, Messerli FH, Oren S, et al. Cardiovascular effects of isradipine in essential hypertension. Am J Cardiol. 1991;68:65–70.
44. Little WC, Cheng CP, Elvelin L, et al. Vascular selective calcium entry blockers in the treatment of cardiovascular disorders: focus on felodipine. Cardiovasc Drugs Ther. 1995;9:657–63.
45. Schmieder RE, Messerli FH, Garavaglia GE, et al. Cardiovascular effects of verapamil in patients with essential hypertension. Circulation. 1987;75:1030–6.
46. Ventura HO, Messerli FH, Oigman W, et al. Immediate hemodynamic effects of a new calcium-channel blocking agent (nitrendipine) in essential hypertension. Am J Cardiol. 1983;51:783–6.
47. Szlachcic J, Tubau JF, Vollmer C, et al. Effect of diltiazem on left ventricular mass and diastolic filling in mild to moderate hypertension. Am J Cardiol. 1989;63:198–201.
48. Muiesan G, Agabiti-Rosei E, Romanelli G, et al. Adrenergic activity and left ventricular function during treatment of essential hypertension with calcium antagonists. Am J Cardiol. 1986;57:44D–9D.
49. Schulman SP, Weiss JL, Becker LC, et al. The effects of antihypertensive therapy on left ventricular mass in elderly patients. N Engl J Med. 1990;322:1350–6.
50. Granier P, Douste-Blazy MY, Tredez P, et al. Improvement in left ventricular hypertrophy and left ventricular diastolic function following verapamil therapy in mild to moderate hypertension. Eur J Clin Pharmacol. 1990;39(Suppl 1):S45–6.
51. Weiss RJ, Bent B. Diltiazem-induced left ventricular mass regression in hypertensive patients. J Clin Hypertens. 1987;3:135–43.
52. Senda Y, Tohkai H, Kimura M, et al. ECG-gated cardiac scan and echocardiographic assessments of left ventricular hypertrophy: reversal by 6-month treatment with diltiazem. J Cardiovasc Pharmacol. 1990;16:298–304.
53. Gottdiener JS, Reda DJ, Massie BM, et al. Effect of single-drug therapy on reduction of left ventricular mass in mild to moderate hypertension: comparison of six antihypertensive agents. The Department of Veterans Affairs Cooperative Study Group on antihypertensive agents. Circulation. 1997;95:2007–14.
54. van Leeuwen JT, Smit AJ, May JF, et al. Comparative effects of diltiazem and lisinopril on left ventricular

structure and filling in mild-to-moderate hypertension. J Cardiovasc Pharmacol. 1995;26:983–9.
55. Leenen FH, Fourney A. Comparison of the effects of amlodipine and diltiazem on 24-hour blood pressure, plasma catecholamines, and left ventricular mass. Am J Cardiol. 1996;78:203–7.
56. Ferrara LA, de Simone G, Mancini M, et al. Changes in left ventricular mass during a double-blind study with chlorthalidone and slow-release nifedipine. Eur J Clin Pharmacol. 1984;27:525–8.
57. Phillips RA, Ardeljan M, Shimabukuro S, et al. Effect of nifedipine GITS on left ventricular mass and diastolic function in severe hypertension. J Cardiovasc Pharmacol. 1991;17:S172–4.
58. Totteri A, Scopelliti G, Campanella G, et al. [Evaluation of regression of left ventricular hypertrophy after antihypertensive therapy. Comparative echo-Doppler study of ace inhibitors and calcium antagonists]. Italian. Minerva Cardioangiol. 1993;41:231–7.
59. Yamakado T, Teramura S, Oonishi T, et al. Regression of left ventricular hypertrophy with long-term treatment of nifedipine in systemic hypertension. Clin Cardiol. 1994;17:615–8.
60. Kirpizidis HG, Papazachariou GS. Comparative effects of fosinopril and nifedipine on regression of left ventricular hypertrophy in hypertensive patients: a double-blind study. Cardiovasc Drugs Ther. 1995;9:141–3.
61. Myers MG, Leenen FH, Tanner J. Differential effects of felodipine and nifedipine on 24-h blood pressure and left ventricular mass. Am J Hypertens. 1995;8:712–8.
62. Ferrara LA, Fasano ML, de Simone G, et al. Antihypertensive and cardiovascular effects of nitrendipine: a controlled study vs. placebo. Clin Pharmacol Ther. 1985;38:434–8.
63. Drayer JI, Hall WD, Smith VE, et al. Effect of the calcium channel blocker nitrendipine on left ventricular mass in patients with hypertension. Clin Pharmacol Ther. 1986;40:679–85.
64. Giles TD, Sander GE, Roffidal LC, et al. Comparison of nitrendipine and hydrochlorothiazide for systemic hypertension. Am J Cardiol. 1987;60:103–6.
65. Machnig T, Henneke KH, Engels G, et al. Nitrendipine vs. captopril in essential hypertension: effects on circadian blood pressure and left ventricular hypertrophy. Cardiology. 1994;85:101–10.
66. Costantino G, Di Lorenzo L, Buonissimo S, et al. Echocardiographic analysis of anatomical and functional changes in the left heart ventricle during antihypertensive treatment with nicardipine. G Ital Cardiol. 1988;18:644–8.
67. Gokce C, Oram A, Kes S, et al. Effects of nicardipine on left ventricular dimensions and hemodynamics in systemic hypertension. Am J Cardiol. 1990;65:680–2.
68. Sumimoto T, Hiwada K, Ochi T, et al. Effects of long-term treatment with sustained-release nicardipine on left ventricular hypertrophy and function in patients with essential hypertension. J Clin Pharmacol. 1994;34:266–9.
69. Langan J, Rodriguez-Manas L, Sareli P, et al. Clinical experience in hypertension. Cardiology. 1997;88(Suppl 1):56–62.
70. Kloner RA, Sowers JR, DiBona GF, et al. Effect of amlodipine on left ventricular mass in the amlodipine cardiovascular community trial. J Cardiovasc Pharmacol. 1995;26:471–6.
71. Bignotti M, Grandi AM, Gaudio G, et al. One-year antihypertensive treatment with amlodipine: effects on 24-hour blood pressure and left ventricular anatomy and function. Acta Cardiol. 1995;50:135–42.
72. Skoularigis J, Strugo V, Weinberg J, et al. Effects of amlodipine on 24-hour ambulatory blood pressure profiles electrocardiographic monitoring, and left ventricular mass and function in black patients with very severe hypertension. J Clin Pharmacol. 1995;35:1052–9.
73. Carr AA, Prisant LM. The new calcium antagonist isradipine. Effect on blood pressure and the left ventricle in black hypertensive patients. Am J Hypertens. 1990;3:8–15.
74. Saragoca MA, Portela JE, Abreu P, et al. Regression of left ventricular hypertrophy in the short-term treatment of hypertension with isradipine. Am J Hypertens. 1991;4:188S–90S.
75. Vyssoulis GP, Karpanou EA, Pitsavos CE, et al. Regression of left ventricular hypertrophy with isradipine antihypertensive therapy. Am J Hypertens. 1993;6:82S–5S.
76. Manolis AJ, Kolovou G, Handanis S, et al. Regression of left ventricular hypertrophy with isradipine in previously untreated hypertensive patients. Am J Hypertens. 1993;6:86S–8S.
77. Modena MG, Masciocco G, Rossi R, et al. Evaluation of the effectiveness of isradipine SRO in the treatment of hypertensive patients with left ventricular hypertrophy. Cardiovasc Drugs Ther. 1994;8:153–60.
78. Galderisi M, Celentano A, Garofalo M, et al. Reduction of left ventricular mass by short-term antihypertensive treatment with isradipine: a double-blind comparison with enalapril. Int J Clin Pharmacol Ther. 1994;32:312–6.
79. Grandi AM, Bignotti M, Gaudio G, et al. Ambulatory blood pressure and left ventricular changes during antihypertensive treatment: perindopril versus isradipine. J Cardiovasc Pharmacol. 1995;26:737–41.
80. Pringle SD, Barbour M, Simpson IA. Effect of felodipine on left ventricular mass and Doppler-derived hemodynamics in patients with essential hypertension [abstract]. Proceedings of the 4th international symposium on calcium antagonists: pharmacology and clinical research, Florence, Italy, May 25–27, 1989.
81. Cerasola G, Cottone S, Nardi E, et al. Reversal of cardiac hypertrophy and left ventricular function with the calcium antagonist felodipine in hypertensive patients. J Hum Hypertens. 1990;4:703–8.
82. Wetzchewald D, Klaus D, Garanin G, et al. Regression of left ventricular hypertrophy during long-term anti-

hypertensive treatment – a comparison between felodipine and the combination of felodipine and metoprolol. J Intern Med. 1992;231:303–8.
83. Leenen FH, Holliwell DL. Antihypertensive effect of felodipine associated with persistent sympathetic activation and minimal regression of left ventricular hypertrophy. Am J Cardiol. 1992;69:639–45.
84. Nalbantgil I, Onder R, Killiccioglu B, et al. The efficacy of felodipine ER on regression of left ventricular hypertrophy in patients with primary hypertension. Blood Press. 1996;5:285–91.
85. Klingbeil AU, Schneider M, Martus P, et al. A meta-analysis of the effects of treatment on left ventricular mass in essential hypertension. Am J Med. 2003;115:41–6.
86. Kohlhardt M, Fleckenstein A. Inhibition of the slow inward current by nifedipine in mammalian ventricular myocardium. Naunyn Schmiedeberg's Arch Pharmacol. 1977;298:267–72.
87. Nayler WG, Szeto J. Effect of verapamil on contractility, oxygen utilization, and calcium exchangeability in mammalian heart muscle. Cardiovasc Res. 1972;6:120–8.
88. Sung RJ, Elser B, McAllister RG. Intravenous verapamil for termination of re-entrant supraventricular tachycardias: intracardiac studies correlated with plasma verapamil concentrations. Ann Intern Med. 1980;93:682–9.
89. Bonow RO, Rosing DR, Bacharach SL, et al. Effects of verapamil on left ventricular systolic function and diastolic filling in patients with hypertrophic cardiomyopathy. Circulation. 1981;64:787–96.
90. Brooks N, Cattell M, Pidgeon J, et al. Unpredictable response to nifedipine in severe cardiac failure. Br Med J. 1980;281:1324.
91. Chew CY, Hecht HS, Collett JT, et al. Influence of severity of ventricular dysfunction on hemodynamic responses to intravenously administered verapamil in ischemic heart disease. Am J Cardiol. 1981;47:917–22.
92. de Buitleir M, Rowland E, Krikler DM. Hemodynamic effects of nifedipine given alone and in combination with atenolol in patients with impaired left ventricular function. Am J Cardiol. 1985;55:15E–20E.
93. Elkayam U, Weber L, McKay C, et al. Spectrum of acute hemodynamic effects of nifedipine in severe congestive heart failure. Am J Cardiol. 1985;56:560–6.
94. Ferlinz J, Easthope JL, Aronow WS. Effects of verapamil on myocardial performance in coronary disease. Circulation. 1979;59:313–9.
95. Klein HO, Ninio R, Oren V, et al. The acute hemodynamic effects of intravenous verapamil in coronary artery disease. Assessment by equilibrium gated radionuclide ventriculography. Circulation. 1983;67:101–10.
96. Lamping KA, Gross GJ. Differential effects of intravenous vs. intracoronary nifedipine on myocardial segment function in ischemic canine hearts. J Pharmacol Exp Ther. 1984;228:28–32.
97. Serruys PW, Brower RW, ten Katen HJ, et al. Regional wall motion from radiopaque markers after intravenous and intracoronary injections of nifedipine. Circulation. 1981;63:584–91.
98. Thomas P, Sheridan DJ. Vascular selectivity of felodipine: clinical experience. J Cardiovasc Pharmacol. 1990;15(Suppl 4):S17–20.
99. Packer M, O'Connor CM, Ghali JK, et al. Effect of amlodipine on morbidity and mortality in severe chronic heart failure. Prospective randomized amlodipine survival evaluation study group. N Engl J Med. 1996;335:1107–14.
100. Cohn JN, Ziesche S, Smith R, et al. Effect of the calcium antagonist felodipine as supplementary vasodilator therapy in patients with chronic heart failure treated with enalapril: V-HeFT III. Vasodilator-heart failure trial (V-HeFT) study group. Circulation. 1997;96:856–63.
101. Nissen SE, Tuzcu EM, Libby P, Thompson PD, Ghali M, Garza D, Berman L, Shi H, Buebendorf E, Topol EJ, Investigators CAMELOT. Effect of antihypertensive agents on cardiovascular events in patients with coronary disease and normal blood pressure: the CAMELOT study: a randomized controlled trial. JAMA. 2004;292(18):2217–25.
102. Bangalore S, Parkar S, Messerli FH. Long-acting calcium antagonists in patients with coronary artery disease: a meta-analysis. Am J Med. 2009;122(4):356–65.
103. Wright JM, Musini VM, Gill R. First-line drugs for hypertension. Cochrane Database Syst Rev. 2018;4:CD001841.
104. Jamerson K, Weber MA, Bakris GL, Dahlof B, Pitt B, Shi V, et al. Benazepril plus amlodipine or hydrochlorothiazide for hypertension in high-risk patients. N Engl J Med. 2008;359:2417–28.
105. Bangalore S, Fakheri R, Toklu B, Messerli FH. Diabetes mellitus as a compelling indication for use of renin angiotensin system blockers: systematic review and meta-analysis of randomized trials. BMJ. 2016;352:i438.
106. Wang JG, Li Y, Franklin SS, Safar M. Prevention of stroke and myocardial infarction by amlodipine and angiotensin receptor blockers: a quantitative overview. Hypertension. 2007;50(1):181–8.
107. Hjalmarson A, et al. Major outcomes in high-risk hypertensive patients randomized to angiotensin-converting enzyme inhibitor or calcium channel blocker vs diuretic: The antihypertensive and lipid-lowering treatment to prevent heart attack trial (ALLHAT). JAMA. 2002;288(23):2981–97.
108. Dahlof B, Sever PS, Poulter NR, Wedel H, Beevers DG, Caulfield M, et al. Prevention of cardiovascular events with an antihypertensive regimen of amlodipine adding perindopril as required versus atenolol adding bendroflumethiazide as required, in the Anglo-Scandinavian cardiac outcomes trial-blood pressure lowering arm (ASCOT-BPLA): a multicentre randomised controlled trial. Lancet. 2005;366(9489):895–906.

109. Opie LH. First line drugs in chronic stable effort angina – the case for newer, longer-acting calcium channel blocking agents. J Am Coll Cardiol. 2000;36(6):1967–71.
110. Staessen JA, Fagard R, Thijs L, Celis H, Arabidze GG, Birkenhager WH, et al. Randomised double-blind comparison of placebo and active treatment for older patients with isolated systolic hypertension. The systolic hypertension in Europe (Syst-Eur) trial Investigators. Lancet. 1997;350(9080):757–64. Epub 1997/09/23. PubMed PMID: 9297994.
111. Lund-Johansen P, Omvik P. Central hemodynamic changes of calcium antagonists at rest and during exercise in essential hypertension. J Cardiovasc Pharmacol. 1987;10(Suppl 1):S139–48.
112. Rinkenberger RL, Prystowsky EN, Heger JJ, Troup PJ, Jackman WM, Zipes DP. Effects of intravenous and chronic oral verapamil administration in patients with supraventricular tachyarrhythmias. Circulation. 1980;62(5):996–1010.
113. Page RL, Joglar JA, Caldwell MA, Calkins H, Conti JB, Deal BJ, et al. 2015 ACC/AHA/HRS guideline for the management of adult patients with supraventricular tachycardia: a report of the American College of Cardiology/American Heart Association task force on clinical practice guidelines and the Heart Rhythm Society. J Am Coll Cardiol. 2016;67(13):e27–e115.
114. Alabed S, Sabouni A, Providencia R, Atallah E, Qintar M, Chico TJ. Adenosine versus intravenous calcium channel antagonists for supraventricular tachycardia. Cochrane Database Syst Rev. 2017;10:Cd005154.
115. Delaney B, Loy J, Kelly AM. The relative efficacy of adenosine versus verapamil for the treatment of stable paroxysmal supraventricular tachycardia in adults: a meta-analysis. Eur J Emerg Med. 2011;18(3):148–52.
116. Rosei EA, Dal Palu C, Leonetti G, Magnani B, Pessina A, Zanchetti A. Clinical results of the verapamil in hypertension and atherosclerosis study. VHAS investigators. J Hypertens. 1997;15(11):1337–44.
117. Zanchetti A, Rosei EA, Dal Palu C, Leonetti G, Magnani B, Pessina A. The verapamil in hypertension and atherosclerosis study (VHAS): results of long-term randomized treatment with either verapamil or chlorthalidone on carotid intima-media thickness. J Hypertens. 1998;16(11):1667–76.
118. Black HR, Elliott WJ, Grandits G, Grambsch P, Lucente T, Neaton JD, et al. Results of the Controlled ONset Verapamil INvestigation of Cardiovascular Endpoints (CONVINCE) trial by geographical region. J Hypertens. 2005;23(5):1099–106.
119. Pepine CJ, Handberg EM, Cooper-DeHoff RM, Marks RG, Kowey P, Messerli FH, et al. A calcium antagonist vs a non-calcium antagonist hypertension treatment strategy for patients with coronary artery disease. The international verapamil-Trandolapril study (INVEST): a randomized controlled trial. JAMA. 2003;290(21):2805–16.
120. Lee TH, Salomon DR, Rayment CM, Antman EM. Hypotension and sinus arrest with exercise-induced hyperkalemia and combined verapamil/propranolol therapy. Am J Med. 1986;80(6):1203–4.
121. Joyal M, Cremer KF, Pieper JA, Feldman RL, Pepine CJ. Systemic, left ventricular and coronary hemodynamic effects of intravenous diltiazem in coronary artery disease. Am J Cardiol. 1985;56(7):413–7.
122. Kenny J, Daly K, Bergman G, Kerkez S, Jewitt DE. Beneficial effects of diltiazem in coronary artery disease. Br Heart J. 1984;52(1):53–6.
123. Tsuneda T, Yamashita T, Fukunami M, Kumagai K, Niwano S, Okumura K, et al. Rate control and quality of life in patients with permanent atrial fibrillation: the quality of life and atrial fibrillation (QOLAF) study. Circ J. 2006;70(8):965–70.
124. Goldstein RE, Boccuzzi SJ, Cruess D, Nattel S. Diltiazem increases late-onset congestive heart failure in postinfarction patients with early reduction in ejection fraction. The adverse experience committee; and the multicenter diltiazem postinfarction research group. Circulation. 1991;83(1):52–60.
125. Sugimoto T, Ishikawa T, Kaseno K, Nakase S. Electrophysiologic effects of diltiazem, a calcium antagonist, in patients with impaired sinus or atrioventricular node function. Angiology. 1980;31(10):700–9.
126. Zeltser D, Justo D, Halkin A, Rosso R, Ish-Shalom M, Hochenberg M, et al. Drug-induced atrioventricular block: prognosis after discontinuation of the culprit drug. J Am Coll Cardiol. 2004;44(1):105–8.
127. Hansson L, Hedner T, Lund-Johansen P, Kjeldsen SE, Lindholm LH, Syvertsen JO, et al. Randomised trial of effects of calcium antagonists compared with diuretics and beta-blockers on cardiovascular morbidity and mortality in hypertension: the Nordic diltiazem (NORDIL) study. Lancet. 2000;356(9227):359–65.

7 Pressor Agents, Pure Inotropes, Mixed Function Agents

Paul Anaya and Tracy E. Macaulay

Introduction

In critically ill patients presenting with shock, hemodynamic stability can be achieved using mechanical support with intra-aortic balloon pumps, ventricular assist devices, or extracorporeal membrane oxygenation (ECMO); however, an initial pharmacologic approach is typically undertaken and often preferred. The primary objective of using vasoactive medications is to maintain adequate tissue perfusion and optimize oxygen delivery by improving mean arterial pressure and cardiac output [1, 2]. When considering the use of vasodilators, inotropes, and vasopressors, it is important to be mindful of the balance sought in providing adequate oxygen delivery by maintaining the minimal effective perfusion pressure while simultaneously limiting myocardial oxygen demand and preventing tissue ischemia.

A working knowledge of the hemodynamic effects of these vasoactive agents is the key to guide therapeutic decision-making regarding the choice of vasoactive agent for any given clinical setting. A detailed discussion of basic hemodynamic principles is provided in Part I of this book. To briefly review, cardiac performance is dependent on the physiologic elements of preload and afterload. According to the Frank-Starling principle, stroke volume (or cardiac output) will increase with an increase in preload (Fig. 7.1).

Left ventricular (LV) preload can be estimated by measures of left atrial pressure, pulmonary capillary wedge pressure, or left ventricular end-diastolic pressure. Right ventricular (RV) preload can be estimated by measuring right atrial pressure, central venous pressure, or right ventricular

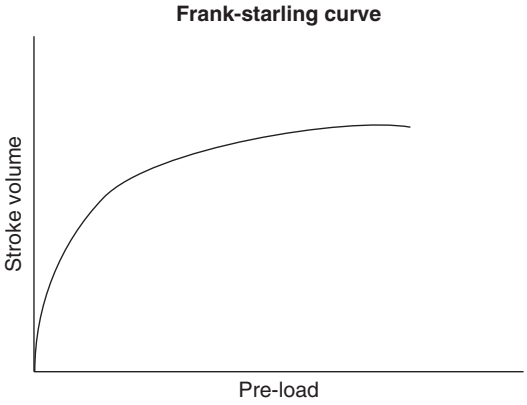

Fig. 7.1 The Frank-Starling curve as it applies in cardiac hemodynamics depicts the relationship between preload and stroke volume or cardiac output

P. Anaya (✉) · T. E. Macaulay
Gill Heart Institute, University of Kentucky, Lexington, KY, USA
e-mail: paulanaya@uky.edu; tracy.macaulay@uky.edu

A. T. Askari, A. W. Messerli (eds.), *Cardiovascular Hemodynamics*, Contemporary Cardiology,
https://doi.org/10.1007/978-3-030-19131-3_7

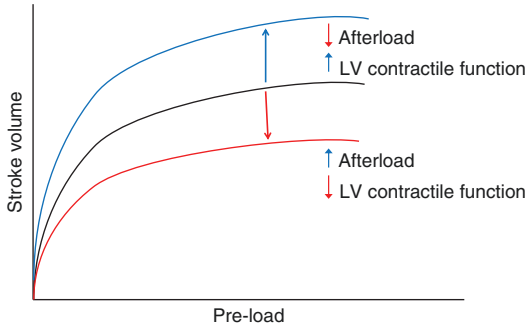

Fig. 7.2 The effects of afterload and intrinsic LV contractility on the Frank-Starling relationship

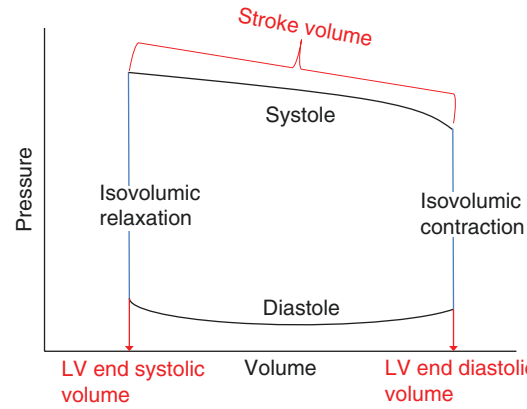

Fig. 7.3 The pressure-volume relation depicts the volumetric and pressure changes that occur through a single cardiac cycle. As is illustrated, the phases of the cardiac cycle include diastole (or filling phase) which begins at the time of mitral valve opening, isovolumetric contraction defined as the time from mitral valve closure until aortic valve opening, systole (or ejection phase) which begins at the time of aortic valve opening, and isovolumetric relaxation defined by the time between aortic valve closure until mitral valve opening heralds the next diastolic phase. Stroke volume is defined as the difference between the volume contained within the ventricle at end diastole and the volume contained at the end of ejection

end-diastolic pressure. In simple terms, preload can be viewed as the distending capacity of the ventricle, and is often referred to as the ventricular filling pressure. An important concept to understand is that in an intact heart surrounded by pericardium, there is a physical limit imposed on the degree of ventricular distention achieved with progressive increases in preload. Furthermore, the distending pressure of the LV is counteracted by, and therefore, determined in part by the surrounding pericardial (or RV) pressure [3]. In mathematical terms, the distending pressure is equal to the ventricular filling pressure minus the pericardial pressure. Under normal physiologic circumstances, the pericardial pressure is negligible and can be ignored such that the distending pressure is equal to the filling pressure. In the setting of acute decompensated heart failure associated with volume overload, the pericardial pressure rises and can no longer be ignored. Thus, while measures of left atrial pressure (or PCWP) may be elevated, the actual distending pressure (i.e., preload) is lower, thereby shifting the relationship of stroke volume to preload leftward along the Frank-Starling curve, resulting in a lower stroke volume. Additionally, as illustrated in Fig. 7.2, regardless from where a patient lies on their specific Frank-Starling curve, a shift of the curve downward for any given preload would imply either an increase in afterload forces or a decrease in the intrinsic contractility of the ventricle. Conversely, a shift of the curve upward for any given preload state would imply either a decrease in afterload or an increase in the intrinsic contractility of the ventricle. Afterload influences cardiac performance in a reciprocal manner such that increases in afterload result in lower cardiac output whereas reduced afterload generally results in improved cardiac output. Left ventricular pressure-volume relations contain information regarding cardiac performance, intrinsic contractile function, preload, and afterload (Fig. 7.3). Historically, these have been generated in the cardiac catheterization laboratory using intracardiac pressure sensors and altering intracardiac volume by pharmacologic or mechanical means. Such alterations in volume produce a series of pressure-volume loops whereby the end-systolic pressure-volume points align (Fig. 7.4). This linear relation is known as the left ventricular end-systolic elastance and defines the intrinsic contractile function of the left ventricle. Additionally, a line drawn from the end-systolic pressure-volume point to the end-diastolic pressure-volume point is known as the arterial elastance and defines the ventricular afterload.

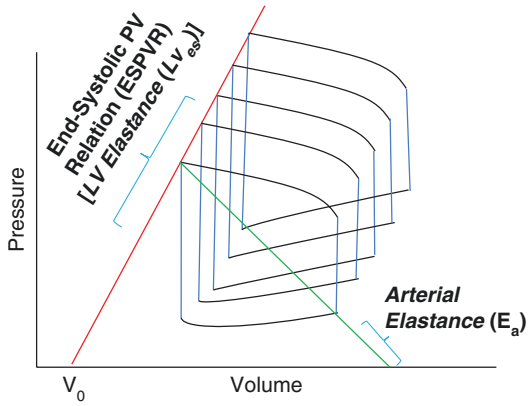

Fig. 7.4 By altering preload, a series of pressure-volume loops can be generated. These can be used to define ventricular end-systolic elastance (LV E_{es}). This end-systolic pressure-volume linear relation is generally accepted as a measure of LV contractility with steeper slopes indicating greater contractility and less steep slopes indicating reduced contractility. Similarly, a linear relationship between the end-systolic pressure-volume point and the end-diastolic pressure–volume point defines arterial elastance (Ea) from which the LV afterload is derived. Black = diastolic and systolic phases of the cardiac cycle; blue = isovolumetric phases; red = LV elastance (LV contractility); green = arterial elastance (afterload)

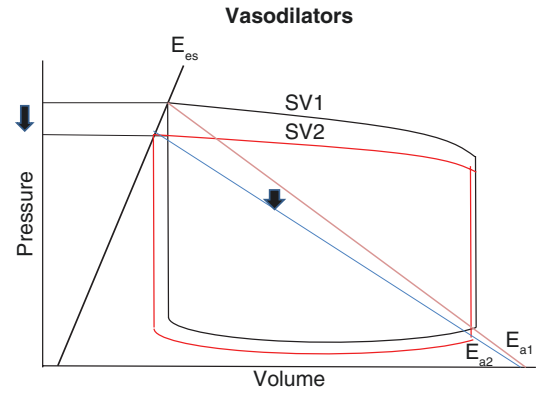

Fig. 7.5 Hemodynamic effects of vasodilators. A reduction in afterload is depicted as a downward shift in the arterial elastance ($E_{a1} \rightarrow E_{a2}$) and a decrease in the end-systolic pressure. This results in an increase in the stroke volume (SV2 > SV1). Vasodilators do not affect the LV contractility. Black = baseline hemodynamic profile; red = hemodynamic profile after intervention

Pharmacologic Fundamentals and Hemodynamic Effects

Vasodilators

Vasodilator therapy is most frequently used in the treatment of hypertension. It is also useful in patients with left ventricular systolic dysfunction (LVSD) with or without pulmonary edema, and has demonstrated a mortality reduction in both acute and chronic management [4, 5]. The primary site of action for vasodilators is the peripheral vasculature where they facilitate the effects of nitric oxide (NO), or act as direct NO donors, to potentiate vasodilatation. Vasodilators used in acute decompensated heart failure or cardiogenic shock include nitroprusside and nitroglycerin. While ace inhibitors, angiotensin receptor blockers, beta-blockers, calcium channel blockers, hydralazine, and long-acting oral nitrates can also achieve vasodilatation, these are more typically used in the management of chronic heart failure or hypertensive crisis [6–8]. Since the primary effect of vasodilators is to reduce the systemic vascular resistance, the expected pressure-volume relation would yield a tracing in which stroke volume is augmented simply by decreasing the LV afterload (Fig. 7.5). These agents also have variable effects on venodilation and therefore may also cause a slight reduction in preload. No change to LV contractility occurs, so the end-systolic pressure-volume relation remains constant.

Nitroglycerin

Nitroglycerin (NTG) is a direct NO donor, providing an exogenous source of NO which increases vascular cGMP resulting in smooth muscle relaxation (Table 7.1). Nitroglycerin acts as a preferential venodilator, thereby reducing cardiac preload. It also is an effective coronary artery vasodilator, making it an ideal choice for the patient with myocardial ischemia, hypertension, and/or elevated pulmonary capillary wedge pressure. Contraindications include right ventricular failure, hypertrophic cardiomyopathy, pericardial disease, or pericardial tamponade. Despite favorable hemodynamic effects, no mortality reduction from the use of intravenous nitrates has been demonstrated in large clinical trials [6, 7].

Table 7.1 Vasodilators

Generic (brand)	Starting dose	Maintenance and titration	Adverse drug Rxn	Precautions and contraindications	Uses
Nitroglycerin (Nitrostat IV)	5 mcg/min	Increase every 3 min to max 200 mcg/min	Headache, tachyphylaxis	RV failure, pericardial dz, restrictive cardiomyopathy	Used to treat symptoms of ischemia (low doses), hypertension (high doses), and pulmonary edema
Nitroprusside (Nipride)	0.5 mcg/kg/min	Increase every 5 min to max 5–10 mcg/kg/min; ideally 48 h	Cyanide toxicity and methemoglobinemia with prolonged use and/or high dose	Severe renal, liver impairment	Acute decompensated heart failure due to high afterload, cardiogenic pulmonary edema
Diltiazem (Cardizem)	Arrhythmias – 10 mg IVP (0.25 mg/kg)	5–20 mg/h infusion	AV nodal blockade	Congestive heart failure, bradycardia, sick sinus syndrome, WPW	Atrial fib/flutter, PSVT
Verapamil (Isoptin)	Arrhythmias – 2.5–5 mg IVP	N/A	AV nodal blockade	Congestive heart failure, bradycardia, sick sinus syndrome, WPW	Atrial fib/flutter, PSVT
Nicardipine (Cardene)	No bolus	3–15 mg/h	Low BP, tachycardia, edema	Aortic stenosis	Hypertensive crisis
Nesiritide (Natrecor)	2 mcg/kg IV	0.01 mcg/kg/min; max 0.03 mcg/kg/min; titrate by 0.005 mcg/kg/min q3 h	Low BP, renal failure	Valvular heart dz, pericardial dz, hypotension, restrictive cardiomyopathy	Acute decompensated heart failure with volume overload

Tachyphylaxis can develop within 24 h of continuous therapy, but can generally be overcome by increasing the dose or providing a nitrate-free interval if possible [8].

Sodium Nitroprusside

Sodium nitroprusside is an endothelium-independent vasodilator like nitroglycerin, serving as a direct NO donor within the vasculature. Unlike nitroglycerin, nitroprusside is associated with preferential arterial vasodilating properties [9]. Therefore, while capable of reducing cardiac preload much like nitroglycerin, it has a more potent afterload reducing capability. Unlike other vasodilators, nitroprusside causes only mild increases in heart rate and an overall decrease in myocardial oxygen demand. The molecular composition of sodium nitroprusside includes five cyanide ions which can accumulate as either cyanide or thiocyanate in patients with liver or renal failure, respectively, thereby limiting its applicability. Patients receiving high doses (10 mcg/kg/min) for a prolonged time (>2 days) are particularly at risk of toxicity. Despite this, nitroprusside is considered to be the gold standard intravenous antihypertensive for its remarkable effectiveness and rapid onset of action (Table 7.2).

Other Vasodilators

Intravenous calcium channel blockers, specifically diltiazem, have several important roles in the management of various clinical conditions. Blockade of calcium entry into coronary and peripheral arterial smooth muscle cells results in vasodilation and has a negative chronotropic and negative inotropic effect on the myocardium. The negative chronotropic effects are useful for the management of rapid ventricular heart rates, particularly in patients with supraventricular tachycardia. It is important to note that the significant negative inotropy means diltiazem is only recommended in patients with normal ejection fraction and absence of clinical heart failure. Diltiazem may also play a role in the management of hypertensive urgency and emergency; however, its long biological half-life of 3–4.5 h, makes it less useful than medications with a more rapid onset and easier titration. Also, due to the delayed onset of action, an intravenous bolus of IV diltiazem would typically precede initiation of a continuous infusion.

Esmolol is a β-1 selective adrenergic receptor blocker that has a very rapid onset and short duration of action, making it easily titratable. Unlike labetolol and carvedilol, esmolol exhibits very weak vasodilator effects and therefore is *not* clinically useful as a vasodilator. Rather, its negative chronotropic effect predominates, hence its utility in the treatment of tachyarrhythmias. A resurgent interest in use of esmolol in the treatment of septic shock, mainly due to his negative chronotropic effects, has recently emerged and is a topic of current investigations [10].

Nesiritide is a recombinant B-type natriuretic peptide. Early studies demonstrated that the main clinical effect of nesiritide is peripheral vasodilatation [11]. Nesiritide also induces a

Table 7.2 Comparison of intravenous vasodilators

	NTG	Nitroprusside	Diltiazem	Verapamil	Nicardipine
Mech. of action	Nitric oxide donor, ↑cGMP	Nitric oxide donor, ↑cGMP	Calcium channel blocker	Calcium channel blocker	Calcium channel blocker
Hemodynamic effect	Venodilation>arterial	Arterial and venous vasodilator	Decrease HR, vasodilator	Decrease HR, vasodilator	Vasodilator
Contractility	No effect	No effect	Decrease	Decrease	No effect
Heart rate (HR)	No direct effect (possible reflex tachycardia)	↑ (reflex)	0/↓	0/↓	↑ (reflex)
SA automaticity	No effect	No effect	Decrease	Decrease	No effect
AV conduction	No effect	No effect	Decrease	Decrease	No effect
Vasodilation	↑↑	↑↑↑↑	↑↑↑	↑↑↑↑	↑↑↑↑↑

cGMP cyclic guanosine monophosphate

Table 7.3 Inotrope overview

Generic name	Brand name	Starting dose	Maintenance and titration	Pharmacokinetic properties	Adverse effects
Dobutamine	Dobutrex	1 mcg/kg/min	20 mcg/kg/min	Metabolized by methylation and conjugation, inactive metabolites are renally excreted, *t*1/2 ¼ 2 min	Angina, hypertension, tachyarrhythmia, headache
Isoproterenol	Isuprel	0.01 mcg/kg/min	Increase every 5 min to maximum 0.3 mcg/kg/min	Hepatic metabolism, *t*1/2 ¼ 3–7 h	Syncope, tachyarrhythmia, confusion, tremor
Milrinone	Primacor	0.25 mcg/kg/min	0.75 mcg/kg/min	Renally excreted (83% unchanged), *t*1/2 ¼ 2.3 h (prolonged in renal failure)	Ventricular arrhythmias, hypotension, headache
Levosimendan	Simdax	6–12 mcg/kg IVP	0.05–0.2 mcg/kg/min	Hepatic metabolism with over 10 min active metabolite; $t_{1/2}$ 70 h (prolonged in renal failure)	Hypotension

natriuresis and enhances diuresis, which is associated with a reduction in the PCWP. The combined effects would be expected to improve cardiac performance and increase ventricular stroke volume through a reduction in ventricular afterload and preload. Although initially touted for its clinical effect at reducing dyspnea, subsequent randomized clinical trials failed to demonstrate any meaningful clinical outcomes in terms of renal function or rates of death or rehospitalization [11–13].

Inotropes

Intravenous inotropic therapy is indicated for the treatment of low-output heart failure and cardiogenic shock [14]. In cardiogenic shock, the decrease in cardiac output results in inadequate tissue perfusion, thereby increasing adrenergic drive. Although the release of endogenous catecholamines is temporarily effective acutely, chronic adrenergic stimulation ultimately leads to down-regulation of β_1-receptors and reduced contractile function. The use of inotropic agents such as dobutamine, milrinone, or levosimendan through the direct stimulation of existing β_1-receptors, inhibition of phosphodiesterase III, or calcium sensitization, respectively to augment cardiac output and achieve adequate tissue perfusion may be necessary. Adverse effects of inotropic agents include both supraventricular and ventricular tachyarrhythmias. Therefore, these agents should only be used in acutely ill patients and only for the shortest duration necessary. Additionally, despite their beneficial hemodynamic effects, these agents have not been shown to provide a mortality benefit [15, 16].

The net physiologic effect of inotropic support is an increase in myocardial contractile function and an increased heart rate, resulting in an increased cardiac output. While these effects improve cardiac performance, this occurs at the expense of an increased myocardial oxygen demand (Table 7.3). Pressure-volume relation plots would result in a leftward shift of the LV end-systolic elastance (pressure-volume linear relation) (Fig. 7.6). This leads to an increase in the stroke volume and hence the cardiac output. Despite an increased cardiac output, the blood pressure changes minimally, and any expected increase in the pulsatile pressure is offset by the afterload reduction derived from the peripheral effects of these agents, particularly milrinone.

Dobutamine

Dobutamine is a synthetic catecholamine that acts as a pure inotrope. It binds with high affinity to the β_1- and β_2-receptors in a 3:1 ratio and with lesser affinity to alpha-receptors (B1 > B2 > alpha) [8, 14, 15]. The overarching effect of dobutamine is to augment myocardial contractile function through direct binding of the Gs-protein-coupled β_1-receptor which activates

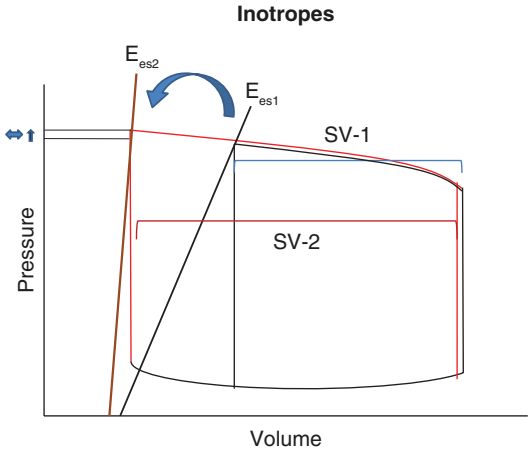

Fig. 7.6 The hemodynamic effect of inotropes. The net effect is a leftward shift in the end-systolic pressure-volume relation (LV end-systolic elastance ($E_{es1} \rightarrow E_{es2}$)) indicating augmented contractility, which results in improved cardiac performance as indicated by the increased stroke volume (SV2 > SV1). Black = baseline hemodynamic profile; red = hemodynamic profile after intervention

adenylate cyclase to produce cyclic AMP (cAMP). The generation of cAMP in turn stimulates calcium influx into the cytoplasm, facilitating actin-myosin interactions with the troponin complex to increase inotropy. In the setting of left ventricular heart failure, dobutamine doses as low as 1 mcg/kg/min and up to 20 mcg/kg/min have been used. At infusion rates of dobutamine above 5 mcg/kg/minute, peripheral vascular effects are seen. Binding of dobutamine to β_2-receptors in the smooth muscle cells of the vasculature also leads to the generation of cAMP. In contrast to its actions on the heart, cAMP activates cAMP-dependent protein kinase (CAMK) within the smooth muscle cells of the vasculature, which causes intracellular reuptake of cytoplasmic calcium by the sarcoplasmic reticulum, thereby leading to vessel relaxation [15]. This effect is counteracted to some extent by the stimulation of alpha-receptors within the vessel wall, which causes peripheral vasoconstriction. The overall effect of dobutamine, however, favors increased myocardial contractility and mild vasodilatation. Advantages of dobutamine include its short half-life (2 minutes) and minimal peripheral effects, which allows infusion through a peripheral vein. It is metabolized by the liver without known active metabolites and is safe to use in patients with renal dysfunction.

Isoproterenol

Isoproterenol is a non-selective beta-receptor agonist which acts as a potent chronotropic and inotropic agent. It is most often used in the setting of cardiogenic shock due to bradycardia in post cardiac transplantation patients. It is also effective in suppressing some ventricular tachycardia arrhythmias [17]. While isoproterenol can augment cardiac output, it has peripheral vasodilatory effects, so no significant change in blood pressure is noted. Therefore, it is not indicated as monotherapy for cardiogenic shock. Like dobutamine, isoproterenol possesses minimal alpha-receptor activity and may therefore be administered through a peripheral vein.

Milrinone

Milrinone is a selective phosphodiesterase (PDE) III inhibitor that prevents the degradation of cAMP and therefore increases intracellular cAMP in cardiac tissue [14, 18]. Hence, this agent operates downstream of the ß-receptor pathway but through its effects results in an increase in intracellular calcium, which augments myocardial contractile function. Compared to dobutamine, milrinone has slightly more potent vasodilatory effects in the periphery through the inhibition of PDE III actions within the pulmonary and peripheral vasculature. Thus, in addition to its positive inotropic effects on the heart, milrinone also reduces afterload and left atrial pressure and enhances LV diastolic relaxation effects. Like dobutamine, milrinone is indicated for severe left ventricular dysfunction. Milrinone may be more beneficial than dobutamine in patients already receiving chronic beta-blockade therapy [19]. In patients with resolving cardiogenic shock, milrinone allows the addition of beta-blocker oral therapy when patients are clinically better compensated, thereby ensuring a more optimal transition to oral heart failure medical management [20]. However, short-term use of milrinone for mild-to-moderate heart failure

exacerbations has not been shown to decrease hospital length of stay and has been associated with an increase in arrhythmias [14]. Compared to dobutamine, no difference in clinical outcomes or arrhythmogenicity has been demonstrated [19]. One disadvantage of milrinone is that it is eliminated by the kidneys, so it should be avoided or administered at a reduced dose in patients with severe renal dysfunction.

Levosimendan

Levosimendan is a calcium-sensitizing agent indicated for the short-term treatment of severe acute decompensated heart failure. It is associated with increased calcium sensitivity of the troponin protein complex, thereby improving myocardial contractility [21, 22]. This is achieved without altering the intracellular concentration of calcium, which minimizes any effects on diastolic relaxation properties. Additionally, it activates potassium-ATP channels in the smooth muscle cells of the vasculature and mitochondria, promoting vasodilatation and possibly affording cardioprotection from myocardial ischemia (although this latter property is controversial and requires further study) [21]. The drug is contraindicated in the setting of severe liver or kidney impairment, and is limited by its side effects, which include an increased risk of atrial fibrillation, ventricular arrhythmias, hypotension, and hypokalemia. Although used in many countries it is not yet approved by the federal drug administration (FDA) for use in the United States.

Vasopressors

Vasopressor agents act predominantly in the peripheral vasculature to achieve vasoconstriction. Consequently, use of these agents typically requires administration through a central line to avoid tissue ischemia that can arise when administered through a peripheral intravenous line or as a consequence of extravasation. These agents include dopamine, norepinephrine, epinephrine, and phenylephrine (Table 7.4). The hemodynamic effects of vasopressor agents are illustrated in Figs. 7.7 and 7.8. The predominant vasoconstrictive properties of these agents results in an increase in cardiac afterload via increased systemic vascular resistance. Thus, while capable of increasing the systemic blood pressure, they do

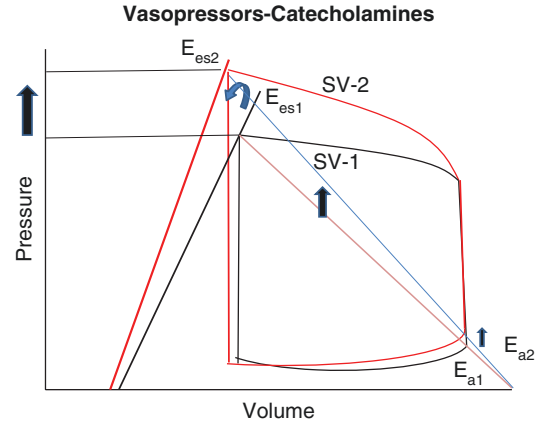

Fig. 7.7 Hemodynamics of catecholamine vasopressor agents. The actions of catecholaminergic vasopressors result in improved contractile function denoted by the slightly leftward shift in the end-systolic pressure-volume relation ($E_{es1} \rightarrow E_{es2}$). However, the dominant effect from these agents is peripheral vasoconstriction leading to an increase in afterload ($E_{a2} > E_{a1}$). Depending on the inotropic effect that these agents confer in comparison to the increased afterload, stroke volume might be expected to increase although to a lesser extent as compared to pure inotropic agents, remain unchanged, or in the setting of an overwhelming increase in afterload, actually decrease (SV1 ≈ SV2). These agents are therefore best suited in cases of vasodilatory shock where their effect in maintaining adequate tissue perfusion pressure is required. Black = baseline hemodynamic profile; red = vasopressor effect; pink = arterial elastance (afterload) at baseline; blue = arterial elastance (afterload) vasopressor effect

Table 7.4 Vasopressor agents

Drug	Brand name	Starting dose	Maintenance and titration
Dopamine	Intropin	3–10 mcg/kg/min	20 mcg/kg/min
Epinephrine	Adrenalin	0.05 mcg/kg/min	0.2–0.8 mcg/kg/min
Norepinephrine	Lovephed	0.02–0.04 mcg/kg/min	0.4–1 mcg/kg/min
Phenylephrine	Neo-Synephrine	100 mcg/min	40–60 mcg/min
Vasopressin	Pitressin	0.01 units/min	0.04 units/min

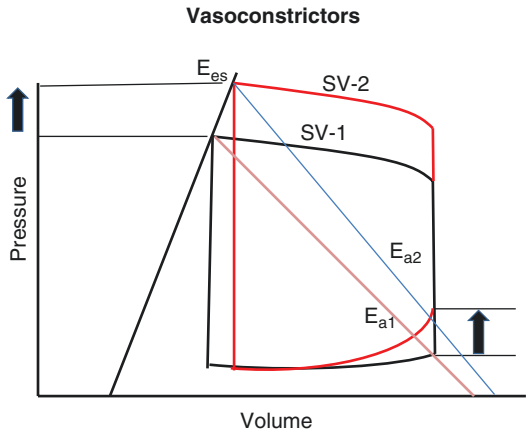

Fig. 7.8 Hemodynamics of pure vasoconstrictors. These agents act primarily to increase the systemic vascular resistance resulting in an upward shift of the pressure-volume relationship. The increase in afterload does not affect intrinsic contractile function but does result in an increase in the end-systolic blood pressure, increased LV end-diastolic pressure, and an increase in the LV afterload ($E_{a1} \rightarrow E_{a2}$). The combined effects result in elevated myocardial oxygen demand and a reduced stroke volume (SV2 < SV1). Therefore, while systemic blood pressure is improved, it comes at the expense of the cardiac output. Black = baseline hemodynamic profile; red = vasoconstrictor effect; pink = arterial elastance (afterload) at baseline; blue = arterial elastance (afterload) vasoconstrictor effect

so at the price of an increased myocardial oxygen demand through elevated heart rate and increased afterload, thereby potentially reducing stroke volume. In the case of the endogenous catecholamine agents such as dopamine, norepinephrine, and epinephrine, these effects are somewhat ameliorated by the slightly enhanced cardiac inotropy.

Catecholamines

Dopamine

Dopamine is an endogenous catecholamine that exhibits unique, dose-dependent pharmacologic actions. Low doses (<5 mcg/kg/min) primarily have dopaminergic receptor (DA1) activity, resulting in vasodilation and increased renal, mesenteric, and coronary blood flow [15]. Historically, low-dose (≤5 mcg/kg/min) dopamine infusion was thought to be renal protective and could aid in the prevention of contrast-induced nephropathy. However, study results have been conflicting and overall show no evidence of a true renal-protective benefit or clinical outcome improvement with renal-dose dopamine [23–25]. Dopamine doses of 3–10 mcg/kg/min will stimulate β_1- and β_2-receptors ($\beta 1 > \beta 2$), enhancing inotropy and chronotropy. At maximal doses of 10–20 mcg/kg/min, alpha-receptor stimulation is dominant and overrides the inotropic effects thereby providing blood pressure support through peripheral vasoconstriction and increased systemic vascular resistance. Due to the increased systemic vascular resistance with doses in this range, myocardial oxygen demand is increased. Pulmonary vein vasoconstriction can occur in patients receiving dopamine, which might compromise the reliability of PCWP measurements as an estimate of left ventricular end-diastolic filling pressures [14, 15].

Norepinephrine and Epinephrine

Norepinephrine and epinephrine are endogenous catecholamines derived from dopamine and characteristically demonstrate mixed receptor activity. Norepinephrine has β_1- and alpha-receptor activity, with lesser affinity for β_2-receptors. This translates clinically into more potent vasoconstrictive properties and less inotropic effects at all dose ranges as compared with dopamine. For this reason, norepinephrine remains the initial catecholamine of choice for septic or vasodilatory shock. Epinephrine is the most potent agonist for the β_1-, β_2-, and alpha-receptors. Use of continuous epinephrine infusion is limited by adverse effects such as cardiac arrhythmias, tissue ischemia, tachycardia, hyperglycemia, cerebral hemorrhage, pulmonary edema, and diminished splanchnic blood flow. As such, epinephrine should be reserved for patients who are unresponsive to dopamine or norepinephrine [8, 14, 26].

Epinephrine bolus dosing in the range of 0.5–1 mg IV (0.1–0.5 mg intracardiac or 0.1 mg/kg via endotracheal tube) has a role in advanced cardiac life support algorithms such as treatment of pulseless ventricular tachycardia, ventricular fibrillation, asystole, or pulseless electrical activity. Another emergent use is in anaphylactoid

reactions to medications, or more commonly contrast. In this setting, depending on the degree of compromise, different doses and routes of epinephrine administration may be appropriate. For systemic anaphylactoid reactions (i.e., hypotension, vasodilatory shock), epinephrine should be given emergently as an intravenous bolus dose of 10 mcg. This dose should be repeated in 1-minute intervals until an intravenous infusion of epinephrine can be initiated or until the patient's hemodynamics have been adequately stabilized. For less severe reactions, epinephrine 0.3–0.5 mg (0.3–0.5 mL of 1:1000 solution) can be given subcutaneously or intramuscularly. Repeated doses are often necessary while steroids and other symptomatic treatments take effect.

Pure Vasoconstrictors

Phenylephrine

Phenylephrine acts as a pure alpha-receptor agonist with almost no β-receptor activity. Consequently, it is a potent vasoconstricting agent and is ideal for the treatment of anesthetic- or vasovagal-induced hypotension as well as vasodilatory shock. Dosing typically begins at 100–180 mcg/min until blood pressures are stable and then infusion is decreased to a maintenance dose of 40–60 mcg/min. The potent vasoconstrictor activity may cause a reflexive decrease in adrenergic drive. Hemodynamically, the dominant effect is an increase in afterload (Fig. 7.8). Therefore, caution should be used in patients with myocardial ischemia or heart failure-induced shock, where inotropy and reduced afterload is needed. Table 7.5 summarizes the hemodynamic effects of vasopressors and inotropes.

Vasopressin

Vasopressin is an endogenous non-catecholamine vasopressor agent secreted primarily by the pituitary gland in response to various physiological stimuli including hypotension, intravascular volume depletion, increased serum osmolality, pain, and hypoxia [8, 14]. It can also be released to a lesser extent by the adrenal glands and myocar-

Table 7.5 Hemodynamic effects of vasopressors and inotropes[a]

Drug type, generic (brand)	HR	MAP	PCWP	SVRI	CO	Receptor activity
Vasopressors						
Dopamine	↑↑					
<3		0	0	0	0	D > b1
3–10		↑	↑	0	1	b1 > b2 > D
>10		↑↑	↑↑	↑	↑	a1 > b1 >> b2
Epinephrine	↑↑↑					
<0.05		0	0	0/↓	↑↑↑	b1 >> b2
0.05–0.15		↑	↑↑	↑	↑↑↑	b1 > a1 > b2
>0.15		↑↑	↑↑	↑↑↑	↑↑	a1 > b1
Norepinephrine	↑↑	↑↑↑	↑↑↑	↑↑↑	0	a1 >> b1
Phenylephrine	0	↑↑	↑↑	↑	0	a1
Vasopressin						
Inotropes						
Dobutamine (Dobutrex[1])	↑					b1 > b2 > a1
2–10		↑	↓	↑	↑	
10–20		0/↓	↓	0/↓	↑↑	
Isoproterenol (Isuprel[1])		↓↓	↓↓	↓↓↓	↑↑↑	b1 >> b2
Amrinone (Inocor[1])	↑	0	↓	↓↓	↑	PDE III inhibitor
Milrinone	↑	↓↓	↓	↓↓	↑↑	PDE III inhibitor
Levosimendan	0	↓↓	↓	↓↓	↑↑	Ca sensitizer

[a]All listed doses are in mcg/kg/min

D dopamine receptor, *b1* beta 1, *b2* beta 2, *a1* alpha, *v1* vasopressin receptor; *PDE* phosphodiesterase, *Ca* calcium

dium in response to circulating catecholamines and increased wall stress, respectively. Vasopressin binds to two receptors, V_1 and V_2. The V_1 receptors are further classified into V_{1a} and V_{1b} subtypes depending on their localization. For example, V_{1a} receptors are primarily found in the smooth muscle cells of the blood vessels, and V_{1b} receptors are localized to the pituitary gland. V_2 receptors are found exclusive in the renal collecting duct. Whereas stimulation of V_{1a} receptors through binding by vasopressin results in vasoconstriction, binding of V_2 receptors causes retention of water by the kidney. These effects result in an increase in both afterload and preload, thereby raising systemic blood pressure and potentially augmenting cardiac output by invoking Frank-Starling forces on the heart [26, 27]. The effect on afterload, however, predominates and limits any potential increase in cardiac output. Additionally, its vasoconstrictive effects on the coronary and cerebral circulations are relatively mild in comparison to catecholaminergic vasopressor agents. Its primary utility is in the treatment of vasodilatory shock and advanced cardiac life support for cardiac arrest algorithms [28]. One potential advantage of vasopressin, over epinephrine is in patients with acidosis, as catecholamine response is diminished in patients with low pH and in hypoxic environments. Fixed-dose vasopressin infusions are recommended as add-on therapy to norepinephrine in patients with vasodilatory shock as vasopressin may augment the vascular sensitivity to norepinephrine and improve its vasopressor effect.

Conclusion

Although advances in mechanical circulatory support have greatly aided the management of patients presenting with cardiogenic shock, vasoactive pharmacologic agents remain the mainstay of treatment. Therefore, it is imperative that cardiac critical care practitioners understand the pharmacologic and hemodynamic effects of these agents in order to provide better patient care.

Bullet Point Summary

- Intravenous vasodilators, such as nitroglycerin, nitroprusside, and nesiritide play an important role in the management of patients with acute decompensated heart failure associated with volume overload and elevated systemic vascular resistance.
- Inotropic agents dobutamine and milrinone operate at different levels along the ß-receptor pathway to augment ventricular contractility.
- Vasopressors should be used for short-term improvement in perfusion pressures in patients with shock (following adequate fluid resuscitation).
- Selection between vasoactive agents is based on the differences in pharmacology, hemodynamic expectations, and specific clinical scenarios.
- Vasopressin provides only mild vasoconstriction as monotherapy but the effect is magnified when co-administered with IV catecholamine in patients with vasodilatory shock.
- Epinephrine is versatile and may be administered IV, via ET tube, or intracardiac in ACLS, as continuous infusion in certain patients with shock, or IM or SQ in anaphylaxis.
- Esmolol is not a vasodilator and currently has a very limited role in the management of patients presenting with shock.

Case 1

A 57-year-old man with a history of non-ischemic cardiomyopathy (LVEF 30%) presents to the emergency department after 4 weeks of progressive dyspnea, non-productive cough, leg swelling, and reduced urine output. He had been treated at urgent care facilities for community acquired pneumonia but his symptoms persisted and worsened. On presentation, his vital signs are BP 120/95 mmHg, HR 104 bpm. He is afebrile and breathing at a rate of 30 breaths per minute. Oxygen saturation on room air is 90%. Physical examination findings show a well-developed male in respiratory distress. Neck examination shows jugular venous distension and bilaterally

diminished carotid upstrokes. The chest reveals bilateral crackles up to the middle lung fields bilaterally. Cardiac examination demonstrates a regular rate, tachycardia, with a sustained and displaced PMI, soft S1S2, audible S3 gallop, and 3/6 systolic murmur heard best at the apex. The abdomen shows evidence of hepatoabdominal reflux and hepatomegaly. The extremities are warm. An ECG shows diffusely low voltage, sinus tachycardia, 105 bpm, a left anterior fascicular block and no evidence of acute myocardial ischemia. A chest x-ray shows bilateral pulmonary edema. An arterial line and central line are placed and nitroprusside is administered. He is placed on supplemental oxygen and given IV diuretics. Within several minutes, the BP is now 100/60 mmHg, HR 90 bpm and the patient reports being able to breath easier. His urine output and his oxygenation have improved.

Question 1:

In the triage of this patient, which of the following hemodynamic profiles would best describe this patient?

A. Warm, dry
B. Warm, wet
C. Cold, dry
D. Cold, wet

Question 2:

The hemodynamic effect of the treatment given is expected to result in which of the following?

A. Shift the end-systolic pressure-volume relation leftward, thereby increasing stroke volume.
B. Shift the end-systolic pressure-volume relation rightward, thereby increasing stroke volume.
C. Reduce afterload and thereby increase stroke volume.
D. Reduce preload more than afterload and thereby increase stroke volume.

Question 3:

The patient develops a fever on hospital day 2 and becomes hypotensive and tachycardic. Physical examination demonstrates resolved jugular venous distention, improved peripheral edema, and warm extremities. Laboratory studies show a mild leukocytosis. Blood cultures are drawn although results are not yet available. The next best course of action would be which of the following:

A. Start broad-spectrum IV antibiotics, continue IV nitrate and diuretic therapy for decompensated heart failure.
B. Discontinue IV nitrate and diuretic therapy. Withhold antibiotics until culture results are returned.
C. Obtain a procalcitonin level and continue with IV nitrate and diuretic therapy.
D. Start broad-spectrum IV antibiotics, discontinue IV nitrate and diuretic therapy, and consider the need for vasopressor support.

Case 2

A 70-year-old man with CAD and ischemic cardiomyopathy returned from a trip abroad with complaints of fatigue, chest pressure, and progressive dyspnea with minimal exertion. At his last clinic visit 6 months ago prior to his trip, the patient was able to play golf and climb 2 flights of stairs without difficulty. He has been compliant with his medical therapy which includes carvedilol 25 mg BID, sacubitril/valsartan 49/51 mg BID, hydralazine 50 mg TID, isosorbide mononitrate 30 mg daily, and spironolactone 25 mg daily. He was hospitalized with acute decompensated heart failure and pulmonary edema, and treated with IV diuretics. Although he responded initially to this treatment, by hospital day 2 he no longer responded to treatment and his urine output declined precipitously. He developed respiratory failure and was ultimately placed on mechanical ventilatory support. A right heart catheterization was performed which showed the following: SBP 85/50 mmHg, HR 110 bpm, RAP 18 mmHg, RV 68/15, PA pressure 70/30/43, PCWP 28 mmHg, CO 3.6 L/min by thermodilution, CI 1.8 L/min/m^2.

Question 4:

The most appropriate next step in the management of this patient would be which of the following?

A. Discontinue oral medications and begin IV inotropic support.
B. Stop beta-blocker and begin dopamine IV infusion.

C. Discontinue oral medications except carvedilol; add milrinone infusion for inotropic support; continue IV diuresis.
D. Continue oral medications, begin milrinone infusion, and continue IV diuresis.

Question 5:
The combined effect of inotropic support and vasodilator medical therapy would be expected to cause which of the following hemodynamic profiles?

A. A shift of the end-systolic pressure-volume relation leftward, causing stroke volume to increase.
B. A reduced afterload and shift of the end-systolic pressure-volume relation leftward.
C. A reduced afterload and no net change in the end-systolic pressure-volume relation.
D. A reduced preload and afterload and a shift of the end-systolic pressure-volume relation to the left.

Case 3

A 60-year-old woman with a history of diabetes mellitus, HTN, and CKD4 is admitted with an acute anterior ST elevation myocardial infarction. She is immediately transferred to the cardiac catheterization laboratory where she undergoes an emergent diagnostic cardiac catheterization and percutaneous coronary intervention to a thrombotic occlusion of the proximal left anterior descending coronary artery. The patient is noted to have obstructive coronary artery disease in the right coronary artery and a large obtuse marginal branch of the left circumflex coronary artery as well, but these were not intervened upon. A right heart catheterization is also performed and shows the following: RAP 10, RV 35/12, PA pressure 40/25/30, PCWP 25, CO 4.1 L/min/m^2, CI 2.3 L/min/m^2. The patient emerges from the cardiac catheterization lab intubated and sedated. She is receiving infusions of dobutamine, norepinephrine, dopamine, and phenylephrine. Her vitals are as follows: BP 100/70 mmHg, HR 120 bpm, T 37C. An echocardiogram is performed demonstrating severe LV systolic dysfunction with an estimated LV ejection fraction of 20% and global hypokinesis.

Question 6:
In order to optimize cardiac performance, which of the following strategies is most appropriate for this patient?

A. Continue current medical therapy.
B. Wean vasopressor agents while maintaining inotropic support.
C. Add IV diuretic therapy.
D. Prepare for mechanical circulatory support.

Answers

1. B

   The clinical profile that best describes this patient is warm and wet. Clinical findings indicate signs of volume overload are present, and hence, the patient is wet. Furthermore, the patient is warm to palpation, a clinical finding that suggests adequate perfusion. This information can be further supplemented by laboratory and imaging studies. In contrast, a warm/dry profile implies either a normal hemodynamic profile or a patient with adequate perfusion who is intravascular volume depleted. A cold/wet profile implies grossly inadequate tissue perfusion and volume overload, whereas a cold/dry profile suggests inadequate perfusion and intravascular volume depletion.

2. C

   The primary hemodynamic effect of IV vasodilator therapy is a reduction in afterload. This reduction in afterload improves cardiac performance, which may result in an increased stroke volume. This is accomplished without changing the end-systolic pressure-volume relation and without appreciably altering preload. Although the improved cardiac performance can enhance diuresis and therefore reduce preload, the dominant effect of vasodilator therapy is a reduction in afterload.

3. D

   A change in the patient's clinical status is often accompanied by a change in hemodynamics. Therefore, recognition of these changes is imperative to guide changes in treatment strategy. In the case scenario, the patient has developed a bacteremia and clinical signs of septic shock. Thus, despite the

fact that the patient presented initially with signs of acute decompensated heart failure associated with volume overload and was treated with IV vasodilator therapy and diuretics, the clinical circumstances now dictate that the patient requires treatment for septic shock which includes IV antibiotics, volume resuscitation, and potentially vasopressor therapy.

4. D

This patient presents with cardiogenic shock characterized by abnormally low cardiac output and elevated right and left heart filling pressures. The calculated systemic vascular resistance is normal, likely a manifestation of the patient's chronic heart failure therapy. Therefore, the patient is most likely to be helped by an augmentation of LV contractility with the use of inotropes. The elevated right and left ventricular filling pressures are consistent with a volume-overloaded state and suggest that aggressive diuresis is indicated. Discontinuation of the patient's chronic heart failure therapy would likely increase afterload and compromise any potential gain from using inotropic agents. In the event that oral therapy cannot be administered, IV vasodilators may be given. Several studies have also shown that abrupt discontinuation of beta-blockers is associated with adverse clinical outcomes, including an increased risk of ventricular arrhythmias.

5. B

The expected hemodynamic effects of combined vasodilator and inotropic effects include a leftward shift in the end-systolic pressure-volume relation (steeper slope) indicating an improvement in LV contractile function. Simultaneously, the predominant effect of vasodilator therapy would be to reduce afterload, resulting in a reduction of end-systolic pressure. The combined effect is to improve cardiac performance and increase cardiac output.

6. B

According to the right heart catheterization findings, the patient is maintaining a cardiac index, which is borderline normal. Calculated systemic vascular resistance is elevated and the patient is normotensive and tachycardic. Together, these findings suggest that the patient's afterload is inordinately high and is likely due to the effects of the vasopressor agents the patient is receiving. Therefore, the gradual removal of these agents would be expected to further improve cardiac performance and may allow for the eventual discontinuation of inotropic support as well. Ultimately, revascularization of the remaining non-culprit obstructive CAD lesions identified at the time of diagnostic cardiac catheterization prior to hospital discharge will provide the best chance for recovery of LV systolic function.

References

1. Tuchschmidt J, Fried J, Astiz M, et al. Elevation of cardiac output and oxygen delivery improves outcome in septic shock. Chest. 1992;102(1):216–20.
2. Felker GM, O'Connor CM. Inotropic therapy for heart failure: an evidence based approach. Am Heart J. 2001;142(3):393–401.
3. Taylor RR, Covell JS, Sonnenblick EH, Ross J Jr. Dependence of ventricular distensibility on filling of the opposite ventricle. Am J Phys. 1967;213(3):711–8.
4. The CONSENSUS Trial Study Group. Effects of enalapril on mortality in severe congestive heart failure. Results of the Cooperative North Scandinavian Enalapril Survival Study (CONSENSUS). N Engl J Med. 1987;316(23):1429–35.
5. Mullens W, Abrahams Z, Francis GS, et al. Sodium nitroprusside for advanced low-output heart failure. J Am Coll Cardiol. 2008;52(3):200–7.
6. Gruppo Italiano per lo Studio della Sopravvivenza nell'infarto Miocardico. GISSI-3: effects of lisinopril and transdermal glyceryl trinitrate singly and together on 6-week mortality and ventricular function after acute myocardial infarction. Lancet. 1994;343(8906):1115–22.
7. Flather M, Pipilis A, Collins R, et al. Randomized controlled trial of oral captopril, of oral isosorbide mononitrate and of intravenous magnesium sulphate started early in acute myocardial infarction: safety and haemodynamic effects. ISIS-4 (Fourth International Study of Infarct Survival) Pilot Study Investigators. Eur Heart J. 1994;15(5):608–19.
8. Opie L, Gersch B, editors. Drugs for the heart. 6th ed. Philadelphia: Elsevier; 2005. p. 161–2.
9. Dell'Italia LJ, Starling MR, Blumhardt R, et al. Comparative effects of volume loading, dobutamine, and nitroprusside in patients with predominant right ventricular infarction. Circulation. 1985;72(6):1327–35.

10. Morelli A, Ertmer C, Westphal M, et al. Effect of heart rate control with esmolol on hemodynamic and clinical outcomes in patients with septic shock. A randomized clinical trial. JAMA. 2013;310(16):1683–91.
11. Publication committee for the VMAC Investigators. Intravenous nesiritide vs nitroglycerin for treatment of decompensated congestive heart failure. A randomized controlled trial. JAMA. 2002;287(15):1531–40.
12. Silver MA, Horton DP, Ghali JK, et al. Effect of nesiritide versus dobutamine on short-term outcomes in the treatment of patients with acutely decompensated heart failure. J Am Coll Cardiol. 2002;39(5):798–803.
13. O'Connor CM, Starling RC, Hernandez AF, et al. Effect of nesiritide in patients with acute decompensated heart failure. N Engl J Med. 2011;365:32–43.
14. Overgaard CB, Dzavik V. Inotropes and Vasopressors: review of physiology and clinical use in cardiovascular disease. Circulation. 2008;118:1047–56.
15. Leier CV, Heban PT, Huss P, et al. Comparative systemic and regional hemodynamic effects of dopamine and dobutamine in patients with cardiomyopathic heart failure. Circulation. 1978;58(3 pt 1):466–75.
16. Unverferth DV, Magorien RD, Lewis RP, et al. Long-term benefit of dobutamine in patients with congestive cardiomyopathy. Am Heart J. 1980;100(5):622–30.
17. Viskin S. Long QT syndromes and torsade de pointes. Lancet. 1999;354(9190):1625–33.
18. Cuffe MS, Califf RM, Adams KF Jr, et al. Short-term intravenous milrinone for acute exacerbation of chronic heart failure: a randomized controlled trial. JAMA. 2002;287(12):1541–7.
19. Lowes BD, Tsvetkova T, Eichhorn EJ, et al. Milrinone versus dobutamine in heart failure subjects treated chronically with carvedilol. Int J Cardiol. 2001;81:141–9.
20. Kumar A, Choudhary G, Antonio C, et al. Carvedilol titration in patients with congestive heart failure receiving inotropic therapy. Am Heart J. 2001;142:512–5.
21. Nieminem MS, Fruhwald S, Heunks LMA, et al. Levosimendan: current data, clinical use and future development. Heart Lung Vessel. 2013;5(4):227–45.
22. Schumann J, Henrich EC, Strobl H, et al. Inotropic agents and vasodilator strategies for the treatment of cardiogenic shock or low output syndrome. Cochrane Database Syst Rev. 2018:CD009669.pub3. https://doi.org/10.1002/14651858.
23. Bellomo R, Chapman M, Finfer S, et al. Low-dose dopamine in patients with early renal dysfunction: a placebo-controlled randomised trial. Australian and New Zealand Intensive Care Society (ANZICS) Clinical Trials Group. Lancet. 2000;356(9248):2139–43.
24. Marik PE, Iglesias J. Low-dose dopamine does not prevent acute renal failure in patients with septic shock and oliguria. NORA- SEPT II Study Investigators. Am J Med. 1999;107(4):387–90.
25. Kellum JA, M Decker J. Use of dopamine in acute renal failure: a meta-analysis. Crit Care Med. 2001;29(8):1526–31.
26. Bassi G, Radermacher P, Calzia E. Catecholamines and vasopressin during critical illness. Endocrinol Metab Clin N Am. 2006;35(4):839–57.
27. Barrett LK, Singer M, Clapp LH. Vasopressin: mechanisms of action on the vasculature in health and in septic shock. Crit Care Med. 2007;35(1):33–40.
28. Lindner KH, Dirks B, Strohmenger HU, et al. Randomised comparison of epinephrine and vasopressin in patients with out-of-hospital ventricular fibrillation. Lancet. 1997;349(9051):535–7.

8 Recently Approved Pharmacologic Agents to Improve Outcomes in Heart Failure

David C. Booth and Navin Rajagopalan

Introduction and Background

Over the past 5 years, two novel FDA-approved agents for the treatment of heart failure have been introduced, the angiotensin receptor-neprilysin inhibitor (ARNi), sacubitril/valsartan (Entresto), and the funny current (I_f) inhibitor ivabradine (Corlanor). Prior to the approval of these agents, hemodynamic optimization – using vasodilators including hydralazine and isosorbide [1, 4, 5] – and neuro-humoral inhibition, combining angiotensin-converting enzyme inhibition, ß-blockade, and mineralocorticoid-receptor antagonism [2, 3, 6–11], have been the evidence-based pharmaceutical approaches to improve outcome in chronic systolic heart failure. The majority of the agents tested in the referenced trials rested on a background of proven hemodynamic benefit. There is a relative paucity of published hemodynamic data for sacubitril/valsartan and ivabradine, as randomized trials for these agents in systolic heart failure have been endpoint-driven. This chapter summarizes the outcome data, quality of life results, and available hemodynamic data for these two drugs. Other modalities which have been shown to improve survival in systolic heart failure include the implantable cardioverter defibrillator, cardiac resynchronization therapy, and left ventricular assist device implantation, but these are not discussed here.

Rationale and Research Leading to Sacubitril/Valsartan

Heart failure activates the sympathetic nervous system (SNS) and the renin-angiotensin-aldosterone system (RAAS), leading to vasoconstriction and increased sympathetic tone, in turn resulting in downregulation of the ß-receptors. Activation of RAAS leads to increased secretion of angiotensin II and aldosterone, which also results in increased ADH secretion. These neurohormonal maladaptations result in fluid retention, perpetuating the cycle of heart failure. ACE inhibition, or angiotensin receptor blockade, ß-blockade, and mineralocorticoid antagonism modulate the effects of the SNS and RAAS.

Since the early 1980s, the natriuretic peptide system (NPS) began to receive attention as a potential target in heart failure treatment. Within the NPS are three hormones, atrial natriuretic peptide (ANP), B-type natriuretic peptide (BNP),

D. C. Booth (✉)
The Gill Heart and Vascular Institute, University of Kentucky Medical Center, Lexington, KY, USA
e-mail: dcbooth@email.uky.edu

N. Rajagopalan
Heart Failure/Cardiac Transplant Program, The Gill Heart and Vascular Institute, Lexington, KY, USA
e-mail: n.rajagopalan@uky.edu

A. T. Askari, A. W. Messerli (eds.), *Cardiovascular Hemodynamics*, Contemporary Cardiology,
https://doi.org/10.1007/978-3-030-19131-3_8

and C-type atrial natriuretic peptide (CNP). While CNP is secreted from endothelial cells and cardiac fibroblasts and has vasodilatory and anti-remodeling effects, ANP and BNP are secreted, respectively, from the atria and the ventricles, are released in response to fiber stretch and volume overload and promote diuresis, natriuresis, and vasodilation, counteracting the maladaptive effects of SNS and RAAS activation [12]. With the development of angiotensin receptor blockers, which exert their effects primarily at the Type 1 angiotensin II receptor, there was hope that a more specific RAAS antagonist would result in further survival improvement in heart failure outcomes. However, while the Valsartan Heart Failure Trial (Val HeFT) [13] (2001) demonstrated reduced heart failure hospitalizations, leading to an FDA-approved indication in heart failure, overall mortality in the valsartan and placebo groups was similar. The demonstration of the beneficial effects of the natriuretic peptides led to the development of human recombinant BNP, namely nesiritide, which was FDA-approved for use in 2001 on the basis of improvement in dyspnea in decompensated heart failure. However, a larger randomized trial released in 2011, the Acute Study of Clinical Effectiveness of Nesiritide in Decompensated Heart Failure (ASCEND-HF) [14], demonstrated no improvement in dyspnea, 30-day mortality, or readmission rates in the nesiritide group. Hypotension was significant in the nesiritide group. As a result, nesiritide is used rarely in practice today, but natriuretic peptide levels remain well established as biomarkers.

Research efforts have been directed at toward identifying agents that could inhibit the enzyme that breaks down endogenous natriuretic peptides, namely, neprilysin. Neprilysin (NEP) is a neutral endopeptidase, and its inhibition increases bioavailability of natriuretic peptides, bradykinin, and substance P, resulting in natriuretic, vasodilatatory, and anti-proliferative effects. The natural hypothesis was that combined inhibition of the RAAS and NEP would result in a better heart failure treatment (Fig. 8.1). This led to the development of omapatrilat, a combined ACEi/NEPi. Several trials of the agent were conducted in heart failure, culminating in the Omapatrilat Versus Enalapril Randomized Trial of Utility in Reducing Events (OVERTURE) Trial [15] in patients with NYHA Functional Class II–IV heart failure. While post hoc analyses appeared to demonstrate potential benefit, there was an increased incidence of life-threatening angioedema, which was substantiated in a subsequent study of the agent in hypertension. These results effectively thwarted ACEi-NPi as a treatment in heart failure.

An important advantage of ARBs over ACE is is that ARBs do not block the degradation of bradykinin, the principal instigator of cough, a side effect noted in at least 10% of patients on an ACE, and do not cause angioedema which can occur in about 0.1% of patients on an ACE [16]. Omapatrilat was subsequently demonstrated to inhibit an enzyme responsible for bradykinin metabolism. A logical solution to the adverse effects of omapatrilat was to combine an ARB with an NEPi, termed ARNI or angiotensin receptor-neprilysin inhibitor – LCZ696, Sacubitril/Valsartan. Sacubitril is a prodrug which is converted in the body to sacubitrilat, which inhibits neprilysin and thereby the degradation of NPs. A Phase III trial [17] published in 2010 comparing sacubitril/valsartan to valsartan showed greater reduction in systolic, diastolic, and pulse pressures with sacubitril/valsartan. The Prospective Comparison of ARNI with ARB on Management of Heart Failure with Preserved Ejection Fraction (PARAMOUNT) Trial [18], published in 2012 was a Phase II randomized trial that assessed NT-proBNP after 12 weeks of sacubitril/valsartan compared to valsartan in patients with heart failure with preserved left ventricular ejection fraction (HFpEF). At 12 weeks, NT-proBNP was significantly lower in the sacubitril/valsartan group, and an echocardiographic reduction in left atrial volume and size was also demonstrated. The NT-proBNP lowering effect appeared to be independent of a blood pressure lowering effect of the drug.

Published in 2014, the Prospective Comparison of ARNI with ACEI to Determine Impact on Global Mortality and Morbidity in Heart Failure (PARADIGM-HF) trial randomized 8399 patients with HFrEF (LVEF $\leq$40%) and NYHA Class II–IV symptoms to sacubitril/valsartan 200 mg PO BID or enalapril 10 mg PO BID (the

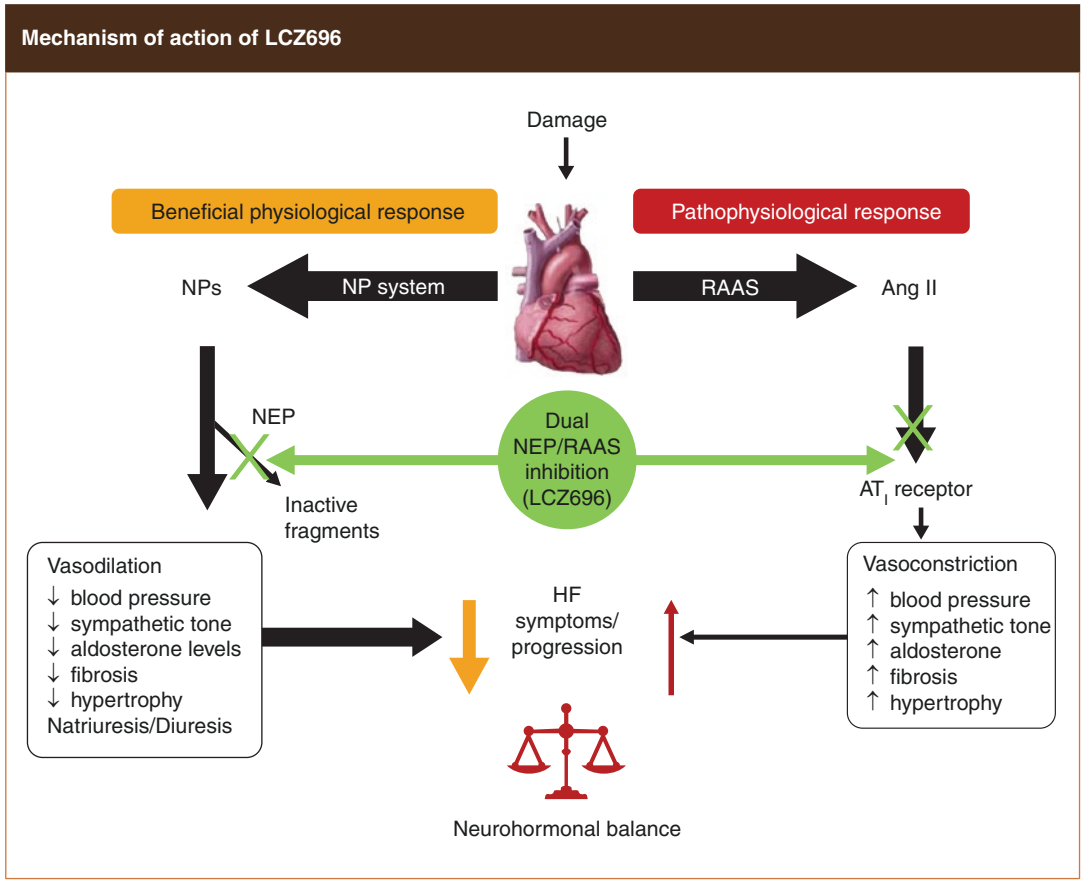

Fig. 8.1 Angiotensin receptor-neprilysin inhibitors have the potential to modulate two counter-regulatory neurohormonal systems in HF: the renin-angiotensin-aldosterone system and natriuretic peptide system. ANG angiotensin, AT1 angiotensin type 1, HF heart failure, NP natriuretic peptide, RAAS renin-angiotensin-aldosterone system. (Indian Heart Journal Volume 70, Supplement 1, July 2018, Pages S102–S110)

goal dose from CONSENSUS and SOLVD), in addition to standard therapy for chronic systolic heart failure. The majority of the study population was receiving ß-blockers and mineralocorticoid antagonists. The primary end point of the trial was the combination of death from cardiovascular causes and heart failure hospitalization. There being insufficient Phase II safety data for sacubitril/valsartan, the PARADIGM protocol stipulated safety and tolerability run-ins for all participants in the trial. If participants tolerated both sacubitril/valsartan and enalapril, they were randomly assigned to the two study arms. This approach allowed assessment not only of the end point of the trial but also provided safety and tolerability data. The study was stopped early, after median follow-up of 27 months, when the study met the prespecified cutoff for significant benefit. The ARNI combination resulted in a 20% decrease in the primary end point, HR = 0.80, $P < 0.001$, giving a Number Needed to Treat of 21. The study drug also reduced the individual components of the combined end point, death from cardiovascular cause by 20% and heart failure hospitalizations by 21%, both $p < 0.001$. All-cause mortality in the sacubitril/valsartan arm was reduced by 16%, HR = 0.84, $p < 0.001$. While sacubitril/valsartanb resulted in 14% experiencing hypotension as compared to 9% in the enalapril arm, the discontinuation rate was not significantly different (sacubitril/valsartan 0.9%, enalapril 0.7%). No significant difference was noted in the occurrence of non-serious angioedema between the two groups.

In secondary analyses, sacubitril/valsartan demonstrated clinical benefits in other indices of heart failure progression, including improved NYHA class, reduced need for intensification of medical treatment, and reduction in the need for emergency department visits, intensive care, and inotropic support. Other findings from PARADIGM-HF include significantly lower NT-proBNP and troponin levels in the sacubitril/valsartan group, significant reduction in the incidence of sudden cardiac death and death from worsening heart failure independent of cardioverter defibrillation implantation, and a nonsignificant reduction in the need for left ventricular assist device implantation and cardiac transplantation. The PARADIGM-HF investigators also carried out a comparison of the sacubitril/valsartan arm with the treatment arms of the SOLVD Trial (enalapril) and the CHARM-Alternative Trial [19] (candesartan) and found substantial relative risk reductions for both the composite end point and for cardiovascular death. Using the Kansas City Cardiomyopathy Questionnaire, the PARADIGM-HF investigators [20] demonstrated remarkable improvement in physical and social activity limitations with sacubitril/valsartan compared to enalapril. The largest improvements were reported in household chores ($p < 0.001$) and sexual relationships ($p = 0.002$); these benefits persisted through 36 months of assessment. In another secondary analysis [21], the PARADIGM-HF investigators found the frequency of episodes of hyperkalemia to be significantly greater in the enalapril arm compared to ARNI, (3.1 versus 2.2 incidents per 100 patient-years, HR = 1.37, CI 1.06–1.76, $p = 0.02$) for patients already taking a mineralocorticoid antagonist.

Criticisms of the PARADIGM-HF Trial include that the study was predominantly white (66%), male (78%), and enrolled predominantly NYHA Functional Class II (70%) patients. Only 5% of the study population was black, perhaps limiting the ability of the study to accurately detect the incidence of angioedema. It has also been suggested that the enalapril dose in PARADIGM-HF was too low [22]. Narrowly defined, only patients with systolic heart failure and an ejection fraction of ≤35% would be candidates for the drug, based on PARADIGM-HF entry criteria. An additional criticism is that neprilysin has been shown to have a role in maintaining homeostasis of amyloid-ß peptide, raising the issue that a neprilysin inhibitor might lead to increased deposits of this protein in brain [11]. However, in a randomized, double-blind trial measuring sacubitril/valsartan levels in cerebrospinal fluid in healthy human subjects [23], sacubitril/valsartan did not cause changes in aggregable amyloid β isoforms compared with placebo, despite achieving CSF concentrations of a metabolite of sacubitril/valsartan sufficient to inhibit neprilysin.

The Prospective Comparison of ARNI with ARB Global Outcomes in HF With Preserved Ejection Fraction (PARAGON-HF Trial) [24], a prospective randomized trial of the impact of sacubitril/valsartan in HFpEF, has completed enrollment and has an estimated study completion date of March 15, 2019 (clinicaltrials.gov). Serial cognitive testing is being carried out in PARAGON-HF in an effort to assess the impact of sacubitril/valsartan on cognition.

In summary, in prespecified measures of nonfatal clinical deterioration of heart failure, the PARADIGM-HF investigators demonstrated that the combination of sacubitril/valsartan prevented the clinical progression of surviving heart failure patients more effectively than did enalapril alone [25]. On the basis of the PARADIGM-HF Trial, sacubitril/valsartan was FDA-approved in July 2015 to reduce the risk of death and hospitalization for heart failure in patients with chronic heart failure (NYHA Class II–IV) and reduced ejection fraction.

The comParIson Of sacubitril/valsartaN versus Enalapril on Effect on nt-pRo-bnp in patients stabilized from an acute Heart Failure (PIONEER-HF) trial (PMID:30415601) enrolled 881 patients with heart failure with reduced ejection fraction who were hospitalized for acute decompensated heart failure at 129 sites in the United States. After hemodynamic stabilization, patients were randomly assigned to receive either sacubitril–valsartan (target dose, 97 mg of sacubitril with 103 mg of valsartan twice daily) or enalapril (target dose, 10 mg twice daily). The primary efficacy outcome was the time-averaged proportional change in the N-terminal pro–B--type natriuretic peptide (NT-proBNP) concentra-

tion from baseline through weeks 4 and 8. Key safety outcomes were the rates of worsening renal function, hyperkalemia, symptomatic hypotension, and angioedema.

The investigators noted that time-averaged reduction in the NT-proBNP concentration was significantly greater in the sacubitril–valsartan group than in the enalapril group. In addition, the two drugs appeared to be equally safe; the rates of worsening renal function, hyperkalemia, symptomatic hypotension, and angioedema did not differ significantly. In an analysis of exploratory clinical outcomes, the in-hospital initiation of sacubitril–valsartan therapy was associated with a lower rate of rehospitalization for heart failure at 8 weeks than enalapril therapy.

Pharmacokinetics of Sacubitril/Valsartan

Absorption of sacubitril/valsartan is rapid, with maximum levels of sacubitril, sacubitrilat, and valsartan all achieved by 2–3 h [26]. With twice-daily dosing, steady-state concentrations are reached within 3 days. Sacubitril is eliminated as predominantly sacubitrilat by the kidney, while valsartan is eliminated by the biliary route. In heart failure patients, area under the concentration-time curves for sacubitril, sacubitrilat, and valsartan was higher. Renal impairment had no impact on sacubitril or valsartan, but increased the area under the concentration-time curve for sacubitrilat. Moderate hepatic impairment increased the area under the concentration-time curve of valsartan and sacubitrilat approximately two-fold. Regarding drug-drug interactions, sacubitril/valsartan increased plasma concentrations of atorvastatin. Pharmacokinetics of the drug were not affected by age, sex, or ethnicity.

Hemodynamic Impact of Sacubitril/Valsartan

Surprisingly little specific functional and hemodynamic data are available regarding sacubitril/valsartan. A post hoc analysis of the PARAGIGM-HF demonstrated that the drug was effective at reducing cardiovascular death and heart failure hospitalization across the spectrum of left ventricular ejection fraction (LVEF), when assessed in stepwise 5-point reductions in LVEF [27]. Addition of sacubitril/valsartan in patients with advanced systolic heart failure may be a useful strategy to improve hemodynamics and to potentially facilitate the transitioning from intravenous HF therapies.

Ivabradine

Background and Pharmacology

The search for a direct sinoatrial node inhibitor began four decades ago. Ivabradine was the first drug specifically developed as a heart rate lowering agent, and in Europe was initially considered for the treatment of angina pectoris. Sinoatrial myocytes have the capacity to develop slow diastolic depolarizations, driving membrane voltage toward the threshold for initiating an action potential (Fig. 8.2). Sinoatrial node activity involves several ionic currents flowing through channels, including the funny or hyperpolarization-activated cyclic nucleotide-gated channel that regulates the I_f current, so-called for its unusual properties compared with other channels at the time of its discovery. The I_f current is carried across the sarcolemma by both sodium and potassium ions, is directly activated by cyclic adenosine monophosphate (cAMP), and is related to I_h neuronal channels. Ivabradine has substantial selectivity for inhibiting the I_f channel at doses that allow heart rate slowing [28]. Studies in experimental models have demonstrated that ivabradine has a pure heart rate lowering effect, does not affect LV contractile state [29], and does not have negative lusitropic properties. In healthy volunteers, equipotent doses of ivabradine (30 mg) and propranolol (40 mg) had similar effects on heart rate and heart rate variability, whereas propranolol was associated with significant systolic and mean blood pressure lowering, and a greater decrease in cardiac output measured noninvasively, compared to ivabradine, placebo, or both [30]. Under fasting conditions, peak plasma ivabradine concentrations are reached in approximately

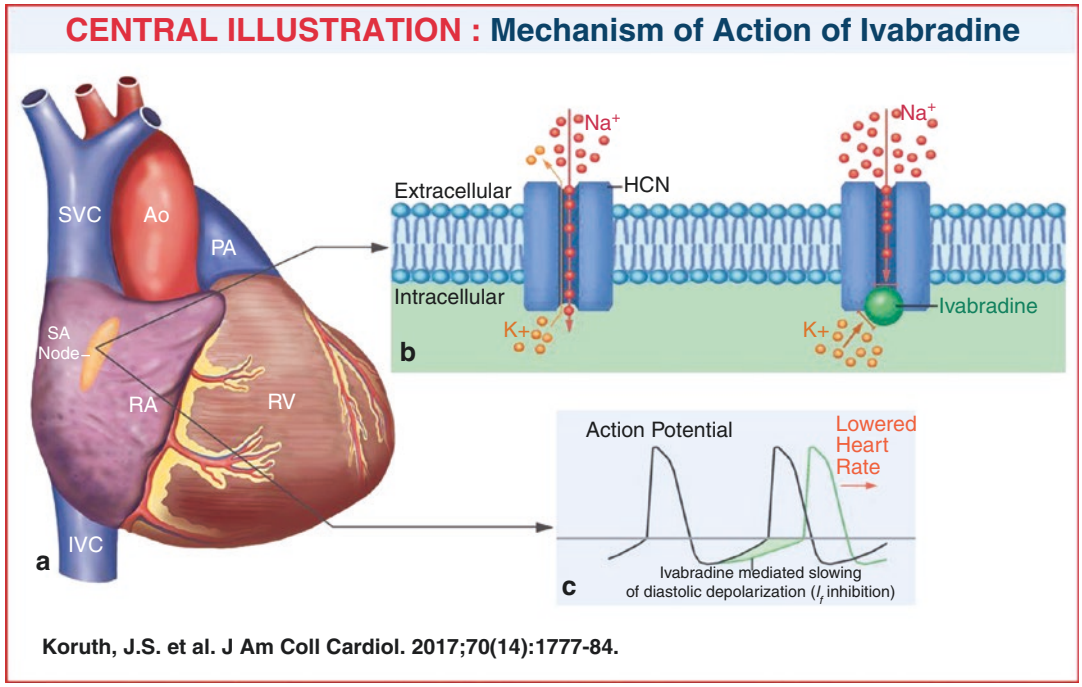

Fig. 8.2 Ivabradine's primary mechanism of action on cardiac tissue is on the sinoatrial (SA) node, which occupies a predominantly subepicardial position at the junction of the superior vena cava (SVC) and the right atrium (RA). (**a**) Heart with position of the Sinoatrial (SA) node. (**b**) In the sinoatrial node, ivabradine blocks the intracellular aspect of the hyperpolarization-activated cyclic nucleotide-gated (HCN) transmembrane channel, which is responsible for the transport of sodium (Na^+) and potassium (K^+) ions across the cell membrane, in the open state. This results in the inhibition of the inward funny current ($\mathbf{I_f}$), which is specifically activated at hyperpolarized membrane potentials. (**c**) By selectively inhibiting $\mathbf{I_f}$, there is a reduction in the slope of diastolic depolarization of the pacemaker action potential (shaded region) and an increase in the duration of diastole, without altering other phases of the action potential. This results in heart rate reduction. Ao aorta, IVC inferior vena cava, PA pulmonary artery, RV right ventricle. (PMID:28958335)

1 hour. Food delays absorption by approximately 1 hour but appears to increase plasma levels of the drug. Ivabradine is extensively metabolized in the liver. The excretion of ivabradine and its metabolites is both renal and hepatic. The half-life of ivabradine and its metabolites requires twice-daily dosing. There is no direct effect of ivabradine on the QT interval. Phosphenes, the off-target effect of ivabradine, are bright sensations not mediated by retinal stimuli, due to effects on hyperpolarization-activated channels in the retina.

While ivabradine was initially targeted as a drug for heart rate control, randomized data failed to demonstrate a significant advantage in patents with stable coronary artery disease without clinical heart failure [31]. Similarly, ivabradine compared to placebo did not significantly improve the change in physical limitation score at 1 year in patients with anginas pectoris [32], although ivabradine patients had better angina scores compared to placebo on the Seattle Angina Questionnaire on every visit to 36 months. Ivabradine did not result in significant exercise tolerance testing benefit, compared to low-dose atenolol, and no advantage was noted when added to full-dose amlodipine [33, 34].

Because of the documented beneficial effect of heart rate lowering in heart failure with reduced ejection fraction, ivabradine was tested in this setting, beginning with the Morbidity-Mortality Evaluation of the I_f Inhibitor Ivabradine in Patients With Coronary Artery Disease and Left Ventricular Dysfunction (BEAUTIFUL) Trial [35], a randomized double-blind, placebo-controlled trial of

10,917 patients. Enrollment characteristics included LVEF <40%, 85% NYHA Class II and III, 83% male, and 87% were taking ß-blockers. At a median of 19 months of follow-up, no difference was found between the ivabradine and placebo groups for the composite end point of cardiovascular death, hospitalization for myocardial infarction (MI), or hospitalization for worsening heart failure. A subgroup analysis of 14% of patients with activity-limiting angina had reduction in hospitalization for MI and borderline reduction in the composite end point ($p = 0.05$); the difference was statistically significant for patients in this subgroup with baseline heart rate ≥ 70 [36].

To investigate the potential benefits on ischemia seen in this subgroup, the SIGNIFY [37] Trial was undertaken, enrolling 19,102 patients with stable coronary artery disease who did not have clinical heart failure. This study again enrolled predominantly male patients; 75% had angina pectoris, and the mean LV ejection fraction was 56%. While heart rate was significantly reduced by ivabradine, there was no significant benefit of ivabradine on the primary composite end point of cardiovascular death or nonfatal MI after median follow-up of 28 months. When the prespecified subgroup with activity-limiting angina was analyzed for the composite outcome, there was in fact evidence of harm with ivabradine therapy; an absolute increase in the composite end point of 1.1% ($p = 0.02$). The reason or reasons for this adverse outcome remain unclear, but the conclusion to be drawn from trials of ivabradine in angina pectoris without LV systolic dysfunction is that no benefit occurs, and even though there may be symptomatic improvement, those patients appear to be at greater risk of an adverse effect of the drug.

The Systolic Heart Failure Treatment with the I_f-inhibitor Ivabradine (SHIFT) Trial [38] randomized 6505 patients with ischemic and nonischemic heart failure, NYHA Class II–IV but predominantly Class II–III, LVEF ≤35%, to ivabradine or placebo. The trial randomized no patients from the United States; most patients were male, 89% taking ß-blockers, 91% ACEi or ARB, 60% aldosterone antagonists, 22% a digitalis preparation. More than two-thirds achieved the target dose of 7.5 mg ivabradine twice daily. Compared to placebo, the composite end point of cardiovascular death or first hospitalization for heart failure was significantly reduced (hazard ratio 0.82, $p < 0.0001$, driven primarily by reduction in HF hospitalization) (Fig. 8.3) Trends were detected for less benefit in patients also receiving ß-blockers and greater benefit for nonischemic patients. There were significant improvements in the NYHA Class and Kansas City Cardiomyopathy Questionnaire summary scores [39]. When patients with baseline heart rate ≥70 from BEAUTIFUL and SHIFT were pooled, no significant impact on mortality could be demonstrated. An echo substudy [40] from SHIFT of 275 patients demonstrated a small but significant increase on LVEF after 8 months of ivabradine therapy (4 ± 10%, $p = 0.004$).

Shortcomings of the SHIFT Trial include that 25% of trial participants were not taking a ß-blocker for HRrEF and that ivabradine did not significantly reduce any end point in patients with baseline HR ≤ 75 bpm. Whereas trials of carvedilol, metoprolol succinate, and bisoprolol demonstrated consistent survival benefit, a similar heart rate reduction by ivabradine resulted in no all-cause survival benefit. Another SHIFT subgroup analysis demonstrated that a statistically significant improvement for the primary end point occurred only for patients <50% of target ß-blocker doses [41]. Thus, ivabradine appeared to exert a beneficial effect only in patients who were also being treated with ß-blockers in whom a heart rate goal of ≤75 bpm had not been achieved. Regarding adverse effects, ivabradine increased the frequency of bradycardia, both asymptomatic and symptomatic, was associated with an increased incidence of atrial fibrillation, and resulted in some ivabradine withdrawals due to phosphenes, which resolved upon discontinuation of drug. The 1.7% increase in the risk of atrial fibrillation noted in pooled BEAUTIFUL and SHIFT data underscore the importance of observing patients on ivabradine for this rhythm disturbance, especially in view of the negative prognostic impact of atrial fibrillation on systolic heart failure. The FDA approved ivabradine in April 2015 for patients with HFrEF

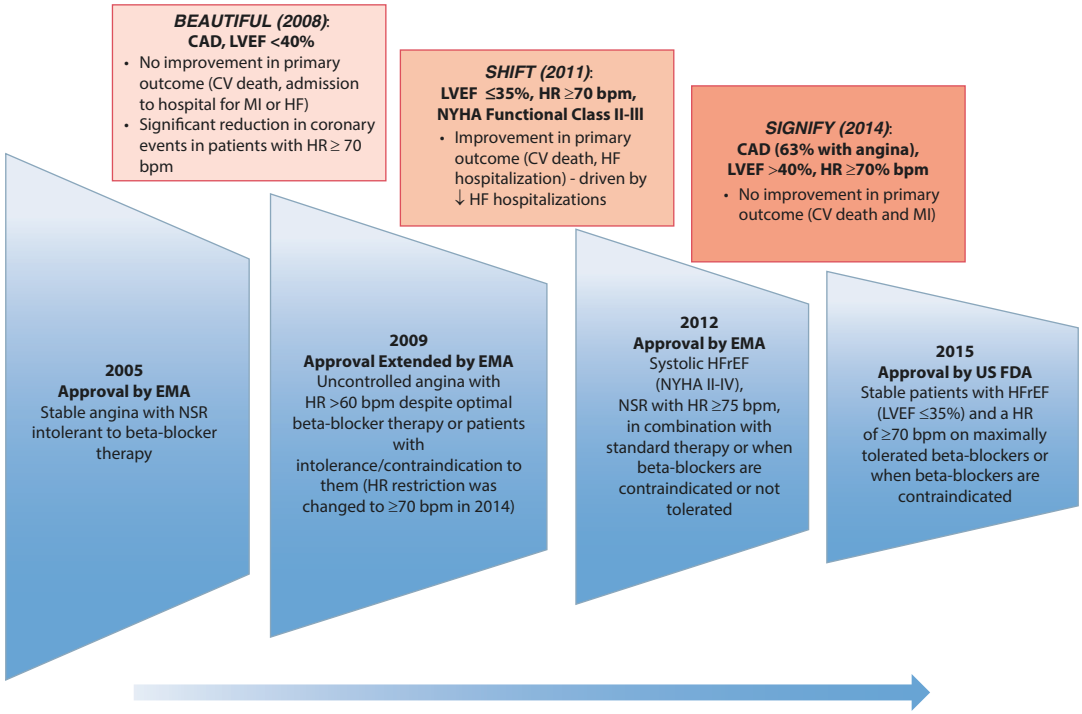

Fig. 8.3 Approval timeline of ivabradine across Europe and the United States. The indications for the use of ivabradine have evolved over time and differ based on region. Since it was first approved for use in angina by the European Medicines Agency (EMA) in 2005, the findings of several randomized controlled trials have resulted in expanded indications to include select heart failure patients and only recent approval by the US Food and Drug Administration (FDA) for this indication. BEAUTIFUL Morbidity-Mortality Evaluation of the I_f-Inhibitor Ivabradine in Patients With Coronary Disease and Left Ventricular Dysfunction, CAD coronary artery disease, CV cardiovascular, HFrEF heart failure with reduced ejection fraction, LVEF left ventricular ejection fraction, MI myocardial infarction, NYHA New York Heart Association, NSR normal sinus rhythm, SHIFT Systolic Heart Failure Treatment with the I_f-Inhibitor Ivabradine Trial, SIGNIFY Study Assessing the Morbidity-Mortality Benefits of the I_f-Inhibitor Ivabradine in Patients With Coronary Artery Disease. (PMID:28958335)

with LVEF ≤35% on a ß-blocker at the maximum tolerated dose, with HR ≥ 70 bpm (Fig. 8.4). The drug is contraindicated in patients with sinus node dysfunction or atrioventricular block. The FDA approval underscores the prerequisite for guideline-based treatment with maximally tolerated ß-blockers proven effective in HFrEF. In such patients in whom HR remains >70–75 beats per minute, the addition of ivabradine is reasonable. For patients with HFrEF who are proven intolerant of ß-blockers, treatment with ivabradine appears reasonable, keeping in mind that while ivabradine results in decreased heart rate, the exact mechanism of benefit remains uncertain.

Questions remain regarding the efficacy of ivabradine. From a recent meta-analysis of the ivabradine trials [42], the authors concluded that while use of ivabradine in patients with HFrEF in sinus rhythm with HR ≥ 70 to reduce HF hospitalization was supported by the literature, the strength of the evidence was such that more widespread adoption of ivabradine in HF would require additional randomized trials. Recent guideline updates [43] emphasize adherence to the ivabradine FDA package indication.

On the other hand, the guidelines advise that for any patient in NYHA Class II–IV HFrEF not on an ARNI, the threshold to consider discontinuing an ACEi or ARB in favor of sacubitril/valsartan should be low [44]. The number of women and ethnicities different from white in many of the foregoing trials is low enough that one might

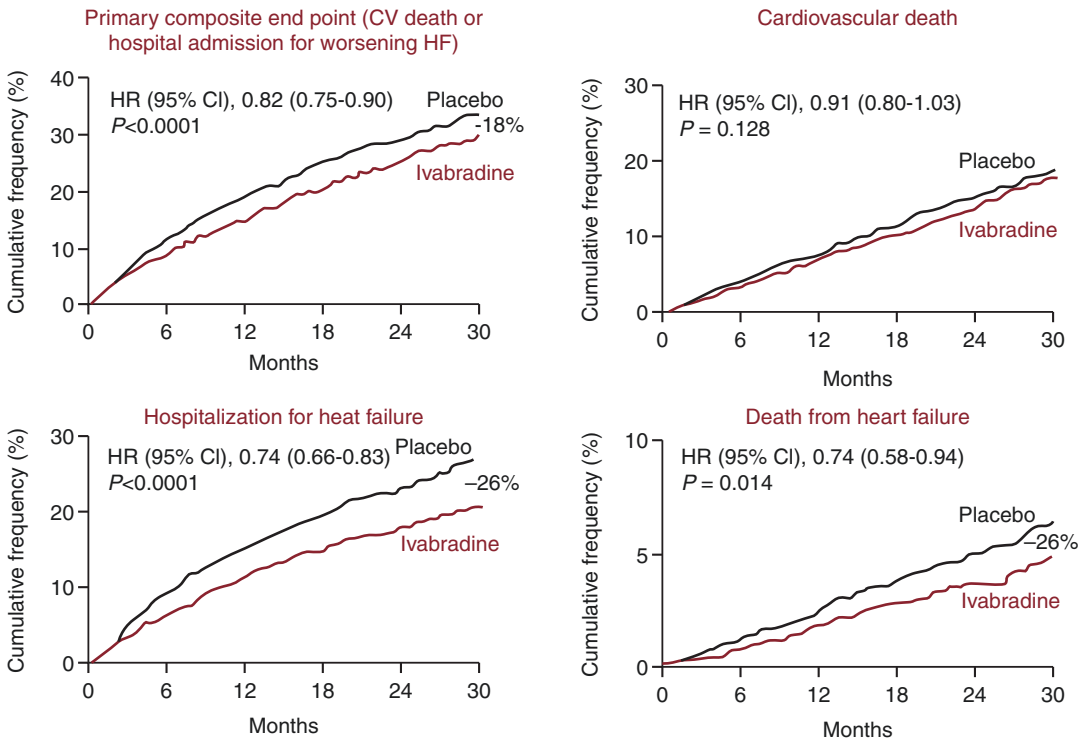

Fig. 8.4 Kaplan-Meier cumulative event curves for different end points in SHIFT. Primary composite outcome (**Panel A**); cardiovascular mortality or heart failure hospitalization and its two components cardiovascular mortality (**Panel B**); heart failure hospitalizations (**Panel C**) and heart failure deaths (**Panel D**) in the ivabradine and the placebo arms. CV cardiovascular, HF heart failure, SHIFT Systolic Heart Failure Treatment with the I_f-Inhibitor Ivabradine Trial. (Swedberg et al.; SHIFT Investigators. Lancet. 2010;376:875–885)

question scientific efficacy of these agents in these populations. For further guidance on the use of sacubitril/valsartan and ivabradine, the reader is referred to the 2017 ACC/AHA/HFSA focused update of the 2013 ACCF/AHA Guideline for the Management of Heart Failure [43] and the 2017 ACC Expert Consensus Decision Pathway for Optimization of Heart Failure Treatment [44].

References

1. Cohn JN, Archibald DG, Ziesche S, et al. Effect of vasodilator therapy on mortality in chronic congestive heart failure. N Engl J Med. 1986;314:1547–52.
2. CONSENSUS Trial Study Group. Effects of enalapril on mortality in severe congestive heart failure. N Engl Med. 1987;316:1429–35.
3. SOLVD Investigators. Effect of enalapril on survival in patients with reduced left ventricular ejection fractions and congestive heart failure. N Engl J Med. 1991;325:293–302.
4. Cohn JN, Johnson G, Ziesche S, et al. A comparison of enalapril with hydralazine-isosorbide dinitrate in the treatment of chronic congestive heart failure. N Engl J Med. 1991;325:303–10.
5. Taylor AL, Ziesche S, Yancy C, et al. Combination of isosorbide dinitrate and hydralazine in blacks with heart failure. N Engl J Med. 2004;351:2049–57.
6. Packer M, Coats AJ, Fowler MB, et al. Effect of carvedilol on survival in severe chronic heart failure. N Engl J Med. 2001;344:1651–8.
7. MERIT-HF Study Group. Effect of metoprolol CR/XL in chronic heart failure: metoprolol CR/XL randomised intervention trial in congestive heart failure (MERIT-HF). Lancet. 1999;353:2001–7.
8. Pitt B, Zannad F, Remme WJ, et al. The effect of spironolactone on morbidity and mortality in patients with severe heart failure. Randomized aldactone evaluation study investigators. N Engl J Med. 1999;341:709–17.
9. Kagawa CM, Sturtevant FM, Van Arman CG. Pharmacology of a new steroid that blocks salt

activity of aldosterone and desoxycorticosterone. J Pharm Exp Ther. 1959;126:123–30.
10. Zannad F, McMurray JJ, Frum H, et al. Eplerenone in patients with systolic heart failure and mild symptoms. N Engl J Med. 2011;364:11–21.
11. Digitalis Investigation Group. The effect of digoxin on mortality and morbidity in patients with heart failure. N Engl J Med. 1997;336:525–33.
12. Srikanth Y, Aronow WS, Mondal P, Chabbott DR. The evolution of natriuretic peptide augmentation in management of heart failure and the role of sacubitril/valsartan. Arch Med Sci. 2017;13:1207–16.
13. Cohn JN, Tognoni G, for the Valsartan Trial Investigators. A randomized trial of the angiotensin receptor blocker valsartan in chronic heart failure. N Engl J Med. 2001;345:1667–1675.
14. O'Connor CM, Starling RC, Hernandez AF, et al. Effect of nesiritide in patients with acute decompensated heart failure. N Engl J Med. 2011;365:32–43.
15. Packer M, Califf RM, Konstam MA, et al. Comparison of omapatrilat and enalapril in patients with chronic heart failure: the Omapatrilat Versus Enalapril Randomized Trial of Utility in Reducing Events (OVERTURE). Circulation. 2002;106:920–6.
16. Braunwald E. The path to an angiotensin receptor neprilysin inhibitor in the treatment of heart failure. J Am Coll Cardiol. 2015;65:1029–41.
17. Ruilope LM, Dukat A, Bohm M, et al. Blood-pressure reduction with LCZ696, a novel dual-acting inhibitor of the angiotensin II receptor and neprilysin: a randomised, double-blind, placebo-controlled, active comparator study. Lancet. 2010;375:1255–66.
18. Solomon SD, Zile M, Pieske B, et al. The angiotensin receptor neprilysin inhibitor LCZ696 in heart failure with preserved ejection fraction: a phase 2 double-blind randomised controlled trial. Lancet. 2012;380:1387–95.
19. Young JB, Dunlap ME, Pfeffer MA, et al. Mortality and morbidity reduction with candesartan in patients with chronic heart failure and left ventricular systolic dysfunction: results of the CHARM low-left ventricular ejection fraction trials. Circulation. 2004;110:2618–26.
20. Chandra A, Lewis EF, Claggett BL, et al. Effects of sacubitril/valsartan on physical and social activity limitations in patients with heart failure: a secondary analysis of the PARADIGM-HF trial. JAMA Cardiol. 2018;3:498–505. https://doi.org/10.1001/jamacardio.2018.0398 . Published online April 4.
21. Desai AS, Vardeny O, Claggett B, et al. Reduced risk of hyperkalemia during treatment of heart failure with mineralocorticoid receptor antagonists by use of sacubitril/valsartan compared with enalapril: a secondary analysis of the PARADIGM-HF trial. JAMA Cardiol. 2017;2:79–85.
22. Bernardez-Pereira S, Ramires FJA, de Melo RFT, Pereira-Barretto AC. Was the enalapril dose too low in the PARADIGM-HF trial? Cardiol Rev. 2018; https://doi.org/10.1097/CRD.0000000000000193. [Epub ahead of print]
23. Langenickel TH, Tsubouchi C, Ayalasomayajula S, et al. The effect of LCZ696 (sacubitril/valsartan) on amyloid-ß concentrations in cerebrospinal fluid in healthy subjects. Br J Clin Pharmacol. 2016;81:878–90.
24. Solomon SD, Rizkala AR, Gong J, et al. Angiotensin receptor neprilysin inhibition in heart failure with preserved ejection fraction: rationale and design of the PARAGON-HF Trial. JACC Heart Fail. 2017;5:471–82.
25. Packer M, McMurray JJ, Desai AS, et al. Angiotensin receptor neprilysin inhibition compared to enalapril on the risk of clinical progression in surviving patients with heart failure. Circulation. 2015;131:54–61.
26. Ayalasomayajula S, Langenickel T, Pal P, et al. Clinical pharmacokinetics of sacubitril/valsartan (LCZ696): a novel angiotensin receptor neprilysin inhibitor. Clin Pharmacokinet. 2017;56:1461–78.
27. Solomon SD, Claggett B, Desai AS, et al. Influence of ejection fraction on outcomes and efficacy of sacubitril/valsartan (LCZ696) in heart failure with reduced ejection fraction. The prospective comparison of ARNI with ACEI to determine impact on global mortality and morbidity in heart failure (PARADIGM-HF) trial. Circ Heart Fail. 2016;9:e002744.
28. Sulfi S, Timmis AD. Ivabradine – the first selective sinus node I_f channel inhibitor in the treatment of stable angina pectoris. Int J Clin Pract. 2006;60:222–8.
29. Vilaine JP, Bidouard JP, Lesage L, et al. Anti-ischemic effects of ivabradine, a selective heart rate-reducing agent, in exercise-induced myocardial ischemia in pigs. J Cardiovasc Pharmacol. 2003;42:688–96.
30. Joannides R, Moore N, Iacob M, et al. Comparative effects of ivabradine, a selective heart rate lowering agent, and propranolol on systemic and cardiac haemodynamics at rest and during exercise. Br J Clin Pharmacol. 2006;61:127–37.
31. Borer JS, Fox K, Jaillon P, et al. Antianginal and antiischemic effects of ivabradine, and I_f inhibitor, in stable angina: a randomized, double-blind, multicentered, placebo-controlled trial. Circulation. 2003;107:817–23.
32. Tendera M, Chassany O, Ferrari R, et al. Quality of life with ivabradine in patients with angina pectoris. The study assessing the morbidity and mortality benefits of the I_f inhibitor ivabradine in patients with stable coronary artery disease quality of life substudy. Circ Cardiovasc Qual Outcomes. 2016;9:31–8.
33. Tardif JC, Ponikowski P, Kahan T, et al. Efficacy of the I_f current inhibitor ivabradine in patients with chronic stable angina receiving beta blocker therapy: a 4-month, randomize, placebo-controlled trial. Eur Heart J. 2009;30:540–8.
34. European Medicines Agency. Ivabradine: European public assessment report – scientific discussion. http://www.ema.europa.eu/docs/en_GB/document_library/EPAR_-_Scientific_Discussion/human/000597/WC500043587.pdf
35. Fox K, Ford I, Steg PG, et al. Ivabradine for patients with stable coronary artery disease and left-

ventricular systolic dysfunction (BEAUTIFUL): a randomised, double-blind, placebo-controlled trial. Lancet. 2008;372:807–16.
36. Fox K, Ford I, Steg PG, et al. Relationship between ivabradine treatment and cardiovascular outcomes in patients with stable coronary artery disease and left ventricular systolic dysfunction with limiting angina: a subgroup analysis of the randomized, controlled BEAUTIFUL trial. Eur Heart J. 2009;30:2337–45.
37. Fox K, Ford I, Steg PG, et al. Ivabradine in stable coronary artery disease without clinical heart failure. N Engl J Med. 2014;371:1091–9.
38. Swedberg K, Komaida M, Bohm M, Borer JS, et al. Ivabradine and outcomes in chronic heart failure (SHIFT): a randomised placebo-controlled trial. Lancet. 2010;376:875–85.
39. Ekman I, Chassany O, Komajda M, et al. Heart rate reduction with ivabradine and health related quality of life in patients with chronic heart failure: results from the SHIFT study. Eur Heart J. 2011;32:2395–404.
40. Tardif JC, O'Meara E, Komajda M, SHIFT Investigators, et al. Effects of selective heart rate reduction with ivabradine on left ventricular remodelling and function: results from the SHIFT echocardiography substudy. Eur Heart J. 2011;32:2507–15.
41. Böhm M, Borer J, Ford I, et al. Heart rate at baseline influences the effect of ivabradine on cardiovascular outcomes in chronic heart failure: analysis from the SHIFT study. Clin Res Cardiol. 2013;102:11–22.
42. Narayanan MA, Reddy YNV, Baskaran J, et al. Ivabradine in the treatment of systolic heart failure – a systematic review and meta-analysis. World J Cardiol. 2017;9:182–90.
43. Yancy CW, Jessup M, Bozkurt B, et al. 2017 ACC/AHA/HFSA focused update of the 2013 ACCF/AHA guideline for the management of heart failure: a report of the American College of Cardiology/American Heart Association Task Force on Clinical Guidelines and the Heart Failure Society of America. J Am Coll Cardiol. 2017;70:776–803.
44. Yancy CW, Januzzi JL, Allen LA, et al. 2017 ACC expert consensus decision pathway for optimization of heart failure treatment: answers to 10 pivotal issues about heart failure with reduced ejection fraction: a report of the American College of Cardiology Task Force on Expert Consensus Decision Pathways. J Am Coll Cardiol. 2018;71:201–30.

Mechanical Circulatory Support

9

Daniel H. Katz and Marwa A. Sabe

Hemodynamics of Cardiogenic Shock

A clear understanding of the unique hemodynamic changes in CS is critical to understanding the downward spiral of CS (Fig. 9.1) and the unique benefits of various MCS devices. The loop in Fig. 9.2a shows a standard pressure-volume loop for a normal heart. As a reminder, the end-systolic pressure-volume relationship (ESPVR) represents the intrinsic systolic function of the heart, and the slope of the ESPVR, the end-systolic elastance (Ees), is an approximation of contractility. The end-diastolic pressure-volume relationship (EDPVR) defines the diastolic function of the heart. The specific pressure-volume loop assumed by the heart depends on the preload and afterload at any given time but is bounded by the ESPVR and EDPVR. The shift in Fig. 9.2b represents the expected change when the heart suffers an acute insult to intrinsic contractile function, such as an AMI. In general, the contractile function of the heart decreases, which manifests as a drop in the slope of the ESPVR. The resulting pressure-volume loop represents a dilated left ventricle (increased end-diastolic volume) and a weak contractile force that produces a much smaller stroke volume.

A critical problem that drives cardiogenic shock can be demonstrated by considering the energetics of the normal heart compared to the acutely insulted heart. The heart requires energy according to the space bounded by the ESPVR, EDPVR, and the pressure-volume loop. It can be divided into the energy needed to maintain the heart shape and electrical function, termed potential energy (PE), and the energy of actually pumping blood, termed stroke work (SW). Together these make up the pressure-volume area which is directly proportional to myocardial oxygen demand. As you can see by comparing Fig. 9.2c, d, in an acute insult, SW may decrease substantially, but PE remains relatively high. Since SW represents not only a demand for oxygen, but also the supply of oxygen, it is easy to see how such a change in the energetics of the heart could precipitate an imbalance in myocardial demand and supply. This imbalance leads to further ischemia, even in the absence of further coronary obstruction, and drives the downward spiral of CS.

To intervene on this pathophysiologic process, clinicians have several tools at their disposal. In the setting of an AMI, urgent reperfusion remains

D. H. Katz
Beth Israel Deaconess Medical Center,
Boston, MA, USA
e-mail: dkatz@bidmc.harvard.edu

M. A. Sabe (✉)
Beth Israel Deaconess Medical Center,
Boston, MA, USA

Harvard Medical School, Boston, MA, USA
e-mail: msabe@bidmc.harvard.edu

A. T. Askari, A. W. Messerli (eds.), *Cardiovascular Hemodynamics*, Contemporary Cardiology,
https://doi.org/10.1007/978-3-030-19131-3_9

the standard of care [1]. However, several CS states are not driven by coronary occlusion, so thrombolysis and/or percutaneous coronary intervention will offer limited benefit. Traditionally, vasopressors and inotropes have formed the basis of management in CS, as these agents are widely available, have rapid onset of action, and require minimal staff resources to uti-

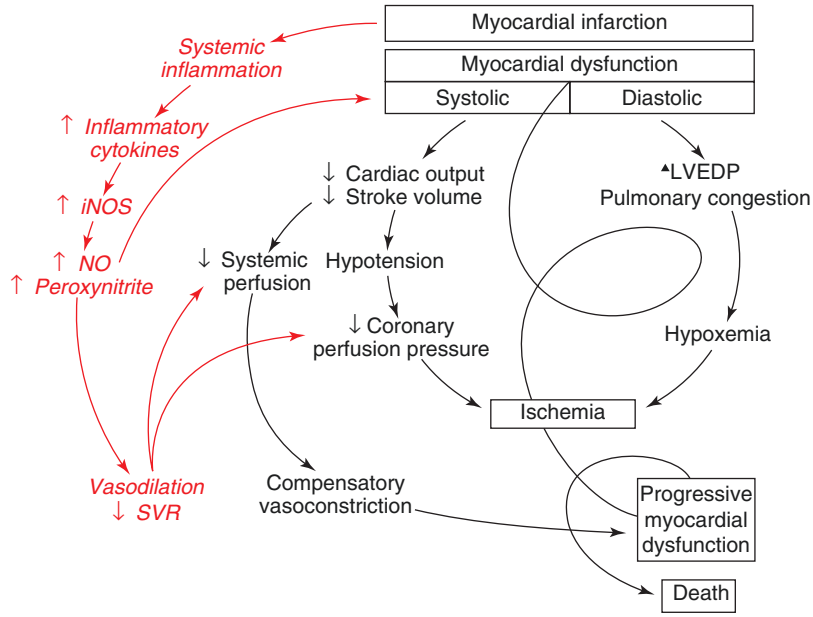

Fig. 9.1 Cardiogenic shock paradigm. Red indicates the effects of inflammatory pathways (Reproduced with permission from Judith Hochman and Harrison's Principles of Internal Medicine)

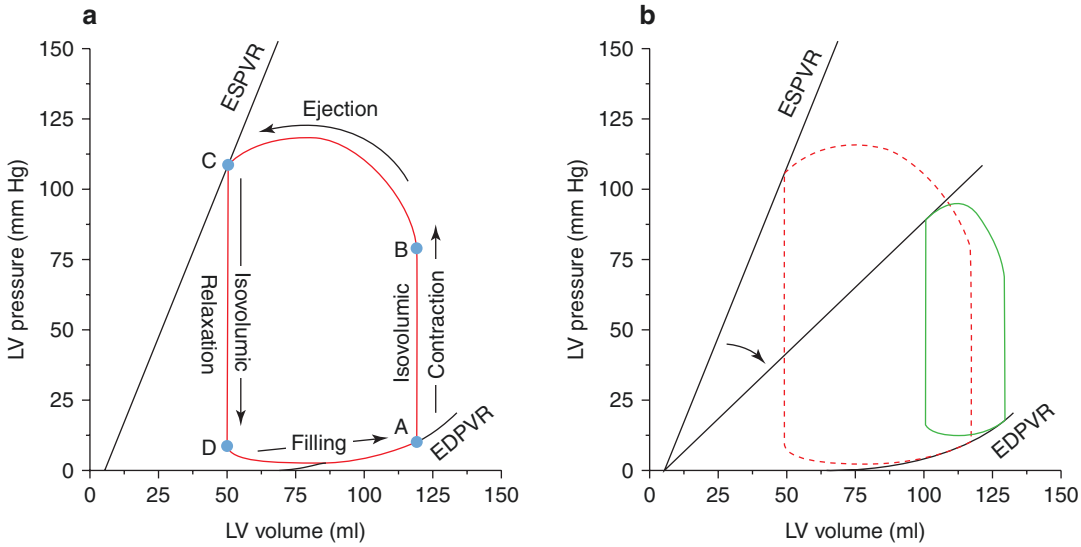

Fig. 9.2 (**a**) The standard pressure-volume loop for a normal heart is shown. The process from point A to point B represents isovolumic contraction where pressure increases without a change in volume. The aortic valve opens at B and ejection occurs with a drop in volume. Ejection occurs until point C when the aortic valve closes, which is followed by isovolumic relaxation to point D. The mitral valve opens at point D and the left ventricle fills. (**b**) In an acute insult, the systolic function of the heart weakens and the ESPVR decreases in slope. This results in a smaller volume of ejection and dilation of the ventricle overall. (**c**) Highlights the components of the pressure-volume area (PVA), which is made up of the stroke work (SW) and the potential energy (PE). (**d**) Shows the change in PE and SW when there is an acute insult to the heart. (Adapted from Uriel et al. JACC 2018 with permission [2])

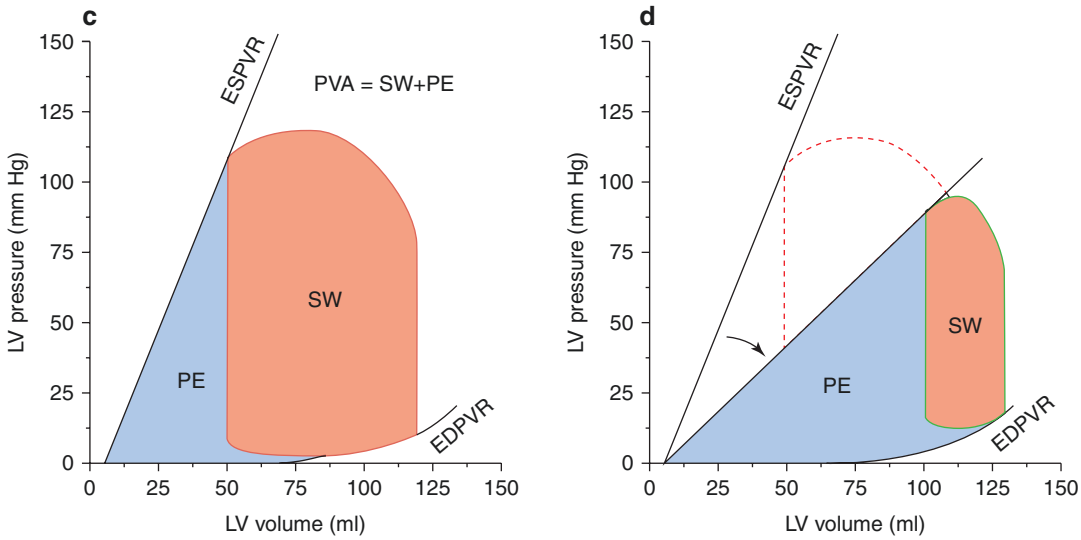

Fig. 9.2 (continued)

lize. However, they also increase myocardial oxygen demand, and may impair end-organ microcirculation, and, thus far, no randomized trials have in fact shown benefit [3]. While these agents are useful for short-term stabilization of hemodynamic collapse, MCS provides a therapeutic intervention that not only supports cardiac output and improves tissue perfusion but also *reduces* myocardial oxygen demand by unloading the ventricle and therefore directly interrupts the spiral of ischemia and myocardial dysfunction that leads toward death [2].

Systems for Temporary Mechanical Circulatory Support

There are numerous devices that provide direct left ventricular (LV) unloading in the setting of CS. They vary in the degree of cardiac output they contribute, and each has unique benefits and challenges. What follows is a general review of the most commonly used devices in clinical practice.

Intra-Aortic Balloon Pump (IABP)

The IABP is the most commonly used form of MCS [4], likely due to the ease of implantation and familiarity in practice. It consists of a conical balloon loaded on a catheter, which is then inserted peripherally so that it may sit in the descending aorta between the left subclavian artery and the renal arteries [5]. Insertion is typically through the femoral artery, but can also be done via the axillary artery directly or through a conduit [6]. Balloon sizes range from 25 cc to 50 cc, and the inflation of the balloon, typically with helium gas, is timed along with the intrinsic heart rate, guided either by the ECG or with fiber-optic monitoring of blood flow. The access cannula is usually 7.5F, the smallest of the various MCS systems.

Hemodynamic Effects

The IABP performs two useful functions in each cardiac cycle. During diastole, the balloon inflates (Fig. 9.3a). This significantly enhances the diastolic pressure within the proximal aorta and therefore enhances the coronary perfusion pressure and the resulting coronary flow [7], thereby directly improving myocardial oxygen supply. The balloon deflates during systole, which results in a significant decrease in afterload. The decrease in afterload allows for earlier opening of the aortic valve, which decreases oxygen demand during isovolumic contraction. In a heart with available contractile reserve, this

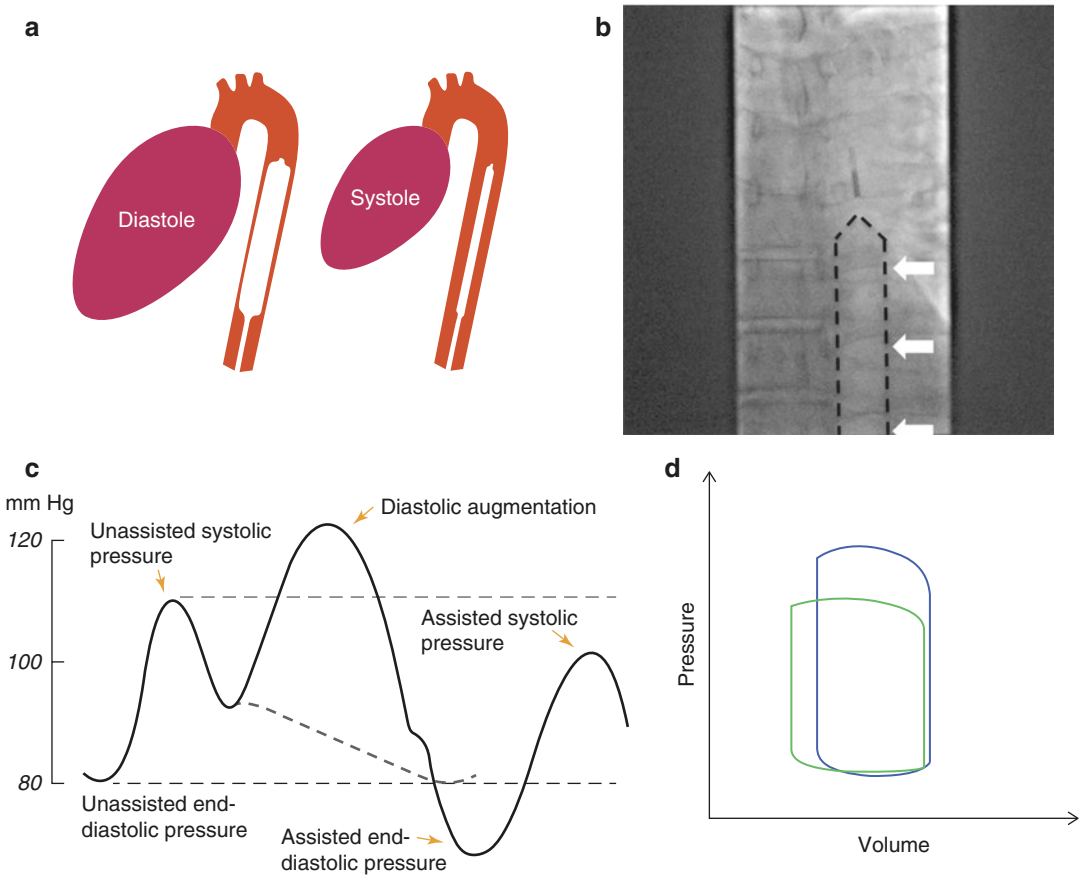

Fig. 9.3 (**a** and **b**) The Intra-aortic balloon pump is peripherally inserted in the descending aorta under fluoroscopy. It inflates during diastole and deflates during systole. (**c**) Diagram of the IABP's effects on systemic blood pressure. When the balloon inflates during diastole, it augments the diastolic pressure, ideally above the normal (unassisted) systolic pressure. Then, with deflation during systole, the systolic pressure is reduced slightly below what it is normally. This is referred to as the assisted systolic pressure. (**d**) Pressure-volume loop with insertion of the IABP is shown in green. Note that with reduction in the afterload, the aortic valve opens at a lower pressure and there is greater volume of ejection. (Reproduced with permission from Briceno et al. [8])

unloading leads to greater stroke volume (Fig. 9.3) [2, 5]. The decrease in systemic vascular resistance without a significant decrease in systemic blood pressure can be extremely useful in cases of acute severe mitral regurgitation or when systemic vascular resistance is high but blood pressure remains low, a state that limits use of afterload reducing medications such as sodium nitroprusside.

Limitations

IABPs are estimated to increase cardiac output somewhere between 0.5 and 1.0 L/min, although this augmentation can be variable in different individuals [5]. However, IABPs themselves provide little intrinsic cardiac output. The LV unloading they provide can enhance LV systolic ejection, similar to vasodilators in acute heart failure (without the side effect of peripheral hypotension, as noted above), but the increase in cardiac output is quite modest. IABPs are also more limited in patients with very high heart rates and arrhythmias due to issues with inflation timing, although this is somewhat mitigated in newer devices that operate by fiberoptic monitoring rather than ECG. IABPs also are contraindicated in patients with any more than mild aortic insufficiency, as inflation during diastole will

exacerbate the degree of aortic insufficiency. Access site bleeding is a present but controllable risk, as the insertion sheath is modest in size.

Study Data

The most important randomized clinical trial of IABPs was the IABP SHOCK II trial which compared IABP to standard treatment in approximately 600 patients with CS related to AMI. There was no benefit in mortality seen at 30 days; however, the trial is noted to have substantial issues with crossover with ~10% of patients in the conventional group receiving IABP, and there are ongoing questions regarding timing of placement, particularly in AMI [3, 8, 9]. This has decreased the strength of recommendations for the use of IABP, but in practice the hemodynamic benefits and the caveats of the IABP-SHOCK II trial have led to continued high-volume use of IABPs.

Ultimately, IABPs are likely to be best suited for situations when the need to increase systemic perfusion is modest, coronary ischemia is a predominant driver of CS, or when a reduction in afterload is expected to be of substantial benefit. IABPs continue to be used for temporizing patients with AMI awaiting CABG, acute mitral regurgitation awaiting surgery, and in selected chronic heart failure patients presenting with cardiogenic shock.

Impella

The Impella (Abiomed, Danvers, Massachusetts) is a percutaneously implanted left ventricular assist device that utilizes an axial flow impeller to pump blood from the LV to the aorta. There are three models presently used in practice which include the Impella 2.5, the Impella CP (3.5), and the Impella 5.0. Access site cannulae are 12F, 14F, and 21F respectively. The model numbers correspond to the upper limit of flow rate achievable, with the CP achieving a maximum of ~4.0 L/min, though actual flow rates are usually somewhat lower than these maximums. The impeller is fixed to a pigtail catheter which is advanced across the aortic valve to the LV either through the femoral artery or through the axillary artery (used frequently for the 5.0 model given the much larger size) (Fig. 9.4).

Hemodynamics

Unlike the IABP, which only reduces afterload, the Impella actively reduces the LV pressure and volume, reducing both preload and afterload. As can be seen in Fig. 9.4, the Impella reduces both wall stress (afterload) and end-diastolic pressure (preload), which leads to a dramatic reduction in both myocardial stroke work and potential energy. This leads to a reduction in myocardial oxygen demand. At the same time, the Impella directly increases cardiac output, which can increase myocardial oxygen supply (Fig. 9.4d). The resulting change in the balance of supply and demand suggests a direct interruption of myocardial ischemia that improves the dangerous spiral of CS.

Limitations

Impella use is growing, though operator familiarity and adequate staff training remain a barrier to use in some care settings. Impellas also use larger access cannulae compared to IABPs, which can lead to an increased bleeding risk. This can be exacerbated by hemolysis related to the axial pump [10], acquired von Willebrand syndrome [11], as well as the necessity of anticoagulation, which is not always necessary for IABPs when the balloon inflates with every beat (1:1). The limitations of duration for Impella use are somewhat uncertain. The FDA has approved the device for 6 days, but some sites have used the Impella 5.0 up to a maximum of 35 days [12]. Femoral access duration is more limited than axillary access due to immobility issues.

Study Data

The small ISAR SHOCK trial observed that even the Impella 2.5 had superior hemodynamic effects compared to the IABP [13]. As a corollary of the benefit of greater cardiac output achieved with this device, registry data also suggested a benefit for patients who received an upgrade from Impella 2.5 to Impella 5.0 [14]. Unfortunately, randomized data for hard out-

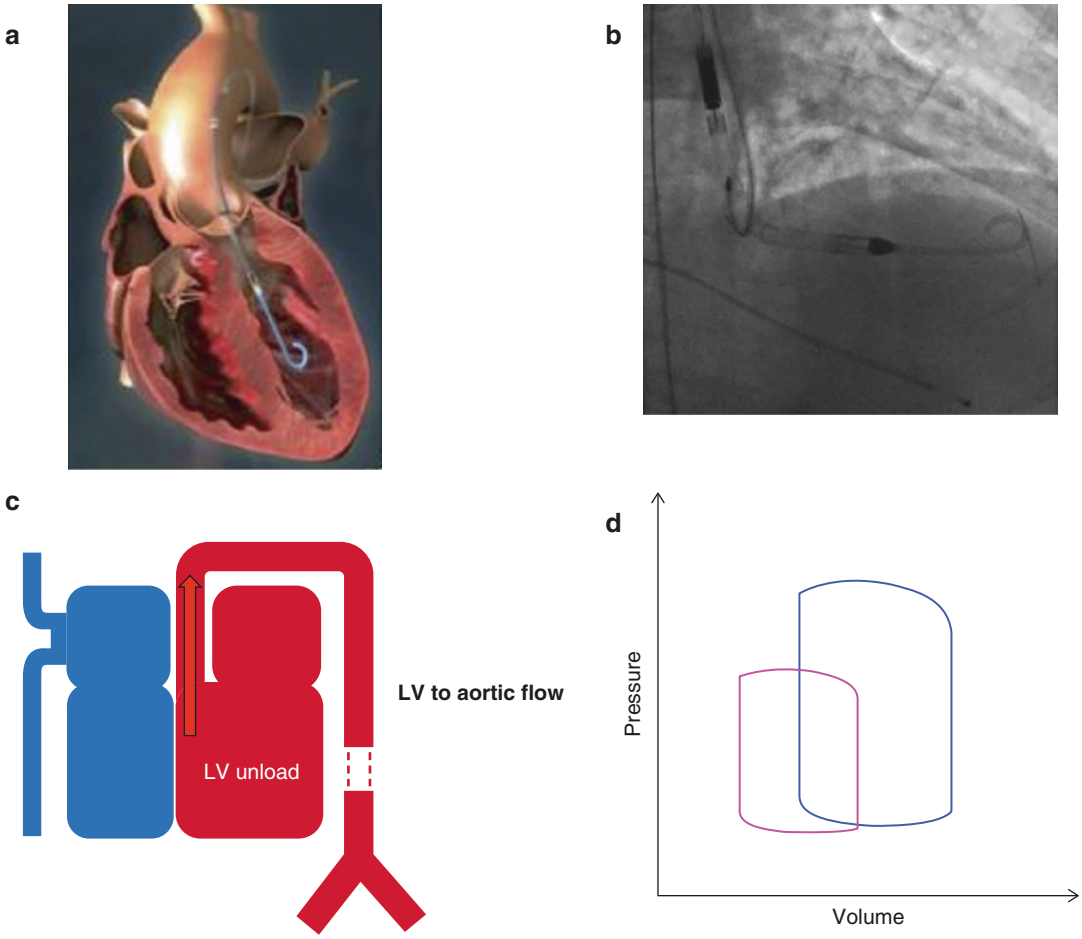

Fig. 9.4 (**a** and **b**) The Impella is inserted fluoroscopically across the aortic valve. (**c**) The Impella directly unloads the LV into the aorta. (**d**) The resulting pressure-volume loop (purple) reflects the unloading of the Impella, as the left ventricular end-diastolic volume significantly decreases. Note that the loop reflects a lower LV stroke volume; however, overall global cardiac output is supported by the Impella. (Reproduced with permission from Briceno et al. [8])

comes are lacking. The Impella CP and IABP were compared in 48 patients with AMI and CS, with no observable difference in 30-day mortality [15]. There is registry data to suggest that for those patients in whom an AMI is the trigger for CS, Impella use prior to coronary intervention was superior to its use afterward [16]. As a result of the experience with Impella at the time of coronary intervention, these devices are frequently deployed in AMI complicated by CS. However, there are some data for use in acute decompensated heart failure, as a bridge to a decision regarding heart transplantation or left ventricular assist device (LVAD) implantation [17, 18].

Extracorporeal Pumps

IABPs and Impellas are both peripherally placed, intracorporeal pumps. As a result, the volume of flow they can deliver, the durability of their use, and their anatomic flexibility are limited. Extracorporeal pumps, on the other hand, use large, robust centrifugal pumps capable of higher flow rates. The inflow and outflow cannulae can be placed in numerous orientations, either peripherally or centrally, depending on anatomy and the desired effect on hemodynamics. A membrane oxygenator can also be placed in-line with an extracorporeal pump to provide blood oxygenation if needed. Like the Impella, these

systems require anticoagulation to reduce the risk of thromboembolism. This section covers the more commonly encountered platforms.

TandemHeart

In many ways, the TandemHeart (CardiacAssist Inc., Pittsburgh, Pennsylvania) mimics the Impella. It is percutaneously placed and directly unloads the LV; however, it uses an extracorporeal centrifugal pump. A 21F inflow cannula is inserted into the femoral vein up to the right atrium and passes across the septum (by transseptal puncture) into the left atrium. The blood is pumped directly into the femoral artery through a 17F cannula (Fig. 9.5) [19]. The hemodynamic profile is similar to that of the Impella. In addition to the routine risks of percutaneous femoral access (bleeding, infection, limb ischemia, etc.), trans-septal puncture increases the possibility of tamponade. Trans-septal puncture is also more technically difficult, and thus this system is not as widely used as the Impella [8]. When compared to IABP, the TandemHeart improved hemodynamic parameters but showed no mortality benefit [20, 21].

CentriMag

The CentriMag (Abott Laboratories, Abbott Park, Illinois) is quite similar to the TandemHeart. It also consists of an extracorporeal centrifugal

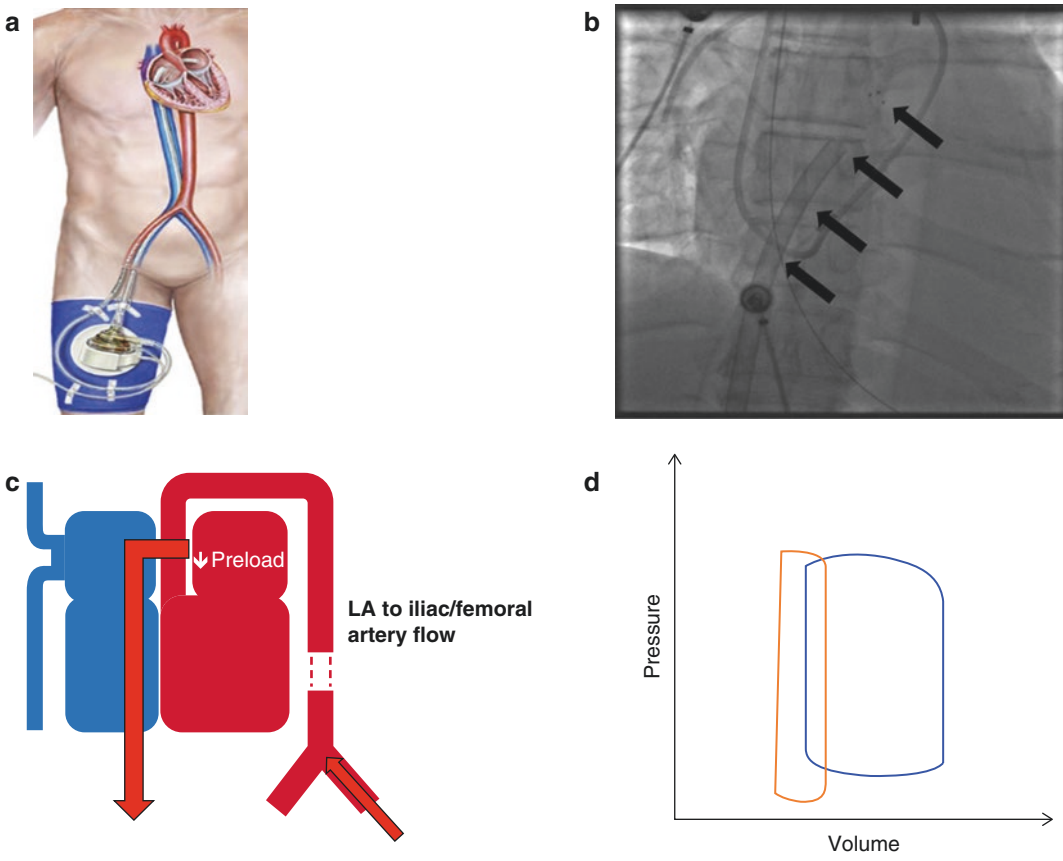

Fig. 9.5 (**a** and **b**) The TandemHeart is placed percutaneously under fluoroscopic guidance. (**c**) The inlet cannula advances up the femoral vein to the right atrium, and crosses to the left atrium, where it drains blood and reduces LV preload. (**d**) Hemodynamic benefits include reduction in preload and reduction in the left ventricular end-systolic volume. Note that the TandemHeart increases afterload on the LV by delivering blood to the femoral artery (Reproduced with permission from Briceno et al. [8])

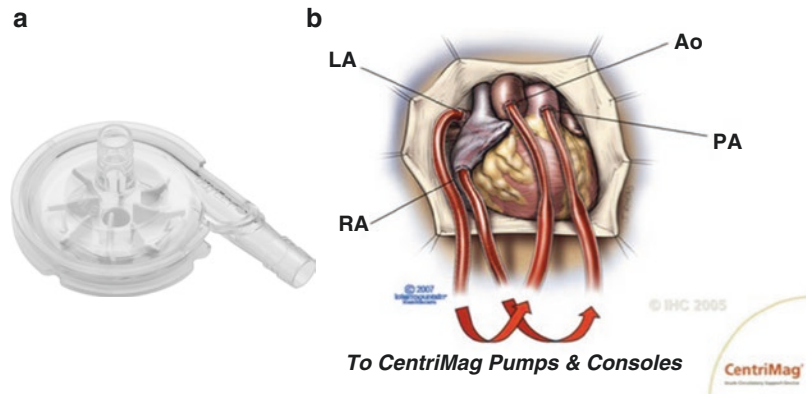

Fig. 9.6 (**a**) The CentriMag is a high flow centrifugal pump. (**b**) The CentriMag can pump blood from the right atrium to the pulmonary artery or the left atrium to the aorta. Other configurations are possible. (Images reproduced with permission from Abbott Laboratories)

pump. The key difference is that the system is implanted through central cannulation (usually by a cardiothoracic surgeon), rather than peripherally. Most commonly the inflow cannula is in the left atrium, and the outflow cannula is in the aorta (Fig. 9.6). However, depending on the situation, the inflow cannulae can be placed in the pulmonary vein or in the left ventricle directly, and for right-sided support can be placed in the right atrium. It is noted that CentriMag is somewhat more flexible in the cannulae it can use and the range of flows it can provide (up to 10 L/min). As a result, surgeons find it useful in post-pericardiotomy syndrome, and the extended duration makes it useful in patients for whom extended mechanical support is needed, as either a bridge to recovery, durable LVAD, or orthotopic heart transplantation [22].

Venoarterial Extracorporeal Membrane Oxygenation (VA-ECMO)

ECMO is any system that uses an external membrane to provide oxygenation and removal of carbon dioxide, and is thus suitable for refractory respiratory failure. If that is all that is required, and the patient does not need hemodynamic support, then veno-venous ECMO (VV-ECMO) is adequate. In the setting of CS complicated by respiratory failure, where support of cardiac output is also needed, the membrane oxygenation is paired with a high flow centrifugal pump, and oxygenated blood is pumped from the venous system into the arterial system, hence, venoarterial ECMO (VA-ECMO). Blood is typically removed from the right atrium and returned to the femoral artery after oxygenation, although central cannulation of the aorta by a surgeon is also possible. Alternately, if needed, the inflow can come via the right internal jugular vein and the outflow returned to the right subclavian artery. The venous cannulae range from 19F to 25F and the arterial cannulae are 15F to 24F. Whatever the orientation, the heart and lungs are all bypassed and replaced by the system, such that VA-ECMO is essentially the same as cardiopulmonary bypass (Fig. 9.7). This arrangement takes over the work of both ventricles and therefore is most commonly used in the setting of acute biventricular failure, also complicated by hypoxemic respiratory failure. This is most often seen in AMI, myocarditis, or primary graft failure following orthotopic heart transplant [23].

Hemodynamics

The hemodynamic effects of VA-ECMO are notably different than other MCS systems discussed thus far. Because VA-ECMO drains the venous system, usually from the right atrium, the right ventricle is unloaded, but the LV is not; blood still crosses the pulmonary and coronary vascular circuits and drains into the LV. In fact, not only does ECMO not unload the LV, it then delivers blood flow to the aorta, which in fact increases the afterload on the LV. If left unmanaged, an LV incapable of unloading itself against the afterload of ECMO may develop increased filling pressures and LV distension, which can lead to both increased myocardial oxygen demand and ischemia, as well as pulmonary edema. Furthermore, if the ventriculo-aortic

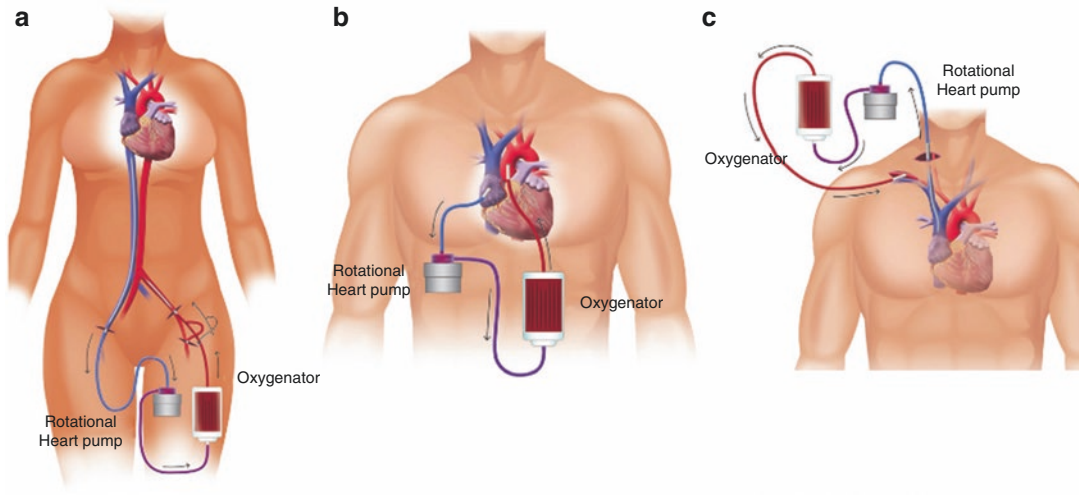

Fig. 9.7 Three possible configurations for VA ECMO. The heart pump and the oxygenator connect a venous inflow to an arterial outflow. Configurations include (**a**) femoral vein to femoral artery, (**b**) right atrium to aorta ("central cannulation"), or (**c**) right internal jugular vein to right subclavian artery. (Reproduced with permission from Rao et al. [23])

coupling is so adverse that the aortic valve does not open, stasis of blood in the LV can increase the patient's risk for thromboembolic events [23].

To manage this problem, ECMO flows could be reduced, though this is limited by the demands of adequate tissue perfusion. Instead, a variety of left ventricular venting options can be employed (Fig. 9.8). Venting options include inotropes or vasodilators, IABP or Impella placement, atrial septostomy (to allow for left atrial to right atrial shunting), or simply a cannula placed directly in the left atrium or LV that drains into the ECMO circuit [23]. Impellas are a frequently used ventilation strategy in patients on VA-ECMO, and simultaneous use of Impella with ECMO support ("ECPELLA") has been shown to be associated with improved 30-day mortality and lower inotrope use in patients requiring VA-ECMO [24].

While it is critical for the LV to be adequately vented to prevent the aforementioned complications, it should also be noted that in patients with substantial respiratory compromise, the blood coming from the LV is poorly oxygenated. If the LV vents itself vigorously, or is supported by any of the strategies listed, enough flow can be generated such that deoxygenated blood preferentially finds its way into the peripheral circulation.

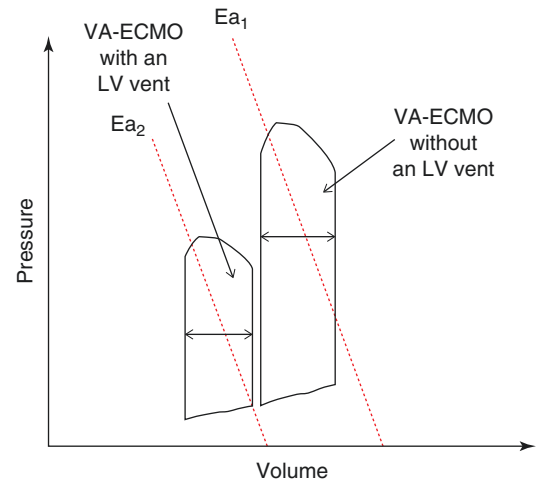

Fig. 9.8 Effect of an LV vent on LV hemodynamics. The vent reduces LV end-diastolic volume and also reduces end-systolic pressure. (Reproduced with permission from Kapur et al. [25])

The at-risk organs are those most proximal, namely, the heart, upper extremities, and head. Thus, this phenomenon is known as North-South syndrome, or Harlequin syndrome (Fig. 9.9) [26]. The phenomenon is best monitored using pulse oximetry or radial artery access in the right arm, wherein arterial supply comes from the

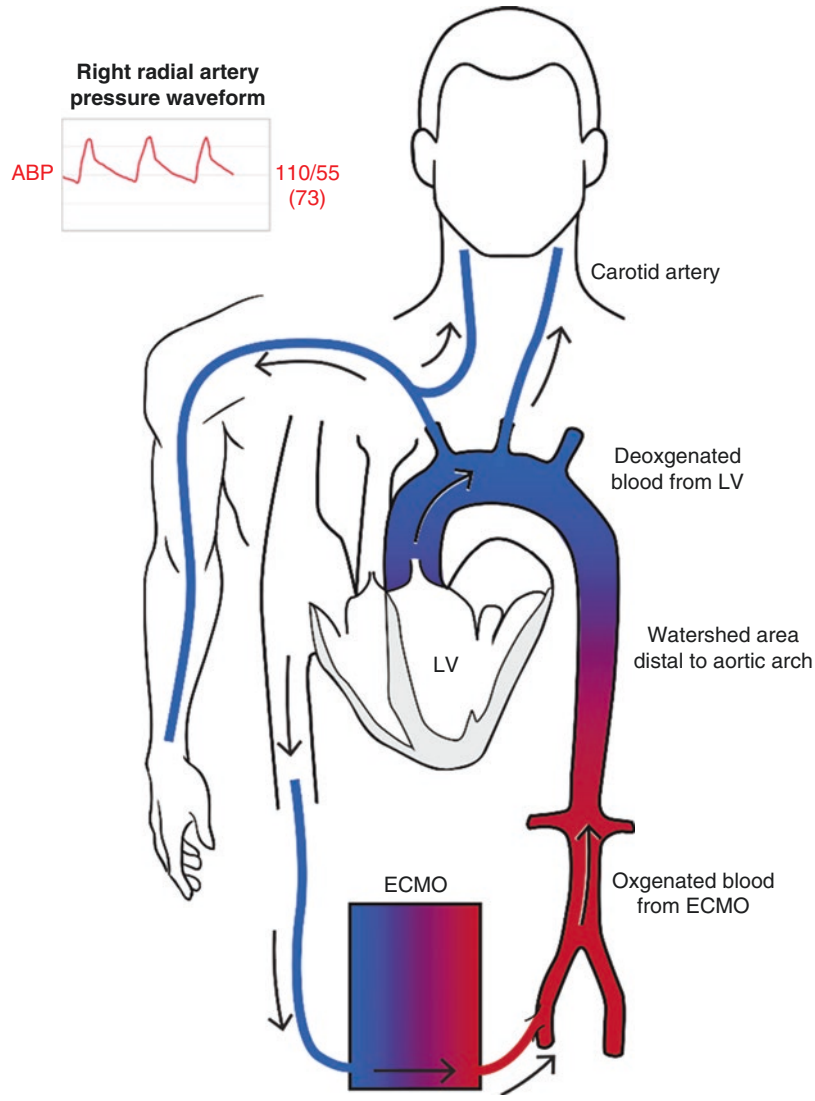

Fig. 9.9 North-South syndrome or Harlequin syndrome. Oxygenated blood from the ECMO circuit mixes with deoxygenated blood from the LV. If this mixing occurs distal to the aortic arch, oxygen to the upper extremities and head can be compromised (Reproduced with permission from Rao et al. [23])

most proximal branch of the aortic arch. If oxygen saturation dips relative to the left arm, or the arterial wave form looks more like the pulsatile work of the LV rather than the continuous flow of ECMO, this can indicate North-South syndrome (or Harlequin syndrome) [23]. If it occurs, increasing ECMO flows can be helpful. Alternative solutions include weakening the stronger LV with an esmolol drip or returning some oxygenated blood back to the RA (which would then make its way to the LV by the normal route), a system referred to as veno-arterio-venous ECMO (VAV-ECMO) [27].

Risks and Limitations

Here again the risks of peripheral cannulation and anticoagulation must be considered: infection, bleeding, and limb ischemia. Because of the particularly large cannulae used with ECMO, the leg distal to the insertion site is frequently cannulated to provide direct antegrade flow and prevent limb ischemia [28]. The ECMO circuit also tends to be more thrombogenic and inflammatory than systems with just a pump, and as a result, peripheral vasodilation and thrombotic events are an ever-present concern [29].

Indications and Contraindications

The principal indication for VA-ECMO is in patients requiring biventricular support as well as respiratory support. The membrane oxygenator carries much of the added risk of ECMO compared to other forms of MCS discussed above, so adding this element should only be done if it is necessary to support the patient. The most important contraindication to initiation of VA-ECMO is the absence of an exit strategy to allow removal of the circuit, whether that is recovery of the heart, durable MCS (discussed below), or heart transplant. Relative contraindications include coagulopathy, obesity, age, and other life-limiting comorbidities particularly malignancy. These issues factor into the likelihood of the patient surviving their time on the ECMO circuit.

Durable Mechanical Circulatory Support

The MCS systems described above are temporary interventions in the setting of cardiogenic shock. In this sense, they are utilized as a bridge to some other more permanent outcome. In some cases, this is a bridge to myocardial recovery, for example, following reperfusion, or of certain types of myocarditis by means of immunosuppressive therapy. However, in patients with CS due to acute on chronic decompensated heart failure or in whom myocardial recovery does not occur, temporary MCS should not even be initiated unless some sort of exit strategy is possible. For more and more patients, that exit strategy is a durable LVAD, and for those who are not heart transplant candidates, durable LVADs represent destination therapy.

Durable LVAD Systems

In general terms, the continuous flow LVADs that are most commonly used in clinical practice are not substantially different from the extracorporeal systems covered above. A high flow pump directly unloads the left ventricle and pumps blood into the proximal aorta. The critical difference is that the pump is surgically implanted in the chest or abdomen. Only a driveline, which powers the pump, is tunneled externally to the skin.

Two categories of pumps are in common use: centrifugal and axial flow pumps, both of which are continuous flow pumps. The HeartWare HVAD (Medtronic, Minneapolis, Minnesota) and the HeartMate 3 (HM3) (Abbott Laboratories, Abbott Partk, Illinois) use centrifugal flow pumps which are implanted with a short inflow cannula into the LV apex, while the HeartMate II (HMII) is an axial flow pump that is implanted just below the diaphragm with a slightly longer inflow cannula connected to the LV apex (Fig. 9.10) [30]. All three systems have a driveline that tunnels out through the abdominal wall and connects externally to a controller which can be powered by

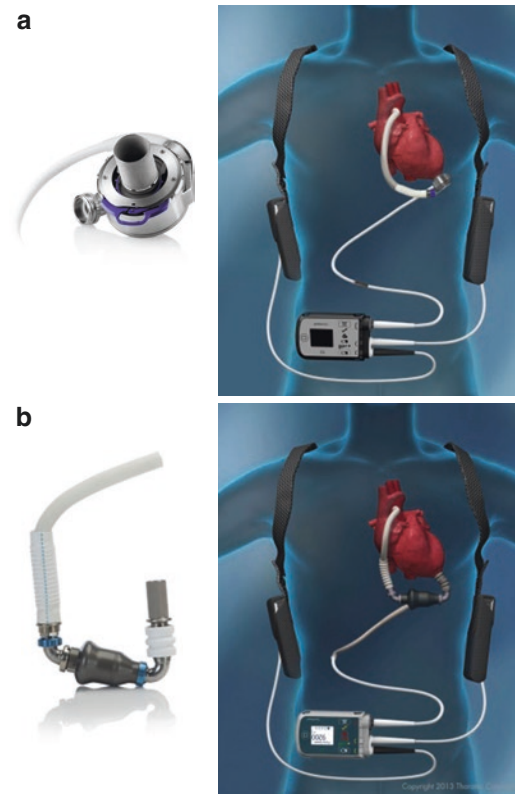

Fig. 9.10 Left ventricular support devices. (**a**) Shows the centrifugal flow pump the HeartMate 3 device. HeartWare (not shown here) is also a centrifugal flow pump. (**b**) Shows the axial flow pump HeartMate II device. Both are connected to external systems with a driveline. Inflow cannulas sit in the LV and outflow cannulas in the aorta. (Reproduced with permission from Abbott Laboratories)

battery or wall outlet. These devices support cardiac output, allowing patients to leave the hospital and resume daily living.

Hemodynamics

In the acute setting, LVADs are hemodynamically similar to other LV-to-aorta MCS systems discussed, such as Impella. However, because the patient's total cardiac output is a combination of their intrinsic LV function, which is pulsatile, and part continuous flow pump, it is worth considering how the two interact. The only externally controllable setting on the LVAD is the speed, measured in rotations per minute. The actual flow that this generates, however, depends on multiple factors, including the preload, afterload, and viscosity of the blood. More directly, as seen in Fig. 9.11, the flow generated by the device is indirectly proportional to the head pressure, which is the pressure gradient between the LV and the aorta. In diastole, the head pressure is high, since LV pressure is relatively low. The high head pressure means flow across the LVAD is lower. During systole, the head pressure is much lower as the LV generates higher pressures at the LVAD inflow cannula. With the low head pressure, LVAD flow increases. Therefore the actual flow generated by the device fluctuates with the cardiac cycle. Because of this effect on flow, increases in the afterload experienced by the LVAD lowers the flow generated by the LVAD, while increases in preload increases flow based on their effect on the head pressure [30]. In fact, the LVAD is more sensitive than the heart to these changes, and it is therefore critical to tightly control blood pressure and volume status in LVAD patients.

The unloading that the LVAD provides manifests in several ways. First, it directly reduces the LV volume and pressure, with subsequent decrease in LV size on echocardiogram. There is evidence that the unloading of the LV myocytes can have long-term beneficial effects on LV remodeling [2]. The direct unloading of the LV also means that the LV itself provides a reduced component of the cardiac output. As a result, the peripheral arterial flow is less pulsatile and more continuous; the greater the LVAD's contribution to the total cardiac output, the lower the pulsatility observed in peripheral arteries [30]. Because of this hemodynamic effect, LVAD patients often do not have blood pressure that can be measured by a typical cuff. Rather a Doppler probe is used to determine the pressure at which flow returns to a peripheral artery. This is commonly referred to as the opening pressure, and it is recommended to keep this below 80 mmHg, given the afterload sensitivity of these devices [31].

LVADs also directly impact the RV. LV unloading reduces left-sided filling pressures, resulting in a drop in RV afterload. However, there are negative consequences for the RV as well. The increased flow from the LVAD can return to the RV and cause RV distension and dysfunction. At the same time, the intraventricular septum can be pulled toward the inflow cannula by the pump, decreasing the septal contribution to RV contractility, and weakening RV performance. For those at risk, these issues can cause early RV failure after LVAD implantation. There is also evidence for late RV failure, the cause of which remains unclear, but may be related to chronic impacts of the above phenomena [30].

Pump Parameters

When in clinic or in the hospital, the HeartMate and HeartWare systems are connected to interfaces that display relevant information about function. Each system uses a different interface for displaying these pump parameters, but in general, pump speed, pump power, pump flow, and some indication of the degree of pulsatility should be readily apparent. The pump speed is set directly. The pump power is directly measured by the VAD and is directly proportional to the amount of actual flow through the VAD. Flow itself is not directly measured by the VAD, but rather calculated from pump power, pump speed, and blood viscosity, with viscosity derived from the hematocrit which has to be entered into the interface (in the HeartWare and HM3 device; this option is not available in the HMII device). For this reason, entering a new hematocrit can cause a sudden shift in the calculated flow.

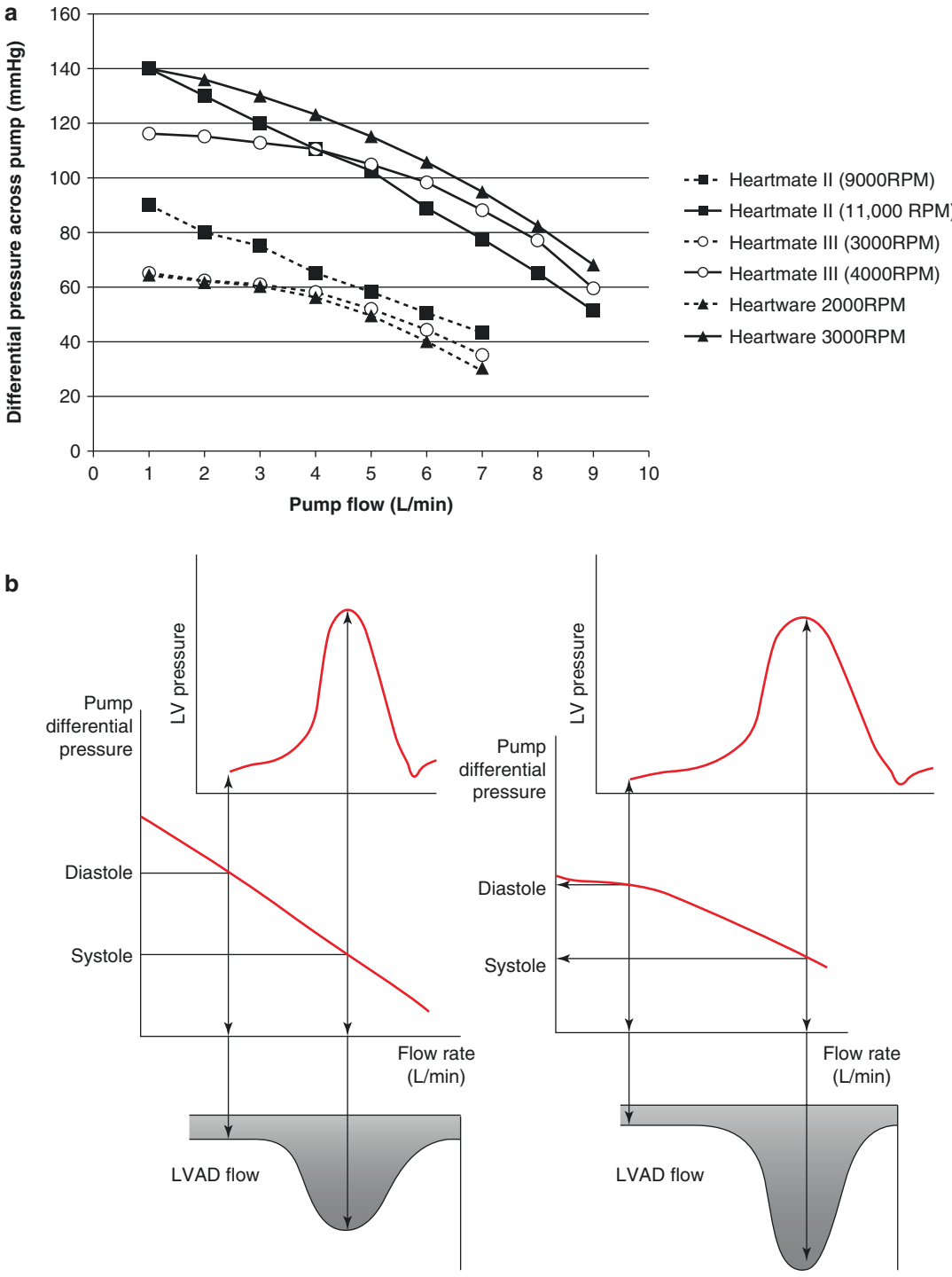

Fig. 9.11 LVAD hemodynamics. (**a**) The actual flow generated by an LVAD varies by the type, speed, and head pressure. (**b**) Actual flow rates in an LVAD vary throughout the cardiac cycle. During systole, the pressure gradient between the LV and the aorta shrinks, so flow increases. The right panel shows an LVAD that is more sensitive to changes in head pressure, with larger fluctuations in flow rate. (Reproduced with permission from Lim et al. [30])

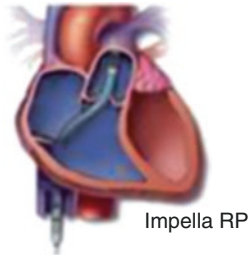

Fig. 9.12 Impella RP. The impeller pumps blood from the inferior vena cava to the pulmonary artery. (Reproduced with permission from Kapur et al. [32])

Right Ventricular Support

The above examples of MCS all focused on left ventricular support, save for ECMO which provides biventricular support. RV support, either in addition to LV support or in isolation can also be achieved with many of the systems already covered. Percutaneous VADs can be placed with cannulae in the right atrium and pulmonary artery, thereby unloading the right heart. There is also an Impella RP, specifically designed for RV support (Fig. 9.12) [25, 32]. Simultaneous use of Impella 2.5, CP, or 5.0 and Impella RP can be used for hemodynamic support in patients with biventricular shock [33]. Durable RVAD is also an option, both in patients with RV failure related to LVAD implantation and in patients with biventricular failure requiring bridge support prior to orthotopic heart transplantation.

Review Questions

Case 1: A 34-year-old female with no past medical history presents with 4 days of progressive dyspnea. She had a mild upper respiratory infection 2 weeks ago. Her vital signs show a temperature of 37 °C, heart rate of 132 in sinus rhythm with frequent ventricular ectopy, blood pressure of 78/59, and an oxygen saturation of 82% on BiPAP with 60% FiO2. On exam, she has an elevated jugular venous pulsation to 14 cm H_2O, crackles in both lung fields, an S3 gallop, and cool, mottled extremities. She is in visible distress. Bedside echocardiogram shows biventricular systolic dysfunction, 2+ mitral regurgitation and no aortic insufficiency. During the echocardiogram, she becomes unresponsive and a code is called for PEA arrest. She is intubated, and after two rounds of CPR and one dose of epinephrine, she has return of spontaneous circulation, though her oxygen saturation remains 83% on appropriate ventilator support and her blood pressure is 76/58.

1. What type of support would be most appropriate at this time?
   A. Dobutamine and norepinephrine
   B. Transfer to the OR for emergent durable RVAD and LVAD
   C. Impella 5.0 via axillary cutdown
   D. VA-ECMO

This patient presents with likely myocarditis with profound biventricular failure and respiratory compromise. This situation favors VA-ECMO. Inotropes and vasopressors are less likely to provide adequate support, and an Impella fails to support the RV. While durable RVAD and LVAD could offer adequate circulatory support, it fails to address the respiratory failure and is potentially unnecessary as near term recovery is possible.

2. The above patient is started on VA-ECMO via right femoral vein and left femoral artery cannulation. Twelve hours after initiation the patient is noted to have frothy secretions in the endotracheal tube. Bedside echo shows a markedly dilated LV with 4+ mitral regurgitation without flail. The aortic valve is not noted to open.

   What is the next best step in management?

A. Placement of an Impella CP
B. Transfer to the OR for emergent mitral valve repair
C. Increasing ECMO pump speed
D. Increasing ventilator oxygenation support

This patient needs LV unloading given their very poor LV function, which can be achieved with an Impella device, acting as a direct LV vent. The mitral regurgitation is a functional con-

sequence of LV dilation, and is not the primary driver of the situation. Increasing ECMO pump speed will increase flow in the proximal aorta and worsen the situation. Increasing ventilator oxygenation support may increase overall oxygenation to a small extent, but does not address LV unloading.

Case 2: A 59-year-old man with a history of hypertension and diabetes presents after 4 days of intermittent chest pressure at rest. Today his chest pressure has persisted for several hours, and he is markedly short of breath prompting his presentation. Vital signs show a heart rate of 95, blood pressure of 92/68, and an oxygen saturation of 92% on room air. His EKG shows ST elevations in V1-V4 with associated q-waves and reciprocal ST depressions. He is given aspirin, ticagrelor, and a bolus of heparin. The catheterization laboratory is activated. Via right radial artery access, he is found to have a proximal LAD occlusion. As the intervention is about to begin, blood pressure is noted to be 75/55, and the patient becomes less responsive.

3. What is the next best action?
   A. Complete the procedure while closely monitoring vital signs
   B. Place an Impella CP
   C. Start a norepinephrine drip
   D. Cannulate for VA-ECMO

This patient is developing cardiogenic shock from an AMI. The primary need is for rapid left ventricular support. Fixing the lesion without support could allow the cycle of CS to continue. It is preferred to start some form of hemodynamic support and then complete the procedure. Norepinephrine would not be an ideal agent as it does not decrease myocardial demand or increase coronary perfusion. VA-ECMO is not necessary as the patient does not have RV or respiratory failure.

Case 3: A 52-year-old male with diabetes, hypertension, and hyperlipidemia with infrequent medical care presents with 3 days of progressive dyspnea and fatigue. He has noted 10 lbs weight gain in the last week. He is noted to be tachycardic to 105 bpm and his blood pressure is 85/56. His extremities are cool to the touch and he is noted to have trouble paying attention during the history. EKG shows inferolateral T-wave inversions with ST depressions. Troponins are sent. Bedside echocardiogram shows EF 15% with wall motion abnormalities. He is given 325 mg aspirin and bolused with 5000 U of IV heparin for presumed acute coronary syndrome. He is started on a dopamine drip and transferred to the cath lab which shows severe three vessel coronary disease with small distal vessels. There is no culprit vessel on which to intervene.

4. What is the next best intervention?
   A. Start sodium nitroprusside
   B. Place an IABP
   C. Book the OR for placement of a left atrium to aortic CentriMag
   D. Book the OR for placement of a durable LVAD

The patient has exacerbation of likely long-standing ischemic coronary disease. He is developing CS and reperfusion is not an option. Temporary MCS with an IABP would be valuable here. It would help to unload the struggling ventricle and increase coronary perfusion pressure to the likely ischemic heart. Sodium nitroprusside would be risky given low blood pressure. A CentriMag would provide hemodynamic support, but is much more invasive than an IABP and may not be necessary at this point. Similarly durable LVAD would be premature as LV recovery is possible in the near term.

After 3 days on the IABP, his mentation has improved and he is diuresed back to his dry weight. However, there is no improvement in the patient's intrinsic LV function, and the cardiothoracic surgeons have decided his coronaries are insufficient for coronary artery bypass surgery. The IABP is unable to be weaned without decrease in blood pressure. He and his family would like to know what further options he has at this point.

5. What option would be best at this time?
   A. Continued monitoring on IABP
   B. Upgrade to CentriMag

C. Evaluate for LVAD/orthotopic heart transplant
D. Transition to comfort care

This patient should begin an urgent evaluation for LVAD and/or heart transplant. Upgrading to CentriMag at this time is not necessary as the patient is adequately supported on IABP, but further monitoring on IABP is unlikely to yield further improvement in his LV function, and is not worth the daily risk for complications from IABP. Transitioning to comfort care is not appropriate as LVAD support is an option and the patient and family are seeking further care.

References

1. van Diepen S, Katz JN, Albert NM, et al. Contemporary management of cardiogenic shock: a scientific statement from the American Heart Association. Circulation. 2017;136(16):e232–68. https://doi.org/10.1161/CIR.0000000000000525.
2. Uriel N, Sayer G, Annamalai S, Kapur NK, Burkhoff D. Mechanical unloading in heart failure. J Am Coll Cardiol. 2018;72(5):569–80. https://doi.org/10.1016/j.jacc.2018.05.038.
3. Thiele H, Ohman EM, Desch S, Eitel I, de Waha S. Management of cardiogenic shock. Eur Heart J. 2015;36(20):1223–30. https://doi.org/10.1093/eurheartj/ehv051.
4. Stretch R, Sauer CM, Yuh DD, Bonde P. National trends in the utilization of short-term mechanical circulatory support: incidence, outcomes, and cost analysis. J Am Coll Cardiol. 2014;64(14):1407–15. https://doi.org/10.1016/j.jacc.2014.07.958.
5. Parissis H, Graham V, Lampridis S, Lau M, Hooks G, Mhandu PC. IABP: history-evolution-pathophysiology-indications: what we need to know. J Cardiothorac Surg. 2016;11. https://doi.org/10.1186/s13019-016-0513-0.
6. Naqvi SY, Salama IG, Yoruk A, Chen L. Ambulatory intra aortic balloon pump in advanced heart failure. Card Fail Rev. 2018;4(1):43–5. https://doi.org/10.15420/cfr.2018:22:1.
7. Kern MJ, Aguirre FV, Tatineni S, et al. Enhanced coronary blood flow velocity during intraaortic balloon counterpulsation in critically ill patients. J Am Coll Cardiol. 1993;21(2):359–68.
8. Briceno N, Kapur NK, Perera D. Percutaneous mechanical circulatory support: current concepts and future directions. Heart. 2016;102(18):1494–507. https://doi.org/10.1136/heartjnl-2015-308562.
9. Thiele H, Zeymer U, Neumann F-J, et al. Intraaortic balloon support for myocardial infarction with cardiogenic shock. N Engl J Med. 2012;367(14):1287–96. https://doi.org/10.1056/NEJMoa1208410.
10. Badiye AP, Hernandez GA, Novoa I, Chaparro SV. Incidence of hemolysis in patients with cardiogenic shock treated with Impella percutaneous left ventricular assist device. ASAIO J. 2016;62(1):11–4. https://doi.org/10.1097/MAT.0000000000000290.
11. Flierl U, Tongers J, Berliner D, et al. Acquired von Willebrand syndrome in cardiogenic shock patients on mechanical circulatory microaxial pump support. PLoS One. 2017;12(8):e0183193. https://doi.org/10.1371/journal.pone.0183193.
12. Castillo-Sang MA, Prasad SM, Singh J, Ewald GA, Silvestry SC. Thirty-five day Impella 5.0 support via right axillary side graft cannulation for acute cardiogenic shock. Innovations (Phila). 2013;8(4):307–9. https://doi.org/10.1097/IMI.0000000000000009.
13. Seyfarth M, Sibbing D, Bauer I, et al. A randomized clinical trial to evaluate the safety and efficacy of a percutaneous left ventricular assist device versus intra-aortic balloon pumping for treatment of cardiogenic shock caused by myocardial infarction. J Am Coll Cardiol. 2008;52(19):1584–8. https://doi.org/10.1016/j.jacc.2008.05.065.
14. Engström AE, Cocchieri R, Driessen AH, et al. The Impella 2.5 and 5.0 devices for ST-elevation myocardial infarction patients presenting with severe and profound cardiogenic shock: the Academic Medical Center intensive care unit experience. Crit Care Med. 2011;39(9):2072–9. https://doi.org/10.1097/CCM.0b013e31821e89b5.
15. Ouweneel DM, Eriksen E, Sjauw KD, et al. Percutaneous mechanical circulatory support versus intra-aortic balloon pump in cardiogenic shock after acute myocardial infarction. J Am Coll Cardiol. 2017;69(3):278–87. https://doi.org/10.1016/j.jacc.2016.10.022.
16. O'Neill WW, Schreiber T, Wohns DHW, et al. The current use of Impella 2.5 in acute myocardial infarction complicated by cardiogenic shock: results from the USpella registry. J Interv Cardiol. 2014;27(1):1–11. https://doi.org/10.1111/joic.12080.
17. Hall SA, Uriel N, Carey SA, et al. Use of a percutaneous temporary circulatory support device as a bridge to decision during acute decompensation of advanced heart failure. J Heart Lung Transplant. 2018;37(1):100–6. https://doi.org/10.1016/j.healun.2017.09.020.
18. Lima B, Kale P, Gonzalez-Stawinski GV, Kuiper JJ, Carey S, Hall SA. Effectiveness and safety of the Impella 5.0 as a bridge to cardiac transplantation or durable left ventricular assist device. Am J Cardiol. 2016;117(10):1622–8. https://doi.org/10.1016/j.amjcard.2016.02.038.
19. Gilotra NA, Stevens GR. Temporary mechanical circulatory support: a review of the options, indica-

tions, and outcomes. Clin Med Insights Cardiol. 2015;8(Suppl 1):75–85. https://doi.org/10.4137/CMC.S15718.
20. Burkhoff D, Cohen H, Brunckhorst C, O'Neill WW. A randomized multicenter clinical study to evaluate the safety and efficacy of the TandemHeart percutaneous ventricular assist device versus conventional therapy with intraaortic balloon pumping for treatment of cardiogenic shock. Am Heart J. 2006;152(3):469.e1–8. https://doi.org/10.1016/j.ahj.2006.05.031.
21. Thiele H, Sick P, Boudriot E, et al. Randomized comparison of intra-aortic balloon support with a percutaneous left ventricular assist device in patients with revascularized acute myocardial infarction complicated by cardiogenic shock. Eur Heart J. 2005;26(13):1276–83. https://doi.org/10.1093/eurheartj/ehi161.
22. Gregoric ID, Cohn WE, Akay MH, La Francesca S, Myers T, Frazier OH. CentriMag left ventricular assist system. Tex Heart Inst J. 2008;35(2):184–5.
23. Rao P, Khalpey Z, Smith R, Burkhoff D, Kociol RD. Venoarterial extracorporeal membrane oxygenation for cardiogenic shock and cardiac arrest. Circ Heart Fail. 2018;11(9):e004905. https://doi.org/10.1161/CIRCHEARTFAILURE.118.004905.
24. Patel S, Lipinski J, Al-Kindi S, et al. Simultaneous venoarterial extracorporeal membrane oxygenation and percutaneous left ventricular decompression therapy with Impella is associated with improved outcomes in refractory cardiogenic shock. ASAIO J. 2019;65(1):21–8. https://doi.org/10.1097/MAT.0000000000000767.
25. Kapur NK, Esposito M. Hemodynamic support with percutaneous devices in patients with heart failure. Heart Fail Clin. 2015;11(2):215–30. https://doi.org/10.1016/j.hfc.2014.12.012.
26. Hoeper MM, Tudorache I, Kühn C, et al. Extracorporeal membrane oxygenation watershed. Circulation. 2014;130(10):864–5. https://doi.org/10.1161/CIRCULATIONAHA.114.011677.
27. Cakici M, Gumus F, Ozcinar E, et al. Controlled flow diversion in hybrid venoarterial-venous extracorporeal membrane oxygenation. Interact Cardiovasc Thorac Surg. 2018;26(1):112–8. https://doi.org/10.1093/icvts/ivx259.
28. Madershahian N, Nagib R, Wippermann J, Strauch J, Wahlers T. A simple technique of distal limb perfusion during prolonged femoro-femoral cannulation. J Card Surg. 2006;21(2):168–9. https://doi.org/10.1111/j.1540-8191.2006.00201.x.
29. Millar JE, Fanning JP, McDonald CI, McAuley DF, Fraser JF. The inflammatory response to extracorporeal membrane oxygenation (ECMO): a review of the pathophysiology. Crit Care. 2016;20(1):387. https://doi.org/10.1186/s13054-016-1570-4.
30. Lim HS, Howell N, Ranasinghe A. The physiology of continuous-flow left ventricular assist devices. J Card Fail. 2017;23(2):169–80. https://doi.org/10.1016/j.cardfail.2016.10.015.
31. Feldman D, Pamboukian SV, Teuteberg JJ, et al. The 2013 International Society for Heart and Lung Transplantation guidelines for mechanical circulatory support: executive summary. J Heart Lung Transplant. 2013;32(2):157–87. https://doi.org/10.1016/j.healun.2012.09.013.
32. Kapur Navin K, Esposito Michele L, Yousef B, et al. Mechanical circulatory support devices for acute right ventricular failure. Circulation. 2017;136(3):314–26. https://doi.org/10.1161/CIRCULATIONAHA.116.025290.
33. Kuchibhotla S, Esposito ML, Breton C, et al. Acute biventricular mechanical circulatory support for cardiogenic shock. J Am Heart Assoc. 2017;6(10). https://doi.org/10.1161/JAHA.117.006670.

Part III

Methods of Hemodynamic Evaluation

Key Clinical Findings

10

Sachin S. Goel and William J. Stewart

From inability to let well alone;
from too much zeal for the new and contempt for what is old;
from putting knowledge before wisdom, science before art, and cleverness before common sense;
from treating patients as cases;
and from making the cure of the disease more grievous than the endurance of the same, Good Lord, deliver us.

– Sir Robert Hutchison MD FRCP (1871–1960)

Case 1

A 65-year-old male, with history of coronary artery disease, anterior wall myocardial infarction 10 years ago, and ischemic cardiomyopathy with left ventricular ejection fraction of 30%, presents to the emergency room with worsening dyspnea on exertion and orthopnea for 1 week. On examination, his heart rate is 88 beats per minute and regular, blood pressure is 126/74 mm Hg, and respiratory rate is 18 per minute with oxygen saturation measuring 94% at room air. The jugular venous pressure is elevated to 14 cm of water. Examination of the lungs is notable for bibasilar rales. Cardiovascular exam reveals a laterally displaced apical impulse. The S1 is normal, S2 is physiologically split, and there is a moderately loud S3. There is no audible murmur. Abdominal examination reveals mild hepatomegaly, with the edge 2 cm below the costal margin, with no evidence of ascites. The lower extremities demonstrate moderate pitting edema to the mid-calf bilaterally.

This patient is in acute decompensated heart failure (ADHF), which, even today, remains a clinical diagnosis performed at the bedside, based primarily on history and physical examination, rather than on laboratory data. The most important clues to this diagnosis are symptoms related to dyspnea and signs related to biventricular congestion and volume overload. Of the symptoms, orthopnea correlates best with elevated pulmonary capillary wedge pressure (PCWP), with a sensitivity approaching 90% [1]. Clinically evident edema usually indicates a volume excess of at least 3–4 L. Measuring blood pressure is of critical importance in patients with ADHF since hypotension is one of the strongest predictors of poor outcomes [2] and has important implications for therapy.

Jugular venous pressure (JVP) is a cardinal aspect of the cardiovascular examination in the assessment of volume status in patients in general, and in those with ADHF in particular. However, estimation of JVP is highly dependent on examiner skill, experience, and patience. An abnormally elevated JVP is a pressure defined as >5 cm of water. If the patient is sitting at a 45 degree angle to the bed, there should be no visible pulsations above the angle of Louis. JVP reflects right atrial (RA) pressure. It is often used

S. S. Goel (✉)
Prairie Heart Institute, St John's Hospital, Springfield, IL, USA
e-mail: Sachin.Goel@prairieheart.com

W. J. Stewart
Department of Cardiovascular Medicine, Cleveland Clinic, Cleveland, OH, USA

A. T. Askari, A. W. Messerli (eds.), *Cardiovascular Hemodynamics*, Contemporary Cardiology,
https://doi.org/10.1007/978-3-030-19131-3_10

as a surrogate for left ventricular filling pressure; however right heart failure is often absent in patients with left-sided heart failure. The most common cause of right ventricular failure is left ventricular failure. In a study consisting of 1000 consecutive patients with advanced heart failure undergoing right heart catheterization, RA pressure was found to somewhat reliably predict PCWP (r = 0.64), and the positive predictive value of RA pressure >10 mm Hg for PCWP >22 mm Hg was 88% [3]. Hepatojugular reflux (HJR) is jugular venous distension induced by firm pressure over the liver. An increase in JVP >3 cm by this maneuver is a positive HJR, which is a sign of right-sided volume overload. The presence of jugular venous distension, at rest or inducible, is the bedside clinical sign that has the best combination of sensitivity (81%), specificity (80%), and predictive accuracy (81%) for prediction of elevation of PCWP (≥18 mm Hg) [4].

The third heart sound (S3) occurs in early diastole due to abrupt cessation of rapid early diastolic left ventricular inflow as a consequence of increased LV filling pressures and an abnormally stiff, non-compliant left ventricle [5]. It is a fairly specific marker for LV dysfunction and correlates with BNP levels [6]. However, it is not as sensitive as other bedside findings. In a comprehensive analysis evaluating all studies published between 1966 and 2005 which assessed the precision and diagnostic accuracy in diagnosing the cause of dyspnea, the S3 was found to increase the likelihood of ADHF more than any other part of the physical examination (likelihood ratio 11, 95% Confidence Interval 4.9–25.0) [7]. The S3 is associated with elevated LV filling pressures [8]. In a comprehensive study of the physiology of the S3 comparing findings from phonocardiography, tissue Doppler echocardiography, BNP, and invasive LV hemodynamics, patients with an audible S3 were found to have a higher early mitral inflow velocity (E), a more rapid deceleration time (DT) of early mitral inflow, reduced mitral annular velocity (e'), and therefore higher E/e' ratio. The E/e' ratio has been correlated with elevated LV filling pressures [9, 10].

Hepatomegaly results from increased central venous pressure and is often accompanied by right upper quadrant tenderness. Based on various components of the history and physical examination, patients with ADHF can be assigned to one of the quadrants of a 2 × 2 table, each of which represents a distinct hemodynamic profile defined by the presence or absence of congestion (wet or dry) and low or normal perfusion (cold or warm) (Fig. 10.1) [11]. This strategy is very useful in selecting initial therapy and identifying prognosis in patients with ADHF.

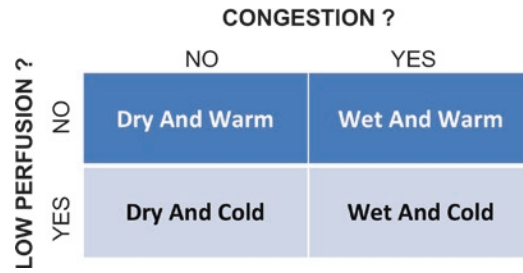

Fig. 10.1 Hemodynamic profiles in ADHF. Evidence for *congestion* (the "yes-no" delineation of the two columns) includes orthopnea, elevated JVP, hepatojugular reflux, S3, rales, hepatomegaly, ascites, peripheral edema, and a loud P2. Evidence *for low perfusion* (the "yes-no" delineation of the two rows) includes narrow pulse pressure, cool and clammy extremities, altered mentation, and oliguria

Case 2

A 54-year-old lady with known history of a heart murmur for over two decades presents with symptoms of worsening fatigue, dyspnea on exertion, and palpitations for the last 2 years. On examination, her pulse is irregular with a heart rate of 110 beats per minute and her blood pressure is 132/84 mm Hg. The jugular venous pressure is elevated to 12 cm of water. Cardiovascular exam reveals laterally displaced, brisk, enlarged, and hyperdynamic apical impulse. The S1 is normal and there is a loud 3/6 holosystolic murmur radiating to the axilla and to the left paravertebral region. In addition, a parasternal right ventricular heave is palpable and a loud P2 is audible. The pulmonary exam is notable for bibasilar rales. Abdominal examination is unremarkable and there is trace bilateral pedal edema.

This patient has chronic severe mitral regurgitation (MR), likely secondary to mitral valve

prolapse (MVP). Although this patient's history and physical findings are classic, clinical findings in MR vary depending on acuity, severity, and the mechanism. For example, in acute severe MR, sometimes caused by acute papillary muscle rupture or endocarditis, the apical LV impulse is not displaced because the LV has not had a chance to dilate. In acute severe MR, the systolic murmur may be early in timing and decrescendo in configuration due to rapid systolic equalization of pressures between the left ventricle and the left atrium (LA). The LA pressure would have a large "V" wave during ventricular systole. MVP is sometimes associated with (1) one or more systolic clicks, produced by sudden tensing of the elongated chordae tendineae as the leaflets prolapse, and (2) a holosystolic or late systolic murmur. In less than severe MR, it is useful to observe the onset of the murmur and the timing of systolic click in MVP, both of which move earlier in systole with maneuvers which reduce left ventricular end diastolic volume (such as standing and the Valsalva maneuver), while the murmur becomes louder. Conversely, the onset of the murmur and the timing of systolic click in MVP are delayed later in systole with maneuvers that increase left ventricular end diastolic volume (such as squatting) and the murmur becomes softer (Fig. 10.2) [12]. Severe MR is often associated with a holosystolic murmur that radiates

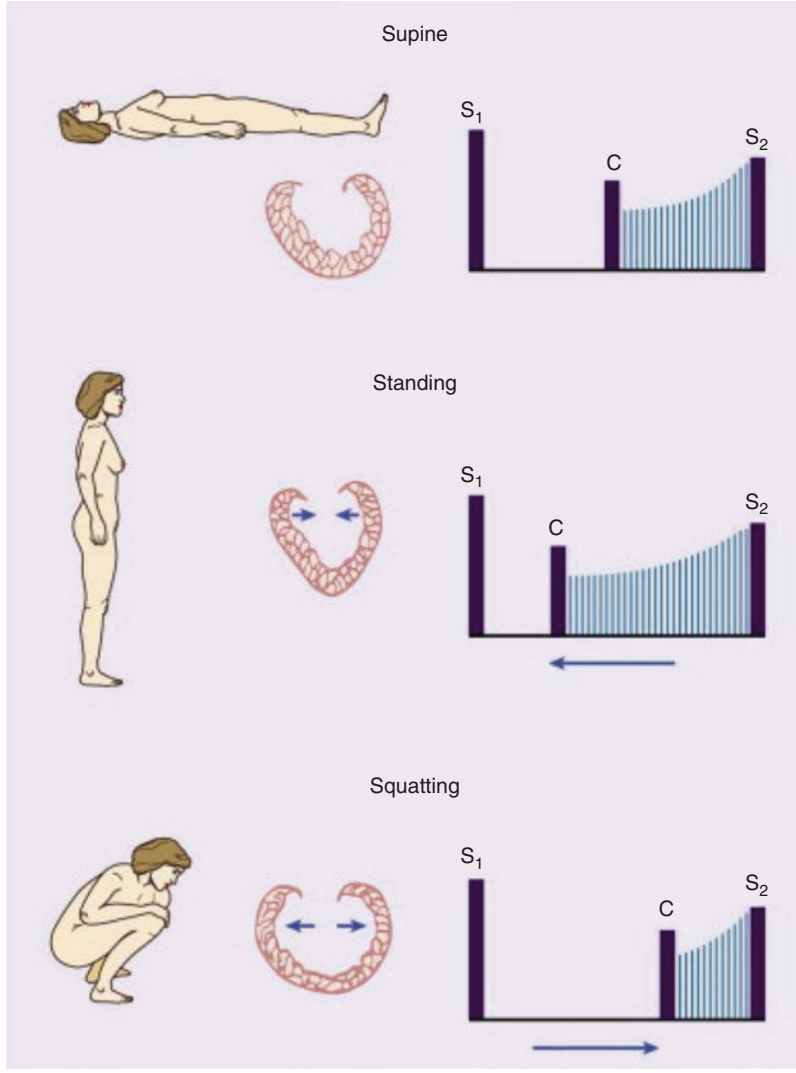

Fig. 10.2 Behavior of the nonejection click (C) and systolic murmur of mitral valve prolapse. The top panel shows the first heart sound (S1), the mid-systolic click (C), and the second heart sound (S2), with the late systolic murmur of moderate mitral regurgitation while the patient is supine. With standing, (middle panel) venous return decreases, the heart becomes smaller, and the prolapse occurs earlier in systole. The click and murmur move closer to S1. With squatting, (lower panel) venous return increases, causing an increase in left ventricular chamber size. The click and murmur occur later in systole and move away from S1. (From Shaver et al. [27])

posteriorly to the axilla and around to the left paravertebral region in the back, irrespective of which mitral leaflet is involved. As mitral regurgitation becomes chronic, left ventricular volume overload leads to left atrial enlargement and atrial fibrillation is common. With development of pulmonary hypertension, the P2 component of the second heart sound becomes louder. The S2 splitting may widen with more severe MR, due to a combination of early A2 as a result of decrease in left ventricular ejection time and delay in P2.

Case 3

A 64-year-old man with history of coronary artery bypass grafting (CABG) 15 years ago presents with complaints of increasing dyspnea on exertion over the last 12 months. Recently he has also noted worsening leg edema and increasing abdominal girth. On examination, his heart rate is 90 beats per minute and regular, and his blood pressure is 108/74 mm Hg. The jugular venous pressure is elevated to 14 cm of water with a prominent, rapidly collapsing *y* descent and a positive Kussmaul sign. The apical impulse is not displaced. The S1 and S2 are normal and there is a high-pitched early diastolic sound, corresponding with the prominent y descent seen in jugular venous waveform, which is heard best at the LV apex. Abdominal examination reveals pulsatile hepatomegaly with evidence of ascites. Bilateral lower extremity edema is present.

This patient likely has pericardial constriction, based on his history and physical findings. Subsequent imaging and cardiac catheterization confirmed this diagnosis. Constriction is characterized by thickened, scarred, and/or calcified pericardium that markedly limits diastolic filling of the heart. The jugular venous waveforms help clarify hemodynamics in constrictive pericarditis. Jugular venous pressure contour normally has two distinct positive waves (*a* and *v* wave) and two negative waves (*x* and *y* descent) (Fig. 10.3a). The *a* wave occurs with right atrial systole and follows the P wave on EKG and precedes the first heart sound (S1). The *x* descent normally occurs as RA pressure falls after the *a* wave and ventricular systole pulls the tricuspid valve and the RA downward. The *c* wave interrupts the *x* descent

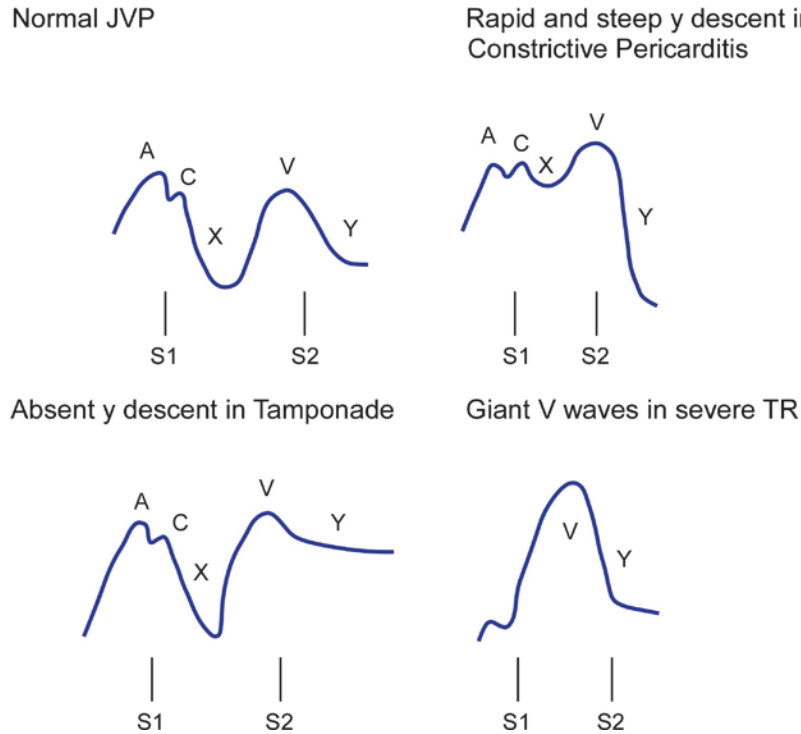

Fig. 10.3 Jugular venous waveform patterns – (**a**) normal patients, (**b**) (constrictive pericarditis), (**c**) pericardial tamponade and (**d**) (severe tricuspid regurgitation) (TR). JVP jugular venous pressure, S1 first heart sound, S2 second heart sound. The A, C, and V positive waves, and the X and Y negative waves, are explained in the text

during early ventricular systole as the tricuspid valve is briefly pushed in to the right atrium as the ventricle begins contracting, thereby elevating RA pressure briefly. The *v* wave occurs with RA filling at the end of ventricular systole, just after the second heart sound (S2). The *y* descent follows the v wave and occurs with fall in RA pressure after the tricuspid valve opens and fills the RV in diastole. Regarding the abnormal jugular venous pressure waveform in constrictive pericarditis, the most prominent wave is the rapid *y* descent, as the ventricles fill rapidly during early diastole due to elevated atrial pressures. Once the pericardial constraining volume is reached, however, ventricular filling slows abruptly due to the development of high ventricular pressure, which is manifested as the characteristic dip and plateau in ventricular diastolic pressures. The JVP contour therefore has an M or W-shaped contour (Fig. 10.3b), with a prominent, rapidly collapsing *y* descent, along with a normal or reduced *x* descent. Another feature of constriction is the respirophasic changes in jugular venous pressure. In normal individuals, JVP falls with inspiration as a reflection of the reduction in the intrathoracic pressure; the increased venous return is accommodated by the compliant right ventricle. In constrictive pericarditis, the increased venous return is not accommodated well; the increased venous return meets the stiff and inelastic pericardium, resulting in a rise in jugular venous pressure with inhalation, characteristically referred to as Kussmaul sign [13]. The classic (sometimes the only) auscultatory finding in constrictive pericarditis is a high-pitched early diastolic sound, referred to as pericardial knock, which occurs due to the abrupt cessation of blood during early diastolic ventricular filling. The pericardial knock corresponds in timing with the prominent y descent in JVP [14].

Case 4

A 66-year-old lady with history of metastatic breast carcinoma presents with worsening dyspnea on exertion for the last 3 days. On examination, her heart rate is 110 beats per minute, blood pressure is 88/56 mm Hg, and there is a paradoxical pulse of 20 mm Hg. The jugular venous pressure is markedly elevated to the angle of the jaw, with an absent *y* descent. The apical impulse is reduced and the heart sounds are muffled and distant. Pulmonary examination reveals clear breath sounds bilaterally.

The triad of hypotension, elevated JVP, and muffled heart sounds, also known as Beck's triad, should alert one to the possibility of cardiac tamponade. This was first described in 1935 by Claude Schaeffer Beck, who was Professor of Cardiovascular Surgery at Case Western Reserve University. Cardiac tamponade occurs when fluid of any kind accumulates in the pericardial space, to an extent where high intrapericardial pressure limits cardiac filling. This leads to markedly elevated venous pressures and reduced cardiac output, which can be rapidly fatal if not treated promptly. A relatively small amount of fluid that accumulates rapidly in the pericardial space can lead to tamponade. In case of a slowly accumulating pericardial effusion, a much larger volume of fluid may be necessary to cause tamponade as the pericardial pressure-volume relation shifts to the right, with greater compliance of the parietal pericardium [15, 16]. In either situation, once a critical amount of fluid has accumulated in the pericardial space, the intrapericardial pressure rises significantly even with relatively smaller rises in volume. The increased intrapericardial pressure may impair cardiac filling and reduce cardiac output. As a compensatory mechanism for maintaining cardiac output and blood pressure, tachycardia is nearly always present in tamponade. One exception to this rule is when the underlying cause for pericardial effusion and resultant tamponade is hypothyroidism. The JVP in pericardial tamponade is almost always elevated, and is sometimes associated with venous distension in the forehead and scalp. The jugular venous waveform is characterized by an absent *y* descent (Fig. 10.3c) due to restricted or diminished ventricular filling even in early diastole with the markedly elevated pericardial pressure. This pattern is in contrast to constrictive pericarditis where ventricular filling in early diastole is rapid and abbreviated prior to its cessation in mid-diastole due to the pericardial constraint.

Pulsus paradoxus, described by Adolf Kussmaul in 1873, is a helpful sign of cardiac tamponade. Pulsus paradoxus is defined as an abnormally large (>10 mm Hg) decline in systolic blood pressure during inhalation and is a consequence of exaggerated ventricular interdependence and exaggerated effects on left- and right-sided filling due to changes in intrathoracic pressure (Fig. 10.4). Normally, the inspiratory decrease in intrathoracic pressure causes an increase in systemic, venous return and a decrease in pulmonary venous return, with a small movement of

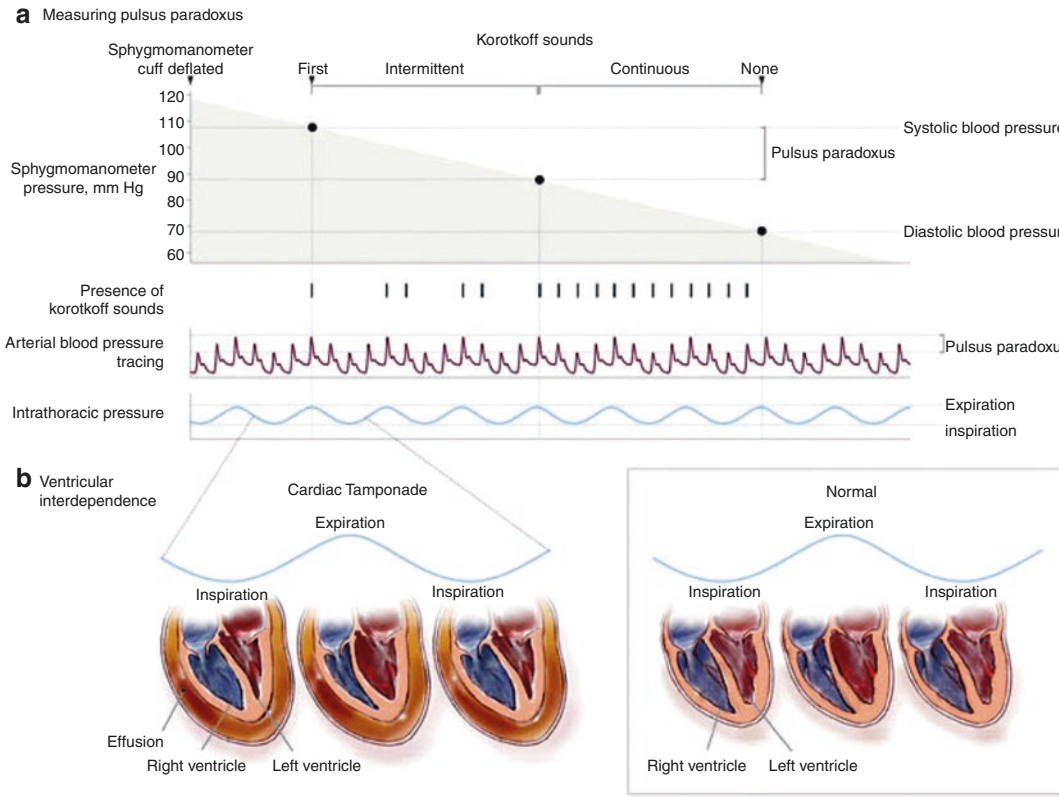

Fig. 10.4 Measurement and mechanism of pulsus paradoxus (**a**) The examiner inflates the sphygmomanometer cuff fully, listens for Korotkoff sounds as the cuff is slowly deflated, and then notes the pressure at which Korotkoff sounds are initially audible only during expiration. As the cuff is further deflated, the examiner notes the pressure at which Korotkoff sounds become audible during expiration and inspiration. The difference between these two pressures is the pulsus paradoxus, which can normally be from 0 to 10 mm Hg. In cardiac tamponade, the pulsus paradoxus measures greater than 10 mm Hg. Inspiratory diminution in the arterial blood pressure tracing represents the pulsus paradoxus. A similar phenomenon may be observed on a pulse oximeter waveform. (**b**) During inspiration in the normal heart, negative intrapleural pressures increase venous return to the right ventricle and decrease pulmonary venous return to the left ventricle by increasing the pulmonary reservoir for blood. As a result of increased right ventricular distention, the interventricular septum bows slightly to the left, and the filling and stroke volume of the left ventricle are mildly reduced. In expiration, these changes are reversed, resulting in the septum bowing to the right and a mild reduction in right ventricular filling. In the presence of cardiac tamponade, the reciprocal changes seen in the normal heart are exaggerated when the pericardial sac is filled with fluid, thus limiting distensibility of the entire heart. This results in a more dramatic reduction in filling of the left ventricle during inspiration, exacerbating the normal inspiratory decrease in stroke volume and blood pressure. (From Roy et al. [28])

the interventricular septum toward the left. The small decrease in left ventricular stroke volume and aortic peak systolic blood pressure results primarily due to inspiratory decrease in LV filling from the decrease in intrathoracic pressure. With tamponade, in presence of pericardial fluid compressing all the walls of the heart, these respiratory changes in venous return are exaggerated. With inhalation, the drop in left-sided filling reduces left ventricular stroke volume and the systemic systolic blood pressure drops by a greater extent than in normal physiology, i.e., more than 10 mm Hg. In patients with true tamponade, pulsus paradoxus can be masked by the presence of numerous conditions, including severe hypotension, pericardial adhesions, right ventricular hypertrophy, severe aortic regurgitation, a stiff left ventricle or other conditions which elevate LV filling pressure, and atrial septal defect [16].

Case 5

A 78-year-old male with history of hypertension, hyperlipidemia, and diabetes mellitus presents with worsening dyspnea on exertion over the last 2 years. On examination, he has a slow-rising, late-peaking, low-amplitude carotid contour by palpation. His heart rate is regular at 88 beats per minute and blood pressure 108/66 mm Hg. The jugular venous pressure is normal. The apical impulse is sustained and non-displaced. Cardiac auscultation reveals normal S1, a soft S2 without splitting, and a 3/6 late peaking systolic ejection murmur, best heard in the right second intercostal space and radiating to the carotids. Pulmonary examination reveals clear breath sounds bilaterally. Abdominal examination is unrevealing and he has no pedal edema.

Based on clinical findings, this patient likely has severe aortic stenosis (AS). Hemodynamically, AS is characterized by a pressure gradient between the left ventricle and aorta during systole (Fig. 10.5a), and the magnitude of this pressure gradient is an indication of the severity of AS. Several physical findings have been shown to correlate with severity of AS, including the characteristic carotid pulse contour, a reduced or absent S2, and the timing and intensity of murmur (Table 10.1) [17]. The quality of carotid pulse in severe AS has classically been described as "parvus et tardus," i.e., weak and slow-rising and delayed. This can be best assessed best by simultaneously palpating the carotid pulse and auscultating the heart. In severe AS, the weak and delayed carotid pulse reflects severe obstruction, with a reduced early systolic rate of blood flow across the aortic valve into the arterial circulation. Delay between brachial and radial pulse (brachioradial delay) has also been described as a clinical indicator of severe AS [18]. With worsening AS, the aortic valve leaflets become increasingly calcified and immobile, leading to a soft or inaudible A2 component of the second heart sound. A normal intensity of A2 implies flexible and mobile aortic valve leaflets and can essentially be very helpful in ruling out severe senile AS. However, the A2 may still be normal in severe AS in young people whose stenosis reflects more congenital fusion of the cusps and less calcific restriction. The gradient between the left ventricle and aorta in AS is greatest in mid-systole and is relatively small early and late in systole. The murmur therefore has a diamond shape; it starts soft and builds to a peak in mid-systole and then becomes quiet in late systole immediately before S2 (Fig. 10.5a). It is referred to as a systolic ejection murmur, since it begins after S1 and ends before S2. The intensity of murmur correlates generally with severity of AS, but there are many exceptions to that correlation. It is best heard at the base of the heart in the second right intercostal space and radiates to the carotids. The timing of the peak intensity of systolic ejection murmur also corresponds to the severity of AS. With mild AS, the maximum instantaneous gradient between the left ventricle and aorta occurs early in systole;

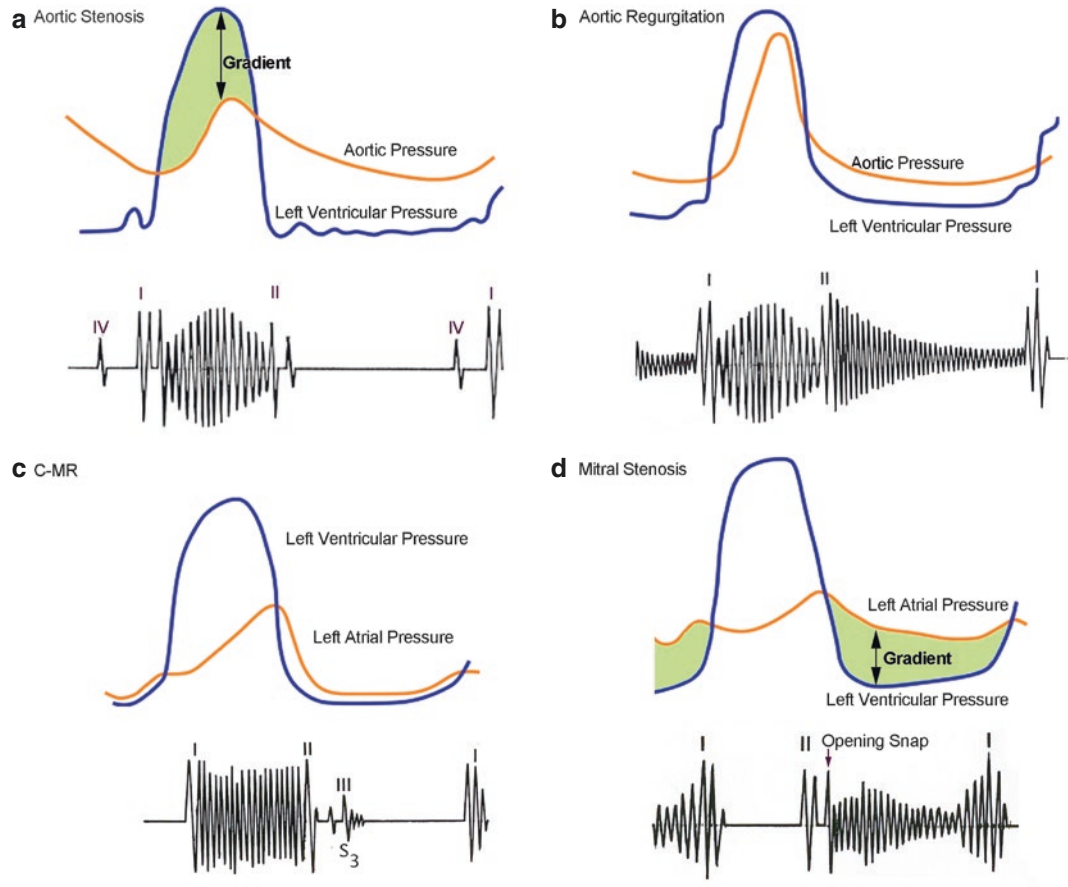

Fig. 10.5 Relationship of murmurs to LV, aortic, and LA pressure waveforms and hemodynamics in various valve diseases. (**a**) *Aortic stenosis (AS).* The gradient between the left ventricle and aorta in AS is greatest in mid-systole and is relatively small early and late in systole. The murmur therefore has a diamond shape, i.e., starts soft and builds to a peak in mid-systole and then becomes quiet in late systole immediately before S2. In young AS patients, there may be an early ejection sound. In senile AS, A2 becomes diminished or absent. An S4 is common due to LV noncompliance. (**b**) *Aortic regurgitation (AR)*. The early diastolic murmur (EDM) begins with S2 and has a decrescendo contour. The duration of the murmur continues for a variable time in diastole, depending on severity and acuity of AR. Notice that aortic diastolic pressure is low. (**c**) *Mitral regurgitation*. There is a pansystolic murmur with a flat profile due to the regurgitant flow into the left atrium. Note that the left atrial pressure rises during systole, a "v" wave. An early diastolic S3 or flow rumble may occur. (**d**) *Mitral stenosis (MS)*. A loud S1 is heard since the mitral gradient is high and the leaflets are not very thickened or calcified. An important indicator of the severity of MS is the time interval between the S2 and opening snap (OS), which is the time it takes for LV pressure to fall from late systolic aortic pressure to early diastolic left atrial pressure. The mitral valve snaps open due to the increased gradient, causing an opening snap (OS). The diastolic murmur correlates with the gradient across the mitral valve, which is largest in early diastole, and increases again in late diastole in this patient in sinus rhythm

hence the systolic murmur peaks in early systole. As the severity of AS worsens, the maximum instantaneous gradient between the left ventricle and the aorta occurs progressively later in systole, and correspondingly the murmur peaks late. No single physical examination finding rules in or rules out severe AS; however, a combination of slow and delayed carotid impulse, reduced intensity of S2, and mid to late peaking systolic ejection murmur at the base radiating to the neck is fairly accurate in diagnosing severe AS clinically [19].

Table 10.1 Physical findings in severe aortic stenosis

Examination	Finding
Carotid pulse	Weak, slow rising, and delayed carotid pulse (pulsus parvus et tardus)
Second heart sound (S2)	Soft or inaudible A2 component of S2
Murmur	Mid to late peaking in systole, radiating to the neck

Case 6

A 56-year-old asymptomatic male is referred for evaluation after his primary care physician heard a heart murmur. On examination, he has a rapidly collapsing pulse with a regular heart rhythm, heart rate of 90 beats per minute and blood pressure of 144/40 mm Hg, and therefore a pulse pressure of 104 mm Hg. Cardiac examination reveals a wide and hyperdynamic apical impulse that is displaced laterally and inferiorly. A high-frequency, blowing decrescendo diastolic murmur is heard, best at the left sternal border in end expiration with the patient sitting up. There is also a short early systolic murmur of moderate intensity. In addition, a systolic and diastolic bruit is heard when the femoral artery is partially compressed and popliteal systolic cuff pressure is >170 mm Hg. Pulmonary and abdominal exam are unremarkable.

No other disease condition in cardiovascular medicine has more eponymous signs associated with it than chronic aortic regurgitation (AR) (Table 10.2). The principal hemodynamic abnormality in chronic AR responsible for these signs is the wide pulse pressure (Fig. 10.5b). The low diastolic arterial pressure results from the rapid run-off of blood from the aorta back into the left ventricle. There is an increase in left ventricular end diastolic volume and hence an increase in left ventricular stroke volume and the pulse pressure. The arterial pulse contour has a rapidly rising and collapsing pulse referred to as "water hammer" pulse, or Corrigan's sign, first described by Sir Dominic Corrigan in 1832. The carotid upstroke is rapid resulting from the increased stroke volume. Few studies have systematically assessed the predictive value of these eponymous signs in Table 10.1; however Duroziez's sign, Corrigan pulse, and Hill's sign are perhaps most important useful signs in detecting severe chronic AR [20]. In a literature review, the presence of a diastolic decrescendo murmur as heard by a cardiologist was the most useful finding for detecting AR (positive likelihood ratio of 8.8), and its absence was most useful in ruling out AR [21]. The diastolic murmur of chronic AR is high-pitched and blowing in character and is best heard along the left sternal border at the left third or fourth intercostal space, with the patient sitting up and leaning forward, with held exhalation. The severity of chronic AR correlates somewhat with the duration of the murmur, while its intensity varies widely. With severe chronic AR, the murmur can be holodiastolic. However, in very severe AR, particularly sudden onset acute AR, the murmur may be early diastolic and short, due to rapid equilibration of LV and aortic pressure. Most patients with severe AR also have an early peaking systolic flow murmur which results from the increased stroke volume even in the absence of concomitant AS. Finally, an apical mid-late diastolic rumble, referred to as the Austin-Flint murmur is audible

Table 10.2 Eponymous signs of chronic aortic regurgitation

Sign	Description
Hill's sign	Exaggerated difference in lower and upper extremity blood pressure
Corrigan's sign	Rapidly collapsing arterial pulse
Duroziez's sign	Systolic and diastolic bruit heard on partial femoral artery compression
Quincke's sign	Exaggerated capillary pulsations of the nail beds
deMusset's sign	Head bobbing with each heart beat
Traube's sign	Pistol shot sound heard over the femoral artery
Mueller's sign	Pulsatile uvula
Becker's sign	Pulsatile retinal arteries
Rosenbach's sign	Pulsatile liver
Gerhard's sign	Pulsatile spleen
Mayne's sign	More than 15 mm hg drop in diastolic blood pressure with arm elevated compared to arm in standard position

in occasional patients with chronic severe AR, reflecting the impact of the AR jet on the anterior mitral valve leaflet; this should not be confused with the diastolic rumble of mitral stenosis.

Case 7

A 62-year-old male with 30 pack-year history of smoking, hypertension, hyperlipidemia, and diabetes mellitus presents to the ER after experiencing worsening substernal chest discomfort radiating to the left arm for 8 hours. On arrival, he appears diaphoretic with a heart rate of 104 beats per minute, blood pressure of 90/68 mm Hg and he is tachypneic with a respiratory rate of 20 per minute and an oxygen saturation of 94% on room air. He is drowsy and somewhat disoriented. Stat 12 lead EKG reveals widespread 3 mm ST segment elevation in precordial leads V1 through V6 and reciprocal ST segment depression in inferior limb leads. Cardiovascular examination reveals elevated JVP at 12 cm and normal heart sounds with no murmurs, rubs or gallops. Pulmonary examination reveals bibasilar rales. Abdominal examination is unrevealing and he has no lower extremity edema, but his extremities are cold and clammy. With a diagnosis of acute ST segment elevation myocardial infarction (STEMI) and cardiogenic shock, he is emergently taken to the cardiac catheterization laboratory. The proximal left anterior descending coronary artery (LAD) is found to be totally occluded, so it is opened and stented. Pulmonary artery catheterization shows a PCWP of 28 mm Hg, with a cardiac index of 1.7 L/min per m^2, and an intra-aortic balloon pump (IABP) is placed. Emergent echocardiogram did not show any evidence of mechanical complications of MI.

Cardiogenic shock is characterized by end-organ hypoperfusion due to cardiac dysfunction and is hemodynamically defined by persistent hypotension (systolic blood pressure <80 to 90 mmHg or mean arterial pressure 30 mmHg lower than baseline) with severe reduction in the cardiac index (<1.8 L/min per m^2 without support or <2.0 to 2.2 L/min per m^2 with support) and adequate or elevated filling pressures [22]. The most common cause of cardiogenic shock is acute myocardial infarction (MI) with left ventricular failure. In the setting of MI, it is very important to rule out mechanical complications such as acute severe MR secondary to papillary muscle dysfunction, ventricular free wall rupture, or ventricular septal defect, all of which can contribute to cardiogenic shock. Other causes of these alarming hemodynamics include acute severe LV or RV dysfunction of any etiology, valvular heart disease such as acute mitral or aortic regurgitation, pericardial tamponade, massive pulmonary embolism, acute aortic dissection, hypertrophic obstructive cardiomyopathy, and acute myocarditis. The hallmark of cardiogenic shock is hypoperfusion of the extremities and vital organs. Loss of cardiac output from any cause increases sympathetic activation, which increases arteriolar constriction and systemic vascular resistance, in an attempt to maintain blood pressure and tissue perfusion. Clinically, cardiogenic shock manifests with signs of reduced end-organ perfusion such as altered mental status, oliguria, respiratory distress due to pulmonary congestion, and cool, clammy extremities. Such patients are typically in the bottom right on the hemodynamic profile chart presented in Fig. 10.1, i.e., wet and cold. However, not all patients in cardiogenic shock have vasoconstriction and elevated systemic vascular resistance. Almost a fifth of patients with cardiogenic shock studied in the SHOCK trial had hemodynamic findings of low systemic vascular resistance, similar to patients with sepsis. This probably results from inappropriate vasodilation, which may represent a systemic inflammatory response state (SIRS) similar to sepsis [22, 23]. Cardiogenic shock can be diagnosed based on clinical findings, but invasive hemodynamic monitoring helps confirm and quantify the degree of vasoconstriction or vasodilation, quantifying filling pressures and cardiac output and ultimately guiding therapy.

Case 8

A 78-year-old woman is brought to the ER with fever, cough, shortness of breath, and altered mental status. She has had intermittent fever

and cough with productive sputum for the last 3 days. On arrival to the ER, she is drowsy but arousable and confused. She is febrile with a temperature of 39 °F, heart rate of 120 beats per minute and regular, blood pressure of 80/50 mm Hg, tachypneic with a respiratory rate of 22 beats per minute, and an oxygen saturation of 90% on room air. Cardiovascular examination reveals no jugular venous distension and rapidly collapsing jugular vein distension even when supine. She has normal heart sounds and no murmurs, rubs, or gallops. Pulmonary exam reveals bronchial breath sounds and rales in the right lower zone with egophony and dullness on percussion. Abdominal exam is unrevealing, and peripheral extremities are warm to touch with capillary refill >3 seconds and mottling of skin. Chest X-ray confirms right lower lobe consolidation.

This patient is in septic shock. It is similar to the patient in case 7; however the mechanism and pathophysiology are different. Also called distributive or vasodilatory shock, the hallmark of septic shock is profound vasodilation and inadequate tissue extraction of oxygen. Vasodilation is mediated by three mechanisms: activation of ATP-sensitive potassium channels in the vascular smooth muscle cell plasma membranes, activation of inducible nitric oxide synthetase, and deficiency of vasopressin [24]. This is followed by leukocyte migration and activation and release of pro-inflammatory markers such as tumor necrosis factor (TNF) and interleukins, which lead to tissue damage and organ dysfunction, which manifest as a systemic inflammatory response state (SIRS).[25] SIRS is defined by the presence of one of the following:

- Temperature >38.5 °F or <35 °F
- Heart rate >90 beats per minute
- Respiratory rate >20 per minute or PaCO2 <32 mm Hg
- WBC >12,000 cells/mm^3, <4000 cells/mm^3, or >10% immature band forms

Sepsis is defined as SIRS in presence of an infection. Similarly, severe sepsis and septic shock are largely clinical diagnoses [25]. Severe sepsis is defined as the presence of sepsis and one of the following signs of organ dysfunction:

- Areas of mottled skin.
- Capillary refilling requires 3 seconds or longer.
- Urine output <0.5 mL/kg for at least 1 hour, or the need for renal replacement therapy.
- Elevated blood lactate levels >2 mmol/L.
- New decrease in mental status.
- Platelet count <100,000 platelets/mL.
- Disseminated intravascular coagulation.
- Acute lung injury or acute respiratory distress syndrome (ARDS).
- Cardiac dysfunction, as defined by echocardiography or direct measurement of the cardiac index.

Septic shock is defined by the presence of severe sepsis and one of the following:

- Systemic mean blood pressure <60 mm Hg (<80 mm Hg if previous hypertension) after adequate fluid resuscitation or PCWP between 12 and 20 mm Hg
- Need for dopamine >5 mcg/kg per min or norepinephrine or epinephrine <0.25 mcg/kg per min to maintain mean blood pressure above 60 mm Hg (80 mm Hg if previous hypertension)

Thus sepsis has a continuum of severity ranging from sepsis manifesting as SIRS to severe sepsis and septic shock. Despite optimal management, mortality from severe sepsis and septic shock can range from 40% to 50% or higher. The key for successful outcome is early identification of the severity of this continuum and of a potential infectious focus.

Case 9

A 54-year-old man with history of chronic alcohol abuse and liver cirrhosis presents with hematemesis. On examination, he is afebrile with a heart rate of 78 beats per minute and blood pressure of 130/80 mm Hg when supine and 110 beats

per minute and 102/60 mm Hg when standing. He feels dizzy on standing. His tongue, axillae, and mucous membranes are moist. Cardiac, pulmonary, and abdominal exams are unrevealing.

This patient has hypovolemia likely secondary to blood loss, in this case, bleeding esophageal varices. Hypovolemia occurs when extracellular sodium and fluid are lost at a rate greater than intake. This may occur by way of gastrointestinal losses (hemorrhage, vomiting, diarrhea), renal losses (diuresis, salt wasting), loss from skin (burns), or third space sequestration (acute pancreatitis, acute intestinal obstruction, fracture). One of the most common causes of hypovolemia is excessive use of diuretic medications. History and physical examination are important in identifying the presence, etiology, and severity of hypovolemia, perhaps even more so than laboratory testing. For example, the initial hemoglobin correlates poorly with the degree of blood loss, even in patients whose hypovolemia is due to gastrointestinal hemorrhage. Similarly prerenal azotemia is a late finding in acute dehydration. Postural assessment of systolic blood pressure is the most rapid and reliable bedside tool, in the absence of autonomic neuropathy or over-use of antihypertensive drugs. A drop of more than 10 mm Hg when the patient goes from supine to standing is indicative of at least a 10% deficit in intravascular volume. In a systematic review of physical findings in assessment of patients with blood loss and hypovolemia, severe postural dizziness and an increase in pulse rate $\geq$ 30 beats per minute were found to be the most sensitive and specific findings for large blood loss [26]. In the same study, the presence of dry axilla supported the diagnosis of hypovolemia in patients with vomiting, diarrhea, or decreased oral intake. Moist mucous membranes and a normal furrowed appearance of the tongue were found to argue against it. It is important to remember that postural blood pressure and heart rate should be measured with the intervention of the patient standing still for 1 minute. Jugular venous pressure is usually low in patients with hypovolemia, and it may be necessary to lay the patient down to see the venous pulsations above the clavicle. Normal skin has elasticity or turgor, i.e., it immediately returns to its normal position after being pinched and released. This is due to elastin content in the subcutaneous tissue, which is affected by moisture content and age. In younger individuals, poor skin turgor may represent hypovolemia.

Case 10

A 53-year-old lady with history of rheumatic heart disease with long-standing history of mitral stenosis, s/p balloon mitral valvotomy 15 years ago, and mitral valve replacement 8 years ago presents with worsening fatigue, exercise intolerance, abdominal distension, and lower extremity swelling. On examination, she has an irregularly irregular pulse with a heart rate of 80 beats per minute, blood pressure of 110/68 mm Hg, and respiratory rate of 16 per minute. Jugular venous pressure is elevated to 14 cm of water with a prominent V wave and a sharp y descent. Cardiac exam reveals a palpable right ventricular heave. On auscultation, the P2 is loud and a 3/6 holosystolic murmur is audible at the left lower sternal border. The murmur increases in intensity with inspiration. Abdominal examination reveals a pulsatile and enlarged liver with evidence for ascites. Moderate bilateral pedal edema is also present.

Tricuspid regurgitation (TR) is a valve lesion that occurs commonly, as a result of right ventricular dilatation from any cause, through the effects of secondary pulmonary hypertension. The most frequent cause is left-sided heart failure due to mitral valve disease or left ventricular dysfunction. TR also occurs in the setting of cor pulmonale, from intrinsic lung disease, or from primary pulmonary hypertension. Pathophysiologically, long-standing pulmonary hypertension causes right ventricular pressure overload, which causes dilatation of the right ventricle and tricuspid annulus. In patients with chronic severe TR, the JVP waveform is characterized by the loss of x descent and a prominent systolic V wave (or C-V wave) caused by markedly increased right atrial pressure during ventricular systole, which is followed by a rapid y descent (Fig. 10.3d). Auscultation usually reveals a loud P2 in pres-

ence of pulmonary hypertension. There may be a pansystolic murmur, loudest in about the fourth intercostal space in the left or right parasternal region. Classically, the systolic murmur intensity increases with inspiration (Carvallo sign) as the venous return on the right side of the heart increases; however, this finding is inconsistent. Many patients with significant TR do not have respirophasic variation, and some have an unimpressive murmur. In the absence of pulmonary hypertension, TR may also occur as a primary valve abnormality, due to trauma, or endocarditis classically in patients who have used intravenous drugs, but increasingly in patients with infected pacemaker leads. In severe TR, there is an increase in diastolic flow, so many patients have a diastolic rumble (sometimes quite loud) along the left sternal border and/or a right sided S3. With severe long-standing TR, the pressure gradient between the right atrium and right ventricle is minimized, and the TR murmur may be short early systolic, barely audible, or absent. A pulsatile liver is often present in severe TR, and ascites and extremity edema are commonly present.

Case 11

A 52-year-old male, with no risk factors for coronary artery disease, presents with symptoms of shortness of breath on exertion and two episodes of near syncope. He has family history of sudden death. On examination, his carotid pulse has a rapid upstroke, followed by a second peak. His heart rate is 60 beats per minute and blood pressure 120/80 mm Hg. His jugular veins are not distended. The apical impulse is wide, sustained, and laterally displaced. On cardiac auscultation, S1 is normal and S2 is paradoxically split. A harsh crescendo-decrescendo 3/6 systolic murmur, heard best at the left sternal border, increases in intensity with the Valsalva maneuver, breath holding with increased abdominal pressure. His lungs are clear on auscultation, and abdominal examination is unrevealing.

Based on physical findings, this patient has hypertrophic cardiomyopathy (HCM). HCM is a common genetic cardiovascular disease and is defined as significant myocardial hypertrophy in the absence of an identifiable cause. The most common sites of ventricular hypertrophy are, in decreasing order, the septum, apex, and mid ventricle. It is further classified as obstructive or non-obstructive, depending on whether a dynamic left ventricular outflow tract (LVOT) gradient is present, either at rest or with provocative maneuvers. LVOT obstruction is the main pathophysiologic mechanism in HCM. The hypertrophied proximal interventricular septum combines with systolic anterior motion (SAM) of the mitral valve leaflets toward the septum, which causes LVOT obstruction and also mitral regurgitation. LVOT obstruction in HCM is dynamic, in contrast to valvular or membranous AS where obstruction to LV outflow is fixed. In dynamic LVOT obstruction, the degree of obstruction varies with cardiac contractility and loading conditions, whereas in case of fixed obstruction such as AS, the degree of obstruction doesn't vary as much with maneuvers. Purposeful alterations in cardiac hemodynamics can be very useful at the bedside in differentiating systolic murmurs of HCM and AS (Table 10.3). Almost all cardiac murmurs decrease in intensity with the Valsalva maneuver except the murmur of HCM. The Valsalva maneuver decreases preload which results in reduced filling of the left ventricle and hence an increase in LVOT obstruction, thus increasing the intensity of systolic murmur in HCM. Similarly, change in position from squatting to standing reduces venous return and preload, thus increasing

Table 10.3 Effect of maneuvers on hypertrophic cardiomyopathy and aortic stenosis

Maneuver	Hemodynamic effect	AS murmur intensity	HCM murmur intensity
Valsalva	Decreased preload	Decreases	Increases
Squat to stand	Decreased preload	Decreases	Increases
Stand to squat	Increased preload	Increases	Decreases
Amyl nitrite inhalation	Decreased preload	No change	Increases

murmur intensity in HCM. Inhalation of amyl nitrite results in vasodilation and decreased preload, which again worsens LVOT obstruction in HCM and the murmur intensity increases. The gradient also increases in the beat after a premature ventricular complex (PVC) and during other types of positive inotropic activity, such as intravenous or endogenous catecholamines. Presence of a loud murmur of at least grade 3/6 usually implies LVOT outflow gradient of greater than 30 mm Hg. The carotid pulse in patients with HCM is characterized by an initial rapid upstroke as no LVOT obstruction exists in early systole. This is followed by a collapse in the pulse as LVOT obstruction develops, followed by a second peak as left ventricular pressure increases to overcome the obstruction. This is referred to as bisferiens pulse, which contrasts markedly from the carotid contour in valvular AS, as mentioned above. The second heart sound in HCM is normal in intensity, and can be paradoxically split due to prolonged ejection time with severe LVOT obstruction.

Case 12

A 45-year-old female, who immigrated from India, presents with new onset palpitations and dyspnea on exertion. She recalls having a prolonged febrile illness during childhood, followed by a murmur. On examination she has an irregularly irregular pulse with a heart rate of 84 beats per minute at rest and a blood pressure of 110/70 mm Hg. Her jugular veins are not distended. The apical impulse has a tapping quality and is undisplaced. A parasternal RV heave is felt along with a palpable P2. On auscultation, S1 is loud, P2 is loud, and an opening snap is heard just after the second heart sound. A low-pitched "rumbling" early diastolic murmur is heard at the apex with the bell of the stethoscope, with the patient in left lateral decubitus position, in held exhalation. Bibasilar rales are heard on lung auscultation. Abdominal and lower extremity exam is unrevealing.

This patient likely has significant mitral stenosis (MS) secondary to rheumatic heart disease. MS is characterized by a pressure gradient between the left atrium and left ventricle during diastole (Fig. 10.5d). The transmitral pressure gradient for any given valve area depends on the transvalvular flow rate. Increase in transmitral flow, most commonly due to exercise, leads to increased pressure gradient and elevated left atrial pressure, which in turn raises pulmonary venous and pulmonary capillary pressures, resulting in dyspnea. Atrial fibrillation or any pathologic state involving an increased heart rate, such as anemia, hyperthyroidism, or others, shortens diastole more than systole. Because the time available for flow across the mitral valve is shorter, the heart spends more percentage of the time in the early phase of diastolic mitral valve flow, when gradients are higher, contributing to marked elevation in left atrial pressure. Chronic pulmonary venous and capillary hypertension leads to pulmonary arterial hypertension and often right-sided heart failure, though not yet in this patient. Atrial fibrillation with rapid ventricular response is often a precipitating or exacerbating factor of the onset of symptoms in patients with MS and may result in pulmonary edema. In fact, MS with rapid AF is a condition where pulmonary edema responds well to beta blocker therapy. Diastolic filling time increases with reduction in heart rate, which reduces the left atrial pressure (because the mitral flow spends more time in "mid to late diastole" when the gradient is lower) and hence the pulmonary venous and capillary pressures are lower.

The physical findings in MS are attributable to two aspects of the inflammatory rheumatic process that leads to fibrosis: (1) thickening and fibrosis of the valve cusps and (2) commissural fusion. The classic auscultatory signs in mild MS, before the leaflets are very thickened, calcified, or markedly immobile, include a loud S1 and an audible opening snap (OS) after S2. The intensity of S1 and presence of the opening snap (OS) reflect the pandiastolic pressure gradient. An important indicator of the severity of MS is the time interval between the S2 and OS, which is the time it takes for LV pressure to fall from late systolic aortic pressure to early diastolic

left atrial pressure. With more severe MS, the left atrial pressure is higher and mitral valve opening occurs closer to S2, causing the S2-OS interval to decrease (Fig. 10.5d). With marked calcification and immobility of the mitral valve leaflets, both S1 and the OS become softer. The murmur of MS is a low-pitched rumbling diastolic murmur at the apex, best heard with the bell of the stethoscope with the patient in left lateral decubitus position. Listening in held exhalation brings the heart closer to the stethoscope and stops the interference of respiratory sounds. The diastolic murmur of MS can be accentuated by brief period of exercise, even just walking or running in place, due to the increased heart rate and the increase in cardiac output. In severe MS, the murmur is usually longer. In patients in sinus rhythm, the rumble is loudest when the gradients are highest, in very early and late diastole (during the atrial kick). The pre-systolic (late diastolic) accentuation of the diastolic murmur is lost when atrial fibrillation occurs.

Self-Assessment Questions

1. A 40-year-old asymptomatic lady presents for evaluation of a murmur that was heard by her primary care physician. On examination, her vital signs are normal. Her jugular veins are not distended and carotid upstrokes are normal. There is a systolic click followed by a 2/6 mid-late systolic murmur at the apex. In order to confirm your suspicion of mitral valve prolapse, you ask the patient to perform squatting and standing maneuvers. What happens to the click and the murmur with squatting and standing maneuvers in a patient with mitral valve prolapse?
   A. The click and murmur move closer to S1 with squatting and away from S1 with standing.
   B. The click and murmur move closer to S1 with standing and away from S1 with squatting.
   C. There is no change in the click or the murmur with standing or squatting.
   D. The click and the murmur decrease in intensity with standing and increase in intensity with squatting.
2. Each of the following statements regarding the JVP waveform and cardiac hemodynamics is true *except*:
   A. Constrictive pericarditis is characterized by a prominent and steep or rapidly collapsing y descent.
   B. Cardiac tamponade is characterized by an absent y descent.
   C. Cannon A wave is present in severe tricuspid regurgitation.
   D. The x descent is lost in severe tricuspid regurgitation.
3. A 52-year-old lady with history of rheumatic heart disease, with history of open mitral commissurotomy 20 years ago, presents with new onset dyspnea on exertion and worsening palpitations. On examination she has an irregularly irregular pulse with a heart rate of 118 beats per minute and a blood pressure of 100/60 mm Hg. Her jugular veins are distended. The apical impulse has a tapping quality and is undisplaced. A parasternal RV heave is felt along with a palpable P2. On auscultation, a low-pitched rumbling mid-diastolic murmur is heard at the apex with the bell of the stethoscope, with the patient in left lateral decubitus position. Bibasilar rales are heard on lung auscultation. What is the next best step in the management of this patient?
   A. Sodium nitroprusside for afterload reduction
   B. Intravenous nitroglycerin infusion for preload reduction
   C. Intravenous morphine
   D. Intravenous beta blocker therapy for rate control
4. All of the following increase the murmur intensity in patients with hypertrophic obstructive cardiomyopathy, except:
   A. Squatting
   B. Standing
   C. Valsalva maneuver
   D. Inhalation of amyl nitrite
5. Each of the following is a finding in severe aortic stenosis, except:
   A. Pulsus parvus et tardus
   B. Soft or inaudible A2
   C. Mid-late peaking systolic murmur
   D. Bisferiens pulse

Answers to Self-Assessment Questions

1. B.
   Standing leads to reduction in venous return and preload. The left ventricle therefore becomes smaller, and prolapse occurs earlier in systole, i.e., closer to S1. Concurrently the intensity of the murmur increases. Squatting leads to increase in preload, causing an increase in LV chamber size; therefore the click and murmur occur later in systole and move away from S1.
2. C.
   Cannon A wave is present in tricuspid stenosis or complete heart block where the right atrium contracts against a closed tricuspid valve due to atrio-ventricular dissociation. All other statements are true.
3. D.
   This patient has rheumatic mitral stenosis and is in heart failure secondary to atrial fibrillation with rapid ventricular response. Tachycardia shortens diastole more than systole, thus reducing the time available for flow across the mitral valve and contributing to marked elevation in left atrial pressure and pulmonary edema. Pure mitral stenosis is the only condition where acute heart failure is treated with beta blocker therapy for heart rate control.
4. A.
   Decrease in preload, secondary to any maneuver (valsalva, standing, and inhalation of amyl nitrite) results in reduced filling of the left ventricle and hence LVOT obstruction increases, thus increasing the intensity of systolic murmur in HCM. Squatting on the other hand increases preload, increasing ventricular volume and reducing the LVOT gradient, hence making the murmur softer in intensity.
5. D.
   In severe AS, the weak and delayed (parvus et tardus) carotid pulse reflects severe obstruction of blood flow across the aortic valve into the peripheral circulation. With worsening AS, the aortic valve leaflets become increasingly calcified and immobile, leading to a soft or inaudible A2 component of S2. With mild AS, the maximum instantaneous gradient between the left ventricle and aorta occurs early in systole; hence the systolic murmur peaks in early systole. As the severity of AS worsens, the maximum instantaneous gradient between the left ventricle and the aorta occurs progressively later in systole, and correspondingly the murmur peaks late. Bisferiens pulse is seen in patients with severe AR or HOCM.

References

1. Stevenson LW, Perloff JK. The limited reliability of physical signs for estimating hemodynamics in chronic heart failure. JAMA. 1989;261:884–8.
2. Gheorghiade M, Abraham WT, Albert NM, Greenberg BH, O'Connor CM, She L, Stough WG, Yancy CW, Young JB, Fonarow GC. Systolic blood pressure at admission, clinical characteristics, and outcomes in patients hospitalized with acute heart failure. JAMA. 2006;296:2217–26.
3. Drazner MH, Hamilton MA, Fonarow G, Creaser J, Flavell C, Stevenson LW. Relationship between right and left-sided filling pressures in 1000 patients with advanced heart failure. J Heart Lung Transplant. 1999;18:1126–32.
4. Butman SM, Ewy GA, Standen JR, Kern KB, Hahn E. Bedside cardiovascular examination in patients with severe chronic heart failure: importance of rest or inducible jugular venous distension. J Am Coll Cardiol. 1993;22:968–74.
5. Braunwald EPJ. Physical examination of the heart and circulation. New York: Elsevier; 2005. p. 817–8.
6. Marcus GM, Gerber IL, McKeown BH, Vessey JC, Jordan MV, Huddleston M, McCulloch CE, Foster E, Chatterjee K, Michaels AD. Association between phonocardiographic third and fourth heart sounds and objective measures of left ventricular function. JAMA. 2005;293:2238–44.
7. Wang CS, FitzGerald JM, Schulzer M, Mak E, Ayas NT. Does this dyspneic patient in the emergency department have congestive heart failure? JAMA. 2005;294:1944–56.
8. Marcus GM, Vessey J, Jordan MV, Huddleston M, McKeown B, Gerber IL, Foster E, Chatterjee K, McCulloch CE, Michaels AD. Relationship between accurate auscultation of a clinically useful third heart sound and level of experience. Arch Intern Med. 2006;166:617–22.
9. Shah SJ, Marcus GM, Gerber IL, McKeown BH, Vessey JC, Jordan MV, Huddleston M, Foster E, Chatterjee K, Michaels AD. Physiology of the third heart sound: novel insights from tissue Doppler imaging. J Am Soc Echocardiogr. 2008;21:394–400.

10. Nagueh SF, Mikati I, Kopelen HA, Middleton KJ, Quinones MA, Zoghbi WA. Doppler estimation of left ventricular filling pressure in sinus tachycardia. A new application of tissue doppler imaging. Circulation. 1998;98:1644–50.
11. Nohria A, Mielniczuk LM, Stevenson LW. Evaluation and monitoring of patients with acute heart failure syndromes. Am J Cardiol. 2005;96:32G–40G.
12. Weis AJ, Salcedo EE, Stewart WJ, Lever HM, Klein AL, Thomas JD. Anatomic explanation of mobile systolic clicks: implications for the clinical and echocardiographic diagnosis of mitral valve prolapse. Am Heart J. 1995;129:314–20.
13. Little WC, Freeman GL. Pericardial disease. Circulation. 2006;113:1622–32.
14. Tyberg TI, Goodyer AV, Langou RA. Genesis of pericardial knock in constrictive pericarditis. Am J Cardiol. 1980;46:570–5.
15. Freeman GL, LeWinter MM. Pericardial adaptations during chronic cardiac dilation in dogs. Circ Res. 1984;54:294–300.
16. Spodick DH. Acute cardiac tamponade. N Engl J Med. 2003;349:684–90.
17. Munt B, Legget ME, Kraft CD, Miyake-Hull CY, Fujioka M, Otto CM. Physical examination in valvular aortic stenosis: correlation with stenosis severity and prediction of clinical outcome. Am Heart J. 1999;137:298–306.
18. Leach RM, McBrien DJ. Brachioradial delay: a new clinical indicator of the severity of aortic stenosis. Lancet. 1990;335:1199–201.
19. Etchells E, Glenns V, Shadowitz S, Bell C, Siu S. A bedside clinical prediction rule for detecting moderate or severe aortic stenosis. J Gen Intern Med. 1998;13:699–704.
20. Babu AN, Kymes SM, Carpenter Fryer SM. Eponyms and the diagnosis of aortic regurgitation: what says the evidence? Ann Intern Med. 2003;138:736–42.
21. Choudhry NK, Etchells EE. The rational clinical examination. Does this patient have aortic regurgitation? JAMA. 1999;281:2231–8.
22. Reynolds HR, Hochman JS. Cardiogenic shock: current concepts and improving outcomes. Circulation. 2008;117:686–97.
23. Kohsaka S, Menon V, Lowe AM, Lange M, Dzavik V, Sleeper LA, Hochman JS. Systemic inflammatory response syndrome after acute myocardial infarction complicated by cardiogenic shock. Arch Intern Med. 2005;165:1643–50.
24. Landry DW, Oliver JA. The pathogenesis of vasodilatory shock. N Engl J Med. 2001;345:588–95.
25. Annane D, Bellissant E, Cavaillon JM. Septic shock. Lancet. 2005;365:63–78.
26. McGee S, Abernethy WB 3rd, Simel DL. The rational clinical examination. Is this patient hypovolemic? JAMA. 1999;281:1022–9.
27. Shaver JA, Leonard JJ, Leon DF. Examination of the heart. Part IV: auscultation of the heart. Dallas: American Heart Association; 1990. p. 13.
28. Roy CL, et al. Does this patient with pericardial effusion have cardiac tamponade. JAMA. 2007;297:1810–8.

Echocardiography

11

Omeed Zardkoohi and Richard A. Grimm

Introduction

Echocardiography is a powerful, noninvasive imaging tool that can provide useful hemodynamic information to guide patient management. Intracardiac pressures, cardiac output, vascular resistance, shunt fractions, and valve lesions can be assessed by using a combination of two-dimensional imaging, color Doppler, pulse and continuous wave Doppler, and tissue Doppler. While echocardiography can provide data complementary to catheter-derived measurements and in some situations has even supplanted invasive monitoring, its application requires meticulous technique, an understanding of basic principles of physics, and an appreciation of potential limitations of the method.

Basic Physics of Echocardiography

Doppler Principle

The Doppler principle explains that the frequency of a wave increases as the source of the wave moves toward an observer, while the frequency of a wave decreases as the source moves away from an observer [1]. The change in the frequency of the sound wave depends on the velocity of the moving object, the velocity of sound, and the angle at which the sound wave hits the object. Echocardiography extrapolates this principle of frequency shift to determine the velocity of blood flow in the heart. When a sound wave is transmitted from the transducer crystal at a given frequency, it is reflected by a red blood cell at a certain frequency back to the transducer (Fig. 11.1). If the red blood cell is moving toward the sound waves, the frequency will increase, but if the red blood cell is moving away from the sound wave, the frequency will decrease. The Doppler shift is the change in frequency between the transmitted sound and the reflected sound and is expressed in the following Doppler equation [2]:

$$\Delta f = f_r - f_0 = \frac{2 f_0 (\cos\theta)(v)}{c}$$

where f_0 = transmitted frequency; f_r = reflected frequency; θ = angle between the ultrasound beam and blood flow; v = velocity of red blood cells; and c = speed of ultrasound in blood (1540 m/s).

Algebraic rearrangement of the equation allows one to solve for velocity:

$$v = \frac{(c)(\Delta f)}{2(f_0)(\cos\theta)}$$

O. Zardkoohi (✉)
Northwestern Medicine, Chicago, IL, USA
e-mail: omeed.zardkoohi@nm.org

R. A. Grimm
Cleveland Clinic, Cleveland, OH, USA
e-mail: grimmr@ccf.org

A. T. Askari, A. W. Messerli (eds.), *Cardiovascular Hemodynamics*, Contemporary Cardiology,
https://doi.org/10.1007/978-3-030-19131-3_11

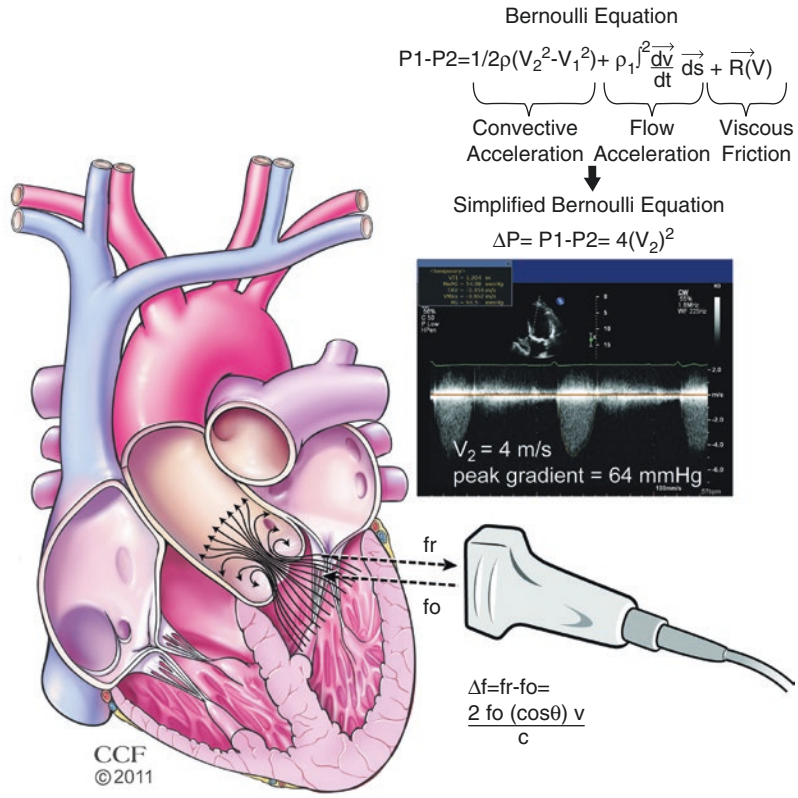

Fig. 11.1 The Doppler principle and Bernoulli equation. *Bottom right*: The echo transducer sends ultrasound waves at a given frequency (f_0) to the heart, and the sound waves are reflected back to the transducer at a different frequency (f_r). The difference between (f_0) and (f_r) is the *Doppler shift*. As shown in the equation, the Doppler shift is directly proportional to the transmitted frequency (f_0), the cosine of the angle of incidence θ (angle between the ultrasound wave and vector of the red blood cell), and the velocity of the red blood cells, however, is inversely proportional to the speed of ultrasound in the medium (c). Rearrangement of the equation allows one to determine the velocity of the red blood cells. *Top right*: The Bernoulli equation enables one to determine the pressure gradient across a stenosis, in this case, a stenotic aortic valve. Flow accelerates just before and at the level of the stenosis. The velocity proximal to the stenosis is V_1, and the velocity distal to the stenosis is V_2. Based on certain assumptions (see text), the Bernoulli equation can be simplified to $P1 - P2 = \Delta P = 4(V_2)^2$. In this case, the peak gradient is 64 mmHg based on the peak velocity across the aortic valve (V_2) of 4 m/s. Reprinted with permission, Cleveland Clinic Center for Medical Art & Photography © 2011

Note that the number "2" in the equation results from the fact that there are actually two Doppler shifts: one when the sound wave sent from the transducer strikes the red blood cell, and the other when the wave reflected from the red blood cell is sent back to the transducer. Doppler echocardiography is highly angle-dependent. *The angle should ideally be <20 ° which results in <10% underestimation of true flow velocity* [2]. When the ultrasound beam is ideally oriented parallel to the direction of blood flow, that is, when the angle θ is 0 °, the equation is simplified since the cosine of 0 ° is 1. Using the simplified Bernoulli principle (Fig. 11.1), it follows that velocity can be used to estimate pressures.

Continuous Wave Versus Pulse Wave Doppler

Two forms of Doppler echocardiography are pulse wave (PW) Doppler and continuous wave (CW) Doppler. Pulse wave Doppler employs a single crystal that emits short bursts or pulses of

ultrasound at a certain rate per second, known as the *pulse repetition frequency (PRF)*, which is dependent on the depth of interrogation. These pulses are sent to a particular sampling location or depth, and the same crystal waits for the reflected frequency (Fig. 11.2a). Because the same crystal sends and receives the ultrasound wave, the maximum velocity that can be measured is limited by the time it takes to send and receive the wave. This is called the *Nyquist limit*, which is one-half the PRF. *The PRF and the Nyquist limit are solely determined by the depth of the sample volume and not by the transducer frequency*. The shallower the sample volume, the higher the PRF or number of pulses sent per second by the transducer. If the Doppler frequency shift is greater than the Nyquist limit, then the velocities above this limit are cut off the spectral

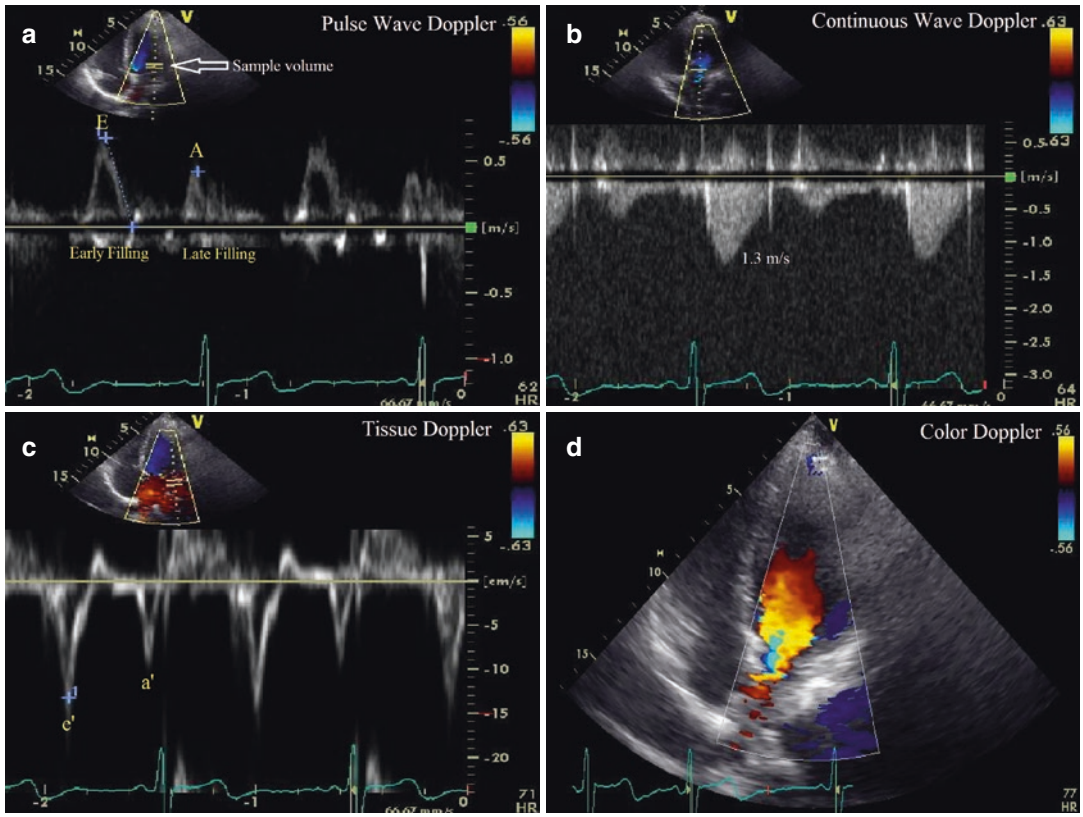

Fig. 11.2 Various forms of Doppler in echocardiography. (**a**) Pulse wave (PW) Doppler of the mitral inflow with the sample volume placed at the leaflet tips. In PW, the same transducer crystal sends and receives waves to determine the Doppler shift at a particular sample volume, marked by the *white arrow*. Because PW obtains information about a particular location, it is said to have "range specificity or range resolution," but it is prone to aliasing. Note that in diastole there is early filling (*E* wave) and Late Filling (*A* wave). Diastasis is known as the period between the *E* and the *A* wave. The *E* velocity is 68 cm/s. (**b**) Continuous wave (CW) Doppler across the aortic valve. In CW, one crystal sends sound waves continuously and another crystal receives the sound waves. Because the CW profile represents all the velocities along the path of interrogation (represented by the *dotted line*), the peak velocity cannot be localized based on the CW signal alone. This phenomenon is known as "range ambiguity." The *y* axis is velocity and the *x* axis is time, and therefore the area under the curve is the velocity time integral (VTI), or the aortic valve VTI, in units of distance (cm). In this example, the peak velocity is 1.3 m/s and the Aortic Valve VTI is 22 cm. (**c**) Tissue Doppler of the mitral annulus characterizes annular velocities, with the corresponding annular e' and a' waves. These waves correspond temporally with the *E* and *A* waves of the mitral inflow. Because $E = 68$ cm/s and $e' = 13$ cm/s, the ratio E/e' is roughly 5, suggesting normal PCWP pressures. (**d**) Color Doppler in which the color pixels represent the mean velocity vector at a particular location

Doppler profile and wrap around to the opposite direction, a phenomenon known as aliasing [1]. Anyone who has watched a wagon wheel in a Western movie appreciates this phenomenon. As the wagon starts to move away, the wheel appears to be moving clockwise. But as the wagon wheel picks up speed and exceeds the "Nyquist limit" of the movie camera, the wheel appears to be moving counterclockwise, which is the equivalent of aliasing. An example of aliasing in echocardiography can be found in Fig. 11.4c, in which PW is used to determine the right ventricular outflow tract (RVOT) velocity. Note that during diastole, the pulmonary regurgitation jet velocity exceeds the Nyquist limit of 1 m/s and wraps around (aliases) to the negative portion of the spectral Doppler profile. Therefore, PW *is suited for measuring low velocity flow (<2 m/s) at specific locations in the heart*, such as the left ventricular outflow tract (LVOT), right ventricular outflow tract (RVOT), mitral inflow, tricuspid inflow, and hepatic vein inflow. PW has the property of "range specificity" in that it provides information at a specific location. Figure 11.2a shows PW of the mitral inflow with sample volume at the leaflet tips, demonstrating the three phases of diastole: early filling (*E* wave), diastasis, and late filling (*A* wave).

Because continuous wave (CW) Doppler employs two crystals, one continuously emitting ultrasound waves and the other continuously receiving reflected waves, it does not fall under the Nyquist limitation (Fig. 11.2b). This allows for interrogation of higher velocities without aliasing. *In CW, all the velocities along the ultrasound beam are recorded, rather than the velocities at one particular location. The peak velocity cannot be localized based on the CW signal alone, a phenomenon known as* "range ambiguity." CW is used to assess gradients in aortic stenosis and mitral stenosis, peak mitral regurgitation velocity, peak tricuspid regurgitation velocity, and intracardiac shunt velocity.

Finally, tissue Doppler is a specialized form of PW that allows the interrogation of myocardial and annular velocities by focusing on lower velocities of higher amplitude with a high frame rate (Fig. 11.2c). Tissue Doppler imaging is employed in the estimation of intracardiac pressures, quantification of wall motion in stress echo, detection of diastolic dysfunction, and intraventricular dyssynchrony, among other applications.

Color Doppler

Color Doppler provides a visual representation of intracardiac flow by translating the velocity vector into color: red and yellow represent flow moving toward the transducer while blue hues represent flow moving away from the transducer (Fig. 11.2d). Note that in the color scale which appears to the right of Fig. 11.2d, the darker the color shade, the closer to zero the velocity becomes, with black representing 0 m/s. The color image is constructed by the summation of multiple scanning lines which translates Doppler shifts into mean velocity, and then the mean velocity into a color based on the color scale. To determine real-time, accurate blood velocities along the path of multiple scanning lines, the transducer must rapidly send multiple groups of pulses or "packets" with pulse wave Doppler. While having more pulses per "packet" increases the accuracy of velocity measurements, this occurs at the expense of temporal resolution because more time is needed to acquire the information from the pulses. Because color Doppler relies on PW, if the velocity of flow is greater than the Nyquist limit, color aliasing occurs, in which color may reverse from blue to yellow, for example.

Bernoulli Equation

The *Bernoulli equation* has applications for echocardiography-based hemodynamic assessment. It is used to calculate the gradient across a stenosis, a regurgitant valve, or a septal defect between two cardiac chambers, and it consists of three components: *convective acceleration, flow acceleration*, and *viscous friction* (Fig. 11.1) [3].

$$P1 - P2 = \underbrace{\frac{1}{2}\rho\left(V_2^2 - V_1^2\right)}_{\text{Convective acceleration}} + \underbrace{\rho\int_1^2 \frac{\overrightarrow{dV}}{dt}\overrightarrow{ds}}_{\text{Flow acceleration}} + \underbrace{R\left(\vec{V}\right)}_{\text{Viscous friction}}$$

where $P1$ = pressure proximal to stenosis; $P2$ = pressure distal to the stenosis, ρ = mass density of blood (1.06×10^3 kg/m^3); V_1 = velocity at proximal location; V_2 = velocity at distal location; ds = acceleration distance; and R = viscous resistance.

Convective acceleration is the increase in kinetic energy that corresponds to the pressure drop across the orifice, and is analogous to the conversion of potential energy to kinetic energy that occurs when an object falls by gravity [3]. The *flow acceleration* component describes the pressure drop required to accelerate the blood by overcoming the blood's inertial forces. Finally, the *viscous friction* component describes the frictional, viscous force that results from neighboring blood cells moving at different velocities.

There are some features of blood flow in the human heart that allow for simplification of the Bernoulli equation. First, the *viscous friction* term is negligible because the velocity profile of blood through a stenotic valve is relatively flat (little variation in blood velocity and therefore little friction), as well as because orifice diameters in the heart are relatively large, minimizing the effect of friction at the center of the orifice. In addition, previous studies have indicated that in most clinical situations the *flow acceleration* component is negligible [3]. In single, stenotic lesions, the proximal velocity term V_1 is typically small (<1 m/s) and can be ignored. Therefore, because in most clinical scenarios the *viscous friction*, *flow acceleration*, and V_1 components are negligible, the Bernoulli equation is simplified to $P1 - P2 = \Delta P = 4(V_2)^2$ (Fig. 11.1).

Intracardiac Pressures

The guide through echocardiographic assessment of various cardiac chamber pressures will follow the same sequence as during a diagnostic right heart catheterization, beginning with the right atrium. A summary of the equations discussed is presented at the end of the chapter (Fig. 11.10).

Right Atrium

Right atrial pressure is reflected in the size of the inferior vena cava (IVC), its response to changes in intrathoracic pressure, and the hepatic vein Doppler profile. Interrogation of the IVC by transthoracic echocardiography can be performed with the subcostal view (Fig. 11.3a, c). An *IVC diameter ≤2.1 cm that collapses >50% with sniffing (which causes an acute drop in intrathoracic pressure resulting in decreased venous return) suggests a normal RA pressure of 3 mmHg (range 0–5 mmHg)* [4]. *An IVC diameter >2.1 cm that collapses <50% with a sniff suggests a high RA pressure around 15 mmHg (range 10–20 mmHg)*. IVC profiles that do not fit into these two categories (i.e., IVC ≤ 2.1 cm but <50% collapse or IVC > 2.1 cm but >50% collapse) can be designated as an intermediate RA pressure of 8 mmHg. Other additional parameters such as hepatic vein profile can be used to further refine this estimated pressure. Young healthy adults may have dilated IVCs but normal RA pressure, and estimation of RA pressure using the IVC index may not be reliable in patients who are intubated [4]. An additional estimate of right atrial pressure is derived from the ratio of the tricuspid inflow diastolic E wave velocity and the right ventricular annular e' velocity, which is the right-sided correlate of estimating left atrial pressure by tissue Doppler. A ratio of $E/e' > 6$ is suggestive of high right atrial pressures. This method can be used in situations where IVC measurements are unobtainable or inaccurate [5].

Because the hepatic vein drains into the IVC, which then drains into the RA, the hepatic vein Doppler profile can provide complementary information regarding right atrial and ventricular hemodynamics. The hepatic vein profile consists of two main antegrade flow waves (systolic (S) and diastolic (D) waveforms) and a retrograde atrial wave (a) (Fig. 11.3b). The S, D, and a waves correspond to the x, y, and a waves of the jugular venous pressure waveform, respectively.

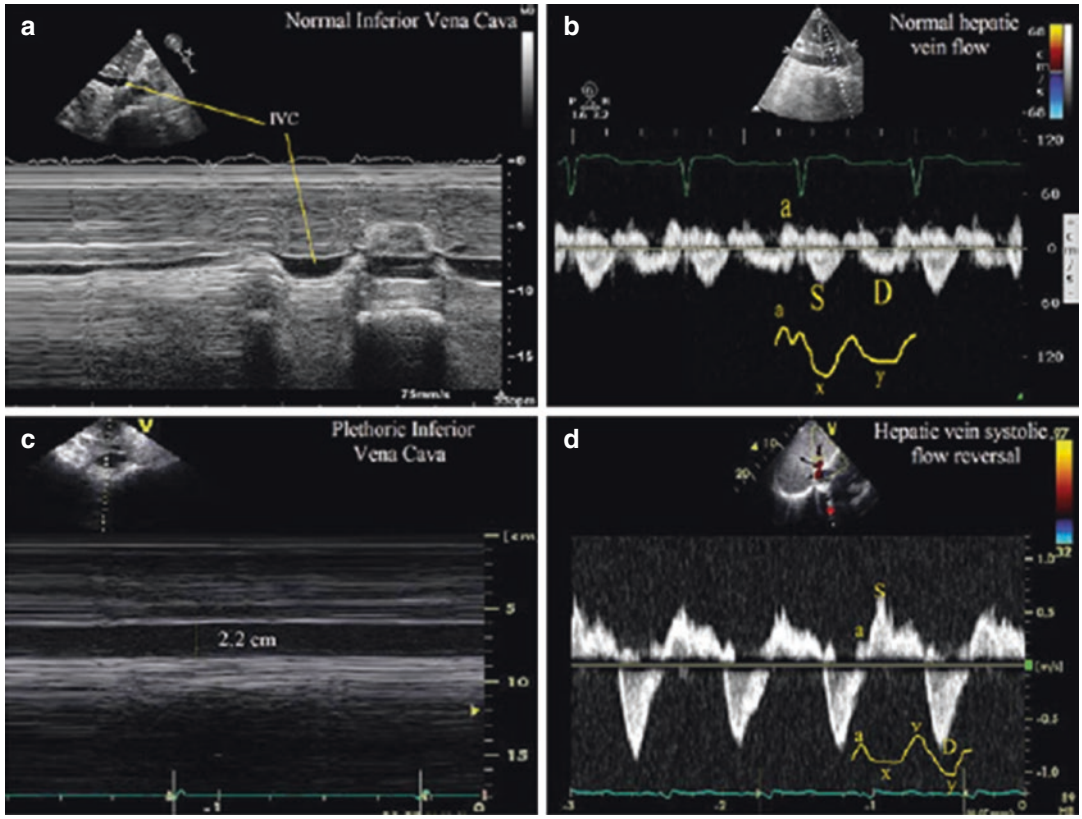

Fig. 11.3 Right-sided pressures. (**a**) M-mode through the IVC from the subcostal view. Note that the IVC size is <2.1 cm and collapses greater than 50%, suggesting normal right atrial pressure (0–5 mmHg). (**b**) Pulse wave (PW) Doppler of the hepatic vein showing normal hepatic vein flow. Note that there are two antegrade waves (*S* and *D*) and one retrograde wave (*a* reversal). The representative portions on the JVP waveform are shown (*S* corresponds to the *x* descent, and *D* corresponds to the *y* descent). The onset of the *S* wave corresponds to the onset of the QRS (isovolumic contraction), although the peak occurs in mid to late systole. In this example, the velocity of the *S* wave is larger than the *D* wave, indicating normal right atrial pressures. (**c**) A plethoric IVC greater than 2.1 cm in width which does not collapse, suggesting a right atrial pressure between 10 and 20 mmHg. (**d**) Systolic flow reversal in the hepatic veins in severe tricuspid regurgitation. Notice that the *S* wave is above the baseline, indicating flow reversal. This corresponds to the blunted *x* descent and tall *v* wave in the JVP waveform

Flow in the hepatic vein is sensitive to respiration, with increasing antegrade flow during inspiration and decreasing flow during expiration. With normal RA pressure, there is a predominance of the *s* wave in the antegrade waveform, whereas with elevated RA pressure, because the pressure gradient between the RA and the hepatic vein is lower, the *s* wave is blunted and the *d* wave predominates. *More quantitatively, a ratio of the s wave velocity divided by the sum of the s and d wave velocity* $[V_s/(V_s + V_d)]$ *less than 55% is highly correlated with an elevated RA pressure* [6]. In addition, in severe tricuspid regurgitation, there may even be systolic wave reversal, which is the echocardiographic equivalent of the loss of the *x* descent in the jugular venous waveform (Fig. 11.3d). In pulmonary hypertension, there may be prominent flow reversal during atrial systole (prominent *a* wave) due to high pulmonary pressures transmitting back to the atrium during diastole. Utilizing the ECG to accurately differentiate systolic flow reversal in the hepatic vein (which should occur coincident with isovolumic contraction) from a prominent (*a*) wave can be

key to avoiding misinterpretation of quite different hemodynamic conditions.

Right Ventricle

In the absence of tricuspid stenosis, the right ventricular end-diastolic pressure should equal the RA pressure as estimated from the IVC measurement. If tricuspid regurgitation (TR) is present, the peak velocity (v_{TR}) measured at end-expiration can be used to estimate the pressure gradient between the right ventricle and right atrium during systole ($\Delta P = 4V_{TR}^2$) (Fig. 11.4a). This pressure gradient can be added to the RA pressure to estimate the right ventricular systolic pressure (RVSP = RA + $4V_{TR}^2$). A TR velocity greater than 2.8–2.9 cm/s, in the setting of a normal RA pressure (0–5 mmHg), corresponds roughly to an RVSP of 36 mmHg, which

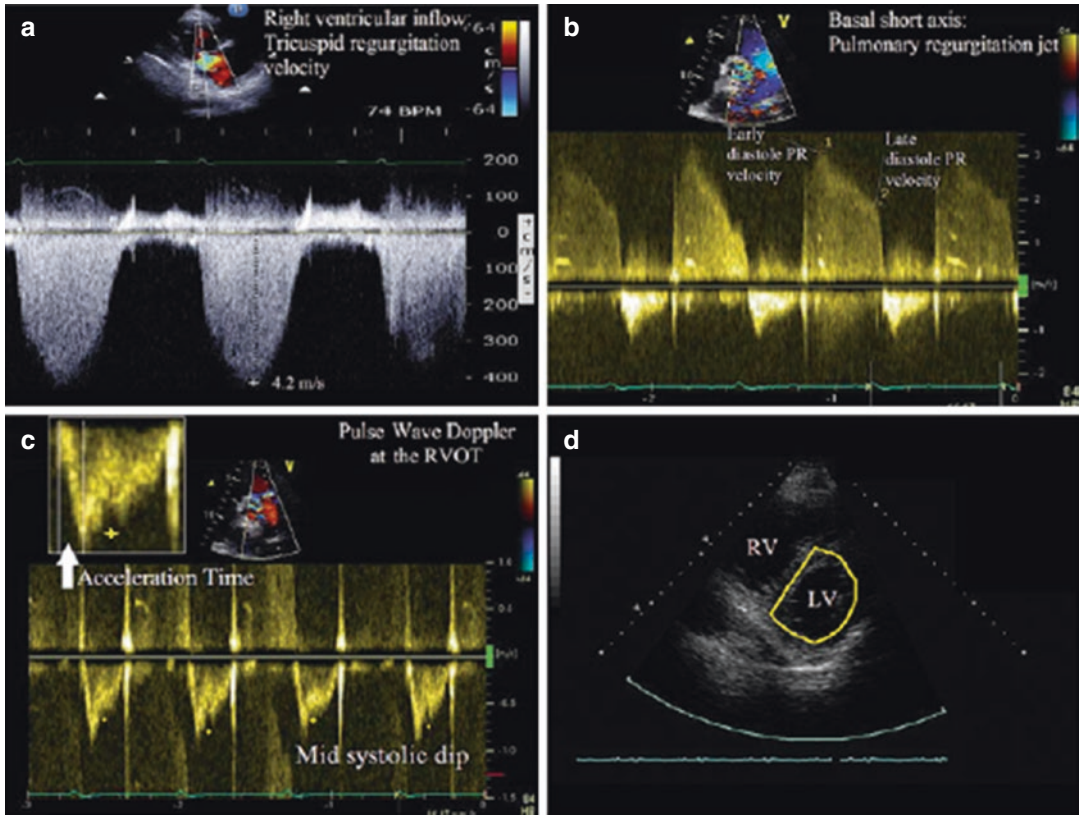

Fig. 11.4 Pulmonary pressures and signs of pulmonary hypertension. (**a**) The right ventricular systolic pressure can be estimated from the peak tricuspid regurgitation velocity obtained in the right ventricular inflow view (*see Question 1*). (**b**) The continuous wave (CW) Doppler profile of the pulmonary regurgitation jet. The early peak velocity can be used to determine the mean pulmonary artery (PA) pressure by the following formula: Mean PA Pressure = $4v_{EarlyDPR}^2$. In this case, early pulmonary regurgitation (PR) jet velocity is 3.9 m/s and the end-diastolic PR velocity is 1.9 m/s. Therefore, the mean PA pressure is roughly 39 mmHg. Also, the pulmonary artery end-diastolic pressure (PAEDP) can be determined from the end-diastolic velocity and estimated right atrial (RA) pressure: PAEDP = RA + $4v_{EDPR}^2$ (*see Question 2*). Note that in pulmonary hypertension, there is absence of the typical end-diastolic dip in the pulmonary regurgitation CW profile that normally corresponds to atrial systole. (**c**) The sample volume is in the RVOT, just below the pulmonic valve. In pulmonary hypertension, there is a steep slope in early systole (acceleration phase becomes shorter, *upper left corner*) and there can be a mid-systolic dip in the RVOT profile (*yellow stars*), due to high afterload. A simplified formula to calculate the mean pulmonary artery pressure (MPAP) is MPAP = 80 − 0.5 (acceleration time (ms)). Acceleration time is roughly 90 ms, yielding a MPAP of 35 mmHg. (**d**) Note the D-shaped septum during systole, suggestive of RV pressure overload

indicates the presence of mild pulmonary hypertension [4].

In cases of severe TR, in which the tricuspid valve is essentially "wide-open" during systole and there is no longer a fixed orifice with a significant pressure drop across the orifice, the RVSP may be underestimated. This is due to the fact that the flow acceleration (inertance) component of the Bernoulli equation is no longer negligible (a pressure drop must occur to overcome the inertance of the large volume of blood), while the convective flow component is less important (large orifice). Therefore, the simplified Bernoulli equation, which includes only the convective component, typically underestimates the RVSP in this scenario [4, 7].

If there is no RVOT obstruction or pulmonary stenosis, then the RVSP should be equal to the pulmonary artery systolic pressure (PASP). In the presence of pulmonary stenosis, because the peak gradient across the pulmonary valve during systole represents the pressure drop from the RV to the pulmonary artery (PA), the PASP can be derived from subtracting the peak gradient across the pulmonary valve during systole (obtained by CW) from the RVSP obtained from the TR jet [8].

Pulmonary Artery

As stated above, the PASP is equal to the right ventricular systolic pressure in the absence of RVOT obstruction. The end-diastolic pressure gradient between the pulmonary artery and the right ventricle is extrapolated from the end-diastolic velocity of the pulmonary regurgitation jet ($\Delta P = 4V_{\mathrm{PRed}}{}^2$) (Fig. 11.4b). Because this jet represents the difference between pulmonary artery end-diastolic pressure (PAEDP) and RVEDP (i.e., $\Delta P = 4V_{\mathrm{PRed}}{}^2 = \mathrm{PAEDP} - \mathrm{RVEDP}$), and RVEDP equals RA pressure in the absence of tricuspid stenosis, it follows by algebraic manipulation that $\mathrm{PAEDP} = \mathrm{RA} + 4V_{\mathrm{EDPR}}{}^2$ [9]. Also, the mean PA pressure can be estimated from the peak pulmonary regurgitation jet velocity (Mean PA Pressure = $4V_{\mathrm{EarlyDPR}}{}^2$) or the RVOT flow measured by PW Doppler using the formula $80 - 0.5 * (\text{pulmonic acceleration time(ms)})$ (Fig. 11.4c) [10]. These formulae can be useful when TR velocity signal is weak and unreliable. Estimation of pulmonary vascular resistance can be made by determining the ratio of the Peak TR velocity and the RVOT VTI (right ventricular outflow tract velocity time integral) in the following formula [11]:

$$\mathrm{PVR}\ (\text{Woods units}) = \frac{10 * (\text{peak TR velocity}(\mathrm{m/s})}{\text{RVOT VTI}(\mathrm{cm})) + 0.16}.$$

Echocardiographic signs of pulmonary hypertension include a D-shaped left ventricle, loss of the atrial systolic dip in the pulmonary regurgitation jet, and a mid-systolic decrease in the pulmonary outflow velocity (Fig. 11.4).

Pulmonary Capillary Wedge/Left Atrial Pressure

One method of estimating the left atrial (LA) pressure is to determine the peak mitral regurgitation velocity (V_{MR}), from which one can derive the pressure gradient between the left ventricle (LV) and LA (LV systolic pressure − LA pressure = $4V_{\mathrm{MR}}{}^2$) [12]. Because the LV systolic pressure equals the systolic blood pressure (SBP) in the absence of LVOT obstruction, the LA pressure = $\mathrm{SBP} - 4V_{\mathrm{MR}}{}^2$. A more common method of estimating the left atrial pressure is to determine the ratio of the mitral inflow *E* velocity to septal mitral annular velocity (*e′*), or *E/e′* [13]. *An E/e′ ratio of >15 is highly correlated with a pulmonary capillary wedge pressure (PCWP) >20, while an E/e′ ratio less than 8 corresponds to a normal PCWP* [13]. This method is valid for patients with

normal and abnormal systolic function. Tissue Doppler-derived estimates of PCWP can be used in patients with atrial fibrillation as well. However, in patients with constriction the exaggerated e' velocity, which corresponds to the rapid y descent on JVP waveform, yields a low E/e' ratio in spite of the fact that the left atrial pressures are elevated. This is the so-called *annulus paradoxus* [14].

Finally, in patients with aortic insufficiency, because the end-diastolic velocity of the aortic regurgitation jet ($4V_{AI}^2$) represents the pressure gradient between the aorta (diastolic blood pressure or DBP) and the LV end-diastolic blood pressure (LVEDP), one can estimate the LVEDP using the following formula: $\text{LVEDP} = \text{DBP} - 4V_{EDAI}^2$. Measurement error inherent with sphygmomanometric readings provides the primary limitation of this method. In the case of severe acute AI, where the end-diastolic velocity of the aortic insufficiency jet approaches zero, the LVEDP approaches the DBP.

Cardiac Output and System Vascular Resistance

The flow rate through a vessel is the product of the cross-sectional area of the vessel and the velocity of blood. However, because velocity varies over time throughout the cardiac cycle due to pulsatility, one cannot take an instantaneous velocity to measure overall flow rate. Rather, an integral of the velocities over time, called the VTI from the Doppler profile, is used to characterize integrated velocity in a given time period to determine flow (volume), rather than flow rate (volume/time) (Fig. 11.5a, b). VTI is essentially a measure of stroke distance. When the VTI (distance) is multiplied by the cross-sectional area (distance squared), the product is a volume (distance cubed). Therefore, stroke volume of the left ventricle can be estimated by multiplying the cross-sectional area of the LVOT ($\pi r^2 = \pi(D/2)^2 = \pi D^2/4 = D^2 * 0.785$, where r is radius and D is diameter) obtained in the parasternal long axis view and multiplying it by the VTI of the PW Doppler profile obtained in the apical long axis view (Fig. 11.5a). The PW cursor is typically placed about 0.5–1 cm below the valve to obtain a laminar flow curve. It is important to measure the PW Doppler profile at the same location as the measured cross-sectional area to maintain accuracy. This stroke volume can be multiplied by the heart rate to give an estimated cardiac output (in the absence of significant aortic regurgitation). If there is no regurgitation or intracardiac shunts, then the stroke volume through the tricuspid, pulmonary, mitral, and aortic valves should be equivalent, and therefore, the principle of multiplying the cross-sectional area of these valves by the VTI of flow across the valves can be applied throughout the heart. Practically speaking, however, stroke volume is typically measured in the LVOT.

If a left to right shunt is present (i.e., ASD or VSD), then it is clinically relevant to estimate the severity of the shunt by determining the ratio of pulmonary blood flow (Q_p) to systemic blood flow (Q_s). Figure 11.6 shows an example of a secundum ASD with left to right flow. Systemic stroke volume is measured by multiplying the LVOT area ($D^2*0.785$) by the LVOT VTI from the parasternal long axis views and the apical long axis views, respectively. The pulmonary stroke volume is measured by multiplying the RVOT Area by the RVOT VTI, measured in the basal short axis view across the pulmonary valve. The ratio of Q_p/Q_s, which equals [(RVOT VTI) (RVOT $D^2*0.785$)]/[(LVOT VTI) (LVOT $D^2*0.785$)], gives an estimate of the shunt fraction (Fig. 11.6). The term 0.785 cancels, and the ratio simplifies to (RVOT VTI) (RVOT D^2)/(LVOT VTI) (LVOT D^2). A ratio greater than 1.5 is considered a significant left to right shunt.

Just as pulmonary vascular resistance correlates with the TR velocity/RVOT VTI, systemic vascular resistance (SVR) correlates relatively well with *MR velocity/LVOT VTI*. A ratio of *MR velocity/LVOT VTI > 0.27* has a relatively high sensitivity and specificity for *SVR > 14 Woods units* [15].

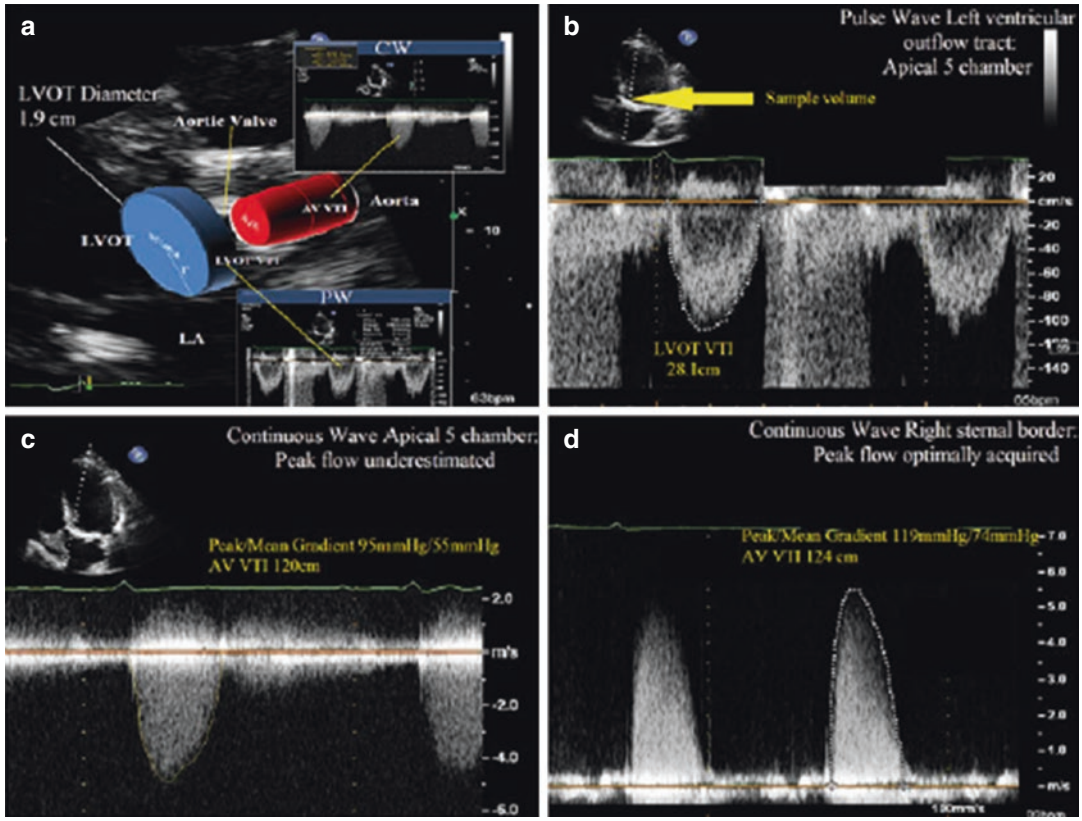

Fig. 11.5 Stroke volume and aortic valve area (AVA) calculation using the continuity equation. (**a**) Based on the continuity equation, the flow through the left ventricular outflow tract (LVOT), or the volume of the *blue cylinder*, must equal the flow through the aortic valve, or the volume of the *red cylinder*. The stroke volume (represented by the *blue cylinder*) is estimated by multiplying the LVOT area by the LVOT VTI. The LVOT area is obtained using the equation Area = πr^2 = (Diameter)^2∗0.785, with the diameter measured in the parasternal long axis view. Because the LVOT diameter in this case is 1.9 cm, the LVOT area is 2.84 cm^2. From the apical 5 chamber or apical long axis view, the LVOT VTI is obtained, which in this case is 28.1 cm (*bottom right* and (**b**)). Therefore, the stroke volume = 28.1 cm∗2.84 cm^2 = 79.8 cm^3. The product of the stroke volume and the heart rate (SV∗HR) can give an estimate of cardiac output. The volume of the *red cylinder* is the product of the AVA and the AV VTI (**c**, **d**). Because the volume of the *blue cylinder* (LVOT Area∗LVOT VTI) must equal the volume of the *red cylinder* (AVA∗AV VTI) to satisfy the continuity equation, it follows that AVA = [LVOT VTI ∗ (LVOT diameter)^2 ∗ 0.785]/[AV VTI] = Stroke volume/AV VTI (*see Question 3*). (**b**) Pulse wave Doppler Sample volume is placed just below the aortic valve in the 5 chamber view, and the LVOT VTI is traced. (**c**) Continuous wave Doppler measures the highest velocity along its path to estimate the peak and mean gradient across the aortic valve. The peak and mean gradients are 95/55 mmHg from the 5 chamber view, which is an underestimation of peak flow in this particular patient. Multiple views are necessary to obtain the highest, most representative jet velocity, as seen in (**d**). Right sternal border view obtains peak and mean gradients of 119/74 mmHg, higher than the peak gradient of 95 mmHg from the apical 5 chamber view

Valve Disease

It is important to recognize that an integrated approach using multiple echocardiographic methods of analysis and clinical context to determine severity of valve lesions is crucial, rather than relying on one specific measurement.

Aortic Stenosis

Echocardiography is currently the standard method to evaluate aortic valve stenosis. Application of the continuity equation is central to the calculation of aortic valve area (AVA). Based on the conservation of mass, the flow in

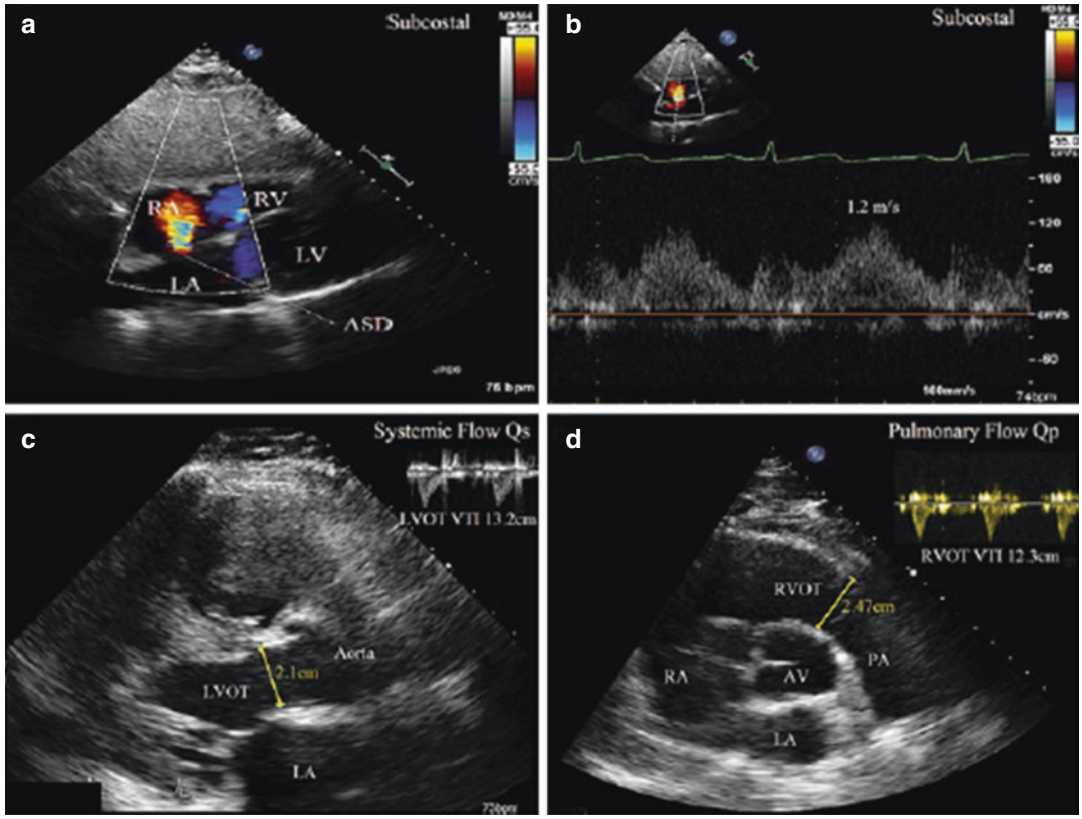

Fig. 11.6 Shunt calculation in a patient with a secundum atrial septal defect (ASD). (**a**) Color flow Doppler demonstrates left to right flow across the ASD in this subcostal view. (**b**) Pulse wave Doppler at the level of the ASD confirms that there is left to right continuous flow. During peak systole, based on the velocity of 1.2 m/s, the pressure gradient between the right atrium (RA) and the left atrium (LA) is $4v^2 = 4(1.2)^2 = 5.8$ mmHg. The RA pressure was estimated at 10 mmHg, so the LA pressure during systole is estimated at 15.8 mmHg (LA = RA + $4v^2$). (**c**) Measurement of systemic flow (Q_s) based on the LVOT area and LVOT VTI (pulse wave Doppler from the apical 5 chamber view, *right upper corner*). (**d**) Measurement of pulmonary flow (Q_p) based on the RVOT area and the RVOT VTI (pulse wave Doppler from the basal short axis view, *right upper corner*). The Q_p/Q_s or shunt fraction is 1.3:1 (*see Question 4 for calculation of Q_p, Q_s, and shunt fraction*)

the left ventricular outflow tract (LVOT) should be equal to the flow through the aortic valve orifice. First, one must determine the flow in the LVOT, or the stroke volume, by multiplying the cross-sectional area of the LVOT by the LVOT VTI determined by PW Doppler in the apical long axis or 5 chamber view (Fig. 11.5a, b). The PW sample volume should be located in the LVOT beneath the valve, and a crisp laminar Doppler signal with no contamination from the pre-stenotic flow acceleration should be sought. This is typically 0.5–1.0 cm from the aortic valve. The LVOT diameter should be measured from the septum to the anterior mitral leaflet in mid-systole, roughly 0.5–1.0 cm from the aortic valve in the parasternal long axis view to approximate the location where the PW was measured in the other echocardiographic view [16]. This flow should equal the product of the cross-sectional area of the aortic valve (AVA) and the AV VTI as determined by CW Doppler, typically the highest VTI obtained from a given view (suprasternal, apical, right parasternal) (Fig. 11.5c, d). The volume of blood in the cylinder in the LVOT (blue cylinder) must equal the volume of blood in the cylinder at the aortic valve (red cylinder) to not violate the law of mass conservation. The AV VTI obtained by CW Doppler is highly dependent on technique and the ability to obtain a good signal that is parallel to flow. Occasionally the right parasternal approach is used to obtain the highest gradient (Fig. 11.5d).

Based on the continuity equation:

$$\text{LVOT Cylinder Volume or Stroke Volume} = \text{AV Cylinder Volume}$$
$$\text{LVOT VTI} * \text{LVOT area} = \text{AV VTI} * \text{AVA}$$
$$\text{LVOT VTI} * (\text{LVOT diameter})^2 * 0.785 = \text{AV VTI} * \text{AVA}$$

Rearrangement yields [17] (Fig. 11.5):

$$\text{AVA} = \frac{\left[\text{LVOT VTI} * (\text{LVOT diameter})^2 * 0.785\right]}{\left[\text{AV VTI}\right]}$$

This equation gives a reliable estimate of the AVA; less than 1.0 cm^2 is considered severe aortic stenosis [16, 18]. Because the LVOT diameter is squared and measurements can vary, this is the greatest source of error in the formula.

The AVA is just one method among many to assess severity of aortic stenosis. Other methods include identifying the peak and mean gradient across the aortic valve, peak velocity across the aortic valve, and dimensionless index [17]. The peak velocity across the aortic valve is obtained from the CW Doppler profile, from which the peak gradient is calculated (from the peak velocity using $\Delta P = 4V^2$), and the mean gradient is calculated by averaging the instantaneous gradients during the ejection period [17]. A mean gradient >40 mmHg is considered severe. Echocardiographic assessment of peak gradient provides the instantaneous gradient between the LV and the aorta, which is different from cardiac catheterization in which often a peak to peak gradient is reported, a less physiologic value. Importantly, the mean gradient on cardiac catheterization correlates well with the Doppler-derived mean gradient. Table 11.1 shows the stages of severity of aortic stenosis based on the AHA/ACC 2014 Valve Guideline Update [16].

Although the peak velocity and estimated AVA are usually concordant (i.e., either velocity >4 m/s and AVA <1.0 cm^2 or velocity <4 m/s and AVA >1.0 cm^2), there may be scenarios in which the jet velocity and AVA may be discordant. In the case of velocity >4 m/s and AVA >1.0 cm^2, possibilities include a high stroke volume, concomitant moderate-to-severe aortic regurgitation, and a large body size. In the case of velocity <4 m/s and AVA <1.0 cm^2, possibilities include low stroke volume, severe concomitant mitral regurgitation, and small body size [16]. In either situation, the peak velocity is the better predictor of clinical outcome, and it is suggested that it be used to determine valve stenosis severity [16].

In patients who have left ventricular dysfunction (LVEF <40%) with concomitant aortic stenosis, the calculated AVA may be severe (<1.0 cm^2), but the mean gradient may not be severe (<30–40 mmHg). It is important to then determine if the aortic stenosis is truly severe and causing left ventricular dysfunction, which would imply improved left ventricular function with valve replacement, or if the aortic stenosis is only moderate in the presence of LV dysfunction from another cause (i.e., coronary disease, nonvalvular cardiomyopathy, etc.), in which the perceived small AVA is related to the inability of the left ventricle to generate the necessary valve opening forces (pseudostenosis). In the latter scenario, valve replacement would not be expected to improve left ventricular dysfunction. Low-dose dobutamine stress protocols (described in detail elsewhere [16]) can distinguish the two clinical scenarios. Recall from the continuity equation that the AVA is proportional to the *LVOT VTI/AV VTI*. If the patient truly has severe aortic stenosis, with the administration of dobutamine, the LVOT VTI and AV VTI should increase proportionally due to increased flow across a fixed,

Table 11.1 Aortic stenosis stages based on the recent AHA/ACC 2014 valve guidelines update [16]

Stage	Definition	Valve anatomy	Valve hemodynamics	Hemodynamic consequences	Symptoms
A	At risk of AS	Bicuspid aortic valve, aortic valve sclerosis, or other congenital anomaly	Aortic V_{max} <2 m/s	None	None
B	Progressive AS	Mild-to-moderate leaflet calcification with some reduced systolic motion or rheumatic commissural fusion	Mild AS: Aortic V_{max} 2.0–2.9 m/s or mean ΔP < 20 mmHg Moderate AS: Aortic V_{max} 3.0–3.9 m/s or mean ΔP 20 - 39 mmHg	Early LV dysfunction may be present but LVEF is preserved	None
C1	Asymptomatic severe AS	Severe leaflet calcification or congenital stenosis with severely reduced leaflet motion	Aortic $V_{max} \geq 4$ m/s Mean $\Delta P \geq 40$ mmHg AVA ≤ 1.0 cm^2 Very severe AS is an aortic $V_{max} \geq 5$ m/s or Mean $\Delta P \geq 60$ mmHg	LV diastolic dysfunction Mild LV hypertrophy Normal LVEF	None: exercise testing is reasonable to confirm symptom status
C2	Asymptomatic severe AS with LV dysfunction	Severe leaflet calcification or congenital stenosis with severely reduced leaflet motion	Aortic $V_{max} \geq 4$ m/s Mean $\Delta P \geq 40$ mmHg AVA ≤ 1.0 cm^2	LVEF <50%	None
D1	Symptomatic severe high gradient AS	Severe leaflet calcification or congenital stenosis with severely reduced leaflet motion	Aortic $V_{max} \geq 4$ m/s Mean $\Delta P \geq 40$ mmHg AVA ≤ 1.0 cm^2	LV diastolic dysfunction, LVH, pulmonary HTN may be present	Exertional dyspnea, angina, or reduced exercise tolerance, syncope or presyncope
D2	Symptomatic severe low-flow/low-gradient AS with reduced LVEF	Severe leaflet calcification with severely reduced leaflet motion	AVA ≤ 1.0 cm^2 with resting aortic $V_{max} < 4$ m/s or mean $\Delta P < 40$ mmHg Dobutamine stress echo shows AVA ≤ 1.0 cm^2 with $V_{max} \geq 4$ m/s at any flow rates	LV diastolic dysfunction, LVH, LVEF <50%	HF, angina, syncope or presyncope
D3	Symptomatic severe low-gradient AS with normal LVEF or paradoxical low-flow severe AS	Severe leaflet calcification with severely reduced leaflet motion	AVA ≤ 1.0 cm^2 with aortic V_{max} <4 m//s or mean ΔP < 40 mmHg Indexes AVA ≤ 0.6 cm^2/m^2 *Stroke volume index <35 mL/m^s* *Measured when patient is normotensive*	Increased relative wall thickness with preserved ejection fraction Small LV chamber with low stroke volume Restrictive diastolic filling	HF, angina, syncope, or presyncope

stenotic orifice, so the AVA should remain relatively unchanged. However, if the aortic stenosis only appears severe because of concomitant left ventricular dysfunction, dobutamine infusion will increase the LVOT VTI without a concomitant increase in AV VTI because of improved valve opening, thereby resulting in an increased calculated AVA. It follows that if the AVA increases above 1.0 cm^2 with dobutamine infusion, it is not likely to be severe aortic stenosis. Severe AS is suggested by a peak jet velocity >4.0 m/s provided that the valve area does not increase to >1.0 cm^2 [16]. In addition, the presence of contractile reserve (increase in EF or

SV ≥ 20%) during dobutamine stress predicts a lower mortality rate (<10%) with AVR than if contractile reserve is absent (>30%) [19].

The velocity ratio, also known as the dimensionless index, which is flow independent, is the ratio of the LVOT peak velocity and the AV peak velocity (can also use VTI ratio). A velocity index <0.25 is considered severe. This is used to compare aortic stenosis severity over time in patients who may have different loading conditions.

Accurate estimation of aortic stenosis severity depends on meticulous technique to obtain both an accurate LVOT diameter assessment, as well as the highest velocity jet which may require multiple echocardiographic views. In general, inaccuracies in measuring gradients by echocardiography typically err on the side of underestimation. However, there are two situations in which echocardiography may overestimate severity of stenosis. First, as stated earlier, the peak gradient estimated by the simplified Bernoulli equation ignores the velocity in the LVOT (V_1) as it is usually very small (<1 m/s). Scenarios in which the proximal velocity is >1.5 m/s or the peak velocity is <3 m/s, the flow velocity and gradient may be overestimated since the V_1 is ignored. Therefore, a more accurate estimate of peak gradient across the valve is $\Delta P = 4\left(V_2^2 - V_1^2\right)$ [16]. Another scenario in which the stenosis severity may be overestimated is the pressure recovery phenomenon. This occurs when some of the potential energy which was converted to kinetic energy at the level of the aortic stenosis is converted back to potential energy as flow decelerates (i.e., increasing pressure distal to the valve in the aorta). This pressure recovery is typically negligible, except in the case of small aortas with gradual widening after the stenosis (typically less than 3 cm in diameter). With larger aortas, much of the kinetic energy is converted to heat due to turbulence and viscous friction, so pressure recovery is not an issue [16]. Pressure recovery can be quantitatively calculated as $\Delta P = 4V^2 * 2(\text{AVA/aorta area}) * (1 - \text{AVA/Aorta area})$. As can be seen by the equation, if the AVA is small, and the aorta area is large, the AVA/aorta area ratio is small, and pressure recovery is minimal [16].

One collateral method to confirm the pressure gradient across the LVOT or aortic valve is to assess the peak mitral regurgitation velocity. As described previously, LV systolic pressure − LA pressure = $4V_{MR}^2$. If the LA pressure is estimated to be between 10 and 20 mmHg, then the LV systolic pressure can be estimated by 10–20 mmHg + $4V_{MR}^2$. If the SBP is known, then the difference between the estimated LV systolic pressure and SBP approximates the peak pressure gradient across the LVOT or aortic valve.

Mitral Stenosis

The most common cause of mitral stenosis (MS) is commissural fusion as a result of rheumatic fever. Several echocardiographically derived measurements can be used to assess mitral stenosis, including pressure gradient, pressure half-time, continuity equation, proximal isovelocity surface area (PISA) method, and planimetry. Although planimetry may well provide the most accurate measurement of the mitral valve area (MVA) provided that the images are acquired at leaflet tip level and are a true on-axis view, this section will focus on the pressure gradient, pressure half-time, and continuity equation to assess the valve area. PISA method and planimetry are discussed in detail in another reference [16]. Peak and mean pressure gradients across the mitral valve in diastole are measured by CW from the apical 4 chamber view (Fig. 11.7). It is essential to interrogate the mitral valve during a regular rhythm and normal heart rate (60–80 bpm). If the patient is in atrial fibrillation, then several cardiac cycles (6–8) should be averaged. Mean gradient is preferred to the peak gradient, since the peak gradient may be influenced by mitral regurgitation, atrial compliance, and left ventricular diastology. One cause of a very high peak gradient out of proportion to the mean gradient, for example, is severe mitral regurgitation. While pressure gradients are important parameters in the assessment of mitral stenosis severity, they are highly influenced by heart rate, cardiac output, and mitral regurgitation [16]. Mean pressure gradients supportive of mild, moderate, and

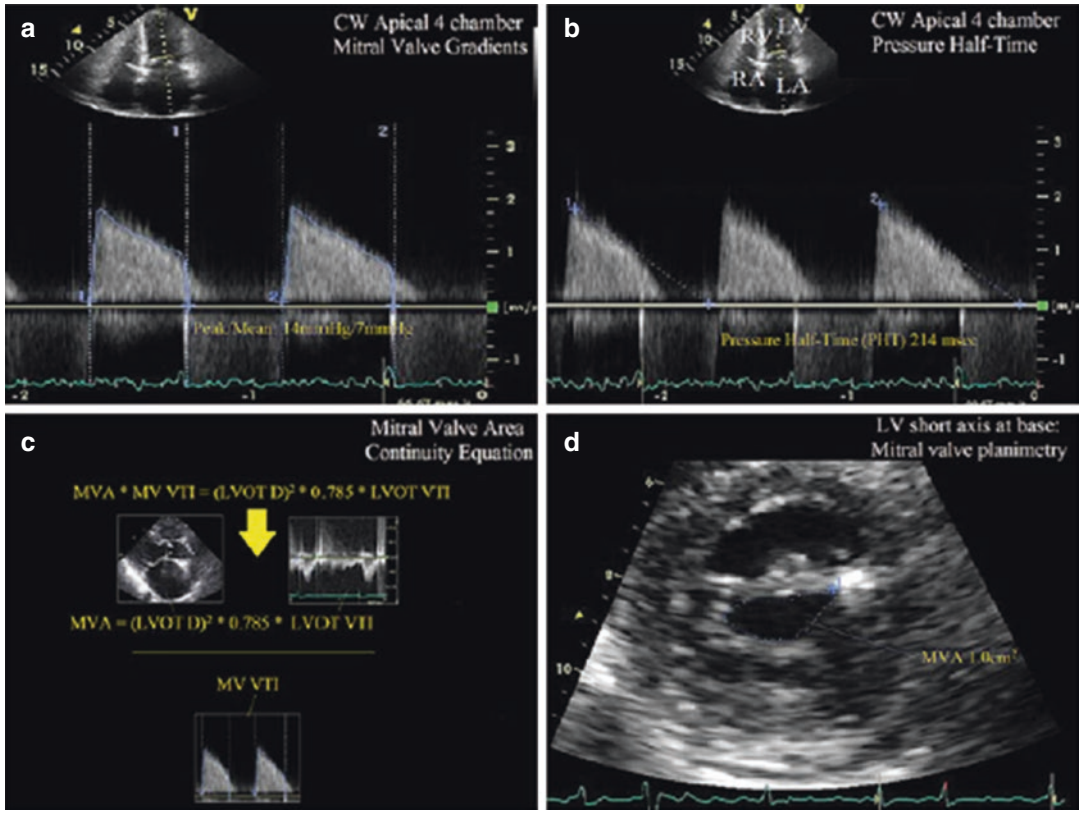

Fig. 11.7 Assessment of mitral stenosis. (**a**) Continuous wave Doppler across the mitral valve yields the peak and mean gradient (14/7 mmHg). Given the irregular heart rhythm, 6–8 beats are measured and averaged to obtain the peak and mean gradient. (**b**) The pressure half-time (PHT) is the time for the pressure gradient to decrease by 50%, and is equal to 0.29∗Deceleration time. Again, multiple beats are averaged (6–8) to obtain the PHT of 214 ms. The mitral valve area (MVA) is estimated by the following empiric equation: MVA = 220/PHT, giving a MVA of 220/214, or 1.0 cm^2, by the PHT method. (**c**) Calculation of MVA using the continuity equation. The flow across the mitral valve must equal the flow across the aortic valve, and therefore, MVA ∗ MV VTI = LVOT a ∗ LVOT VTI. In this case, the LVOT diameter is 1.9 cm, the LVOT VTI is 20 cm, and the MV VTI is 56.4 cm. Therefore, the calculated MV area is 1.0 cm^2. Note that the MV VTI is measured using CW and the LVOT VTI is measured using PW in this situation. (**d**) Planimetry is another method of estimating the MVA. Note the commissural fusion and "fish-mouth" appearance of the mitral opening, characteristic of rheumatic mitral valve disease. In this example, planimetry yields a MVA of 1.0 cm^2, concordant with the PHT and continuity methods

severe MS are <5 mmHg, 5–10 mmHg, and >10 mmHg, respectively [20].

Pressure half-time (PHT) is the time (in ms) it takes for the peak pressure gradient across the mitral valve in diastole to decrease by 50%. Based on the relationship between pressure and velocity, it is also the time in ms it takes for the peak velocity to decrease by 29%. This measurement is obtained by tracing the slope of the *E* wave during early diastole (Fig. 11.7b). It has been found that there is an inverse relationship between PHT and MVA by the following equation: MVA (cm^2) = 220/PHT [21]. In addition, the MVA (cm^2) = 759/Deceleration Time (ms). See Table 11.2 for measurements and valve stenosis severity.

Pressure half-time may be low even in severe MS if atrial compliance is low. In severe aortic insufficiency, due to the increase in the LVEDP during diastole as a result of regurgitation, the pressure between the LV and LA will equilibrate sooner, so the PHT will be reduced and the MVA estimate using the PHT will be inaccurate.

Table 11.2 Stage of mitral stenosis

Stage	Definition	Valve anatomy	Valve hemodynamics	Hemodynamic consequences	Symptoms
A	At risk of MS	Mild valve doming during diastole	Normal transmitral flow velocity	None	None
B	Progressive MS	Rheumatic valve changes with commissural fusion and diastolic doming of the mitral valve leaflets, MVA > 1.5 cm^2	Increased transmitral flow velocities MVA > 1.5 cm^2 Diastolic pressure half-time <150 msec		None
C	Asymptomatic severe MS	Rheumatic valve changes with commissural fusion and diastolic doming of the mitral valve leaflets Planimetered MVA ≤ 1.5 cm^2 MVA ≤ 1.0 cm^2 with very severe MS	MVA ≤ 1.5 cm^2 MVA ≤ 1.0 cm^2 with very severe MS Diastolic pressure half-time >150 ms, or >220 ms with very severe MS	Severe LA enlargement Elevated PASP>30 mmHg	None
D	Symptomatic severe MS	Rheumatic valve changes with commissural fusion and diastolic doming of the mitral valve leaflets Planimetered MVA ≤ 1.5 cm^2	MVA ≤ 1.5 cm^2 MVA ≤ 1.0 cm^2 with very severe MS Diastolic pressure half-time > 150 ms, or ≥220 ms with very severe MS	Severe LA enlargement Elevated PASP>30 mmHg	Decreased exercise tolerance Exertional dyspnea

MVA mitral valve area, *PASP* pulmonary artery systolic pressure

The continuity equation estimates the MVA if there is no aortic insufficiency or mitral regurgitation. The flow through the mitral valve should equal the flow through the LVOT by conservation of mass. The formula for flow through the LVOT (i.e., stroke volume), as described previously, is LVOT VTI ∗ (LVOT diameter)^2 ∗ 0.785. Again, this can be thought of as a cylinder, in which the base of the cylinder is the area of the LVOT and the height is the LVOT VTI. The flow through the mitral valve equals the product of the cross-sectional area of the mitral orifice (base of the cylinder) multiplied by the MV VTI (height of the cylinder). The MV VTI is determined by the computer package from the tracing of the CW mitral inflow from the 4 chamber view (Fig. 11.7c).

$$\text{LVOT Cylinder Volume or Flow} \quad \text{MV Cylinder Volume or Flow}$$

$$\text{LVOT VTI} * \text{LVOT area} = \text{MV VTI} * \text{MVA}$$

$$\text{LVOT VTI} * \left(\text{LVOT diameter}\right)^2 * 0.785 = \text{MV VTI} * \text{MVA}$$

$$\text{MVA} = \frac{\left[\text{LVOT VTI} * \left(\text{LVOT diameter}\right)^2 * 0.785\right]}{\left(\text{MV VTI}\right)}$$

Because MS elevates LA pressures, pulmonary hypertension may result. In general, the more severe the MS is, the more severe the pulmonary hypertension becomes. Pulmonary artery (PA) pressures can be assessed using the estimated RVSP, assuming there is no RVOT obstruction or pulmonic stenosis. A resting PASP > 50 mmHg or exercise-induced pulmo-

Table 11.3 Mitral regurgitation severity [16]

Grade	Definition	Valve anatomy	Valve hemodynamics	Hemodynamic consequences	Symptoms
A	At risk of MR	Mild mitral valve prolapse Mild valve thickening and leaflet restriction	No MR jet or small central jet <20% LA on Doppler Small vena contracta <0.3 cm	None	None
B	Progressive MR	Severe mitral valve prolapse with normal coaptation Rheumatic valve changes with leaflet restriction and loss of central coaptation Prior infective endocarditis(IE)	Central jet MR 20–40% LA or late systolic eccentric jet MR Vena contracta <0.7 cm Regurgitant volume <60 mL Regurgitant fraction <50% ERO <0.40 cm^2 Angiographic grade 1–2+	Mild LA enlargement No LV enlargement Normal pulmonary pressure	None
C	Asymptomatic severe MR	Severe mitral valve prolapse with loss of copatation or flail leaflet Rheumatic valve changes with leaflet restriction and loss of central coaptation Prior IE Thickening of leaflets with radiation heart disease	Central jet MR >40% LA or holosystolic eccentric jet MR Vena contracta ≥0.7 cm Regurgitant volume ≥60 mL Regurgitant fraction ≥50% ERO ≥0.40 cm^2 Angiographic grade 3–4+	Moderate or severe LA enlargement LV enlargement Pulmonary hypertension may be present at rest or with exercise C1 LVEF >60% and LVESD <40 mm C2 LVEF ≤60% and LVESD ≥40 mm	None
D	Symptomatic severe MR	Severe mitral valve prolapse with loss of coaptation or flail leaflet Rheumatic valve changes with leaflet restriction and loss of central coaptation Prior IE Thickening of leaflets with radiation heart disease	Central jet MR >40% LA or holosystolic eccentric jet MR Vena contracta ≥0.7 cm Regurgitant volume ≥60 mL Regurgitant fraction ≥50% ERO ≥0.40 cm^2 Angiographic grade 3–4+	Moderate or severe LA enlargement LV enlargement Pulmonary hypertension present	Decreaesd exercise tolerance Exertional dyspnea

nary hypertension (PASP > 60 mmHg) in the absence of other causes implies hemodynamically significant mitral stenosis [22].

Mitral Regurgitation

Echocardiographic assessment of mitral regurgitation severity relies on a "weighted average" of the information obtained from multiple modalities (Table 11.3). Color Doppler is the most readily apparent and visualized method of assessing mitral regurgitation. The jet area in the atrium on color Doppler is highly dependent on PRF and color scale. Typically, a large jet area spanning more than 40% of the atrium is considered severe MR. However, there are many caveats to using jet area. The appearance of the color is highly

technique-dependent, and can be affected by hemodynamic changes and atrial size. In addition, a very eccentric jet may "hug" the wall and appear to be smaller than a more central jet, giving the false impression that the eccentric MR is not severe. In addition, in the case of acute, severe mitral regurgitation, the jet duration may be very short given the acute rise in LA pressure, and technical factors such as insufficient color resolution may lead to underestimation [23]. Given its many limitations, jet area should not be the sole method used for quantification of mitral regurgitation.

Another method of MR assessment is the flow convergence or PISA method, which is an extension of the continuity principle and has been shown to correlate well with angiographically determined severity [24]. As flow converges toward a regurgitant orifice, the flow organizes into several concentric hemispheres, each with a specific velocity (Fig. 11.8a). As blood approaches the regurgitant orifice, the radius of the hemisphere decreases, while the velocity of blood at the surface of the hemisphere increases. Since the surface area (cm^2) of the hemisphere can be derived from the radius (surface area of hemisphere = $2\pi r^2$), and the velocity of the blood cells (cm/s) at the surface of the hemisphere (aliasing velocity, V_a) can be obtained from the color scale, the product of these two values (in units of cm^3/s) gives the flow rate proximal to the orifice (Fig. 11.8a). The flow rate distal to the orifice, which must equal the flow rate proximal to the orifice, can be calculated from the effective regurgitant orifice area (EROA) multiplied by the peak mitral regurgitant velocity, obtained from the CW Doppler in the 4 chamber view (Fig. 11.8c). To determine the velocity of the hemisphere of the proximal flow convergence, the color baseline or Nyquist limit are shifted downward toward the direction of flow (Fig. 11.8a). As shown in the figure, this maneuver increases the radius of the hemisphere, allowing easy visualization of color transition from blue to yellow, which is the location where the velocity is equal to the aliasing velocity. By having a larger radius and a lower aliasing velocity, propagation of error in radius measurement is reduced.

It follows that:

$$\text{Flow rate proximal to orifice} = \text{Flow rate distal to the orifice}$$

$$\text{Hemisphere surface area} * V_a = \text{EROA} * \text{peak mitral velocity}$$

$$2\pi r^2 * V_a = \text{EROA} * V_{MR}$$

$$\text{EROA} = \frac{\left(6.28 r^2 * V_a\right)}{V_{MR}}$$

This, of course, assumes that the hemisphere radius is measured at the time that the peak MR velocity occurs, so attempts must be made and standardizing the timing of measurement (i.e., mid-systole). As seen in Table 11.2, ERO > 0.4 is severe MR, and <0.2 is mild MR. The PISA method is not very accurate in situations of very eccentric MR jets (may overestimate severity) and noncircular orifices. A geometric correction factor for eccentric jets that create a wedge of a hemisphere instead of a full hemisphere has been described [25]. The angle created by the wedge (α) is divided by 180° and multiplied by the EROA to obtain the geometrically corrected EROA. Therefore, Geometrically corrected ER OA = $(\alpha/180) * (6.28r^2 * V_a)/V_{MR}$. Furthermore, flow velocity calculated by the PISA method represents an instantaneous flow rate. For instance, in mitral valve prolapse, the instantaneous EROA may be large but if the regurgitation only occurs in mid to late systole, the total regurgitant volume may not be very large. So perhaps a more accurate measurement of MR severity in this situation would be regurgitant volume.

To determine the regurgitant volume (RV), the EROA is multiplied by the MV VTI.

$$\text{RV} = \text{EROA} * \text{MV VTI}$$

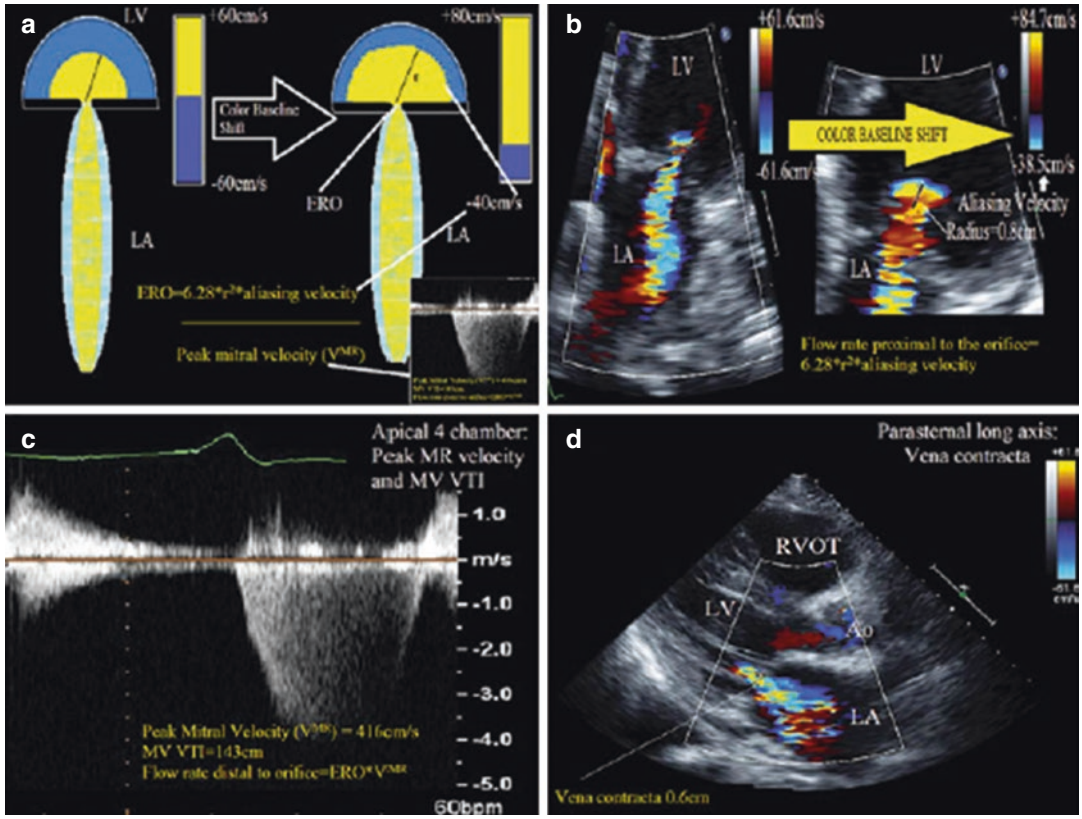

Fig. 11.8 PISA (proximal isovelocity surface area) method for mitral regurgitation and vena contracta. (**a**) Artistic rendition of the PISA concept. As flow converges during systole toward the regurgitant orifice, it accelerates and forms concentric hemispheres of increasing velocity and decreasing radius. For example, the velocity at the edge of the *yellow hemisphere* is higher than the velocity at the edge of the *blue hemisphere*. First the image should be optimized and zoomed. Next, the color baseline is shifted downward toward the direction of flow, from −65 to −40 cm/s, creating the *larger yellow hemisphere* with a lower velocity on the right. The velocity at the boundary between the *yellow* and *blue hemisphere* is the aliasing velocity (V_a = −40 cm/s). The flow proximal to the orifice equals the product of the hemisphere surface area ($2\pi r^2$) and the aliasing velocity (V_a). This proximal flow should equal the flow distal to the orifice, which is the product of the regurgitant orifice area (EROA) and peak MR velocity (V_{MR}). Therefore, EROA = $(2\pi r^2 * V_a)/V_{MR}$. (**b**) Similar to *panel A*, after creating a zoomed-in image, the color baseline is shifted toward the direction of flow, and a larger hemisphere with a known radius (0.8 cm) and aliasing velocity (V_a = 38.5 cm/s) is created. Based on the above equation, the proximal flow rate is 154.7 cm^3/s. (**c**) Continuous wave Doppler across the mitral valve to obtain the peak mitral regurgitant velocity (V_{MR}) = 416 cm/s and MV VTI. The distal flow rate is V_{MR}*EROA. The EROA, which is equal to $(2\pi r^2 * V_a)/V_{MR}$, is 0.37 cm^2, consistent with moderately-severe MR. Regurgitant volume can be calculated with the information in this figure (*see Question 5*). Using the simplified PISA formula, $r^2/2$, estimated EROA is 0.32 cm^2, likely slightly underestimated because the aliasing velocity is 38.5 cm/s, not the 40 cm/s assumed in the simplified formula. (**d**) The vena contracta, the narrowest jet width at the orifice, measured in the parasternal long axis view, is 0.6 cm, consistent with moderately-severe MR

EROA calculation using the PISA may be cumbersome, which can discourage its routine use. A simplified formula can be used if certain assumptions are made [26]. First, one assumes a pressure gradient between the LV and LA of 100 mmHg, which yields a mitral velocity (V_{MR}) of 5 m/s or 500 cm/s (from the Bernoulli equation, LV systolic pressure − LA pressure = $4V_{MR}^2$). If aliasing velocity (V_a) is set to 40 cm/s, then plugging these into the equation:

$$\text{EROA} = \frac{\left(6.28r^2 * V_a\right)c}{V_{MR}}$$

$$\text{EROA} = \frac{\left(6.28r^2 * 40\ \text{cm/s}\right)}{500\ \text{cm/s}}$$

$$\text{EROA} \oplus \frac{r^2}{2}$$

The vena contracta is the narrowest color flow at or upstream of the valve orifice [16]. For mitral regurgitation, it is typically assessed in the parasternal long axis view, and is considered to be independent of flow and pressure for a fixed orifice, even for eccentric jets (Fig. 11.8d). A vena contracta width of <0.3 cm is considered mild MR, and >0.7 cm is considered severe [16]. This parameter, when measurable, should always be considered a key component to the integrated approach to determining mitral regurgitation severity.

Other signs of severe MR are a triangular shape in the CW profile of the mitral regurgitant (early peaking) rather than a smooth parabolic profile, which implies rapid equilibration of LV and LA pressure from severe MR [16]. In addition, in the mitral inflow PW profile, severe MR is typically associated with a tall *E* wave >120 cm/s. Stage 1 diastolic dysfunction pattern on mitral inflow virtually excludes severe MR. In severe MR, the elevated LA pressures during systole decrease the gradient between the LA and the pulmonary veins, so the pulmonary vein *s* wave may be blunted or even reversed.

Aortic Insufficiency

In the parasternal long axis view, the percentage of the LVOT width that the regurgitant jet occupies has been correlated with aortic insufficiency (AI) severity [16]. If the jet width in diastole occupies more than 65% of the LVOT diameter, then it is considered severe. However, just as with jet area in MR, jet width in AI is not valid for eccentric jets in which severity may be underestimated (Fig. 11.9a) [27]. The vena contracta is the narrowest neck of the jet at the level of the valve. The width of the vena contracta correlates with regurgitant orifice area and is unaffected by jet eccentricity [28]. To accurately measure the vena contracta width, a zoomed-in parasternal long axis view should be obtained that shows the flow convergence zone, the vena contracta, as well as the regurgitant jet in the LVOT. A vena contracta width ≥6 mm suggests severe AI (Table 11.4). The utility of this method is limited if there are multiple jets [16]. The PISA method has been applied for the calculation of the aortic regurgitant EROA. This measurement should be made in the apical 5 chamber or apical long axis view in early diastole but is technically more difficult to obtain than the PISA for MR. The same principle applies as with MR, in that the flow rate proximal to the orifice (aorta) which is the product of the hemisphere area and the aliasing velocity ($2\pi r^2 * V_a$) equals the flow rate distal to the orifice in the LVOT (EROA∗peak aortic regurgitant velocity). However, the color baseline is shifted up rather than down, as this is toward the direction of flow. EROA ≥0.3 cm^2 correlates with severe AI (Table 11.4). The simplified PISA method used for MR ($r^2/2$) does not apply to AI.

Pulse wave Doppler in the upper descending thoracic aorta from the suprasternal view can both qualitatively and quantitatively assess aortic regurgitation severity [27]. Holodiastolic flow reversal in the proximal descending aorta is specific for at least moderately-severe aortic insufficiency, and is considered to be the echocardiographic equivalent of the *Duroziez's sign* [16] (Fig. 11.9b). This is a much more specific finding if there is flow reversal is present when sampling in the abdominal aorta. The ratio of the reverse flow (diastolic VTI∗cross-sectional area of the aorta in diastole) to the forward flow (systolic VTI∗cross-sectional area of the aorta in systole) is proportional to the regurgitant fraction [29].

PHT of the aortic regurgitation jet reflects the rate of equalization between the aortic and LV pressures (Fig. 11.9c). Therefore, this PHT is not only influenced by the severity of aortic insufficiency but also by LV pressure, LV compliance, and afterload conditions. Hence, it may be the least reliable method for assessing regurgitation

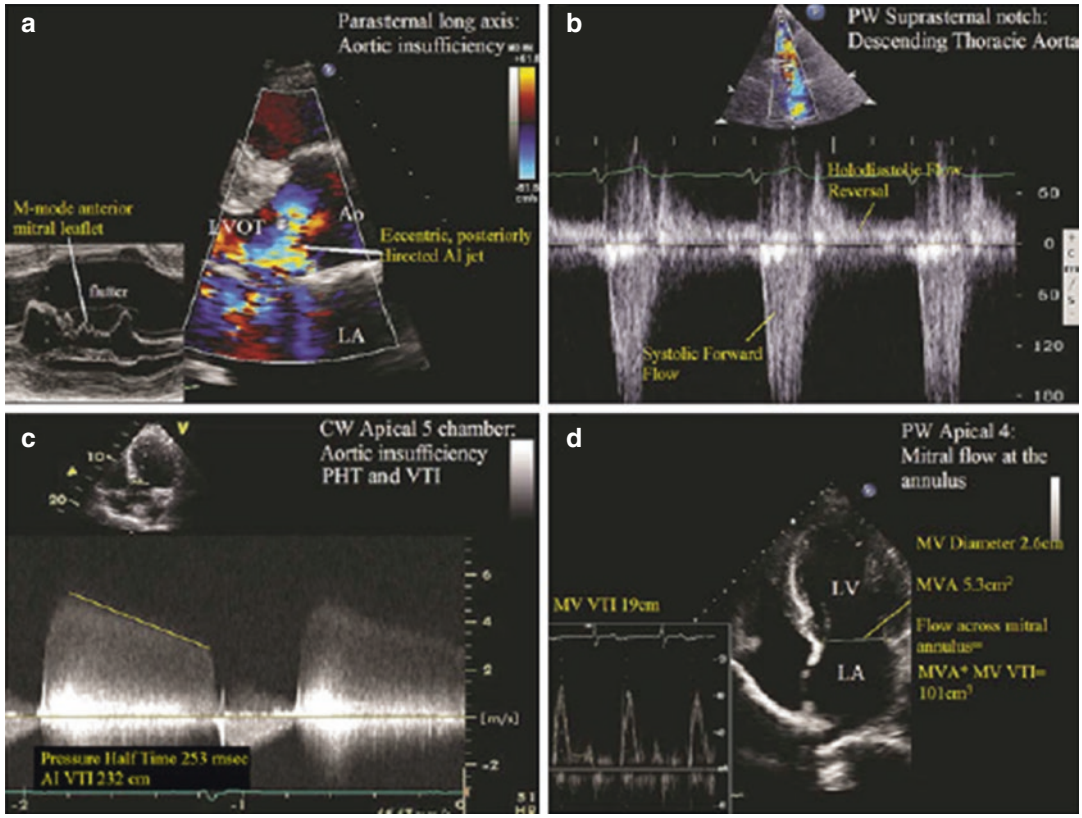

Fig. 11.9 Severe aortic insufficiency (AI). (**a**) Parasternal long axis view color Doppler demonstrates a very severe, eccentric, and posterior directed jet. Note that the M-Mode across the mitral leaflet shows fluttering of the anterior leaflet due to the aortic insufficiency jet (*lower left corner inset*). Given the eccentricity, one cannot use the LVOT jet area to assess severity. (**b**) Pulse wave Doppler with sample volume in the upper descending thoracic aorta, demonstrating holodiastolic flow reversal, a sign of severe AI. (**c**) Continuous wave Doppler across the aortic valve in the apical 5 chamber view. The PHT is 253 ms, consistent with severe AI. The aortic insufficiency VTI is 232 cm based on the CW profile. (**d**) Application of the continuity equation allows for the calculation of the regurgitant AI volume. Flow across the mitral valve plus the regurgitant volume should equal the flow across the aortic valve (Stroke volume). The MVA is determined by measuring the mitral valve diameter, and this area (5.3 cm^2) is multiplied by the MV VTI at the annulus (19 cm) to yield a flow of 101 cm^3. Flow across the aortic valve is determined by the product of the LVOT VTI and LVOT area, which yields a volume of 169 cm^3, calculation not shown. Therefore, the aortic insufficiency regurgitant volume is 169 cm^3 − 101 cm^3 = 68 cm^3, consistent with severe AI. The regurgitant orifice area (EROA) of the aortic valve is calculated by dividing the regurgitant volume (68 cm^3) by the AI VTI (232 cm), which equals 0.3 cm^2, also consistent with severe AI

severity [16]. A PHT <200 ms is supportive of severe aortic insufficiency, and a pressure half-time greater than 400 ms is unlikely to represent more than moderate AR. However, even in severe AI, if the LV has dilated as a chronic adaptation to the increased preload and afterload, then the pressure half-time could be normal since the LV and aorta pressures would not rapidly equilibrate. If vasodilators are given or LV pressures increase for a given degree of AI, the PHT would decrease.

The continuity equation can also be applied to aortic insufficiency if there is no more than mild mitral insufficiency. Think of the flow across the aortic valve as gross income, the regurgitant volume as the tax, and the flow across the mitral valve as the net income. The difference between the flow across the aortic valve ("gross" systolic stroke volume) and the flow across the mitral valve ("net" forward stroke volume) is equal to the "tax" or regurgitant volume per beat. The "gross"

Table 11.4 Stages of aortic insufficiency [16]

Stage	Definition	Valve anatomy	Valve hemodynamics	Hemodynamic consequences	Symptoms
A	At risk for AR	Bicuspid aortic valve (or other congenital valve anomaly) Aortic valve sclerosis Diseases of the aortic sinuses or ascending aorta History of rheumatic fever or known rheumatic heart disease IE(infective endocarditis)	AR severity: none to trace	None	None
B	Progressive AR	Mild-to-moderate calcification Dilated aortic sinuses Rheumatic valve changes Previous IE	Mild AR: jet width <25% of LVOT; vena contracta <0.3 cm; RVol <30 mL/beat; RF <30%; ERO <0.10 cm^2; angiography grade 1+ Moderate AR: Jet width 25–64% of LVOT; vena contracta 0.3–0.6 cm; RVol 30–59 mL/beat; RF 30–49%; ERO0.10–0.20 cm^2;angiography grade 2 + _	Normal LV systolic function Normal LV volume or mild LV dilation	-None
C	Asymptomatic severe AR	Calcific aortic valve disease Bicuspid valve Dilated aortic sinuses or ascending aorta Rheumatic valve changes IE with abnormal leaflet closure or perforation	Severe AR: Jet width ≥65% of the LVOT Vena contract>0.6 cm Holodiastolic flow reversal in the proximal abdominal aorta RVol ≥60 mL/beat RF ≥50% ERO ≥0.3 cm^2 Angiography grade 3–4+ LV dilation	C1: Normal LVEF ≥50% and mild-to-moderate LV dilation (LVESD ≤ 50 mm) C2: Abnormal LV systolic function with depressed LVEF (<50%) or severe LV dilatation(LVESD > 50 mm or indexed LVESD > 25 $mm.m^2$)	None, exercise testing is reasonable to confirm symptom status
D	Symptomatic Severe AR	Calcific aortic valve disease Bicuspid valve Dilated aortic sinuses or ascending aorta Rheumatic valve changes IE with abnormal leaflet closure or perforation	Severe AR: Jet width ≥65% of the LVOT Vena contract > 0.6 cm Holodiastolic flow reversal in the proximal abdominal aorta RVol ≥60 mL/beat RF ≥50% ERO ≥0.3 cm^2 Angiography grade 3–4+ LV dilation	Symptomatic severe AR may occur with normal systolic function (LVEF ≥50%), mild-to-moderate LV dysfunction(LVEF 40–50%), or severe LV dysfunction(LVEF <40); Moderate-to-severe LV dilation is present	Exertional dyspnea or angina or more severe HF symptoms

EROA effective regurgitant orifice area, *RV* regurgitant volume, *RF* regurgitant fraction, *DA* descending aorta, *LV* left ventricle

stroke volume can be obtained either from the LVOT VTI method or from the difference between the LV volumes in systole and diastole. To calculate "net" forward flow across the mitral valve, it is important to use PW and place the sample volume at the annulus of the mitral valve to measure and accurate flow across the mitral valve during diastole (Fig. 11.9d).

$$\text{Regurgitant volume}(\text{RV}) = \text{Stroke volume across aortic valve} - \text{Flow across mitral valve annulus}$$

$$\text{RV} = (\text{LVOT VTI} * \text{LVOT area}) - (\text{MV VTI}(\text{diastole}) * \text{MV annulus area})$$

$$\text{RV} = \left[\text{LVOT VTI} * (\text{LVOT diameter})^2 * 0.785\right] - [\text{MV VTI} * (\text{MV diameter})^2 * 0.785]$$

Once the regurgitant stroke volume is obtained, it can be divided by the regurgitant jet VTI obtained from CW in diastole to calculate the EROA [16]. If the EROA is in the severe range but the RV is not, it may be because in acute AI, the rapid increase in the LVEDP shortens the time for regurgitation, so the regurgitant volume may not be as large as expected from the EROA (Fig. 11.10).

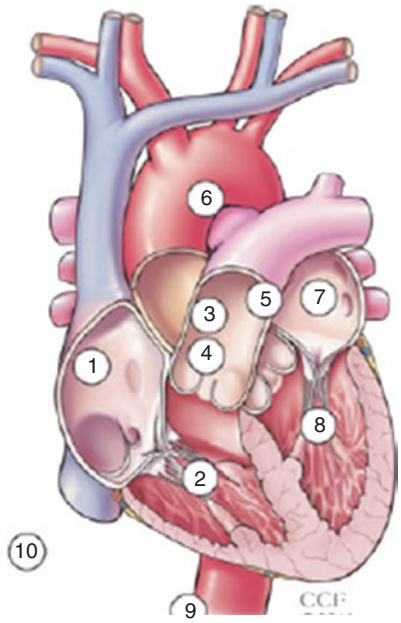

1. RA=(0-5 mmHg) if IVC ≤ 2.1 cm and collapses > 50%
   RA=(10-20 mmHg) if IVC>2.1 cm and collapses <50%
2. RVSP=$4V_{TR}^2$+ RA
3. PASP=RVSP if no RVOT obstruction or PS
4. PAEDP=RA + $4(V_{EDPR})^2$
5. Mean PAP=$4(V_{Early\ DPR})^2$ OR 2(PADP)/3 + PASP/3
   PVR(Woods Units)=$10*(V_{TR}/\text{RVOT VTI}) + 0.16$
6. CO=(LVOT VTI)(LVOT D)^2(0.785)(Heart Rate)
7. LA=SBP+ $4(VMR)^2$ if no outflow tract obstruction or Aortic stenosis
   E/e'> 15 = PCWP >20; E/e'<8 =normal PCWP
8. LVEDP=DBP-$4(V_{EDAI})^2$
9. SVR>14 Woods Units if V_{MR}/LVOT VTI>0.27
10. Q_p/Q_s=[(RVOT VTI)(RVOT D)^2]/[(LVOT VTI)(LVOT D)^2]

Fig. 11.10 Summary of intracardiac pressure calculations. RA right atrial pressure, IVC inferior vena cava, RVSP right ventricular systolic pressure, V_{TR} peak tricuspid regurgitation velocity, PASP pulmonary artery systolic pressure, RVOT right ventricular outflow tract, PS pulmonic stenosis; PAEDP pulmonary artery end-diastolic pressure, V_{EDPR} end-diastolic pulmonary regurgitation velocity, PAP pulmonary artery pressure, $V_{EarlyDPR}$ early diastolic pulmonary regurgitation velocity, PVR pulmonary vascular resistance, VTI velocity time integral, LVOT left ventricular outflow tract, D diameter, LA left atrial pressure, SBP systolic blood pressure, V_{MR} peak mitral regurgitation velocity, PCWP pulmonary capillary wedge pressure, LVEDP left ventricular end-diastolic pressure, DBP diastolic blood pressure, V_{EDAI} end-diastolic aortic insufficiency velocity, SVR systemic vascular resistance, Q_p pulmonary flow, Q_s systemic flow. (Reprinted with permission, Cleveland Clinic Center for Medical Art & Photography © 2011)

3D Echocardiography

The advent of 3D echocardiography has provided clinicians with more anatomic detail regarding valve structure and function. One arena in particular in which 3D echo provided value is the assessment of valves during valve interventions, either surgical or in the catheterization lab. For instance, 3D echo assists the operator in the transcatheter placement of the Mitra-clip for the treatment of mitral regurgitation. Beyond informing the clinical regarding anatomic structure and function, 3D echo has some limited clinical applications in the assessment of valve hemodynamics. In mitral stenosis, 3D echo can be used for measuring valve area. In addition, in the same way that a PISA is calculated using 2D echo, 3D Doppler can be used to assess the radius of the proximal isovelocity surface area. The 2D PISA assumes a hemispheric shape of the PISA, which may not be true in all regurgitant lesions, and, for example, in functional mitral regurgitation, the geometry may be more ellipsoid. By applying the hemi-ellipsoid formula for instance, the mitral regurgitation severity can be more accurately measured [30, 31]. *Although its current clinical application in valve hemodynamics is somewhat limited, with time this method will likely receive wider adoption.*

Review Questions

1. What is the estimated right ventricular systolic pressure (RVSP) in the patient in Fig. 11.4a if the inferior vena cava (IVC) measures 2.5 cm and there is no collapse with sniff?
   A. 60 mmHg
   B. 70 mmHg
   C. 30 mmHg
   D. 85 mmHg
2. What is the estimated end-diastolic pulmonary artery pressure in Fig. 11.4b?
   A. 14.4 mmHg
   B. 14.4 mmHg + RA pressure
   C. 38.5 mmHg
   D. 38.5 mmHg + RA pressure
3. Based on the continuity equation, what is the estimated aortic valve area (AVA) in Fig. 11.5? Is this severe AS or moderate AS?
   A. 1.2 cm^2, moderate AS
   B. 1.2 cm^2, severe AS
   C. 0.6 cm^2, severe AS
   D. 0.6 cm^2, moderate AS
4. The patient in Fig. 11.6 has a known secundum atrial septal defect, and as shown in panel (a), there is left to right flow across the atrial septal defect. The echocardiogram was performed to estimate the shunt fraction. Based on the information provided in Fig. 11.6, what is the estimated Q_p/Q_s ratio?
   A. 1:1
   B. 1.3:1
   C. 0.5:1
   D. 2:1
5. In Fig. 11.8, the regurgitant orifice area is 0.37 cm^2. Based on the information in panel (c), what is the estimated regurgitant volume per beat?
   A. 143 mL/beat
   B. 416 mL/beat
   C. 53 mL/beat
   D. 100 cc/beat

Answers

1. The peak TR velocity is 420 cm/s, or 4.2 m/s. Based on the simplified Bernoulli equation, the difference between the RV and RA pressure is $4V_{TR}^2$, or $4*(4.2)^2 = 70.56$ mmHg, roughly 70 mmHg. The RA pressure is estimated at 15 mmHg based on the dilated IVC that does not collapse greater than 50% with the sniff. Therefore, because the RVSP is equal to RA pressure plus the $4V_{TR}^2$, RVSP = 70 mmHg + 15 mmHg = 85 mmHg, compatible with severe pulmonary hypertension.
2. In Fig. 11.4b, the spectral Doppler shows the CW across the RVOT and pulmonic valve. From the pulmonary regurgitation jet, the late diastolic pulmonary regurgitation velocity represents the pressure difference between the pulmonary artery and the right ventricle at end diastole (note the timing just at the onset of the QRS). Therefore, the $4v_{PRed}^2$ = RVEDP − PAEDP. It

follows that PAEDP = RVEDP + $4v_{PRed}^2$. Because the RVEDP is equal to RA pressure, PAEDP = RA + $4v_{PRed}^2$. Here the end-diastolic velocity is 1.9 m/s. Therefore, PAEDP = RA + $4(1.9)^2$ = 14.4 mmHg + RA pressure.

3. Based on the continuity equation, AVA = [LVOT VTI ∗ (LVOT diameter)^2 ∗ 0.785]/[AV VTI]. The LVOT VTI from Fig. 11.5b is 28.1 cm, and the LVOT diameter from Fig. 11.5a is 1.9 cm. The highest AV VTI was obtained from the right sternal border view, which is 124 cm. Note that this corresponded to a peak and mean gradient of 119/74 mmHg, severe aortic stenosis (AS) by gradients. Using the continuity equation, AVA = [28.1 ∗ $(1.9)^2$ ∗ 0.785]/[124] = 0.6 cm^2, also compatible with severe AS.
4. The ratio of pulmonary blood flow to systemic blood flow is the Q_p/Q_s, or shunt fraction. The systemic blood flow (Q_s) is estimated by multiplying the LVOT area, (LVOT D)^2∗0.785, by the LVOT VTI. As shown in Fig. 11.6c, the LVOT diameter is 2.1 cm and the LVOT VTI is 13.2 cm. Therefore, the systemic flow is $(2.1)^2$ ∗ 0.78 5 ∗ 13.2 = 45.7 cm^3. The pulmonary blood flow (Q_p) is estimated by multiplying the RVOT area, (RVOT D)^2∗0.785, by the RVOT VTI. As shown in Fig. 11.6d, the RVOT diameter is 2.47 cm and the RVOT VTI is 12.3 cm. Therefore, the pulmonary blood flow is $(2.47)^2$ ∗ 0.785 ∗ 12.3 = 58.9 cm^3. The Q_p/Q_s ratio is 45.7/58.9 = 1.3:1. Note that because the 0.785 constant is present in both the numerator and denominator, the Q_p/Q_s calculation can be simplified to [(RVOT D)^2 ∗ (RVOT VTI)]/[(LVOT D)^2 ∗ (LVOT VTI)].
5. The regurgitant volume is equal to the product of the regurgitant orifice area (EROA, cm^2) and the MV VTI (cm). In this case, the product of the EROA (0.37 cm^2) and the MV VTI (143 cm) gives a regurgitant volume of 53 mL/beat, which is consistent with moderately-severe MR.

References

1. Anavekar NS, Oh JK. Doppler echocardiography: a contemporary review. J Cardiol. 2009;54(3):347–58.
2. Quinones MA, Otto CM, Stoddard M, Waggoner A, Zoghbi WA, Doppler Quantification Task Force of the Nomenclature and Standards Committee of the American Society of Echocardiography. Recommendations for quantification of Doppler echocardiography: a report from the Doppler Quantification Task Force of the Nomenclature and Standards Committee of the American Society of Echocardiography. J Am Soc Echocardiogr. 2002;15(2):167–84.
3. Hatle L, Angelsen B. Doppler ultrasound in cardiology: physical principles and clinical applications. 2nd ed. Philadelphia: Lea & Febiger; 1985. p. 331.
4. Rudski LG, Lai WW, Afilalo J, et al. Guidelines for the echocardiographic assessment of the right heart in adults: a report from the American Society of Echocardiography endorsed by the European Association of Echocardiography, a registered branch of the European Society of Cardiology, and the Canadian Society of Echocardiography. J Am Soc Echocardiogr. 2010;23(7):685–713; 786–8.
5. Nageh MF, Kopelen HA, Zoghbi WA, Quinones MA, Nagueh SF. Estimation of mean right atrial pressure using tissue Doppler imaging. Am J Cardiol. 1999;84(12):1448–51, A8.
6. Nagueh SF, Kopelen HA, Zoghbi WA. Relation of mean right atrial pressure to echocardiographic and Doppler parameters of right atrial and right ventricular function. Circulation. 1996;93(6):1160–9.
7. Firstenberg MS, Vandervoort PM, Greenberg NL, et al. Noninvasive estimation of transmitral pressure drop across the normal mitral valve in humans: importance of convective and inertial forces during left ventricular filling. J Am Coll Cardiol. 2000;36(6):1942–9.
8. Lima CO, Sahn DJ, Valdes-Cruz LM, et al. Noninvasive prediction of transvalvular pressure gradient in patients with pulmonary stenosis by quantitative two-dimensional echocardiographic Doppler studies. Circulation. 1983;67(4):866–71.
9. Masuyama T, Kodama K, Kitabatake A, Sato H, Nanto S, Inoue M. Continuous-wave Doppler echocardiographic detection of pulmonary regurgitation and its application to noninvasive estimation of pulmonary artery pressure. Circulation. 1986;74(3):484–92.
10. Beard JT II, Newman JH, Loyd JE, Byrd BF III. Doppler estimation of changes in pulmonary artery pressure during hypoxic breathing. J Am Soc Echocardiogr. 1991;4(2):121–30.
11. Scapellato F, Temporelli PL, Eleuteri E, Corra U, Imparato A, Giannuzzi P. Accurate noninvasive estimation of pulmonary vascular resistance by Doppler echocardiography in patients with chronic failure heart failure. J Am Coll Cardiol. 2001;37(7):1813–9.

12. Gorcsan J III, Snow FR, Paulsen W, Nixon JV. Noninvasive estimation of left atrial pressure in patients with congestive heart failure and mitral regurgitation by Doppler echocardiography. Am Heart J. 1991;121(3 pt 1):858–63.
13. Ommen SR, Nishimura RA, Appleton CP, et al. Clinical utility of Doppler echocardiography and tissue Doppler imaging in the estimation of left ventricular filling pressures: a comparative simultaneous Doppler-catheterization study. Circulation. 2000;102(15):1788–94.
14. Ha JW, Oh JK, Ling LH, Nishimura RA, Seward JB, Tajik AJ. Annulus paradoxus: transmitral flow velocity to mitral annular velocity ratio is inversely proportional to pulmonary capillary wedge pressure in patients with constrictive pericarditis. Circulation. 2001;104(9):976–8.
15. Abbas AE, Fortuin FD, Patel B, Moreno CA, Schiller NB, Lester SJ. Noninvasive measurement of systemic vascular resistance using Doppler echocardiography. J Am Soc Echocardiogr. 2004;17(8):834–8.
16. 2014 AHA/ACC Guideline for Management of Patients with Valvular Heart Disease. A report of the American College of Cardiology/American Heart Association Task Force on Practice Guidelines. Circulation. 2014;129:2440–92.
17. Baumgartner H, Hung J, Bermejo J, et al. Echocardiographic assessment of valve stenosis: EAE/ASE recommendations for clinical practice. J Am Soc Echocardiogr. 2009;22(1):1–23; 101–2.
18. Oh JK, Taliercio CP, Holmes DR Jr, et al. Prediction of the severity of aortic stenosis by Doppler aortic valve area determination: prospective Doppler-catheterization correlation in 100 patients. J Am Coll Cardiol. 1988;11(6):1227–34.
19. Monin JL, Quere JP, Monchi M, et al. Low-gradient aortic stenosis: operative risk stratification and predictors for long-term outcome: a multicenter study using dobutamine stress hemodynamics. Circulation. 2003;108(3):319–24.
20. Rahimtoola SH, Durairaj A, Mehra A, Nuno I. Current evaluation and management of patients with mitral stenosis. Circulation. 2002;106(10):1183–8.
21. Thomas JD, Weyman AE. Doppler mitral pressure half-time: a clinical tool in search of theoretical justification. J Am Coll Cardiol. 1987;10(4):923–9.
22. Bonow RO, Carabello BA, Chatterjee K, et al. 2008 focused update incorporated into the ACC/AHA 2006 guidelines for the management of patients with valvular heart disease: a report of the American College of Cardiology/American Heart Association Task Force on Practice Guidelines (Writing Committee to revise the 1998 guidelines for the management of patients with valvular heart disease). Endorsed by the Society of Cardiovascular Anesthesiologists, Society for Cardiovascular Angiography and Interventions, and Society of Thoracic Surgeons. J Am Coll Cardiol. 2008;52(13):e1–142.
23. Smith MD, Cassidy JM, Gurley JC, Smith AC, Booth DC. Echo Doppler evaluation of patients with acute mitral regurgitation: superiority of transesophageal echocardiography with color flow imaging. Am Heart J. 1995;129(5):967–74.
24. Bargiggia GS, Tronconi L, Sahn DJ, et al. A new method for quantitation of mitral regurgitation based on color flow Doppler imaging of flow convergence proximal to regurgitant orifice. Circulation. 1991;84(4):1481–9.
25. Pu M, Vandervoort PM, Griffin BP, et al. Quantification of mitral regurgitation by the proximal convergence method using transesophageal echocardiography. Clinical validation of a geometric correction for proximal flow constraint. Circulation. 1995;92(8):2169–77.
26. Pu M, Prior DL, Fan X, et al. Calculation of mitral regurgitant orifice area with use of a simplified proximal convergence method: initial clinical application. J Am Soc Echocardiogr. 2001;14(3):180–5.
27. Zoghbi WA, Enriquez-Sarano M, Foster E, et al. Recommendations for evaluation of the severity of native valvular regurgitation with two-dimensional and Doppler echocardiography. J Am Soc Echocardiogr. 2003;16(7):777–802.
28. Tribouilloy CM, Enriquez-Sarano M, Bailey KR, Seward JB, Tajik AJ. Assessment of severity of aortic regurgitation using the width of the vena contracta: a clinical color Doppler imaging study. Circulation. 2000;102(5):558–64.
29. Touche T, Prasquier R, Nitenberg A, de Zuttere D, Gourgon R. Assessment and follow-up of patients with aortic regurgitation by an updated Doppler echocardiographic measurement of the regurgitant fraction in the aortic arch. Circulation. 1985;72(4):819–24.
30. Schmidt FP, Gniewosz T, Jabs A, Münzel T, Hink U, Lancellotti P, von Bardeleben RS. Usefulness of 3D-PISA as compared to guideline endorsed parameters for mitral regurgitation quantification. Int J Cardiovasc Imaging. 2014;30(8):1501–8.
31. Matsumura Y, Fukuda S, Tran H, et al. Geometry of the proximal isovelocity surface area in mitral regurgitation by 3-dimensional color Doppler echocardiography: difference between functional mitral regurgitation and prolapse regurgitation. Am Heart J. 2008;155:231–8.

Suggested Reading

Hatle L, Angelsen B. Doppler ultrasound in cardiology: physical principles and clinical applications. 2nd ed. Philadelphia: Lea & Febiger; 1985. p. 331.

Quinones MA, Otto CM, Stoddard M, Waggoner A, Zoghbi WA, Doppler Quantification Task Force of the Nomenclature and Standards Committee of the American Society of Echocardiography. Recommendations

for quantification of Doppler echocardiography: a report from the Doppler Quantification Task Force of the Nomenclature and Standards Committee of the American Society of Echocardiography. J Am Soc Echocardiogr. 2002;15(2):167–84.

Baumgartner H, Hung J, Bermejo J, et al. Echocardiographic assessment of valve stenosis: EAE/ASE recommendations for clinical practice. J Am Soc Echocardiogr. 2009;22(1):1–23; 101–2.

Zoghbi WA, Enriquez-Sarano M, Foster E, et al. Recommendations for evaluation of the severity of native valvular regurgitation with two-dimensional and Doppler echocardiography. J Am Soc Echocardiogr. 2003;16(7):777–802.

CT and MRI Cardiovascular Hemodynamics

12

Andrew O. Zurick

Introduction

Noninvasive cardiac imaging has experienced dynamic improvements over the past several decades. Multiple, complementary technologies, including magnetic resonance imaging (MRI), computed tomography (CT), echocardiography, nuclear scintigraphy, fluoroscopy, and angiography, are now capable of directly or indirectly providing information on cardiac and great vessel anatomy, volumes and function, myocardial perfusion, valvular morphology and function, coronary artery blood flow, and presence or absence of myocardial fibrosis or scar. Further, several of these technologies now are capable of providing a noninvasive hemodynamic assessment, which has otherwise primarily in the past been the domain and strength of echocardiography and invasive catheterization. Both CT and MRI have been proven to be accurate and reproducible, with each now capable of providing noninvasive hemodynamic information which is capable of enhancing clinical decision-making and impacting patient care. However, the use of this information must be based on a thorough knowledge of the strengths and weaknesses of the various noninvasive methods of hemodynamic assessment. Understanding the applications and limitations of these modalities will permit their effective and efficient usage in the future (Table 12.1).

A. O. Zurick (✉)
St. Thomas Heart, Nashville, TN, USA
e-mail: andrew.zurick@ascension.org

General Overview of MR and CT Physics and Techniques

Physics Overview

MRI is based on the resonance, or increased amplitude of oscillation of a system exposed to a periodic force, of atomic nuclei. Following the application of radio waves, MRI measures the electromagnetic signals that are emitted from atomic nuclei. Hydrogen is the most simple and abundant element in the human body, consisting of a single proton and electron, and therefore, it represents an ideal substrate for clinical MRI. There exists a unique relationship between electricity and magnetism, namely moving electrical charges are capable of generating a magnetic field, and a time-varying magnetic field can create electric fields that can promote the flow of electrical charges. Atomic nuclei of several atoms behave as small magnets with angular momentum, and when placed within a magnetic field, they have a tendency to align with the direction of an electric field applied, and process, or rotate, about their own axis, as would a top.

Most current clinical MRI involves superconducting magnets, where a magnetic field is

A. T. Askari, A. W. Messerli (eds.), *Cardiovascular Hemodynamics*, Contemporary Cardiology,
https://doi.org/10.1007/978-3-030-19131-3_12

Table 12.1 CT and MRI advantages and disadvantages

	Advantages	Disadvantages
Computed tomography	Rapid image acquisition	Radiation exposure
	Excellent spatial resolution (<1 mm)	Potential need for iodinated contrast dye
	3D dataset acquisition for ability for post-processing/reconstruction	Limited temporal resolution (best temporal resolution with current generation scanners on order of 75 ms)
	Typically well tolerated by patients	Limited hemodynamic assessment options currently
	Not contraindicated in patients with ferromagnetic/metallic implants	
Magnetic resonance imaging	Tissue characterization	Increased image acquisition time
		Potential for patient claustrophobia
	Excellent spatial resolution (1–2 mm)	Possibility, although rare, for NSF following gadolinium contrast administration
	Temporal resolution better than CT (typically 25–50 ms)	Inability to image patients with absolute contraindications including those with ferromagnetic implants (i.e., pacemakers, ICDs, intracerebral vascular coils, etc.)
	Unlimited imaging plane orientation and ability to acquire 3D datasets	
	No need for contrast (i.e., can be performed on patients with decreased GFR)	
	Increased ability to assess cardiovascular hemodynamics noninvasively via volumetric and phase-contrast analysis	

generated perpendicular to an electrical current flowing along a cylindrical coiled wire. The creation of MR images involves the excitation of protons, within a magnetic field, using pulses of radiofrequency energy, which can be specifically applied to body parts of interest through the concurrent application of magnetic field gradients. Following excitation of a tissue, a signal is created within a "receive" coil, which subsequently undergoes analog-to-digital conversion (ADC), which is then processed by the MRI computer as raw data into "k-space." The "Fourier transform" of the raw data ultimately generates 2D or 3D MR images that can be viewed for interpretation. MR imaging of the heart must contend with both cardiac and respiratory motion, conflicting requirements for both high temporal and spatial resolution, and do all of this both accurately and reproducibly in the clinical setting, in a timely fashion.

As with CMR, the small dimensions of the coronary arteries and rapid motion of cardiac structures pose significant challenges to effective imaging with cardiac computed tomography (CT). Current generation multirow detector CT (MDCT) scanners involve a rotating X-ray source, which emit photons, which pass through a patient, as they are moved through the machine gantry. Due to continued improvements in gantry rotation times, and the development of dual-source CT, temporal resolution has improved. Slice collimation, or thickness, has also continued to improve, resulting in greater spatial resolution. Increased X-ray tube strength has also resulted in decreased image noise and recent generation scanners have continued to improve simultaneous slice acquisition, now up to as many as 320 slices per rotation, which allows one to cover a larger volume per rotation, decrease overall data acquisition time, and reduce duration of required breath hold. Through the simultaneous registration of the ECG, it is possible to synchronize image reconstruction with the relative cardiac phase. Ongoing developments in tube-current modulation, prospective ECG-gated scanning, and improved table pitch (speed with which the patient table is advanced through the scanner) continue to lower patient radiation exposure (effective dose).

MRI Techniques

Phase-Contrast Imaging

Phase-contrast imaging (PCI) is an MRI technique for quantifying velocity and blood flow in the heart, across valves, and through great vessels. By measuring the phase shift, or change in precessional frequency, of protons in blood as they move through a magnetic field with a bipolar gradient, velocity, direction, and volume of blood flow can be determined. The amount of relative phase difference is proportional to the velocity of the moving spin, and these phase shifts are measured in degrees within a range of ±180°. Similar to aliasing velocity in Doppler echocardiography, the encoding velocity (VENC) chosen for this technique should optimally be chosen to correspond to a phase shift of 180°. If the phase shift exceeds 180°, then the spins will be interpreted as having a different orientation, which would therefore result in abnormal velocity interpretation. Ultimately, phase-contrast MR imaging produces velocity-encoded images where signal intensity is proportional to the velocity of blood moving through or within the slice plane. Unlike echocardiography, which is constrained by acoustic windows, PCI, utilizing a single imaging plane that is most commonly perpendicular to the direction of blood flow, generates a velocity-encoded image of multiple phases of the heart cycle either with or without breath-holding. No intravenous contrast is necessary to generate these images. Quantification of blood flow is subsequently determined by various software applications that require the user to manually outline the vessel of interest for each cardiac phase, which then produces time-velocity and time-flow curves (Fig. 12.1a,b). Many studies have now demonstrated the reliability of PCI with CMR; however it must be noted that the accuracy of the technique can be significantly affected by the presence of eddy currents [1].

Myocardial Tagging

Myocardial tagging is a series of techniques that impose a saturation grid or series of saturation lines across the myocardium [1]. Deformation of these lines due to myocardial contraction and relaxation are then monitored and can be used to assess myocardial function by tracking the motion of the myocardium during the various phases of the cardiac cycle [2] (Fig. 12.2). When combined with cine imaging, myocardial tagging can provide complementary information regarding myocardial contraction, performance, and can be used to measure myocardial strain in three dimensions. In clinical practice, myocardial tag lines are typically evaluated subjectively to differentiate normal and hypokinetic myocardial segments. While predominantly used as a supplementary technique to cine imaging to evaluate cardiac wall motion, the research applications of myocardial tagging are continuing to evolve, particularly with recent advances in image acquisition speed and improved signal-to-noise ratios.

Volumetric and Functional Assessment

Through continued improvement in hardware and software, MRI has evolved into the "gold standard" for ventricular volumetric and function assessment owing to its excellent accuracy and reproducibility. With manual or automated contours of multiphase, ECG-gated epi- and endocardial contours, ventricular volumes, function, and mass can be determined. In addition, while Doppler echocardiography has typically been considered the reference standard for assessment of diastolic dysfunction, recent studies have also demonstrated the utility and reproducibility of CMR techniques for flow and phase-contrast data analysis to extract velocity-related diastolic parameters [3]. The degree of myocardial fibrosis is related to the degree of left ventricular stiffness. Malaty et al. evaluated 50 patients with dilated cardiomyopathy (DCM) with Doppler echocardiography and breath-hold segmented inversion recovery sequence imaging following intravenous gadolinium administration to determine amount of left ventricular scar burden. Hyperenhancement (HE) was present in 31 patients with a mean scar burden of 4 ± 7.6%, and patients with DCM without HE had significantly higher septal E/E' ratio than patients with scar ($p = 0.05$) suggesting that factors other than scar burden likely contribute to LV stiffness to a greater extent than replacement fibrosis in this

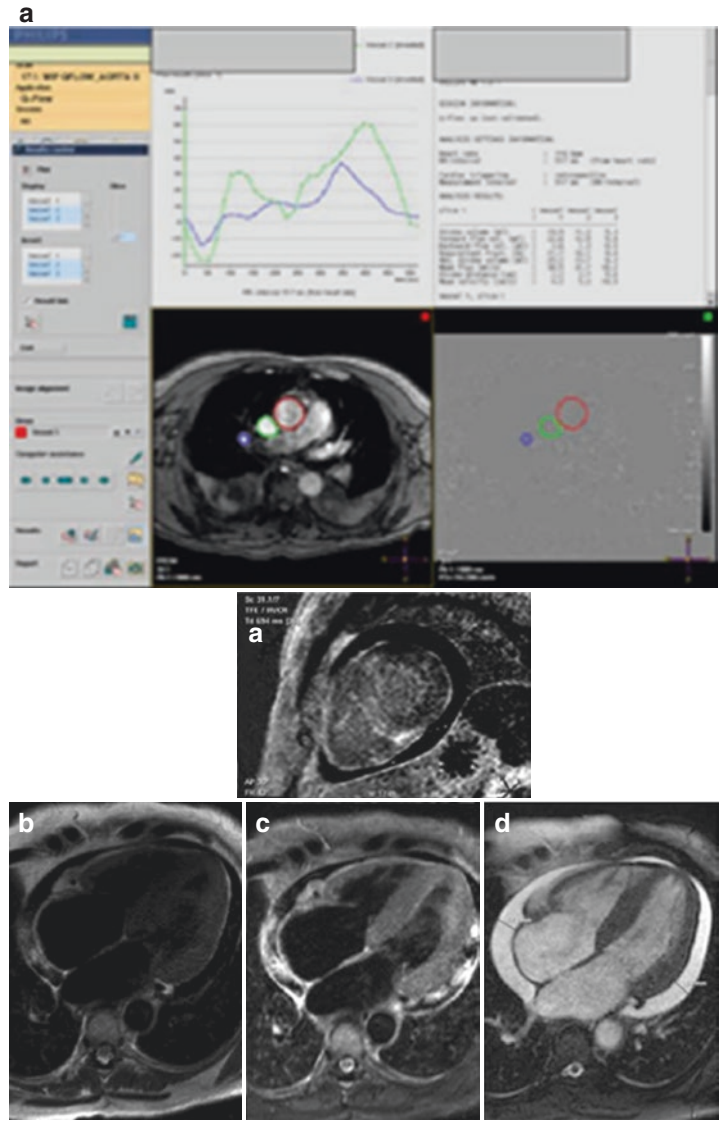

Fig. 12.1 (**a**) Cardiac amyloidosis. Image at *top* are from representative phase-contrast image demonstrating manual contouring of the ascending aorta, superior vena cava, and right upper pulmonary vein. Flow curves in *upper left panel* demonstrate systolic blunting consistent with diastolic dysfunction. Images at *bottom* demonstrate tissue characterization of myocardium in cardiac amyloidosis, with associated circumferential pericardial effusion, through multiple different cardiac MRI pulse sequences. (**b**) Hypertrophic cardiomyopathy with severe systolic anterior motion of the mitral valve (SAM). Representative phase-contrast image (*top*) demonstrating manual contouring of the left ventricular outflow tract. Contours are propagated to images from multiple cardiac phases. Image at *bottom left* represents single cardiac-phase magnitude gradient echo image at end-systole. Peak left ventricular outflow tract velocity can be measured and converted to pressure gradient through utilization of modified Bernoulli equation

b

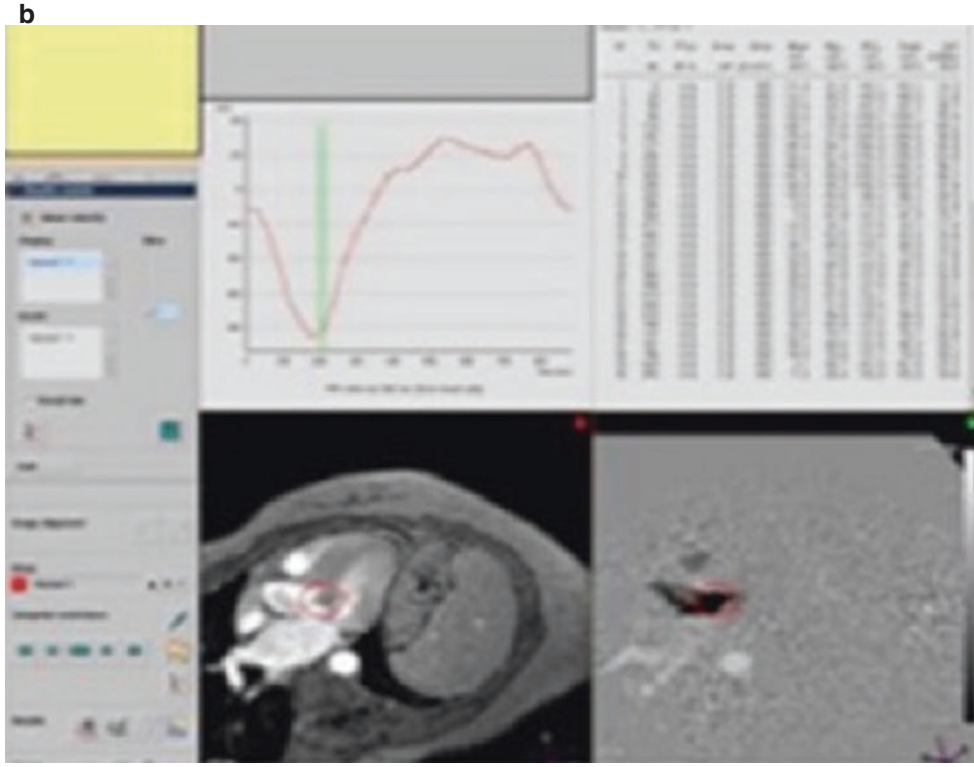

Fig. 12.1 (continued)

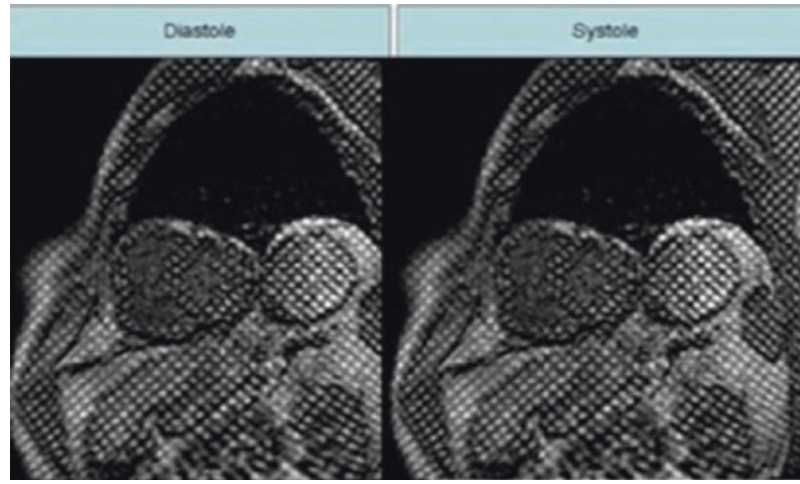

Fig. 12.2 Myocardial tagged image (short axis orientation) with saturation lines depicted across the myocardium in both systole (*right*) and diastole (*left*)

patient population [4]. However, other groups have also shown that cardiac fibrosis correlates with impaired LV diastolic function and functional capacity, elevated NT-pro BNP, and adverse cardiac remodeling in patients with non-ischemic DCM [5]. Other groups have utilized CMR phase-contrast velocity mapping (i.e., tissue phase mapping) to evaluate regional wall motion patterns and longitudinally and circumferentially directed movements of the left ventricle [6]. The complex pattern of ventricular twisting and longitudinal motion in the normal

human heart can be better understood through applications such as these, ultimately helping to provide a better understanding of the complex mechanics of the normal heart.

Stress cardiac MRI has continued to evolve and is capable of providing a multiparametric examination of cardiac function, perfusion, and valvular function and assessing for interstitial fibrosis or myocardial scar. Lipinksi M et al. performed a meta-analysis to understand the role that stress cardiovascular MRI plays in the assessment of patients with known or suspected coronary artery disease [7]. A total of 11,636 patients were evaluated, and those with ischemia were noted to have a higher rate of myocardial infarction or cardiovascular death compared with patients that had a non-ischemic study.

The combined outcome annualized events rates were 4.9% for a positive versus 0.8% for a negative stress CMR ($p < 0.0001$), 2.8% versus 0.3% for cardiovascular death ($p < 0.0001$), and 2.6% versus 0.4% for MI ($p < 0.0005$). The presence of late gadolinium enhancement was significantly associated with a worse prognosis. More recently, Liu A et al. published the first prospective validation of stress T1 mapping against invasive coronary measurements for detecting obstructive coronary artery disease [8]. Sixty patients with angina and 30 normal patients were imaged with CMR adenosine stress/rest T1-mapping. Ischemic viable myocardium downstream from obstructive CAD showed nearly abolished T1 reactivity, while myocardium downstream from non-obstructive coronary artery disease with microvascular dysfunction showed a lesser degree of blunting of T1 reactivity. This method of evaluating patients with coronary artery disease for ischemia may prove to obviate the need for routine intravenous gadolinium contrast administration.

Delayed Enhancement Imaging

The intensity of voxels in an MR image is a direct result of the amount of signal that can be measured by a receiver coil. MR intravenous contrast agents are useful for depicting anatomy and physiology, evaluating vascular supply to both normal and pathologic tissues, and assessing myocardial viability. Most MR contrast agents work by shortening T1 relaxation times, which results in increased signal intensity. The most commonly used MR contrast agents are chelates of gadolinium (Gd3+), a lanthanide heavy metal ion.

Inversion recovery imaging is capable of selectively suppressing signal from certain tissues based on their T1 recovery times and is useful for assessing myocardial infarction and viability. Following gadolinium administration, infarcted myocardium demonstrates a delayed pattern of gadolinium washout, and through the use of inversion recovery techniques, normal myocardium is "nulled" so that infarcted myocardium appears bright by comparison.

Tissue Characterization (T1- and T2-Weighted Imaging)

One of the unique features of cardiac MRI is the ability to characterize normal and pathologic tissues through the use of various pulse sequences. In addition to fat suppression and gadolinium contrast enhancement, T1- and T2-weighted imaging are the most widely utilized techniques. Tissues that tend to appear brighter on T1-weighted images include lipid, hemorrhagic products, proteinaceous fluid, and gadolinium. T2-weighted images of the heart help to characterize tissues with longer T2-times and are typically performed with concurrent blood nulling.

CT Techniques

ECG-Triggering

Through the simultaneous registration of the ECG, it is possible to synchronize CT image reconstruction with the relative cardiac phase. Due to cardiac and respiratory movements, motion artifacts can significantly affect cardiovascular CT images. Appropriate collimation size and image acquisition speed are important to obtain images free from artifacts. Currently, the collimation size for coronary artery calcium screening and angiography is 0.6–3 mm and acquisition speed ranges from 50 to 250 ms. Currently, two ECG-trigger techniques are utilized in cardiac CT

imaging, retrospective and prospective triggering. Prospective triggering can be performed with R wave triggering, end-systolic triggering, and both end-systolic and end-diastolic combined triggering. Alternatively, retrospective triggering is widely used and synchronized to an ECG signal that is recorded simultaneously with images. Changes in heart rate or rhythm can induce misregistration artifact in both prospective and retrospective triggered images.

Contrast Media

The primary purpose of contrast media injection is to increase contrast between the structure of interest and surrounding tissues by increasing the CT Hounsfield units. Care must be taken regarding circulation time for contrast media, the time interval that it takes blood to move from the point of venous access, the structure/region of interest, with several factors having influence, including cardiac output, injection rate, and venous anatomy. Circulation time can be measured using a small contrast bolus injection with serial scanning of a single image slice to obtain peak enhancement time through the time density curve. Alternatively, automatic bolus triggering utilizes a monitoring scan obtained 10–12 s following the start of contrast injection, and when the Hounsfield unit (HU) reaches a pre-specified threshold (typically 120 HU), imaging is initiated.

Clinical Applications

Shunts

Cardiac MRI has become a valuable tool in the evaluation of both cardiac anatomy and quantification of physiologic function. CMR can detect, provide morphologic information about, and quantify both intra- and extra-cardiac shunts. Shunt volume can be calculated through the use of volumetric cine MR imaging or PCI. Provided that there is absence of concurrent valvular regurgitation, total forward flow through the proximal ascending aorta and main pulmonary artery can be utilized to determine shunt fraction (Shunt fraction % (Q_p/Q_s) = total PCI pulmonary artery volume flow (mL)/total PCI ascending aortic volume flow (mL)). Alternatively, shunt severity can be calculated by comparing the ratio of right ventricular to left ventricular stroke volumes (Q_p/Q_s), again provided that there is not significant simultaneous valvular regurgitation. In addition, MR angiography can provide excellent 3D anatomic examination of vessels including the presence of anomalous pulmonary veins.

Cardiac CT is a useful adjunctive imaging modality in the assessment of intra- and extracardiac shunts. It is typically reserved for patients with contraindications for CMR or when there are issues associated with severe claustrophobia. Excellent spatial resolution provides the ability to visualize interatrial and interventricular septal defects (VSDs) [9]. Cardiac CT permits detailed imaging the heart, but also affords additional assessment of several noncardiac structures including mediastinum, lungs, pulmonary artery system, aorta, esophagus, chest wall, and airways [10]. Previous studies have shown that cine CT, through evaluation of indicator dilution curves, provides a precise, noninvasive technique for measuring shunt lesions in congenital and acquired heart diseases [11].

Atrial Septal Defect

Atrial septal defect (ASD) is the most common shunt lesion detected de novo in adulthood [12]. Sinus venosus, septum secundum, and primum defects can clearly be identified with MR imaging in the transverse plane or along the short axis. Further, spin-echo MR imaging has been found to have a greater than 90% sensitivity and specificity for identification of atrial septal defects [13]. PCI enables more precise evaluation of both size and shape of atrial septal defects and permits more accurate quantification of the degree of shunting present [14, 15]. In addition, cardiac CT has been also shown to detect and characterize ASDs with high sensitivity (66–100%) and specificity (86–100%) [16] (Fig. 12.3).

Ventricular Septal Defect

VSD is the second most common congenital defect of the heart, accounting for nearly 20% of

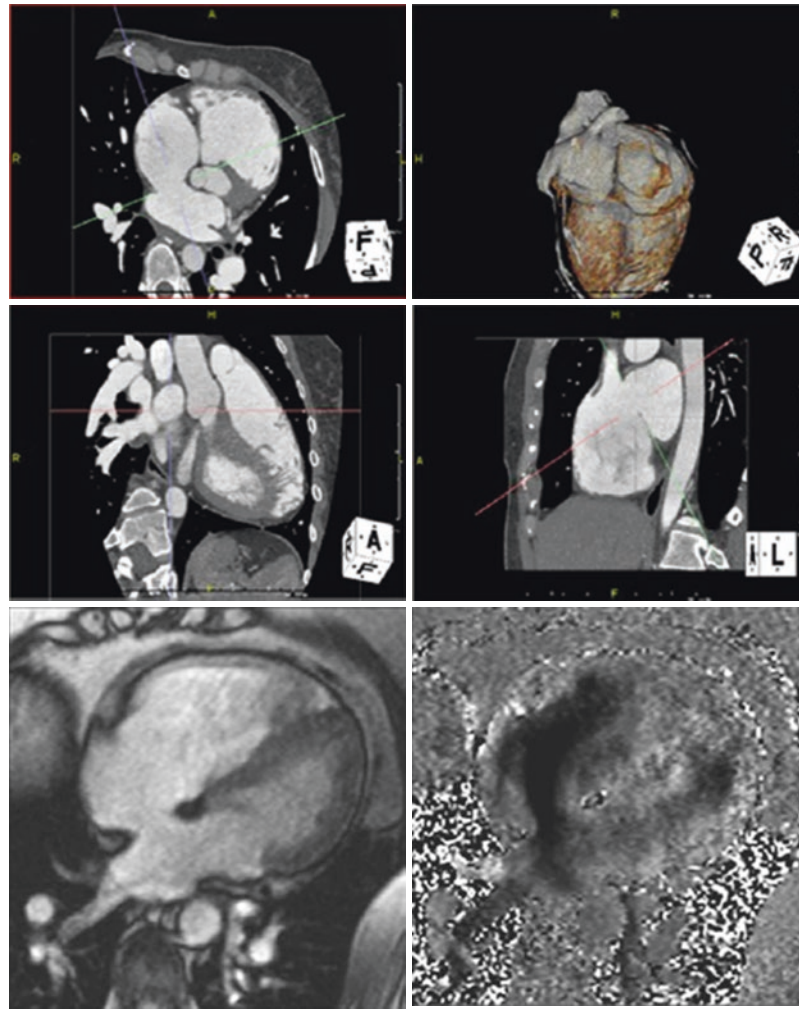

Fig. 12.3 ECG-gated cardiac computed tomography with iodinated contrast axial image demonstrating atrial septal defect (ASD), ostium secundum type (*top*). Cardiac MRI (*bottom*) steady-state free precession 4-chamber image demonstrating ASD, ostium secundum type (*right*), and phase-contrast image demonstrating left to right shunt across ASD (*left*)

all cardiac malformations [12]. VSD can be further categorized into four groups based on location and margin: outlet, membranous, trabecular, and inlet [17]. Membranous is the most common. MR imaging possesses greater than 90% sensitivity for the detection of VSD [18].

Atrioventricular Septal Defect

Atrioventricular septal defects present as a common atrioventricular valve with abnormal arrangement of the valvular leaflets, and variable defects in the primum atrial septum and ventricular inlet septum [19]. In the most severe form of atrioventricular septal defect, there exists bidirectional shunting, where all four chambers of the heart communicate. CMR is a particularly valuable tool in the evaluation of atrioventricular septal defects to delineate anatomical features which are important for surgical planning, cardiac chamber dimension, and presence and size of ventricular component of defects.

Patent Ductus Arteriosus

Before birth, the ductus arteriosus allows blood to bypass the baby's lungs by connecting the pulmonary arteries with the aorta. Patent ductus arteriosus (PDA) is a congenital disorder within the great vessels wherein a neonate's ductus arteriosus fails to close after birth. PDA accounts for 10–12% of all congenital heart disease [12].

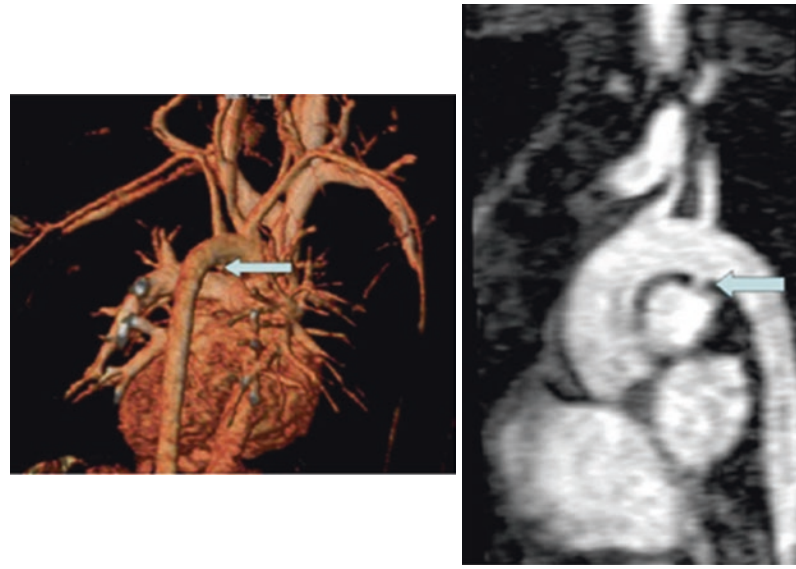

Fig. 12.4 Patent ductus arteriosus. Image at right is 3D, volume rendered MR image of PDA (*arrow*). Image at *left* is MR angiography sagittal image demonstrating PDA in an alternate orientation (*arrow*)

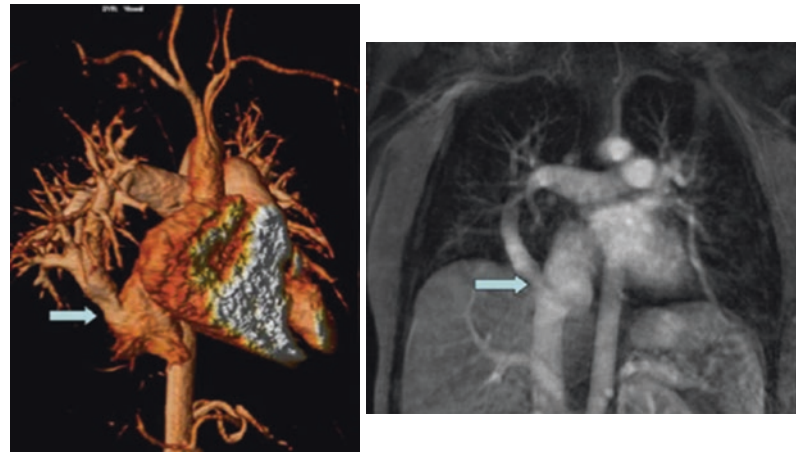

Fig. 12.5 Scimitar syndrome patient (partial anomalous pulmonary venous drainage). Image at *left* demonstrates 3D volume-rendered MR image of anomalous pulmonary venous return with right inferior pulmonary vein draining via antrum on inferior vena cava. Image at right is coronal MR maximum intensity projection (MIP) depicting same

CMR is capable of clearly demonstrating the persistent communication between the aorta and pulmonary artery; however due to the often small size of these defects (<3 mm), echocardiography remains the primary diagnostic tool for their identification and evaluation (Fig. 12.4).

Partial Anomalous Pulmonary Venous Return

Partial anomalous pulmonary venous return (PAPVR) involves one or more pulmonary veins returning aberrantly to the superior or inferior vena cava, right atrium, or coronary sinus. PAPVR is present in 10–15% of patients with secundum-type atrial septal defects and 100% of patients with sinus venosus-type defects [19]. Children with PAPVR are typically asymptomatic, whereas adults with the condition will typically present with dyspnea and palpitations. CMR is a particularly attractive imaging modality for identifying PAPVR as it provides a large field of view and can be performed without ionizing radiation or contrast material. CMR has been reported to have greater sensitivity (95%) for identification of PAPVR compared with echocardiography and angiography [20] (Fig. 12.5).

Diastology

CMR is now playing an increasing role in understanding the physiology of diastolic function. CMR is capable of evaluating myocardium in both active and passive phases, providing insight into relaxation and compliance characteristics. Further, CMR through PCI can assess inflow and myocardial velocities. Previous studies comparing CMR to TTE in the assessment of diastolic function have shown that velocities of mitral valve flow (E and A wave) measured by CMR correlated well with TTE ($r = 0.81$; $p < 0.001$), but also demonstrated systematic underestimation by CMR compared to TTE [21, 22]. Myocardial tagging with CMR can provide complementary information regarding myocardial contraction performance and can be used to measure myocardial strain in three dimensions.

While not typically thought of as a reliable source for assessment of diastolic function, recent studies have demonstrated that CT is capable of providing information regarding cardiac diastolic function. Boogers et al. evaluated 70 patients who had undergone CT and 2D echocardiography with TDI. Good correlations were observed between cardiac CT and 2D echocardiography for assessment of E ($r = 0.73$; $p < 0.01$), E/A ($r = 0.87$; $p < 0.01$), E_a ($r = 0.82$; $p < 0.01$), and E/E_a ($r = 0.81$; $p < 0.01$). In addition, a good diagnostic accuracy (79%) was found for detection of diastolic dysfunction using cardiac CT [23]. Other groups have evaluated the arterial enhancement of the aortic-root lumen on contrast-enhanced CT and plotted its change over time to determine the time-enhancement curve. Nakahara et al. evaluated 30 patients with suspected coronary artery disease who underwent MDCT and echocardiography. On univariate analysis, the slope of the time-enhancement curve was found to correlate with the e' ($r = 0.686$; $P = 0.000$) and E/e' ($r = -0.482$; $P = 0.007$) ([24]).

Valvular Heart Disease

While echocardiography remains the primary first-line imaging modality for the assessment of valvular heart disease, over the past several years, complementary uses of cardiovascular MRI and CT for the assessment of valvular heart disease have been demonstrated. MRI and CT can provide a comprehensive assessment of cardiac valvular anatomy and function. MRI offers the additional capability of assessing blood flow through a variety of imaging sequences.

The unlimited imaging planes offered by cardiac MRI are advantageous for assessment of the complex mitral valve anatomy. The primary benefit of MRI for the assessment of mitral regurgitation is the ability to quantitate regurgitant volume in conjunction with ventricular volumes and function. The primary method for quantification of mitral regurgitation involves subtracting aortic forward flow (calculated from aortic phase-contrast imaging) from the left ventricular stroke volume. Quantification of mitral regurgitation with MRI correlates only modestly with echocardiography but offers lower inter- and intra-observer variability [25]. More recently however, some data has demonstrated discrepancy between mitral regurgitation severity calculated by echocardiography compared with MRI [26]. Some have argued that since LV volume reductions following mitral valve surgery were more closely related to regurgitant volumes measured by MRI rather than echocardiography, that MRI should be the preferred method of mitral regurgitation assessment [26].

Multi-slice computed tomography (MSCT), while not able to provide information of blood flow like MRI, can provide additional or complementary information on the assessment of mitral valve anatomy. Delgado V et al. evaluated 151 patients with MSCT to assess the anatomy of the mitral valve subvalvular apparatus, mitral valve tenting height, and leaflet tethering [27]. The anatomy of the subvalvular apparatus was noted to be highly variable, particularly the posterior papillary muscle, involving multiple heads and insertion sites. Mitral valve tenting height at the central level and mitral valve sphericity index were the strongest determinants of FMR severity. With the continued growth in structural heart transcatheter therapies, MSCT will certainly play an increasing role in the pre-procedural planning of these complex cases over the coming years.

Further, MRI PCI has been demonstrated to help in the stratification of aortic regurgitant (AR) severity. Holodiastolic reversal in the mid-descending thoracic aorta using PCI has been shown to indicate severe AR and can be used with quantified regurgitant values obtained from PCI to further stratify AR severity [28].

One measure of severity of a valvular stenosis involves the peak transvalvular pressure gradient that is generated across the area of narrowing. For stenotic valvular lesions, PCI can be positioned through-plane or in-plane to estimate the maximum transvalvular velocity (V_{max}). As is seen with spectral Doppler echocardiography, if the imaging slice does not pass through the area of maximum velocity, then the pressure gradient, estimated using the modified Bernoulli equation (pressure gradient (mmHg) = $4 \times V_{max2}$), will be underestimated. Aliasing will have a similar appearance as in Doppler echocardiography, and if this is seen at the time of image acquisition, this sequence must be repeated using an alternate phase encoding velocity (V_{enc}). Additionally, PCI can also evaluate volume flow rates by measuring the mean velocity of blood across its lumen (V_{mean}) and multiplying by the cross-sectional area of the vessel lumen (volume flow (mL/s) = V_{mean} (cm/s) × area (cm^2)).

Aortic valve stenosis continues to be one of the most common valvular disorders in older adults with a prevalence of 8% at age 85 [29]. Open surgical aortic valve replacement is the only treatment that has been demonstrated to improve symptoms, survival, and functional status [30]. However, certain patient subsets are deemed high-risk for surgical repair, which lead to the development of transcatheter aortic valve replacement (TAVR). CT now plays a vital role in assessing patients prior to percutaneous aortic valve implantation. 3D reconstructed multi-planar images allow assessment of the aortic valve in multiple phases of the cardiac cycle and permit direct valve and annular area planimetry (Fig. 12.6). These measurements tend to be slightly larger than what is reported by 3D transesophageal echocardiography. Additionally, cardiac CT permits estimation of optimal valve implantation angles via fluoroscopy in the catheterization laboratory. Further, ECG-gated imaging of the thoracic aortic permits accurate assessment of aortic anatomy and morphology. Contrasted imaging of the abdominal aorta and peripheral arteries is also very important for determining whether the peripheral arteries are large enough to accommodate the large diameter of the delivery catheters. The results of the PARTNER trial have shown that at 1 year, the rate of death from any cause was 30.7% with TAVR, compared to 50.7% with standard therapy. However, at 30 days, TAVR as compared to standard therapy was associated with a high incidence

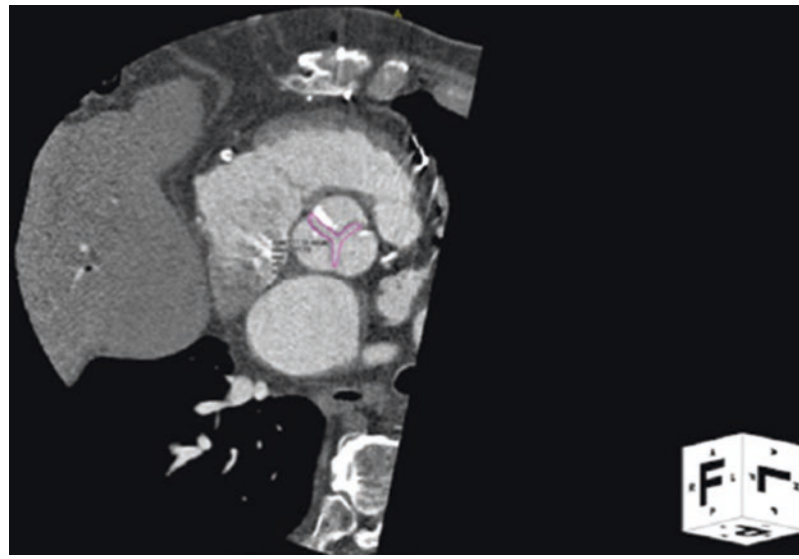

Fig. 12.6 Aortic stenosis. Cardiac CT 3D reconstructed multi-planar image of the aortic valve in short axis at end-systole with planimetry of aortic valve area

of major strokes (5 vs. 1.1%, $p = 0.06$) and major vascular complications (16.2 vs. 1.1%, $p < 0.001$) [31]. With the continued expansion of structural and valvular heart disease therapies in the coming years, CT will continue to play a larger role in pre-procedural planning.

CT is also capable of assessing ventricular volumes on multiphase-gated images to help in the determination of ventricular dilatation with regurgitant valvular lesions. Further, in patients with mechanical valves, CT provides a rapid, low-radiation exposure technique to image the valve in multiple phases of the cardiac cycle to determine opening and closure angles.

Cardiomyopathies

CMR provides excellent qualitative as well as quantitative assessment of ventricular function. When compared with Doppler echocardiography, phase-contrast measurements correspond well, and show fair correspondence when compared with invasive techniques utilizing the Fick principle, indicator-ink method, or thermodilution [32, 33]. Volumetric and functional assessment of the ventricles typically involves retrospectively gated steady-state free precession imaging of the chambers either in short- or long-axis orientations. Utilizing post-processing software, contours of the epi- and endocardium are typically drawn manually for each imaging slice, though more recently with progressive developments in artificial intelligence (AI), contouring can now more commonly be done automatically and edited by a reviewer for accuracy. Post-processing software generates quantitative data regarding cardiac function (ejection fraction, stroke volume, cardiac output), mass, and volumes. Alternatively, determination of cardiac output can be performed with phase-contrast imaging. By comparing cardiac output of the left ventricle in the ascending aorta with the cardiac output of the right ventricle in the main pulmonary artery, there is an internal control of these measurements, with gross differences typically indicating either unknown intra- or extra-cardiac shunt or more commonly, error in the initial prescription of the phase-contrast technique with either incorrectly selected imaging plane or phase encoding velocity.

CMR is now evolving as an important imaging modality in the assessment of patients with hypertrophic cardiomyopathy [34]. Cine imaging provides anatomic and morphologic assessment, allowing for measurement of myocardial wall thickness, papillary muscle anatomy, and left ventricular outflow tract obstruction. Phase-contrast imaging has proven useful in the assessment of gradients in patients with hypertrophic obstructive cardiomyopathy [35]. In patients with left ventricular outflow tract obstruction, PCI (both in plane and through plane) is useful to determine the peak velocity in a manner similar to Doppler echocardiography [34]. Post-gadolinium contrast delayed enhancement imaging also permits assessment of myocardium for scar. CMR also has proven useful in the evaluation of myocardial sarcoidosis [36], amyloidosis [37–39], and hemochromatosis [39, 40].

Through the simultaneous registration of the ECG, it is possible to synchronize image reconstruction with the relative cardiac phase with cardiac CT imaging. In patients with suspected or documented heart disease, precise, accurate quantification of cardiac function is vital for diagnosis, risk stratification, treatment, and prognosis. The same data that is acquired for coronary arterial evaluation, as part of coronary CT angiography, can also be used for evaluation of cardiac function. Previous studies have demonstrated that multiphase, gated cardiac CT demonstrates good correlation when compared with 2D surface echocardiography [41, 42].

Pericardial Disease

CMR is an excellent modality for assessing pericardial disease. CMR can accurately demonstrate pericardial thickness, effusion, pericardial cysts and through various pulse sequences, also demonstrate pericardial edema and/or inflammation. Real-time gradient-echo CMR in a single imaging slice can evaluate ventricular function with simultaneous respiration visualization and assess for

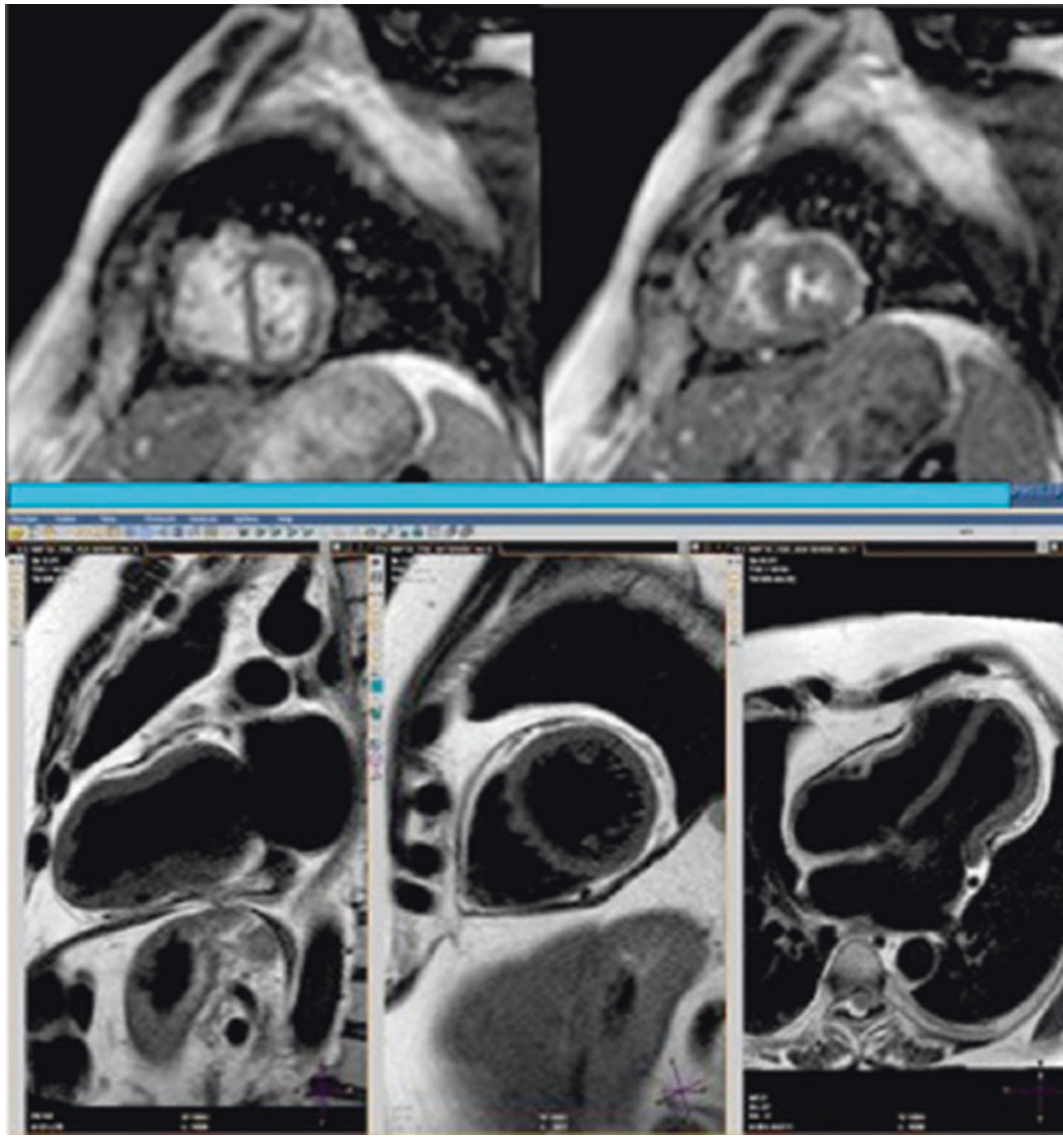

Fig. 12.7 Constrictive pericarditis cardiac MRI. Images at *top* demonstrate real-time free-breathing gradient echo short axis image of the left ventricle demonstrating ventricular interdependence in patient with constrictive pericarditis. Images at *bottom* are spin-echo "dark-blood" images in multiple orientations demonstrating pericardial thickening

ventricular interdependence that might suggest tamponade or constrictive physiology (Fig. 12.7). One area where CMR has significant limitations is in the assessment of pericardial calcification. Pericardial calcium causes significant susceptibility artifact on bright-blood cine MRI sequences.

Cardiac CT provides the ability, whether gated or non-gated, with iodinate contrast or without, to visualize the pericardium and assess and quantify pericardial thickening, calcification, or effusion. Multiphase, retrospectively ECG-gated cardiac CT imaging with iodinated contrast also allows for a functional assessment of interventricular septal motion and ventricular interdependence, although with a somewhat lesser temporal resolution (Fig. 12.9).

Vascular Hemodynamics

Vascular anatomy and pathology can be imaged using CMR with or without gadolinium-based contrast. Black-blood imaging provides excellent vascular anatomic detail with nulling of the blood pool. Alternatively, cine bright-blood CMR imaging provides additional information about vascular wall pathology and flow dynamics. First pass gadolinium-enhanced magnetic resonance angiography (MRA) can now be performed on nearly any MR scanner and produces high-spatial resolution images with broad anatomic coverage (Fig. 12.8). Artifacts with MRA may occasionally result in misdiagnosis of pseudostenosis in a vessel due to metal artifacts, susceptibility artifact from concentrated gadolinium, and volume averaging.

Phase-contrast imaging has also proven useful in the assessment of gradients across aortic coarctation [5]. With aortic coarctation, collateral flow can be assessed by measuring blood flow within 2 cm of the coarctation and above the diaphragm. In patients with significant coarctation, the flow within the coarctation increases toward the diaphragm due to retrograde perfusion of the dilated intercostal arteries, which are providing collateral circulation [43]. Additionally, measurements within the coarctation can help determine peak velocity and therefore pressure gradient within the stenosis. Pressure gradients greater than 20 mmHg measured during cardiac catheterization have been previously considered an indication for intervention [44].

Alternatively, CT angiography can also provide excellent spatial resolution when imaging arterial phase vascular images. Typically, vascular imaging with CT angiography does not necessitate ECG-gating, unless there is specific concern regarding the aortic root, which will typically be affected by cardiac motion artifact on non-ECG-gated images.

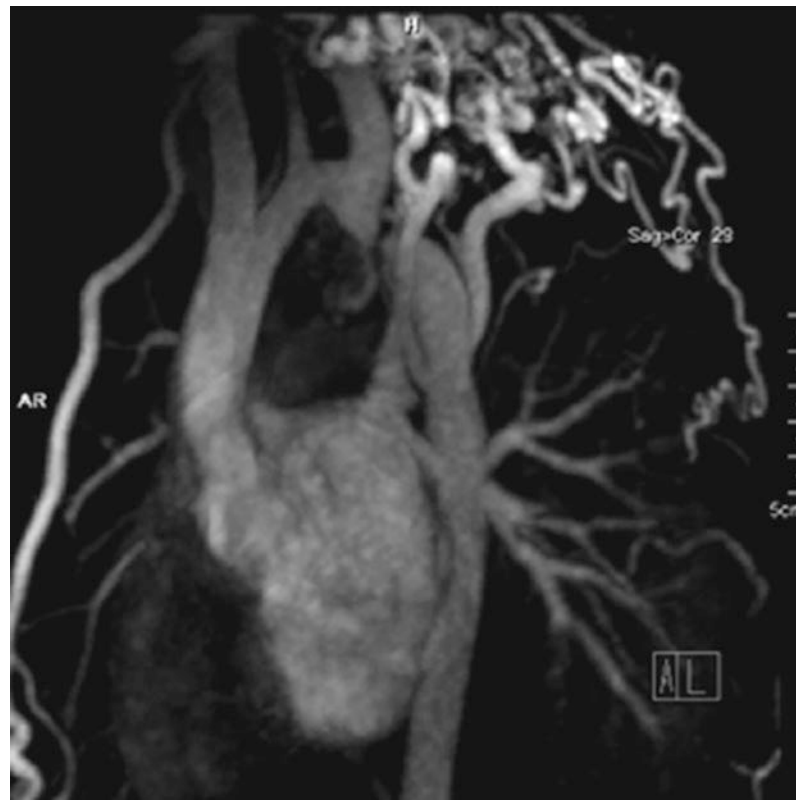

Fig. 12.8 3D volume rendered MR angiography image of aortic coarctation (*arrow*) with significant collateral vessels

Coronary Angiography

Through the simultaneous administration of intravenous iodinated contrast material, oral and intravenous beta-blockers to lower the heart rate, and sublingual nitroglycerin for coronary vasodilation, imaging of the coronary arteries has become increasingly feasible (Fig. 12.9). Several multicenter clinical studies have now shown the high diagnostic yield with coronary CT angiography, with sensitivities reported between 83% and 99% and specificities ranging from 93% to 98% [45]. Further, due to very high negative predictive values (95–100%), modern CCTA can be used to reliably rule out the presence of significant coronary artery stenoses.

While the strength of coronary CT is its excellent spatial resolution and anatomic definition, its most commonly cited weakness had been its inability to provide hemodynamic data. Coronary artery stenosis severity does not always correlate well with lesion functional severity at time of invasive FFR. Several studies have now been performed with coronary CT angiography that not only assess anatomy and morphology, but also provide functional physiologic information on coronary flow. New methods have been developed that utilize the anatomic data provided by CCTA in conjunction with computational fluid dynamic modeling that can calculate coronary fractional flow reserve (CT-FFR) from resting CCTA datasets [46], under estimated hyperemic flow conditions (Figs. 12.10 and 12.11). This provides for lesion-specific decreases in FFR, noninvasively. HeartFlow CT-FFR analysis uses an off-site, supercomputer, three-dimensional modeling technique and has now been validated against invasive FFR measurements and was approved by US Food and Drug Administration (FDA) for clinical use in 2014. Siemens Healthcare has also developed a one-dimensional analysis (cFFR) that can be performed at on-site workstations, but this technology is not yet commercially available as of the time of this writing.

During the past several years, multiple studies have been published that evaluated the diagnostic performance of CT-FFR and cFFR compared with invasive FFR as the reference standard [47–53]. Compared with CCTA anatomic assessment of stenosis severity alone, cFFR and CT-FFR

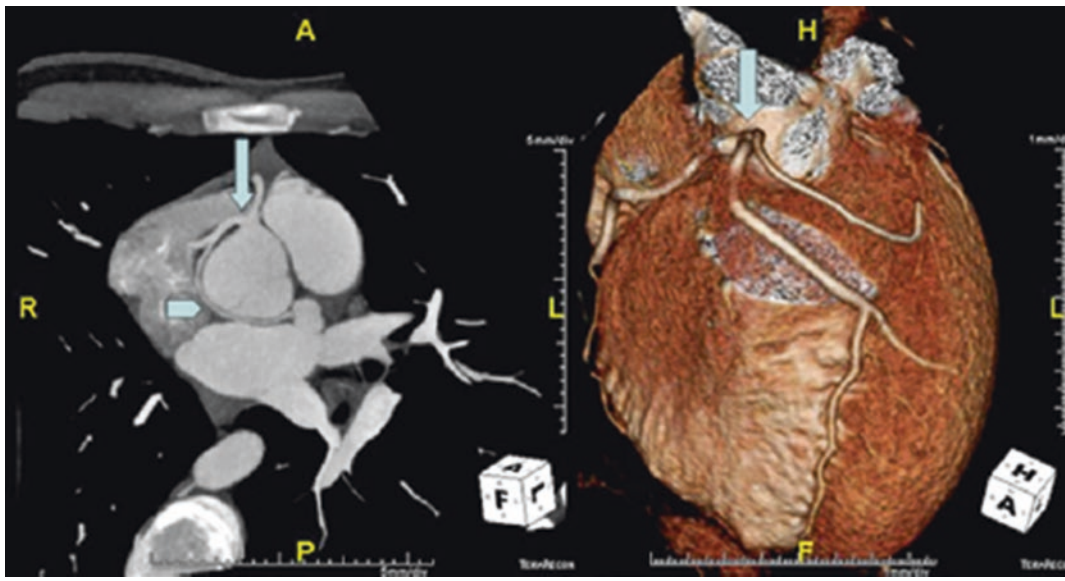

Fig. 12.9 Anomalous origin of the coronary arteries. Image at left demonstrates a maximum intensity projection (MIP) image of a common origin of both the left and right coronary arteries from a single, common ostium with the circumflex coronary artery passing retro-aortic (*arrowhead*). Image at left is a 3D volume-rendered image depicting same (*arrow*)

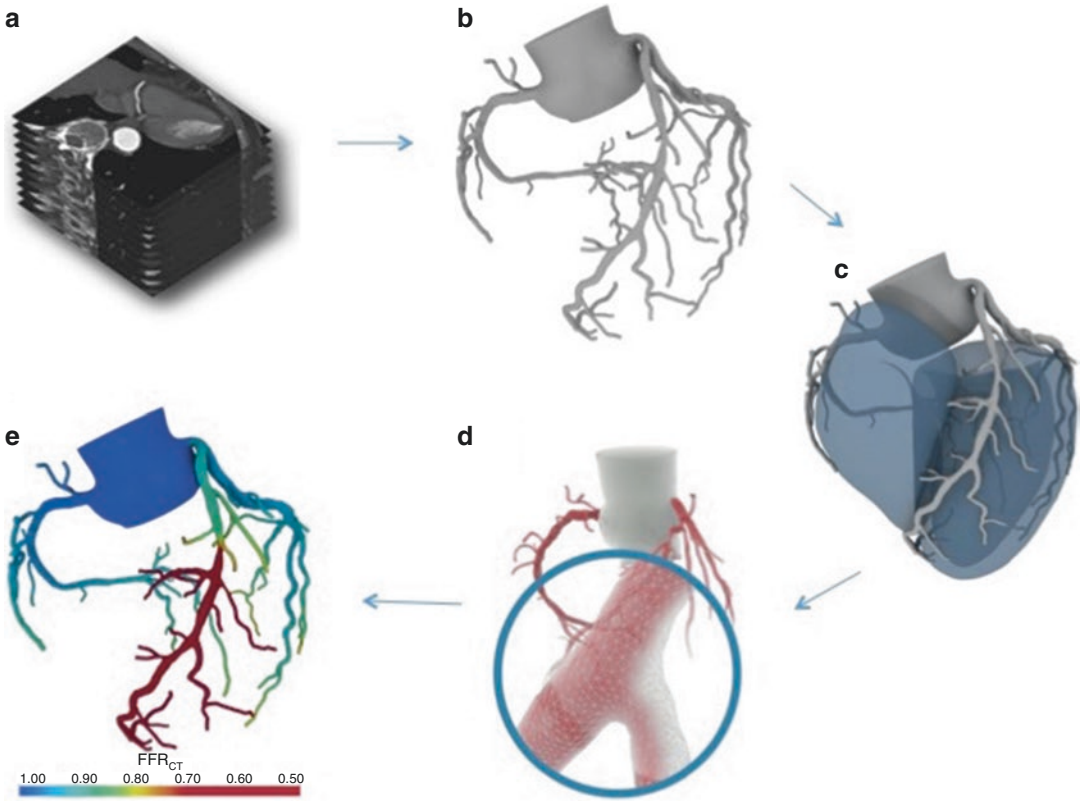

Fig. 12.10 (**a**) Coronary CT angiography image dataset, acquired using standard imaging protocol. (**b**) Image segmentation produces an anatomic model of the root of aorta and epicardial coronary arteries including all second and third order branchings to approximately 1 mm in diameter. (**c**) Physiologic model of coronary flow with specified inflow and outflow boundary conditions is created. Resting coronary flow is based on left ventricular myocardial volume extracted from CT image data and the microcirculation model is based on epicardial vessel size. (**d**) Computational fluid dynamics methods are used to simulate coronary blood flow under maximal hyperemia with simultaneous computation of coronary pressure and flow at millions of discrete points throughout the coronary tree. (**e**) Three-dimensional display of FFR_{CT} values in each coronary artery and its branches with color coding of numerical FFR_{CT} values as shown on the scale. (Images courtesy of Dr. Christopher Zarins, HeartFlow)

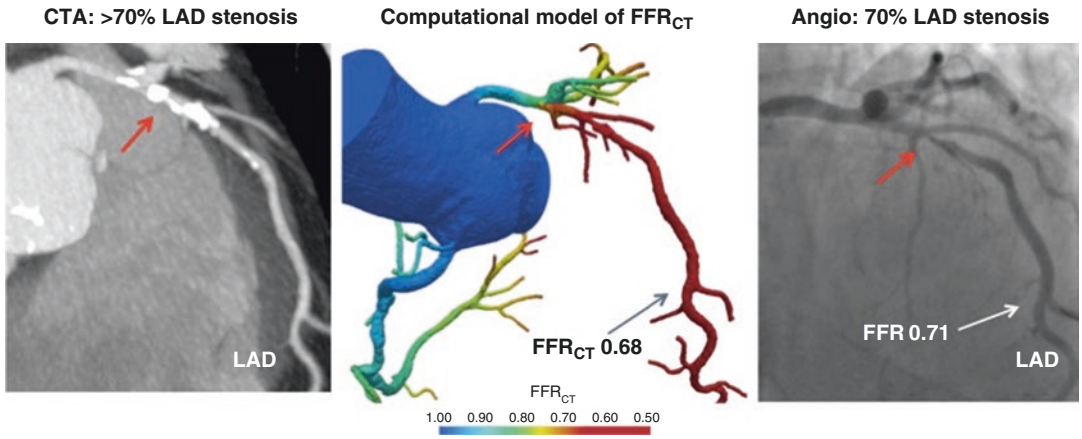

Fig. 12.11 CT-FFR. Case example. CCTA demonstrates heavily calcified LAD lesion with >70% stenosis. HeartFlow FFR_{CT} analysis shows functionally significant proximal LAD stenosis with FFR_{CT} 0.68. Coronary angiogram confirms 70% LAD stenosis with measured FFR 0.71. (Images courtesy of Dr. Christopher Zarins, HeartFlow)

both demonstrated improved test specificity. Good correlations with both cFFR and CT-FFR compared to invasive FFR were reported, ranging from 0.63 to 0.82. Certainly, overall image quality plays a vital role in overall CCTA imaging, and prior studies evaluating cFFR and CT-FFR have demonstrated that 10–13% of cases could not be utilized due to suboptimal image quality. In a sub-analysis of the NXT trial, among patients with CAC score 400, the accuracy, sensitivity, and specificity of FFR_{CT} for the determination of lesion-causing pressure drop were 75% (95% CI, 62%–84%), 88% (95% CI, 64%–97%), and 69% (95% CI, 54%–81%), which were higher than those of CCTA with 44% (95% CI, 31%–56%), 94% (95% CI, 79%–100%), and 23% (95% CI, 11%–37%), respectively [50].

Several groups have now started to look at the potential role of stress and rest myocardial perfusion imaging with CT [54–56]. Pontone G et al. evaluated 100 consecutive symptomatic patients scheduled for invasive coronary angiography with resting coronary CCTA and stress static computed tomography myocardial perfusion (CTP). Patients were evaluated for overall diagnostic accuracy and overall effective dose compared with those of invasive coronary angiography and FFR. Coronary CTA alone demonstrated a per-vessel and per-patient sensitivity, specificity, negative predictive value, positive predictive value, and accuracy of 98%, 76%, 99%, 63%, and 83% and of 98%, 54%, 96%, 68%, and 76%, respectively. Combining coronary CTA with stress CTP, per-vessel and per-patient sensitivity, specificity, negative predictive value, positive predictive value, and accuracy were 91%, 94%, 96%, 86%, and 93% and 98%, 83%, 98%, 86%, and 91%, with a significant improvement in specificity, positive predictive value, and accuracy in both models. The mean effective dose for coronary CTA and stress CTP were 2.8± 1.4 mSv and 2.5± 1.1 mSv [53].

Coronary artery disease remains the leading cause of morbidity and mortality in the industrialized world. While conventional coronary angiography remains the "gold standard" for evaluation of coronary arterial disease, it does possess limitations, namely its invasive nature, cost, and need for radiation and iodinated contrast exposure. Due to these limitations, alternative noninvasive imaging modalities have evolved for the evaluation of coronary artery disease that can avoid some of these undesirable attributes. While CT coronary angiography provides excellent spatial and temporal resolution, its use still requires patient breath-holding, exposure to radiation, and use of iodinated contrast agents. MR imaging of the coronary arteries does not require radiation exposure, can be performed either with or without administration of contrast material, and is capable of being accomplished with or without patient breath-hold. Similar to other noninvasive modalities, MR imaging of the coronary arteries is limited by both cardiac and respiratory motion. In addition, the small size and tortuosity of the coronary vessels, coupled with rapid spatial displacement and increased distance from the body or surface coils, present challenges for accurate imaging.

Initial studies with coronary MRA demonstrated that this technique was capable of accurate diagnosis of left main coronary artery and three-vessel disease [57]. With the continued development and improvement in MRI software and hardware, improvements in spatial resolution and image quality have been possible. Additional studies have now reported that contrast-enhanced MRA (CE-MRA) at 3.0 T is able to depict significant coronary artery stenoses with high sensitivity (94.6%), and negative predictive values of 98.5% and 97.7% on a per-segment and per-vessel basis respectively [58]. Additional studies have compared the visual and quantitative analysis high-spatial resolution CMR perfusion at 3.0 T against invasively determined fractional flow reserve (FFR) [59]. At an FFR threshold <0.75 to define hemodynamically significant lesions, visual CMR analysis reported sensitivity and specificity of 0.82 and 0.94 ($p < 0.0001$), respectively.

Further developments in coronary artery imaging have come through the use of ECG and respiratory triggered, segmented, 3D data acquisition. During free-breathing, monitoring of diaphragmatic motion is performed by a unique navigator echo, and the decision to accept or

reject image data are made based on the position of the diaphragm [60]. In addition, stress-induced myocardial ischemia can now be assessed noninvasively with the use of blood oxygen level-dependent (BOLD) CMR [59]. Perfusion CMR imaging has been compared with quantitative coronary angiography (QCA) and fractional flow reserve (FFR). Futamatsu et al. evaluated 37 patients with perfusion CMR imaging, quantitative coronary angiography, and FFR. Myocardial perfusion reserve (MPR) using a cutoff of 2.06 was found to have sensitivity and specificity for identification of hemodynamically significant CAD (defined as FFR ≤0.75) of 92.9 and 56.7% respectively. Sensitivity and specificity of anatomically significant CAD (>50% diameter stenosis) were 87.2% and 49.2% respectively [61].

Future Directions

The future of cardiac imaging is dynamic. With ever-increasing advances in both hardware and software, cardiac MRI and CT will continue to evolve and improve. Increasing magnetic field strength coupled with multiphased array coils promises to improve CMR spatial resolution. Continued improvements in gantry rotation times, table pitch, X-ray tube strength, and improved simultaneous slice acquisition are all promising areas of improvement in cardiac CT technology at present. Additionally, the coming decade will likely see continued advancements in artificial intelligence and software processing algorithms. With these continued advancements, cardiac CT and MRI will continue to play an ever-increasing role in the noninvasive hemodynamic evaluation of our patients.

Review Questions

1. A 47-year-old female has developed increasing shortness of breath over the preceding 6 months. Transthoracic echocardiogram has demonstrated severe ventricular hypertrophy. Subsequent cardiac MRI is performed to assess LVOT gradients and papillary muscle morphology.

   Among the following, CMR can best evaluate diastolic dysfunction via:

   A. Phase-sensitive inversion recovery imaging (PSIR) post-gadolinium contrast.
   B. Phase-contrast imaging.
   C. Non-breath-hold T2-weighted axial images of the myocardium.
   D. Magnetic resonance angiography.

   Answer B: Phase-contrast imaging (PCI) is capable of assessing both inflow and myocardial velocities, and plotting flow curves relative to the various phases of the cardiac cycle. This modality can provide insight into both myocardial relaxation and compliance characteristics. PCI has been shown to correlate well with TTE in the assessment of diastolic function; however, it tends to underestimate velocities of mitral valve flow (*E* and *A* waves) compared to TTE.

2. A 69-year-old African American male previously underwent coronary artery bypass graft surgery and mitral valve repair 10 years ago. Over the past 9 months, he has developed increasing shortness of breath, lower extremity edema, and abdominal fullness. Transthoracic echocardiogram demonstrates septal bounce and tubular shaped left ventricle with atrial tethering. Subsequent cardiac MRI is performed to evaluate for constrictive pericarditis.

   Among the following, which method is most useful for evaluating for ventricular interdependence?

   A. Real-time gradient echo CMR.
   B. Breath-hold, four-chamber steady-state free precession cine imaging.
   C. Short-axis, breath-hold delayed-hyperenhancement imaging post-gadolinium contrast.
   D. Short-tau inversion recovery imaging (STIR).

   Answer A: Real-time gradient echo CMR typically provides a single image slice, the short axis left ventricle is most often chosen. Through simultaneous evaluation of both ventricular function with respiration, it is possible to assess for ventricular interdependence. Breath-hold, four-chamber steady-state free precession cine imaging is a good method for assessing ventricular function. Short-axis, breath-hold delayed-hyperenhancement

imaging post-gadolinium contrast has been shown to be an effective method for evaluating for active pericardial inflammation; however, this in and of itself does not necessarily reflect evidence of constriction. Short-tau inversion recovery imaging (STIR) is an effective method for evaluating for myocardial and/or pericardial inflammation.

3. With cardiac CT, it is possible to synchronize image reconstruction with the relative cardiac phases via:
   A. Iterative reconstruction.
   B. ECG-triggering.
   C. Filtered back-projection.
   D. Myocardial tagging.

   Answer B: ECG-triggering, through the simultaneous registration of the ECG at the time of image acquisition, can allow for image reconstruction that is synchronized to the relative cardiac phase. ECG-triggering can be performed both prospectively and retrospectively. Iterative reconstruction is a method or group of algorithms used in 2D and 3D image sets. Filtered back-projection is also a reconstruction technique used for CT that applies a filter to the raw data collected during CT and attenuation information is simultaneously collected that are then utilized in image creation. Myocardial tagging is a cardiac MRI technique that applies saturation grid lines to the myocardium, and their subsequent deformation can be used to assess myocardial contraction and relaxation.
4. Shunt volume and shunt fraction (Q_p/Q_s) using MRI can be calculated through use of:
   A. Volumetric cine MRI.
   B. Phase-contrast imaging (PCI).
   C. Neither.
   D. Both A and B.

   Answer D: Both volumetric cine MRI and PCI can be used to calculate shunt volume and shunt fraction (Q_p/Q_s) provided that there is no significant concurrent valvular regurgitation. Specifically, total forward flow through the proximal ascending aorta and main pulmonary artery can be used to determine shunt fraction (Shunt fraction % (Q_p/Q_s) = total PCI pulmonary artery volume flow (mL)/total PCI ascending aortic volume flow (mL)) Alternatively, by using the ratios of the right ventricular to left ventricular stroke volumes, acquired by use of volumetric cine MRI, the shunt fraction can be calculated—provided there is again no significant simultaneous valvular regurgitation.
5. A 17-year-old girl is found to have bicuspid aortic valve by echocardiography. What imaging modality, among those listed below, would be best suited to assess for a common associated cardiovascular anomaly with this condition?
   A. CT.
   B. Chest X-ray.
   C. PET.
   D. MRI.

   Answer D: Patients with bicuspid aortic valve often have other congenital aortic and cardiac abnormalities [62]. The most common association is with coarctation of the aorta, which in autopsy series has been reported to be found in 6% of cases. Alternatively, 30–40% of patients with coarctation are subsequently found to have a bicuspid aortic valve. MRI not only is an excellent modality for assessing the aortic valve morphology and function, but also provides excellent spatial resolution and a large field of view (see Fig. 12.7) to evaluate noncardiac thoracic anatomy. While CT also is a versatile modality with excellent spatial resolution and broad field-of-view, the radiation exposure in this young patient is less than desirable. Chest X-ray is an indirect method of assessing for additional complications associated with coarctation such as notching noted along the ribs. PET has no significant role in imaging coarctation.

References

1. Finn JP, Nael K, Deshpande V, Ratib O, Laub G. Cardiac MR imaging: state of the technology. Radiology. 2006;241:338–54.
2. Hillenbrand HB, Lima JA, Bluemke DA, Beache GM, McVeigh ER. Assessment of myocardial systolic function by tagged magnetic resonance imaging. J Cardiovasc Magn Reson. 2000;2:57–66.
3. Bollache E, Redheuil A, Clément-Guinaudeau S, Defrance C, Perdrix L, Ladouceur M, Lefort M, De Cesare A, Herment A, Diebold B, Mousseaux E, Kachenoura N. Automated left ventricular diastolic function evaluation from phase – contrast magnetic resonance and comparison with Doppler echocardiography. J Cardiovasc Magn Reson. 2010;12:63.
4. Malaty AN, Shah DJ, Abdelkarim AR, Nagueh SF. Relation of replacement fibrosis to left ventricular diastolic function in patients with dilated cardiomyopathy. J Am Soc Echocardiogr. 2011;24:333–8.
5. Karaahmet T, Tigen K, Dundar C, et al. The effect of cardiac fibrosis on left ventricular remodeling, diastolic function, and N-terminal pro-B-type natriuretic peptide levels in patients with non-ischemic dilated cardiomyopathy. Echocardiography. 2010;27:954–60.
6. Codreanu I, Robson MD, Golding SJ, et al. Longitudinally and circumferentially directed movements of the left ventricle studied by cardiovascular magnetic resonance phase contrast velocity mapping. J Cardiovasc Magn Reson. 2010;12:48.
7. Lipinski MJ, et al. Prognostic value of stress cardiac magnetic resonance imaging in patients with known or suspected coronary artery disease. J Am Coll Cardiol. 2013;62:826–38.
8. Liu A, et al. Gadolinium-free cardiac MR stress T1-mapping to distinguish epicardial from microvascular coronary artery disease. J Am Coll Cardiol. 2018;71:957–68.
9. MacMillan RM, Rees MR, Eldredge WJ, Maranhao V, Clark DL. Quantitation of shunting at the atrial level using rapid acquisition computed tomography with comparison with cardiac catherization. J Am Coll Cardiol. 1986;7:946–8.
10. Rajiah P, Kanne JP. Computed tomography of septal defects. J Cardiovasc Comput Tomogr. 2010;4:231–45.
11. Garrett JS, Jaschke W, Botvinick EH, Higgins CB, Lipton MJ. Quantitation of intracardiac shunts by cine CT. J Comput Assist Tomogr. 1988;12:82–7.
12. Diethelm L, Dery R, Lipton MJ, Higgins CB. Atrial-level shunts: sensitivity and specificity of MR in diagnosis. Radiology. 1987;162:181–6.
13. Holmvang G, Palacios IF, Vlahakes GJ, et al. Imaging and sizing of atrial septal defects by magnetic resonance. Circulation. 1995;92:3473–80.
14. Hundley WG, Li HF, Lange RA, et al. Assessment of left-to-right intracardiac shunting by velocity-encoded, phase-difference magnetic resonance imaging: a comparison with oximetric and indicator dilution techniques. Circulation. 1995;91:2955–60.
15. Anderson RH, Lenox CC, Zuberbuhler JR. The morphology of ventricular septal defects. Perspect Pediatr Pathol. 1984;8:235–68.
16. Williamson EE, Kirsch J, Araoz PA, Edmister WB, Borgeson DD, Glockner JF, Breen JF. ECG- gated cardiac CT angiography using 64-MDCT for detection of patent foramen ovale. AJR Am J Roentgenol. 2008;190:929–33.
17. Didier D, Higgins CB. Identification and localization of ventricular septal defect by gated magnetic resonance imaging. Am J Cardiol. 1986;57:1363–8.
18. Higgins CB. Radiography of congenital heart disease. In: Higgins CB, editor. Essentials of cardiac radiology and imaging. Philadelphia: Lippincott; 1992. p. 49–90.
19. Ferrari VA, Scott CH, Holland GA, Axel L, Sutton MS. Ultrafast three-dimensional contrast-enhanced magnetic resonance angiography and imaging in the diagnosis of partial anomalous pulmonary venous drainage. J Am Coll Cardiol. 2001;37:1120–8.
20. Rathi VK, Doyle M, Yamrozik J, Williams RB, Caruppannan K, Truman C, Vido D, Biederman RW. Routine evaluation of left ventricular diastolic function by cardiovascular magnetic resonance: a practical approach. J Cardiovasc Magn Reson. 2008;8:36.
21. Rathi VK, Biederman RW. Expanding role of cardiovascular magnetic resonance in left and right ventricular diastolic function. Heart Fail Clin. 2009;5:421–35.
22. Boogers MJ, van Werkhoven JM, Schuijf JD, Delgado V, El-Naggar HM, Boersma E, Nucifora G, van der Geest RJ, Paelinck BP, Kroft LJ, Reiber JH, de Roos A, Bax JJ, Lamb HJ. Feasibility of diastolic function assessment with cardiac CT feasibility study in comparison with tissue Doppler imaging. JACC Cardiovasc Imaging. 2011;3:246–56.
23. Nakahara T, Jinzaki M, Fukuda N, Takahashi Y, Ishihara T, Takada A, Suzuki K, Manita M, Imanari T, Kanesawa N, Kuribayashi N, Kuribayashi M. Estimation of the left ventricular diastolic function with cardiac MDCT: correlation of the slope of the time-enhancement-curve with the mitral annulus diastolic velocity. Eur J Radiol. 2011;81(2):234–8.. [Epub ahead of print]
24. Bolen MA, Popovic ZB, Rajiah P, Gabriel RS, Zurick AO, Lieber ML, Flamm SD. Cardiac MR assessment of aortic regurgitation: holodiastolic flow reversal in the descending aorta helps stratify severity. Radiology. 2011;260(1):98–104.. [Epub ahead of print]
25. Cawley PJ, Hamilton-Craig C, Owens DS, Krieger EV, Strugnell WE, Mitsumori L, et al. Prospective comparison of valve regurgitation quantitation by cardiac magnetic resonance imaging and transthoracic echocardiography. Circ Cardiovasc Imaging. 2013;6(1):48–57.
26. Uretsky S, Gillam L, Lang R, Chaudhry FA, Argulian E, Supariwala A, et al. Discordance between echocardiography and MRI in the assessment of mitral regurgitation severity: a prospective multicenter trial. J Am Coll Cardiol. 2015;65(11):1078–88.

27. Delgado V, et al. Assessment of mitral valve anatomy and geometry with multislice computed tomography. J Am Coll Cardiol Img. 2009;2:556–65.
28. Ambler G, Omar RZ, Royston P, Kinsman R, Keogh BE, Taylor KM. Generic, simple risk stratification model for heart valve surgery. Circulation. 2005;112:224–31.
29. Bonow RO, Carabello BA, Kanu C, de Leon AC Jr, Faxon DP, Freed MD, et al. American College of Cardiology/American Heart Association task force on practice guidelines. ACC/AHA guidelines for the management of patients with valvular heart disease: a report of the American College of Cardiology/American Heart Association task force on practice guidelines. Circulation. 2006;114:e84–231.
30. Leon MB, Smith CR, Mack M, Miller DC, Moses JW, Svensson LG, Tuzcu EM, et al. Transcatheter aortic-valve implantation for aortic stenosis in patients who cannot undergo surgery. N Engl J Med. 2010;363:1597–607.
31. Kondo C, Caputo GR, Semelka R, Foster E, Shimakawa A, Higgins CB. Right and left ventricular stroke volume measurements with velocity encoded cine MR imaging: in vitro and in vivo validation. Am J Roentgenol. 1991;157:9–16.
32. Hoeper MM, Tongers J, Leppert A, Baus S, Maier R, Lotz J. Evaluation of right ventricular performance with a right ventricular ejection fraction thermodilution catheter and magnetic resonance imaging in patients with pulmonary hypertension. Chest. 2001;120:502–7.
33. Kwon D, Desai M. Cardiac magnetic resonance in hypertrophic cardiomyopathy: current state of the art. Expert Rev Cardiovasc Ther. 2010;8:103–11.
34. Proctor RD, Shambrook JS, McParland P, Peebles CR, Brown IW, Harden SP. Imaging hypertrophic heart diseases with cardiovascular MR. Clin Radiol. 2011;66:176–86.
35. Cheong BY, Muthupillai R, Nemeth M, Lambert B, Dees D, Huber S, Castriotta R, Flamm SD. The utility of delayed-enhancement magnetic resonance imaging for identifying nonischemic myocardial fibrosis in asymptomatic patients with biopsy-proven systemic sarcoidosis. Sarcoidosis Vasc Diffuse Lung Dis. 2009;26:39–46.
36. Syed IS, Glockner JF, Feng D, Araoz PA, Martinez MW, Edwards WD, Gertz MA, Dispenzieri A, Oh JK, Bellavia D, Tajik AJ, Grogan M. Role of cardiac magnetic resonance imaging in the detection of cardiac amyloidosis. JACC Cardiovasc Imaging. 2010;3:155–64.
37. Austin BA, Tang WH, Rodriguez ER, Tan C, Flamm SD, Taylor DO, Starling RC, Desai MY. Delayed hyper-enhancement magnetic resonance imaging provides incremental diagnostic and prognostic utility in suspected cardiac amyloidosis. JACC Cardiovasc Imaging. 2009;2:1369–77.
38. Desai MY, Lima JA, Bluemke DA. Cardiovascular magnetic resonance imaging: current applications and future directions. Methods Enzymol. 2004;386:122–48.
39. Cheong B, Huber S, Muthupillai R, Flamm SD. Evaluation of myocardial iron overload by T2∗ cardiovascular magnetic resonance imaging. Tex Heart Inst J. 2005;32:448–9.
40. Vural M, Ucar O, Selvi NA, Pasaoglu L, Gurbuz MO, Cicekcioglu H, Aydogdu S, Koparal S. Assessment of global left ventricular systolic function with multidetector CT and 2D echocardiography: a comparison between reconstructions of 1-mm and 2-mm slice thickness at multidetector CT. Diagn Interv Radiol. 2010;16:236–40.
41. Ko SM, Kim YJ, Park JH, Choi NM. Assessment of left ventricular ejection fraction and regional wall motion with 64-slice multidetector CT: a comparison with two-dimensional transthoracic echocardiography. Br J Radiol. 2010;83:28–34.
42. Lotz J, Meier C, Leppert A, Galanski M. Cardiovascular flow measurement with phase-contrast MR imaging: basic facts and implementation. Radiographics. 2002;22:651–71.
43. Campbell M. Natural history of coarctation of the aorta. Br Heart J. 1970;32:633–40.
44. Achenbach S. Computed tomography coronary angiography. J Am Coll Cardiol. 2006;48:1919–28.
45. Chow BJ, Kass M, Gagne O, Chen L, Yam Y, Dick A, Wells GA. Can differences in corrected coronary opacification measured with computed tomography predict resting coronary artery flow. J Am Coll Cardiol. 2011;57:1280–8.
46. Nakanishi R, Budoff M. Noninvasive FFR derived from coronary CT in the management of coronary artery disease: technology and clinical update. Vasc Health Risk Manag. 2016;12:269–78.
47. Coenen A, Lubbers MM, Kurata A, et al. Fractional flow reserve computed from noninvasive CT angiography data: diagnostic performance of an on-site clinician-operated computational fluid dynamics algorithm. Radiology. 2015;274:674–83.
48. Koo BK, Erglis A, Doh JH, et al. Diagnosis of ischemia-causing coronary stenoses by noninvasive fractional flow reserve computed from coronary computed tomographic angiograms. Results from the prospective multicenter discover-flow (diagnosis of ischemia-causing stenoses obtained via noninvasive fractional flow reserve) study. J Am Coll Cardiol. 2011;58:1989–97.
49. Min JK, Leipsic J, Pencina MJ, et al. Diagnostic accuracy of fractional flow reserve from anatomic CT angiography. JAMA. 2012;308:1237–45.
50. Nørgaard BL, Leipsic J, Gaur S, NXT Trial Study Group, et al. Diagnostic performance of noninvasive fractional flow reserve derived from coronary computed tomography angiography in suspected coronary artery disease: the NXT trial (analysis of coronary blood flow using CT angiography: next steps). J Am Coll Cardiol. 2014;63:1145–55.
51. Renker M, Schoepf UJ, Wang R, et al. Comparison of diagnostic value of a novel noninvasive coronary computed tomography angiography method versus standard coronary angiography for assessing fractional flow reserve. Am J Cardiol. 2014;114:1303–8.

52. Baumann S, Wang R, Schoepf UJ, et al. Coronary CT angiography- derived fractional flow reserve correlated with invasive fractional flow reserve measurements – initial experience with a novel physician-driven algorithm. Eur Radiol. 2015;25:1201–7.
53. Pontone G, et al. Incremental diagnostic value of stress computed tomography myocardial perfusion with whole-heart coverage CT scanner in intermediate- to high-risk symptomatic patients suspected of coronary artery disease. J Am Coll Cardiol Img. 2019;12:338–49.
54. Blankstein R, Jerosch-Herold M. Stress myocardial perfusion imaging by computed tomography: a dynamic road is ahead. JACC Cardiovasc Imaging. 2010;3:821–3.
55. Tamarappoo BK, Dey D, Nakazato R, Shmilovich H, Smith T, Cheng VY, Thomson LE, Hayes SW, Friedman JD, Germano G, Slomka PJ, Berman DS. Comparison of the extent and severity of myocardial perfusion defects by CT angiography and SPECT myocardial perfusion imaging. JACC Cardiovasc Imaging. 2010;3:1010–9.
56. Kim WY, Danias PG, Stuber M, Flamm SD, Plein S, Nagel E, et al. Coronary magnetic resonance angiography for the detection of coronary stenoses. N Engl J Med. 2001;345:1863–9.
57. Chen Z, Duan Q, Xue X, Chen L, Ye W, Jin L, Sun B. Noninvasive detection of coronary artery stenoses with contrast-enhanced whole-heart coronary magnetic resonance angiography at 3.0 T. Cardiology. 2010;117:284–90.
58. Lockie T, Ishida M, Perera D, Chiribiri A, De Silva K, Kozerke S, Marber M, Nagel RR, Redwood S, Plein S. High-resolution magnetic resonance myocardial perfusion imaging at 3.0-tesla to detect hemodynamically significant coronary artery stenoses as determined by fractional flow reserve. J Am Coll Cardiol. 2011;57:70–5.
59. Weber OM, Martin AJ, Higgins CB. Whole-heart steady-state free precession coronary artery magnetic resonance angiography. Magn Reson Med. 2003;50:1223–8.
60. Mymin D, Sharma GP. Total and effective coronary blood flow in coronary and noncoronary heart disease. J Clin Invest. 1974;52:363–73.
61. Steffens JC, Bourne MW, Sakuma H, O'Sullivan M, Higgins CB. Quantification of collateral blood flow in coarctation of the aorta by velocity encoded cine magnetic resonance imaging. Circulation. 1994;90:937–43.
62. Therrien J, Webb GD. Congenital heart disease in adults. In: Braunwald E, editor. Heart disease: a textbook of cardiovascular medicine. 6th ed. Philadelphia: Saunders; 2001. p. 1592–621.

13 Objective Evaluation of Hemodynamics in the Outpatient Setting

Gbolahan Ogunbayo and Ahmed Abdel-Latif

Introduction

Noninvasive hemodynamic (HD) monitoring offers a safer and relatively accurate means of monitoring patients' hemodynamics when performed appropriately. Beyond the potential benefit of determining volume status, noninvasive HD monitoring can be of value in evaluating the adequacy of cardiac perfusion and indirect assessment of cardiac index. Some of these HD parameters have been shown to predict or reduce heart failure admissions [1–6]. It can further reduce the complications associated with invasive hemodynamic monitoring [7, 8]. In the outpatient setting, noninvasive hemodynamic assessment helps to optimize medical therapy, titrate mediations, and identify heart failure patients who will require more aggressive therapies and mechanical support. Accordingly, the current American College of Cardiology Foundation/American Heart Association (ACC/AHA) guidelines for the diagnosis and management of patients with heart failure designates hemodynamic assessment in patients with heart failure a Class I indication [9].

Ambulatory hemodynamic monitoring can be done remotely or in an outpatient setting. Continuous remote monitoring usually requires implantation of a device and external equipment for remote (home) monitoring and transmission or on-site (office) measurement. Instantaneous monitoring can be done in an ambulatory (office) setting. Compared to standard scheduled office visits/audible device alerts, remote monitoring has been shown to reduce emergency department or unplanned/urgent office visits by allowing early and rapid detection of events requiring attention and action [10, 11].

History and Physical Examination

Assessment of volume status is an integral part of management and begins with a thorough and systematic history and physical examination. History focuses on severity and changes in symptoms, response to therapy and inquisition about possible etiologies. Although the cardinal symptom of left ventricular failure is shortness of breath (SOB), a patient may present with a myriad of other symptoms in isolation or combination with SOB including cardiac symptoms such as chest discomfort, palpitations, progressive/worsening dyspnea on exertion or at rest, orthopnea, or paroxysmal nocturnal dyspnea. Exertional dyspnea may not be

G. Ogunbayo
Gill Heart Institute and Division of Cardiovascular Medicine, University of Kentucky, Lexington, KY, USA

VA Medical Center, Lexington, KY, USA

A. Abdel-Latif (✉)
VA Medical Center, Lexington, KY, USA

Saha Cardiovascular Research Center, University of Kentucky, Lexington, KY, USA
e-mail: abdel-latif@uky.edu

A. T. Askari, A. W. Messerli (eds.), *Cardiovascular Hemodynamics*, Contemporary Cardiology,
https://doi.org/10.1007/978-3-030-19131-3_13

evident in sedentary patients. A (usually productive) cough is not uncommon due to pulmonary edema and irritation. Downstream effects of congestion include symptoms related to hepatic congestion such as jaundice and other features of resultant hepatic dysfunction as well as pedal edema and resultant symptoms including skin changes. Additional presentations/complaints of cardiac decompensation include weakness, fatigue, symptoms of cerebral hypoperfusion including mental status changes, weight loss (cardiac cachexia), nausea, anorexia, bloating, and early satiety.

Physical findings of volume overload may be subtle or overwhelming depending on the degree of volume overload. Vitals may reveal low blood pressure and even low body temperature from reduced cardiac output. Decompensated patients may have a fast and thread-like pulse. Cardiac signs may include inability to lay flat even during the examination, displaced apical impulse that suggests cardiomegaly, elevated jugular venous pressure (JVP), S3 gallop, pulsus alternans, murmurs, or mitral and tricuspid regurgitation from ventricular enlargement. Pulmonary signs include wheezing, rhonchi, reduced air entry, and crackles. Patient with severe heart failure may exhibit signs of reduced cerebral perfusion and include SOB with use of accessory muscles, anxiety, somnolence or confusion. Other signs on physical examination are cachexia with evidence of malnutrition, cyanosis, distended neck veins, exophthalmos jaundice, ascites, and hepatomegaly that may be tender and pedal edema.

Chest X-Ray

Chest X-ray is a quick and noninvasive tool to assess for pulmonary edema in patients with heart failure. The classic signs of pulmonary edema on a chest X-ray include pulmonary vascular congestion and pleural effusion. However, it is important to note that patients with advanced heart failure may not exhibit the classic signs of pulmonary congestion on chest X-ray despite elevated pulmonary capillary wedge pressure. Thus, chest X-ray is not always a sensitive tool in assessing heart failure and could lag behind other methods such as invasive assessment and physical examination.

Echocardiography

Echocardiography is another noninvasive and quick methods to assess cardiac function and estimate hemodynamics in patients. Classical findings of elevated left ventricular filling pressure include high E/e' ratio (the ratio between the velocity of blood inflow through mitral valve and the tissue Doppler velocity at the mitral valve annulus). This concept has been challenged in new studies and the consensus is to avoid complete reliance on this finding specially in patients with advanced heart failure [12]. Dilated inferior vena cava (IVC) on echocardiography has the highest predictive value for decompensated heart failure and elevated PCWP compared to clinical congestion, elevated JVP, and elevated biomarkers. The addition of echo to the clinical and laboratory tests has an extremely high correlation with invasive PCWP assessment [13].

Biomarkers

Natriuretic peptides are a group of plasma peptides that have been measured routinely in clinical practice to guide the diagnosis and management of patients with heart failure. This family includes B-type natriuretic peptide (BNP) and the N-terminal portion of the pro-brain natriuretic peptide (NT-proBNP). NT-proBNP is the biological inert byproduct of the degradation of pre-proBNP. NT-proBNP has been established as a biological marker in the diagnosis and staging of heart failure and has been recommended as a diagnostic tool by the American College of Cardiology/American Heart Association guidelines [14]. Additionally, BNP and NT-proBNP are important prognostic markers in patients with chronic heart failure [15]. Functionally, NT-proBNP hormone acts to promote natriuresis, diuresis and induce vasodilation [15]. The clearance of NT-proBNP occurs primarily in the

kidneys and the plasma levels are therefore affected by renal dysfunction. Careful consideration should be taken when using NT-proBNP levels for hemodynamic assessment in obese patients in which NT-proBNP levels tend to be low. On the other hand, NT-proBNP levels should be evaluated within the clinical context in patients with other conditions that could elevate their levels such as pulmonary disease. Nonetheless, the addition of NT-proBNP level to careful physical examination and history taking increases the clinical accuracy in diagnosing and managing patients with heart failure [15].

As detailed above, none of these methods provide ideal sensitivity and specificity for hemodynamic assessment in patients with heart failure. Therefore, multiple investigators and clinicians have utilized composite scores combining some or all of the above parameters to achieve better clinical decisions when treating heart failure patients. These scores have been shown to be highly predictive of mortality in heart failure patients and improve the specificity of clinical assessment [16, 17].

Continuous Pulmonary Vascular Pressure Monitoring

Continuous monitoring devices include pulmonary artery measurement, right ventricular (RV) pressure monitoring, left atrial (LA) pressure measurements and measurement of thoracic or cardiac (electrical) impedance via intracardiac device leads. Instantaneous hemodynamics may be obtained in the ambulatory/outpatient setting by thoracic bioimpedance, bioreactance, partial carbon dioxide rebreathing technique, portable Doppler flow measurement, and photoelectric plethysmography.

Implantable (Continuous) Sensors/ Monitoring Devices

Pulmonary Artery Monitoring

Changes in pulmonary artery pressure are good predictors of adverse clinical outcomes and hospital readmission in patients with heart failure [3, 18, 19]. In the absence of mitral valve stenosis, PCWP reflects the left ventricular filling pressure. Chronic pulmonary artery pressure monitoring can be achieved using the CardioMEMS™ HF System (CardioMEMS, Inc./St Jude Medical, Inc., USA) implanted in the pulmonary artery connected to a monitoring device by acoustic ultrasonic signals [20]. Multipe reports have confirmed the feasibility, ease of use, accuracy, and predictive ability in long- and short-term large-scale outcome studies [3, 18, 21–25]. This led to FDA approval of wireless implantable hemodynamic monitors for use in patients with New York heart association II–IV symptoms with a recent hospital admission. The goal of these devices in heart failure patients is to reduce heart failure admissions. This system consists of a sensor, an antenna, and interrogating devices (Fig. 13.1). The sensor is made of a coil and a pressure-sensitive capacitor, which both form a pressure-sensitive electric circuit that resonates at a specific frequency. Pressure applied to this unit causes a deflection that shifts the device's frequency which is electromagnetically coupled through an antenna held against the patient's body either with a wand for outpatient pressure measurement or through a pillow for ambulatory or home use [26].

Pulmonary artery pressure tracings from this system can be used as a marker of volume status to monitor and treat patients. Patients with heart failure and dilated left ventricles function at the end of the pressure-volume curve. Therefore, smaller increases in volume are more likely to cause significant and measurable increase in left ventricular end-diastolic and pulmonary pressures, leading to pulmonary edema. Similarly, heart failure patients with preserved ejection fraction and noncompliant ventricles respond to volume changes as described above, although through a different mechanism. Pulmonary artery pressure measurements can detect these small changes days before the onset of heart failure symptoms and need for heart failure admission. Implantation of the CardioMEMS™ device is safe and requires the initial use of dual

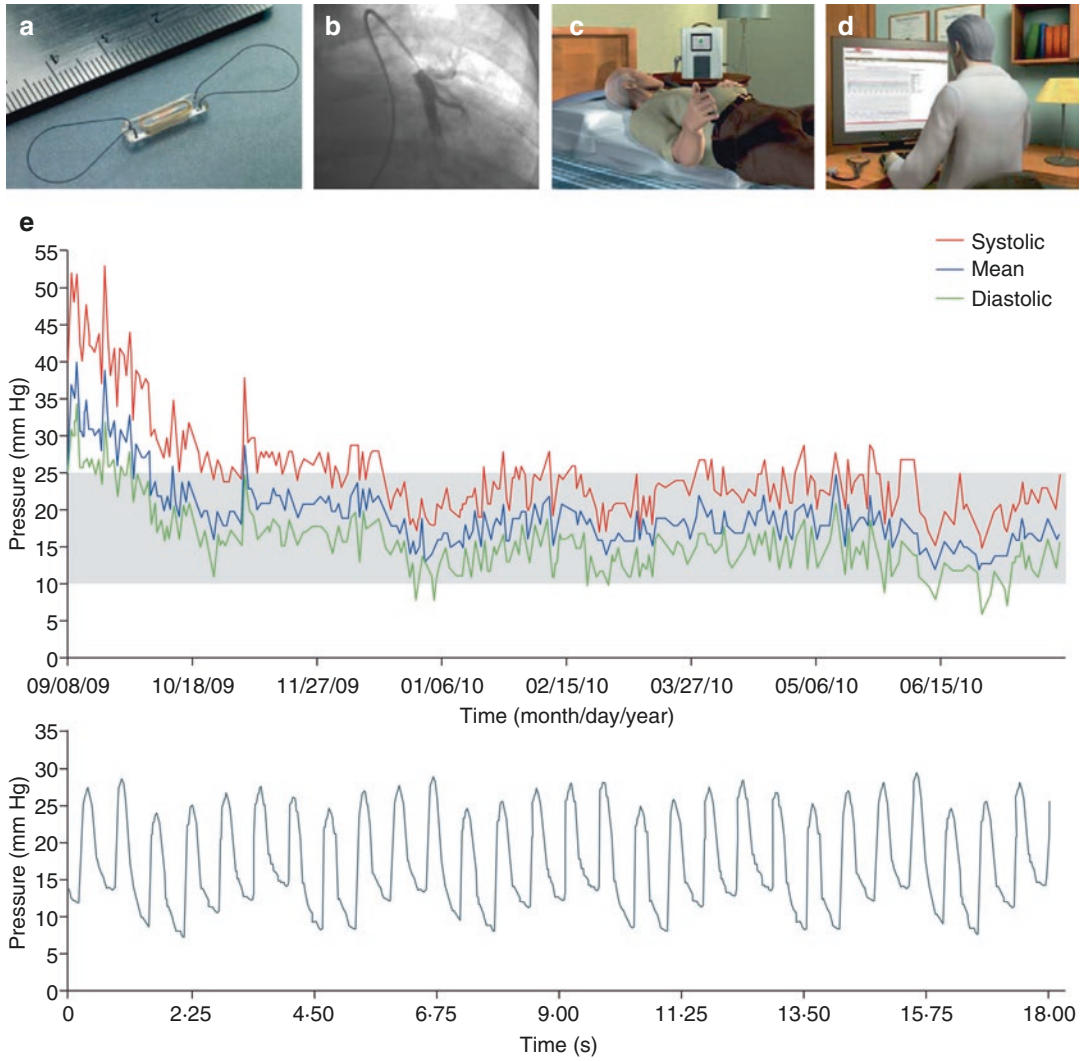

Fig. 13.1 The CardioMEMS™ HF implantable hemodynamic monitoring system. (**a**) CardioMEMS sensor or transmitter; (**b**) transcatheter implantation of the device into a distal branch of the descending pulmonary artery; (**c**) patient is instructed to take daily pressure readings from home using the home monitoring unit; (**d**) information transmitted from the monitoring system to the database is immediately available to treating physicians for review; (**e**) transmitted information consists of pressure trend information and individual pulmonary artery pressure waveforms and are available on the online portal for healthcare providers. (Adapted from Abraham et al. [3])

antiplatelet therapy for 1 month followed by lifelong aspirin use [27–29].

Advantages of this system include accuracy, reproducibility, ease of use, and the relative safe insertion and operation. The sensor does not require a battery and does not need to be replaced or refitted with a battery. Patient compliance with monitoring and medication adhesion are essential to achieve the proposed benefit.

Intracardiac Sensors/Monitoring Devices

Right Ventricular Pressure Sensors

There is no stand-alone right ventricular (RV) sensor device approved by the Food and Drug Administration (FDA). A trial of an implantable monitoring system, the Chronicle® ICD and

Chronicle® implantable hemodynamic monitor (Medtronic, Inc., USA) to measure RV hemodynamics and other parameters showed no clinical effectiveness and therefore it was not approved by the FDA [22].

Left Atrial Pressure Sensors

As with stand-alone RV sensors, there is no FDA-approved left atrial (LA) pressure sensor. An outcomes trial of an investigational LA pressure monitoring device, the HeartPod® (St Jude Medical, Inc., USA) showed feasibility and favorable short- and long-term performance. However, enrollment stopped early because of an excess of implant-related complications [30–32]. These studies, however, show that LA pressure monitoring devices have some promise in the ambulatory and remote management of patients with heart failure.

Intrathoracic Impedance to Measure Volume Status

Intrathoracic impedance is inversely related with volume status and pulmonary capillary wedge pressure. Aortic blood flow is the major determinant of thoracic impedance and therefore, impedance can be used to non-invasively assess cardiac stroke volume and cardiac output/index. These measurements correlate with invasive cardiac output/index [33]. Changes in intrathoracic impedance are noted days or weeks before the onset of symptoms or hospital admission in patients with heart failure [34]. The inverse relationship between intrathoracic impedance and volume accumulation is due to the increased electrical conductance through fluid medium. Feasibility of measuring thoracic congestion by thoracic impedance with the use of an implantable system was almost simultaneously described in human and canine models (Figs. 13.2 and 13.3) [34, 35].

Pacemakers and implantable cardioverter defibrillators (ICDs) are able to measure intrathoracic impedance in humans using the RV bipolar electrode, the LV lead, or ICD electrode. This is done

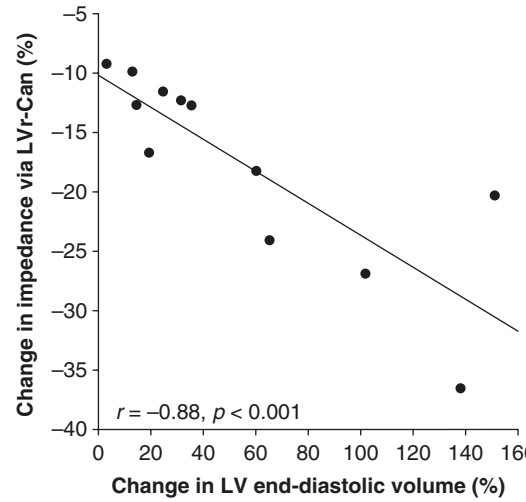

Fig. 13.2 Relationship between LVEDP and impedance. Data shown are for impedance recorded by left ventricular (LV) r–Can in 12 dogs. Correlation coefficient is calculated using Spearman rank order. (Adapted from Khoury et al. [36])

by injecting low-voltage, non-stimulating currents between the device casing and the electrodes. The LV lead has been shown to be the most sensitive to impedance changes in left atrium and left ventricular end-diastolic pressures (LVEDP) [36]. Different devices have patented software that monitor changes in impedance by establishing a baseline using sampling obtained over a period of time. Some programs are able to alert a patient and/or care provider when a predetermined or preset volume threshold is met. Monitoring this parameter has been shown to reduce hospital admissions in patient with heart failure [4, 23, 37, 38]. A 12-week period is required from implantation to impedance measurement. Shorter periods are required for replaced devices.

Advantages of intrathoracic impedance monitoring include the ease of use and the simplicity of the device without the need for additional equipment. When used appropriately and integrated in the clinical management of patients with heart failure, intrathoracic impedance can help reduce hospital admissions due to heart failure (Fig 13.6) [34]. It gives the patient and caregiver the opportunity to be proactive about alteration of hemodynamics and fluid status. Currently, with advances in battery technology,

the impact of impedance monitoring on battery life is small. Instantaneous (ambulatory) impedance measurement is usually inaccurate in settings where there are sources of electrical noise and body motion. Additionally, the system is very sensitive to positioning of the electrodes, body size, humidity, and temperature.

Impedance can also be measured in the ambulatory setting by placing electrodes/sensors on either side of the neck and thorax, two on either side (Fig 13.4). A pair of electrodes inject/transmit alternating electric current while the other pair senses and determines the thoracic impedance. There are two components of impedance: base impedance, which is based on tissue and air in the thoracic cavity and dynamic impedance, which is determined by changing blood volume and velocity in the thoracic aorta. All these parameters have different electrical properties, causing variations in electrical conductance. Ventricular function causes blood flow through the compliant arteries to be pulsatile, thus causing changes in blood volume in the aorta and the thoracic arterial system that results in changes in electrical conductance and impedance.

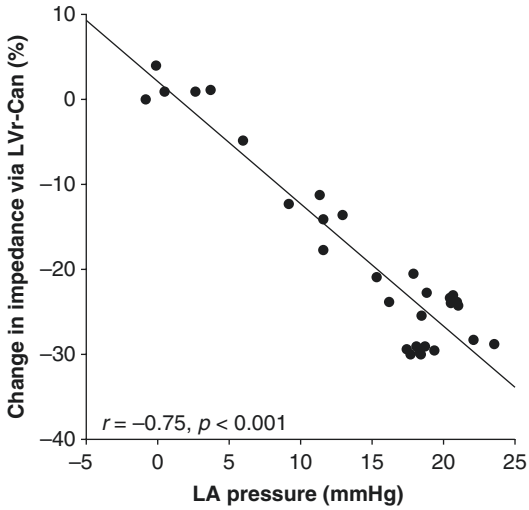

Fig. 13.3 Relationship between LA pressure and Impedance. Data shown are for impedance recorded by left ventricular (LV) r–Can in 1 dog at different time points of the experiment. Correlation coefficient is calculated using Spearman rank order. (Adapted from Khoury et al. [36])

These dynamic, beat-to-beat changes in electric conductance and impedance are used to calculate the stroke volume and other hemodynamic parameters (Fig 13.5). Parameters that can be measured include the stroke volume (SV), cardiac output (CO), central fluid volume, cardiac time intervals, contractility/ejection fraction (EF), acceleration index, total peripheral resistance, aortic compliance, pulmonary capillary wedge pressures (PCWP), and total fluid index (Table 13.1) [40].

The concept of impedance is based on Ohm's Law:

$$\left(I = \frac{E}{R} \right)$$

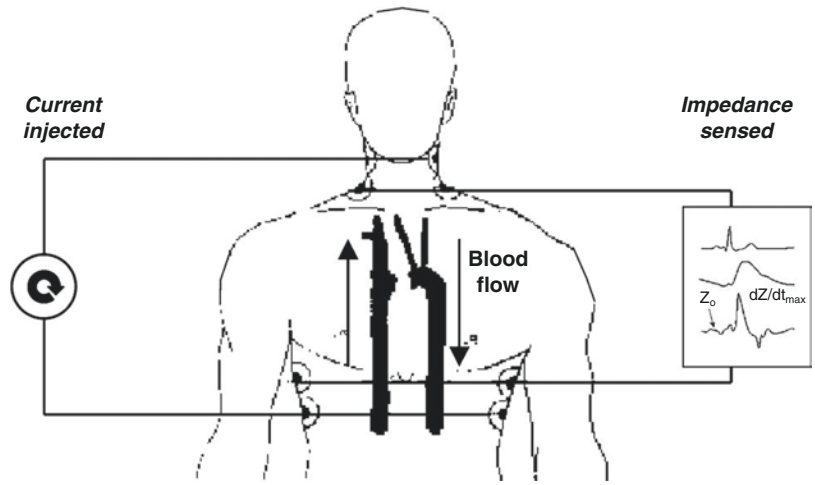

Fig. 13.4 Tetrapolar system of electrodes, separating the current pathway from the sensing pathway. After transmitting electricity by way of the outer electrodes, the impedance to flow of the current through the thorax along the path of least resistance (i.e., the great vessels) is sensed by way of the inner electrodes. (Adapted from Summers et al. [39])

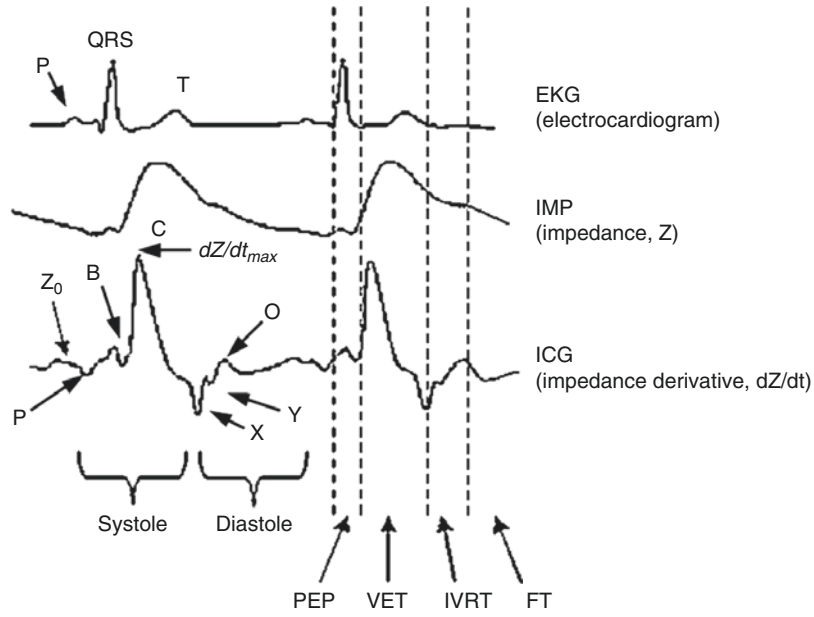

Fig. 13.5 Definition of cardiac and impedance waveforms during the cardiac cycle. *Waveforms* Z_0 baseline impedance, A atrial wave, Baortic valve opening, Cmaximum aortic flow (dZ/dt_{max}), X aortic valve closing, Y pulmonic valve closing, O mitral valve opening, PEP pre-ejection period, VET ventricular ejection time, IVRT isovolumic relaxation time, FT ventricular filling time. (Adapted from Summers et al. [39])

Table 13.1 Electric conductance-based methods for calculating cardiac hemodynamics

Parameters calculated	Formula	Units
Stroke volume (SV)	PF∗ × VET	mL
Stroke index	SV/BSA	mL/beat/m^2
Systolic time ratio	PEP/LVET	
Cardiac output (CO)	SV × HR	L/min
Cardiac index (CI)	CO/BSA	L/min/m^2
Left cardiac work index	(MAP − PCWP) × CI × 0.0144	Kg/m/m^2
Systemic vascular resistance	[(MAP − CVP)/CO] × 80	dyne s cm^5
Systemic vascular resistance index	[(MAP − CVP)/CI] × 80	dyne s cm^5/m^2

BSA body surface area, *CVP* central venous pressure, *HR* heart rate, *LVET* left ventricular ejection time, *MAP* mean arterial pressure, *PEP* pre-ejection period, *PF* peak flow, *PCWP* pulmonary capillary wedge pressure, *VEPT* volume of electrically participating tissue, *VI* velocity index, ∗ derivatives in text

where I is the flow of electric current, E is the voltage drop between the two ends of a circuit, and R is the resistance or impedance [41]. Given a constant current in the circuit, the relationship of changes in voltage across the circuit will be inversely proportional to the impedance. Impedance is related to the resistivity ($_{\varrho}$) (measured in Ωcm), length (L), and cross-sectional area of the conducting medium/material:

$$Z = {}_{\varrho}\left(\frac{L}{A}\right).$$

Since volume is equal to the product of cross-sectional area and length, impedance can be related to changes in the volume according to the following equation [39, 41]:

$$Z = {}_{\varrho}\left(\frac{L^2}{V}\right).$$

In 1940, Nyboer examined the changes in blood volume and flow in the extremities by impedance plethysmography and related the change in impedance (ΔZ) to the change in volume (ΔV) [39, 42]:

$$\Delta V = {}_{\varrho}\left(\frac{L^2}{Z_0^2}\right)\Delta Z$$

With regard to time (t), the equation can be simplified by:

$$\Delta V(t) = {}_{\varrho}\left(\frac{L^2}{Z^2}\right)\Delta Z(t)$$

Changes in impedance in a conductor (thorax) will reflect changes in the volume within the great vessels of the thorax since current will flow through the path of least resistance (resistivity of plasma 65 Ωcm; whole blood 300 Ωcm and muscle, fat, bone and air 200–5000 Ωcm). Using these formulas, the stroke volume can be estimated using a derivative of the impedance waveform $(\delta Z/\delta t)_{max}$, the peak volume change during peak current flow (PF), and the ventricular ejection time (VET) [39, 41, 42]:

$$\mathrm{PF} = {}_{\varrho}\left(\frac{L^2}{Z_0^2}\right)\left(\frac{\delta Z}{\delta t}\right)_{\max}$$

where Z_0 is the baseline impedance of all thoracic tissue, fluid, and air, about 25 Ω for the average adult.

$$\Delta V = \mathrm{SV} = \mathrm{PF} \times \mathrm{VET}$$

$$\Delta V = \mathrm{SV} = {}_{\varrho}\left(\frac{L^2}{Z_0^2}\right)\left(\frac{\delta Z}{\delta t}\right)_{\max} \mathrm{VET}$$

${}_{\varrho}\left(L^2 / Z_0^2\right)$ can be represented by a constant of proportionality, C. Therefore,

$$\Delta V = \mathrm{SV} = \mathrm{C} \times \left(\frac{\delta Z}{\delta t}\right)_{\max} \times \mathrm{VET}$$

The basic assumption of this method is that the change in thoracic impedance is primarily due to increases in the aortic volume. Because the electrical field distribution in the thorax is actually closer to a cone than a cylinder, the initial model was changed from a cylinder to a cone, and therefore the formula was revised [39, 43, 44]:

$$\Delta V = \mathrm{SV} = {}_{\varrho}\left(\frac{L^3}{4.2}\right)\left(\frac{\delta Z}{\delta t}\right)_{\max} \frac{\mathrm{VET}}{Z_0}$$

To avoid the length measurements, the average distance of the thorax (L) is determined to be 17% of the total body height (H); therefore, the equation is revised to:

$$\Delta V = \mathrm{SV} = \left(\frac{(0.17\mathrm{H})^3}{4.2}\right)\left(\frac{\delta Z}{\delta t}\right)_{\max} \frac{\mathrm{VET}}{Z_0},$$

where $(0.17\mathrm{H})^3/4.2$ is defined as the volume of electrically participating thoracic tissue (VEPT).

Finally, when this equation is normalized to an ideal body weight by a factor, δ, the equation would become [39, 44, 45]:

$$\mathrm{SV} = \delta(\mathrm{VEPT})\left(\frac{\delta Z}{\delta t}\right)_{\max} \frac{\mathrm{VET}}{Z_0}$$

Although very sensitive, other changes and pathologies like changes in blood viscosity from anemia and lung pathologies such as pleural effusion or pneumothorax can significantly alter impedance, therefore increasing false positives and reducing its specificity [39, 46]. A study reported that in order to achieve a low false-positive rate, FDA-approved intrathoracic impedance models resorted to algorithms with lower sensitivity for predicting heart failure exacerbation. This may limit the use of thoracic impedance for the prediction/detection of heart failure episodes [47]. More recently, intrathoracic impedance has been used to monitor intravascular volume, aiming to apply knowledge of this method to guide volume therapy in patients with heart failure (Fig. 13.6). Optimal determination of stroke volume by impedance requires patient weight between 67 and 341 pounds and a height of 4–7 feet. Impedance may not be accurate in patients with sepsis, severe aortic regurgitation, and tachycardia (HR > 250 bpm) or patients on intra-aortic balloon pumps [40]. Table 13.2 summarizes the correlation coefficients of different impedance measurements compared to the standard for normal variants and pathologic states.

Intracardiac Impedance Monitoring

Intracardiac impedance has been discussed as an alternative, or a complimentary tool, to other hemodynamic parameters and surrogates in patients with heart failure [46, 48, 49]. It has been used to measure the volume status in patients with cardiac resynchronization therapy (CRT) devices. Intracardiac impedance is a reflection of volume changes in the LV during the entirety of the cardiac cycle. It reduces the false positives encountered with intrathoracic

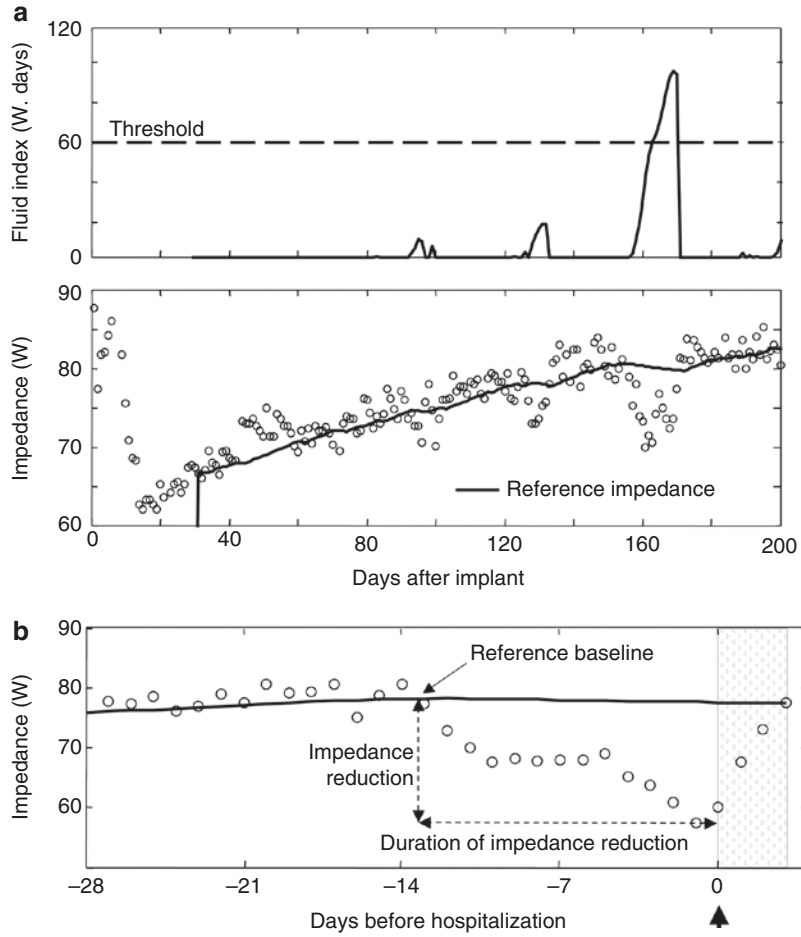

Fig. 13.6 Operational algorithm for detecting changes in impedance over time. (**a**) Differences between measured impedance (bottom; o) and reference impedance (solid line) are accumulated over time to produce fluid index (top). Threshold is then applied to fluid index to detect sustained decreases in impedance. (**b**) Example of impedance reduction before heart failure hospitalization (arrow) for fluid overload and impedance increase during intensive diuresis during hospitalization. Label indicates reference baseline (initial reference impedance value when daily impedance value consistently falls below the reference impedance line before admission). Magnitude and duration of impedance reduction are also shown. Days in hospital are shaded. (Adapted from Yu et al. [34])

impedance measurements associated with other thoracic pathologies. Other theoretical advantages over intrathoracic impedance measurements include reduced delay needed for device pocket maturation and the potentially earlier detection of volume overload as changes in the LVEDP typically occur before pulmonary edema. It can however only be used in patients with CRT devices and these measurements are dependent on lead position which renders them relative rather than absolute values. Additionally, adjustments are needed for postural and diurnal changes commonly encountered with intracardiac impedance measurements.

A combination of multiple parameters that can be recorded from intracardiac devices to form a diagnostic algorithm have been described. These algorithms include various parameters and surrogate markers and have been used to predict heart failure admissions [50, 51]. A list of the devices described above and their proprietary names are summarized in Table 13.3.

Table 13.2 Cumulative correlation coefficients of different impedance measurements compared to a standard for normal variants and pathologic states: How they could affect accurate estimation of cardiac output

Patient	Average correlation	Possible issues with CO estimation
Heathy	0.81 (0.50–0.98)	Hyperdynamic/overestimates
Animals	0.86 (0.41–0.98)	Anatomic landmarks/underestimates
CAD/AMI	0.79 (0.22–0.95)	Weak pulse/underestimates
Chest tubes	0.35	Noise/variable estimates
CHF	0.83 (0.63–0.99)	Lung edema/underestimates
COPD	0.92	Conduction/overestimates
Elderly	0.95	Atherosclerosis/underestimates
Gunshot wound	0.72	Noise/variable estimates
Hemorrhagic shock	0.88 (0.84–0.98)	Low flow/underestimates
Intubated	0.84 (0.1–0.98)	Noise/variable estimates
Obesity	0.76 (0.58–0.94)	Conduction/underestimates
Obstetric patients	0.81 (0.28–0.97)	Anatomic landmarks/underestimates
Pediatric/neonatal patients	0.83 (0.28–0.97)	Lower current/underestimates
Sepsis	0.56 (0.36–0.75)	Runoff/underestimates

Modified from Summers et al. [39]

Table 13.3 Overview of intracardiac impedance monitoring devices

Device	Primary indication	FDA status	Primary measured variable(s)	Implant location	Pertinent contraindications or restrictions
OptiVol® fluid status monitoring system (Medtronic, Inc., USA)	Ambulatory HF surveillance in patients who also meet indication for ICD therapy	Approved Nov 2004	Intrathoracic impedance and heart rate variability	Pectoral muscle region	Patients without an indication for ICD therapy or limited thoracic venous access
Chronicle® ICD and Chronicle® implantable hemodynamic monitor (Medtronic, Inc., USA)	Ambulatory HF surveillance in patients who also meet indication for ICD therapy	Not approved	RV systolic pressure, RV diastolic pressure (an estimate of PADP), maximum change in pressure over time (dP/dt and −dP/dt)	Right ventricle	Patients without an indication for ICD therapy or limited thoracic venous access
HeartPod® (St Jude Medical, Inc., USA)	Ambulatory HF surveillance	Not approved	Mean left atrial pressure	Left atrium	Patients unable to perform Valsalva maneuvers and maintain an airway pressure >39 mmHg for 8 s (required for periodic device calibration)
CardioMEMS™ HF system (CardioMEMS, Inc./St Jude medical, Inc., USA)	Ambulatory surveillance in HF patients with NYHA III symptoms who have preserved EF or reduced EF on OMT, who have had a HF hospitalization in the previous year	Approved May 28, 2014	Systolic, diastolic, and mean pulmonary artery pressure	Left pulmonary artery (ideally, basal segmental branch)	Based on CHAMPION trial criteria (REF), patient should not have any of the following: History of recurrent (>1) pulmonary embolism or deep vein thrombosis inability to tolerate a right heart catheterization recent major cardiovascular event (e.g., myocardial infarction, stroke) within 2 months of monitoring

RT cardiac resynchronization therapy, dP/dT rate of rise of left ventricular pressure (mmHg/sec), *EF* left ventricular ejection fraction, *eGFR* estimated glomerular filtration rate, *HF* heart failure, *ICD* implantable cardioverter defibrillator, *NYHA* New York Heart Association functional class, *OMT* optimal medical therapy, *PADP* pulmonary artery diastolic pressure, *RV* right ventricle
Adapted from Mooney et al. [29]

Bioreactance

Bioreactance is another noninvasive method of measuring cardiac hemodynamics, much like impedance cardiography, but unlike impedance, uses change in signal amplitude of blood flow (Fig. 13.7). Accordingly, bioreactance measures relative phase shifts of the received signals (alternating currents) in comparison to transmitted signals (ΔΦ). These phase shifts are categorized by changes in capacitive and inductive properties of changes in blood flow and intrathoracic volume. This system is less susceptible to noise, and theoretically can be more widely used with fewer limitations compared to impedance cardiography. Also, Unlike hemodynamic measurements by impedance cardiography, bioreactance neither needs static impedance nor utilizes the distance between electrodes for calculation of SV and CO, making hemodynamic calculation less prone to uncertainty [52]. This method has been shown to be accurate and show close overall correlation with hemodynamic measurements obtained using the thermodilution method [53].

Despite the advantages of bioreactance and its improvements over bioimpedance, both methods have similar underlying concepts and hence similar limitations. Changes in aortic dynamics including diseases of the aorta and aortic valve would affect the accuracy of readings. Arrhythmias and heart rates above 150 beats per minute, as well as shunts, edema, abdominal/thoracic pathologies that involve rapid volume shifts between intravascular and extravascular spaces could also make recordings inaccurate.

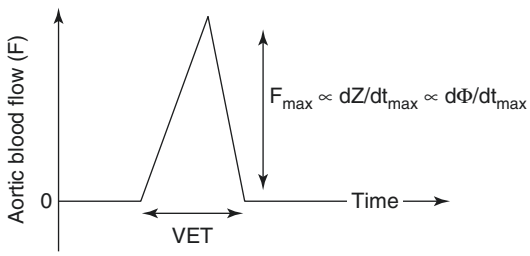

Fig. 13.7 Overview of aortic flow as a function of time and its use to measure cardiac hemodynamics. The basic principle of stroke volume (SV) estimation from changes in the bioimpedance ($\delta Z/\delta t$) or phase shift ($\delta\Phi/\delta t$)

Similar to the cardiac impedance underlying method of measurement, bioreactance is governed by the following physics equation:

$$\Delta V = \mathrm{SV} = {}_{\varrho}\left(\frac{L^2}{Z_0^2}\right)\left(\frac{\delta Z}{\delta t}\right)_{\max} \mathrm{VET}$$

given the tight correlation between rate of blood flow and change in phase shifts, ($\delta\Phi/\delta t$), therefore [52]:

Using a constant of proportionality (C):

$$\Delta V = \mathrm{SV} = \mathrm{C} \times \left(\frac{\delta\Phi}{\delta t}\right)_{\max} \times \mathrm{VET}$$

Partial Carbon Dioxide Rebreathing Technique

This method of hemodynamic measurement uses the carbon dioxide method of the Fick principle which is based on mass conservation [54]:

$$Q = \frac{\mathrm{VCO_2}}{\left(\mathrm{CvCO_2} - \mathrm{CaCO_2}\right)},$$

where Q = cardiac output; VCO_2 = CO_2 elimination (ml/min); $CvCO_2$ = venous CO_2 content (ml/ml of blood); and $CaCO_2$ = arterial CO_2 content (ml/ml of blood). This calculations assume that CO_2 concentrations remain relatively constant.

Since only the pulmonary capillary (nonshunted) blood flow (PCBF) is used in this calculation, accurate measurement of cardiac output requires adding the estimated amount of blood flow not passing through the lungs. In the CO_2 rebreathing method, subjects rebreathe air from a bag, allowing CO_2 to accumulate such that the mixed venous partial pressure is calculated. In the partial rebreathing method, however, in addition to measurements during the rebreathing, measurements are obtained during a non-rebreathing period. These measurements are applied to the Fick equation to obtain cardiac outputs [54].

$$Q_{PCBF} = \frac{VCO_{2NR} - VCO_{2R}}{\left(CvCO_{2NR} - CaCO_{2NR}\right) - \left(CvCO_{2R} - CaCO_{2R}\right)},$$

where NR = non-rebreathing phase and R = rebreathing phase.

Since it is assumed that CO_2 concentrations remain relatively constant during both phases,

$$Q_{PCBF} = \frac{VCO_{2NR} - VCO_{2R}}{CaCO_{2NR} - CaCO_{2R}} \text{ or :}$$

$$Q_{PCBF} = \frac{\Delta VCO_2}{\Delta CaCO_2}$$

Several systems exist for this method of cardiac output calculation. Each one consist of CO_2 measurements, processing of CO_2 signals and several hardware modifications to increase accuracy.

Generally, the first phase is non-rebreathing when baseline measurements are obtained. This lasts about a minute and is followed by a rebreathing phase which lasts for about another minute. During this period, there is repeated inhalation of expired CO_2. The amount of CO_2 inhaled is regulated by a valve attached to the mouthpiece. CO_2 in the rebreathing phase of the test is stored from the preceding exhalation period by the valve system in the mouthpiece, therefore making sure that the inhaled CO_2 is actually from the patient. Repeated inhalation of CO_2 during the rebreathing period increases alveolar CO_2 concentration, arterial CO_2 content and reduces alveolar diffusion of CO_2 and CO_2 clearance from the lungs. In the third and final phase, there is restoration of the patient's CO_2 stores, called the stabilization phase. This also lasts approximately 1 min and restores CO_2 parameters to normal [54].

Although this method is noninvasive, safe, convenient, and applicable in an ambulatory/outpatient setting, it assumes constant cardiac output, partial pressure of mixed venous oxygen, and shunt fraction. Changes during measurements of any of these parameters can significantly change the test results. Also, It is assumed that subjects' hemoglobin concentration is 11 g/dl. A drop of 3 mg/dl can change the estimated cardiac output by about 10%. It may also be inaccurate in patients with lung disease and resultant abnormalities of gas exchange or in patients with a $PaCO_2$ greater than 30 mmHg. Additionally, this method will be technically difficult to use in patients who cannot tolerate the rebreathing phase [7, 54, 55].

Conclusion

Noninvasive cardiac hemodynamic assessment and long-term monitoring have proven beneficial in patients with heart failure. Advances in monitoring devices and technology is allowing accurate and reliable remote monitoring of patients with heart failure. This concept is helping clinicians to manage patients and reduce unnecessary hospital admissions.

References

1. Nakamura N, Koga T, Iseki H. A meta-analysis of remote patient monitoring for chronic heart failure patients. J Telemed Telecare. 2014;20(1):11–7. https://doi.org/10.1177/1357633X13517352.
2. Klersy C, De Silvestri A, Gabutti G, Regoli F, Auricchio A. A meta-analysis of remote monitoring of heart failure patients. J Am Coll Cardiol. 2009;54(18):1683–94. https://doi.org/10.1016/j.jacc.2009.08.017.
3. Abraham WT, Adamson PB, Bourge RC, Aaron MF, Costanzo MR, Stevenson LW, Strickland W, Neelagaru S, Raval N, Krueger S, Weiner S, Shavelle D, Jeffries B, Yadav JS. Wireless pulmonary artery haemodynamic monitoring in chronic heart failure: a randomised controlled trial. Lancet. 2011;377(9766):658–66. https://doi.org/10.1016/S0140-6736(11)60101-3.
4. Small RS, Wickemeyer W, Germany R, Hoppe B, Andrulli J, Brady PA, Labeau M, Koehler J, Sarkar S, Hettrick DA, Tang WHW. Changes in intrathoracic impedance are associated with subsequent risk of hospitalizations for acute decompensated heart failure: clinical utility of implanted device monitoring without a patient alert. J Card Fail. 2009;15(6):475–81. https://doi.org/10.1016/j.cardfail.2009.01.012.

5. Domenichini G, Rahneva T, Diab IG, Dhillon OS, Campbell NG, Finlay MC, Baker V, Hunter RJ, Earley MJ, Schilling RJ. The lung impedance monitoring in treatment of chronic heart failure (the LIMIT-CHF study). Europace. 2016;18(3):428–35. https://doi.org/10.1093/europace/euv293.
6. Boehmer JP, Hariharan R, Devecchi FG, Smith AL, Molon G, Capucci A, An Q, Averina V, Stolen CM, Thakur PH, Thompson JA, Wariar R, Zhang Y, Singh JP. A multisensor algorithm predicts heart failure events in patients with implanted devices: results from the MultiSENSE study. JACC Heart Fail. 2017;5(3):216–25. https://doi.org/10.1016/j.jchf.2016.12.011.
7. Sangkum L, Liu GL, Yu L, Yan H, Kaye AD, Liu H. Minimally invasive or noninvasive cardiac output measurement: an update. J Anesth. 2016;30(3):461–80. https://doi.org/10.1007/s00540-016-2154-9.
8. Belardinelli R, Ciampani N, Costantini C, Blandini A, Purcaro A. Comparison of impedance cardiography with thermodilution and direct Fick methods for noninvasive measurement of stroke volume and cardiac output during incremental exercise in patients with ischemic cardiomyopathy. Am J Cardiol. 1996;77(15):1293–301. https://doi.org/10.1016/S0002-9149(97)89153-9.
9. Yancy CW, Jessup M, Bozkurt B, Butler J, Casey DE, Drazner MH, Fonarow GC, Geraci SA, Horwich T, Januzzi JL, Johnson MR, Kasper EK, Levy WC, Masoudi FA, McBride PE, McMurray JJ V, Mitchell JE, et al. 2013 ACCF/AHA guideline for the management of heart failure: a report of the American college of cardiology foundation/American heart association task force on practice guidelines. Circulation. 2013;128(16). https://doi.org/10.1161/CIR.0b013e31829e8776.
10. Landolina M, Perego GB, Lunati M, Curnis A, Guenzati G, Vicentini A, Parati G, Borghi G, Zanaboni P, Valsecchi S, Marzegalli M. Remote monitoring reduces healthcare use and improves quality of care in heart failure patients with implantable defibrillators: the evolution of management strategies of heart failure patients with implantable defibrillators (EVOLVO) study. Circulation. 2012;125(24):2985–92. https://doi.org/10.1161/CIRCULATIONAHA.111.088971.
11. Varma N, Epstein AE, Irimpen A, Schweikert R. Efficacy and safety of automatic remote monitoring for implantable Cardioverter-defibrillator follow-up. Circulation. 2010;122:325–32. https://doi.org/10.1161/CIRCULATIONAHA.110.937409.
12. Mullens W, Borowski AG, Curtin RJ, Thomas JD, Tang WH. Tissue Doppler imaging in the estimation of intracardiac filling pressure in decompensated patients with advanced systolic heart failure. Circulation. 2009;119(1):62–70. https://doi.org/10.1161/CIRCULATIONAHA.108.779223.
13. Goonewardena SN, Blair JEA, Manuchehry A, Brennan JM, Keller M, Reeves R, Price A, Spencer KT, Puthumana J, Gheorghiade M. Use of hand carried ultrasound, B-type natriuretic peptide, and clinical assessment in identifying abnormal left ventricular filling pressures in patients referred for right heart catheterization. J Card Fail. 2010;16(1):69–75. https://doi.org/10.1016/j.cardfail.2009.08.004.
14. Yancy CW, Jessup M, Bozkurt B, Butler J, Casey DE, Drazner MH, Fonarow GC, Geraci SA, Horwich T, Januzzi JL, Johnson MR, Kasper EK, Levy WC, Masoudi FA, McBride PE, McMurray JJV, Mitchell JE, et al. 2013 ACCF/AHA guideline for the management of heart failure: executive summary: a report of the American College of Cardiology foundation/American Heart Association task force on practice guidelines. J Am Coll Cardiol. 2013;62(16):1495–539. https://doi.org/10.1016/j.jacc.2013.05.020.
15. Berger R, Huelsman M, Strecker K, Bojic A, Moser P, Stanek B, Pacher R. B-type natriuretic peptide predicts sudden death in patients with chronic heart failure. Circulation. 2002;105(20):2392–7. https://doi.org/10.1161/01.CIR.0000016642.15031.34.
16. Gheorghiade M, Follath F, Ponikowski P, Barsuk JH, Blair JEA, Cleland JG, Dickstein K, Drazner MH, Fonarow GC, Jaarsma T, Jondeau G, Sendon JL, Mebazaa A, Metra M, Nieminen M, Pang PS, Seferovic P, et al. Assessing and grading congestion in acute heart failure: a scientific statement from the acute heart failure committee of the heart failure association of the European society of cardiology and endorsed by the European society of intensive care medicine. Eur J Heart Fail. 2010;12(5):423–33. https://doi.org/10.1093/eurjhf/hfq045.
17. Lucas C, Johnson W, Hamilton MA, Fonarow GC, Woo MA, Flavell CM, Creaser JA, Stevenson LW. Freedom from congestion predicts good survival despite previous class IV symptoms of heart failure. Am Heart J. 2000;140(6):840–7. https://doi.org/10.1067/mhj.2000.110933.
18. Adamson PB, Bharmi R, Dalal N, Abraham WT. Impact of pulmonary artery pressure monitoring on all-cause 30-day hf readmissions and associated centers for medicare and medicaid services hospital readmissions reduction program penalty. J Card Fail. 2015;21(8):S115. https://doi.org/10.1016/j.cardfail.2015.06.332.
19. Santas E, de la Espriella-Juan R, Mollar A, Valero E, Miñana G, Sanchis J, Chorro FJ, Núñez J. Echocardiographic pulmonary artery pressure estimation and heart failure rehospitalization burden in patients with acute heart failure. Int J Cardiol. 2018;241:407–10. https://doi.org/10.1016/j.ijcard.2017.04.055.
20. Hoppe UC, Vanderheyden M, Sievert H, Brandt MC, Tobar R, Wijns W, Rozenman Y. Chronic monitoring of pulmonary artery pressure in patients with severe heart failure: multicentre experience of the monitoring pulmonary artery pressure by implantable device responding to ultrasonic signal (PAPIRUS) II study. Heart. 2009;95(13):1091–7. https://doi.org/10.1136/hrt.2008.153486.
21. Adamson PB, Abraham WT, Stevenson LW, Desai AS, Lindenfeld J, Bourge RC, Bauman

J. Pulmonary artery pressure-guided heart failure management reduces 30-day readmissions. Circ Heart Fail. 2016;9(6) https://doi.org/10.1161/CIRCHEARTFAILURE.115.002600.
22. Adamson PB, Magalski A, Braunschweig F, Böhm M, Reynolds D, Steinhaus D, Luby A, Linde C, Ryden L, Cremers B, Takle T, Bennett T. Ongoing right ventricular hemodynamics in heart failure: clinical value of measurements derived from an implantable monitoring system. J Am Coll Cardiol. 2003;41(4):565–71. https://doi.org/10.1016/S0735-1097(02)02896-6.
23. Desai AS, Bhimaraj A, Bharmi R, Jermyn R, Bhatt K, Shavelle D, Redfield MM, Hull R, Pelzel J, Davis K, Dalal N, Adamson PB, Heywood JT. Ambulatory hemodynamic monitoring reduces heart failure hospitalizations in "real-world" clinical practice. J Am Coll Cardiol. 2017;69(19):2357–65. https://doi.org/10.1016/j.jacc.2017.03.009.
24. Heywood JT, Jermyn R, Shavelle D, Abraham WT, Bhimaraj A, Bhatt K, Sheikh F, Eichorn E, Lamba S, Bharmi R, Agarwal R, Kumar C, Stevenson LW. Impact of practice-based management of pulmonary artery pressures in 2000 patients implanted with the CardioMEMS sensor. Circulation. 2017;135(16):1509–17. https://doi.org/10.1161/CIRCULATIONAHA.116.026184.
25. Abraham WT, Stevenson LW, Bourge RC, Lindenfeld JA, Bauman JG, Adamson PB. Sustained efficacy of pulmonary artery pressure to guide adjustment of chronic heart failure therapy: complete follow-up results from the CHAMPION randomised trial. Lancet. 2016;387(10017):453–61. https://doi.org/10.1016/S0140-6736(15)00723-0.
26. Adamson PB, Abraham WT, Aaron M, Aranda JM, Bourge RC, Smith A, Stevenson LW, Bauman JG, Yadav JS. CHAMPION trial rationale and design: the long-term safety and clinical efficacy of a wireless pulmonary artery pressure monitoring system. J Card Fail. 2011;17(1):3–10. https://doi.org/10.1016/j.cardfail.2010.08.002.
27. Abraham WT. The role of implantable hemodynamic monitors to manage heart failure. Cardiol Clin. 2017;35(2):273–9. https://doi.org/10.1016/j.ccl.2016.12.009.
28. Vanoli E, D'Elia E, La Rovere MT, Gronda E. Remote heart function monitoring: role of the CardioMEMS HF system. J Cardiovasc Med. 2016;17(7):518–23. https://doi.org/10.2459/JCM.0000000000000367.
29. Mooney DM, Fung E, Doshi RN, Shavelle DM. Evolution from electrophysiologic to hemodynamic monitoring: the story of left atrial and pulmonary artery pressure monitors. Front Physiol. 2015;6. https://doi.org/10.3389/fphys.2015.00271.
30. Abraham WT, Adamson PB, Costanzo MR, Eigler N, Gold M, Klapholz M, Maurer M, Saxon L, Singh J, Troughton R. Hemodynamic monitoring in advanced heart failure: results from the LAPTOP-HF trial. J Card Fail. 2016;22(11):940. https://doi.org/10.1016/j.cardfail.2016.09.012.
31. Troughton RW, Ritzema J, Eigler NL, Melton IC, Krum H, Adamson PB, Kar S, Shah PK, Whiting JS, Heywood JT, Rosero S, Singh JP, Saxon L, Matthews R, Crozier IG, Abraham WT. Direct left atrial pressure monitoring in severe heart failure: long-term sensor performance. J Cardiovasc Transl Res. 2011;4(1):3–13. https://doi.org/10.1007/s12265-010-9229-z.
32. Ritzema J, Melton IC, Richards AM, Crozier IG, Frampton C, Doughty RN, Whiting J, Kar S, Eigler N, Krum H, Abraham WT, Troughton RW. Direct left atrial pressure monitoring in ambulatory heart failure patients: initial experience with a new permanent implantable device. Circulation. 2007;116(25):2952–9. https://doi.org/10.1161/CIRCULATIONAHA.107.702191.
33. Drazner MH, Thompson B, Rosenberg PB, Kaiser PA, Boehrer JD, Baldwin BJ, Dries DL, Yancy CW. Comparison of impedance cardiography with invasive hemodynamic measurements in patients with heart failure secondary to ischemic or nonischemic cardiomyopathy. Am J Cardiol. 2002;89(8):993–5. https://doi.org/10.1016/S0002-9149(02)02257-9.
34. Yu CM, Wang L, Chau E, Chan RHW, Kong SL, Tang MO, Christensen J, Stadler RW, Lau CP. Intrathoracic impedance monitoring in patients with heart failure: correlation with fluid status and feasibility of early warning preceding hospitalization. Circulation. 2005;112(6):841–8. https://doi.org/10.1161/CIRCULATIONAHA.104.492207.
35. Wang L, Lahtinen S, Lentz L, Rakow N, Kaszas C, Ruetz L, Stylos L, Olson WH. Feasibility of using an implantable system to measure thoracic congestion in an ambulatory chronic heart failure canine model. PACE – Pacing Clin Electrophysiol. 2005;28(5):404–11. https://doi.org/10.1111/j.1540-8159.2005.40009.x.
36. Khoury DS, Naware M, Siou J, Blomqvist A, Mathuria NS, Wang J, Shih HT, Nagueh SF, Panescu D. Ambulatory monitoring of congestive heart failure by multiple bioelectric impedance vectors. J Am Coll Cardiol. 2009;53(12):1075–81. https://doi.org/10.1016/j.jacc.2008.12.018.
37. Vollmann D, Nägele H, Schauerte P, Wiegand U, Butter C, Zanotto G, Quesada A, Guthmann A, Hill MRS, Lamp B. Clinical utility of intrathoracic impedance monitoring to alert patients with an implanted device of deteriorating chronic heart failure. Eur Heart J. 2007;28(15):1835–40. https://doi.org/10.1093/eurheartj/ehl506.
38. Catanzariti D, Lunati M, Landolina M, Zanotto G, Lonardi G, Iacopino S, Oliva F, Perego GB, Varbaro A, Denaro A, Valsecchi S, Vergara G. Monitoring intrathoracic impedance with an implantable defibrillator reduces hospitalizations in patients with heart failure. PACE – Pacing Clin Electrophysiol. 2009;32(3):363–70. https://doi.org/10.1111/j.1540-8159.2008.02245.x.
39. Summers RL, Shoemaker WC, Peacock WF, Ander DS, Coleman TG. Bench to bedside: electrophysiologic and clinical principles of noninvasive

hemodynamic monitoring using impedance cardiography. Acad Emerg Med. 2003;10(6):669–80. https://doi.org/10.1111/j.1553-2712.2003.tb00054.x.
40. Yancy C, Abraham WT. Noninvasive hemodynamic monitoring in heart failure: utilization of impedance cardiography. Congest Heart Fail. 2003;9(5):241–50. https://doi.org/10.1111/j.1751-7133.2003.tb00021.x.
41. Winter UJ, Klocke RK, Kubicek WGNW, editors. Thoracic impedance measurements in clinical cardiology. New York: Thieme Medical Publishers; 1994.
42. Nyboer J. Electrical impedance plethysmography; a physical and physiologic approach to peripheral vascular study. Circulation. 1950;2(6):811–21. https://doi.org/10.1161/01.CIR.2.6.811.
43. Sramek B. Thoracic electric bioimpedance. Basic principles and physiologic relationships. Cesk Fysiol. 1993;42(3–4):111–5.
44. Bernstein DP. A new stroke volume equation for thoracic electrical bioimpedance: theory and rationale. Crit Care Med. 1986;14(10):904–9.
45. Newman DG, Callister R. The non-invasive assessment of stroke volume and cardiac output by impedance cardiography: a review. Aviat Space Environ Med. 1999;70(8):780–9.
46. Lau CP, Siu DCW, Tse HF. Optimizing heart failure therapy with implantable sensors. J Arrhythmia. 2012;28(1):4–18. https://doi.org/10.1016/j.joa.2012.02.003.
47. Heist EK, Herre JM, Binkley PF, Van Bakel AB, Porterfield JG, Porterfield LM, Qu F, Turkel M, Pavri BB. Analysis of different device-based intrathoracic impedance vectors for detection of heart failure events (from the detect fluid early from intrathoracic impedance monitoring study). Am J Cardiol. 2014;114(8):1249–56. https://doi.org/10.1016/j.amjcard.2014.07.048.
48. Liu PS, Tse HF. Implantable sensors for heart failure monitoring. J Arrhythmia. 2013;29(6):314–9. https://doi.org/10.1016/j.joa.2013.06.003.
49. Bocchiardo M, Vilsendorf DMZ, Militello C, Lippert M, Czygan G, Gaita F, Schauerte P, Stellbrink C. Intracardiac impedance monitors stroke volume in resynchronization therapy patients. Europace. 2010;12(5):702–7. https://doi.org/10.1093/europace/euq045.
50. Whellan DJ, Ousdigian KT, Al-Khatib SM, Pu W, Sarkar S, Porter CB, Pavri BB, O'Connor CM. Combined heart failure device diagnostics identify patients at higher risk of subsequent heart failure hospitalizations. Results from PARTNERS HF (program to access and review trending information and evaluate correlation to symptoms in patients with hear). J Am Coll Cardiol. 2010;55(17):1803–10. https://doi.org/10.1016/j.jacc.2009.11.089.
51. Whellan D, Alkhatib S, Kloosterman E, Kutalek S, Manaris A, Oconnor C, Pavri B, Porter C, Singh A, Lung T. Changes in Intrathoracic fluid index predict subsequent adverse events: results of the multi-site program to access and review trending INformation and evaluate CoRrelation to symptoms in patients with heart failure (PARTNERS HF) trial. J Card Fail. 2008;14(9):799–799. https://doi.org/10.1016/j.cardfail.2008.10.015.
52. Keren H, Burkhoff D, Squara P. Evaluation of a noninvasive continuous cardiac output monitoring system based on thoracic bioreactance. 2007;10032:583–9. https://doi.org/10.1152/ajpheart.00195.2007.
53. Cotter G, Moshkovitz Y, Kaluski E. Clinical investigations in critical care accurate, noninvasive continuous monitoring of cardiac output by whole-body electrical bioimpedance∗. 2004. Chest; 125: 1431-1440.
54. Jaffe MB. Partial CO2 rebreathing cardiac output-operating principles of the NICO(TM) system. J Clin Monit Comput. 1999;15(6):387–401. https://doi.org/10.1023/A:1009981313076.
55. Killick C, Parkin W. Non-invasive cardiac output measurement using a fast mixing box to measure carbon dioxide elimination. Anaesth Intensive Care. 2008;36(5):665–73. https://doi.org/10.1177/0310057X0803600506.

14 Cardiac Catheterization: Right- and Left-Heart Catheterization

Michael D. Faulx and Khaled M. Ziada

Introduction

Myocardial performance is determined by the combined effects of preload, afterload, and contractility [1]. *In vivo,* myocardial performance is represented by the cardiac output, while loading conditions are defined by the interplay between volume, pressure, and vascular resistance within the cardiac chambers and great vessels. Catheterization remains the gold standard for cardiovascular hemodynamic assessment because it provides direct, "real-time" hemodynamic information. Catheterization plays a major role in the diagnosis and management of conditions such as valvular heart disease, complex congenital heart disease, acutely decompensated heart failure, shock, and pulmonary hypertension.

Cardiac catheterization is widely available, and in most centers these procedures are performed quite safely. However, one must always respect the fact invasive procedures are inherently risky. In most cases invasive hemodynamic assessment should be pursued only after noninvasive modalities have failed to furnish the desired results.

M. D. Faulx
Cleveland Clinic, Cleveland, OH, USA
e-mail: Faulxm@ccf.org

K. M. Ziada (✉)
Gill Heart and Vascular Institute, University of Kentucky, Lexington, KY, USA
e-mail: kziad2@uky.edu

Invasive Hemodynamic Assessment: Fundamental Concepts

The goal of invasive hemodynamic assessment is to accurately replicate real cardiovascular physiology. The accuracy of the data depends on the means through which it is obtained. A basic understanding of how hemodynamic information is acquired in the laboratory is essential to its correct interpretation.

Pressure Measurements

Complex pressure waves generated by the heart and great vessels are periodic, meaning that each cycle repeats itself at a fundamental frequency determined by the heart rate (expressed as cycles/second or Hertz, Hz). The French physicist Jean Baptiste Fourier (1786–1830) demonstrated that complex periodic waves can be expressed as the sum of any number of simpler sinusoidal waves, each with its own frequency and amplitude. These are referred to as *harmonics* and the frequency of each harmonic is an integral multiple of the fundamental frequency (Fig. 14.1). Fourier's theorem is important because the physical properties of a monitoring system must be configured to accurately reproduce pressures across a broad range of harmonic frequencies.

The challenge of constructing a practical hemodynamic monitoring system was tackled by the

A. T. Askari, A. W. Messerli (eds.), *Cardiovascular Hemodynamics*, Contemporary Cardiology,
https://doi.org/10.1007/978-3-030-19131-3_14

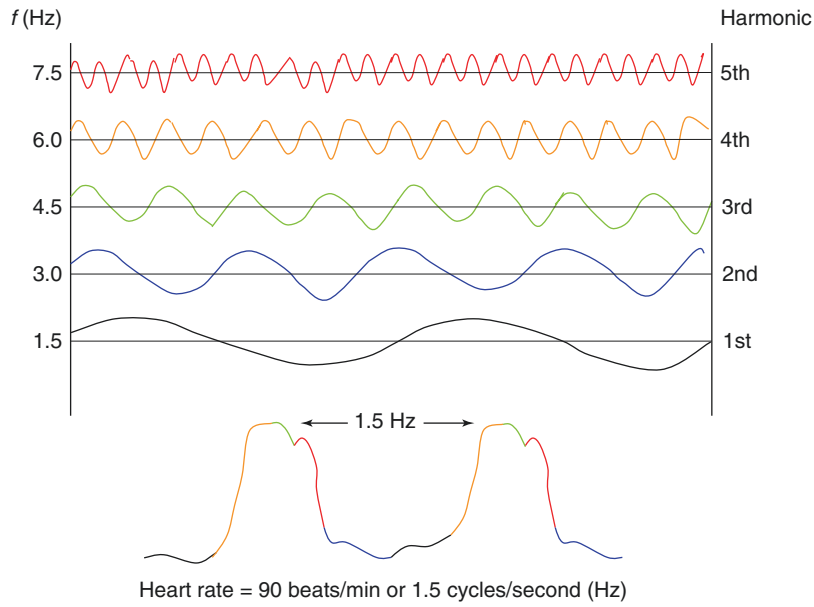

Fig. 14.1 Harmonics in hemodynamic assessment. The aortic pressure waves shown at the bottom are composed of simpler sinusoidal harmonic waves. Each harmonic is a multiple of the fundamental frequency, in this case 1.5 Hz. The data contained within each harmonic contributes in some way to the reconstructed waveform, depicted in this illustration by color. Exclusion of one or more harmonics by a monitoring system can produce a distorted, inaccurate pressure tracing

American physician Carl J. Wiggers (1883–1963). Wiggers employed a fluid-filled catheter system in contact with a rubber diaphragm coupled to a recording device and this design, after several refinements, is still used in monitoring devices today.

The fidelity of pressure measurements obtained by fluid-filled catheters is heavily dependent on the characteristics of the transducer membrane. Flexible membranes are *sensitive* because they can accurately reflect most received amplitudes but they do not respond well to higher frequency harmonics. Conversely rigid membranes respond to a wide range of harmonic frequencies (have better *frequency response*) but tend to be less sensitive. Recording systems used in modern clinical practice tend to have stiffer membranes in order to capture the range of harmonics expected in human physiology, sacrificing sensitivity to some degree.

Another major hindrance to accurate pressure measurement is the fact that transducer membranes resonate in response to stimulation, generating their own pressure waves at a fundamental frequency called the *natural frequency*. When the harmonic frequency of a recorded wave approaches the natural frequency of the monitoring system the amplitudes reflected to the monitor at or near that frequency will be greatly exaggerated. The ability of a catheter system to attenuate the pressure waves produced by the transducer membrane is referred to as *damping*. An ideally damped system is one in which the ratio of input amplitude to output amplitude is maintained close to 1:1 across a broad range of frequencies. Natural frequency (and also frequency response) increases with membrane stiffness and catheter diameter and decreases with catheter length, catheter stiffness, and fluid viscosity. Damping responds in the opposite manner to these factors. Thus, catheters with high-fidelity, tip-mounted transducers (Millar Instruments, Houston, TX) have excellent frequency response and are well suited for capturing high-frequency pressure changes over short time intervals (i.e., measurement of left ventricular dP/dt). Longer, stiffer, fluid-filled catheters coupled to a transducer at the hub are well damped and reasonably sensitive across most of the harmonic frequencies encountered in human studies.

The basic equipment required for pressure measurement in the catheterization lab includes a fluid-filled hollow catheter, multi-port manifold, transducer membrane in contact with an electrical strain gauge, signal amplifier, and a monitor. The catheter tip is placed in the cardiac chamber of interest and connected to the transducer via a dedicated port on the manifold. Pressures at the catheter tip are transmitted through the fluid medium (saline, blood, or contrast) to the transducer membrane, which stretches and vibrates in response to the pressure it sees. The membrane is coupled to a tiny strain gauge contained within a housing unit that has been equilibrated to atmospheric pressure (referred to as *zeroing*). Movement of the piston across the wires of the strain gauge produces an electrical current that is subsequently amplified, reconfigured, and displayed on the monitor.

Hemodynamic waveforms obtained from fluid-filled catheters are subject to a variety of artifacts. Common encountered artifacts are demonstrated and extensively reviewed in Fig. 14.2a–e.

Blood Flow Measurements

Accurate measurement of cardiac output is vital not only as an index of myocardial performance but also as a component in the quantification of valvular stenoses, vascular resistances, and shunts. In clinical practice, cardiac output is assessed by two methods: Fick method and thermodilution.

Oxygen Extraction and Utilization: The Fick Method

The German physiologist Adolph Fick (1829–1901) theorized that the utilization of any substance by an organ can be expressed as the product of the blood flow to the organ and the difference between the arterial and venous concentrations of the substance. When this principle is applied to the lungs, oxygen uptake (VO_2) would be equal to pulmonary blood flow x the difference between pulmonary arterial ($A[O_2]$) and venous ($V[O_2]$) oxygen content. Assuming that there is no pulmonary-systemic shunt and that flow through the pulmonary and systemic circuits are equal, the Fick equation can provide a measure of cardiac output (CO):

$$\text{Fick equation} \quad \text{CO}\left(\text{L/min}\right) = \frac{\text{VO}_2 \ \left(\text{mL/min}\right)}{\text{A}\left[\text{O}_2\right] - \text{V}\left[\text{O}_2\right] \ \left(\text{mL/L}\right)}$$

Oxygen consumption for an individual patient can be directly measured by devices that employ a closed rebreathing circuit with a CO_2 detector. However, this approach is expensive and technically cumbersome and many laboratories assume a resting VO_2 of 1.25 mL/m^2. The reader should be aware that assumed VO_2 values are based on studies of basal metabolic activity in predominantly young subjects. Measured VO_2 can significantly vary from baseline in subjects with underlying cardiopulmonary disease so the use of assumed oxygen consumption values can introduce significant error in the calculation of cardiac output.

Hemoglobin binds approximately 1.36 mL of elemental oxygen per gram and oxygen bound to the hemoglobin molecule accounts for over 98% of the total oxygen content of human blood. Oxygen dissolved in plasma accounts for the rest and is represented by the product of oxygen solubility in plasma (0.003 mL/dL/mmHg) and the partial pressure of oxygen in plasma, PaO_2. The oxygen content of blood is represented by the following equation:

$$\text{Cb}\left[\text{O}_2\right] = \left\{\left[\text{hemoglobin}\right] \times 1.36 \times \text{SaO}_2 \times 10\right\} + 0.003 \times \text{PaO}_2 \times 10.$$

SaO_2 is the percent oxyhemoglobin as detected by oximetry. For the sake of simplicity the content of dissolved O_2 is often omitted from this calculation, but the reader should be aware that under certain circumstances (i.e., high FiO_2 with positive pressure ventilation) the amount of dissolved oxygen in blood can become clinically relevant.

The Fick method is generally an accurate method of cardiac output measurement but error can be introduced at several levels. The Fick method relies on several key assumptions such as the absence of an intracardiac shunt and the notion that oxygen consumption and cardiac output are constant during measurement. In critically

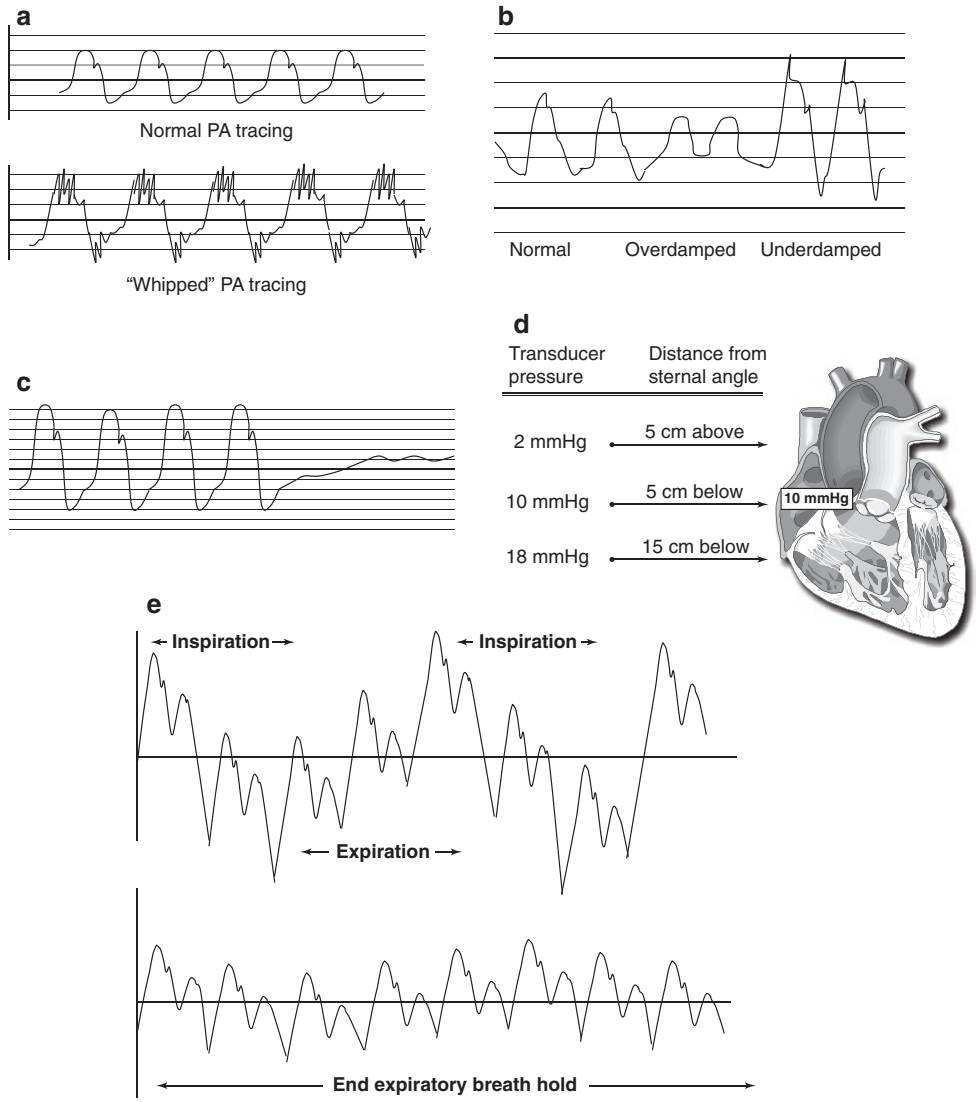

Fig. 14.2 (**a**) Catheter whip in a pulmonary artery (PA) pressure tracing. Whip occurs when the catheter tip vibrates in response to ventricular contraction or valvular motion. Whip causes high-frequency distortion of the waveforms, particularly at the high and low points of the complex. Since the extremes of the waveform are equally affected, the mean pressure obtained from a "whipped" tracing is generally accurate. Whip can be attenuated by catheter repositioning, the use of a high-frequency filter, or increased damping. (**b**) Damping-related artifacts. Overdamping results in a flat, low-amplitude waveform that lacks contour detail. Overdamping can be caused by catheter kinking, air bubbles or blood in the transducer circuit, and the use of long, small-caliber catheters. It can be overcome by removing kinked tubing, flushing of the catheter and manifold, and use of shorter, large-caliber catheters. Under-damping produces exaggerated waveforms with overestimated amplitudes. It occurs when the natural frequency of the catheter system approximates a harmonic frequency in the pressure wave. This can be offset by lowering the natural frequency of the catheter system (longer, smaller-caliber catheters) or the patient (treat tachycardia). (**c**) Positional artifact. This is characterized by flattening of the pressure tracing with a gradual rise in pressure. It most often occurs when the catheter tip is pressed against the wall of a vessel or chamber. Gentle withdrawal and redirection of the catheter typically solves the problem. (**d**) Transducer malposition. In this example, the true mean right atrial pressure is 10 mmHg. When the transducer is zeroed at a level 5 cm below the sternal angle the catheter recording is accurate. When the transducer is zeroed at a level above the chest, the pressure is underestimated. When the transducer is zeroed at a level well below the right atrium, the pressure is overestimated. (**e**) Respiratory variation of right atrial pressure. The thin-walled right-sided chambers are subject to respiratory variation, particularly in subjects with underlying obstructive lung disease. Pressure measurements taken during a few seconds of breath holding at the end of normal expiration (when intrathoracic pressure is theoretically zero) are much less variable

ill patients with pulmonary disease, oxygen consumption can be overestimated since the delivery of oxygen from the lungs to the blood is not uniform. The Fick equation also requires several measurements, each with its own degree of measurement error. The use of an assumed value for oxygen consumption, as mentioned previously, is a major potential source of error; hence, the use of the term "estimated Fick cardiac output" may be the more accurate description of what is actually measured in the routine catheterization laboratory practice.

Indicator Dilution over Time: The Thermodilution Technique

Thermodilution measures the rate of change of blood temperature over time. By injecting a fixed volume (10 mL) of chilled or room air temperature injectate (5% dextrose or 0.9% saline) into the right atrial port of the catheter and continuously measuring temperature with a thermistor located at the catheter tip, we can estimate the rate of flow from the right atrium to the catheter tip. Thermodilution calculations are mathematically complex as they account factors such as the expected degree of catheter warming during injection and the specific heat and gravities of blood and the injectate. Numerical cardiac outputs are provided by computerized analysis of temperature versus time curves and the final cardiac output is typically reported as an average of several injections.

Thermodilution correlates reasonably well with other measures of cardiac output but there are several contributors to measurement error. Pulmonary artery temperature can vary with respiration so injection during the same portion of the respiratory cycle (i.e., end expiration) each time reduces the potential for error. Shorter injection periods (<3 seconds) are preferable to longer ones for similar reasons and the injection periods should be as uniform as possible. Smaller injectate volumes with warmer injectate temperatures (i.e., 5 mL injected at room temperature) produce more measurement error than colder, larger volume injections because the signal-to-noise ratio is lower. Thermodilution is not reliable in the presence of significant tricuspid regurgitation or in low output states because the injectate tends to cycle between the right atrium and right ventricle, resulting in a flattened temperature-time curve.

A recent comparative study indicates that the correlation between thermodilution and estimated Fick methods for the calculation of cardiac output is modest ($r = 0.65$), with a difference of >20% demonstrated in about 38% of patients. Low output by the thermodilution method correlated more closely with 3 and 12 months mortality, indicating that it maybe the preferred method of cardiac output calculation.

Risk of Cardiac Catheterization

Proper informed consent should be obtained from the patient or a designated medical decision maker prior to cardiac catheterization. The major risks related to right and left cardiac catheterization appear in Table 14.1. Decompensated heart failure, shock, acute coronary syndromes, left ventricular dysfunction, morbid obesity, depressed mental status, and advanced kidney disease are all associated with increased procedural risk. The risk for stroke increases significantly with cannulation of the left ventricle. Although debilitating strokes are rare the incidence of small, clinically silent strokes assessed by MRI was found to be 22% in one series of patients with severe aortic stenosis who underwent left ventricular cannulation [2]. For this reason, routine left ventricular catheterization should be avoided in favor of a selective approach, reserving left ventricular cannulation for patients with nondiagnostic or conflicting noninvasive test results.

The most common catheterization complications are related to problems with the vascular access site or subsequent hemostasis. When feasible ultrasound or radiographic guidance should be employed to localize landmarks and guide cannulation of large arteries and veins. Morbid obesity is a common contributor to access-related complications, particularly when femoral access is attempted.

Table 14.1 Complications associated with diagnostic left- and right-heart catheterization[a]

Complication (% risk)	Contributing factors	Prevention
Death (0.11%)	High acuity illness	Reassess necessity of the procedure
	Emergency procedure	Have ACLS equipment on stand by
Myocardial infarction (0.05%)	Acute coronary syndromes	Appropriate medical therapy for ACS
	Profound hypertension	Medical management of hypertension
	Profound tachycardia	Medical management of tachycardia
Stroke (0.07%)	Cannulation of left ventricle	Avoid crossing aortic valve unless absolutely necessary
	Atrial fibrillation	Over-the-wire catheter exchanges
	Ascending aortic atheroma	
Access complications (0.43%)	Anticoagulation	Correction of coagulopathy
Major hematomas	Morbid obesity	Radial artery access
Retroperitoneal bleeds	Agitation	Imaging-guided vascular cannulation
Arteriovenous fistulas		Appropriate conscious sedation
Major arrhythmias (0.38%)	Electrolyte disturbances	Correct metabolic derangements
Ventricular fibrillation	Hypoxemia	Supplement oxygen
Ventricular tachycardia	Right coronary conus branch injection	Cautiously injection of right coronary
Complete heart block		
	Catheter-induced endocardial trauma	Use pigtail catheter in left ventricle
	Underlying bundle branch blocks	
Other embolic events (rare)	Pre-existing deep vein thrombosis	Exclude thromboses prior to study
Pulmonary embolism/ infarction	Prolonged immobility	Limit duration of PA catheterization over-the-wire catheter exchanges
Distal atheroembolism	Aortic atheromatous disease	
Contrast nephropathy (variable)	Pre-existing kidney disease	Adequate hydration
	Diabetes	Use of N-acetylcysteine
	Dehydration	Minimize use of contrast
	Large contrast volume	
Serious allergic reactions	Pre-existing allergies	Pretreatment with corticosteroids and antihistamines
Contrast agents (0.37%)		
Local anesthetic (ester agents)		Use of amide anesthetic agents
Respiratory arrest (variable)	Underlying pulmonary disease	Limit the use of sedatives
	Altered mental status	Optimize heart failure and lung disease prior to the study
	Decompensated heart failure	Frequent airway assessment
	Morbid obesity	Anesthesiology consultation
Other vascular complications (0.28%)	Balloon inflation in small arteriole	Avoid inflation in distal PA
Pulmonary artery perforation	Catheter trauma	Cautious catheter removal
Coronary artery dissection		
Perforation of cardiac chamber	Sub-intimal guide wire route	Use flexible J-tipped wires

[a]Adapted from Noto et al. [4]

ACLS advanced cardiac life support, *ACS* acute coronary syndrome, *PA* pulmonary artery

Right-Heart Catheterization Technique

Right-heart catheterization is generally performed using a 7- or 8-French vascular sheath placed in the common femoral vein or right internal jugular vein using modified Seldinger technique and typically under ultrasound guidance. A balloon tipped pulmonary artery catheter is inserted through the sheath and the balloon is inflated once the tip of the catheter has cleared the sheath. The catheter tip, guided by flow and the manipulation of the operator, traverses the heart from the great veins to the pulmonary artery and the pulmonary artery wedge position [3]. The catheter is then connected to the pressure transducer via a multi-port manifold. Blood can also be withdrawn from the catheter for oximetry and chemistry sampling. There is a proximal lumen at the level of the right atrium to allow for thermodilution assessment of cardiac output. Rarely, situations arise where direct measurement of left atrial pressure is desirable, such as in the evaluation of severe native or prosthetic mitral stenosis. Left atrial cannulation can be performed from the right atrium by fluoroscopy-guided needle puncture of the interatrial septum at the level of the fossa ovalis and the use of a Brockenbrough catheter.

Left-Heart Catheterization Technique

Left-heart catheterization is performed by placing a 4-, 5-, or 6-French sheath into a large artery using Seldinger or modified Seldinger technique. Most contemporary laboratories utilize radial artery access as the preferred choice for arterial access for diagnostic procedures, although the traditional right or left common femoral artery approach remains an important alternative, when radial access is not feasible or when larger bore devices are planned or needed. Ultrasound and fluoroscopic guidance are important tools to optimize the technique and safety of arterial access. Brachial artery access remains as an option for left-sided catheterization, although usually a last resort. Once vascular access is obtained the arterial catheters are advanced retrogradely through the aorta preceded by a J-tipped flexible guidewire. The catheters are controlled by the operator and there are numerous specialized catheters available for use. Endhole catheters are useful for pressure measurements and contrast injection during coronary angiography. They are not ideal for opacification of the aorta or left ventricle because they promote contrast streaming and ventricular ectopy. Multi-hole pigtail catheters record the pressure and are better for the opacification of large structures because they uniformly distribute a larger volume of pressured contrast within a chamber. Aortography and ventriculography should be performed using a pigtail catheter. Some pigtail catheters have proximal and distal transducer ports to allow for simultaneous pressure measurements across a given structure such as the aortic valve.

Data Derived from Right- and Left-Heart Catheterization

Pressure Measurements

When intracardiac pressure measurements are gated to the surface electrocardiogram, systolic and diastolic performance of the heart can accurately be assessed (Fig. 14.3). Pressure measurements are obtained by advancing the catheter to the chamber of interest and recording waveforms over several cardiac cycles. Right-sided pressures can vary greatly with respiration in some patients (see Fig. 14.2e), making interpretation difficult. In this case, a several-second end-expiratory breath hold will maintain thoracic pressure at its theoretical "zero point" for a few cardiac cycles. Normal cardiovascular waveforms and their descriptions follow.

Right Atrial Pressure (Fig. 14.4a)
The normal right atrial pressure wave includes the "a" wave, produced by atrial contraction and the corresponding "x" descent during atrial relaxation. Early in the "x" descent there may be a small positive reflection called the "c" wave which represents closure of the tricuspid valve.

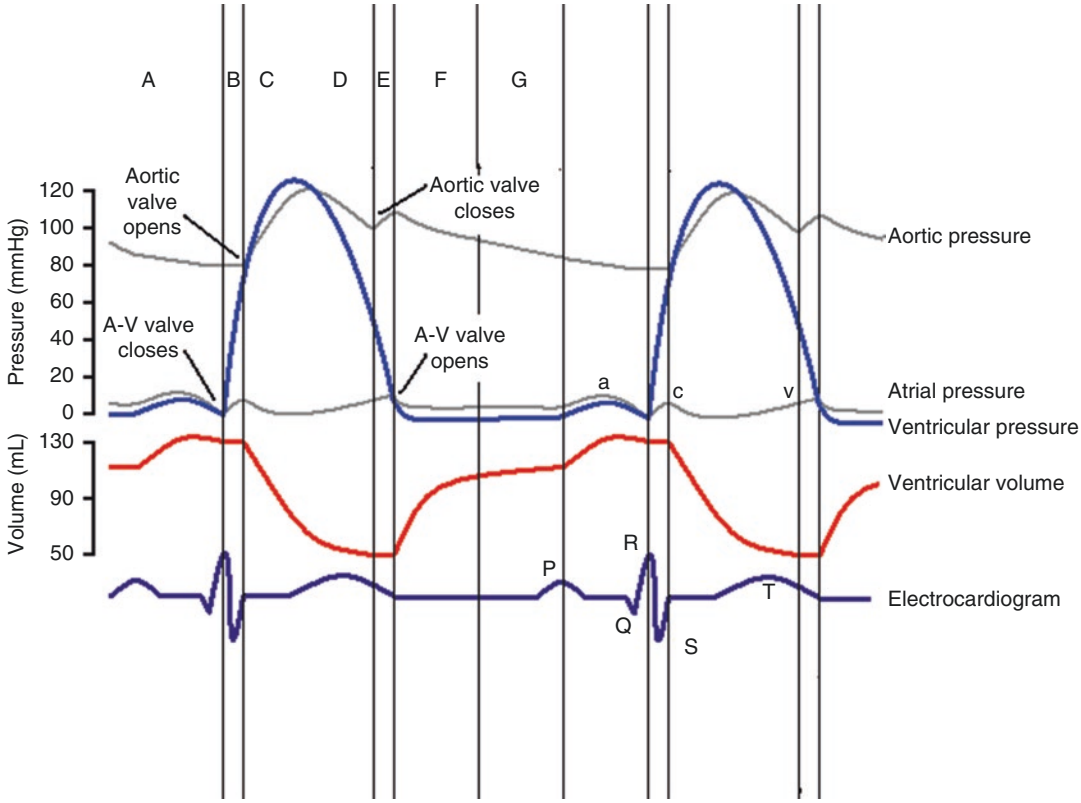

Fig. 14.3 Schematic representation of the major electrical and mechanical events during the cardiac cycle: (**a**) atrial contraction; (**b**) isovolumic contraction; (**c**) rapid ejection; (**d**) reduced ejection; (**e**) isovolumic relaxation; (**f**) rapid ventricular filling; and (**g**) reduced ventricular filling

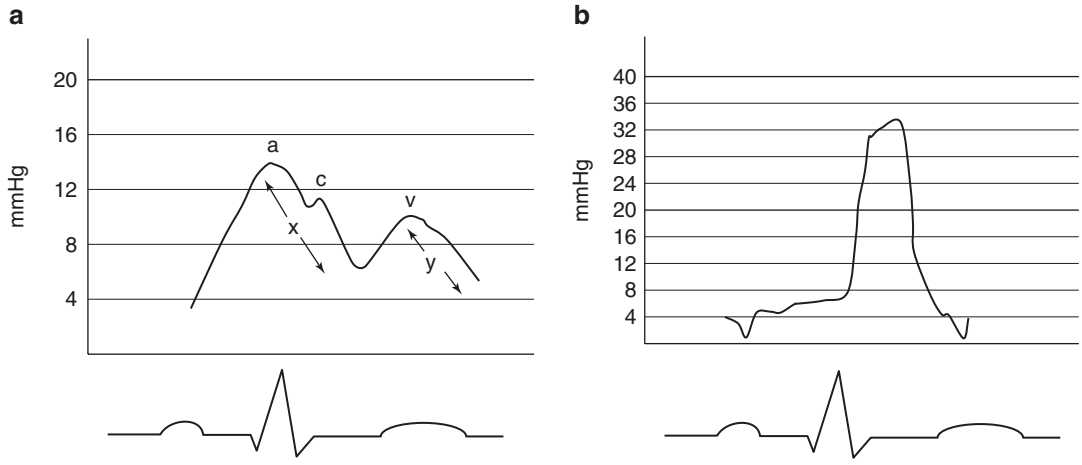

Fig. 14.4 (**a**–**f**) Normal cardiac pressure tracings. Descriptions of each tracing are found within the chapter text. (**g**) Abnormal pressure tracing obtained during selective coronary angiography. In the presence of severe ostial stenosis, the endhole catheter transmits a distorted waveform due to the reflected coronary wedge pressure and appears as a hybrid between aortic and ventricular pressure (ventricularized pressure) waveform

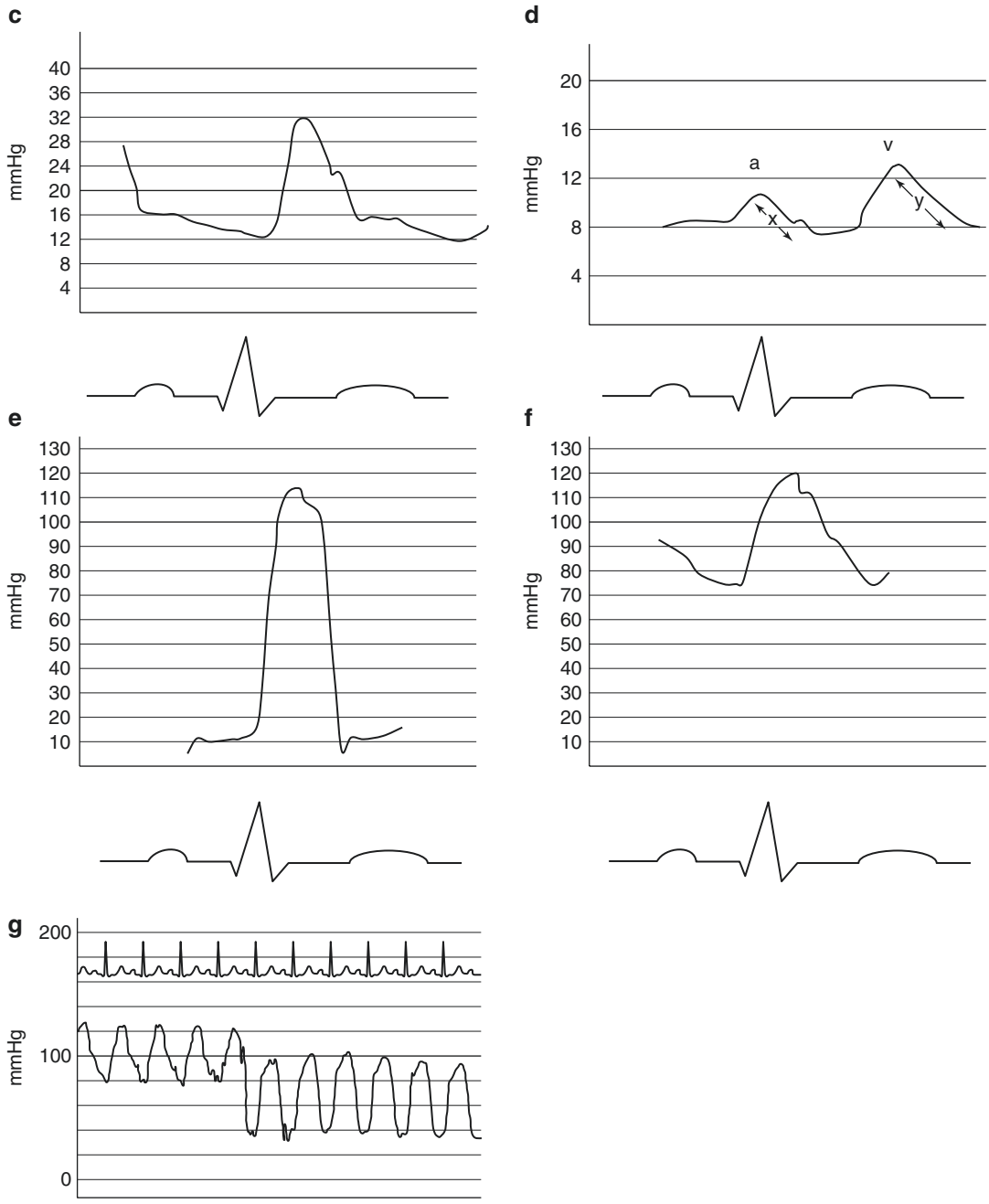

Fig. 14.4 (continued)

The second major wave in the right atrial tracing is the "v" wave, produced by the combination of vena cava flow into the atrium and the upward displacement of the closed tricuspid valve during right ventricular contraction. Once the tricuspid valve opens, the right atrial pressure drops in early diastole, producing the "y" descent. Normal mean right atrial pressure is between 1 and 10 mmHg.

Right Ventricular Pressure (Fig. 14.4b)

The normal right ventricular wave is characterized by a rapid pressure rise during systole followed by

a rapid fall during isovolumic relaxation. Diastolic pressure gradually increases until late systole when the right atrium contracts and right ventricular end-diastolic pressure rises to the level of the atrial "a" wave. Normal right ventricular systolic and diastolic pressure is 15–30 mmHg and 1–10 mmHg, respectively.

Pulmonary Artery Pressure (Fig. 14.4c)

The normal pulmonary artery pressure tracing is a typical arterial waveform with a rapid systolic upstroke. There is a dicrotic notch produced by closure of the pulmonic valve and the diastolic pressure gradually decreases as blood flows from the main pulmonary artery to the lungs. Normal pulmonary artery systolic and diastolic pressure is 15–30 mmHg and 5–10 mmHg, respectively. In intensive care settings, it is common practice to follow the PA end-diastolic pressure as an indirect measure of left atrial pressure. However, this assumption is only true if the pulmonary vascular resistance is close to normal.

Pulmonary Capillary Wedge Pressure, PCWP (Fig. 14.4d)

The PCWP is commonly used as a surrogate for left atrial pressure. This pressure is obtained by cautiously advancing the catheter tip through the pulmonary artery with the balloon inflated until the balloon will no longer advance and appears fixed or "wedged" in the pulmonary bed by fluoroscopy. Inflating the balloon with the catheter tip in the distal pulmonary arterial tree increases the risk for pulmonary artery rupture. The PCWP reflects left atrial pressure because when the balloon is properly wedged there is no longer flow from the proximal PA to the catheter tip. The catheter tip only "sees" the left atrial pressure waves that are reflected back to it through the pulmonary artery capillary bed (Fig. 14.5).

The normal PCWP is analogous to left atrial pressure, with "a" and "v" waves that correspond to left atrial contraction and left ventricular contraction, respectively and their corresponding "x" and "y" descents. It is important to know that left

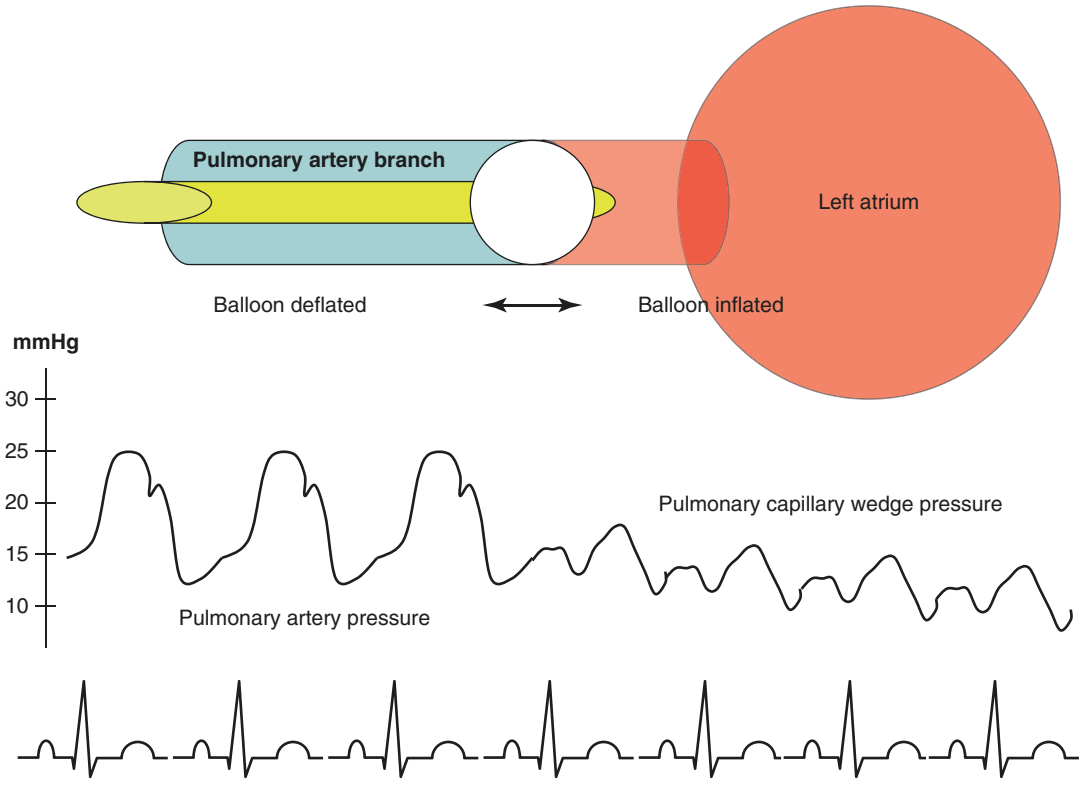

Fig. 14.5 Diagram of the pulmonary capillary wedge technique

atrial activity precedes the reflected wedge pressure by a few milliseconds. This causes the PCWP "v" wave to appear later than the left atrial "v" wave. When the PCWP and left ventricular pressures are superimposed during assessment for mitral stenosis, the result may be overestimation of the transmitral pressure gradient. Normal mean PCWP pressure is between 5 and 12 mmHg, and in the absence of mitral stenosis, it approximates left ventricular end-diastolic pressure.

Left Ventricular Pressure (Fig. 14.4e)
Left ventricular pressure has a rapid upstroke during early systole followed by a rapid descent. Diastolic pressure is low in early diastole and rises slowly until the left atrium contracts. The left ventricular end-diastolic pressure (LVEDP) represents the true preload for the left ventricle, and it is typically measured just prior to abrupt rise in systolic pressure. Normal LVEDP is 5–12 mmHg.

Aortic Pressure and Waveform
(Fig. 14.4f)
Aortic pressure is measured with the catheter tip in the proximal aorta. Central aortic pressures are usually 10–20 mmHg lower than femoral artery pressures due to the greater size and elasticity of the normal aorta. In a normal, high fidelity system, the aortic waveform is characterized by a dicrotic notch which occurs at the closure of aortic valve.

Endhole catheters used for selective coronary angiography should normally transmit a normal waveform of central aortic pressure. In the presence of severe ostial coronary stenosis, the waveform is distorted by the reflected coronary wedge pressure and appears as a hybrid between aortic and ventricular pressure (ventricularized pressure) waveform. The systolic pressure is decreased and the diastolic pressure is markedly decreased, compared to the normal aortic waveform. This should immediately raise concern about severe ostial right or left main coronary stenosis, although the differential diagnosis can simply be a non-coaxial catheter position, with the tip against the wall of the artery (Fig. 14.4g).

Cardiac Output

The Fick method requires sampling of blood from both sides of the pulmonary vascular bed, namely, the pulmonary artery and pulmonary veins or left atrium. Pulmonary artery blood is obtained via aspiration from the distal port of the right-heart catheter. Direct sampling from the left atrium requires transseptal puncture which is impractical for routine diagnostic testing. For this reason, an arterial blood sample (i.e., from the femoral artery sheath) is typically used as a substitute. The thermodilution technique has been previously described.

Normal cardiac output is between 5.0 and 7.5 L/min but varies broadly with patient size and gender (men generally have higher cardiac outputs than women). The human heart can augment its cardiac output over fivefold in certain disease states (i.e., severe anemia, thyrotoxicosis). The cardiac index (cardiac output divided by body surface area, BSA) is a better measure of myocardial performance than cardiac output. The normal range for cardiac index is 2.5–4.0 L/min/m^2. A cardiac index <1.0 L/min/m^2 is not compatible with life.

Vascular Resistance

In a fluid-filled system, resistance (R) is proportional to the pressure difference across the system (ΔP) and inversely proportional to flow (Q); $R = \Delta P/Q$.

By measuring mean aortic pressure (AoP) and mean right atrial pressure (RAP), we can calculate systemic vascular resistance (SVR) in the following manner:

$$\text{Systemic vascular resistance}$$
$$\text{SVR} = \frac{(\text{mean AoP} - \text{mean RAP})}{\text{Cardiac Output}}$$

Similarly, by measuring the mean pulmonary artery pressure (PAP) and left atrial pressure (LAP), either directly or with its surrogate (wedge pressure), we can calculate the pulmonary vascular resistance (PVR):

$$\text{Pulmonary vascular resistance}$$
$$\text{PVR} = \frac{\left(\text{mean PAP} - \text{mean LAP / PCWP}\right)}{\text{Cardiac Output}}$$

Vascular resistances can be expressed in Wood units (mmHg/L/min) or dynes∗s/cm^{-5}. A dyne is the amount of force required to accelerate a 1 gram mass to 1 cm/s^2. 1 Wood unit = 80 dynes∗s/cm^{-5}. Normal systemic vascular resistance is between 8 and 20 Wood units. Normal pulmonary vascular resistance is between 0.25 and 1.6 Wood units.

Shunt Assessment

Shunt flow from the systemic circulation to the pulmonary circulation can be localized and quantified during right-heart catheterization by performing an oximetry saturation run. As the catheter is passed through the great veins to the pulmonary artery, small (2 mL) aliquots of blood are obtained for oximetry from the proximal and distal superior vena cava (SVC), proximal and distal inferior vena cava (IVC), right atrium (low, mid, and high), right ventricle (proximal, mid, and apex), pulmonary artery (main, left, and right), left ventricle, and aorta distal to the ductus arteriosus.

A left-to-right shunt is detected by an oximetry "step-up," where oxygenated left circulation blood mixes with deoxygenated right circulation blood. A "step-up" of ≥7% is considered significant at the level of the great veins and right atrium. A step-up of ≥5% is considered significant at levels distal to the right atrium. Right-to-left shunts are difficult to locate and quantify, and oximetry to detect a "step-down" is generally not performed.

The degree of left-to-right shunting can be quantified by calculating the ratio of pulmonary blood flow (Qp; oxygen consumption divided by the difference in arteriovenous oxygen content across the lungs) to systemic blood flow (Qs; oxygen consumption divided by the difference in arteriovenous oxygen content across the systemic circulation). Systemic mixed venous saturation (MVO_2) is defined as:

$$\text{Mixed venous saturation} \quad \text{MVO}_2 = \frac{\left[(3)\text{SVC saturation} + \text{IVC saturation}\right]}{4}$$

If we assume constant oxygen consumption, hemoglobin concentration, and atmospheric pressure, then many of the terms in this complex calculation cancel out, leaving only the oximetry saturations:

$$\text{Shunt fraction} \quad \text{Qp / Qs} = \frac{\left(\text{Arterial sat}\right) - \left(\text{MVO}_2\text{sat}\right)}{\left(\text{Arterial sat}\right) - \left(\text{pulmonary artery sat}\right)}$$

The pulmonary venous saturation cannot be obtained without transseptal puncture or retrograde catheterization through the mitral and aortic valves. In the absence of a significant right-to-left shunt at the level of the left atrium, ventricle, or proximal aorta, we would expect systemic arterial saturation and pulmonary venous saturation to be the same; thus pulmonary venous saturation is often replaced by systemic arterial saturation in this equation.

Small shunts are defined by Qp/Qs < 1.5 and are often asymptomatic. Large shunts are defined by Qp/Qs > 2.0 and often require closure. Frequently, the location of the shunt is known or suspected from an alternative study such as an echocardiogram, CT scan, or MRI, and catheterization is used to quantify the shunt fraction. In this case, it is not necessary to sample from multiple levels in the same chamber or vessel.

Assessment of Valvular Stenosis

The invasive assessment of valvular stenosis requires measurement of the cardiac output and measurement of the pressure difference across the valve in question. Ideally, pressure measurements should be made simultaneously with two catheters, each coupled to its own transducer and neither crossing the affected valve. The catheters should be placed in the chambers or vessels on either side of the valve, and the pressure tracings should be superimposed to accurately calculate

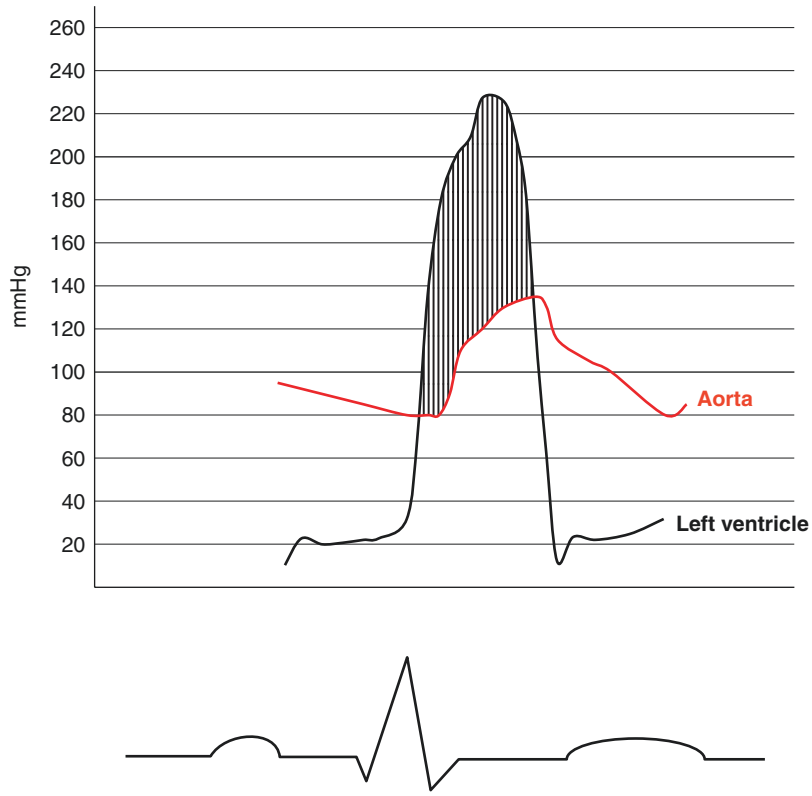

Fig. 14.6 Estimating the transaortic pressure gradient. The pressure waves produced by simultaneous catheterization of the left ventricle and proximal ascending aorta are superimposed. The shaded area under the curve (AUC) is calculated, providing the mean transvalvular gradient

the mean pressure gradient (area under the curve, AUC) (Fig. 14.6).

Assessment of mitral stenosis is performed by measuring simultaneous left ventricular and left atrial pressures. If transseptal puncture is not desired, the pulmonary capillary wedge pressure may be used as a surrogate for the left atrium; however, this may overestimate the magnitude of the gradient since the wedge pressure lags behind true left atrial pressure by a few milliseconds. Assessment of aortic stenosis involves simultaneous measurements in the left ventricle and ascending aorta. Two arterial sheaths can be placed, but this increases the risk for access site complications. Dual lumen pigtail catheters have proximal (ascending aorta) and distal (left ventricle) ports that require two transducers but one arterial access site. Another method is the "pull-back method," where the catheter is withdrawn from the left ventricle into the ascending aorta during continuous recording. This allows for a peak-to-peak measurement of the systolic pressure difference that is not simultaneous and provides a crude approximation of the integrated or mean pressure difference. When aortic stenosis is severe, the catheter itself promotes stenosis, resulting in a higher gradient and potential overestimation of stenosis severity.

The Gorlin formula is typically used to calculate valve areas in the catheterization lab:

$$\text{Gorlin formula} \quad \text{Valve Area}\left(\text{cm}^2\right) = \frac{\text{CO}/[\text{HR}][\text{EP}]}{44.3\times(\text{K})\times\sqrt{\Delta P}},$$

where CO is the cardiac output (L/min), HR is the heart rate (bpm), EP is the ejection period (systolic or diastolic as calculated from the ECG, in seconds/beat), 44.3 is a constant that accounts for energy loss due to acceleration and gravity (cm/s/s), K is a unit-less correction factor (1.0 for the aortic valve and 0.85 for the mitral valve), and $\sqrt{\Delta P}$ is the square root of the mean pressure gradient across the valve. An abbreviated version of

Table 14.2 Criteria for the angiographic assessment of mitral regurgitation

Severity	Grade	Criterion
Mild	1+	Incomplete opacification of left atrium
Moderate	2+	Complete opacification of left atrium but with less relative intensity than the left ventricle
Moderately severe	3+	Complete opacification of left atrium with intensity equal to the left ventricle after 4 beats
Severe	4+	Complete opacification of left atrium with intensity equal the left ventricle within 3 beats

the Gorlin formula, called the Hakki formula, provides a reasonable estimate of valve area as well.

$$\text{Hakki formula} \quad \text{Valve area}\left(\text{cm}^2\right) = \frac{\text{CO}}{\sqrt{\Delta P}}$$

The normal aortic valve orifice area is 3.0–4.0 cm^2. The normal mitral valve orifice area is 4.0–6.0 cm^2.

Assessment of Valvular Regurgitation

The invasive assessment of valvular regurgitation is largely subjective. The severity of aortic and mitral regurgitation can be estimated by applying qualitative criteria to the appearance of aortography and ventriculography, respectively (Table 14.2). The severity of tricuspid and mitral regurgitation can be estimated from the relative magnitude of the "v" waves in the right atrial and PCWP tracings, respectively. However, atrial compliance and ventricular function also influence the amplitude of "v" waves, making this approach fairly non-specific.

References

1. Wiggers CJ. Determinants of cardiac performance. Circulation. 1951;4(4):485–95.
2. Harmon M, Gomes S, Oppenhein C, et al. Cerebral microembolism during cardiac catheterization and risk of acute brain injury: a prospective diffusion-weighted magnetic resonance imaging study. Stroke. 2007;37(8):2035–8.
3. Swan HJ, Ganz W, Forrester J, Marcus H, Diamond G, Chonette D. Catheterization of the heart in man with use of a flow-directed balloon-tipped catheter. N Engl J Med. 1970;283:447–51.
4. Noto TJ Jr, Johnson LW, Krone R, Weaver WF, Clark DA, Kramer JR Jr, Vetrovec GW. Cardiac catheterization 1990: a report of the Registry of the Society for Cardiac Angiography and Interventions (SCA&I). Cathet Cardiovasc Diagn.1991;24(2):75–83.

Suggested Reading

Antman EM, Marsh JD, Green LH, Grossman W. Blood oxygen measurements in the assessment of intracardiac left to right shunts: a critical appraisal of methodology. Am J Cardiol. 1980;46:265–71.

Bashore TM, Bates ER, Berger PB, et al. American College of Cardiology/Society for Cardiac Angiography and Interventions Clinical Expert Consensus Document on cardiac catheterization laboratory standards. A report of the American College of Cardiology Task Force on clinical expert consensus documents. J Am Coll Cardiol. 2001;37:2170–214.

Opotowsky AR, Hess E, Maron BA, et al. Thermodilution vs estimated Fick cardiac output measurement in clinical practice: an analysis of mortality from the Veterans Affairs Clinical Assessment, Reporting, and Tracking (VA CART) program and Vanderbilt University. JAMA Cardiol. 2017;2(10):1090–9.

Sandoval Y, Burke MN, Lobo AS, et al. Contemporary arterial access in the cardiac catheterization laboratory. JACC Cardiovasc Interv. 2017;10(22):2233–41.

Todorovic M, Jensen EW, Thøgerson C. Evaluation of dynamic performance in liquid filled catheter systems for measuring invasive blood pressure. Int J Clin Mon Comp. 1996;13(3):173–8.

Part IV

Specific Hemodynamically Compromised Situations

Tamponade

15

Olcay Aksoy, Begum Sezer,
and Leonardo Rodriguez

Case Presentation

A 47-year-old female with history of systemic lupus erythematosus (SLE) presents with exertional dyspnea. She reports development of peripheral edema in the past month and has had onset of exertional dyspnea in the past few days.

Salient physical examination findings include a heart rate of 92, blood pressure of 136/72, elevated JVP at 16 mmHg, and grade I/VI early systolic murmur at left lower sternal border. The lung fields are clear. There is 2+ pitting lower extremity edema. Pulsus paradoxus is measured to be 8 mmHg.

A chest X-ray shows an enlarged cardiac silhouette. An ECG shows electrical alternans (Fig. 15.1). An urgent echocardiogram shows increased respirophasic variation across mitral and tricuspid valves (Fig. 15.2a, b).

The patient is admitted to the hospital for further evaluation and management. Over the course of the admission, the patient becomes gradually confused. Laboratory evaluation reveals evidence of mild renal dysfunction and a mild transaminitis. She now has a heart rate of 108 and her blood pressure is 92/56. She is transferred to the Intensive Care Unit and a pulmonary artery catheter is placed, which notes right atrial tracings showing blunted *y* descent (Fig. 15.3a). She subsequently receives a pericardiocentesis with improvement in hemodynamics (post-pericardiocentesis tracings shown in Fig. 15.3b). The patient improves clinically and subsequently is discharged on an intensified treatment regimen for SLE. A follow-up echocardiogram is scheduled.

Introduction

Anatomy

The myocardium is encased in a relatively rigid and noncompliant sac called the pericardium. The pericardium is formed by two layers. The outer sac, called the fibrous pericardium, is composed of fibrous tissue and encases the inner layer of pericardium and the heart. The inner sac has two layers – called the parietal and visceral pericardium. The parietal pericardium is attached to the internal surface of the fibrous pericardium and is contiguous with the visceral pericardium as it gets reflected on the cardiac surfaces. In between the visceral and the parietal pericardium is the pericardial space. This space

O. Aksoy (✉)
David Geffen School of Medicine, UCLA Medical Center, Los Angeles, CA, USA
e-mail: oaksoy@mednet.ucla.edu

B. Sezer
UCLA Medical Center, Los Angeles, CA, USA
e-mail: bsezer@mednet.ucla.edu

L. Rodriguez
Cleveland Clinic, Cleveland, OH, USA
e-mail: rodrigl@ccf.org

A. T. Askari, A. W. Messerli (eds.), *Cardiovascular Hemodynamics*, Contemporary Cardiology,
https://doi.org/10.1007/978-3-030-19131-3_15

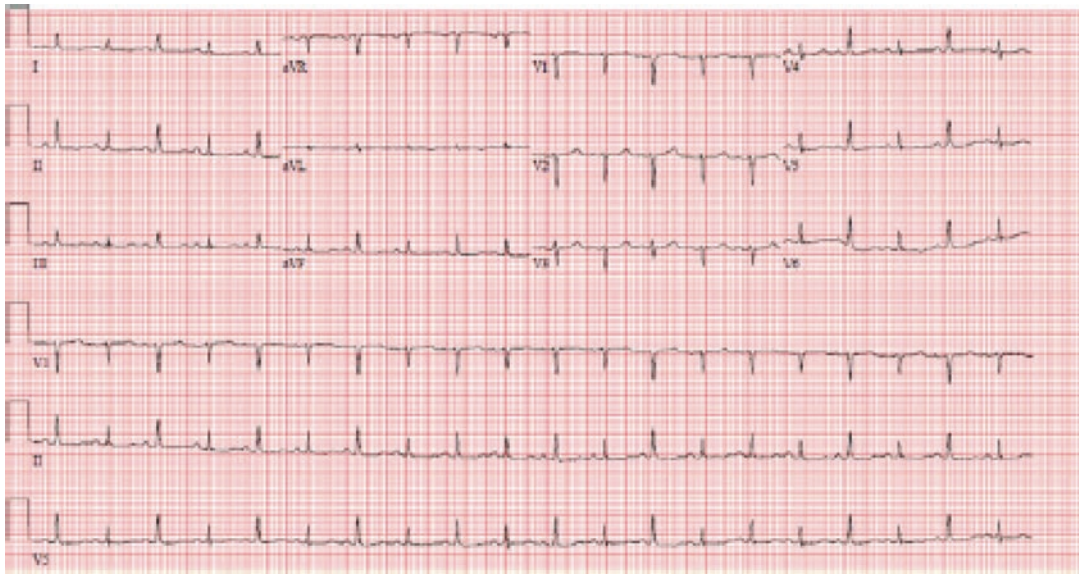

Fig. 15.1 ECG demonstrating electrical alternans

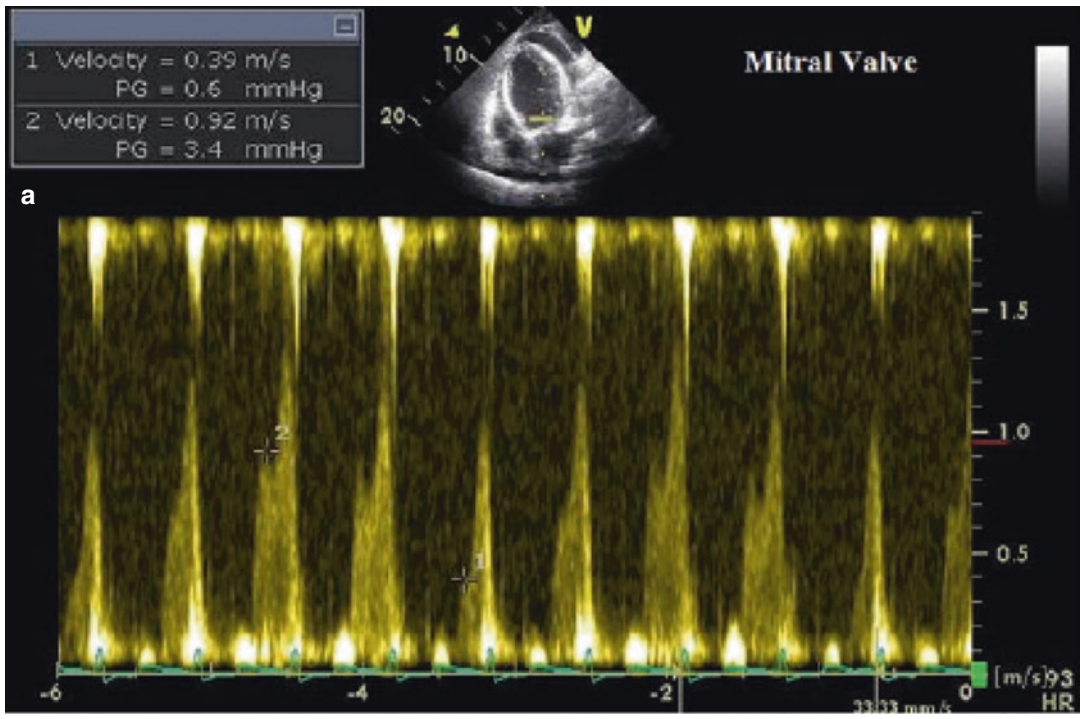

Fig. 15.2 Echocardiogram with Doppler evaluation demonstrating respiratory flow variation across mitral (**a**) and tricuspid valves (**b**)

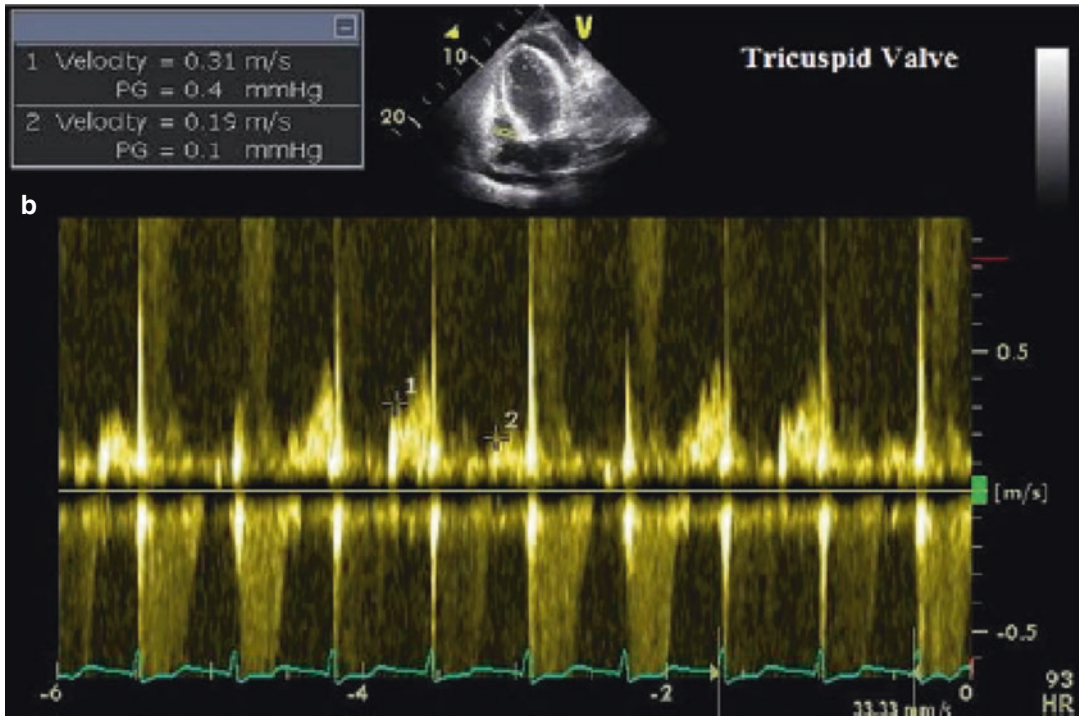

Fig. 15.2 (continued)

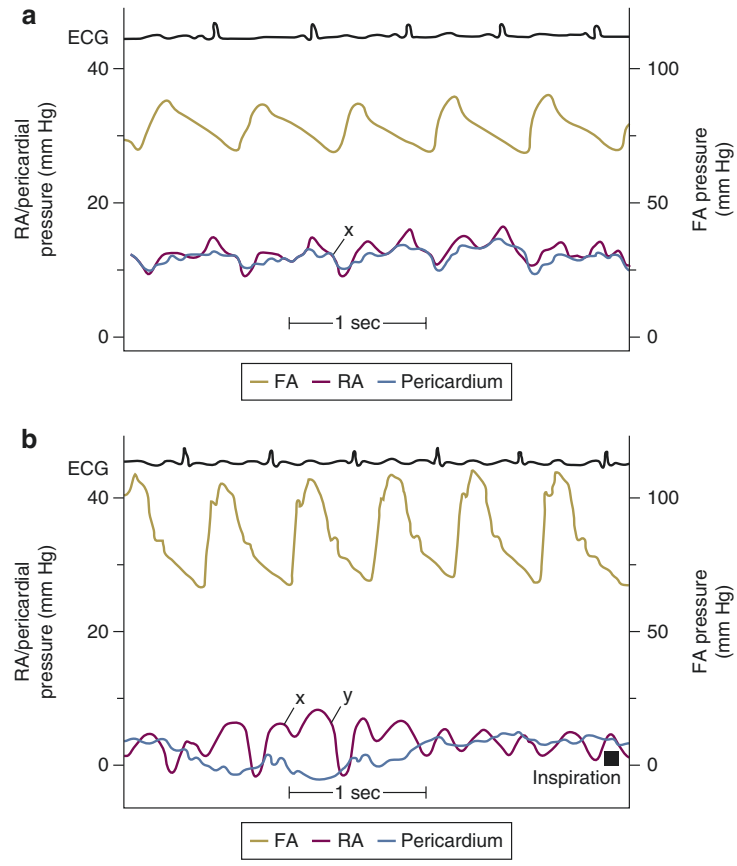

Fig. 15.3 Pre-pericardiocentesis (**a**) and post-pericardiocentesis (**b**). (Reprinted from modification by LeWinter [9])

normally contains up to 50 mL of serous fluid to maintain a low friction environment for the myocardium as it contracts and relaxes within the pericardium throughout the cardiac cycle. The pericardium effectively restrains the cardiac chambers to a confined space and due to this pericardial constraint, any change in the volume of one chamber of the heart is reciprocated by changes in other chambers in the opposite direction [1]. It is this complex interaction of pericardial space with the intracardiac chambers that leads to the hemodynamic consequences of pericardial effusions.

Several diseases and complications of invasive procedures may lead to pathologic accumulation of fluid in the pericardial space, which may impact cardiac output. When the accumulation of pericardial fluid interferes with diastolic filling of the heart, hemodynamic consequences associated with varied clinical presentations including tamponade ensue.

Pathophysiology of Tamponade

Pericardial effusion can be classified according to its onset, size, distribution and composition. The onset can be acute, subacute or chronic (>3 months). The size is based on echocardiogram assessment and is classified as mild (<10 mm), moderate (10–20 mm), or large (>20 mm). Pericardial fluid (exudate, transudate or blood) may distribute in a circumferential or loculated fashion. A variety of different processes can cause pericardial effusion which may eventually lead to cardiac tamponade. Some of these etiologies include malignancy, acute pericarditis, trauma, uremia, iatrogenic, idiopathic, post-acute myocardial infarction, other causes (infection, collagen vascular disease, radiation, heart failure, hypothyroidism).

Progression of a pericardial effusion to tamponade depends on several factors. These include the rate of fluid accumulation, tensile properties of the pericardium, intracardiac pressures, and tensile properties of the myocardium. Ultimately, it is the intrapericardial pressure and its interaction with intracardiac pressures (transmural pressure) that determines the presence of tamponade.

$$\text{Transmural pressure} = \text{intracardiac pressure} - \text{intrapericardial pressure}$$

When the intrapericardial pressure equalizes or exceeds that of the intracardiac chambers, the transmural pressure is then <0, and impaired filling occurs. In patients with pericardial effusions, negative transmural pressure is more often due to increased pericardial pressure but decreased intracardiac pressures also contribute to the development of tamponade.

In cardiac tamponade, increased pericardial pressure from fluid accumulation leads to compression of the cardiac chambers. Hemodynamics of the left and right heart chambers are greatly influenced by each other, which is commonly known as ventricular interdependence. During inspiration, intrathoracic pressure decreases which gets transmitted through the pericardium to the right side of the heart and pulmonary vasculature, causing increased venous return to the right heart. Normally, the free wall expands to accommodate the increased venous return; however, in cardiac tamponade, the free wall cannot expand properly. Hence, the interventricular septum bulges toward the left ventricle to allow right-sided filling, thereby reducing left ventricular compliance and filling during inspiration.

Determinants of intrapericardial pressure include the volume of pericardial fluid and the compliance of the pericardium. The relationship between the size of the effusion and the associated increase in pressure is not linear and is modified by the compliance of the pericardium itself. As such, a larger but chronic effusion might be better tolerated than a smaller but rapidly accumulating one, due to a higher pericardial compliance that develops in the chronic setting (Fig. 15.4). Therefore, the size of the effusion should not be used as a sole criterion for the presence of tamponade.

Progression of a pericardial effusion to tamponade also depends on the intravascular volume status of the patient as well as the compliance of the myocardium. Patients who are intravascularly depleted are more likely to present with compromised hemodynamics due to diminished filling pressures in the cardiac chambers. On the

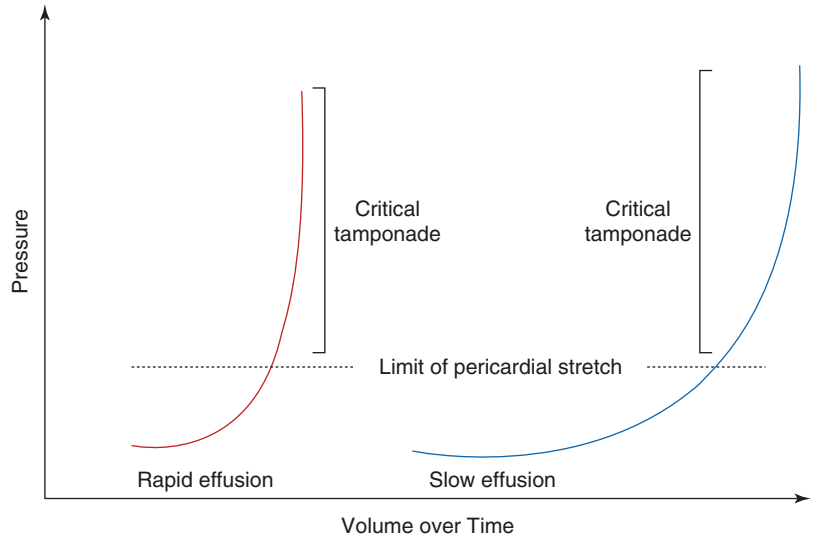

Fig. 15.4 Intrapericardial pressure that is critical in determining the transmural pressure is affected by the time course of fluid accumulation. Rapidly developing effusions reach the limits of the pericardial stretch sooner, whereas slowly developing effusions are better tolerated due to the time allowed for the pericardium to adapt to the changes imposed by the effusion. (Adapted from Spodick [10])

contrary, those with ventricular hypertrophy or restrictive heart disease may not present with tamponade physiology for a given intrapericardial pressure as this pressure is not readily transmitted to the intracardiac chambers due to the diminished compliance of the myocardium.

Table 15.1 Three stages of tamponade

1. Pre-tamponade: no clinical evidence of tamponade as transmural pressure >0; however exaggerated tricuspid and mitral inflow patterns noted
2. Early tamponade: right-sided chambers are affected as the pericardial pressure increases. Clinical presentation might become apparent
3. Tamponade: both right and left-sided chambers are affected as there is equalization of pressures with pericardium. Clinical tamponade is evident

Stages of Pericardial Tamponade

Pericardial tamponade was previously thought of as an "all or none" clinical disorder [2]. However, it is now recognized that patients might present at different stages along the spectrum of tamponade physiology (Table 15.1). The first stage (pre-tamponade) occurs when the pressure in the pericardium is less than right and left ventricular end diastolic pressures (transmural pressure still >0). In this stage, the effusion does not have a clinically significant hemodynamic impact; however, there may be subtle changes in echocardiographic respiratory flow variation across mitral and tricuspid valves and minimally increased pulsus paradoxus pressure (<10 mmHg). In the second stage, the pericardial pressure equals the right ventricular diastolic pressure leading to collapse of the right ventricle during early diastole. In this case, while there is no collapse in the left ventricle, clinical and hemodynamic evidence for tamponade is present with decrease in right ventricular stroke volume. Hypotension, compensatory tachycardia, and elevated pulsus paradoxus might be present. Finally, the most severe stage presents when left ventricular filling is also affected by the increased pericardial pressure. In this case, there is equilibration of pericardial, right ventricular and left ventricular diastolic pressures leading to severely impaired filling of the ventricles and low stroke volume (Fig. 15.5) [3]. Patients in the final stage of tamponade require expeditious diagnosis with direct intervention to drain the pericardial fluid and reestablish hemodynamic stability.

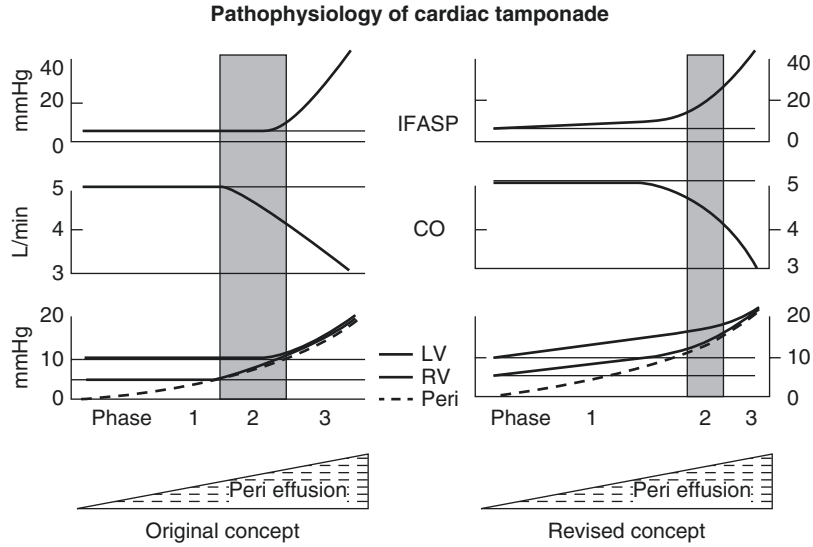

Fig. 15.5 Stages of pericardial tamponade showing pressures in the right atrium, right ventricle, pulmonary capillary wedge pressure, and intrapericardium (peri pericardium, RV right ventricle, LV left ventricle, CO cardiac output, IFASP inspiratory decrease in arterial systolic pressure). Initial concept and its revision with further data are shown below detailing changes in the pressures across stages of tamponade. (Adapted from Reddy et al. [3])

Low-Pressure Tamponade

This condition has been described as a form of tamponade in which relatively low intrapericardial pressure causes cardiac chamber compression in patients with low diastolic pressures (6–12 mmHg). Reported to be present in 20% of patients with tamponade physiology, this condition might be associated with hypovolemia and/or vasodilator and diuretic use [4]. Overall, findings from pulmonary artery catheterization are similar, with equalization of diastolic pressures noted, albeit at lower pericardial and diastolic pressures. Characteristic respiratory fluctuations in transvalvular diastolic Doppler flows are also typically noted. Given the low pressures, patients might not present with typical physical examination findings (elevated JVD, tachycardia); however, they do benefit from pericardiocentesis [4]. When evaluating a patient with a pericardial effusion and hypotension, this clinical entity should be kept in mind.

Diagnosis

Physical Exam Findings

While physical exam might vary in patients with tamponade, there are certain classic findings as defined by Dr. Claude Beck in 1935: low blood pressure, jugular venous distention, and muffled heart sounds. While all three might not be present even in the most advanced cases of tamponade, hypotension and tachycardia, with a narrow pulse pressure, should alert the clinician to its presence.

Pulsus Paradoxus

Originally described by Kussmaul in 1873, pulsus paradoxus is defined by a $\geq$ 10–12 mmHg or a > 9% decline in arterial systemic pressure with inspiration [5]. While the etiology of this drop is debatable, the most widely accepted explanation has to do with intrathoracic pressure changes with

inspiration and the fact that the total volume within the pericardium is fixed. Intrapericardial pressure normally ranges from −5 to +5 cm of water and fluctuates significantly with respiratory cycle. The drop in the intrathoracic pressure with inspiration is transmitted to the pericardium and the right atrium which results in increased venous return to the right side of the heart. The opposite occurs in the left heart, where there is diminished filling of the left ventricle in early inspiration and slightly reduced systemic stroke volume. The reverse is true in expiration: As the intrathoracic pressure increases, the right-sided filling diminishes resulting in improved filling of the left ventricle leading to a higher systemic stroke volume. In a normal individual, these respiratory changes result in a 3–4 mm change in systolic pressure as measured peripherally. When there is a hemodynamically significant tamponade, however, there is interventricular dependence of LV and RV, which leads to exaggeration of the above-described pressure changes with respiration. This is due to the fixed space that the myocardium is constrained within as the increased filling of the RV compromises the filling of the LV, which subsequently leads to the diminished systemic stroke volume with the next contraction. As the underfilled LV cannot generate the normal stroke volume, the blood pressure drops >10 mmHg, which is recognized as pulsus paradoxus on physical exam.

While checking for the presence of pulsus paradoxus allows for quick assessment of patient at the bedside, several coexisting conditions might diminish the accuracy of this test. In patients who have lung disease and shock, pulsus paradoxus might already be present without tamponade. Also, this finding might be absent despite a hemodynamically significant tamponade in the presence of coexisting LV dysfunction with elevated LVEDP, severe aortic insufficiency, pulmonary hypertension, and right ventricular hypertrophy [6, 7].

ECG Findings

Sinus tachycardia, low QRS voltage and electrical alternans are possible ECG findings in tamponade. Sinus tachycardia is the most common finding as heart rate increases to help maintain cardiac output. The amplitudes of the QRS complexes can be low as the fluid collection between the heart and the recording electrodes have a damping effect. Electrical alternans is a phenomenon where QRS complexes alternate in height as the heart swings back and forth within a large fluid filled pericardium (Fig. 15.1). This is a relatively specific finding for tamponade; however, it is not very sensitive.

Echocardiographic Findings

Although tamponade is a clinical diagnosis, echocardiographic evaluation of the patient is a very useful adjunct as it provides direct visualization of the pericardium, the cardiac chambers, and early hemodynamic signs of tamponade physiology. Several echocardiographic parameters may be used to evaluate for evidence of tamponade including M-mode, Doppler interrogation, and 2D visualization. While 2D and M-mode provide visual confirmation of the effusion and the collapse of chambers, Doppler evaluation can be useful in determining the abovementioned flow variations in tamponade (Table 15.2).

Exaggerated diastolic right atrial free wall collapse and diastolic right ventricular outflow tract collapse are early signs of elevated intrapericardial pressure. Brief inversion of the atrial wall can be seen during atrial contraction and does not represent tamponade physiology. Prolonged atrial wall inversion (>1/3 of cardiac cycle) is more indicative of increased intrapericardial pressures. The right ventricular outflow tract is the most easily compressible component of the right ventricle, and may also be affected early

Table 15.2 Evidence of tamponade on echocardiogram

Presence of an effusion. Size, while predictive, is not a reliable determinant of clinical tamponade
Early diastolic collapse of right ventricle
Late diastolic right atrial inversion
Dilated inferior vena cava (>2.5 cm) with failure to collapse of the vessel with inspiration >50%
Respiratory inflow variations across the tricuspid valve (>40%) and the mitral valve (>25%)

Table 15.3 Typical order of findings in tamponade

Tricuspid inflow variation with respiration increased
Mitral inflow variation with respiration increased
Right atrial exaggerated late diastolic collapse (sensitive, nonspecific finding on echocardiogram)
Right ventricular outflow tract collapse (specific finding on echocardiogram)
Right ventricular free wall collapse
Left ventricular free wall collapse

from elevated intrapericardial pressure. As the intrapericardial pressure increases, the right ventricular free wall may also collapse in diastole. Collapse of these above right-sided chambers is indirect evidence that the intrapericardial pressure has exceeded the intracardiac pressures, leading to the inversion of the free walls [1]. As tamponade progresses, further collapse of the left ventricle can also be seen due to similar mechanisms (Table 15.3). Both 2D and M-mode techniques may be used to identify these anatomic manifestations of tamponade.

Doppler evaluation is very helpful in assessing the hemodynamic impact of the pericardial effusion. Outflow across aortic and pulmonary valve (Velocity Time Integral) and inflow across mitral and tricuspid valves (peak velocity) can be measured. In a normal patient, these parameters of flow demonstrate minimal respiratory variation, with the pulmonic and aortic valve velocity time integral varying <10% and the mitral and tricuspid valve peak inflow velocities varying <15% and <25%, respectively. In patients with tamponade, however, respiratory variation across the mitral valve is usually >25% and that across the tricuspid valve >40% (Fig. 15.6). This exaggerated variation in flow across valves provides indirect evidence for ventricular interdependence and suggests a hemodynamically significant effusion.

Also helpful, although often ignored, is the Doppler flow pattern of the hepatic vein. The hepatic vein flow pattern reflects the venous pressure. The normal hepatic vein flow has three major waves: positive systolic and diastolic flows (toward the atrium) and a negative flow corresponding to the atrial contraction (away from the atrium). The systolic flow wave corresponds to the *x* descent and the diastolic flow wave to the *y* descent. In patients with tamponade physiology, blood enters the right atrium only or mostly during ventricular systole. This is reflected in the hepatic vein flow as a predominant systolic wave with decreased or even absent diastolic flow wave (i.e., corresponding to blunted *y* descent on the RA tracing). After pericardiocentesis, the diastolic flow is reestablished (Fig. 15.7).

Pulmonary Artery Catheter Findings

While not routinely used for diagnosis, insertion of a pulmonary artery catheter may provide insight into the pathophysiology of tamponade as it can help clarify the diagnosis.

The cardinal finding on PA catheterization during tamponade is diastolic equalization of pressures of the right atrium, RV diastolic pressure, pulmonary arterial diastolic pressure, and pulmonary capillary wedge pressure. A difference <5 mmHg suffices to establish this equivalency. This pressure is felt to be the passive pressure in the intra-cardiac chambers and should be equal to the intrapericardial pressure in severe tamponade (Fig. 15.8).

As mentioned above, the other abnormal finding is blunted *y* descent following the *v* wave in the right atrial tracing. In tamponade, the *a* wave, *x* descent, and *v* wave remain unaffected as the contraction of the atrium, its relaxation, and rapid filling remain unchanged. The *y* descent, which represents the rapid emptying of the atrium into the right ventricle, is blunted. This is due to the impaired RV relaxation in early diastole due to the effusion-related elevation in RV diastolic pressure. Thus, the rapid emptying of atrium to ventricle, i.e., the *y* descent is blunted (Fig. 15.9). This finding is readily reversed when pericardiocentesis is performed and the intrapericardial pressure is reduced. As the right ventricle is able to relax more efficiently, there is improved flow from the atrium to the ventricle hence a normalized *y* descent.

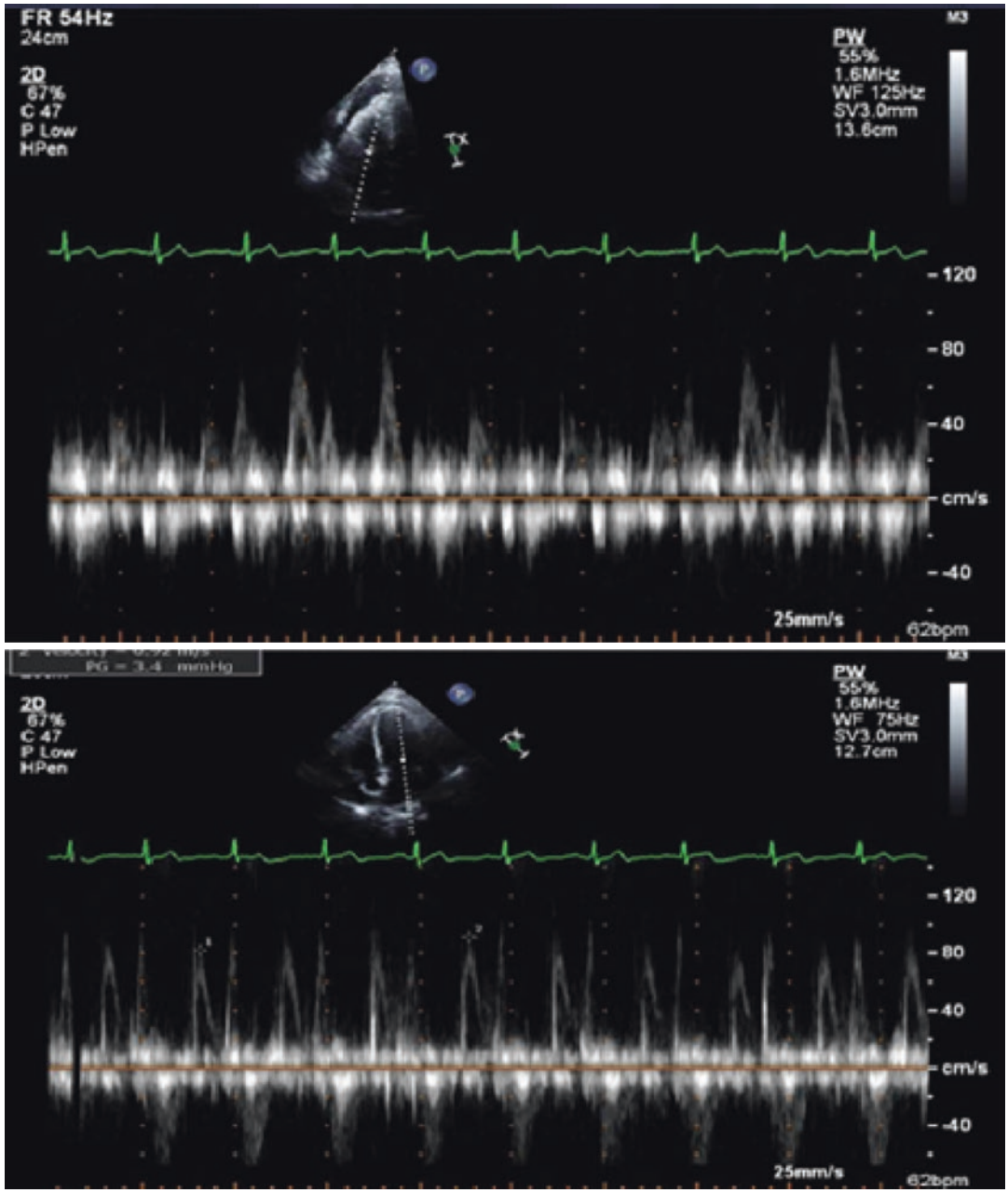

Fig. 15.6 *Top panel* showing tricuspid and *bottom panel* showing mitral valve inflow pattern

Distinction from Constriction

Intrathoracic pressures and changes during inspiration are readily transmitted to the pericardium and the intracardiac chambers in the case of a pericardial effusion with a relatively normal pericardium. In patients who have constrictive pericardium, these pressures are not transmitted, which as a result leads to differences in physical exam and invasive hemodynamic findings. Constriction is notable for lack of decreased right-sided pressure with inspiration, leading to the Kussmaul's sign, a finding not seen in

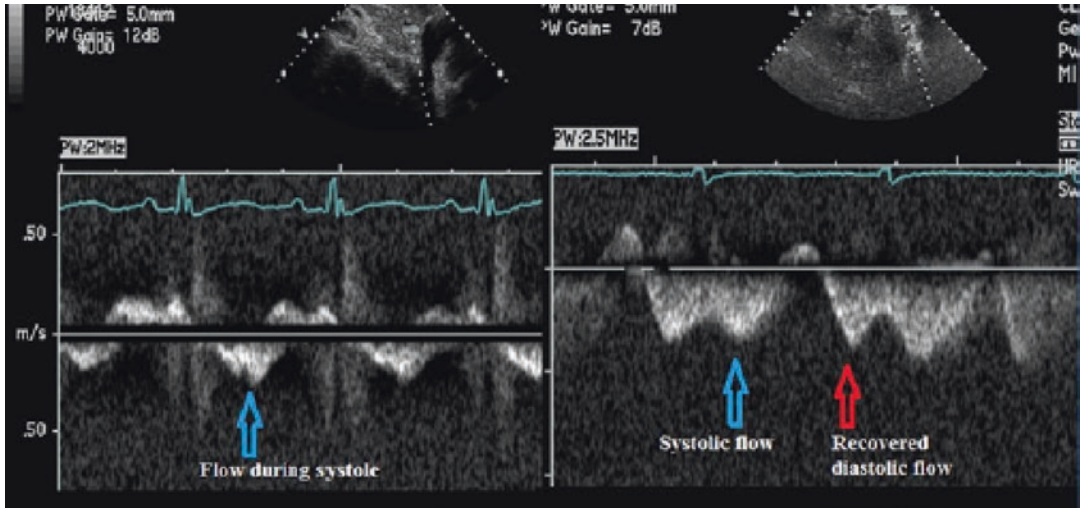

Fig. 15.7 Hepatic vein tracing showing flow to the atrium predominantly during systole and blunted return in diastole. After pericardiocentesis, flow to atrium during diastole is recovered

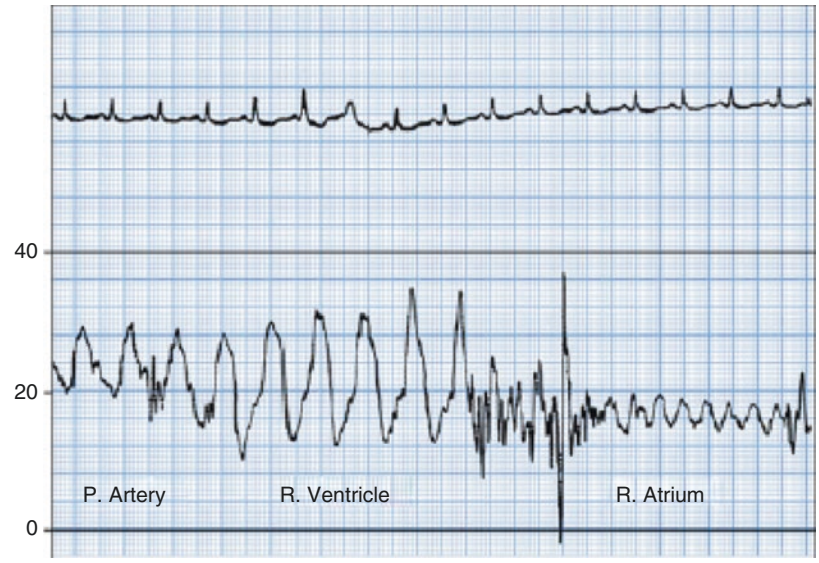

Fig. 15.8 Diastolic equalization of right atrial (mean), right ventricular end diastolic, pulmonary arterial diastolic pressures demonstrated as the PA catheter is pulled back from the pulmonary artery

tamponade. Furthermore, in patients with constriction, there is rapid ventricular filling in early diastole, which is recognized as a prominent *y* descent with a "dip and plateau" appearance (square-root sign) on pulmonary artery catheterization. Such is not the case for tamponade where ventricular filling in early diastole is in fact impaired leading to a blunted *y* descent.

Computed Tomography and Magnetic Resonance Imaging

Advanced imaging such as CT and MRI may be useful to evaluate chronic pericardial effusions but should not be used in the setting of tamponade.

Pericardial effusion might be incidentally diagnosed with these imaging modalities. CT

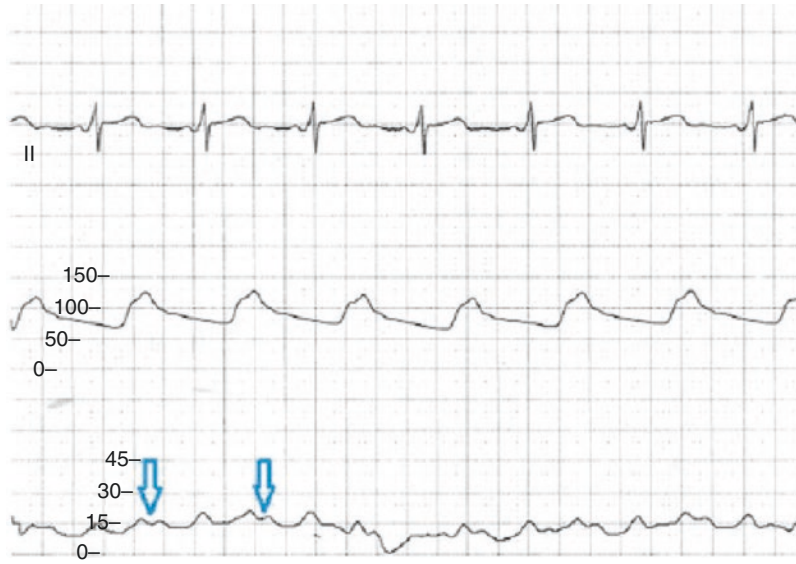

Fig. 15.9 Right atrial pressure waveform with blunted *y* descent

findings of tamponade include enlargement of the inferior vena cava (IVC) with possible reflux of contrast material within the IVC, enlargement of the vena cava, reflux of contrast material within the azygous vein, flattening of the anterior surface of the heart, and enlargement of hepatic and renal veins [8]. These findings are not specific but collectively can suggest tamponade.

When cardiac tamponade is suspected, clinical assessment of the patient should be performed. In the event that there is a question of tamponade, hemodynamic assessment with a focused physical exam and echocardiography should not be delayed. MRI, in fact, can provide further hemodynamic information in these patients; however, when tamponade is suspected, testing and treatment should not be delayed for performing this test.

Pericardial Tamponade in the Postsurgical Patient

While most effusions seen in clinical practice are circumferential, loculated effusions may be seen in postoperative settings and post trauma. Chronic effusions, though initially circumferential, might organize into loculated effusions as well. In this setting, the aforementioned discussions about hemodynamics might not hold true. There may be focal compression of a cardiac chamber that might only be visible by 2D echocardiography. Doppler findings are also less helpful in postsurgical effusions; it is not uncommon to see exaggerated respiratory flow variation even in patients with small effusions. This may be due to increased respiratory effort secondary to pleural effusions or abnormal respiratory dynamics. When a case of focal tamponade is suspected, the clinical status of the patient and location of the effusion should be carefully assessed for further management.

Management

Patients who present with clinical tamponade should be treated emergently. While preparing the patient for removal of the pericardial fluid, intravenous administration of fluids to maintain adequate perfusion pressure is necessary. The administration of fluids improves the intracardiac filling and might stabilize the patient's hemodynamics by increasing the transmural pressure. Either a pericardiocentesis or a pericardial window might be necessary to resolve the compression of the cardiac chambers. Typically anterior,

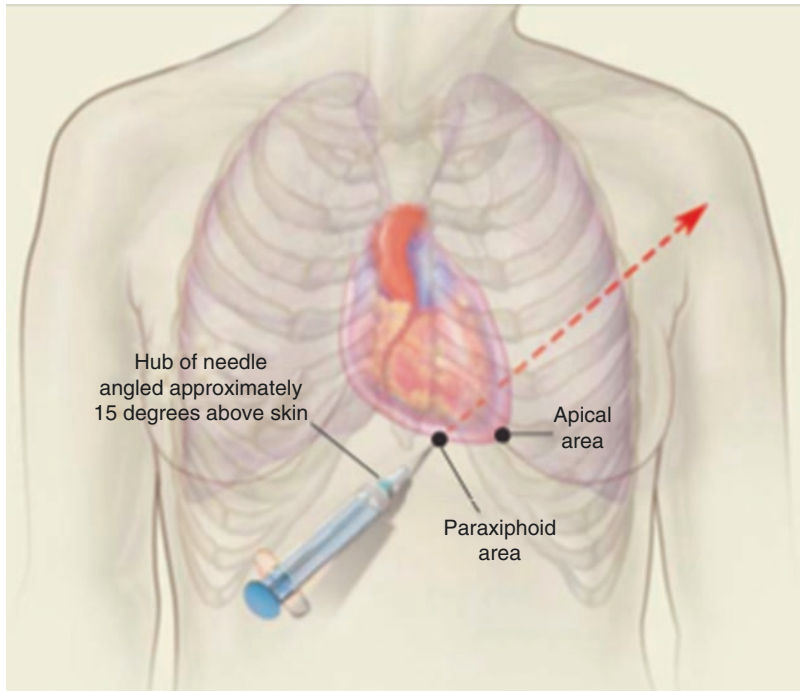

Fig. 15.10 Pericardiocentesis can be performed using paraxiphoid approach where the needle is inserted between xiphoid process and left costal margin at a 15° angle above the skin. In apical approach, the needle is inserted 1–2 cm lateral to the apex within the fifth, sixth, or seventh intercostal space. (Adapted from Spodick [10])

lateral, and apical effusions might be drained by a percutaneous approach; however, surgical drainage is preferred for postoperative patients, loculated, and posterior effusions. The risks and benefits of both approaches in conjunction with the clinical scenario should be taken into account (Fig. 15.10).

Pearls of Assessment

- Pericardial tamponade is a clinical diagnosis.
- Tamponade occurs when transmural pressure is <0.
- When tamponade is in question, all measures for accurate diagnosis and stabilization of the patients should be undertaken.
- Echocardiography is the primary modality to establish the presence of an effusion and support the clinical diagnosis of tamponade.
  - Right atrial and/or ventricular wall inversion.
  - Increased respiratory variation in mitral and tricuspid flows.
  - IVC plethora – dilated IVC with blunted diastolic hepatic vein flow is the most sensitive early echocardiographic finding in tamponade. This may be absent in patients with low-pressure tamponade.
- Pulmonary artery catheterization might be useful to confirm the clinical suspicion in select cases.

Board-Style Questions

1. A 72-year-old man presents with exertional dyspnea and work up including an echocardiogram shows a large pericardial effusion. Which of the following is more specific sign of tamponade?
   A. Systolic flow reversal in hepatic veins
   B. Early diastolic collapse of right atrium
   C. Diastolic collapse of right ventricle
   D. Hypotension in a patient with pericardial effusion
   E. Presence of a large pericardial effusion

2. A 67-year-old female with morbid obesity and rheumatoid arthritis presents with hypotension of unclear etiology. An echocardiogram is performed; however, parasternal and apical windows are difficult to interpret due to body habitus, but there is a moderate circumferential pericardial effusion. Best Doppler hemodynamics are only obtained in the subcostal views. What's expected in the hepatic vein flow pattern in the setting of tamponade?
   A. Diminished forward flow during systole
   B. Diminished forward flow during diastole
   C. Flow reversal during systole
   D. Hepatic vein flow pattern is not expected to change with tamponade
   E. Exaggerated forward flow during diastole
3. Which of the following is not a part of Beck's triad?
   A. Muffled heart sounds
   B. Hypotension
   C. Elevated JVD
   D. Kussmaul's sign
4. A 39-year-old female with a history of tuberculosis as a child presents with pitting peripheral edema and increased fatigue. Echocardiographic evaluation shows pericardial thickening with a moderate effusion. Her heart rate is 102 and blood pressure is 94/64. Which of the following can be helpful in distinguishing tamponade from constriction?
   A. Presence of a pericardial effusion
   B. Absence of Kussmaul's sign
   C. Pericardial thickening seen on CT
   D. Exaggerated flow across tricuspid valve during inspiration
   E. None of the above
5. What's the initial treatment strategy in a hypotensive and tachycardic patient with a pericardial effusion if tamponade is suspected?
   A. Pericardiocentesis
   B. IV fluid infusion
   C. Inotrope infusion
   D. Consultation with cardiothoracic surgery for a pericardial window
   E. Beta blocker administration

Answers to Board-Style Questions

1. Correct answer is C. Systolic flow reversal in hepatic veins is seen in severe tricuspid regurgitation. While options other than C can be seen in tamponade, they are not specific to tamponade.
2. Correct answer is B. Diastolic forward flow is expected to be reduced in the hepatic veins due to elevated right ventricular pressures. Other options do not apply in tamponade.
3. Correct answer is D. Beck's triad consists of muffled heart sounds, hypotension, and elevated neck veins.
4. Correct answer is B. Other options can be seen with both conditions; however, Kussmaul's sign is specific to constriction and is not seen with tamponade.
5. Correct answer is B. An unstable patient in tamponade needs to be fluid repleted emergently in attempt to overcome the pericardial pressure. Further treatment modalities might include pericardiocentesis or a surgical window placement. Beta blockers are contraindicated in compensatory tachycardia.

References

1. Armstrong WF, Ryan T, Feigenbaum H. Feigenbaum's echocardiography. 7th ed. Philadelphia: Wolters Kluwer Health/Lippincott Williams & Wilkins; 2010. xv, 785p.
2. Kern MJ, Lim MJ. Hemodynamic rounds: interpretation of cardiac pathophysiology from pressure waveform analysis. 3rd ed. Hoboken: Wiley; 2009. xxii, 473p.
3. Reddy PS, Curtiss EI, Uretsky BF. Spectrum of hemodynamic changes in cardiac tamponade. Am J Cardiol. 1990;66(20):1487–91.
4. Sagrista-Sauleda J, et al. Low-pressure cardiac tamponade: clinical and hemodynamic profile. Circulation. 2006;114(9):945–52.
5. Curtiss EI, et al. Pulsus paradoxus: definition and relation to the severity of cardiac tamponade. Am Heart J. 1988;115(2):391–8.
6. Sharkey SW. A guide to interpretation of hemodynamic data in the coronary care unit. Philadelphia: Lippincott-Raven; 1997. p. 214.

7. Stouffer GA, Inc E. Cardiovascular hemodynamics for the clinician. Malden: Blackwell Futura; 2008.
8. Restrepo CS, Lemos DF, Lemos JA, Velasquez E, Diethelm L, Ovella TA, Martinez S, Carrillo J, Moncada R, Klein JS. Imaging findings in cardiac tamponade with emphasis on CT. Radiographics. 2007;27:1525–610.
9. LeWinter MM. Pericardial diseases: In: Braunwald's heart disease: a textbook of cardiovascular disease. Philadelphia: Saunders Elsevier; 2008. p. 1836 from original by "Lorell BH, Grossman W. Profiles in constrictive pericarditis, restrictive cardiomyopathy and cardiac tamponade. In: Baum DS, Grossman W, editors. Grossman's cardiac catheterization, angiography, and intervention. Philadelphia: Lippincott Williams & Wilkins; 2000. p. 840".
10. Spodick DH. Acute cardiac tamponade. N Engl J Med. 2003;349(7):684–90.

Suggested Readings

Appleton C. Cardiac tamponade. Cardiol Clin. 2017;35(4):525–37.

Maggiolini S, et al. The role of early contrast-enhanced chest computed tomography in the aetiological diagnosis of patients presenting with cardiac tamponade or large pericardial effusion. Eur Heart J Cardiovasc Imaging. 2016;17:421–8.

Ristic AD, et al. Triage strategy for urgent management of cardiac tamponade: a position statement of the European Society of Cardiology Working Group on Myocardial and Pericardial Diseases. Eur Heart J. 2014;35:2279–84.

Sánchez-Enrique C, et al. Cause and long-term outcome of cardiac tamponade. American J Cardiol. 2016;117(4):664–9.

Constructive Pericarditis and Restrictive Cardiomyopathy

16

Chun Pong Wong and Allan Klein

Introduction

Despite being different disease processes, constrictive pericarditis (CP) and restrictive cardiomyopathy (RCM) are often discussed together due to their similar clinical and hemodynamic features. Physiologically, both processes lead to diastolic dysfunction but mechanisms are different; a rigid, adherent pericardium is noted in constriction while abnormal myocardium is the culprit in restriction. CP is usually a chronic process, and variant forms do exist (effusive-constrictive, subacute, transient, occult) which share many of the clinical findings, but have subtle clinical differences that distinguish each type. In RCM, the pericardium is merely normal, and the pathological process occurs in the myocardium which is often associated with infiltrative diseases such as amyloidosis, hemochromatosis, sarcoidosis, etc. Given the spectrum of disease and the various clinical manifestations of CP and RCM, initial history and physical examination along with hemodynamic considerations and newer non-invasive imaging criteria now lead the way in making the diagnosis. However, using all available data in distinguishing between the two diseases becomes important, as the treatment is very different.

C. P. Wong
Department of Cardiology, Khoo Teck Puat Hospital, National Healthcare Group, Singapore, Singapore

A. Klein (✉)
The Miller Family Heart and Vascular Institute, Cleveland Clinic, Cleveland, OH, USA
e-mail: KLEINA@ccf.org

Pathophysiology

Constrictive Pericarditis

Constrictive pericarditis is a form of diastolic heart failure caused by an inelastic pericardium that inhibits cardiac filling. Because its treatment differs markedly from all other forms of heart failure, accurate diagnosis is imperative.

The overall incidence of clinical CP is rare. After an episode of acute pericarditis, only 1.8% of patients have been found to develop chronic CP. The incidence was lower in patients with idiopathic or viral pericarditis when compared with other etiologies such as rheumatologic disease, malignancy, or bacterial infection. In patients after cardiac surgery, the incidence of chronic, symptomatic CP appears to be similarly low, with the reported rates of 0.2–2.4%. It is unknown how often constrictive physiology is detected on imaging in these diseases.

In Europe and North America, most cases are idiopathic, related to prior cardiac surgery or chest irradiation. There are also increasing number of cases of post cardiac injury syndrome especially in patients after invasive cardiac procedures, e.g. cardiac surgery, radiofrequency

A. T. Askari, A. W. Messerli (eds.), *Cardiovascular Hemodynamics*, Contemporary Cardiology,
https://doi.org/10.1007/978-3-030-19131-3_16

ablation for atrial fibrillation, automated implantable cardioverter defibrillator implantation, etc.

However, in other parts of the world, tuberculosis still remains a dominant cause of CP. Other possible causes include connective tissue disease, infection, malignancy, trauma and asbestosis [1].

Hippocrates (c. 460–370 BC) described the normal pericardium as "a smooth mantle surrounding the heart and containing a small amount of fluid resembling urine" [2]. The pericardium, a roughly flask-shaped membranous sac, envelops almost the entire heart except the region of left atrium around the pulmonary venous ostia. It consists of fibrous and serosal component. The outer fibrous sac is composed primarily of collagen fibers with interspersed short elastic fibrils. The serosal component consists of a single layer of mesothelium that forms a parietal and a visceral layer enclosing the pericardial cavity. The parietal layer lines the fibrous pericardium, and together, these structures form the parietal pericardium (Fig. 16.1a, b). The visceral layer is also known as the epicardium and covers the heart (Fig. 16.1c, d). Between the visceral pericardium and the myocardium is a variable amount of epicardial fat. The pericardial cavity normally contains <50 mL of serous fluid which serves as a lubricant during cardiac motion between the adjoining layers to prevent irritation.

The fibrous pericardium is relatively elastic at low volumes but when stretched it becomes rapidly inelastic. The pericardial pressure-volume relationship is non-linear; initially the slope is flat but subsequently becomes very steep, and this also depends on the rate of fluid accumulation (Fig. 16.2). When a scarred or calcified, noncompliant pericardium becomes adherent to various areas on the surface of the heart, in the case of constriction, the cardiac chambers are unable to relax completely during diastole due to extrinsic limits placed by the pericardium. As a result, in the ventricles, mid- and late-diastolic filling occurs earlier in diastole as the constraining force on the ventricle prevents further expansion and filling of the cavity leading to elevation in end-diastolic pressures and decrease in cardiac output. Once identified, pericardial "stripping"/pericardiectomy is the treatment of choice, as medical therapy alone will typically not provide symptomatic relief.

During inspiration, negative intrathoracic pressure is developed (−6 to 0 mmHg), and it is transmitted to the heart via the pericardium and pericardial space of right atrium (RA). This negative pressure results in increased systemic venous return to the right heart as well as augmenting passive filling of the right ventricle (RV). In the presence of a normal pericardium, as the RV fills, the free walls are able to expand and allow for the capacitance of RV. In CP, this process is impeded as the rigid encasement of the ventricles prevents transmission of the negative intrathoracic pressure to the heart. As the stiff outer shell limits capacitance, the RV free walls are unable to expand and accommodate the increased systemic venous inflow during inspiration. This leads to bowing of the septum toward the left ventricle (LV) to accommodate the volume of the RV inflow. The pulmonary venous circulation, which sits outside of the pericardium, behaves similarly to changes in intrathoracic pressure as the systemic venous system, thus leading to changes in LV filling during the respiratory cycle. On inspiration, the pulmonary venous pressure decreases; however, the negative intrathoracic pressure is not transmitted to the LV, leading to decreased flow gradient across the LV and thus limiting LV filling. During expiration, positive intrathoracic pressure reduces systemic venous return leading to decreased RV end-diastolic pressure. Passive filling of the LV now overcomes RV pressure and the interventricular septum shifts rightward into the RV. This phenomenon is known as *ventricular interdependence*; it occurs to a lesser extent in normal physiology but is exaggerated in CP.

Restrictive Cardiomyopathy

Restrictive cardiomyopathy (RCM) is a myocardial disorder that usually results from increased myocardial stiffness leading to impaired ventricular relaxation with restricted filling. Biventricular chamber size and systolic function are usually normal or near normal until later stages of the

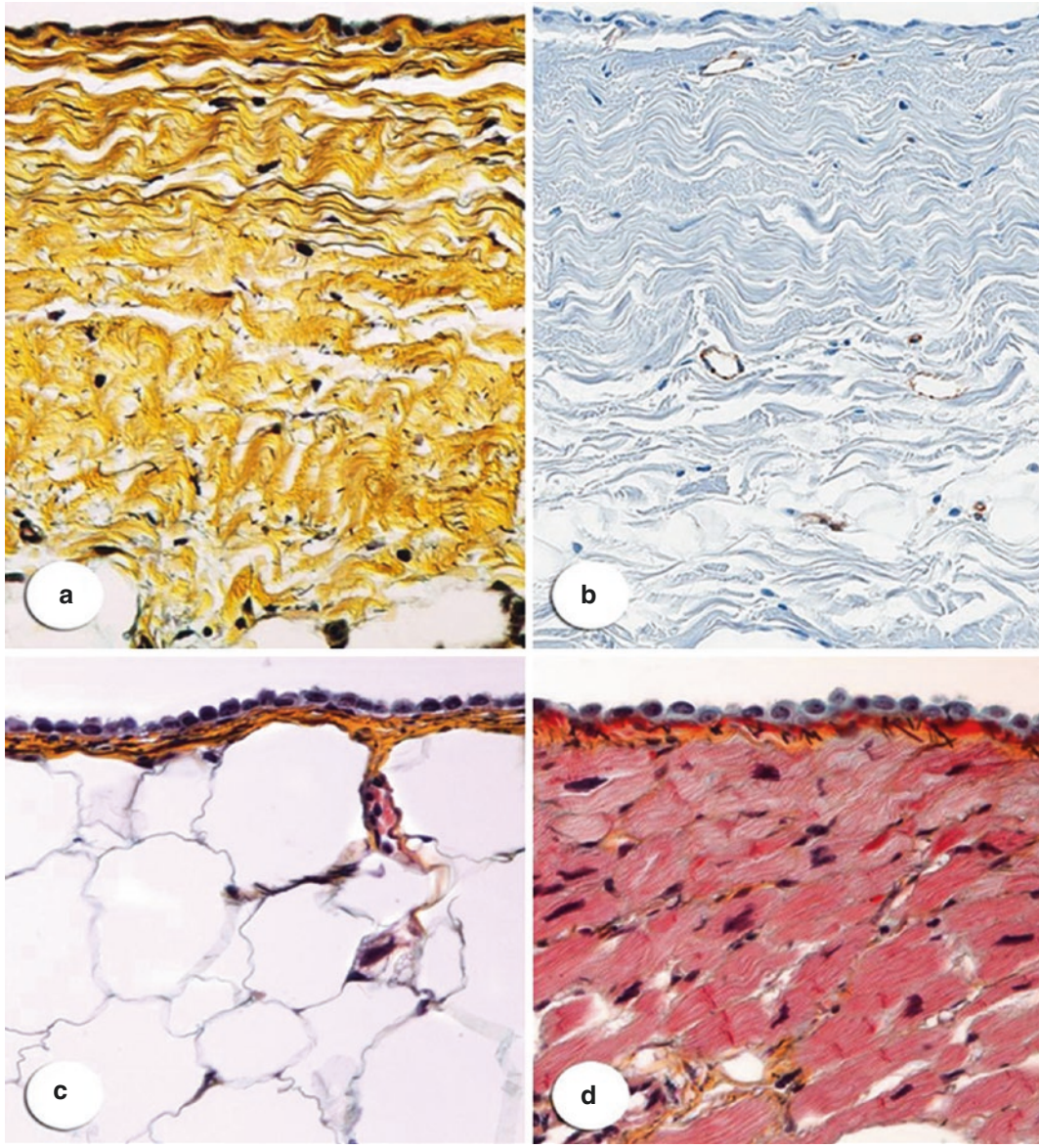

Fig. 16.1 (**a**) Normal, full-thickness parietal pericardium is shown. It consists of a layer of mesothelial cells and compact layers of dense wavy collagen (yellow) with interspersed short elastic fibers (black). (**b**) Fibroblasts with elongated nuclei and scant thin blood vessels are normally present in the parietal pericardium. CD34 immunostaining highlights the endothelial cells of capillaries. (**c**) The visceral pericardium (also called epicardium) consists of a mesothelial cell layer and a thin subepithelial layer of collagen with elastic fibers. The mesothelial cells show distinct microvilli. Beneath the visceral pericardium is epicardial adipose tissue. (**d**) In other areas of the visceral pericardium (or epicardium), only a thin layer of fibrous tissue (yellow) separates the mesothelial cells from the myocardium with absence of epicardial fat. Original magnifications 400×; (**a**, **c**, and **d**): Movat pentachrome stain; (**b**): CD34 immunoperoxidase. (From Klein et al. [9])

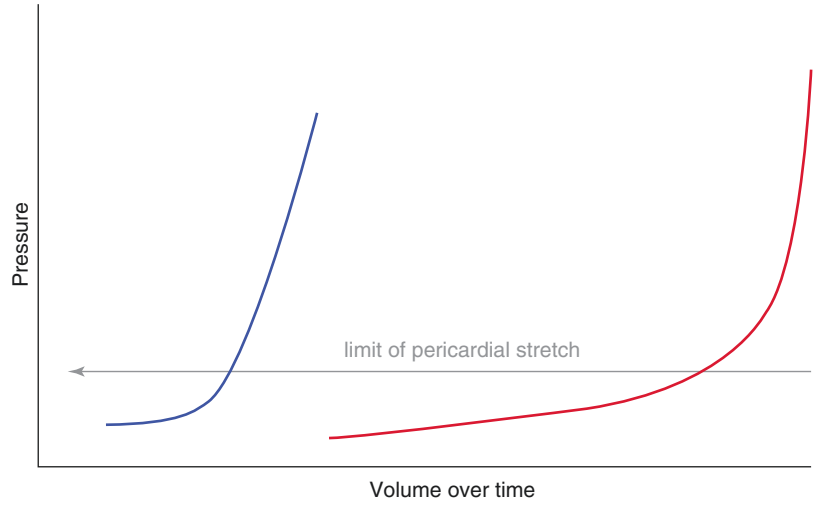

Fig. 16.2 Pericardial pressure-volume curves are shown in which the volume increases slowly or rapidly over time. (Blue curve) Rapidly increasing pericardial fluid first reaches the limit of the pericardial reserve volume (the initial flat segment) and then quickly exceeds the limit of parietal pericardial stretch, causing a steep rise in pressure, which becomes even steeper as smaller increments in fluid cause a disproportionate increase in the pericardial pressure. (Red curve) A slower rate of pericardial filling takes longer to exceed the limit of pericardial stretch, because there is more time for the pericardium to stretch and for compensatory mechanisms to become activated

disease. Affecting either or both ventricles, RCM may cause signs or symptoms of left and/or right heart failure. There may be associated arrhythmias and conduction disturbances. RCM may result from inherited or acquired predispositions and disease or a combination; thereof, which broadly can be classified as infiltrative, storage disease, non-infiltrative, and endomyocardial. Histologically, the infiltrative disorders are associated with deposits in the interstitial space between myocytes, while storage disorders focus primarily on accumulation within the cardiac myocytes. Due to the heterogenous nature of the origins and manifestations of RCM, and the concomitant challenges in diagnosing these diseases, the incidence and prevalence of RCM cannot be accurately estimated.

RCM can also be classified as genetic/familial or non-genetic/non-familial. Familial RCM is often characterized by autosomal dominant inheritance, which in some families is caused by mutations in the desmin gene; in others, familial RCM is associated with conduction defects, caused by mutations in the desmin gene, usually associated with skeletal myopathy. Rarely, familial cases can be associated with autosomal recessive inheritance, e.g. hemochromatosis or glycogen storage disease, or with X-linked inheritance, e.g. Fabry disease [3].

RCM is the least common type of cardiomyopathies [4]. The pericardium and pericardial compliance are normal in pure restrictive cardiomyopathies; however, depending on the cause (e.g. radiation), features of both restriction and constriction can coexist.

Pathophysiologically, the increased stiffness of the LV leads to rapid changes in LV pressure with incremental volume increases. This leads to the characteristic hemodynamic "dip-and-plateau" filling pattern, due to rapid early diastolic filling (dip) and cessation or diastasis of flow in mid- and late-diastole (plateau).

Evaluation

History/Clinical Presentation

Distinguishing between constriction and restriction is often difficult due to similar presenting

symptoms and physical findings. However, there are subtle findings in the history and physical examination that can help to differentiate which process is responsible for the patient's symptoms. The history should be aimed at elucidating any etiologies for either constriction or restriction. For example, an antecedent history of cardiac trauma, cardiac surgery/procedure, or pericarditis would favor constriction, while a prior history of infiltrative or glycogen storage diseases, e.g. amyloidosis, sarcoidosis, or hemochromatosis, suggests restriction. More importantly, a history of radiotherapy especially mantle radiation can lead to symptoms via a myriad of physiological processes including constriction, restriction, pulmonary fibrosis, as well as valvular heart disease. Patients will present with a varying degree of symptoms depending on how advanced the disease process is. Dyspnea on exertion or at rest, edema (lower extremity, ascites, and effusions), pulmonary congestion, and eventually symptoms of low cardiac output are noted in both processes. Late stages of both are heralded by severe heart failure. Table 16.1 lists the different etiologies of CP and RCM.

Physical Examination

Most patients with CP and RCM have elevated jugular venous pressure (JVP). Kussmaul's sign is a paradoxical rise in JVP on inspiration, or a failure in the appropriate fall of the JVP with inspiration. Due to the inability of the RA to accommodate increased venous return, JVP paradoxically increases with inspiration. Kussmaul's sign can be seen in both conditions; however, it is more common in CP. A steep/rapid *Y*-descent of the JVP, i.e. Friedreich's sign, along with peripheral edema, ascites, hepatic congestion, and pleural effusions can also be seen in both conditions as the markers of right-sided heart failure. Physical findings suggestive of CP are the presence of a pericardial knock which occurs at the nadir of the Y-descent and is the diastolic gallop usually heard before S3 consistent with abrupt cessation of ventricular filling; friction rub if active pericarditis; and apical retraction which is secondary to the inability to transmit a palpable ventricular impulse due to a calcified pericardium. An audible S3 and prominent apical impulse are more indicative of restriction. Pulsus

Table 16.1 Causes of constrictive pericarditis and restrictive cardiomyopathy

Constrictive pericarditis	Restrictive cardiomyopathy	
Idiopathic	*Infiltrative*	*Storage diseases*
Viral	Amyloidosis	Fabry disease
Post-surgical	Sarcoidosis	Gaucher disease
Post-radiotherapy	Primary hyperoxaluria	Hemochromatosis
Connective tissue disease	*Endomyocardial*	Glycogen storage disease
Post-MI (Dressler's syndrome)	Carcinoid heart disease	Mucopolysaccharidosis type I (Hurler syndrome)
Post-infectious	Endomyocardial fibrosis	Mucopolysaccharidosis type II (Hunter syndrome)
Uremia	Hypereosinophilic syndrome	Niemann–Pick disease
Sarcoidosis	Chronic eosinophilic leukemia	*Non-infiltrative*
	Drugs (serotonin, methysergide, ergotamine, mercurial agents, busulfan)	Diabetic cardiomyopathy
	Endocardial fibroelastosis	Scleroderma
	Consequence of cancer/cancer therapy	Myofibrillar myopathies
	Metastatic cancer	Pseuxanthoma elasticum
	Drugs (anthracyclines)	Sarcomeric protein disorders
	Radiation	Werner's syndrome

Adapted from Muchtar et al. [4]

paradoxus, which is defined as an abnormal (>10 mmHg) decrease in systolic blood pressure with inspiration, is seen occasionally in CP cases involving pericardial effusion, such as effusive-constrictive pericarditis.

Chest Radiography and Electrocardiography

Pericardial calcification is often seen on chest X-ray and is indicative of CP; however, it is not always present (Fig. 16.8a, b). Cardiomegaly due to biatrial, rather than ventricular enlargement is seen in cases of restrictive cardiomyopathy. Electrocardiography (ECG) findings, such as atrial fibrillation and repolarization abnormalities, are often seen in both conditions, while LV hypertrophy, low voltage QRS, and conduction abnormalities may be a clue to the presence of restriction.

Echocardiography

Echocardiography (TTE) is the first-line and most essential tool in establishing a diagnosis of CP and RCM. In the context of the other diagnostic information, the ability to obtain both anatomic and hemodynamic information is useful in making the diagnosis.

2D and M-Mode

TTE can be used to image the pericardium, regarding the appearance of the pericardium and also the presence of concomitant pericardial effusion. However, measurement of pericardial thickness using TTE is not recommended. Pericardial thickness can also be obtained by transesophageal echocardiography (TEE), though Computed tomography (CT) and cardiac magnetic resonance imaging (CMR) are the gold standard. 2D echocardiography is also useful in assessing atrial and ventricular cavity sizes as well as in characterizing the myocardium. Depending on the etiology, different morphological characteristics can be present, such as thickened myocardium with speckling or a granular pattern which is found in amyloidosis (Fig. 16.3a, b). In RCM, biatrial enlargement, which is less frequent in CP, can be seen on TTE along with a tendency for inter-atrial septal bulging to the right due to increased pressure in the left atrium (LA) as compared to RA (Fig. 16.3b). The characteristic findings of CP on TTE are ventricular septal bounce, myocardial tethering, as well as inferior vena cava (IVC) and hepatic vein plethora. However, ventricular septal shift (VSS) is different from septal bounce. The presence of VSS is defined as any degree of cyclic movement of the ventricular septum toward the left ventricle with inspiration and toward the right ventricle with expiration, which resembles ventricular interdependence. VSS is a sensitive sign of CP with a sensitivity of 93% and specificity of 69% [5]. The features of VSS, septal shudder, and bounce in CP are better appreciated using M-mode imaging due to its high temporal resolution (Fig. 16.4).

Doppler Echocardiography and Tissue Doppler Imaging

Physiologically, both CP and RCM lead to diastolic dysfunction. Information obtained from Doppler echocardiography and tissue Doppler imaging (TDI) has been vital in diagnosing diastolic dysfunction. In additions, TDI information on mitral annular velocities has improved the overall sensitivity and specificity of echocardiography in diagnosing CP while also distinguishing cases of CP from RCM. Doppler has been beneficial by allowing a hemodynamic assessment non-invasively. Specifically, it looks at ventricular filling, i.e., mitral and tricuspid inflow velocities, pulmonary and hepatic venous flow, and especially the respiro-phasic changes brought by CP and RCM in these parameters.

In both CP and RCM, the trans-mitral flow velocity pattern is characteristic of markedly elevated LV filling pressure, i.e. restrictive pattern. The high left atrial pressure (LAP) is associated with high LA–LV gradient at the time of mitral valve opening; therefore, E wave velocity is high, A wave velocity is low, and E/A ratio is high, usually >2.0. However, A wave may not be visible in patients with atrial fibrillation or flutter. Poor LV compliance results in rapid rise of LV

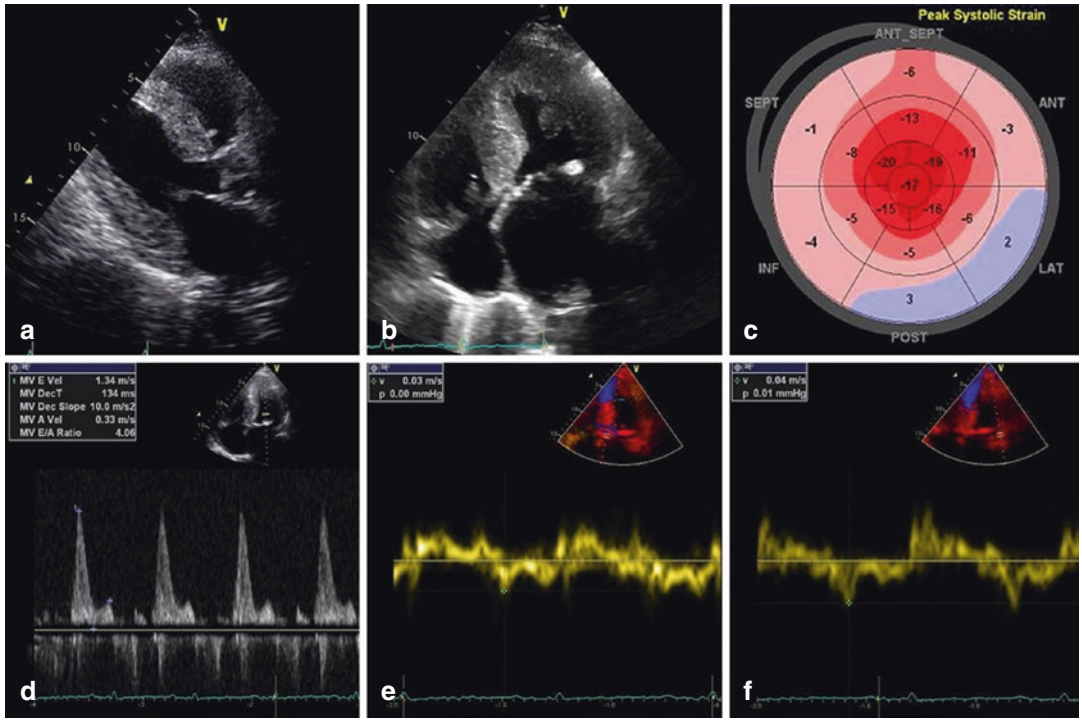

Fig. 16.3 Echocardiography of patient with amyloidosis shows (**a**) thickened myocardium with speckling or a granular pattern and (**b**) biatrial enlargement with inter-atrial septal bulging to the right. (**c**) Global longitudinal strain (GLS) study shows a pattern of apical sparing suggestive of amyloidosis. (**d**) The pulsed wave Doppler study of the mitral inflow shows high E/A ratio of ~4.1 and short deceleration time of ~134 ms. Tissue Doppler imaging (TDI) of mitral annulus shows markedly reduced velocities in both (**e**) septal e' of 3 cm/s and (**f**) lateral e' of 4 cm/s

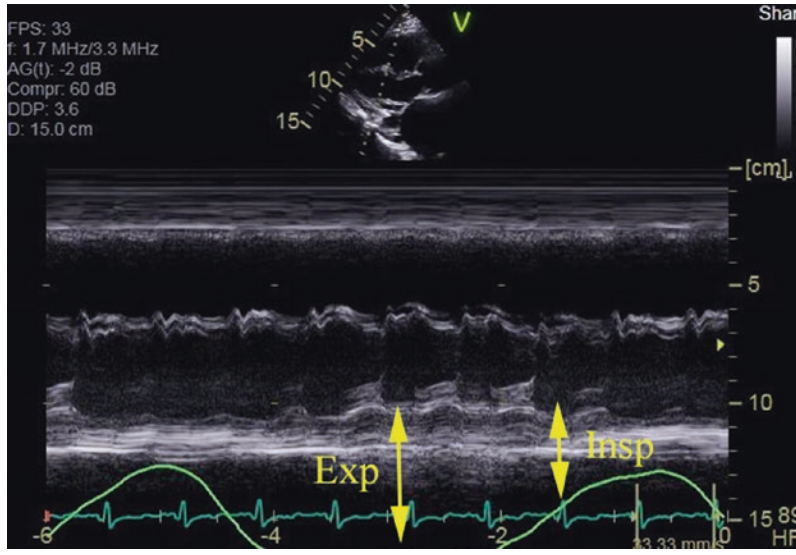

Fig. 16.4 Midventricular septal M-mode recording (parasternal long axis) in a patient with constrictive pericarditis. There is leftward ventricular septal shift in inspiration. Exp indicates expiration and Insp inspiration

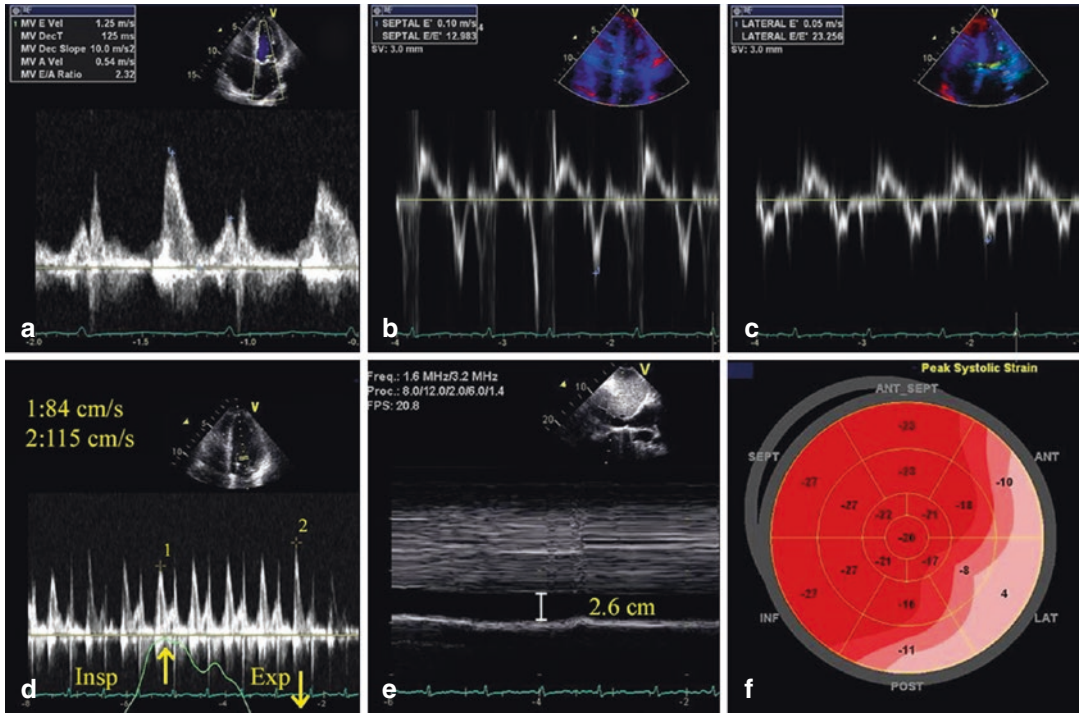

Fig. 16.5 Echocardiography of a patient with constrictive pericarditis. (**a**) The pulse wave Doppler study of the mitral inflow shows high E/A ratio which is ~2.3 and short deceleration time of 125 ms. Tissue Doppler imaging (TDI) of mitral annulus shows "annulus reversus" with (**b**) septal e' of 10 cm/s and (**c**) lateral e' of 5 cm/s. (**d**) There is significant respiratory variation in the mitral inflow [(expiration – inspiration)/expiration; (115–84)/115 × 100% = ~27.0%]. Insp indicates inspiration and Exp, expiration. (**e**) M-mode image shows plethoric inferior vena cava (IVC) with diameter of 2.6 cm and <50% change in diameter during respiration. (**f**) Global longitudinal strain (GLS) study shows LV antero-lateral wall shortening strains were lower than the septal shortening strains

diastolic pressure, which leads to rapid decline of LA–LV pressure gradient. As a result, there is a rapid, early diastolic deceleration of trans-mitral inflow, with shorter than normal deceleration time, i.e., <160 ms (Figs. 16.3d and 16.5a).

Pulmonary artery systolic pressure (PASP), provided pulmonary vascular disease is excluded, can be served as an indirect estimate of LAP and identify patients with increased LV filling pressures. A significant correlation exists between PASP and noninvasively derived LAP. In the absence of pulmonary disease, increased PASP suggests elevated LAP. Calculation of PASP can be done by measuring the peak tricuspid regurgitation (TR) velocity, then applying the modified Bernoulli equation to convert this value into pressure values and adding the estimated right atrial pressure. The American Society if Echocardiography (ASE) recommends the cutoff value for peak TR velocity of >2.8 m/s for diagnosing diastolic dysfunction [5].

TDI of mitral annular velocities have become an integral part of the diastology assessment as well as the diagnosis of CP and restriction. The mitral annular velocity (e′) is measured at the septal/medial and lateral annulus – both of which give information regarding the motion of the annulus with respect to the axis of measurement, i.e., cursor line. These measurements give information about myocardial relaxation and longitudinal motion of the heart, which are affected in CP and restriction. In cases with abnormal relaxation, i.e., restriction, tissue Doppler velocities are predictably reduced (septal e' velocity <7 cm/s or lateral e' velocity <10 cm/s). In RCM, both septal and lateral e' velocities are diminished. In pure CP without myocardial involvement, the septal mitral annulus velocity can be

normal or mildly elevated, i.e., septal e' ≥ 9 cm/s [5]. This is due to the limited lateral expansion of the heart during filling secondary to pericardial encasement which results in a compensatory increase in longitudinal movement of the septum in order to accommodate filling. In patients without pericardial disease, the septal e' is typically lower than the lateral e'. In CP, this relationship reverses; the septal e' velocity is greater than the lateral one, and hence this phenomenon is called "annulus reversus." Tissue Doppler E/e' is a non-invasive estimate of LAP. The ASE guidelines for assessment of diastolic dysfunction recommend using an average of the septal and lateral e' velocities, whereas an average E/e' of >14 indicates elevated LAP [6]. Although LAP is increased in both CP and RCM, E/e' does not increase despite elevated pulmonary capillary wedge pressure (PCWP) in CP, i.e., "annulus paradoxus." However, this only occurs in pure constriction rather than in constriction with myocardial disease [7–8].

The respiratory variation of diastolic inflow velocities across both the mitral and tricuspid valve, i.e., E wave velocities, is different in CP and RCM and can provide compelling evidence for either diagnosis while ruling out other processes. The ASE recommends the calculation of percentage of respiratory variation in CP for mitral and tricuspid inflow as follows:

$$\left(\text{expiration} - \text{inspiration}\right) / \text{expiration} \times 100\%$$

For peak mitral E inflow, the maximal drop occurs with the first beat of inspiration and the first beat of expiration. It usually exceeds 25% respiratory variation (Fig. 16.6d). For peak tricuspid E inflow, the maximal drop is on the first beat in expiration at the same time as the hepatic vein atrial reversal and usually exceeds 40% respiratory variation. The calculated % will be a negative value [9]. These phenomena are manifestations of greatly enhanced ventricular interaction and are not present in either normal subjects or patients with restrictive cardiomyopathy. In restriction, the mitral *E* velocities vary with respiration but to a much lesser degree (usually <10%). These findings can be affected by preload conditions in the LA; an increase in left atrial pressure will diminish the variation with respiration, while volume depleted states will exaggerate it.

Pulmonary and hepatic venous flows represent left and right-sided filling and are also another important measurement in distinguishing constrictive and restrictive physiology. Pulmonary vein systolic flow (*S* wave) is diminished and diastolic flow (*D* wave) is increased irrespective of respiration in restriction. In CP, however, there is increase in both systolic and diastolic flow during expiration as compared to blunted *S* and *D* during inspiration, which is a distinguishing feature (Fig. 16.6).

Hepatic vein flows, designated by *S* and *D* waves can also be used to further identify patients sus-

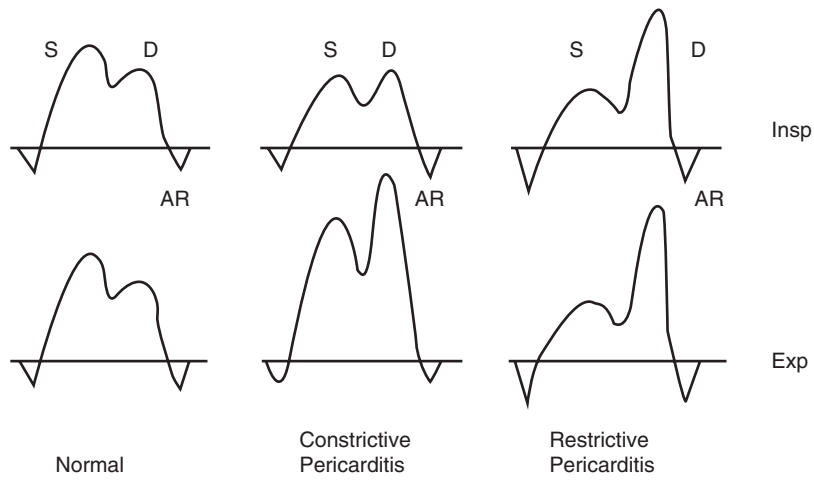

Fig. 16.6 Pulmonary venous flow during different phases of respiration in different conditions. S indicates pulmonary vein systolic flow; D pulmonary vein diastolic flow; AR atrial reversal; Insp inspiration; Exp expiration

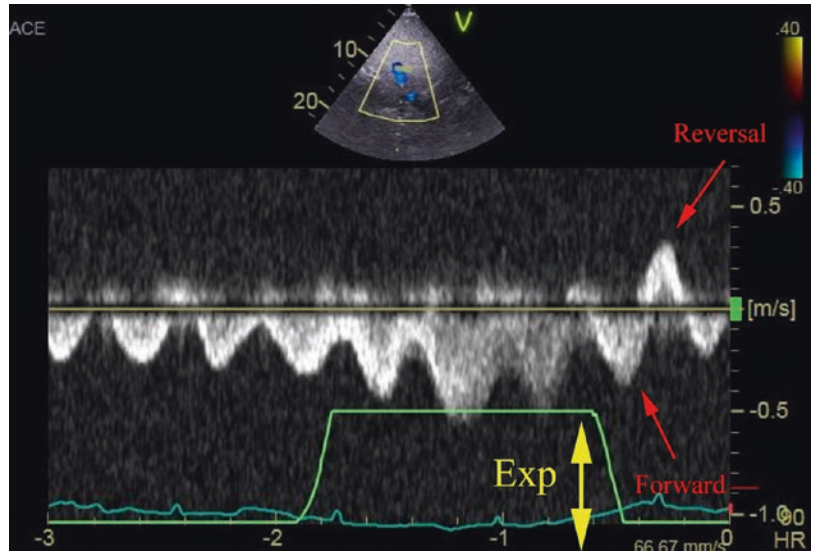

Fig. 16.7 Pulsed-wave Doppler recording (subcostal window) within the hepatic vein in a patient with constrictive pericarditis. Note prominent diastolic flow reversals in expiration, with the diastolic reversal ratio defined as reversal velocity divided by forward velocity (~0.35 m/s reversal velocity divided by ~0.40 cm/s forward flow velocity yields a diastolic reversal ratio of 0.875). Exp indicates expiration

pected of having CP or restriction. Normal patients will have a more prominent *S* wave as compared to the *D* wave; however, there is little to no respiratory variation. In those with CP, there is a significant increase in the diastolic flow, i.e. *D* wave during inspiration and marked blunting during expiration with diastolic flow reversal, whereas restriction patients have an increased diastolic flow, i.e. *D* wave as compared to *S* wave without respiratory variation. However, this is better expressed as the hepatic vein expiratory diastolic reversal ratio, which is defined as follows:

$$\left(\text{diastolic reversal velocity / forward velocity}\right)\text{in expiration.}$$

The finding of a reversal ratio ≥0.79 has a specificity of 88% for CP [5] (Fig. 16.7).

Global Longitudinal Strain (GLS)

Strain in the myocardium can be measured by TDI or speckle-tracking echocardiography (STE). Nowadays, STE is the most widely used strain modality. STE utilizes the phenomenon in which natural acoustic markers in gray scale ultrasound images form interference patterns, i.e., speckles within myocardial tissue. These patterns are quite stable over the short period of time between two consecutive frames, and the 2D displacement for each point in the myocardium is found by automatic search for similar patterns in the two frames (block matching). This process is repeated for all frames through the cardiac cycle to produce a 2D displacement curve for each point in the myocardium. Subsequently, strains are calculated from each LV segment in circumferential, longitudinal, or radial directions [10]. When the information obtained from conventional echocardiography is adequate, GLS is usually not necessary for diagnosis. However, GLS can provide more information in order to exclude other differential diagnosis.

In the cases of RCM, there are often findings of normal or near normal LV systolic function, diastolic dysfunction and left ventricular hypertrophy. The pattern of apical sparing in GLS (Fig. 16.3c) can be an assurance for the diagnosis of amyloidosis in RCM; whereas in hypertrophic cardiomyopathy, myocardial longitudinal deformation is typically reduced at the site of hypertrophy [11]. Due to the tethering of LV free wall in CP, LV septal shortening strains are seen to be higher than the lateral wall shortening strains (Fig. 16.5f), which depends on the location and extent of pericardial calcification. Moreover, the average GLS value is higher in patients with CP than in those with RCM [12].

In distinguishing CP and RCM, Welch TD et al. suggest a relatively simple approach. In the article of the Mayo Clinic diagnostic criteria of constrictive pericarditis, respiration-related ventricular septal shift, preserved or increased septal mitral annular e' velocity, and prominent hepatic vein expiratory diastolic flow reversal are the echocardiographic features which are independently associated with the diagnosis of CP. The presence of VSS with either septal mitral annular e' velocity of ≥9 cm/s or hepatic vein expiratory diastolic reversal ratio of ≥0.79 yields the diagnostic sensitivity of 87% and specificity of 91% for CP [5].

Transesophageal Echocardiography

Given some of the limitations of TTE, TEE may be useful whenever TTE is non-diagnostic or image quality is affected by body habitus or positioning. It can be used in the post-op setting to assess localized effusive-constrictive disease. TEE can be used to image the pericardium to assess thickness and the areas of adherence, as well as to obtain higher fidelity Doppler signals through the MV/TV (*E* velocity) and pulmonary vein flows. Often TEE evaluation is useful as an adjunctive modality since it is better for imaging the posterior aspect of the heart, as well as the RA, RV, and IVC which improves the accuracy of the overall assessment. However, TDI measurement of mitral annulus velocities has not been validated in TEE.

Computed Tomography and Magnetic Resonance Imaging

CT and CMR imaging offer higher resolution and additional information as compared to echocardiography in the evaluation of CP and RCM. CT can assess pericardial thickening (>4 mm) and calcification better than TTE or TEE (Fig. 16.8c, d), though the absence of either does not rule out CP. Talreja DR et al. reported 18% of patients had normal pericardial thickness on histological examination, and 28% of patients had normal pericardial thickness on CT in a study of 143 patients with surgically confirmed CP [13]. It also offers information regarding IVC volume status, as well as ventricular and septal contours associated with constriction. In patients with a prior history of cardiothoracic surgery, CT is useful in assessing the location of important vascular structures prior to surgery as well as assessing for any lung injury or entrapment especially with prior history of radiation exposure.

Gated CMR provides better visualization and resolution of the pericardium than either CT or echocardiography. CT still offers a better assessment of pericardial calcification, but CMR is superior in the evaluation of tissue characterization including pericardial inflammation and edema, pericardial scarring, small pericardial effusions, and myocardial tethering as well as resolving hemodynamic correlates such as IVC plethora and VSS (Fig. 16.9). The ability of CMR for tissue characterization has been used to diagnose and monitor both constrictive physiology and pericardial inflammation in transient CP. Transient CP is an increasingly recognized sub-type of the more typically known CP. It was first described back in 1987, when a small group of subjects with CP demonstrated spontaneous and permanent resolution of constrictive physiology on serial echocardiograms and CMR [14]. Pathologically, transient CP is usually a result of fluctuating pericardial edema, inflammation and fibrin deposition, rather than more fixed pericardial fibrosis or calcification [15]. It may resolve spontaneously or with the assistance of anti-inflammatory therapy. It is likely that in some cases, transient CP may actually represent an early manifestation in the spectrum of CP disease, before chronic inflammation leads to accumulation of fibroblasts and collagen and constrictive physiology becomes irreversible. For the inter-atrial septum (IAS), a thickness of >6 mm is considered significant. This finding is virtually diagnostic of cardiac amyloidosis. Lipomatous hypertrophy can also cause increased thickness of IAS, but it can be easily differentiated by its hyperintense signal on T1-weighted sequence due to fat content [16].

Besides, the delayed enhanced inversion recovery imaging in CMR is the most valuable

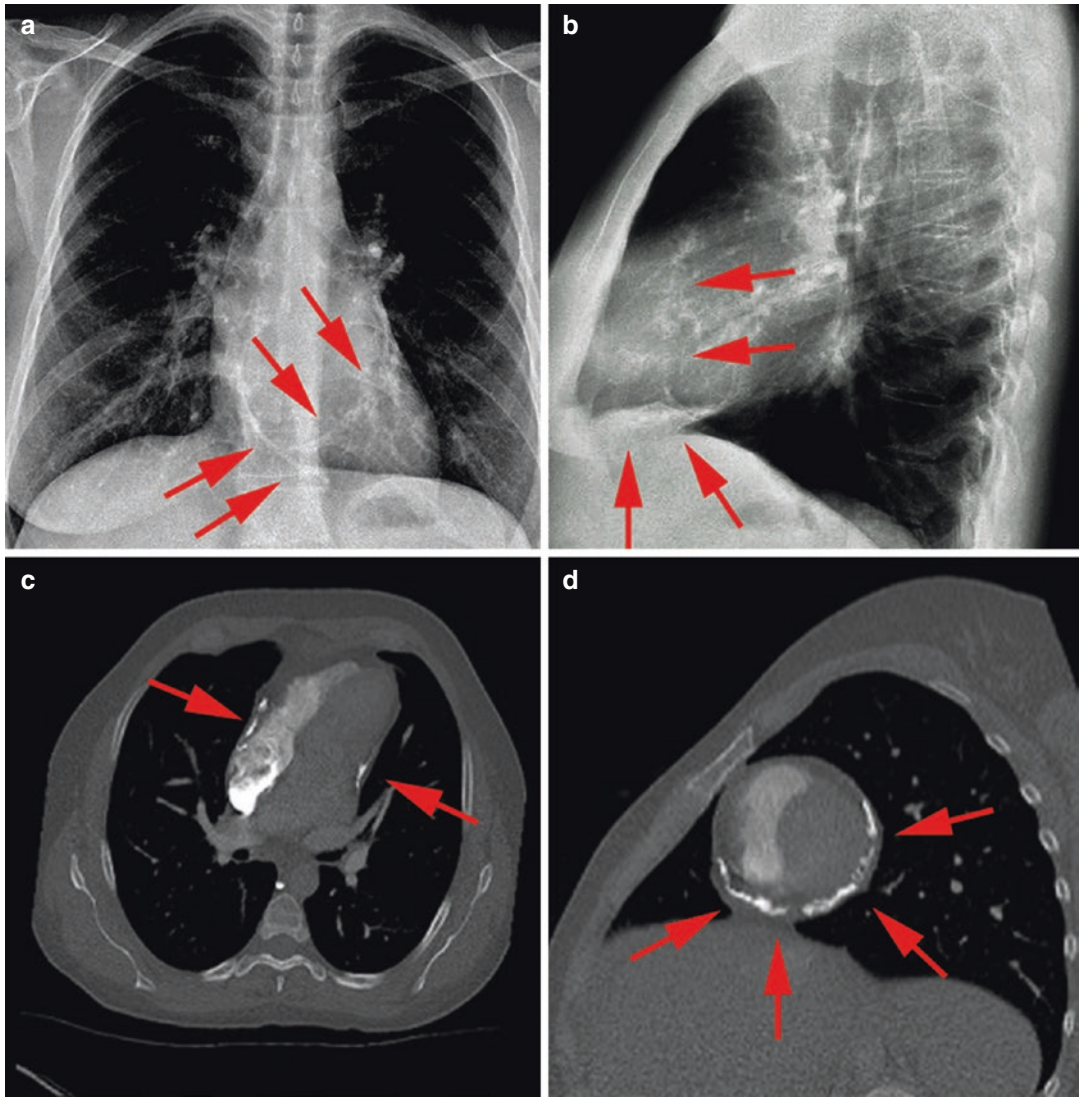

Fig. 16.8 Pericardial calcification seen on CXR (**a** and **b**) and CT scan (**c** and **d**). Red arrows indicate the location of pericardial calcification

sequence for tissue characterization and providing clues as to the underlying cause, especially in the cases of RCM. In cardiac amyloidosis, the late gadolinium enhancement (LGE) is usually global in distribution and predominantly subendocardial but may be transmural. CMR also provides some information about amyloid load (intramyocardial T1 gradient) in the heart, which is helpful in the non-invasive follow-up of patients on treatment [17]. Cardiac sarcoidosis is pathologically characterized by patchy and focal myocardial involvement by granulomatous inflammation, which can leave scar tissue after healing. There are three successive histological stages: edema, non-caseating granulomatous infiltration, and patchy myocardial fibrosis. CMR has been shown to accurately reflect these changes. The acute inflammatory phase shows the presence of focal increased signal on T2-weighted images with myocardial thickening reflecting edema (Fig. 16.10a). Well-formed granulomas are seen as foci of decreased T1 and T2 signal within the area of increased T2 signal. A central low signal area reflects hyaline fibrotic

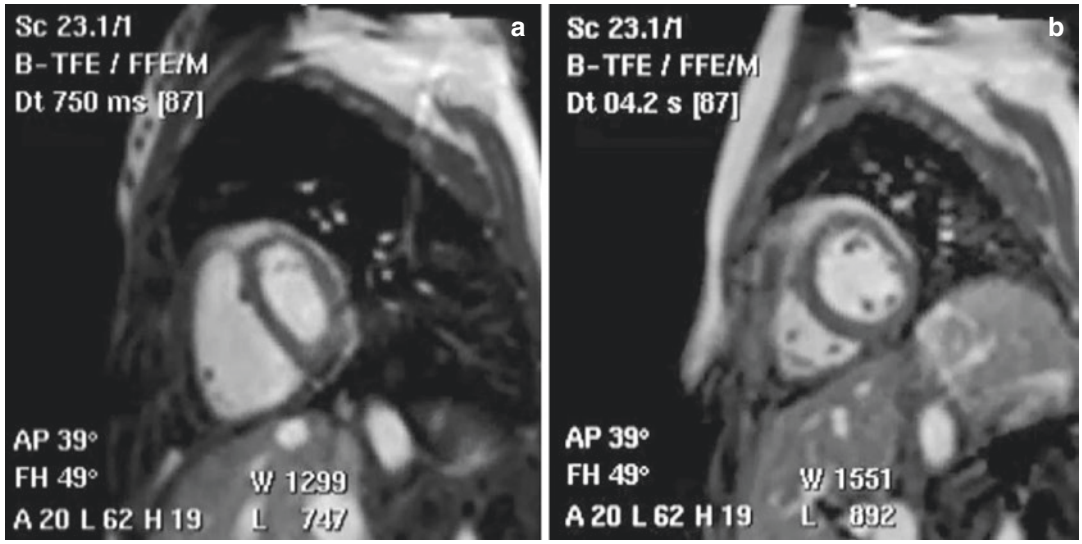

Fig. 16.9 CMR free breathing sequence shows the presence of ventricular septal shift. The ventricular septum moves toward the left ventricle with inspiration during diastole (**a**) and toward the right ventricle with expiration during diastole (**b**)

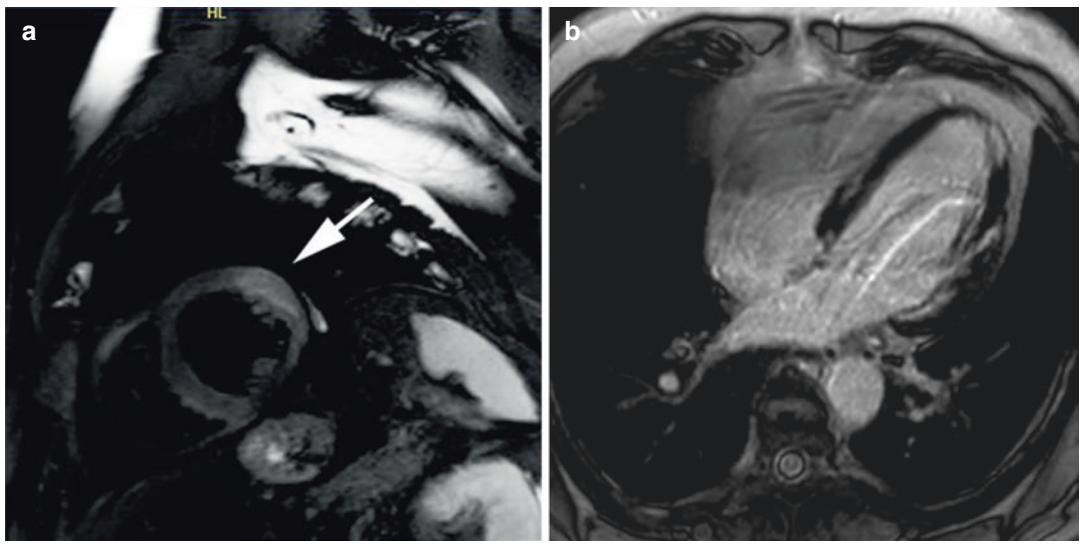

Fig. 16.10 CMR of a patient with sarcoidosis. (**a**) There is increased myocardial signal intensity on T2-STIR imaging to suggest myocardial edema (white arrow). (**b**) Delayed-enhancement imaging reveals late gadolinium enhancement (LGE) in a non-ischemic pattern. There is near transmural LGE in the basal and mid inferoseptum (sparing the endocardium) and mid-myocardial LGE in the mid-anterolateral and transmural LGE at the inferolateral apex

change and peripheral high signal area denotes edema due to granulomatous inflammation. LGE imaging shows hyperenhancement in areas of fibrosis, which does not correspond to any particular coronary artery distribution. These are also more linear in appearance (Fig. 16.10b), compared to the focal, more rounded lesions in the inflammatory stage [16].

In hemochromatosis, CMR is also vital in the detection and quantification of cardiac involvement. Deposition of iron in the myocardium causes a decrease in T2∗ relaxation time, which

can be detected by multi-echo gradient sequences [16]. The ability of CMR to detect myocardial iron overload at an early stage, direct timely institution of chelation therapy, and monitor treatment follow-up have been shown to reduce the morbidity as well as mortality in hemochromatosis [18].

Catheterization/Hemodynamic Assessment

Left and right heart catheterization has been used in the past as the gold standard in distinguishing between CP and RCM. Improvements in non-invasive imaging have helped in increasing the early diagnosis of CP and restriction. Although there are many similar hemodynamic characteristics in CP and RCM, certain unique findings, if present, can help to differentiate the diagnosis.

Hemodynamic findings often seen in patients with CP are increased RA pressure due to the adherent pericardium around RA prevents expansion, Kussmaul's sign (usually present), as well as prominent *x* and *y*-descents of RA pressure tracings because of rapid atrial emptying and underfilled RV (M/W pattern) (Fig. 16.11a). The presence of an increased RV end-diastolic pressure (usually greater than or equal to one-third of the RV systolic pressure) is due to constraint of the RV leading to higher filling pressure. Constriction is generally not known to cause pulmonary hypertension; thus, the RV systolic pressure is not affected. The "dip-and-plateau"/"square-root" sign is seen in the RV and LV pressure tracings as a result of rapid early diastolic flow (dip) and diastasis once pressure equalization occurs (plateau) during mid- and late-diastole. Another key feature is found in the diastolic (plateau) pressures of the LV and RV, which equalize due to the rigid non-elastic pericardium (Fig. 16.11b). This finding is relatively common in patients who undergo catheterization and have constriction; however, in some patients, it is only seen on inspiration, secondary to increased systemic venous return. Lastly, RV and LV systolic pressures exhibit an inverse relation as a result of ventricular interde-

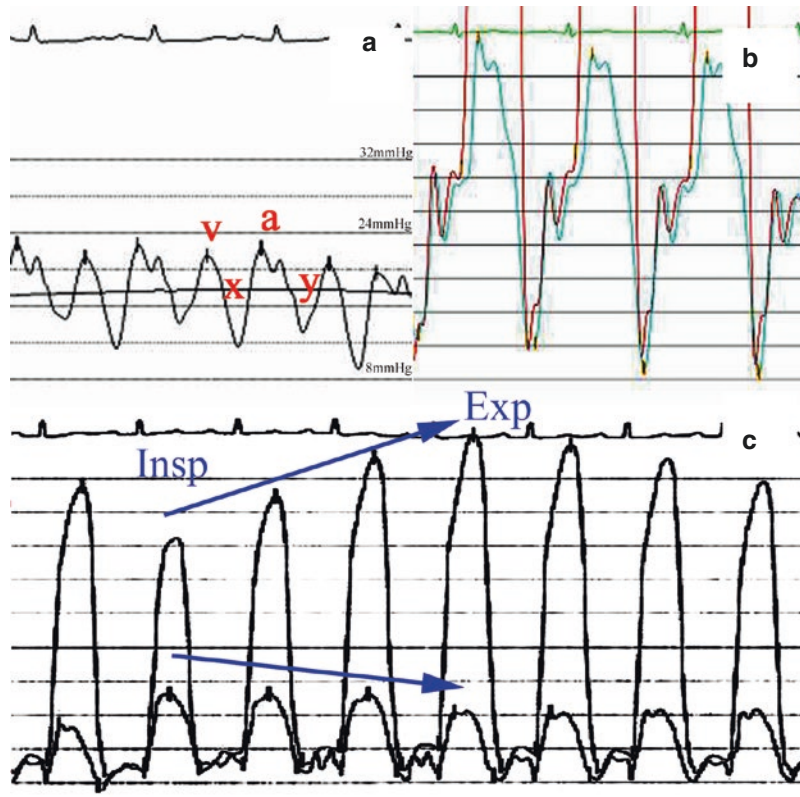

Fig. 16.11 Left and right heart catheterization of a patient with constrictive pericarditis. (**a**) Pressure tracing of the right atrium shows prominent x- and y-descents. v indicates v wave; a, a wave; x, x-descent; and y, y-descent. (**b**) Simultaneous recording of LV and RV pressure tracings shows "dip-and-plateau"/"square-root" sign and equalization of both ventricular diastolic pressures. (**c**) Simultaneous recording of LV and RV pressure tracings with respiratory variation shows ventricular interdependence. LV indicates left ventricle and RV, right ventricle

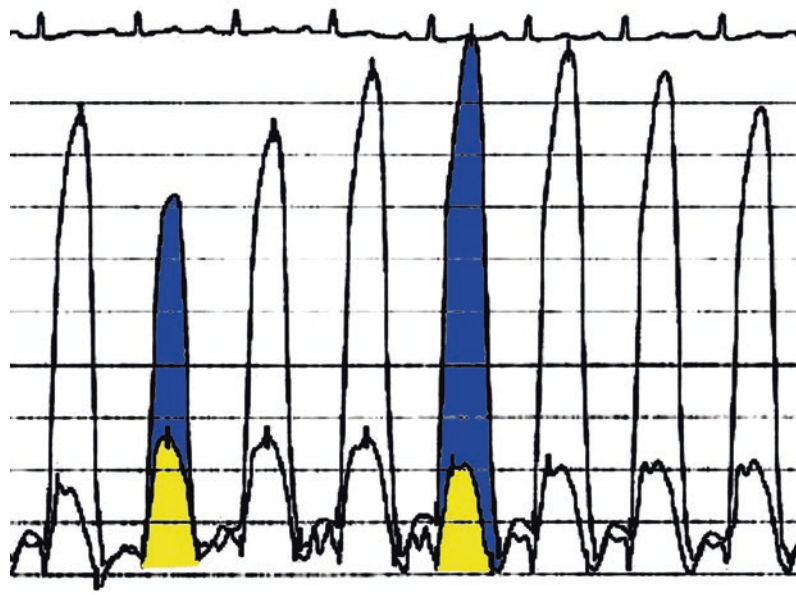

Fig. 16.12 A patient with constrictive pericarditis. During inspiration there is an increase in the area of the RV pressure curve (yellow-shaded area) compared with expiration. The area of the LV pressure curve (blue shaded area) decreases during inspiration as compared with expiration

pendence. With inspiration, the LV systolic pressure falls and the RV systolic pressure rises and vice versa with expiration (Fig. 16.11c). Patients with restrictive cardiomyopathy have ventricular concordance. Systolic area index is used to further quantify this hemodynamic difference. The area under the ventricular pressure curve was used to determine the change in the relative volumes of the LV and RV, which is a better determinant of beat-to-beat stroke volume than the peak pressure alone. The systolic area index is defined as the ratio of the RV area (mmHg × s) to the LV area (mmHg × s) in inspiration versus expiration. An index of greater than 1.1 has been shown to have 97% sensitivity in predicting patients with CP [19] (Fig. 16.12).

Clinical Examples

Calcific Constrictive Pericarditis

A 45-year-old female presented with a history of increasing dyspnea on exertion and progressive heart failure symptoms. She had a history of recurrent pericarditis, otherwise unremarkable. On physical exam, she had bilateral pitting LE edema, elevated JVP, and a pericardial knock. Chest radiography (CXR) showed no pulmonary edema or effusion but was significant for scattered calcification of the pericardium (Fig. 16.8a, b). Echocardiogram showed preserved LV and RV functions, but grade III diastolic dysfunction, VSS and IVC plethora (Fig. 16.5e). Grade III diastolic dysfunction was diagnosed as the LA was dilated with indexed LA volume of ~36 ml/m^2. Transmitral inflow showed high E/A ratio was ~2.3 (Fig. 16.5a). Moreover, the TDI of mitral annulus velocities demonstrated "annulus reversus" with septal e' of 10 cm/s and lateral e' of 5 cm/s (Fig. 16.5b, c), and the average E/e' was ~18.8. The TR signal was insufficient to estimate PASP. Significant respiratory variation in mitral inflow was also present, i.e., >25% respiratory variation in peak mitral E inflow (Fig. 16.5d). GLS study showed LV lateral wall shortening strains were lower than the septal shortening strains (Fig. 16.5f).

Left and right heart catheterization showed normal coronary arteries and confirmed the diagnosis of CP with the hemodynamic finding of CP. There were diastolic equalization of pressures in both the LV and RV and ventricular interdependence (Fig. 16.11b, c).

The patient was referred for pericardiectomy in view of the above findings and persistent symptoms despite medical therapy. She had marked improvement in her symptoms after surgery.

Effusive-Constrictive Pericarditis

A 39-year-old female presents with a history of chest and dyspnea. She had medical history of systolic lupus erythematosus and interstitial lung disease with pulmonary fibrosis. On physical examination, pericardial rubs could be heard. ECG showed sinus tachycardia with diffused ST elevations and PR depressions in lead II. ESR and CRP were both raised. Echocardiography showed large circumferential pericardial effusion with features of cardiac tamponade. Pericardiocentesis was then performed and found exudative pericardial effusion with negative culture and cytology. However, the echocardiography repeated after pericardiocentesis showed small residual pericar-

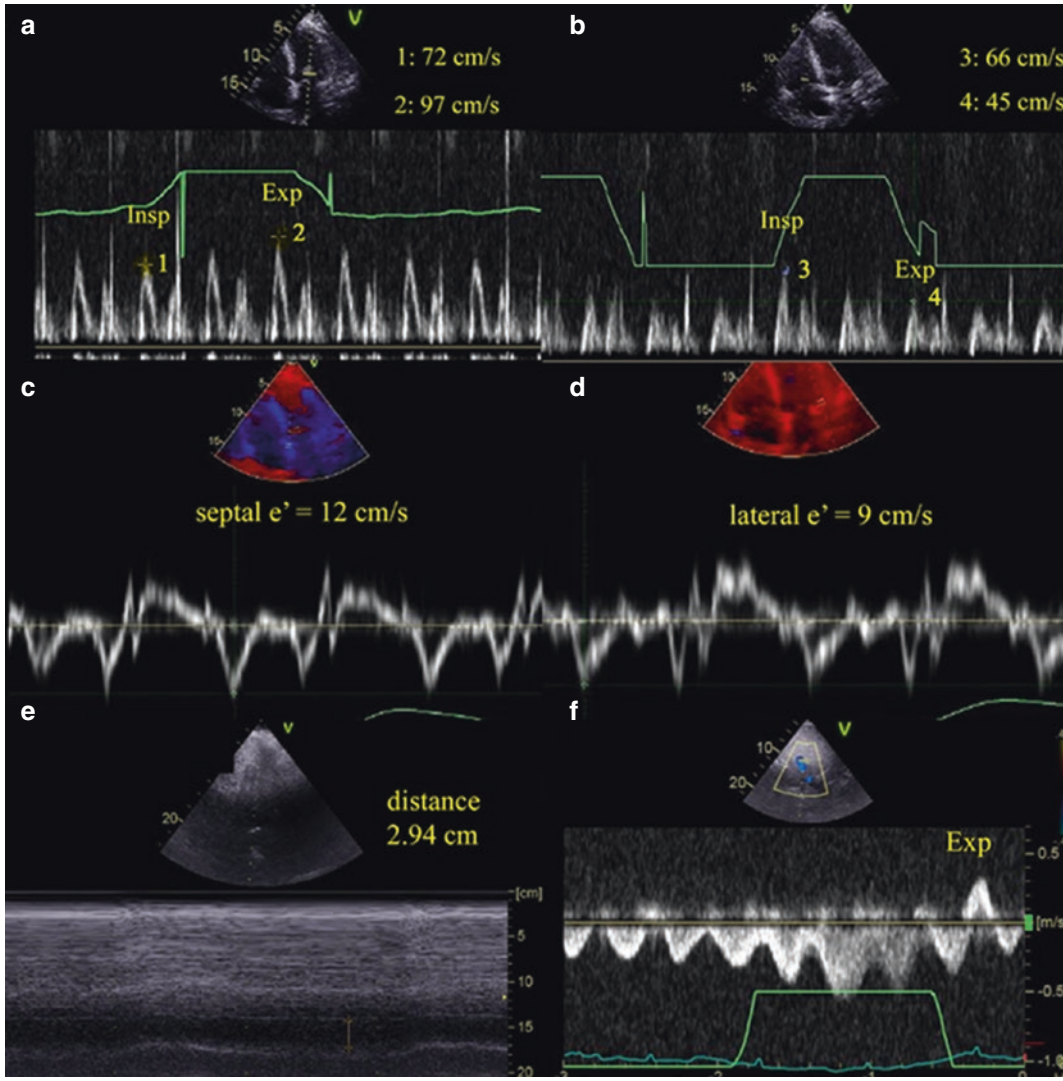

Fig. 16.13 Echocardiography of a patient with effusive-constrictive pericarditis. (**a**) There is significant respiratory variation in the mitral inflow [(expiration – inspiration)/expiration; (97–72)/97 × 100% = ~25.8%]. Insp indicates inspiration and Exp expiration. (**b**) There is significant respiratory variation in the tricuspid inflow [(expiration – inspiration)/expiration; (45–66)/45 × 100% = ~ −46.7%]. Tissue Doppler imaging (TDI) of mitral annulus shows "annulus reversus" with (**c**) septal e' of 12 cm/s and (**d**) lateral e' of 9 cm/s. (**e**) Inferior vena cava is plethoric with diameter of ~2.9 cm and <50% variation in size during respiration. (**f**) Pulsed wave Doppler of hepatic vein flow showed significant end expiratory diastolic flow reversal with hepatic vein expiratory diastolic reversal ratio of ~0.9

dial effusion with features of constriction. There were ventricular septal shift and significant respiratory variation in both mitral and tricuspid inflows, 25.8% and −46.7%, respectively (Fig. 16.13a, b). "Annulus reversus" was present (Fig. 16.13c, d). IVC was still plethoric (Fig. 16.13e). Hepatic vein flow showed significant end expiratory diastolic flow reversal with the hepatic vein expiratory diastolic reversal ratio of ~0.9 (Fig. 16.13f). Since the central venous pressure before and after pericardiocentesis were still >20 mmHg, the diagnosis of effusive-constrictive pericarditis (ECP) is confirmed.

ECP is an uncommon clinical syndrome characterized by the coexistence of tense pericardial effusion and constriction of the heart by the visceral pericardium. Incidence ranges from 2% to 15% of patients with pericarditis, depending on the difference in patient populations, methodologies, and definition. The hallmark of ECP is the presence of the persistently elevated right atrial pressure measured by invasive hemodynamic assessment after intra-pericardial pressure is reduced to a normal level by pericardiocentesis.

Patient was treated with steroids and colchicine. The repeated echocardiography 1 year later did not reveal any more feature of constriction.

Restrictive Cardiomyopathy (Cardiac Amyloidosis)

A 72-year-old male initially presented with new onset atrial fibrillation and dyspnea at rest. Echocardiogram performed was performed during sinus rhythm and showed a depressed ejection fraction of ~40%, marked biatrial enlargement with grade III diastolic dysfunction, moderate pulmonary hypertension, increased left ventricular wall thickness and a speckling pattern of myocardium. GLS study showed the pattern of apical sparing (Fig. 16.3c). The patient was treated with beta-blockers and diuretics presumptively, while serum and urine electrophoresis were negative. The bone marrow biopsy was significant for plasma cell population, and Congo red staining was consistent with amyloidosis. Given the diagnosis of systemic amyloidosis and severe diastolic dysfunction, the patient was presumed to have cardiac amyloidosis and started on treatment for amyloidosis with prednisone and intra-venous melphalan. Due to the chronic nature of the condition and the late presentation as well as the lack of efficacious treatment options, the patient did not respond to therapy and continued to deteriorate over the next few months. Cardiac amyloidosis usually presents later in life with an insidious onset and often is diagnosed as a result of key echocardiographic features. In this case, further testing including CT, MRI, or catheterization was not warranted for diagnosis.

Pearls of Assessment

When assessing a patient with suspected CP or RCM, a focused history and physical examination with emphasis on symptoms as well as clues or signs that suggest either diagnosis is essential. Chest X-ray and ECG are also useful in the initial workup to assess for cardiomegaly and pericardial calcification as well as voltage pattern for possible RCM. Non-invasive imaging is the mainstay and first line of the workup and echocardiography with respirometer to assess for changes in filling velocity and pressures, as well as pericardial thickening is usually the next step. Depending on the echocardiographic results and suspicion for a pericardial or myocardial process, further non-invasive imaging including either a cardiac CT or CMR can be useful to obtain more information that cannot be provided by echocardiography, e.g. pericardial calcification, pericardial inflammation, myocardial fibrosis, etc. If the diagnosis is still inconclusive, left and right heart catheterization with a focus on the hemodynamic findings of "dip-and-plateau" on RV and LV pressure tracings as well as ventricular interdependence which point to a specific diagnosis of CP. Table 16.2 summarizes the key distinguishing features of constrictive pericarditis and restrictive cardiomyopathy. Treatment of symptoms with diuretics is usually a temporizing measure and often patients require surgical pericardiectomy for symptomatic relief of CP. Treatment of RCM depends on the underlying etiology.

Table 16.2 Key distinguishing features of constrictive pericarditis and restrictive cardiomyopathy

	Constrictive pericarditis	Restrictive cardiomyopathy
Physical examination	Pericardial knock	S4 (early) and S3 (late presentation)
	Apical retraction	Prominent apical impulse
Echocardiography		
2D images	Pericardial thickening	Biatrial enlargement
	Ventricular septal shift	Ventricular hypertrophy (usually present)
	Pericardial effusion (may be present)	Myocardial speckling (amyloidosis)
PW mitral inflow	*E*/*A* ratio ≥ 2	*E*/*A* ratio ≥ 2
	>25% respiratory variation in E wave[a]	<25% respiratory variation in *E* wave[a]
PW tricuspid inflow	>40% respiratory variation in E wave[a, b]	<40% respiratory variation in E wave[a, b]
TDI	"Annulus reversus" – lateral e' velocity is reduced, whereas septal e' velocity is normal or higher than normal	Both septal and lateral e' velocities are reduced
PW hepatic vein flow	Hepatic vein flow reversal ratio ≥ 0.79	Hepatic vein flow reversal ratio < 0.79
GLS	LV septum > free wall	Apical sparing (amyloidosis)
Left and right heart catheterization	Diastolic equalization of pressure between LV and RV	LVEDP may be equal to or greater than RVEDP
	Ventricular interdependence	Ventricular concordance
	Systolic area index >1.1	Systolic area index <1.1
	Pulmonary pressure usually normal	Pulmonary hypertension (RVSP >50 mmHg)

GLS Global longitudinal strain, *LV* left ventricle, *LVEDP* left ventricular end-diastolic pressure, *PW* pulse wave Doppler, *RA* right atrium, *RV* right ventricle, *RVEDP* right ventricular end-diastolic pressure, *RVSP* right ventricular systolic pressure, *TDI* tissue Doppler imaging

[a]Respiratory variation = (expiration – inspiration)/expiration × 100%

[b]This is negative value

Review Questions

1. Which of the following(s) is/are cause(s) of pericardial constriction?
   A. Infection
   B. Prior cardiac surgery
   C. Mantle radiation for lymphoma
   D. A and B
   E. All of the above

   Answer: E. Infection, prior cardiac surgery, and mantle radiation for lymphoma are established causes of constrictive pericarditis.
2. Which of the following features of left and right heart cardiac catheterization are seen in constriction?
   A. Diastolic equalization of pressure between LV and RV
   B. Ventricular interdependence
   C. M (or W) pattern on right atrial waveform
   D. Steep or rapid *y*-descent
   E. All of the above

   Answer: E. All of the findings listed above are typically seen in constrictive pericarditis.
3. Which of the following statement is false regarding constrictive pericarditis?
   A. "Annulus reversus" results from a compensatory increase in longitudinal movement of the septum in order to accommodate filling secondary to the limited lateral expansion of the heart during filling secondary to pericardial encasement.
   B. "Pulsus paradoxus" means there is an abnormal (>10 mmHg) decrease in systolic blood pressure with inspiration.
   C. A pericardial knock occurs at the nadir of the x-descent and is consistent with abrupt cessation of ventricular filling.
   D. The American Society of Echocardiography recommends the calculation of percentage of respiratory variation in constrictive pericarditis for mitral and tricuspid inflow is (expiration – inspiration)/expiration × 100%.
   E. Measurement of pericardial thickness using transthoracic echocardiogram is not recommended.

   Answer: C. A pericardial knock occurs at the nadir of the y-descent and is consistent with abrupt cessation of ventricular filling.

4. Which of the following echocardiographic findings is not consistent with restrictive physiology?
   A. Large atria
   B. Blunted *S*/*D* ratio in pulmonary and hepatic vein flows
   C. Low septal and lateral e' velocity on TDI (i.e., septal e' velocity <7 cm/s; lateral e' velocity <10 cm/s)
   D. Decreased mitral inflow velocity (*E* wave) with inspiration
   E. E/A ratio >2

   Answer: D. Decreased mitral inflow (*E* wave) is found in constrictive pericarditis, whereas in restrictive cardiomyopathy, mitral inflow is not changed with respiration. The other findings are all seen in restrictive cardiomyopathy.
5. Which of the following is not the distinguishing features of constrictive pericarditis and restrictive cardiomyopathy?
   A. Ventricular septal shift
   B. Kussmaul's sign
   C. Ventricular interdependence
   D. Hepatic vein flow reversal ratio ≥0.79
   E. Annulus reversus

   Answer: B. Kussmaul's sign can be present in both constrictive pericarditis and restrictive cardiomyopathy.

References

1. Welch TD. Constrictive pericarditis: diagnosis, management and clinical outcomes. Heart. 2017; https://doi.org/10.1136/heartjnl-2017-311683. pii: heartjnl-2017-311683
2. Boyd LJ, Elias H. Contribution to diseases to the heart and pericardium. Bull NY Med Coll. 1955;18:1–31.
3. Elliott P, Andersson B, Arbustini E, et al. Classification of the cardiomyopathies: a position statement from the European Society of Cardiology working group on myocardial and pericardial diseases. Eur Heart J. 2008;29(2):270–6.
4. Muchtar E, Blauwet LA, Gertz MA. Restrictive cardiomyopathy genetics, pathogenesis, clinical manifestations, diagnosis, and therapy. Circ Res. 2017;121(7):819–37. https://doi.org/10.1161/CIRCRESAHA.117.310982.
5. Welch TD, Ling LH, Espinosa RE, et al. Echocardiographic diagnosis of constrictive pericarditis Mayo Clinic criteria. Circ Cardiovasc Imaging. 2014;7(3): 526–34. https://doi.org/10.1161/CIRCIMAGING.113.001613.
6. Nagueh SF, Smiseth OA, Appleton CP, et al. Recommendations for the evaluation of left ventricular diastolic function by echocardiography: an update from the American Society of Echocardiography and the European Association of Cardiovascular Imaging. J Am Soc Echocardiogr. 2016 Apr;29(4):277–314. https://doi.org/10.1016/j.echo.2016.01.011.
7. Alraise MC, Kusunose K, Negishi K, et al. Relation between echocardiographically estimated and invasively measured filling pressures in constrictive pericarditis. Am J Cardiol. 2014;113(11):1911–6. https://doi.org/10.1016/j.amjcard.2014.03.022.
8. Ha JW, Oh JK, Ling LH, et al. Annulus paradoxus: transmitral flow velocity to mitral annular velovity ration is inversely proportional to pulmonary capillary wedge pressure in patients with constrictive pericarditis. Circulation. 2001;104(9):976–8.
9. Klein AL, Abbara S, Agler DA, et al. American Society of Echocardiography clinical recommendations for multimodality cardiovascular imaging of patients with pericardial disease: endorsed by the Society for Cardiovascular Magnetic Resonance and Society of Cardiovascular Computed Tomography. J Am Soc Echocardiogr. 2013;26(9):965–1012.e15. https://doi.org/10.1016/j.echo.2013.06.023.
10. Smiseth OA, Torp H, Opdahl A, et al. Myocardial strain imaging: how useful is it in clinical decision making? Eur Heart J. 2016;37(15):1196–207. https://doi.org/10.1093/eurheartj/ehv529.
11. Urbano-Moral JA, Rowin EJ, Maron MS, et al. Investigation of global and regional myocardial mechanics with 3-dimensional speckle tracking echocardiography and relations to hypertrophy and fibrosis in hypertrophic cardiomyopathy. Circ Cardiovasc Imaging. 2014;7(1):11–9. https://doi.org/10.1161/CIRCIMAGING.113.000842.
12. Amaki M, Savino J, Ain DL, et al. Diagnostic concordance of echocardiography and cardiac magnetic resonance-based tissue tracking for differentiating constrictive pericarditis from restrictive cardiomyopathy. Circ Cardiovasc Imaging. 2014;7(5):819–27. https://doi.org/10.1161/CIRCIMAGING.114.002103.
13. Talreja DR, Edwards WD, Danielson GK, et al. Constrictive pericarditis in 26 patients with histologically normal pericardial thickness. Circulation. 2003;108:1852–7. https://doi.org/10.1161/01.CIR.0000087606.18453.FD.
14. Sagrista-Sauleda J, Permanyer-Miralda G, Candell-Riera J, et al. Transient cardiac constriction: an unrecognized pattern of evolution in effusive acute idiopathic pericarditis. Am J Cardiol. 1987;59:961–6.
15. Taylor AM, Dymarkowski S, Verbeken EK, Bogaert J. Detection of pericardial inflammation with late-enhancement cardiac magnetic resonance imaging: initial results. Eur Radiol. 2006;16:569–74.
16. Gupta A, Singh Gulati G, Seth S, et al. Cardiac MRI in restrictive cardiomyopathy. Clin Radiol.

2012;67(2):95–105. https://doi.org/10.1016/j.crad.2011.05.020.
17. Maceira AM, Joshi J, Prasad SK, et al. Cardiovascular magnetic resonance in cardiac amyloidosis. Circulation. 2005;111(2):186e93.
18. Kondur AK, Li T, Vaitkevicius P, et al. Quantification of myocardial iron overload by cardiovascular magnetic resonance imaging T2∗ and review of the literature. Clin Cardiol. 2009;32(6):E55e9.
19. Talreja DR, Nishimura RA, Oh JK, Holmes DR. Constrictive pericarditis in the modern era: novel criteria for the diagnosis in the cardiac catheterization laboratory. J Am Coll Cardiol. 2008;51(3):315–9. https://doi.org/10.1016/j.jacc.2007.09.039.

Valvular Heart Disease

17

Amar Krishnaswamy and Brian P. Griffin

Introduction

The diagnosis and management of valvular heart disease are challenging and require a knowledge of the relevant historical clues, appreciation of salient physical exam findings, and the ability to critically interpret imaging and invasive hemodynamic data. This chapter will focus on diagnosis of the valve disorders most frequently encountered in the care of patients on the cardiac ward.

Aortic Stenosis

Case Presentation

The patient is a 78-year-old man with a history of hypertension, hyperlipidemia, and percutaneous coronary intervention with drug-eluting stent to the mid-left anterior descending artery 4 years prior. He noted the development of exertional dyspnea over the past 6–12 months, as well as mild chest discomfort over the past 3 months that resolved with rest. Initially attributed to "old age," he finally decided to seek medical attention due to progression of his symptoms.

Salient physical examination findings included mild hypertension (BP 145/90 mmHg) and a normal heart rate (70 bpm). The PMI was not displaced and an S4 gallop was appreciated. A 2/6 systolic crescendo/decrescendo murmur was heard at the upper sternal border peaking late in systole, radiating to the carotids bilaterally. The carotid artery upstrokes were mildly delayed and weak.

Given the symptoms and physical exam findings, transthoracic echocardiography (TTE) was performed. The TTE revealed normal left ventricular function with moderate concentric hypertrophy, a moderately thickened and calcified aortic valve, and severe aortic stenosis (AS) with peak and mean gradients of 85 and 50 mmHg, respectively. With a diagnosis of severe, symptomatic aortic stenosis, the patient was referred for coronary angiography in anticipation of open-heart surgery. Angiography revealed only mild CAD and a patent stent in the mid-LAD, and the patient went to have uneventful valve replacement with an aortic bioprosthesis.

Epidemiology and Pathophysiology

Aortic stenosis (AS) is present in almost 5% of individuals over the age of 75 years [1]. AS may develop due to a congenital valve disorder

A. Krishnaswamy (✉)
Interventional Cardiology, Cleveland Clinic, Cleveland, OH, USA
e-mail: KRISHNA2@ccf.org

B. P. Griffin
Cardiovascular Imaging, Cleveland Clinic, Cleveland, OH, USA
e-mail: GriffiB@ccf.org

A. T. Askari, A. W. Messerli (eds.), *Cardiovascular Hemodynamics*, Contemporary Cardiology,
https://doi.org/10.1007/978-3-030-19131-3_17

(unicuspid or bicuspid valve), as a result of rheumatic valvular heart disease, as a complication of chest radiation, or most commonly due to degenerative ("senile") thickening and calcification. Over time, AS causes increased pressure on the left ventricle (LV) and leads to a chronically increased afterload state. In order to compensate, the ventricle hypertrophies. Due to increased LV mass and worsening diastolic filling mechanics, diastolic dysfunction ensues. With worsening and long-standing stenosis, LV systolic function eventually falls. Furthermore, impaired LV diastolic and/or systolic function may lead to pulmonary hypertension due to left-sided heart disease. Since senile AS shares many risk factors with coronary artery disease (CAD), the clinical presentation may reflect progressive coronary stenosis in these patients in addition to increased myocardial oxygen demand due to the valvular stenosis.

Patients with aortic stenosis may live for years with a "known murmur" that is clinically silent, especially in cases of bicuspid or rheumatic valve disease. It is estimated that the valve area decreases by approximately 0.12 cm^2/year in patients with senile disease, providing a long period of asymptomatic disease [2]. On the other hand, the development of symptoms portends a grave prognosis: without treatment, angina, syncope, and heart failure are associated with a 50% mortality at 5 years, 3 years, and 2 years, respectively [3].

Physical Examination

The physical examination of patients with AS provides a number of characteristic findings. A systolic murmur is best heard in the aortic position (right upper sternal border) and radiates to the carotid arteries. As stenosis worsens, the peak of the murmur moves closer to the second heart sound (S2) since LV ejection across the valve requires a longer ejection time. With very severe disease, the S2 may be almost inaudible due to the proximity of the murmur's peak to the closing of the valve. With severe AS, a murmur mimicking mitral regurgitation (MR) may also be heard at the apex, but does not radiate to the axilla; this is known as Gallivardin's phenomenon. Palpation of the pulse (preferably at the carotid arteries) in patients with severe AS reveals the characteristic slow ascent (*parvus*) and delayed (*tardus*) peak. Additionally, palpation of the pulses at the upper extremity may reveal a "brachio-radial" delay in patients with severe AS that often presents prior to LV failure or clinical symptoms. Of note, the finding is subtle, with a measured delay of 53.5 msec [4]. An S4 gallop may be heard in the setting of left ventricular hypertrophy (LVH) and a stiffened ventricle.

An important differentiation to be made is between the murmur of AS and that of hypertrophic cardiomyopathy (HCM). In patients with AS, a reduction in preload (i.e., with the Valsalva maneuver or moving from squatting to standing) will reduce flow across the stenotic valve and therefore lessen the murmur. Conversely, a reduction in preload causes decreased filling of the LV cavity resulting in a smaller left ventricular outflow tract (LVOT) diameter and worsening systolic anterior motion (SAM) of the mitral valve and therefore augments the murmur in patients with HCM.

Echocardiography

Transthoracic echocardiography (TTE) is the cornerstone of AS assessment and provides information on left ventricular function, aortic valve morphology, degree of stenosis, and an assessment of pulmonary pressures. Rarely, transesophageal echocardiography (TEE) may be necessary for diagnosis if TTE images are limited or for precise planimetry of the valve area (discussed below). In the early stages of AS, LV systolic function is preserved, with varying degrees of compensatory LVH. Over time, with LV stiffening, diastolic filling becomes more dependent upon atrial systole and diastolic dysfunction ensues. Eventually, the chronically afterloaded LV dilates, and left ventricular systolic function declines.

The degree of valvular stenosis can be assessed both qualitatively and quantitatively. The presence of congenital disorders (i.e., unicuspid, bicuspid, etc.) is assessed in the parasternal long-axis (the valve does not coapt in the center line or may have a "doming" appearance) and short-axis

views (the number of cusps can be identified along with the presence of a "raphe"), as well as the degree of thickening and calcification. The short-axis view is also useful for performing planimetry of the aortic orifice.

Hemodynamic assessment of AS by TTE requires an assessment of the following: jet velocity, peak and mean gradients, and the dimensionless index (DI) (Table 17.1) [5]. Peak jet velocity gives a rough estimate of stenosis severity; velocity >4 m/sec is considered severe. The peak gradient is calculated using the peak velocity via the Bernoulli equation ($\Delta P = 4v^2$).

Table 17.1 Echocardiographic evaluation of aortic stenosis severity

	Mild	Moderate	Severe
Peak jet velocity (m/sec)	<3.0	3.0–4.0	>4.0
Mean gradient (mmHg)	<25	25–40	>40
Valve area (cm^2)	>1.5	1.0–1.5	<1.0
Dimensionless index	*	*	<0.25

The mean gradient is calculated using the velocity time integral (VTI), which sums the velocities over an entire cardiac cycle and is provided by tracing the continuous-wave Doppler aortic outflow envelope. The dimensionless index is a ratio of the velocity (or VTI) in the left ventricular outflow tract (LVOT) to that in the aorta; a ratio <0.25 implies an AVA that is <25% of the LVOT area. The DI is helpful in patients for whom LVOT diameter is difficult to measure.

Calculation of aortic valve area (AVA) may be performed by planimetry as above or by using the continuity equation. The continuity equation makes the assumption that flow and volume are constant. Since flow = cross-sectional area (CSA) × velocity, the relationship can also be described as stroke volume = CSA × VTI, and since volume is constant, the equation can be rearranged as $A_{AV}V_{AV} = A_{LVOT}V_{LVOT}$. Calculation of the AVA is demonstrated in Fig. 17.1. Common mistakes in calculation of the AVA

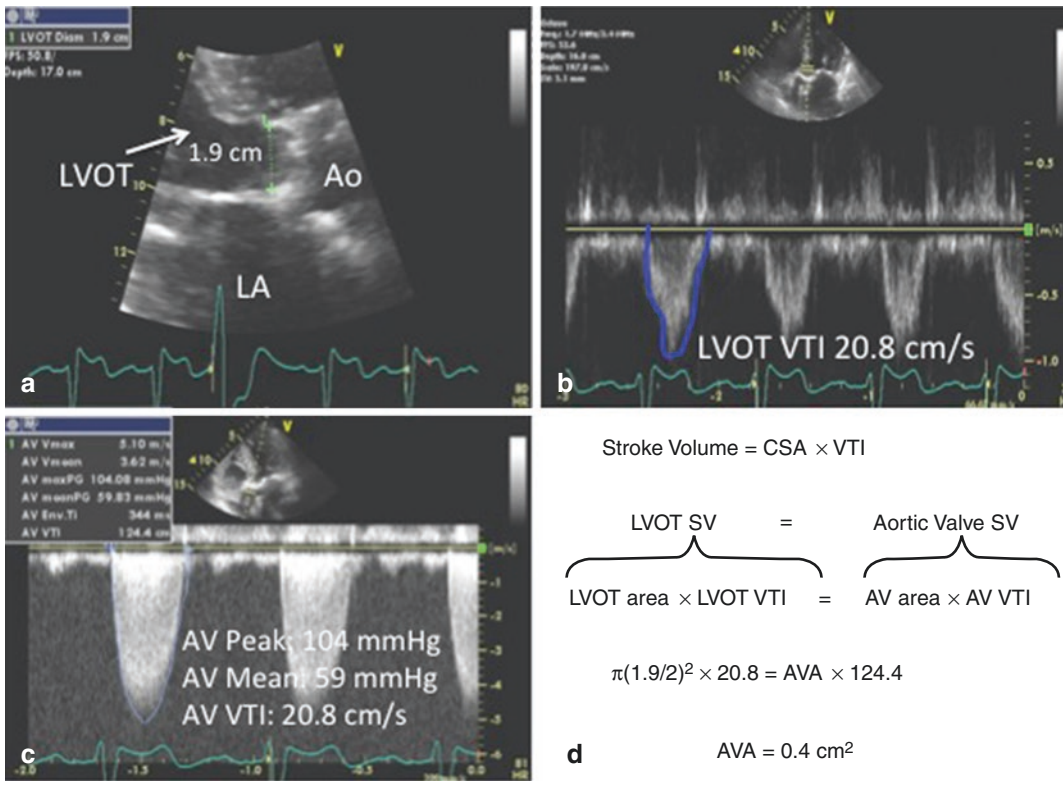

Fig. 17.1 Calculation of aortic valve area (AVA) using the continuity equation. Measurement of the left ventricular outflow tract (LVOT) diameter (**panel A**), velocity time integral (VTI) in the LVOT (**panel B**), and aortic valve (AV) VTI (**panel C**) is necessary to calculate the AVA (**panel D**)

include incorrect measurement of the LVOT diameter (underestimation of the LVOT leads to an underestimation of the AVA) or LVOT/AV outflow gradients.

Low-Flow, Low-Gradient Aortic Stenosis

Patients with chronic pressure overload from AS, CAD, or intrinsic myocardial dysfunction may present with depressed LV function and aortic stenosis with a low gradient. Low-flow/low-gradient (LF/LG) AS is defined as an LVEF <35%, mean gradient <30 mmHg, and AVA < 1.0 cm^2. Evaluation of the true degree of AS in these patients presents a common clinical quandary, as patients may have truly severe AS or "functional" AS caused by poor leaflet excursion in the setting of a low cardiac output (pseudo-AS).

Dobutamine stress echocardiography (DSE) is a common diagnostic tool in this setting. With infusion of increasing doses of dobutamine (DBA; 5–20 mcg), the stroke volume, peak velocity, mean gradient, and AVA are measured/calculated. An increase in SV >20% implies contractile reserve. Increases in peak velocity and/or mean gradient imply true AS; the increased flow across the valve is limited by intrinsic valve disease and results in higher gradients and does not simply cause increased leaflet excursion. An increase in AVA > 0.3 cm^2 implies pseudo-AS; increase in LVOT velocity is greater than the increase in AV velocity due to increased leaflet excursion, providing a higher calculated AVA. The potential outcomes of DSE and the clinical diagnosis are summarized in Table 17.2 [6].

For patients with pseudo-AS, treatment is directed toward the medical management of heart failure. Studies on AVR in patients with LF/LG true AS have shown that perioperative mortality is only mildly increased (5%) in patients with contractile reserve on DSE. On the other hand, patients with LF/LG true AS but without contractile reserve face a significant perioperative mortality (32%) [7]. However, survival thereafter is reasonable, and improvement in ejection fraction is similar in both groups [8].

Table 17.2 Possible outcomes of dobutamine stress echocardiography in low-flow, low-gradient aortic stenosis

Dobutamine response	Diagnosis
Increase in CO and gradient	Contractile reserve present
	True AS
Increase in CO and AVA with constant/decreased gradient	Contractile reserve present
	Pseudo-AS
No response to DBA	No contractile reserve
	Indeterminate re: AS

CO cardiac output, *AVA* aortic valve area, *AS* aortic stenosis, *DBA* dobutamine

Cardiac Catheterization

Outside of the evaluation for coronary artery disease, cardiac catheterization in patients with AS is reserved for situations when the degree of symptoms and severity of AS are contradictory based on noninvasive testing [5]. Catheterization may be used to measure intracardiac pressures, cardiac output, and valve gradient and calculate the AVA.

Historically, measurements of the valve gradient were taken by placing a catheter in the aortic root and another in the LV via transseptal puncture, but this is rarely performed now. Valve gradient may be measured with a dual-lumen pigtail catheter that simultaneously measures pressures in the LV and aorta, or by placing a catheter in the LV and then quickly pulling it back to the aortic root ("pullback gradient"). It should be noted that this "peak-to-peak" gradient is generally lower than the peak gradient obtained by Doppler echocardiography, which is sampled as the peak instantaneous velocity (Fig. 17.2). The peak-to-peak gradient correlates well to the mean gradient.

The valve area is usually calculated using the *Gorlin equation*:

$$\mathrm{AVA} = \mathrm{CO} \div \left(\mathrm{HR} \times \mathrm{SEP} \times 44.3 \times \sqrt{\text{mean gradient}} \right)$$

[CO, cardiac output; HR, heart rate; SEP, systolic ejection period]

Since the Gorlin method is dependent on flow across the aortic valve, patients with LF/LG AS will have a significantly underestimated AVA. In these cases, dobutamine infusion during catheterization may reveal pseudo-AS similar to that

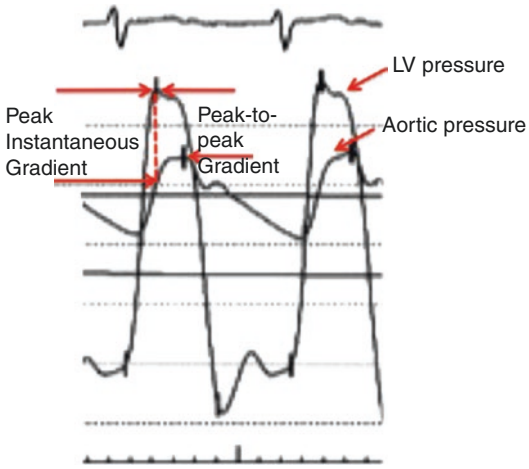

Fig. 17.2 Simultaneous LV and aortic pressure tracing. Peak-to-peak gradient is measured as the difference between peak LV and aortic pressures during cath; peak gradient by echocardiography is an instantaneous peak. Mean gradient is calculated as the average pressure difference between LV and aorta pressures (area between the curves)

described during DSE above (increased cardiac output with increased AVA and stable or decreased gradient).

A simplification of the Gorlin equation is the *Hakki equation*, based upon the assumption that the (HR × SEP × 44.3) approximates 1 under normal conditions [9]:

$$\text{AVA} = \text{CO} \div \sqrt{\text{mean gradient}}$$

For patients with a heart rate >100 bpm, the AVA obtained using the Hakki method should be divided by 1.35 for increased accuracy.

Aortic Regurgitation

Case Presentation

A 42-year-old man presented with progressive dyspnea over a 6-month period. He was quite active previously, running 3 miles every other day, but now required a break after just 2 miles due to dyspnea. He also noticed some dyspnea with walking the three flights of stairs to his apartment, which was new over the prior 1–2 months. He had not experienced orthopnea but has had a few episodes of paroxysmal nocturnal dyspnea over the prior 3 months. He denied chest discomfort or lower extremity edema.

On physical examination, cardiac auscultation was significant for a long, decrescendo, holodiastolic murmur heard best at the left sternal border as the patient leaned forward. Palpation of the brachial pulse revealed a brisk and forceful upstroke and wide pulse pressure. Gentle pressure applied at the tip of the fingernails revealed a "to-and-fro" filling of the nailbeds.

TTE performed revealed a bicuspid aortic valve with fusion of the right and left coronary leaflets and with minimal calcification. There was mild anterior leaflet prolapse resulting in severe, posteriorly directed aortic regurgitation (AR). The aortic root and ascending aorta were normal in size without evidence of dilation. LV systolic function and chamber size were normal.

Given a diagnosis of severe, symptomatic aortic regurgitation, the patient underwent preoperative coronary angiography that revealed minimal atherosclerosis. He then underwent successful aortic valve repair.

Epidemiology and Pathophysiology

Aortic regurgitation (AR) is present in up to 12% of men and may complicate rheumatic valve disease, radiation valvular disease, or bicuspid aortic valve. Infective endocarditis may cause AR due to valve degeneration, leaflet perforation, or paravalvular leakage. Anorectic drugs, such as fenfluramine and phentermine ("fen-phen"), may cause AR through a serotonin-mediated pathway that results in degenerative changes in valve morphology. Additionally, aortic pathology such as ascending dissection or aortic root dilation can cause malcoaptation of the valve and resultant AR. A rare cause of AR is the supracristal VSD, which can result in AR due to prolapse of the noncoronary leaflet.

Of the causes listed above, aortic dissection and endocarditis often cause acute severe AR. This is usually poorly tolerated from a hemodynamic perspective, primarily due to a degree of LV compliance that does not accommodate the

massive increase in volume and leads to acute volume overload and diminished cardiac output. As a result, acute AR is usually a surgical emergency.

The degree of regurgitation is dependent on the diastolic pressure gradient between the aorta and LV, duration of diastole, size of the regurgitant orifice, and LV compliance. In chronic AR, compensatory LV cavity dilation, increase in LV compliance, and LV wall hypertrophy ensue to accommodate the increased filling and afterload. Maintenance of an adequate heart rate (i.e., judicious use of negative chronotropic agents) is also important to minimize diastolic regurgitation time. Together, these changes allow the LVEDP to stay relatively normal and stroke volume to increase. Patients may therefore remain asymptomatic for long periods of time and develop symptoms or LV dysfunction at an average of 4.3% per year [5].

It should also be noted that since diastolic pressure in the aorta is reduced in patients with AR, coronary perfusion pressure is also reduced. Patients may therefore develop symptoms of coronary insufficiency, even in the absence of flow-limiting coronary stenoses, due to decrease coronary flow and increased LV oxygen demand.

Physical Examination

In acute AR, the hallmark diastolic murmur of AR may not be appreciated as easily, since the aortic diastolic and LV diastolic pressures equalize rapidly, and patients are often quite tachycardic due to hemodynamic instability. This also highlights the importance of the judicious use of agents that decrease chronotropy (i.e., beta blockers, non-dihydropyridine calcium-channel blockers, etc.), as slower heart rates allow a longer period of regurgitation.

With chronic AR, however, the long-standing increase in LV volume and concomitant hypertrophy allow the ventricle to accommodate a long period of diastolic backflow through the regurgitant lesion, providing the classic auscultatory diastolic murmur. The murmur is best heard at the aortic position (left sternal border) and may be more easily appreciated with the patient leaning forward. Typically, AR due to aortic dilation is heard at the right sternal border, and that due to valvular disease is heard at the left sternal border. A murmur resembling mitral stenosis (MS) may also be heard at the apex. It is thought that this *Austin Flint* murmur is the result of premature closure of the anterior mitral leaflet due to pressure from the regurgitation jet of AR.

Measurement of the blood pressure often reveals a widened pulse pressure (SBP – DBP). This is due to the fact that the SBP is increased in the setting of higher stroke volume and DBP is decreased due to the regurgitation of blood into the LV.

The peripheral examination in AR provides a number of eponymous findings that have variable degrees of sensitivity and specificity for diagnosis (Table 17.3) [10]. Most of these findings are the result of an increase in stroke volume accompanied by a sudden drop in aortic pressure due to the valvular regurgitation (i.e., wide pulse pressure). Although the majority of these clinical findings lack significant clinical relevance, two signs, Durozier's sign and Hill's sign, have demonstrated clinical correlation with the severity of AR.

Table 17.3 Physical findings in the peripheral examination of severe aortic regurgitation

Physical sign	Description
Corrigan's pulse ("water hammer pulse")	Rapid rise and fall of the arterial pulse
Duroziez's sign	"To-and-fro" murmur heard at the femoral artery elicited with femoral artery compression
Quincke's sign	Capillary pulsations at the nail bed elicited by gentle compression of the distal nail
de Musset's sign	Bobbing of the head
Mueller's sign	Pulsation of the uvula
Hill's sign	Lower extremity BP > upper extremity BP
Rosenbach's sign	Pulsatile liver
Gerhard's sign	Pulsatile spleen

Adapted from Babu et al., Ann Int Med 2003, with permission

Echocardiography

When suggested by history and physical examination, echocardiography provides the definitive diagnosis of AR and provides an assessment of valve morphology, LV size and function, aortic root structure, and of course regurgitation severity.

An assessment of valve anatomy is important to define the etiology of AR. Congenital bicuspid valve disease is responsible for most cases of valvular AR in the developed world, though rheumatic disease remains the most common cause worldwide. In patients with a bicuspid valve, an assessment of the degree of leaflet degeneration and calcification is important to determine whether valve repair may be feasible or whether valve replacement will be necessary. Similarly, assessment for endocarditis is important for antibiotic management and planning the treatment strategy (i.e., large vegetation, presence of abscess, leaflet perforation, etc.).

LV size and systolic function are important to the treatment algorithm. In patients with severe, asymptomatic AR, surgery is not indicated unless there is evidence of LV dilation (end-diastolic dimension >7.5 cm or end-systolic dimension >5.5 cm) or systolic dysfunction (LVEF <50%). It is therefore recommended that patients with chronic AR have close echocardiographic surveillance in the absence of symptoms (every 1 year with mild/moderate AR and every 6 months with severe AR) [5].

Evaluation of ascending aorta and root structure is important for diagnosis and also may dictate the course of management. For instance, in patients with bicuspid AV, dilation of the aorta beyond 5 cm is considered an indication for surgery, and concomitant AV surgery may therefore be performed even in the absence of symptomatic AR. Aortic dissection involving the ascending aorta is a surgical emergency and should be managed accordingly as appropriate.

An accurate assessment of AR severity is nuanced and requires a critical appraisal of numerous parameters taken together. Considerations include regurgitant jet width/LVOT height, vena contracta (VC), calculation of the proximal isovelocity surface area (PISA), subjective appearance of AR jet density and pressure half-time (PHT) of the AR jet on continuous-wave (CW) Doppler, and evidence of diastolic flow reversal in the descending aorta using pulsed-wave (PW) Doppler (Table 17.4).

Table 17.4 Echocardiographic characteristics of severe aortic regurgitation (AR)

Vena contracta	>0.6 cm
Jet width/LVOT height	>60%
PISA	ERO > 0.3 cm^2
Pressure half-time	<250 msec
Descending aorta pulsed-wave Doppler	Pandiastolic reversal of flow with velocity >20 cm/sec

LVOT left ventricular outlflow tract, *ERO* effective regurgitant orifice

The regurgitant jet width is measured in the LVOT in the parasternal long-axis view and compared to the height of the LVOT; a ratio of >60% indicates severe AR. The VC is usually measured in the same view (though the apical five-chamber view may be used) and is the width of the jet at its narrowest point at the AV; a width of >0.6 cm signifies severe AR. By definition, the VC is smaller than the regurgitant jet width.

The PISA method is used most commonly in the assessment of mitral regurgitation (discussed in detail later in this chapter) but can be applied in AR as well to calculate the effective regurgitant orifice (ERO). An ERO >0.3 cm^2 is considered severe.

The basis for measuring PHT (the time required to reduce the gradient across the valve by ½) is as follows: with worsening AR, the aortic diastolic pressure and LVEDP equilibrate more quickly, resulting in a shorter PHT. A PHT < 250 msec signifies severe AR and PHT > 400 msec mild AR. While this method is used clinically, it should be noted that changes in loading conditions (i.e., alterations in SVR, LV compliance) may have effects on the PHT that are contrary to the regurgitant fraction measured. Furthermore, patients with chronic AR may have modified their LV compliance enough that the LV accommodates a long period of diastolic filling (i.e., long PHT). Therefore, the PHT should be used only as a piece of the diagnostic puzzle [11]. Evaluation of the AR jet density on

CW is a subjective measure, and pitfalls include a lack of coaxial alignment of the Doppler signal with the regurgitant flow. Nevertheless, a dense jet with a short PHT may increase the suspicion of severe AR. It should also be noted that due to the large stroke volume ejected by the LV in chronic severe AR, there may be a small outflow gradient measured though this does not reflect true AS.

The presence of some regurgitant flow in the descending aorta in early diastole is common and is due to closure of the AV. Persistent holodiastolic flow reversal with a velocity >20 cm/sec, however, is a marker of severe AR (Fig. 17.3). The presence of diastolic MR (appreciated on the CW or PW Doppler in the apical four-chamber view) may be seen in patients with severely elevated LV pressures, such as in acute severe AR.

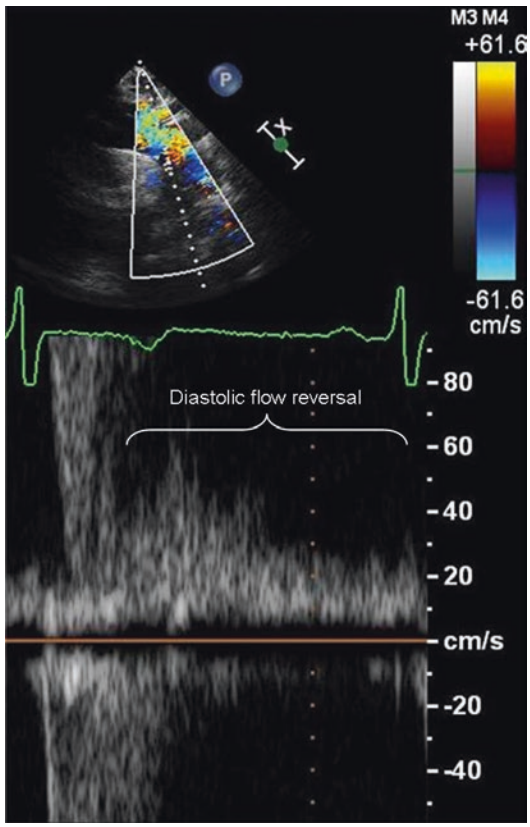

Fig. 17.3 Pulsed-wave Doppler demonstrating pandiastolic flow reversal in the descending thoracic aorta in a patient with severe aortic regurgitation

Cardiac Catheterization

Invasive catheterization holds a diminishing role in the diagnosis of AR. Similar to patients with AS, it is recommended only when the clinical scenario is not substantiated by noninvasive testing. Catheterization can be used to measure the LVEDP, examine the aortic pressure tracing, and quantify the degree of AR.

The aortic pressure tracing reveals elevated SBP (due to increased stroke volume) and a rapid systolic upstroke due to heightened LV contractility. The pulse pressure is widened (as discussed above), and diastolic aortic pressure approximates LVEDP near the end of diastole. In patients with chronic AR, increased LV compliance results in an LVEDP that is near-normal or only mildly elevated. In acute AR, there is a steep, marked rise in LVEDP. The SBP is reduced due to a decline in stroke volume.

The degree of AR is measured using ascending aortography by placing a pigtail catheter in the aortic root, 2 cm above the AV. A left anterior oblique (LAO) projection is selected to properly visualize the ascending aorta and branching arch vessels. Use of a power injector is mandatory, and generally 40 cc of dye is necessary to properly opacify the aorta. The AR is evaluated over two cardiac cycles and quantified as follows: incomplete LV opacification (1+); moderate LV opacification < aortic root opacification (2+); LV opacification = aortic root opacification within two cycles (3+); immediate LV opacification > aortic root opacification (4+).

Mitral Stenosis

Case Presentation

A 48-year-old woman presented to the emergency department with complaints of progressive dyspnea over the past 3 weeks associated with orthopnea and mild lower extremity edema. She had not noticed any chest discomfort or palpitations. She had been having less urine output over the past week, despite a relatively stable diet. She reported a history of rheumatic fever as a teenager, but had

not been followed by a physician for a number of years. She was therefore unaware of any other medical problems.

On examination, she was in mild distress manifest as tachypnea and labored breathing. She was tachycardic with an irregular heart rate of 120 bpm and a BP of 100/65 mmHg. The cardiovascular exam was significant for an opening snap (OS) heard at the left lower sternal border just after the S2, with a short interval between the S2 and OS, followed by a mid-diastolic murmur at the apex heard best in the left lateral position. The JVP was elevated to the angle of the jaw while sitting upright. Examination of the periphery revealed 2+ lower extremity edema bilaterally to the shins and cool extremities.

An ECG revealed atrial fibrillation with a ventricular rate of 125 bpm and no evidence of ischemic changes. Given the examination findings, urgent bedside echocardiography was performed and revealed a low-normal LV ejection fraction (50%) and mild aortic valve thickening and calcification. Most significant was a doming appearance of the anterior mitral leaflet, restricted motion of the posterior mitral leaflet, and fusion of the leaflets at both commissures. The peak and mean gradients across the mitral valve were 34 and 20 mmHg, respectively.

With a clinical diagnosis of suspected cardiogenic shock due to decompensated heart failure and severe mitral stenosis complicated by rapid atrial fibrillation, the patient was moved urgently to the cardiac intensive care unit. Pulmonary artery catheterization (Swan-Ganz) confirmed the diagnosis with a cardiac index of 1.5, PCWP of 35 mmHg, and mixed venous oxygen saturation of 40%. Urgent cardioversion was performed and was successful in restoring a normal sinus rhythm of 70 bpm. With restoration of the rhythm, the patient's urine output increased immediately, and treatment of her volume overload was continued. Repeat TTE revealed a decrease in the mean mitral gradient to 12 mmHg. After successful management of her acute episode, the patient went on to have successful percutaneous mitral balloon valvotomy which decreased her mean mitral gradient to 4 mmHg.

Epidemiology and Pathophysiology

Mitral stenosis (MS) was the first valvular lesion to be diagnosed echocardiographically and treated surgically. Rheumatic heart disease is the leading cause of MS worldwide (prevalence of 6 per 1000 children, compared with 0.5 per 1000 in the United States) [12]. In developed countries, other etiologies such as severe mitral annular calcification due to end-stage renal disease (ESRD), endocarditis, inflammatory disorders (i.e., lupus and rheumatoid arthritis), radiation therapy, and LA myxoma causing MV obstruction are more often considered. MS is a slowly progressive disease that eventually leads to atrial fibrillation (AFib), pulmonary hypertension, and decreased cardiac output. Once symptoms develop, patients face a dismal prognosis, with a 10-year mortality of 70% [13].

In rheumatic fever, inflammation results in nodule formation at the leaflet edge, followed by leaflet thickening, commissural fusion, and chordal thickening and shortening. Smoldering inflammation coupled with turbulent flow across the valve leads to progressive valvular dysfunction [14]. Patients with end-stage kidney disease have disordered calcium metabolism and resultant mitral annular calcification (MAC). As calcification of the annulus progresses to involve the leaflets, obstruction to flow across the valve may occur due to the smaller mitral orifice and restricted leaflet motion [15]. In contrast to rheumatic MS, in which the smallest valve area is at the leaflet tips, obstruction in non-rheumatic MS is predominantly at the annular level.

Physical Examination

The classic findings of MS include the opening snap and mid-diastolic murmur. The source of the OS is mobility of the anterior mitral leaflet and is usually heard best at the LLSB; it is generally not appreciated at the apex. The OS may be differentiated from physiologic splitting of the S2 during exhalation (when the presence of two sounds indicates the OS of MS). A short interval

between the S2 and OS indicates severe MS, as a high LA pressure causes quick opening of the mitral valve in diastole.

The murmur of MS is best heard in the left lateral decubitus position with the stethoscope placed at the ventricular PMI. As with other valve lesions, a louder murmur signifies a large degree of flow (and hence a higher gradient) across the valve. Similarly, in patients with atrial fibrillation, a diastolic murmur leading up to the S1 during a long R-R interval implies severe MS with a persistent gradient even at the end of diastole.

Echocardiography

A subjective assessment of the mitral valve apparatus involves an appraisal of leaflet mobility (typically "doming" of the anterior leaflet and restriction of the posterior leaflet) and thickness, as well as the degree of thickening, calcification, and/or fusion of the commissures and subvalvular apparatus. The systematic scoring system provided by Wilkins and colleagues takes these factors into consideration and is also useful in assessing the feasibility of percutaneous balloon mitral valvotomy (Table 17.5) [16].

The objective evaluation of MS includes a measurement of valve area, valve gradient, and pulmonary artery pressure (PAP) (Table 17.6) [17]. The mitral valve area (MVA) can be assessed using planimetry in the parasternal short-axis projection, though a common pitfall of this method is measuring proximal to the true orifice and thereby overestimating the MVA. Valve area is also estimated using the PHT method, which as with AR is a measure of the time it takes for the gradient across the valve to fall by one-half (Fig. 17.4). Notably, the PHT method is unreliable in patients with severe AR or significant LV diastolic dysfunction since the pressure gradient between the LA and LV equalizes rapidly, providing an abnormally short PHT (thereby overestimating MVA).

The valve gradient in MS is best assessed by tracing the mitral inflow Doppler signal obtained in the apical four-chamber view (Fig. 17.5). The main consideration is the mean gradient, which is automatically calculated by summing the gradient over the cardiac cycle. As shown in the figure,

Table 17.6 Echocardiographic evaluation of mitral stenosis severity

	Mild	Moderate	Severe
Mean gradient	<5 mmHg	5–10 mmHg	>10 mmHg or >15 mmHg with stress
Valve area	>1.5 cm^2	1.0–1.5 cm^2	<1.0 cm^2
Pulmonary artery systolic pressure	<30 mmHg	30–50 mmHg	>50 mmHg or >60 mmHg with stress

Table 17.5 Echocardiographic scoring system for mitral valve stenosis. A score ≤8 is generally associated with favorable outcome from percutaneous mitral balloon valvotomy

Grade	Mobility	Subvalvar thickening	Thickening	Calcification
1	Highly mobile valve with only leaflet tips restricted	Minimal thickening just below the mitral leaflets	Leaflets near normal in thickness (4–5 mm)	A single area of increased echo brightness
2	Leaflet mid and base portions have normal mobility	Thickening of chordal structures extending up to one-third of the chordal length	Mid-leaflets normal, considerable thickening of margins (5–8 mm)	Scattered areas of brightness confined to leaflet margins
3	Valve continues to move forward in diastole, mainly from the base	Thickening extending to the distal third of the chords	Thickening extending through the entire leaflet (5–8 mm)	Brightness extending into the mid-portion of the leaflets
4	No or minimal forward movement of the leaflets in diastole	Extensive thickening and shortening of all chordal structures extending down to the papillary muscles	Considerable thickening of all leaflet tissue (>8–10 mm)	Extensive brightness throughout much of the leaflet tissue

Reproduced with permission from Wilkens et al., Br Heart J. 1988 Oct;60 (4):299–308

a shorter R–R interval results in a marked increase in mitral gradient and highlights the need for appropriate heart rate control in patients with MS, particularly those with concomitant atrial fibrillation.

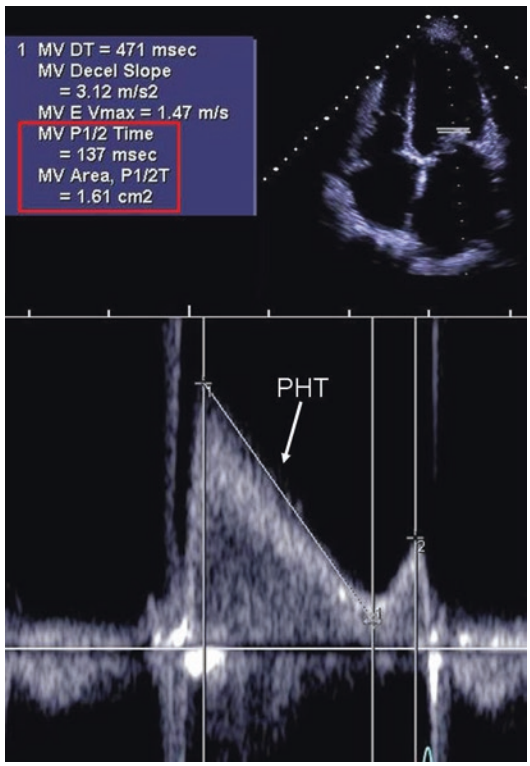

Fig. 17.4 Pulsed-wave Doppler of mitral inflow demonstrating calculation of the mitral valve area (MVA) using the pressure half-time (PHT) method. MVA = 220/PHT

An estimation of pulmonary pressures using the right ventricular systolic pressure (RVSP) is an important part of the evaluation of MS. An RVSP >50 mmHg at rest or > 60 mmHg on exercise TTE is consistent with significant pulmonary hypertension and provides an indication for intervention of MS.

Cardiac Catheterization

As with other valve disorders, catheterization is recommended in the diagnosis of MS when there is discrepancy between the clinical scenario and noninvasive methods [5]. Right heart catheterization (RHC) is often indispensable in the critical care unit to guide management of volume status in patients presenting with pulmonary congestion, depressed cardiac output, and severe mitral stenosis.

The mitral valve gradient is measured by taking simultaneous pressure tracings via an LV catheter and either a pulmonary artery catheter in the wedge position (PCWP) or a direct left atrial catheter (Fig. 17.6). Use of the PCWP is unreliable in patients with pulmonary veno-occlusive disease. It is also important to remember that the "true" wedge pressure is the measured PCWP minus the mean mitral gradient.

As discussed above, the mean gradient is exquisitely sensitive to heart rate, since a faster heart rate leaves less time for diastolic emptying

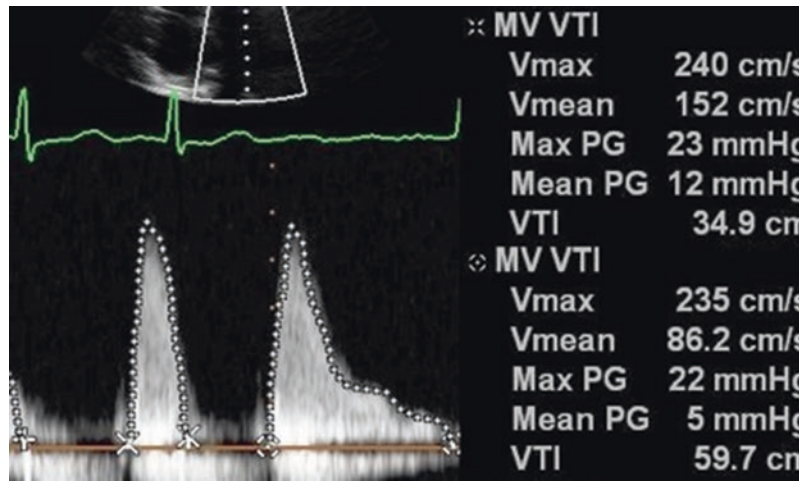

Fig. 17.5 Patient with moderate mitral stenosis and atrial fibrillation. The mean gradient across the mitral valve is significantly increased in the setting of decreased diastolic filling time (i.e., increased heart rate) (beat 1:12 mmHg vs. beat 2:5 mmHg)

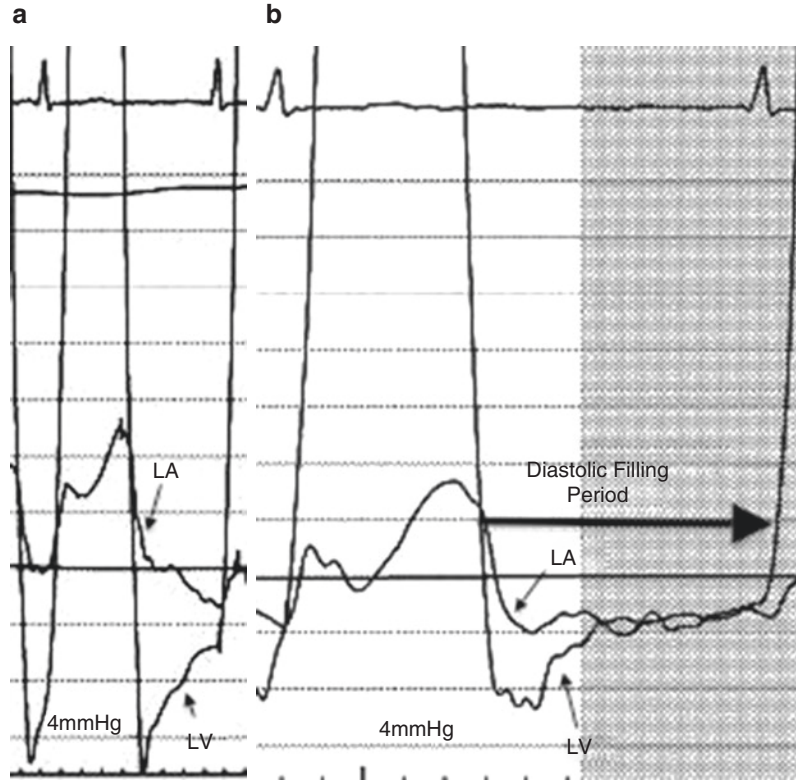

Fig. 17.6 Simultaneous measurement of left atrial (LA) and left ventricular (LV) pressures in a patient with mitral stenosis before (**a**) and after (**b**) percutaneous mitral balloon valvuloplasty. Prior to PMBV, a substantial gradient is present until the end of diastole. In this patient, the pre-procedural resting gradient was 10 mmHg, and post-procedural gradient was 4 mmHg. Paper speed is faster in panel A

of the atrium and results in a higher gradient. In patients with atrial fibrillation, it is therefore recommended to average the gradient over ten cardiac cycles.

The valve area is estimated using the Gorlin formula as follows:

$$\text{MVA} = \left(\text{SV} \div \text{DFP}\right) \div \left(37.7 \times \sqrt{\text{mean gradient}}\right)$$

[SV, stroke volume; DFP, diastolic filling period]

Of note, calculation of the SV using the thermodilution method is not accurate in patients with low cardiac output or significant tricuspid regurgitation. As in patients with AS, the valve area can also be calculated using the Hakki equation:

$$\text{MVA} = \text{CO} \div \sqrt{\text{mean gradient}}$$

In patients with a HR <75 bpm, the value above is divided by 1.35 to provide greater accuracy.

Mitral Regurgitation

Case Presentation

The patient is an 87-year-old man with prior history of diabetes, hypertension, hyperlipidemia, and chronic kidney disease (Stage IV, GFR 25 mL/min/1.73 m^2). He had undergone two prior coronary bypass graft operations, with recent angiography showing patent grafts to the left anterior descending, circumflex, and right coronary arteries. He noted worsening exertional dyspnea over the past 12 months, with recently increasing orthopnea and lower extremity edema. He had initially experienced relief with an increasing dose of diuretics and hydralazine, but his symptoms again worsened.

Physical examination revealed atrial fibrillation with a controlled heart rate of 80 bpm and BP 110/75 mmHg. The PMI was laterally displaced to the mid-axillary line, and there was a 3/6 systolic murmur heard best at the apex and

radiating to the axilla as well as the spine posteriorly. The JVP was elevated at 12 cm H_2O. TTE revealed severely depressed LV function (EF 25%) with moderate LV cavity dilation and moderate LA enlargement. There was severe, posteriorly directed mitral regurgitation due to MV annular dilation, apical displacement of the mitral leaflets, and restriction of the posterior mitral valve.

Given the patient's age, co-morbidities, and two prior open-heart surgeries, he was deemed an inoperable risk for surgical mitral valve repair. He therefore underwent percutaneous mitral valve repair using the MitraClip device (approximating the Alfieri stitch method of surgical repair), which provided a substantial reduction in his degree of MR and improvement in his clinical symptoms.

Epidemiology and Pathophysiology

Mitral regurgitation (MR) affects more than two million people in the United States [18]. Classification of MR is broadly defined by two groups: primary and secondary MR. Primary MR, which is a disorder of the valve itself, is most commonly due to myxomatous (degenerative) disease or mitral valve prolapse (MVP; Barlow's Disease) in the developed world and rheumatic disease in developing countries. Secondary MR is the result of a disordered left ventricular geometry and is usually referred to as "functional" or "ischemic" MR. In secondary MR, annular dilation, apical tethering of the MV leaflets, and/or excessive leaflet motion due to chordal avulsion or papillary muscle rupture lead to the regurgitant lesion.

Acute MR is most often caused by myocardial infarction that leads to papillary muscle rupture or chordal avulsion, supranormal contraction of the non-infarcted papillary muscle, or regional LV dysfunction. Similar to acute AR, it is a severe volume overload state that results in pulmonary edema and depressed cardiac output. Management requires urgent pharmacologic and mechanical afterload reduction and timely surgical referral. Chronic MR, over time, results in a volume overloaded state for the LV and leads to LV dilation and dysfunction, LA enlargement, atrial fibrillation, and pulmonary hypertension.

Physical Examination

A salient physical finding in patients with MR includes the classic high-pitched, holosystolic murmur heard at the apex with radiation to the axilla. If the MR is due to MV prolapse, the murmur may not start until mid-systole, after prolapse of the affected leaflet(s). In patients with severe, posteriorly directed MR (i.e., functional MR or patients with anterior leaflet prolapse), the murmur may also be appreciated by auscultation at the thoracic spine. With posterior prolapse, the regurgitant jet is directed anteriorly and may be best heard at the upper sternal border (similar to AS). The severity of the murmur does not correlate well with the severity of the MR, as other factors including LV cavity dilation and depressed cardiac output can diminish the murmur in the setting of severely decompensated disease. Similar to the murmur in AS, the sound is augmented by increasing afterload (i.e., handgrip) and diminished by reducing venous return (i.e., Valsalva maneuver).

The S1 sound is often diminished due to poor coaptation of the MV leaflets, and the S2 sound may be widely split due to a premature closure of the aortic valve (A2 component) in the setting of poor forward output. In patients with MV prolapse, a mid-systolic click may be appreciated at the time of maximum leaflet prolapse. With heart failure and a dilated LV, an S3 gallop may be also heard. The peripheral exam in severe MR often reveals a prominent upstroke and reflects the increased left ventricular ejection volume, similar to severe AR. In contrast to the pulse in AR, however, the pulse pressure with severe MR is normal.

Echocardiography

Echocardiography is used to quantify MR, evaluate the presence of valve pathology and define

the specific nature of the lesion, and evaluate LV size and systolic function. Quantification of MR is based on a number of parameters including color Doppler, continuous and pulsed-wave Doppler, and pulmonary venous flow pattern (Table 17.7) [19]. Color Doppler imaging can provide an overall impression of the degree of regurgitation based upon the visual estimation of the regurgitant jet in the LA. Slightly more quantitative methods include measurement of the vena contracta (thinnest portion of the regurgitant jet at the regurgitant orifice) and measurement of the regurgitant jet area (RJA) relative to the LA area.

Table 17.7 Echocardiographic determinants of mitral regurgitation severity

	Mild	Moderate	Severe
Color flow mapping			
RJA/LAA	<20%	20–40%	>40%
VC (cm)	<0.40	0.40–0.69	>0.70
ERO (cm^2)	<0.20	0.20–0.40	>0.40
RV (ml/beat)	<30	30–60	>60
Pulsed-wave Doppler			
Mitral E-wave velocity			>1.2 m/sec
PV flow pattern			Systolic blunting or reversal

Reproduced with permission from Krishnaswamy et al. Coron Art Dis 2011

RJA regurgitant jet area, *LAA* left atrial area, *VC* vena contracta, *ERO* effective regurgitant orifice, *RV* regurgitant volume, *PV* pulmonary vein

The proximal isovelocity surface area (PISA) method, as discussed previously in the evaluation of AR, provides the most precise echocardiographic estimation of MR. Briefly, the technique is based upon the idea that as blood converges toward a regurgitant orifice, velocity increases and forms a series of hemispheric shells with the same velocity (hence isovelocity). The velocity at a given shell can be set on the machine as the "aliasing velocity," and calculation of the area bounded by the shell (by measuring the radius) provides the flow at the surface of the shell. Since flow is constant (i.e., conservation of flow principle), the ERO can be calculated as in Fig. 17.7 using the color flow Doppler envelope and the continuous-wave (CW) Doppler tracing to measure MR velocity. If the MR velocity is assumed to be 5 m/sec, and the aliasing velocity set at 40 cm/sec, the PISA formula can be simplified as follows: ERO = $r^2/2$. The regurgitant volume can also be calculated using the

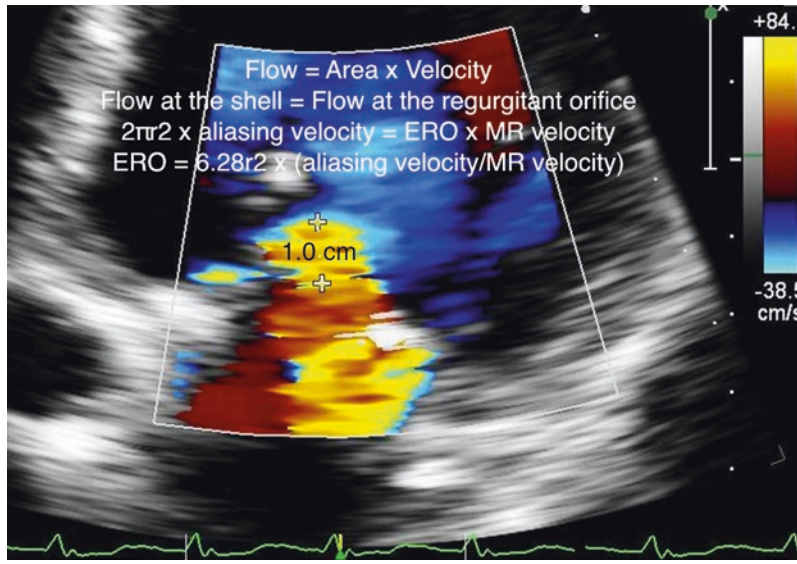

Fig. 17.7 Demonstration of the mitral regurgitation (MR) jet and calculation of the proximal isovelocity surface area (PISA). In this patient with an aliasing velocity set at 38.5 cm/sec and a MR velocity of 500 cm/sec (not shown), the simplified effective regurgitant orifice (ERO) calculation can be used ($r^2/2$), providing an ERO of 0.5 cm^2, which is consistent with severe MR. (Adapted with permission from Krishnaswamy et al., Coron Art Dis 2011)

following: $R_{vol} = ERO \times MR_{VTI}$ (MR_{VTI} is obtained by tracing the MR envelope on CW Doppler).

Pulsed-wave (PW) Doppler is used to interrogate the mitral inflow and stage diastolic function. In the setting of MR, assessment of the peak inflow velocity is useful in quantification. Severe regurgitation results in a higher LA–LV gradient and therefore a higher E-wave velocity during mitral inflow. Use of PW Doppler is also important to evaluate the pulmonary vein flow, specifically for the presence of systolic blunting or reversal in the pulmonary veins that signifies elevated LA pressure (assumedly due to severe MR).

Cardiac Catheterization

Invasive hemodynamic assessment in patients with MR is rarely necessary but may be performed when noninvasive testing is not definitive. In acute MR, the PCWP tracing (or direct LA measurement) demonstrates a large "v" wave due to the large volume of regurgitant blood into a low-compliance LA, and the amplitude of the "v" wave and the LV systolic pressure may be nearly equivalent (Fig. 17.8). It is important to keep this in mind during percutaneous balloon mitral valvotomy as an indicator of complications. The volume overload of the regurgitant lesion on the LV results in elevated LV pressures as well.

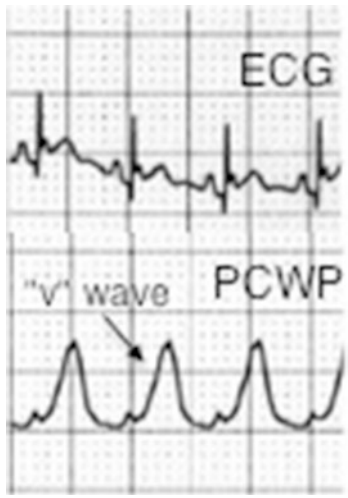

Fig. 17.8 Pulmonary artery catheter pressure tracing in the wedge position (PCWP) in a patient with acute severe mitral regurgitation due to papillary muscle rupture complicating acute myocardial infarction demonstrates a large v-wave

In patients with chronic MR, compliance of the LA increases over time (as does the LV in chronic AR). The "v" wave is therefore smaller than that seen with acute MR. The use of vasodilators in chronic MR produces a similar result. The LV responds to the chronic volume overload of MR as it does in chronic AR and compliance increases, resulting in a less drastic increase in LV pressures than in acute MR.

Ventriculography can also be used to assess the severity of MR. Grading of the regurgitation employs a similar scale as in AR: 1+ = brief LA opacification without LA enlargement; 2+ = moderate LA opacification less than LV opacification and without LA enlargement; 3+ = equal LA and LV opacification that clears over many cycles and with LA enlargement; and 4+ = immediate LA > LV opacification with pulmonary vein filling and LA enlargement. Caution should be exercised in performing ventriculography in patients with MR, in light of the contrast load that it requires in patients who may already be volume overloaded.

Review Questions

Q1. A 74-year-old man presented with exertional dyspnea and orthopnea. Echocardiography revealed a moderately thickened and calcified trileaflet aortic valve with severely restricted motion and an LVEF 20%. Results of interrogation of the AV were performed at rest and with infusion of dobutamine as follows:

Rest		*DBA*	
LVEF	20%	LVEF	25%
LVOT diameter	2.4 cm	LVOT diameter	2.4 cm
LVOT VTI	15.9 cm/sec	LVOT VTI	20.2 cm/sec
Calculated AVA	0.6 cm^2	Calculated AVA	0.9 cm^2

What is the appropriate next step?

(a) Refer for aortic valve replacement
(b) Refer for invasive hemodynamic study
(c) Medical management of LV dysfunction
(d) Refer for balloon aortic valvuloplasty

A1. C. This case demonstrates the diagnosis of "pseudo-AS," for which management of the underlying LV systolic dysfunction is appropriate. In patients with low-flow, low-gradient AS, provocative testing with DBA infusion may be helpful to distinguish true- and pseudo-AS. In this patient, the stroke volume (LVOT area x LVOT VTI) is 71 mL and at stress is 91 mL. This increase of >20% implies the presence of contractile reserve. The increase in calculated AVA of 0.3 cm^2 with stress provides evidence of improved AV leaflet excursion with higher SV; i.e., the "stenosis" is not fixed due to an intrinsic leaflet issue. Surgical intervention or valvuloplasty is not helpful in this setting. An invasive study is not necessary as the diagnosis is clear by echocardiography alone.

Q2. A 45-year-old woman with a history of rheumatic fever presents with worsening exertional dyspnea. Physical examination reveals a regular rate and rhythm. Cardiac auscultation reveals an opening snap and diastolic murmur heard at the apex. There is no lower extremity edema, and the JVP is appreciated at 5 cm above the sternum. Transthoracic echocardiography reveals a normal LVEF, doming of the anterior MV leaflet with restriction of the posterior MV leaflet, and a mean gradient across the MV of 7 mmHg. The estimated RVSP is 40 mmHg. What is the next step in management?

(a) Evaluate noncardiac causes of dyspnea
(b) Perform exercise echocardiography to evaluate the MV
(c) Refer for invasive cardiac catheterization to evaluate the MV
(d) Return for follow-up echocardiogram in 6 months

A2. B. This patient with a history of rheumatic fever presents with exertional dyspnea and a typical echocardiographic appearance of rheumatic mitral valve disease. The mean valve gradient is moderate at best, with a suggestion of borderline pulmonary hypertension (RVSP 40 mmHg). Given the patient's exertional symptoms, however, exercise echocardiography would be the next appropriate step in order to evaluate the MV gradient and pulmonary pressures with exertion. In this patient, TTE during stress revealed a mean MV gradient of 16 mmHg and RVSP of 65 mmHg. She subsequently underwent percutaneous balloon mitral valvuloplasty and was symptom-free with significant exertion afterward. Cardiac catheterization is considered to be less accurate in the evaluation of MS than echocardiography, and is therefore not yet indicated in this patient.

Q3. A 42-year-old man with bicuspid aortic valve seeks to establish a new cardiologist after many years of loss to follow-up. He does not take any medications. He feels well and exercises on a treadmill for 45 minutes 4 times per week. He has no exertional or positional dyspnea. On exam, his HR is 70 bpm and BP 115/50 mmHg. He has a holodiastolic murmur heard best at the left sternal border, and peripheral exam reveals bounding pulses with rapid collapse. TTE reveals normal LVEF 60% with LVIDd 7.2 cm and LVIDs 5.7 cm and a bicuspid aortic valve, and quantification of the degree of AR provides a vena contract of 0.7 cm, PHT 200 msec, and holodiastolic flow reversal in the descending aorta. What is the best next step?

(a) Routine clinical follow-up with TTE in 6 months
(b) Initiation of an ACE-inhibitor
(c) Referral for aortic valve surgery
(d) Exercise stress testing

A3. C. This patient with asymptomatic severe AR demonstrates LV cavity dilation (LVIDd >7.5 cm or LVIDs >5.5 cm), which is a criteria for aortic valve repair or replacement in patients with asymptomatic but severe AR (ACC/AHA Class IIa). For patients with severe AR and normal LV cavity size but without symptoms, follow-up echocardiography is indicated every 6 months (ACC/AHA Class I). Vasodilators are reasonable for symptomatic relief in patients with severe AR (Class IIa), but should not supersede definitive treatment in the setting of LV cavity dilation. Exercise stress testing may be helpful to distinguish whether or not the "asymptomatic" patient is truly asymptomatic (ACC/AHA Class

IIa), but the patient described here has LV cavity dilation and therefore symptoms are not necessary to make the recommendation for surgery.

Q4. A 67-year-old man with hypertension and hyperlipidemia presents with an inferior STEMI and undergoes primary percutaneous coronary intervention to a proximally occluded right coronary artery. The procedure is uneventful, and he is transferred to the cardiac ICU in stable condition. Fourteen hours later, he develops sudden hypotension and dyspnea. There are no new ECG changes. Which of the following would be expected of diagnostic testing:

(a) Large "v"-wave on a PCWP tracing
(b) LA > LV opacification within 1 cycle on a ventriculogram
(c) Pulmonary vein flow reversal during systole on TTE
(d) All of the above

A4. D. The patient above provides a classic presentation of mechanical complication after acute MI, in this case with severe MR due to papillary muscle rupture. Choices A–C all provide diagnostic evidence for severe MR. Appropriate management consists of emergent afterload reduction (using intra-aortic balloon counterpulsation and/or vasodilators if tolerated) and surgical referral for mitral valve surgery.

Q5. A 40-year-old man presents with worsening exertional dyspnea over the past 1 week, along with fevers to 102 degrees. He admits to regular intravenous drug use and claims to have had a "murmur" since childhood. His bedside echocardiogram suggests severe AR. What other diagnostic findings would be expected?

(a) Holodiastolic murmur at the left sternal border
(b) Bradycardia
(c) AR Pressure half-time <250 msec
(d) Systolic murmur resembling MR heard at the apex

A5. C. In acute AR, the rapid rise in LV pressure due to a noncompliant chamber results in rapid equilibration of aortic and LV pressures and results in a short pressure half-time. The hallmark diastolic murmur of AR may not be appreciated as easily in the acute setting for the same reason. Patients with acute AR are often quite tachycardic due to the poorly tolerated hemodynamic consequences of the lesion. The *Austin Flint* murmur of AR resembles the murmur of MS, and is thought to be due to premature closure of the anterior MV leaflet by the regurgitant AR jet.

References

1. Nkomo VT, Gardin JM, Skelton TN, Gottdiener JS, Scott CG, Enriquez-Sarano M. Burden of valvular heart diseases: a population-based study. Lancet. 2006;368:1005–11.
2. Otto CM, Burwash IG, Legget ME, et al. Prospective study of asymptomatic valvular aortic stenosis. Clinical, echocardiographic, and exercise predictors of outcome. Circulation. 1997;95:2262–70.
3. Carabello BA. Clinical practice. Aortic stenosis. N Engl J Med. 2002;346:677–82.
4. Leach RM, McBrien DJ. Brachioradial delay: a new clinical indicator of the severity of aortic stenosis. Lancet. 1990;335:1199–201.
5. Nishimura RA, Otto CM, Bonow RO, et al. 2014 AHA/ACC Guideline for the Management of Patients with Valvular Heart Disease: executive summary a report of the American College of Cardiology/American Heart Association Task Force on Practice Guidelines. Circulation. 2014;129:2440–92.
6. deFilippi CR, Willett DL, Brickner ME, et al. Usefulness of dobutamine echocardiography in distinguishing severe from nonsevere valvular aortic stenosis in patients with depressed left ventricular function and low transvalvular gradients. Am J Cardiol. 1995;75:191–4.
7. Monin JL, Quere JP, Monchi M, et al. Low-gradient aortic stenosis: operative risk stratification and predictors for long-term outcome: a multicenter study using dobutamine stress hemodynamics. Circulation. 2003;108:319–24.
8. Quere JP, Monin JL, Levy F, et al. Influence of preoperative left ventricular contractile reserve on postoperative ejection fraction in low-gradient aortic stenosis. Circulation. 2006;113:1738–44.
9. Hakki AH, Iskandrian AS, Bemis CE, et al. A simplified valve formula for the calculation of stenotic cardiac valve areas. Circulation. 1981;63:1050–5.
10. Babu AN, Kymes SM, Carpenter Fryer SM. Eponyms and the diagnosis of aortic regurgitation: what says the evidence? Ann Intern Med. 2003;138:736–42.
11. Griffin BP, Flachskampf FA, Reimold SC, Lee RT, Thomas JD. Relationship of aortic regurgitant velocity slope and pressure half-time to severity of aortic

regurgitation under changing haemodynamic conditions. Eur Heart J. 1994;15:681–5.
12. Padmavati S. Rheumatic fever and rheumatic heart disease in India at the turn of the century. Indian Heart J. 2001;53:35–7.
13. Selzer A, Cohn KE. Natural history of mitral stenosis: a review. Circulation. 1972;45:878–90.
14. Braunwald E, Bonow RO, Braunwald E. Chapter 57: Valvular heart disease. 7th ed. Philadelphia: Elsevier Saunders; 2005.
15. Muddassir SM, Pressman GS. Mitral annular calcification as a cause of mitral valve gradients. Int J Cardiol. 2007;123:58–62.
16. Wilkins GT, Weyman AE, Abascal VM, Block PC, Palacios IF. Percutaneous balloon dilatation of the mitral valve: an analysis of echocardiographic variables related to outcome and the mechanism of dilatation. Br Heart J. 1988;60:299–308.
17. Baumgartner H, Hung J, Bermejo J, et al. Echocardiographic assessment of valve stenosis: EAE/ASE recommendations for clinical practice. Eur J Echocardiogr. 2009;10:1–25.
18. Enriquez-Sarano M, Akins CW, Vahanian A. Mitral regurgitation. Lancet. 2009;373:1382–94.
19. Zoghbi WA, Enriquez-Sarano M, Foster E, et al. Recommendations for evaluation of the severity of native valvular regurgitation with two-dimensional and Doppler echocardiography. J Am Soc Echocardiogr. 2003;16:777–802.

Pulmonary Hypertension

18

Jordan D. Awerbach and Richard A. Krasuski

Introduction

The pulmonary circulation is normally a low-pressure, low-resistance, and highly compliant system. Pulmonary hypertension (PH) is a pathologic state characterized by an elevation in the mean pulmonary arterial pressure (mPAP). PH may occur as a primary process, though it is most often a complication of other chronic disease states, particularly heart failure and chronic lung disease. Globally, it is helpful to dichotomize PH into precapillary PH, or pulmonary arterial hypertension (PAH), and postcapillary PH, the so-called pulmonary venous hypertension (PVH). Patients may also present with a combination of both. Patients with PAH, regardless of etiology, share common pulmonary vascular changes that define this form of PH. Vasoconstriction and progressive endothelial dysfunction lead to pulmonary vascular remodeling that ultimately results in the obliteration of the pulmonary vasculature and increased pulmonary vascular resistance (PVR) [1].

Right heart catheterization (RHC) remains the gold standard for diagnosing PH and differentiating pre- from postcapillary forms of PH. Classification systems have evolved over time and currently recognize five major etiologies of PH (Table 18.1) [2]: Group 1, PAH; Group 2, PH owing to left-sided heart disease; Group 3, PH due to pulmonary disease or hypoxia; Group 4, chronic thromboembolic PH (CTEPH) and other pulmonary artery (PA) obstructions; and Group 5, PH due to multifactorial mechanisms. PH is hemodynamically defined by a resting mPAP of ≥25 mmHg. Previous definitions have also made reference to mPAP elevation during exercise (to >30 mmHg), but exercise-induced PH in patients with normal resting pressures remains a poorly characterized phenomenon, and recent guidelines have removed this from the definition [3, 4]. PAH is further defined by (1) a PVR >3 Wood units (Wu) and (2) a normal pulmonary capillary wedge pressure (PCWP) (≤15 mmHg).

Epidemiology of Pulmonary Hypertension

The global burden of PH throughout the world has become increasingly recognized [5]. Estimated the prevalence of PH in 2015 at 50–70 million individuals worldwide (about 1% of the global population). Left-sided heart diseases and chronic lung diseases are the most common causes in both industrialized and developing countries. However, the majority of PH is seen in the developing world, where associated diseases including schistosomiasis, rheumatic heart dis-

J. D. Awerbach · R. A. Krasuski (✉)
Division of Cardiovascular Medicine, Duke University Health System, Durham, NC, USA
e-mail: jordan.awerbach@duke.edu; richard.krasuski@duke.edu

A. T. Askari, A. W. Messerli (eds.), *Cardiovascular Hemodynamics*, Contemporary Cardiology,
https://doi.org/10.1007/978-3-030-19131-3_18

Table 18.1 World Health Organization classification system for pulmonary hypertension[a] [2]

Group 1: Pulmonary arterial hypertension
1.1 Idiopathic PAH
1.2 Heritable PAH
1.2.1 BMPR2
1.2.2 ALK-1, ENG, SMAD9, CAV1, KCNK3
1.2.3 Unknown
1.3 Drug- and toxin-induced
1.4 Associated with:
1.4.1 Connective tissue disease
1.4.2 HIV infection
1.4.3 Portal hypertension
1.4.4 Congenital heart diseases
1.4.5 Schistosomiasis
1′ Pulmonary veno-occlusive disease and/or pulmonary capillary hemangiomatosis
1″ Persistent pulmonary hypertension of the newborn (PPHN)
Group 2: Pulmonary hypertension due to left heart disease
2.1 Left ventricular systolic dysfunction
2.2 Left ventricular diastolic dysfunction
2.3 Valvular disease
2.4 Congenital/acquired left heart inflow/outflow tract obstruction and congenital cardiomyopathies
Group 3: Pulmonary hypertension due to lung diseases and/or hypoxia
3.1 Chronic obstructive pulmonary disease
3.2 Interstitial lung disease
3.3 Other pulmonary diseases with mixed restrictive and obstructive pattern
3.4 Sleep-disordered breathing
3.5 Alveolar hypoventilation disorders
3.6 Chronic exposure to high altitude
3.7 Developmental lung diseases
Group 4: Chronic thromboembolic pulmonary hypertension (CTEPH)
Group 5: Pulmonary hypertension with unclear multifactorial mechanisms
5.1 Hematologic disorders: chronic hemolytic anemia, myeloproliferative disorders, splenectomy
5.2 Systemic disorders: sarcoidosis, pulmonary histiocytosis, lymphangioleiomyomatosis
5.3 Metabolic disorders: glycogen storage disease, Gaucher disease, thyroid disorders
5.4 Others: tumoral obstruction, fibrosing mediastinitis, chronic renal failure, segmental PH

[a]Reproduced with permission of publisher [2]

ease, human immunodeficiency virus (HIV), and sickle cell disease are more commonly seen. PH in developing countries predominantly affects a much younger population, whereas it is primarily seen in older patients (above age 65) in industrialized countries.

PAH is overall a rare disease, although it has been the primary focus of most clinical investigation and treatment. Based on registry data primarily from Europe and the United States, the prevalence of PAH is around 12–15 cases per million [4, 6]. The majority of cases (40–50%) are idiopathic (iPAH) or are inheritable/familial forms. Twenty percent of sporadic cases of PAH and 80% of heritable PAH have been linked to mutations in the bone morphogenetic protein receptor type 2 (BMPR2) gene [7]. Presence of the BMPR2 mutation in patients with PAH is associated with increased mortality, and these patients typically present at a younger age with more severe disease [8]. Historically, iPAH commonly affected people in their fourth decade of life, but contemporary registries have demonstrated that the mean age of this population has increased to 50–65 years old [9]. Women are affected 3–4 times as often, though men diagnosed with iPAH have an overall worse prognosis [10]. Prior to the era of targeted PAH pharmacotherapies, long-term survival in iPAH was grim, with a median survival of 2.8 years and 1-, 3-, and 5-year survival rates of 68%, 48%, and 34%, respectively [11]. In the current treatment era, those rates have improved to 91%, 74%, and 65% for the same time intervals [12].

Additional important causes of PAH include connective tissue disease (CTD) and congenital heart disease (CHD). Approximately 15–25% of PAH is associated with CTDs. Systemic sclerosis is the most common cause of CTD-associated PAH in the majority of the world, and survival in patients with CTD-PAH is overall worse compared to those with iPAH [5, 12]. CHD-associated PAH accounts for approximately 10% of cases of PAH. The development of PAH in patients with CHD is generally due to the presence of a hemodynamically significant left-to-right (systemic-to-pulmonary) shunt exposing the pulmonary vascular bed to excessive blood flow and, in some cases, chronically elevated pressures. The risk of PAH developing in this population is related to both the chronicity of the shunt as well as its location, with lesions

distal to the tricuspid valve posing the greatest risk, as they permit the transmission of systemic blood pressures to the pulmonary vascular bed. Thus, PAH may also develop in patients with repaired CHD, particularly when the defect is corrected later in life. If CHD is unrepaired, PAH can progress and ultimately result in Eisenmenger syndrome, characterized by shunt reversal, cyanosis, and right heart failure. Interestingly, patients with Eisenmenger syndrome demonstrate better long-term survival in comparison with untreated iPAH patients, with a 77% 3-year survival [4].

Clinical Presentation

The suspicion for PH requires an astute clinician, especially in iPAH, where patients are comparatively younger and typically otherwise healthy. Many patients are often diagnosed years after the onset of symptoms [13]. Initial symptoms are often nonspecific and may be discounted by both the patient and their physician or attributed to other causes such as deconditioning. The clinician must also be proactive in screening for PAH in patients who have associated chronic illnesses, such as systemic sclerosis or HIV infection.

Dyspnea is the most common presenting symptom, seen in 60% of patients diagnosed with PAH [14]. Patients may also complain of fatigue and weakness early in the course of the disease. When untreated, symptom severity will progress as patients develop right heart dysfunction, and patients may present with syncope, arrhythmias, or overt heart failure [4]. The World Health Organization (WHO) functional classification (FC) schema provides one of the most powerful clinical tools for assessing disease severity and prognosis [4]. WHO FC I patients have no physical limitations. FC II patients are asymptomatic at rest but will experience symptoms with ordinary physical activities. FC III patients continue to be asymptomatic at rest but have marked limitations in physical activity. Patients who are FC IV are unable to carry out any physical activity without significant symptoms. They often have rapid progression of symptoms, may be symptomatic at rest, and have signs of right heart failure on exam; frank syncope may occur with exertion and helps define patients between FC III and IV as being FC IV. Patients who are FC IV have a poor prognosis, and when newly diagnosed generally require hospitalization and initiation of IV prostaglandins.

A measured 6-min walk distance (6MWD) performed in clinic provides an objective assessment of functional status. Using the modified Borg dyspnea scale (see Fig. 18.1 – below) to assess for patient effort and monitor oxygen saturation with noninvasive pulse oximetry may add additional prognostic value. Although baseline numbers provide predictive insight into survival, the significance of changes over time remains controversial. Patients who initially walk >440 m demonstrate improved 1-year survival, whereas those who walk <165 m have significantly worse outcome [15]. Formal exercise testing with measurement of oxygen consumption is also an independent predictor for survival and closely correlates with 6MWD.

Physical exam findings vary with disease severity, although most patients will have an

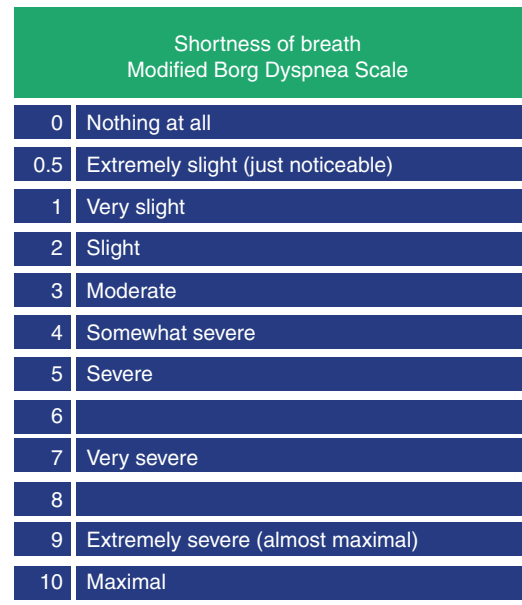

Fig. 18.1 The modified Borg scale has the potential to provide quick, easy, and rapid information about a patient's subjective state of dyspnea

accentuated P2 component of their second heart sound, even with mild disease. Additional auscultatory findings that become present with increasing right heart failure include the low-frequency holosystolic murmur of tricuspid regurgitation (TR), best heard over the left lower sternal border, and a right ventricular (RV) gallop (an S3 and/or S4 may be present). With increasing RV dilation, the patient will develop a palpable parasternal lift. Signs of fluid overload will also become evident with worsening RV failure, including jugular venous distension with prominent *a*- and *v*-wave pulsations associated with decreased RV compliance and worsening TR respectively. The lungs should be dry in isolated PAH; the presence of pulmonary edema suggests postcapillary PH is present, and an alternative diagnosis should be explored.

Noninvasive Testing in PH

The initial evaluation of patients with suspected PH typically involves multiple diagnostic modalities. Laboratory assessments are rarely helpful in the diagnosis of PAH, but may be important when other etiologies of PH, such as rheumatologic diseases, are suspected. Trending brain natriuretic peptide (measured as either BNP or NT-proBNP) values may be helpful to the clinician, as they are correlated with RV dysfunction and prognosis in patients with known PAH [4].

Chest radiography (CXR) is abnormal in 90% of patients presenting with PAH [4]. Right heart dilation, PA enlargement, and loss of distal pulmonary architecture with clear lung fields may all be seen on CXR [14]. A ventilation-perfusion (V/Q) scan should be performed in all patients with suspected PAH to rule out CTEPH, as patients with this disorder may be candidates for curative intervention (pulmonary thromboendarterectomy) or balloon pulmonary angioplasty. The sensitivity and specificity of V/Q scan for both diagnosing and excluding CTEPH approaches 95–100% [4, 16]. Computed tomography (CT) is often performed in patients with known or suspected underlying parenchymal lung disease. Pulmonary function testing (PFT) can elucidate underlying airway disease, such as chronic obstructive pulmonary disease (obstructive pattern) or interstitial lung disease (restrictive pattern). It is important to note, however, that the severity of lung disease as judged by PFTs is often poorly correlated with the presence or severity of PH [17]. A hint to the presence of PH itself is a low diffusing capacity (DLCO) that is out of proportion to the degree of lung disease suggested by the PFTs.

Transthoracic echocardiography should be performed in all patients with suspected PH. It is an excellent screening tool and can also be used assess the severity of PH. Quantifying right ventricular systolic pressure (RVSP) is most traditionally done by measuring the peak velocity of the TR jet, which provides an estimate of the RV systolic pressure (RVSP), a surrogate for pulmonary systolic pressure (in the absence of right ventricular outflow obstruction). There is a high probability of PH in the presence of a TR velocity > 2.8 m/s [4]. However, the absence of a measurable TR jet does not exclude PH and additional echocardiographic parameters can be helpful in this regard. These include dilation of the main PA, increased pulmonary regurgitant velocities, systolic flattening of the intraventricular septum, the presence of RV dilation and/or RV hypertrophy, and elevated right atrial pressure. Tricuspid annular plane systolic excursion (TAPSE) should be measured in all PH patients, with a distance <1.8 cm associated with increased mortality [18]. The presence of a pericardial effusion is an ominous sign in advanced PAH. The echocardiogram is also useful to evaluate for potential cardiac etiologies of PH, including significant valvular disease, left-sided heart failure (systolic and diastolic dysfunction), and the presence of an intracardiac shunt.

Cardiac magnetic resonance (CMR) can provide high-resolution structural information and with phase-contrast studies hemodynamic data as well. However, because of the limited availability and the high cost involved, this modality should not be used for screening.

Hemodynamic Evaluation

The cornerstone for the diagnosis of PH remains the RHC. Measurement of right heart and particularly PA pressures, cardiac output/cardiac index (CO/CI), PVR, and assessment of vasoreactivity are key elements for establishing diagnosis, collecting prognostic indicators, and assisting in the selection of therapy. RHC is recommended in all patients with PAH to confirm the diagnosis, evaluate severity of PH, and assess the need for PAH-specific drugs [4]. RHC is also recommended in patients diagnosed with PAH at 6–12 months surveillance intervals, 3–6 months after a change in therapy and when there is clinical deterioration [4]. There is often trepidation about performing RHC in patients with PAH, who are frequently viewed as being fragile. At experienced PH centers, cardiac catheterization is performed safely, and the risk of major complications is under 1% [19].

PH assessment is best performed in euvolemic states of low or normal CO. Transient high cardiac output states such as anemia, pregnancy, or sepsis will lead to elevated pulmonary pressures, but the PVR should remain normal. Current guidelines recommend that CO be measured by thermodilution, the reliability of which has been validated even in patients with low CO and severe TR [4, 20]. However, this method is prone to errors in measurement in the setting of intracardiac shunting. The direct Fick method is the gold standard for measuring CO, but is rarely performed today due to the cumbersome nature of directly measuring oxygen consumption (VO_2). The indirect Fick method has become the most widely accepted measure of CO; it is less reliable and results should be interpreted cautiously, particularly in patients who are severely obese [21].

We recommend performing a full oxygen saturation run to rule out CHD in all patients undergoing initial RHC for PAH. A left-to-right shunt should be suspected when the absolute PA saturation is >75% or if a step-up of >7% is seen between the superior vena cava (SVC) and PA. A shunt run should consist of measurements from the innominate vein, SVC, inferior vena cava (IVC), RA, RV, and PA. Both high and low SVC saturations should be obtained to identify the presence of anomalous pulmonary venous drainage to the SVC. Whenever a full saturation run is performed, it is important to recognize that the RA receives three different sources of blood return (SVC, IVC, and coronary sinus). The mixed venous saturation is thus estimated by adding three times the SVC saturation to the IVC saturation and dividing by four. Treatment decisions of which shunts benefit from repair and the timing of repair in the setting of PAH are beyond the scope of the chapter (see Chap. 20), but these patients should ideally be referred to cardiologists with expertise in managing adults with congenital heart disease.

The RA pressure waveform (and consequently the central venous waveform) of PH may have several distinctive features. A prominent *a*-wave is common when the RV diastolic pressure is elevated, and the normal *y*-descent may be attenuated reflecting reduced RV compliance. A prominent *v*-wave suggests the presence of significant TR and a fused *cv*-wave is sometimes seen. Severe elevation in mean RA pressure (>20 mmHg) has been associated with increased mortality [22]. Additionally, the expected decrease in RA pressure with inspiration may not occur in patients with severe PH and significant TR; on occasion RA pressure may even increase with inspiration creating confusion that pericardial disease (effusive or constrictive physiology) is present. Pulsus alternans in the RV and PA tracing can occasionally be seen in severe PH and suggests considerable RV dysfunction. It is characterized by alternating strong and weak beats, resulting from the altered Frank–Starling relationship and dyssynchrony of the noncompliant RV.

In normal adults the resting mPAP should not exceed 20 mmHg. PH is defined by a resting mPAP ≥25 mmHg. There remains uncertainty about patients with "borderline" mPAPs of 21–24 mmHg; these patients may simply be early in the disease process [23], though it is reasonable to suspect that future guidelines will lower the threshold of mPAP for defining PH. Previous definitions of PH also included a mPAP of >30 mmHg during exercise. However,

this has been removed from recent guidelines, as further understanding is needed to determine the best methodology for exercising these patients in the catheterization lab [4, 23]. Aging also plays a role in the degree of exercise-induced mPAP elevations; patients >50 years old may demonstrate significantly higher mPAPs, even with slight levels of exertion [23]. In general, however, severe elevations in mPAP (>45 mmHg) are typically only seen in patients with PAH and CTEPH.

Obtaining an accurate assessment of the PCWP is critical in patients with PAH. The PCWP allows for a direct measurement of mean LA pressure, a surrogate for the left ventricular end diastolic pressure (LVEDP) in the absence of mitral valve stenosis or pulmonary venous occlusive disease (PVOD). It is recommended that wedge pressures be sampled in several different segments of the pulmonary vasculature, preferably in the lower lobes of the pulmonary vasculature (West Zone 3). Zone 3 is the only location in the pulmonary circulation where one can be certain that the PA pressure is both greater than the pulmonary venous and pulmonary alveolar pressures, thus minimizing their contribution to the measured PA pressure. Multiple samples should also be obtained in patients with suspected or confirmed CTEPH; obstructive thrombi in some PA segments may lead to the erroneous interpretation of an elevated wedge pressure. An elegant way to document whether PAH is present is continuous recording of the PCWP and then the PAP after balloon deflation and careful withdrawal of the catheter (Fig. 18.2a, b). A significant step-up in the pressure waveform should be noted, resuming the PAP waveform almost immediately after deflation.

If the PCWP waveform has large v-waves, this suggests increased left atrial stiffness or possibly significant mitral regurgitation. In severe pulmonary hypertension, accurate measurement of PCWP may be difficult due to hybrid tracings resulting from incomplete seal of the balloon against the arterial wall. One must be careful not to overinflate the balloon or when performing repeat inflations and deflations in the wedge position, as these can cause rupture of the pulmonary artery, a rare but potentially fatal complication [23].

Measurement of the PCWP should take place during end-expiration (PCWP-exp), when the effects of intrathoracic pressure are minimized. This has been shown to be particularly important in obese and hypoxemic patients, who tend to generate larger intrathoracic pressure changes [23]. A mean pressure will typically be calculated by most cath lab software; however this represents a derived calculation measured over several seconds [24]. The discrepancies between the measured end-expiratory pressure and the digitally calculated mean pressure can be significant and lead to misclassification of patients with pre- and postcapillary PH, with potentially deleterious results (Fig. 18.3) [24]. If the PCWP is normal but clinical concern remains for impaired LV diastology, a small fluid bolus of 500 mL over 5–10 min can be safely administered to help unmask heart failure with preserved ejection fraction (HFpEF) [4, 23]. It is also possible that obtaining hemodynamics during exercise may help to uncover patients with diastolic heart failure, but this is not currently recommended for similar reasons as noted above for testing for PH with exercise [23]. If doubt exists about the accuracy of the PCWP measurement, direct measure of the LVEDP should be performed via retrograde crossing of the aortic valve.

PVR in the normal individual increases with age and decreases with elevations in cardiac output. PVR may be expressed either as Wood units (Wu; mmHg/L/min) or dynes (dyn/s/cm^{-5}),[1] with normal PVR being <1.1 Wu (88 dynes) [25]. PVR is calculated by dividing the transpulmonary pressure gradient (mPAP-PCWP) by the pulmonary blood flow (Qp), which is equal to CO in the absence of intracardiac shunting. A PVR >3 Wu is required for the definition of PAH. Pre- and postcapillary PH may coexist and can be difficult to distinguish clinically when seen together. When precapillary PH is present, the transpulmonary gradient will be higher, at least >12 mmHg, and often markedly elevated. The diastolic pressure

[1] Values given in Wu may be multiplied by 80 to convert to dynes.

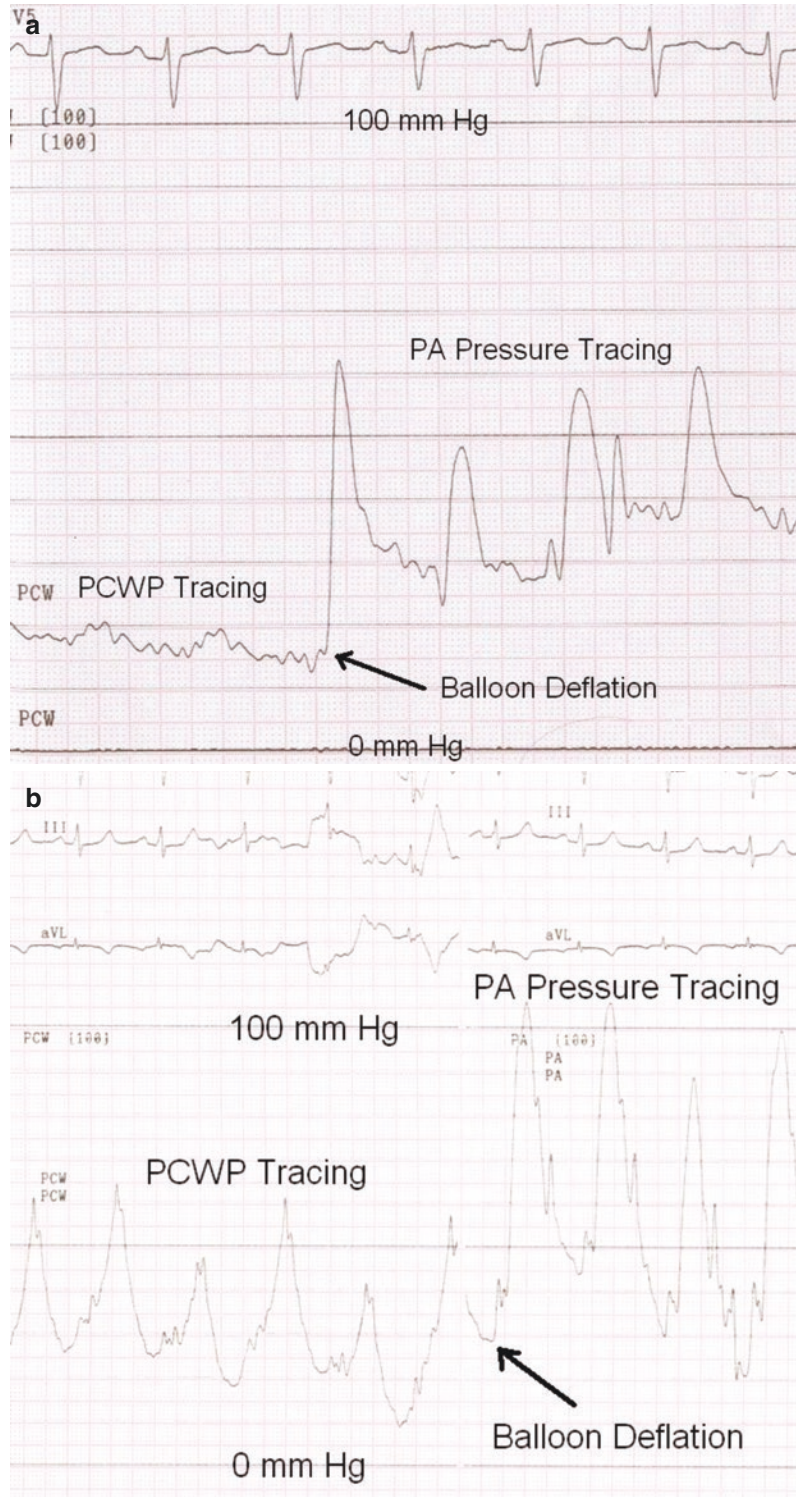

Fig. 18.2 (**a**) Deflation of the wedged pulmonary capillary balloon catheter results in a rapid increase in the pressure recordings identifying the pulmonary artery pressure. In this case the mPAP is >25 mmHg and PCWP is <15 mmHg consistent with a diagnosis of PAH. (**b**) Identification of pulmonary venous hypertension using continuous right heart pressure monitoring during acute balloon inflation and deflation. The PA pressure is elevated but the mPCWP is well in excess of 15 mmHg with large *v*-waves, reflecting the impact of severe mitral regurgitation in this case

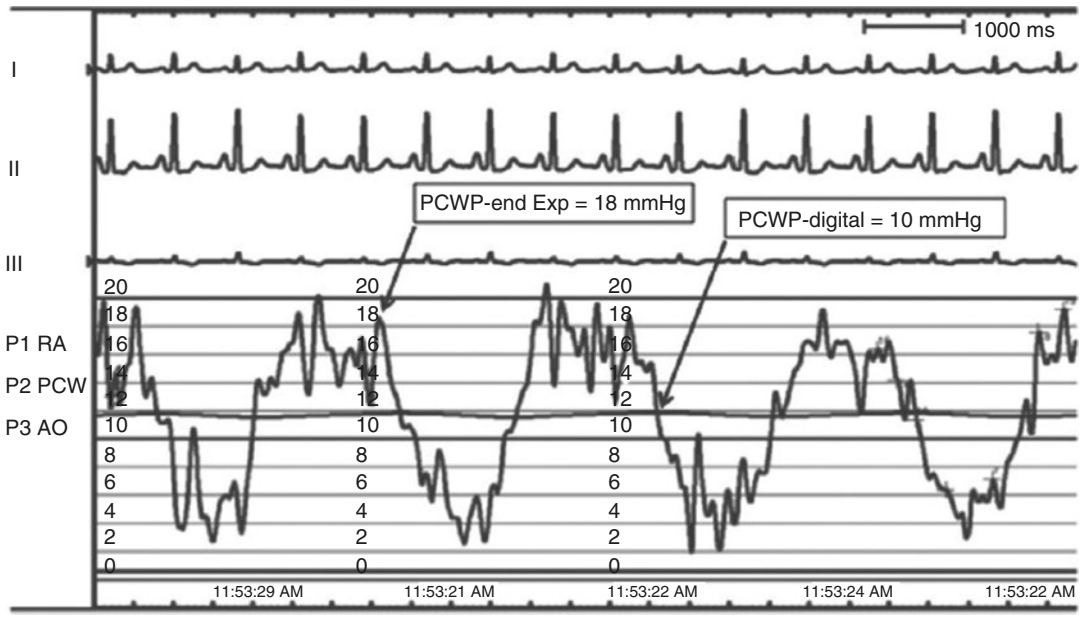

Fig. 18.3 This wedge tracing illustrates the respirophasic waveforms with the digitized means and the difference between PCWP–exp versus the automatically derived mean PCWP, thereby resulting in misclassification. (Reprinted with permission of publisher [24])

gradient (diastolic PAP – PCWP) is also very helpful. In pure postcapillary PH, this difference is typically close to 0, whereas a gradient ≥7 mmHg is consistent with the presence of precapillary PH.

All patients with suspected idiopathic, hereditary or drug-induced PAH should undergo pulmonary vasoreactivity testing as part of their initial RHC. Only a small minority of PAH patients (5–10%) will be vasoresponsive; however responders demonstrate a more favorable prognosis with a 5-year survival rate of 90% when treated with calcium channel blockers (CCBs) [26]. Responsiveness suggests the pulmonary vasculature has satisfactory amounts of vasodilatory reserve, likely representing an earlier stage of disease.

Inhaled nitric oxide (iNO) is most commonly used for vasoreactivity testing because of its specificity in targeting the pulmonary vasculature and neutral effects on coronary blood flow (intravenous prostacyclin and adenosine administration, alternative agents for vasodilatory testing, can reduce coronary blood flow). Also beneficial is the extremely short half-life of iNO, which is particularly important in the event a patient with masked LV diastolic failure or PVOD develops acute pulmonary edema. A substantial increase in the v-wave of the PCWP tracing during inhalation suggests that this may be occurring.

Unfortunately, the equipment used for the setup of iNO administration is cumbersome, and it requires the patient to wear a full facemask for delivery, which can be difficult to tolerate. Newer inhalation agents and smaller delivery devices are being developed (such as modification of the iNeb device to be able to deliver iloprost in a reusable circuit) that may be equally safe and at least as sensitive as iNO.

The maximal effect of iNO is obtained following 5–10 min of inhalation at 40 ppm, after which time the operator should repeat measurements of mPAP and PCWP, and collect PA and systemic saturations to reassess the cardiac output [27]. A positive response has most recently been defined as a reduction in mPAP by 10 mmHg to an absolute value of ≤40 mmHg with preserved CO. Although vasoreactivity testing has traditionally been used to identify patients with iPAH who may be candidates for CCB therapy, recent

studies have suggested that testing may also provide independent prognostic information that extends to other WHO Group I PH patients (PAH) and even those with non-Group I PH [28–30].

Our Approach to Hemodynamic Assessment of PH

1. Patients are taken to the catheterization laboratory in the fasting state and under minimal sedation (to prevent any adverse effect on oxygen saturation or CO).
2. Femoral venous and arterial access is obtained for the initial RHC and brachial, neck or femoral access (based on patient preference) for repeat assessments. If initiation of IV therapy is anticipated, neck access is preferred, as this facilitates leaving the right heart catheter in place after the procedure for more prolonged hemodynamic monitoring in an intensive care setting. In such cases radial access can be considered for left heart requirements. Arterial access permits measurement of the LVEDP if PCWP is questionable or grossly elevated. It also facilitates trouble-free arterial blood gas collection during the shunt run and provides for arterial pressure monitoring and arterial blood gas collection during AVT. It also allows for coronary angiography or ventriculography as necessary.
3. Ideally two transducers should be utilized – this facilitates monitoring of the pulmonary arterial and aortic pressures simultaneously during AVT.
4. A full oxygen saturation run is performed for the initial RHC. This includes innominate vein (or high SVC), SVC, IVC, RA, RV, PA, and aortic saturations. Saturations should immediately be reviewed and repeated if any measurements are questionable. The Fick CO should also be calculated at this time.
5. As the saturations are collected, pressures should be measured in each chamber as the catheter is advanced forward. Collected pressures include RA mean; RV systolic and diastolic; PA systolic, diastolic, and mean; PCWP systolic, diastolic, and mean; and aortic systolic, diastolic, and mean.
6. Measurement of the PCWP should be taken at end-expiration in West zone 3. If there is any question about the validity of the PCWP measurement or if the PCWP is unexpectedly >15 mmHg, measurement of the LVEDP should be performed.
7. Before AVT is performed, thermodilution CO should be performed if that modality is being utilized. At least three measures should be performed with individual results that do not vary more than 15%. If not the case, measures should be repeated until three measures that vary ≤15% have been collected.
8. AVT with iNO (or appropriate alternative agent) should be performed in all patients for whom initiation of advanced medical therapy for PAH is being considered. An increase in the PCWP during testing is generally a contraindication to use of these therapies. A positive response (decrease in mPAP of ≥10 mmHg to a mPAP ≤40 mmHg, without a decrease in CO) may permit initiation of calcium channel blocker therapy in iPAH. If this therapy is selected, very close follow-up is advised, as treatment failure is common.
9. Immediate communication of the results to the referring and treating physicians is essential for prompt recognition and initiation of therapy.

Treatment of PAH

A detailed discussion of the treatment of PAH is beyond the scope of this chapter. The goals of medical management are to achieve normal hemodynamics and a good quality of life – WHO FC I or II symptoms [31]. Treatment must be individualized to the patient and is best undertaken at centers with expertise treating PAH. Most patients will require diuretics to optimize volume status and may require supplemental oxygen to maintain saturations >90% [31]. Vasodilator testing responders should be started on high-dose CCBs (typically amlodipine, diltiazem, or nifedipine). There has been tremendous growth in the field of targeted PAH pharmacotherapies since IV epoprostenol was first approved in 1995. The major classes of PAH drugs currently include phospho-

diesterase type 5 inhibitors (PDE5), endothelin receptor antagonists (ERA), prostaglandins, guanylate cyclase stimulators, and selective prostacyclin IP receptor agonists. Lower-risk patients can be started on a single agent, though it is now common to initiate combination therapy with agents from different classes, particularly in higher-risk patients. Additionally, non-Group 1 patients with precapillary PH, including some with combined pre- and postcapillary PH, may derive benefit from these therapies [32, 33]. These uses should be considered off-label, however, and should be limited to carefully monitored clinical investigations. Ultimately, patients who progress despite advanced therapies may require lung or combined heart-lung transplant to survive.

Several interventional cardiology procedures may be considered to palliate patients with severe, medically refractory PAH and RV failure. Balloon atrial septostomy (BAS) creates an atrial-level right to left shunt that decompresses the RV and increases CO at the expense of worsening hypoxia. BAS has been shown to improve hemodynamics and functional capacity in the short term, although data on long-term survival benefits following the procedure are lacking [34]. The procedure should only be performed at experienced centers and is contraindicated in patients with a mean RA pressure > 20 mmHg or resting oxygen levels <85% on room air [4]. In 2013, Esch et al. [35] described the first-in-human experience, creating a transcatheter pulmonary-to-systemic shunt between the left pulmonary artery and descending thoracic aorta (Potts shunt). Surgical Potts shunts were previously utilized to palliate cyanotic congenital heart disease, but recent interest in their use in the pediatric and adult PAH populations is growing. The advantage of the Potts shunt over a BAS is that the former maintains fully oxygenated blood flow to the head and coronary arteries [34]. An emerging area of research is PA denervation via catheter-based ablation as a treatment of PAH. This is based on experimental evidence showing increased adrenergic signaling is present in patients with PAH and is linked to the development of pulmonary vascular disease and maladaptive RV remodeling [36]. A recent study of 66 patients with PH (39 with Group 1 PAH) demonstrated a >10 mmHg decrease in mPAP in 94% of patients immediately after the procedure, and sustained reductions in mPAP and improvements in CO and WHO FC at 1 year [37]. Though early data looks promising, extensive further studies will be necessary before this paradigm-shifting therapy can be approved.

Case Examples

Case 1

M.H. is a 53-year-old gentleman with scleroderma diagnosed 10 years ago and well-controlled essential hypertension who presented with complaints of worsening exertional dyspnea. A pulmonologist evaluated him 5 years ago and diagnosed him with mild interstitial lung disease. His fatigue and dyspnea had progressively worsened over the previous 3 months to the point of WHO FC III symptoms. There was no prior cardiac history.

His examination showed a JVP of 12 cm, a mildly prominent P2, a II/VI holosystolic murmur consistent with TR and 1+ peripheral edema. An echocardiogram revealed a dilated IVC, right heart enlargement, and mild RV systolic dysfunction with an estimated RVSP of 60 mmHg. There was grade 1 LV diastolic dysfunction; LA size was normal. He was taken to the cardiac catheterization laboratory where pressures included: mean RA 12 mmHg, RV 66/12 mmHg, PA 71/41 with a mean of 51 mmHg, PCWP of 41 mmHg, CI of 2.3 L/min/m^2 and a calculated PVR of 1.9 Wu. He was treated with diuretics by his physician but then developed hypotension and mild acute renal failure resulting in hospitalization.

After seeing the patient in consultation, we felt that the hemodynamics (suggesting PVH) did not match the clinical story (suggesting PAH). We then reviewed the hemodynamic tracings, which brought the measured PCWP into question (Fig. 18.4). It had been measured in only one position and the tracing suggested incomplete balloon occlusion of the PA. The patient begrudgingly agreed to repeat catheterization, where data revealed RA mean 8 mmHg,

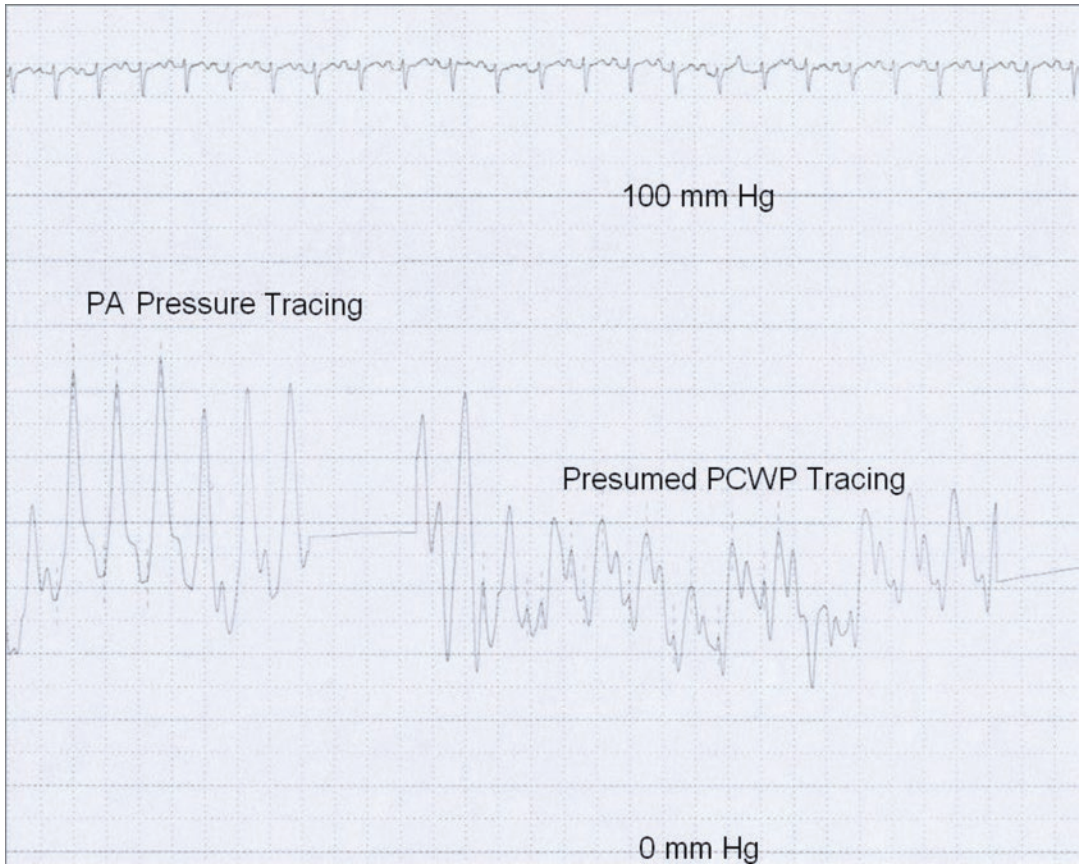

Fig. 18.4 Initial RHC in a patient with scleroderma that suggests the presence of PVH. There is limited respiratory variation in the PCWP tracing and the tracing appears to be a hybrid (fusion of PAP and PCWP waveforms) suggesting incomplete balloon occlusion of the pulmonary artery. These tracing were not consistent with the expected findings. In such cases multiple measurements should be obtained in different locations, and the LVEDP should then be measured for confirmation. This patient required repeat hemodynamic assessment to obtain proper measurements

RV 60/8 mmHg, PAP 60/33 with mean 40 mmHg, PCWP 12 mmHg, CI 2.2 L/min/m^2, and PVR 6.4 Wu (Fig. 18.5). LVEDP was also directly measured via retrograde left heart catheterization and was 11 mmHg. Vasodilatory testing was performed and resulted in a mPAP drop to 36 mmHg with stable PCWP pressure and CI and a decrease in PVR to 5.4 Wu. He was started on an ERA, and on follow-up he experienced a 50 m increase in 6MWD and had improved to WHO FC II.

This patient presents the dilemma of an RHC where data has not been properly collected. In cases like this, it is important to review the actual waveforms and assess if measurements were appropriately performed. In this case the initial RHC evaluated a hybrid PCWP waveform that grossly overestimated the PCWP. With repeat RHC and confirmation with measurement of the LVEDP, the appropriate diagnosis of PAH was made and proper therapy was initiated. Other techniques to ensure appropriate PCWP measurement include repeat measurements in both lung fields in different segments, assurance of appropriate respiratory variation in the tracing, collection of a wedge saturation (which should be ≥95%) and a small (2–3 cc), gentle injection of contrast dye, which should not be washed out until the balloon is deflated (Fig. 18.6).

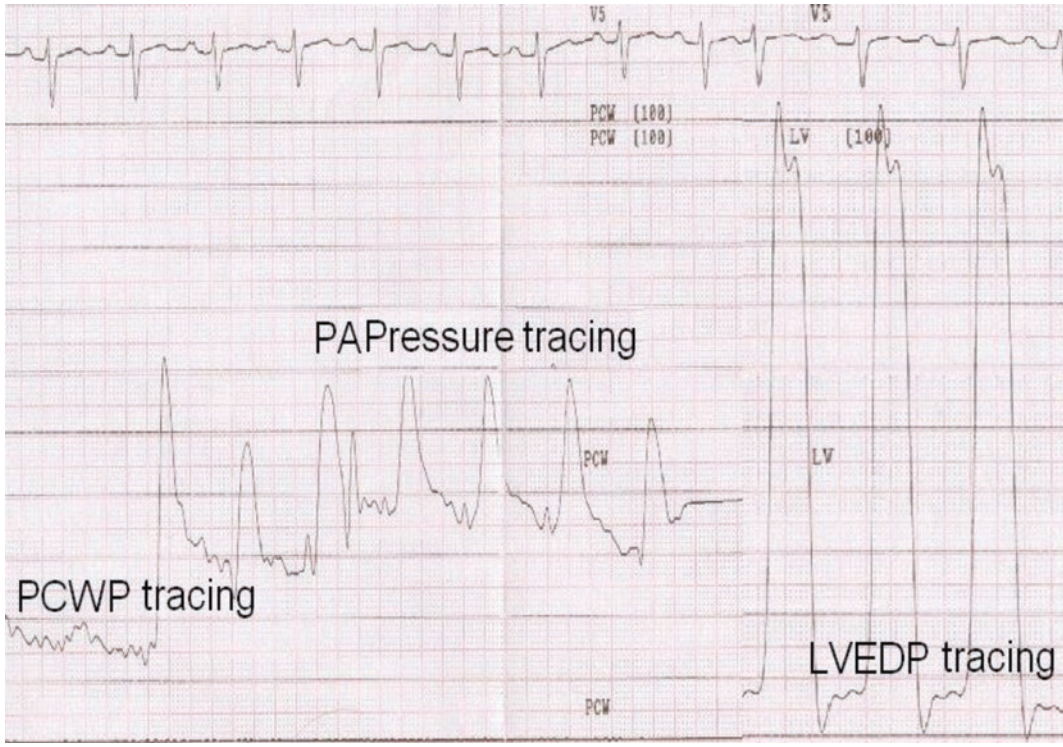

Fig. 18.5 Repeat RHC which indicates the presence of PAH (the expected finding given the clinical history). The LVEDP confirms that the PCWP is low in this case

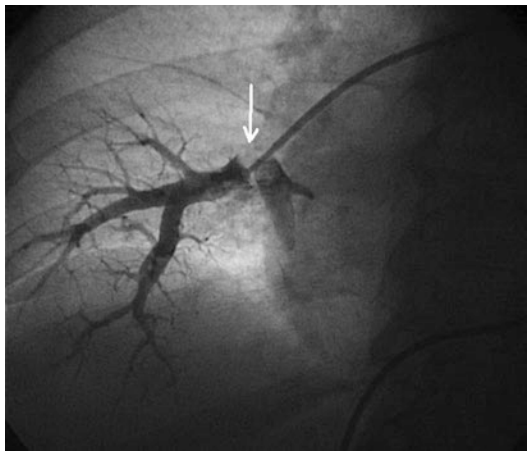

Fig. 18.6 Gentle contrast injection into the right pulmonary artery under balloon inflation (pulmonary wedge angiogram). The tip of the balloon is highlighted by the arrow. Dye is seen filling a branch pulmonary artery proximal to the balloon and suggests incomplete occlusion. In such a case, a hybrid tracing would be present and would lead to an inappropriately high PCWP recording

Case 2

R.B. is a concerned 36-year-old gentleman who presented with progressive exertional dyspnea and fatigue that had significantly limited his ability to work in construction over the last few years. A recent echo suggested right-sided enlargement and borderline elevated RVSP. A bubble study was performed that suggested the presence of a patent foramen ovale (PFO). His right heart catheterization revealed mean RA pressure 10 mmHg, RV 40/9 mmHg, PA 40/18 with mean 25 mmHg, PCWP mean 12 mmHg, cardiac index 4.0 L/min/m^2, and PVR 1.3 Wu. O_2 saturation measurements were SVC 75%, IVC 76%, RA 89%, RV 88%, and PA 88% and a systemic saturation of 98%.

This case highlights the diagnostic capability of a properly performed shunt run. In this case there is a clear increase in saturation at the RA

level. A contrast injection was subsequently performed that showed an anomalous right upper pulmonary vein draining into the border of the SVC and RA and the presence of a right-to-left shunt in the superior septum. This was most consistent with a sinus venosus atrial septal defect and concomitant partial anomalous pulmonary venous return (PAPVR). It is important to recognize that PAPVR can also be present in isolation, and in such cases the echo bubble study may be negative. Performing a shunt run or at least SVC and PA saturations during RHC ensures that such a shunt will not be missed. The anomalous vein can be entered quite easily and safely (providing a careful technique using a flexible wire is utilized), and a gentle contrast injection can delineate its entry point into the heart (Fig. 18.7). A blood gas drawn in the vein should demonstrate a saturation ≥95%.

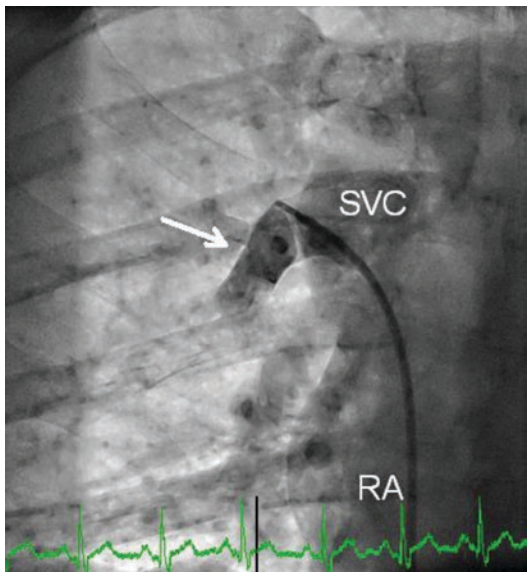

Fig. 18.7 Limited pulmonary vein angiogram (AP projection) of an anomalous right upper pulmonary vein performed via right femoral vein access (hand injection via end-hole catheter). The white arrow highlights the distal segment of the pulmonary vein which drains into the SVC at the RA junction. Samples drawn from this vein showed oxygen saturations >95%. A high CO at catheterization in the presence of right heart enlargement and a negative bubble study should prompt careful assessment for possible anomalous pulmonary venous return

A major clue to the presence of an underlying shunt is revealed in the cardiac index. Most patients with PH will have at least slightly reduced CO (if not grossly decreased). If the CO/CI is normal or high in a patient with echocardiographic evidence of right-sided enlargement (as it was in this case), a shunt is probable and should be carefully sought out. A PFO does not usually result in left-to-right shunting and would certainly not be expected to result in right heart enlargement. The patient in this case was referred to cardiac surgery and underwent successful repair. Repeat echocardiography has demonstrated normalization of his right-sided pressures and chamber sizes after repair.

Case 3

J.T. is a 66-year-old woman with multiple medical problems including advanced renal disease, dilated cardiomyopathy (LVEF~20%), and resultant severe mitral and tricuspid regurgitation. She was admitted to the coronary care unit for further management of worsening congestive heart failure and hemodynamic instability. On examination she was severely volume-overloaded and in respiratory distress with JVD above the angle of the jaw at 45° and a large cv wave. There was a prominent P2 present and a III/VI holosystolic murmur heart best over apex, a laterally displaced point of maximal impulse and a palpable RV heave. Lungs showed bibasilar rales and there was 2+ pitting peripheral edema.

Echo showed four chamber dilatation with severe mitral and tricuspid regurgitation. Estimated RV systolic pressure was 80 mmHg. RHC at the bedside revealed RA pressure 24 mmHg, RV 96/22 mmHg, PA 96/40 with mean 62 mmHg, mean PCWP 34 mmHg, CI 1.8 L/min/m^2, and PVR 10 Wood units. She was seen in consultation for possible initiation of pulmonary-selective therapies, and we instead recommended continued aggressive diuresis and afterload reduction with hydralazine and nitrates (baseline creatinine was 2.5 mg/dl) with the plan

for repeat hemodynamic assessment when stable.

RHC in the cath lab 10 days later showed RA pressure 15 mmHg, RV 73/15 mmHg, PA 73/28 with mean 44 mmHg, PCWP 16 mmHg, CI 1.5 L/min/m^2, and PVR 12.2 Wood units (Fig. 18.8). During inhalation of 40 ppm of nitric oxide, the PA pressure remained essentially unchanged (73/30 with mean 46 mmHg), but the pulmonary capillary wedge increased to a mean of 30 with v-waves to 65 mm Hg (Fig. 18.9). The team was instructed that the patient was not a candidate for selective pulmonary vasodilator therapy and surgical consultation for consideration of mitral and tricuspid valve repair was recommended.

This patient had long-standing RV dysfunction that likely arose from pulmonary venous hypertension consequent to high left-sided filling pressures from left ventricular dysfunction and mitral regurgitation. The PH in this case is therefore the offshoot of long-standing left heart disease and is likely compensatory to "protect" the left ventricle. AVT provides some insight into what would happen with pulmonary-selective therapy and the results suggest that the patient would be poorly tolerant of this therapeutic approach. In such cases this type of therapy could worsen her clinical course and precipitate decompensation and even death. Thorough assessment of hemodynamics in this case led to better understanding of the physiology and avoided a potential pharmacologic misadventure.

Pearls of Assessment of Pulmonary Hypertension

- Clinical suspicion for PH should remain high, especially in young patients with vague complaints such as dyspnea. Family and social history can provide important clues to a possible diagnosis.
- PAH is a diagnosis of exclusion, and patients must undergo a complete workup before a diagnosis of PAH is entertained. Secondary causes resulting in PVH are a far more common cause of PH.

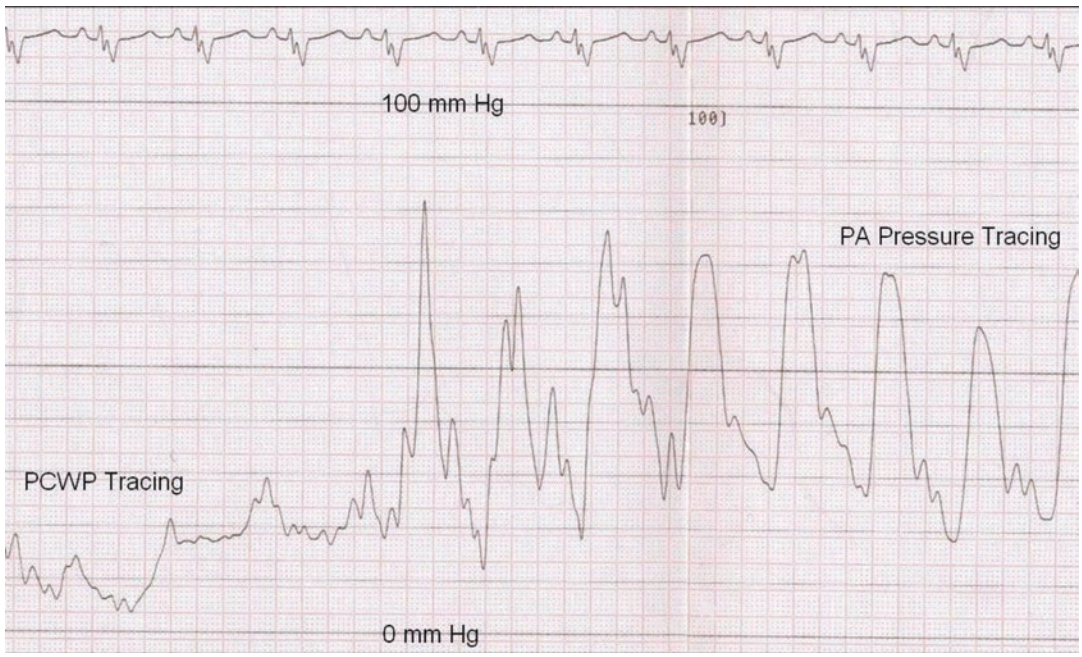

Fig. 18.8 Collected right heart catheterization waveforms in patient with heart failure and severe mitral regurgitation leading to pulmonary hypertension after aggressive diuresis. These suggest the presence of PAH and initially supported a potential role for selective pulmonary vasodilator therapy in this patient

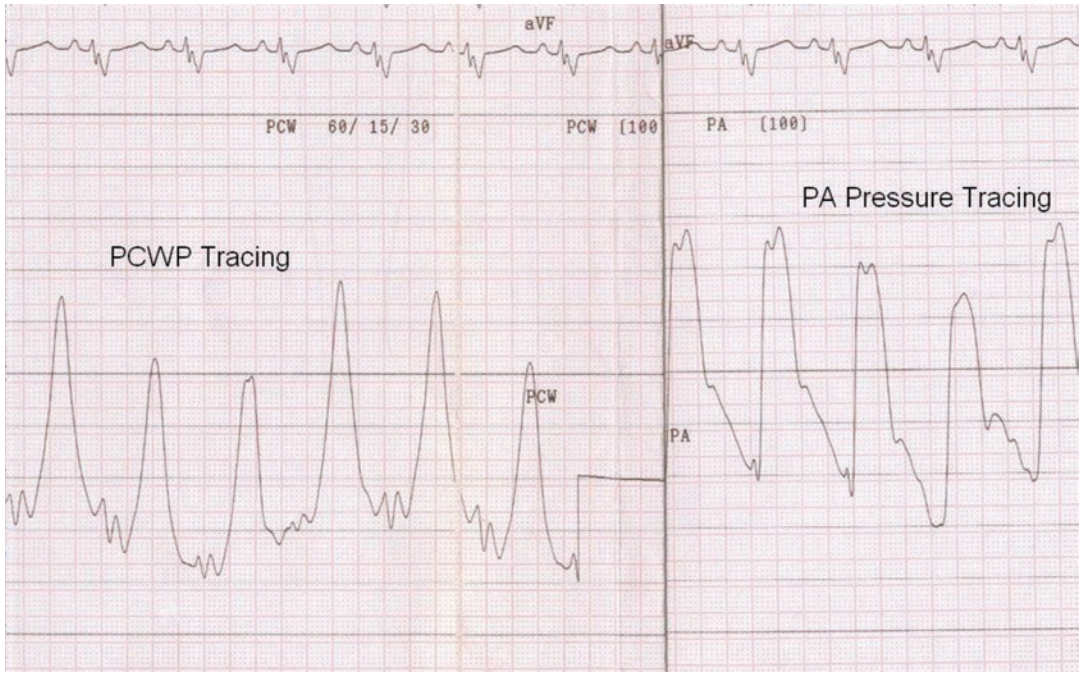

Fig. 18.9 Collected right heart catheterization waveforms during inhalation of 40 ppm of inhaled nitric oxide. Note the dramatic increase in mPCWP to ~30 mmHg and prominent *v*-waves to >65 mmHg. The PA pressure remained essentially unchanged (73/30 with mean 46 mm Hg) compared to baseline (Fig. 18.7). In this case acute vasodilator testing unmasked the left heart pathology leading to pulmonary venous hypertension in this patient

- The use of echocardiography is not adequate for evaluating mild to moderate PH. Only in severe PH does Doppler echocardiography provide reliable data for estimating RVSP. Echocardiography is essential for exclusion of left heart disease.
- The diagnosis of PAH can only be confirmed with RHC. Guidelines define PAH as mPAP >25 mmHg, PCWP ≤15 mmHg, and PVR >3 Wu in the absence of other causes of precapillary PH (e.g., CTEPH, chronic lung disease).
- Appropriate patients undergoing RHC should be further evaluated with vasodilator testing. This aids in selecting therapy and helps determine prognosis.
- Beware of hybrid tracings and confirm that an accurate PCWP measurement has been recorded. For patients in whom PCWP is not believed to be reliable, LVEDP should be directly measured.
- PCWP measurements should be taken at the end of the expiratory phase and in multiple PA segments to confirm accuracy, particularly in the setting of CTEPH or PVOD.
- Prognostic information and therapeutic decision-making are dependent on hemodynamics. Thus, appropriate techniques and proper and immediate interpretation are vital to performing RHC in patients with PH.
- Communication with referring and treating physicians is essential to streamline appropriate patient therapy in this very serious clinical disorder.

Review Questions

1a. A 46-year-old African American woman presents to clinic complaining of cough, lower extremity edema, and dyspnea on exertion over the last 3 months. Her medical history is significant for sarcoidosis diagnosed at 35 years of age and she has a 30-pack year history of smoking. Vitals are blood pressure 135/78 mmHg, pulse 87,

respiratory rate 20, and oxygen saturation 88% on room air. Her cardiac exam is notable only for a prominent P2. EKG shows sinus rhythm with right axis deviation. An arterial blood gas demonstrates a PO_2 of 49 mmHg and a PCO_2 of 35 mmHg. A chest x-ray demonstrates bilateral infiltrates, perihilar lymphadenopathy, and pulmonary vascular dilatation.

What is the best next step in the management of this patient?

A. PFTs
B. Transthoracic echocardiogram
C. CT angiography of chest
D. RHC
E. NT-pro-BNP

Answer C is correct. Although clinical suspicion for PH remains high, other more acute causes of hypoxemia must be ruled out. A CT scan can evaluate the lung parenchyma, which is likely to be abnormal, given this patient's history, and obtaining a contrasted angiography study will evaluate for acute pulmonary embolism or CTEPH as potential causes of hypoxia and PH, respectively. Subsequent evaluations with echocardiogram, PFTs, laboratory testing, and ultimately RHC are all appropriate if other workup is suggestive of PAH.

1b. The patient's CT scan shows the expected findings of sarcoidosis and no pulmonary embolism. An echocardiogram is obtained revealing an RVSP of 70 mmHg with enlargement of right-sided heart structures and normal left heart function. She desaturates to 83% on 6MWT and is only able to complete 280 m. RHC is scheduled.

Which of the following hemodynamics is most consistent with PAH?

A. mPAP 28 mmHg, PCWP 15 mmHg, CO 4.9 L/min, PVR 4.7 Wu
B. mPAP 40 mmHg, PCWP 26 mmHg, CO 5.2 L/min, PVR 2.7 Wu
C. mPAP 52 mmHg, PCWP 14 mmHg, CO 13.4 L/min, PVR 2.8 Wu
D. mPAP 18 mmHg, PCWP 12 mmHg, CO 5.5 L/min, PVR 1.1 Wu
E. mPAP 54 mmHg, PCWP 10 mmHg, CO 5.1 L/min, PVR 8.6 Wu

Answer E is correct. The hemodynamics for this patient are most consistent with the current guidelines for a diagnosis of PAH. Answer B is more indicative of postcapillary PH such as would be seen in patients with heart failure with preserved ejection fraction (HFpEF). The transpulmonary gradient is grossly elevated in answer C, but the CO is also grossly elevated suggesting the presence of an acute high output state such as sepsis or an intracardiac shunt. This patient should have a full saturation run performed to investigate the latter possibility more thoroughly. Answer D is consistent with completely normal hemodynamics. Answer A would have been correct if the PVR had not been calculated incorrectly. The actual PVR is (28–15)/4.9 = 2.7 Wu, which does not meet the formal criteria for PAH.

1c. Acute vasoreactivity testing with iNO at 40 ppm is performed. After 5 min, which of the following hemodynamics is most consistent with a positive response (baseline mPAP 54 mmHg, PCWP 10 mmHg, CO 5.1 L/min)?

A. mPAP 42 mmHg, PCWP 10 mmHg, and CO 5.1 L/min
B. mPAP 38 mmHg, PCWP 10 mmHg, and CO 5.6 L/min
C. mPAP 50 mmHg, PCWP 25 mmHg, and CO 4.9 L/min
D. mPAP 68 mmHg, PCWP 8 mmHg, and CO 4.8 L/min

Answer B is correct. The current definition of a positive test is a drop in mPAP $\geq$10 mmHg to an absolute value $\leq$40 mmHg with the CO remaining stable or increasing. Answer A shows a substantial drop in mPAP, but not to $\leq$40 mmHg. Answer C shows a slight drop in mPAP but also an increase in PCWP and slight decrease in CO. Her PVR calculates as (50–25/4.9) = 5.1 Wu, consistent with combined pre- and postcapillary PH with the predominant driver being left-sided diastolic dysfunction. Although some patients with combined pre- and postcapillary PH benefit from initiation of targeted PAH therapies, this patient's left-sided heart failure should first be optimized and RHC

then repeated to determine the best next steps. Answer E is illogical as the mPAP is not expected to rise, or the PWCP to fall, during vasodilatory testing.

2. A 45-year-old man undergoes RHC for suspected mild PAH. He weighs 80 kg, is 1.75 m tall and his body surface area is 1.97 m^2. His hemoglobin is 12.5 g/dL. Systemic saturation on arterial blood gas is 95%. A shunt run is performed. Which of the following would be most suspicious for PAH secondary to a congenital heart lesion?
   A. SVC saturation 75%, IVC saturation 77%, and PA saturation 74%
   B. SVC saturation 78%, IVC saturation 84%, and PA saturation 68%
   C. SVC saturation 70%, IVC saturation 74%, and PA saturation 72%
   D. SVC saturation 74%, IVC saturation 77%, and PA saturation 90%
   E. SVC saturation 69%, IVC saturation 72%, and PA saturation 71%

   Answer D is correct. The mixed venous saturation is estimated by (3 × SVC + IVC)/4. If the PA saturation is at least 7% greater than the mixed venous saturation, a shunt is highly likely. In answer D, the estimated mixed venous saturation is (3 × 74 + 77)/4 = 75% with a PA saturation of 90%. The pulmonary venous saturation (if not collected) is estimated at 95%. The degree of shunting can be calculated by dividing the Qp by the systemic blood flow (Qs). A rough estimate of the shunt can be calculated using the obtained saturations: (systemic-mixed venous saturations)/(pulmonary vein-PA saturations), which in this case yields a calculated Qp:Qs of (95–75)/(95–90) = 5:1, consistent with a large left-to-right shunt. None of the other choices show a step-up in saturation. The PA saturation in B must be incorrect as a step-down in saturation in the right heart is not possible. This saturation should be repeated ensuring to tap out any residual air bubbles from the syringe (which can lead to aberrant readings) before analysis.
3. A 44-year-old man with vasoresponsive iPAH has been stable on a regimen of 20 mg amlodipine daily for the past 3 years. He presents for follow-up and reports increasing dyspnea and fatigue over the last 3 months. He is comfortable at rest and able to perform some activities of daily living but has fatigue and light-headedness with repetitive actions such as brushing his teeth while standing up. On 6MWD, he desaturates to 83% after 50 m. One year ago, he desaturated to 92% after 100 m. What FC should he be classified as and what is the next step in the care of this patient?
   A. FC II: Change CCB therapy to verapamil or diltiazem
   B. FC III: Change CCB therapy to verapamil or diltiazem
   C. FC III: Repeat RHC for consideration of starting targeted PAH therapies
   D. FC VI: Change CCB therapy to verapamil or diltiazem
   E. FC VI: Admit to the hospital for initiation of IV prostacyclin therapy

   Answer C is correct. This patient presents with clinical worsening consistent with WHO FC III symptoms. It is important to note that the currently utilized definition of responsiveness was derived from a cohort of patients with iPAH with the goal of identifying patients who did well treated solely with CCBs [38]. In this cohort, only ~5% of patients did well with CCB monotherapy long-term. With the proliferation of targeted PAH therapies in the modern era, such a strategy is hard to justify. As such, the modern use of vasoresponsiveness helps to identify, by lack of a response, a high-risk cohort that may only benefit from the most aggressive of therapies. As such, this patient should undergo RHC and initiation of targeted PAH therapies should be considered. There is no evidence to suggest a benefit from switching to an alternative CCB agent as suggested in answers A, B, and D; verapamil is typically avoided in PAH patients out of concern for negative inotropic effects. Answer E is incorrect as the patient's FC is not yet at a VI. Although patients with FC VI often do require admission and initiation of IV prostacyclin therapy, an RHC should also be performed first and prior to a step-up in PAH therapy.

References

1. Galie N, Torbicki A, Barst R, Dartevelle P, Haworth S, Higenbottam T, et al. Guidelines on diagnosis and treatment of pulmonary arterial hypertension. The task force on diagnosis and treatment of pulmonary arterial hypertension of the European Society of Cardiology. Eur Heart J. 2004;25(24):2243–78.
2. Simonneau G, Gatzoulis MA, Adatia I, Celermajer D, Denton C, Ghofrani A, et al. Updated clinical classification of pulmonary hypertension. J Am Coll Cardiol. 2013;62(25 Suppl):D34–41.
3. Kovacs G, Berghold A, Scheidl S, Olschewski H. Pulmonary arterial pressure during rest and exercise in healthy subjects: a systematic review. Eur Respir J. 2009;34(4):888–94.
4. Galie N, Humbert M, Vachiery JL, Gibbs S, Lang I, Torbicki A, et al. 2015 ESC/ERS guidelines for the diagnosis and treatment of pulmonary hypertension: the joint task force for the diagnosis and treatment of pulmonary hypertension of the European Society of Cardiology (ESC) and the European Respiratory Society (ERS): endorsed by: Association for European Paediatric and Congenital Cardiology (AEPC), International Society for Heart and Lung Transplantation (ISHLT). Eur Heart J. 2016;37(1):67–119.
5. Hoeper MM, Humbert M, Souza R, Idrees M, Kawut SM, Sliwa-Hahnle K, et al. A global view of pulmonary hypertension. Lancet Respir Med. 2016;4(4):306–22.
6. Lai YC, Potoka KC, Champion HC, Mora AL, Gladwin MT. Pulmonary arterial hypertension: the clinical syndrome. Circ Res. 2014;115(1):115–30.
7. Soubrier F, Chung WK, Machado R, Grunig E, Aldred M, Geraci M, et al. Genetics and genomics of pulmonary arterial hypertension. J Am Coll Cardiol. 2013;62(25 Suppl):D13–21.
8. Evans JDW, Girerd B, Montani D, Wang X-J, Galiè N, Austin ED, et al. BMPR2 mutations and survival in pulmonary arterial hypertension: an individual participant data meta-analysis. Lancet Respir Med. 2016;4(2):129–37.
9. Hoeper MM, Simon RGJ. The changing landscape of pulmonary arterial hypertension and implications for patient care. Eur Respir Rev. 2014;23(134):450–7.
10. McGoon MD, Miller DP. REVEAL: a contemporary US pulmonary arterial hypertension registry. Eur Respir Rev. 2012;21(123):8–18.
11. D'Alonzo GE, Barst RJ, Ayres SM, et al. Survival in patients with primary pulmonary hypertension: results from a national prospective registry. Ann Intern Med. 1991;115(5):343–9.
12. Benza RL, Miller DP, Barst RJ, Badesch DB, Frost AE, McGoon MD. An evaluation of long-term survival from time of diagnosis in pulmonary arterial hypertension from the REVEAL registry. Chest. 2012;142(2):448–56.
13. Brown LM, Chen H, Halpern S, Taichman D, McGoon MD, Farber HW, et al. Delay in recognition of pulmonary arterial hypertension: factors identified from the REVEAL registry. Chest. 2011;140(1):19–26.
14. Runo JR, Loyd JE. Primary pulmonary hypertension. Lancet. 2003;361(9368):1533–44.
15. Benza RL, Miller DP, Gomberg-Maitland M, Frantz RP, Foreman AJ, Coffey CS, et al. Predicting survival in pulmonary arterial hypertension: insights from the registry to evaluate early and long-term pulmonary arterial hypertension disease management (REVEAL). Circulation. 2010;122(2):164–72.
16. Gopalan D, Blanchard D, Auger WR. Diagnostic evaluation of chronic thromboembolic pulmonary hypertension. Ann Am Thorac Soc. 2016;13(Suppl 3):S222–39.
17. Seeger W, Adir Y, Barbera JA, Champion H, Coghlan JG, Cottin V, et al. Pulmonary hypertension in chronic lung diseases. J Am Coll Cardiol. 2013;62(25 Suppl):D109–16.
18. Forfia PR, Fisher MR, Mathai SC, Housten-Harris T, Hemnes AR, Borlaug BA, et al. Tricuspid annular displacement predicts survival in pulmonary hypertension. Am J Respir Crit Care Med. 2006;174(9):1034–41.
19. Zuckerman WA, Turner ME, Kerstein J, Torres A, Vincent JA, Krishnan U, et al. Safety of cardiac catheterization at a center specializing in the care of patients with pulmonary arterial hypertension. Pulm Circ. 2013;3(4):831–9.
20. Hoeper MM, Maier R, Tongers J, Niedermeyer J, Hohlfeld JM, Hamm M, et al. Determination of cardiac output by the Fick method, thermodilution, and acetylene rebreathing in pulmonary hypertension. Am J Respir Crit Care Med. 1999;160:535–41.
21. Narang N, Thibodeau JT, Levine BD, Gore MO, Ayers CR, Lange RA, et al. Inaccuracy of estimated resting oxygen uptake in the clinical setting. Circulation. 2014;129(2):203–10.
22. Benza RL, Gomberg-Maitland M, Miller DP, Frost A, Frantz RP, Foreman AJ, et al. The REVEAL registry risk score calculator in patients newly diagnosed with pulmonary arterial hypertension. Chest. 2012;141(2):354–62.
23. Hoeper MM, Bogaard HJ, Condliffe R, Frantz R, Khanna D, Kurzyna M, et al. Definitions and diagnosis of pulmonary hypertension. J Am Coll Cardiol. 2013;62(25 Suppl):D42–50.
24. Ryan JJ, Rich JD, Thiruvoipati T, Swamy R, Kim GH, Rich S. Current practice for determining pulmonary capillary wedge pressure predisposes to serious errors in the classification of patients with pulmonary hypertension. Am Heart J. 2012;163(4):589–94.
25. Kovacs G, Olschewski A, Berghold A, Olschewski H. Pulmonary vascular resistances during exercise in normal subjects: a systematic review. Eur Respir J. 2012;39(2):319–28.
26. Thenappan T, Ormiston ML, Ryan JJ, Archer SL. Pulmonary arterial hypertension: pathogenesis and clinical management. BMJ. 2018;360:j5492.

27. Krasuski RA, Warner JJ, Wang A, Harrison JK, Tapson VF, Bashore TM. Inhaled nitric oxide selectively dilates pulmonary vasculature in adult patients with pulmonary hypertension, irrespective of etiology. J Am Coll Cardiol. 2000;36(7):2204–11.
28. Krasuski RA, Devendra GP, Hart SA, Wang A, Harrison JK, Bashore TM. Response to inhaled nitric oxide predicts survival in patients with pulmonary hypertension. J Card Fail. 2011;17(4):265–71.
29. Skoro-Sajer N, Hack N, Sadushi-Kolici R, Bonderman D, Jakowitsch J, Klepetko W, et al. Pulmonary vascular reactivity and prognosis in patients with chronic thromboembolic pulmonary hypertension: a pilot study. Circulation. 2009;119(2):298–305.
30. Post MC, Janssens S, Van de Werf F, Budts W. Responsiveness to inhaled nitric oxide is a predictor for mid-term survival in adult patients with congenital heart defects and pulmonary arterial hypertension. Eur Heart J. 2004;25(18):1651–6.
31. McLaughlin VV, Shah SJ, Souza R, Humbert M. Management of pulmonary arterial hypertension. J Am Coll Cardiol. 2015;65(18):1976–97.
32. Andersen CU, Mellemkjær S, Nielsen-Kudsk JE, Bendstrup E, Hilberg O, Simonsen U. Pulmonary hypertension in chronic obstructive and interstitial lung diseases. Int J Cardiol. 2013;168(3):1795–804.
33. Opitz CF, Hoeper MM, Gibbs JS, Kaemmerer H, Pepke-Zaba J, Coghlan JG, et al. Pre-capillary, combined, and post-capillary pulmonary hypertension: a pathophysiological continuum. J Am Coll Cardiol. 2016;68(4):368–78.
34. Leopold JA. Catheter-based therapies for patients with medication-refractory pulmonary arterial hypertension. Circ Cardiovasc Interv. 2015;8(11):e003332.
35. Esch JJ, Shah PB, Cockrill BA, Farber HW, Landzberg MJ, Mehra MR, et al. Transcatheter Potts shunt creation in patients with severe pulmonary arterial hypertension: initial clinical experience. J Heart Lung Transplant. 2013;32(4):381–7.
36. Maron BA, Leopold JA. Emerging concepts in the molecular basis of pulmonary arterial hypertension: part II: neurohormonal signaling contributes to the pulmonary vascular and right ventricular pathophenotype of pulmonary arterial hypertension. Circulation. 2015;131(23):2079–91.
37. Chen SL, Zhang H, Xie DJ, Zhang J, Zhou L, Rothman AM, et al. Hemodynamic, functional, and clinical responses to pulmonary artery denervation in patients with pulmonary arterial hypertension of different causes: phase II results from the pulmonary artery denervation-1 study. Circ Cardiovasc Interv. 2015;8(11):e002837.
38. Sitbon O, Humbert M, Jais X, Ioos V, Hamid AM, Provencher S, et al. Long-term response to calcium channel blockers in idiopathic pulmonary arterial hypertension. Circulation. 2005;111(23):3105–11.

19 Acute Decompensated Heart Failure

Andrew D. M. Grant, Michael A. Hanna, and Mazen A. Hanna

Epidemiology of Acute Decompensated Heart Failure (ADHF)

Heart failure is estimated to affect 2% of the adult population. There are over one million hospitalizations for ADHF in the USA per year, and, among the Medicare population, it is the leading discharge diagnosis [1, 2]. About 25% of these patients present as de novo heart failure, and 75% present as an exacerbation of chronic heart failure. When not due to an arryhthmia or primary valvular disease, heart failure may arise in those with either reduced (≤40%), preserved (≥50%), or mid-range (40–50%) left ventricular ejection fraction [3, 4]. The inpatient mortality ranges from 3% to 25% depending on associated comorbidites and clinical characteristics [5]. The readmission rate at 30 days is a staggering 20–25% [6].

Hemodynamics of Decompensated Heart Failure

The hemodynamic perturbations in the syndrome of decompensated heart failure are characterized by elevated intracardiac filling pressures, normal or reduced cardiac output, and abnormalities in the systemic and pulmonary vascular resistance (PVR). Although there are syndromes in which the cardiac output is abnormally elevated, these will not be discussed in this chapter.

Intracardiac Filling Pressures

When volume overload (increased preload) and increased afterload occur, there is an elevation of left ventricular end-diastolic pressure from baseline (which may already be elevated). This leads to a rise in left atrial pressure and thus pulmonary capillary wedge pressure (PCWP). The elevation in the PCWP leads to passive *pulmonary hypertension* (pulmonary venous hypertension, WHO Group 2). Either volume overload or pulmonary hypertension (or both) leads to elevation of the right atrial pressure (RAP). The extent of pulmonary hypertension depends on the degree and chronicity of elevation of the PCWP and the degree of superimposed pulmonary vasoconstriction and vascular remodeling (see section "Vascular Resistance").

In patients with ADHF, PCWP is usually >22 mmHg and right atrial pressure >10 mmHg; such a patient is typically classified as "wet." In the average ADHF patient, a RAP >10 mmHg correlates to a PCWP >22 mmHg about 80% of the time [7–10]. In these "concordant" cases, PCWP

A. D. M. Grant
Libin Cardiovascular Institute, Calgary, AB, Canada
e-mail: andrew.grant@ahs.ca

M. A. Hanna · M. A. Hanna (✉)
Cleveland Clinic, Cleveland, OH, USA
e-mail: hannam@ccf.org

A. T. Askari, A. W. Messerli (eds.), *Cardiovascular Hemodynamics*, Contemporary Cardiology,
https://doi.org/10.1007/978-3-030-19131-3_19

is usually about 2–2.5 times RAP. About 20% of the time, there is "discordance" in this relationship; one example is in patients with disproportionate RV failure in whom RAP is significantly elevated with a normal or only mildly elevated PCWP. The other example is when RAP is normal with a significantly elevated PCWP as one may see in acute left-sided heart failure without volume overload or a very noncompliant LV with high resting filling pressure despite euvolemia. These are important hemodynamic concepts to understand as they may affect management.

Cardiac Output

Cardiac output is a product of stroke volume and heart rate (see Chap. 4). Stroke volume is determined by preload (filling pressure), myocardial contractility, and afterload (mainly systemic vascular resistance). In patients with ADHF, a decrease in cardiac output is more likely due to low stroke volume but occasionally can be due to an inappropriately low heart rate. It is important to note that in the majority of cases of ADHF, the cardiac output remains normal. Low cardiac output, as measured by Fick or thermodilution (we more often use the Fick method at our institution), occurs in a minority of patients who have advanced heart failure or excessively low filling pressures due to overdiuresis. Arbitrarily, a cardiac index (cardiac output/body surface area) of <2.2 is considered low, and such a patient is typically classified as "cold" while a patient with a cardiac index >2.2 is classified as "warm [11]." A patient with a low cardiac index may be compensated and have no signs or symptoms of low perfusion at rest; thus, it is important to consider the overall clinical picture in addition to the calculated cardiac index when deciding treatment options and prognosis.

When evaluating a patient with ADHF, it is useful to categorize the patient according to the estimation or measurement of left-sided filling pressures and cardiac output. The classification scheme shown in Fig. 19.1 is a simple and efficient way to clinically categorize patients and help guide appropriate treatment strategies.

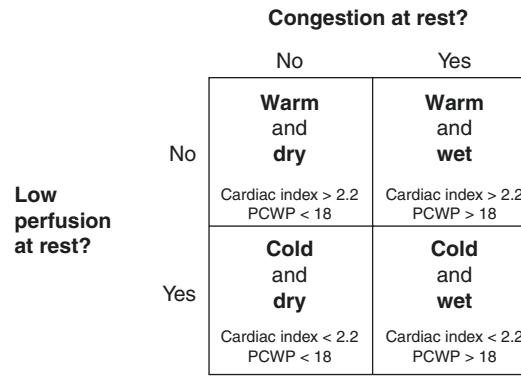

Fig. 19.1 Hemodynamic profiles in patients with left-sided heart failure

Vascular Resistance

Systemic vascular resistance (SVR) is measured as the difference between mean arterial pressure and right atrial pressure divided by cardiac output. Classically, in ADHF, SVR is high as a result of an increased level of vasoconstricting neurohormones such as norepinephrine, angiotension II, and endothelin. However, in the contemporary era in which treatment with agents that block the renin angiotensin aldosterone system (ACE inhibitors/angiotensin receptor blockers/angiotensin receptor blocker + neprilysin inhibitors) and beta blockers is common, the SVR can be normal or sometimes even low. Patients with right-sided heart failure and renal insufficiency are more likely to have normal or low SVR. Knowing the blood pressure and/or the SVR is important with respect to determining treatment options.

Pulmonary vascular resistance (PVR) is measured as the difference between mean pulmonary artery pressure and PCWP (left atrial pressure surrogate) divided by cardiac output. It is important to note that in some patients, in addition to passive pulmonary hypertension due to elevated left atrial pressure, there is an additional component of pulmonary arterial vasoconstriction, raising pulmonary vascular resistance and thus further raising pulmonary artery pressure (pulmonary arterial hypertension). Long-standing elevation of PCWP can also lead to pulmonary vascular remodeling. This component of pulmonary vascular resistance

cannot be reversed by acutely lowering PCWP or with the use of pulmonary vasodilators. Reversal of pulmonary vascular remodeling can be accomplished by long-term consistent lowering of left atrial pressure (e.g., correction of mitral stenosis, left ventricular assist device placement). Patients with an elevated PVR that cannot be reversed have a worse prognosis.

Hemodynamic Evaluation of Decompensated Heart Failure

There are many ways to evaluate hemodynamics in heart failure. The initial and most practical strategy is starting with the clinical history and the physical examination (H&P). Further important hemodynamic information can be gleaned from echocardiography. The most invasive and accurate way to assess hemodynamics is with right heart catheterization using a pulmonary artery catheter, which is reserved for special situations.

Clinical Assessment

The H&P, together with a chest X-ray and basic labs, provides the majority of the hemodynamic information needed to treat patients with acute decompensated heart failure (ADHF). The shortcomings of an H&P are important to acknowledge however, and some of these will be highlighted as we discuss each of the clinical cases at the end of the chapter.

Clinical Estimation of Filling Pressures

Using the H&P, experienced clinicians can estimate, with reasonable accuracy, the intracardiac filling pressures [12, 13]. Some of the important signs and symptoms of elevated filling pressures are outlined in Table 19.1. Symptoms of elevated right atrial pressure, depending on the degree and chronicity, include abdominal bloating and discomfort, early satiety, and RUQ pain that can mimic an abdominal etiology. Signs of elevated right atrial pressure include lower extremity edema, hepatomegaly, and, in advanced right heart failure, ascites. However, the most reliable sign of elevated right atrial pressure is elevation of the jugular venous pressure (JVP), and depending on the skill of the examiner, the right atrial pressure can be reliably assessed at the bedside in most heart failure patients. Indeed, patients with elevation of right atrial pressure may have no edema or ascites, and the only sign may be elevated jugular venous pressure. It is in these patients that congestion is often missed and the patient is incorrectly assumed to be euvolemic.

Table 19.1 Symptoms and signs of elevated intracardiac filling pressures

	↑ RA pressure	↑ PCWP
Symptoms	Leg swelling	Dyspnea at rest or on exertion
	Abdominal bloating	Orthopnea
	Early satiety	PND
	Nausea, anorexia	Positional cough
	RUQ pain	
Signs	Elevated JVP[a]	S_3gallop
	Ascites	+ Abdominojugular reflux
	Enlarged/tender liver	Rales[b]
	Lower extremity edema[c]	

[a]Most specific and sensitive sign of elevated RA pressure and may often be the only sign
[b]Rare in chronic heart failure
[c]Nonspecific and can be due to venous insufficiency, DVT, calcium channel blockers, etc.

Elevation of left atrial pressure/PCWP pressure leads to symptoms of exertional/resting dyspnea, dry cough (worse in the recumbent position), orthopnea, and paroxysmal nocturnal dyspnea. In fact, orthopnea and particularly paroxysmal nocturnal dyspnea are the most specific symptoms of elevated PCWP. The physical exam finding that is most specific for an elevated PCWP (in the absence of mitral stenosis) is an S3 gallop; however, it is not a sensitive finding as most patients with an elevated PCWP do not have an S3 gallop. One of the best clues that a heart failure patient has an elevated PCWP is elevation in the jugular venous pressure. This is because elevated right

Table 19.2 Signs and symptoms of low cardiac output

Symptoms	Fatigue
	Decreased memory/mentation
	Lightheadedness
Signs	Cool extremities
	Sleepy/obtunded
	Narrow pulse pressure
	Oliguria

atrial pressure is predictive of an elevated PCWP in most chronic heart failure patients (see section "Intracardiac Filling Pressures").

Clinical Estimation of Cardiac Output

Estimating cardiac output is more difficult at the bedside [12], but there are several clues to low cardiac output (see Table 19.2). General fatigue, impaired mentation, cool extremities, low urine output, and increased lactate level are useful clues. An objective measure is to calculate the "proportional pulse pressure" which is the systolic blood pressure minus the diastolic blood pressure divided by the systolic blood pressure. A proportional pulse pressure <25% suggests a cardiac index of <2.2 [11].

Echocardiography

The echocardiogram is an important tool in the assessment of heart failure. In patients presenting with a new diagnosis, it is essential in establishing the mechanism of heart failure (preserved versus reduced ejection fraction or valvular etiology; see Chap. 6). Performing a baseline echocardiogram is given a Class I (should be performed) recommendation in patients with a new diagnosis of heart failure according to the ACC/AHA guidelines [14]. For patients with an acute exacerbation of chronic heart failure, it is not always necessary to obtain an echocardiogram. This is particularly true when there is an obvious precipitant for the change in clinical status. When the patient is critically ill or the symptomatic decline is precipitous, the echocardiogram can exclude new structural abnormalities. This is given a IIa (reasonable to perform) recommendation by the ACC/AHA guidelines [14] and has been shown to provide reliable estimates of invasive hemodynamics in this setting [15].

Echo Assessment of Filling Pressures

The measured size of the inferior vena cava (IVC) and its changes with respiration is traditionally used to estimate right atrial pressure [16]. Using this method, there is an assumption that there is continuity between central veins and the right atrium, the same assumption used in interpreting the jugular venous pressure as a reflection of right atrial pressure. Patients with an IVC measuring ≤2.2 cm in diameter that collapses by 50% or more with a sniff are designated as having a low RA pressure (assigned a value of 3 mmHg for the purposes of calculations). Patients with a distended IVC that does not collapse with sniff are designated as having a high RA pressure (15 mmHg). Patients with intermediate findings are assigned an RA pressure of 8 mmHg [16]. An example of this technique is given in Case 3.

Echocardiographic estimation of left ventricular end-diastolic pressures is a continued area of active investigation. The ratio of early diastolic inflow velocity across the mitral valve (E) to the early peak velocity of the mitral valve annulus (E′) has been shown to have a reasonably good correlation with LVEDP [17, 18]. This technique is used in a semiquantitative fashion. An E:E′ ratio of <8 suggests a normal LVEDP. An E:E′ ratio of >15 suggests an LVEDP of greater than 15 [17]. The E:E′ ratio was shown to be less predictive among patients with advanced heart failure admitted to the ICU [19]. Research is underway to find more consistent and precise echocardiographic predictors of LVEDP.

Echo Estimation of Pulmonary Pressures

The most well-accepted means of estimating pulmonary pressures with echocardiography is to

calculate the pressure gradient across the tricuspid valve using the peak velocity of the tricuspid regurgitation jet [16]. Using a simplified Bernoulli equation, the pressure gradient between the right ventricle and the right atrium can be estimated as $P=4v^2$. This is also discussed in detail in Chap. 6, and an example will be reviewed in Case 3.

Echo Assessment of Cardiac Output

Stroke volume (and therefore cardiac output) can be estimated by echocardiography, although it requires several important assumptions be made [20]. The technique for making this estimation is as follows (see also Chap. 6).

The Doppler profile of flow through the LV outflow tract is a graph of velocity vs. time. Taking the integral of this curve gives a unit of distance. When this distance is multiplied by the surface area of the left ventricular outflow tract (LVOT), the resulting number (a volume) is the stroke volume. The LVOT area can be estimated by using 2D echo measurements of its diameter in long axis and then assuming that it is a circle. Although this method is not frequently employed, it should yield a reasonably accurate estimate of stroke volume and therefore of cardiac output (when multiplied by heart rate).

Right Heart Catheterization

Right heart catheterization remains the gold standard for measuring many of the hemodynamic parameters important in the management of heart failure. As noninvasive methodology has improved, however, there are now fewer situations in which this information is necessary [14]. Additionally, a large randomized study showed no benefit to the routine use of a pulmonary artery catheter to manage patients with ADHF in terms of the combined endpoint of mortality and days outside of hospital at 6 months [21].

Right heart catheterization should be considered in a patient who is refractory to initial therapy, whose volume status and cardiac filling pressures are unclear, who has clinically significant hypotension (typically SBP <80 mmHg) or worsening renal function during therapy, or who is being considered for cardiac transplant and needs assessment of the degree and reversibility of pulmonary hypertension and PVR [14, 22]. This latter issue will be discussed further in Case 3.

In each of Cases 1–3, pressures in the right atrium (RA) and pulmonary artery (PA) as well as PCWP as derived from right-heart catheterization are displayed. RA pressure and PCWP are commonly used clinically as descriptors of right and left ventricular "preload" respectively (see Chapter 1). The PA pressure is reported as systolic PA pressure/diastolic PA pressure (mean PA pressure). The cardiac index, as estimated using the Fick principle (see Chap. 4), is also shown. The cardiac index is calculated by dividing the cardiac output by the patient's body surface area. This factor in the size of the patient which is clearly important as normal cardiac output varies with size.

Implantable Hemodynamic Monitoring

There has been recent interest in the use of implantable hemodynamic monitoring systems in the management of heart failure. The CardioMEMS HF system (St. Jude Medical), approved by the FDA in 2016, is a small device implanted in a branch of the pulmonary artery allowing for continuous monitoring of PA pressure. A large randomized clinical trial using this device in patients with chronic NYHA III heart failure demonstrated a reduction in heart failure hospitalizations [23].

General Principles of Management

The majority of patients who present with ADHF are congested and have elevated filling pressures. The central goal of therapy is to decongest the patient and optimize filling pressures to normal or near normal levels. This is most effectively

achieved with the use of an intravenous loop diuretic. In instances of diuretic resistance, combining a loop diuretic with a thiazide, amiloride, and/or spironolactone can be highly effective. If this approach is not successful, as can be the case in advanced renal dysfunction, ultrafiltration may be considered [24, 25].

To further optimize hemodynamics, vasodilators which reduce filling pressures can be used in conjunction with diuretics. Vasodilators, in addition to lowering filling pressures, improve cardiac output by reducing afterload, decreasing functional mitral regurgitation (and thereby increasing forward cardiac output), and reducing wall stress [26–28]. The patients who benefit the most from vasodilators are those with elevated blood pressure and high SVR. It is important to note, however, that a patient with "normal" blood pressure may still have an elevated SVR and benefit from vasodilator therapy. Both "wet and warm" and "wet and cold" patients may be treated with vasodilators.

Intravenous vasodilators used in heart failure are nitroprusside, nitroglycerin, and nesiritide. The vasodilator of choice at our own institution is nitroprusside, which should be administered in an ICU setting with hemodynamic monitoring using a right heart catheter and, in most instances, a blood pressure cuff (as opposed to an arterial line). This is well tolerated and the incidence of cyanide or thiocyanate toxicity is extremely rare to nonexistent [29, 30]. A mean arterial pressure of approximately 65 mmHg is targeted, but this depends on the patient and may need to be higher if renovascular or coronary artery disease is present or suspected, or if the patient is chronically hypertensive with an altered renal autoregulatory threshold. Excessive or overexuberant vasodilation with decrease in blood pressure beyond the renal autoregulatory threshold often leads to decreased renal perfusion, worsening renal function, and should be avoided. Once patients have clinically and hemodynamically improved on intravenous vasodilators, they may be transitioned to an oral vasodilator regimen of either ACE inhibitors, the combination of hydralazine and isosorbide dinitrate, or a combination of all three agents [31].

Intotropic therapy (milrinone or dobutamine) should be reserved for low output states associated with hypotension and end-organ hypoperfusion [32]. The typical patient has advanced systolic dysfunction, a low proportional pulse pressure, cool extremities, and worsening renal function despite adequate filling pressure (need to rule out hypovolemia) and is unresponsive to or intolerant of intravenous vasodilators. These patients constitute no more than 5% of the total ADHF population. Inotropes can also be used as palliative therapy for end-stage heart failure or as a bridge to transplantation.

It is important to note that inotropes increase myocardial oxygen consumption by increasing heart rate and myocardial contractility and can precipitate atrial and ventricular arrhythmias as well as myocardial ischemia. In contrast to dobutamine, milrinone has a long half-life (2.5 h) and is renally excreted, and the dose should be adjusted for renal function. Also, given that milrinone is a more powerful vasodilator, hypotension is more common with this agent and therefore should be used with caution or even avoided when the systolic blood pressure is <90 mmHg. In the setting of background beta blocker therapy, dobutamine will be ineffective unless used in high doses, and milrinone is favored [33, 34]. In rare circumstances, vasopressors are used (dopamine, norepinephrine, vasopressin), when the patient is vasodilated with a low SVR and profound hypotension.

In patients who are managed on a telemetry floor without invasive monitoring, the goal of therapy is to normalize intravascular volume as reflected by relief of edema and normalization of the jugular venous pressure (<8 cmH_2O). When this is achieved, most patients will no longer have orthopnea or dyspnea. Signs of overdiuresis consist of orthostatic decrease in blood pressure and worsening renal function. A common clinical error is incorrectly assuming euvolemia has been achieved when edema has resolved yet unrecognized elevation of the jugular venous pressure persists. By the same token, one may have normalized the jugular venous pressure and achieved intravascular euvolemia but may still have residual edema due to low albumin, venous

insufficiency, or drug side effect (e.g., calcium channel blockers) and wrongly assumed to be intravascularly volume overloaded.

In patients managed with hemodynamic monitoring with a right heart catheter, vasodilator therapy (both intravenous and oral) and diuretics are "tailored" to certain hemodynamic goals. Typically a PCWP of ≤16 mmHg, an RA pressure of ≤8 mmHg, and an SVR of about 1000–1200 dyn are targeted. A common misconception that patients with dilated dysfunctional ventricles require higher filling pressures to maintain cardiac output based on the Starling curve has been dispelled by data showing that most of these patients can maintain and even improve cardiac output with normal or near normal PCWP [30, 35]. As far as RA pressure goals, patients with primarily RV failure may require a higher RA pressure than 8 mmHg to maintain cardiac output and renal perfusion. It has been shown that patients with very elevated RA pressure can have worsening renal function on the basis of renal venous congestion. By lowering RA pressure with diuretics and vasodilators, the kidney is "decongested" or decompressed and renal function often improves [36–38] (see Fig. 19.2).

The goal of cardiac index is usually >2.2, but one has to acknowledge that using the Fick equation, oxygen consumption is estimated and not measured and that up to a 20% variation in cardiac output can be seen [39]. Thus, targeting a specific number per se is simplistic, and the entire clinical picture needs to be considered (e.g., a patient with a cardiac index of 1.8 who with normal PCWP feels well may not need further intervention). Although cardiac output frequently improves, the cardiac output is not the primary target of therapy, rather the reduction of the filling pressures [40]. The general principles of management for the different presentations of heart failure are shown in Fig. 19.3.

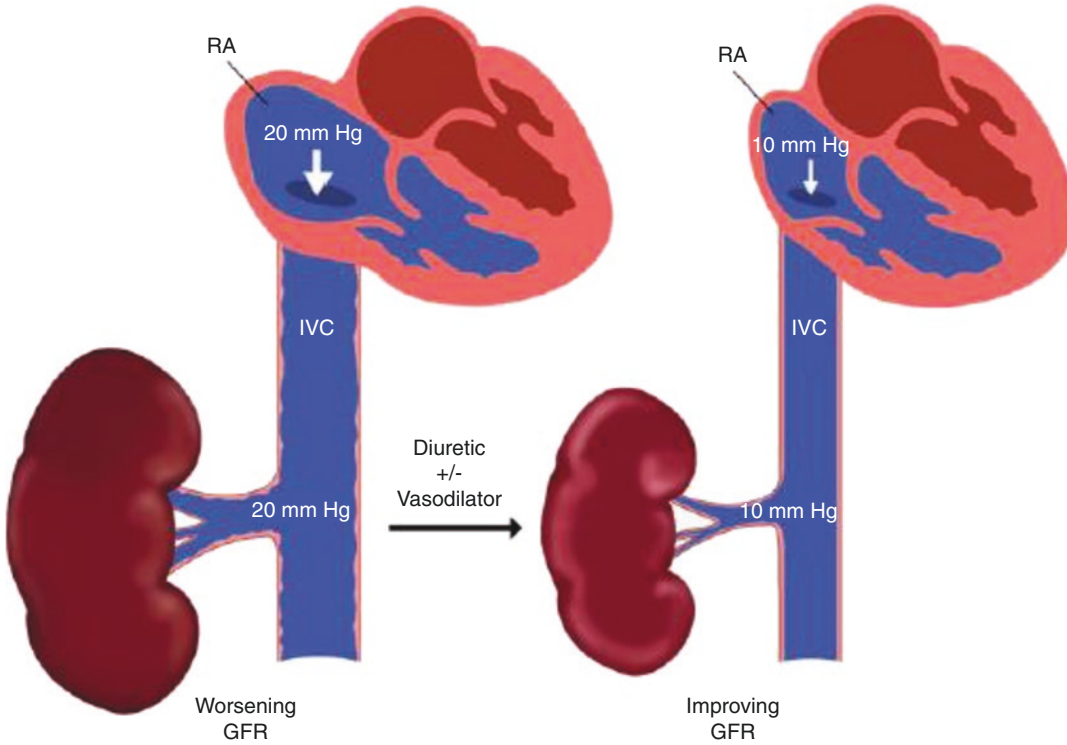

Fig. 19.2 Renal venous congestion: increased right atrial pressure leading to elevated pressure in the IVC and thus the renal vein (especially when coupled with low mean arterial pressure) can lead to worsening renal function by "congesting the kidney." Decreasing right atrial pressure and thus the renal venous pressure can lead to improved renal function

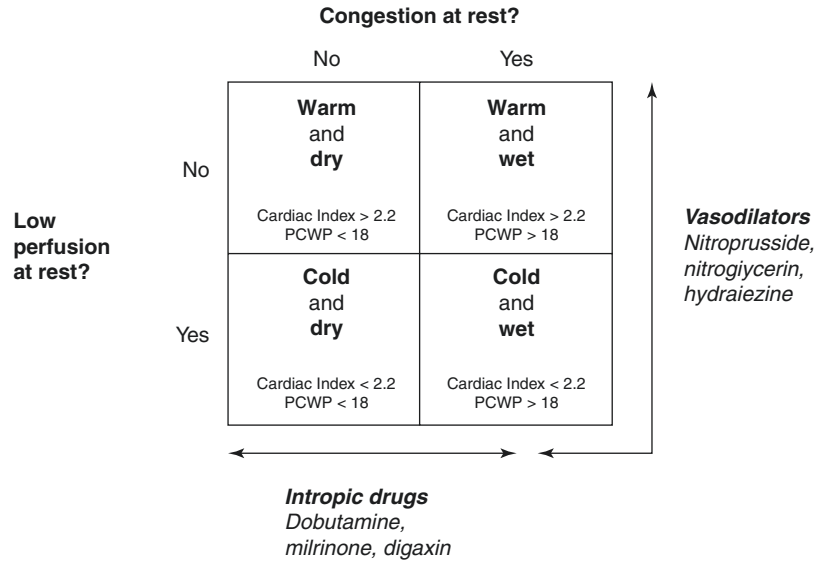

Fig. 19.3 Treatment paradigm in patients with left-sided heart failure

Clinical Presentations of Acute Heart Failure

Case 1

A 46-year-old male with a history of diabetes and hypertension presents with sudden onset of retrosternal chest pain. He is brought by emergency medical services to the hospital where he is found to have an elevated jugular venous pressure, bilateral rales, and edematous and well-perfused extremities. His electrocardiogram reveals ST segment elevation in the inferior leads (ECG leads II, III, and aVF). He is transferred to the cardiac catheterization laboratory but becomes dyspneic and hypoxic lying flat on the table. On examination, his HR is 90 bpm and BP measures 130/90 mmHg. His oxygen saturation is 93% on a high-flow oxygen mask.

A left heart catheterization is performed. The right coronary artery is found to be completely occluded, and the patient undergoes successful angioplasty and stenting to the vessel with good results. A pulmonary artery catheter is placed yielding the following hemodynamics:

RA	PA	PCWP	Cardiac index
12	38/25 (30)	24	3.2

Fig. 19.4 Case 1: left ventricular pressure tracing

A sample from his left heart catheterization is shown in Fig. 19.4. The LVEDP is elevated and correlates closely with the PCWP obtained with right heart catheterization. An echocardiogram is performed which demonstrates severe akinesis of

the inferior wall from base to apex. The overall left ventricular systolic function is described as mildly decreased. Right ventricular function is reported as normal.

Case 1: Hemodynamic Assessment

This is an example of so-called "warm and wet" heart failure (based clinically on his JVP, lower extremity edema and warm extremities, and hemodynamically on an elevated PCWP with a cardiac index in the normal range). Occlusion of the right coronary artery led to systolic and diastolic dysfunction of the left ventricle. This resulted in elevation of the left-sided filling pressures with pulmonary edema.

The orthopnea and hypoxia suggested an acute rise in PCWP. The relationship between PCWP and clinical signs of pulmonary congestion has been well characterized in patients with acute myocardial infarction. The onset of pulmonary congestion generally occurs at a PCWP between 18 and 20, and acute pulmonary edema generally correlates with a PCWP of greater than 30 [41]. These data have been challenged, however [42], and were collected prior to the use of reperfusion techniques such as fibrinolysis and primary percutaneous coronary intervention.

In this case, the importance of echocardiography was to confirm that the main problem was a left ventricular wall motion abnormality and not acute mitral regurgitation, which can be a mechanical complication of inferior myocardial infarction. Suspicion was low for this patient as such cases generally present with cardiogenic shock. However, a high index of suspicion is important. Another known complication of inferior myocardial infarction can be right ventricular infarction. This occurs in some patients when there is proximal occlusion of the right coronary artery but would generally be manifested by an elevated JVP and hypotension without pulmonary congestion. The right heart catheterization provided accurate measurement of cardiac output which has important prognostic implications [43].

In this case, the underlying cause of left ventricular dysfunction is acute coronary occlusion. This is best treated by promptly opening the culprit vessel (here with emergent PCI) in efforts to improve contractility by restoring flow to the compromised ischemic myocardium. Diuretic therapy was also provided to facilitate reduction of volume overload and clearance of pulmonary edema. This is generally considered to be a mainstay of the treatment of decompensated heart failure with increased RA pressure and PCWP. The patient was treated with intravenous furosemide with excellent response. After several days, he no longer required supplemental oxygen, and clinical and radiographic evidence of pulmonary congestion had improved.

Case 2

A 19-year-old G_1P_1 female presents to the emergency department with profound fatigue and right upper quadrant discomfort. Two weeks prior, she gave birth to a healthy baby boy via an uncomplicated vaginal delivery. Since the delivery, she has noticed gradual progression of tiredness to the point where she is no longer able to carry out basic activities of daily living and is short of breath at rest. There is no orthopnea or leg swelling but occasional paroxysmal nocturnal dyspnea. She complains of a dull aching discomfort in the right upper quadrant of her abdomen.

On examination, she is tachycardic with a HR of 120 bpm and BP of 106/88 mmHg. Her extremities are warm. The JVP is elevated to 8 cm above the sternal angle at 60°. The chest is clear to auscultation. In addition to loud first and second heart sounds, a prominent S3 is heard. There is right upper quadrant abdominal tenderness with no rebound tenderness or guarding. A chest X-ray is performed and shows an enlarged cardiac silhouette. An ECG shows sinus tachycardia with low voltages and a nonspecific ST abnormality. Labs are notable for elevated liver enzymes.

Echocardiography shows severe left ventricular dysfunction with an LVEF of 10%, moderate mitral regurgitation, and moderate right

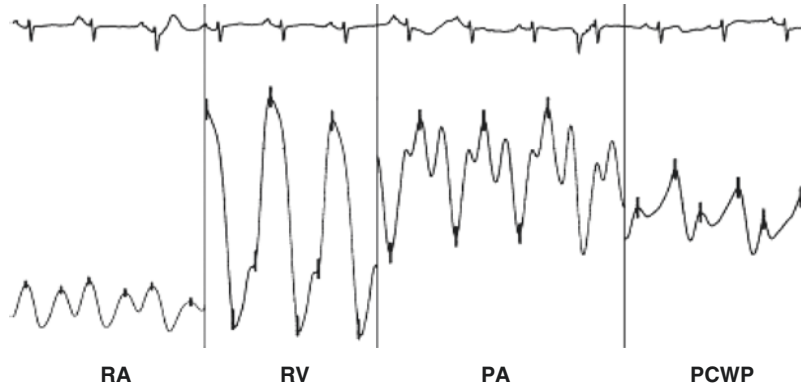

Fig. 19.5 Case 2 sample hemodynamic tracings: Pressures were recorded with the catheter positioned in the right atrium (RA), right ventricle (RV), and pulmonary artery (PA) as well as with pulmonary capillary "wedging" (PCWP). The following pressures were noted: RA mean pressure of 10 mmHg (normal, 0–8 mmHg); RV, pressure of 46/10 mmHg (normal 15–30/0–8 mmHg); PA, pressure of 46/30 mmHg (normal 15–30/4–12 mmHg); and PCWP, mean pressure of 32 mmHg (normal 1–10 mmHg)

ventricular dysfunction. She is given a presumptive diagnosis of a peripartum cardiomyopathy. She is admitted to a heart failure intensive care unit and a pulmonary artery catheterization is performed. Samples from the tracings are seen in Fig. 19.5. Note the somewhat exaggerated waveforms on the section of the tracing labeled pulmonary artery, a commonly encountered artifact.

Her reported hemodynamics are as follows:

RA	PA	PCWP	Cardiac index
10	46/30 (35)	32	2.0

Case 2: Hemodynamic Assessment

This is a case of a patient with so-called "cold and wet" heart failure. The cardiac index is reduced, and both the RA pressure and the PCWP are increased. When accompanied by findings of impaired end-organ function, this state would be termed cardiogenic shock (see Chap. 14). For this patient, there is no clinical evidence of a low perfusion state, such as hypotension, decreased level of consciousness, cool extremities, or renal failure.

The right upper quadrant pain and elevated liver enzymes reflect passive congestion of the liver. The physical examination disclosed an elevated JVP which corresponds to the elevated RA pressure. Note that there were no rales on chest examination and only minimal pulmonary edema on chest X-ray. These findings may have led the clinician to suspect that PCWP was not elevated. Unfortunately, such findings of elevated PCWP are frequently not present among chronic heart failure patients when the time-course of the decompensation is gradual. In such cases, pulmonary lymphatic drainage is enhanced and sufficient to prevent the accumulation of interstitial edema in the lungs. The finding of an S3 should definitely steer the clinician in the right direction, however. The low cardiac output was not recognized at the bedside due to the lack of cool extremities, altered mentation, and low urine output underscoring the insensitivity of these findings [12, 44]. However, if one calculates the proportional pulse pressure in this patient (106–88/106), a value of 17% is obtained suggesting a low cardiac index of <2.2 (see section "Clinical Estimation of Cardiac Output") [11].

The presence of a significant resting sinus tachycardia is ominous however. It suggests that the patient is compensating for a reduced stroke volume by increasing heart rate to maintain cardiac output.

The echocardiogram was crucial in confirming that severe biventricular dysfunction was the cause of the heart failure syndrome. The right heart catheterization was performed because of a concern that the patient was potentially unstable

and needed invasive monitoring. In this case, the right heart catheterization also shows mild elevation in pulmonary artery pressure. The calculated pulmonary vascular resistance (see Chap. 12 for more details) is normal at 1.0 Wood unit:

$$\text{PVR} = \frac{(\text{Mean PA pressure} - \text{PCWP})}{\text{Cardiac output}}$$

$$\text{PVR} = \frac{35-32}{3*} = 1$$

*Cardiac index of 2.0 corresponded to cardiac output of 3 L/min because of body surface area of 1.5 m^2.

This suggests that the patient's pulmonary hypertension is passive and there is no element of pulmonary vasoconstriction or pulmonary vascular remodeling.

The patient was treated with diuretic therapy, ACE inhibitors, and digoxin and observed carefully in an ICU setting. *Beta blockers should not be initiated in such a patient until they become euvolemic and hemodynamically stable*. She was discharged from the hospital 7 days later. Over the next 6 months, the patient was followed closely as an outpatient and had dramatic improvement in symptoms and complete resolution of LV dysfunction. She was advised to avoid pregnancy in the future due to the high risk of recurrent heart failure.

Case 3

A 58-year-old male is referred to a specialized heart failure clinic for evaluation. He has been followed for several years for a non-ischemic dilated cardiomyopathy with severe limitation of his exercise tolerance. His physician sends him for evaluation for the possible need for heart transplantation due to end-stage heart failure. When questioned, he reports that over the past 3 weeks, he has had worsened symptoms of weight gain and leg swelling. These symptoms began after he had started taking a nonsteroidal anti-inflammatory drug for arthritis. On examination, his HR is 90 bpm and his BP measures 98/70 mmHg. He is grossly edematous with pitting edema of both legs as well as scrotal edema. His JVP is elevated with prominent *v* waves. Auscultation of the chest reveals normal breath sounds with no rales or wheeze. On examination of the precordium, there is a loud pulmonic component of the second heart sound and an S3 gallop.

Echocardiography shows severe left ventricular dysfunction with an LVEF of 10% and moderate mitral regurgitation. Severe right ventricular dysfunction is also noted. The estimated RVSP by echocardiography is 88 mmHg (see Fig. 19.6).

The patient is admitted to the hospital, and a right heart catheterization is performed with the following results:

RA	PA	PCWP	Cardiac index
19	88/44 (59)	39	1.5

Case 3: Hemodynamic Assessment

This is another case of so-called "cold and wet" heart failure with reduced cardiac output and elevated right- and left-sided filling pressures. Note again that the patient was not hypoxic and auscultation of the chest did not reveal rales despite a very high PCWP. In contrast to the previous case, the pulmonary hypertension is severe with pulmonary artery pressures approaching the systemic pressures. The loud pulmonic component of S2 is consistent with these high pressures, although it is not a sensitive finding.

The calculated pulmonary vascular resistance is very high (see calculations below) suggesting that there is a pulmonary arterial component to the pulmonary hypertension that would not be immediately reversed if the PCWP was lowered.

$$\text{PVR} = \frac{(\text{Mean PA pressure} - \text{PCWP})}{\text{Cardiac output}}$$

$$\text{PVR} = \frac{59-39}{2.5} = 8 \text{ Wood units}$$

Note how closely the PA pressure was estimated by the transthoracic echocardiogram. Studying the parasternal short-axis images from the echocardiogram also gives us some idea of the relative left- and right-sided intracardiac pressures (Fig. 19.7). The flattened configuration of the interventricular septum during both systole

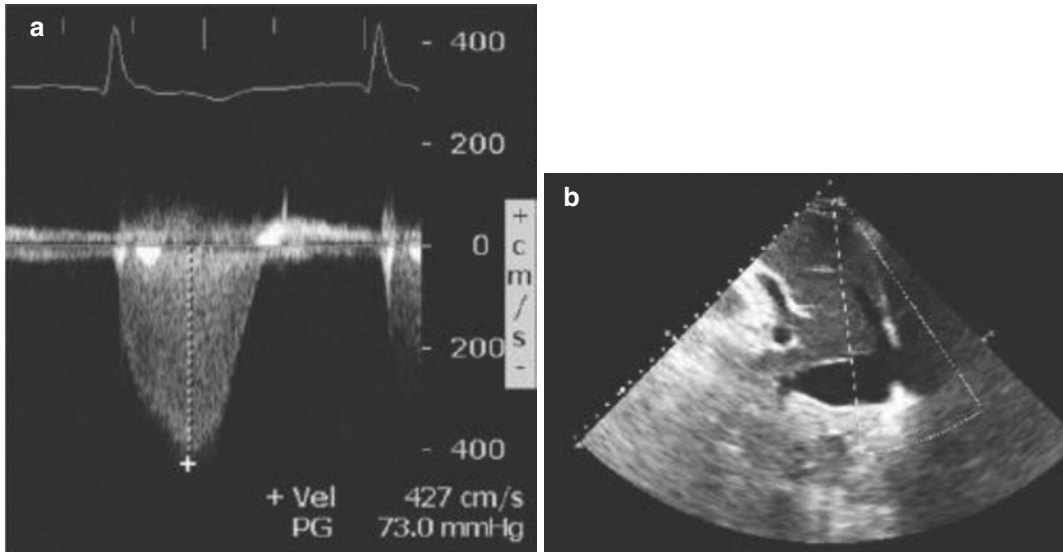

Fig. 19.6 Case 3: estimation of pulmonary artery systolic pressure by echocardiography. Peak velocity of the tricuspid regurgitation jet is 4.27 m/s (**a**) – this suggests a gradient from the RV to the RA of ~73 mmHg. [RV to RA gradient = $4v^2 = 4 \times (4.27)^2 = 72.9$ mmHg. The IVC is dilated (**b**) with a diameter of 2.8 cm and less than 50% variation with respiration – these findings suggest an RA pressure of 15 mmHg. Estimated peak pulmonary artery pressure is 88 mmHg (assuming no pulmonary valve stenosis) (73 + 15 = 88)

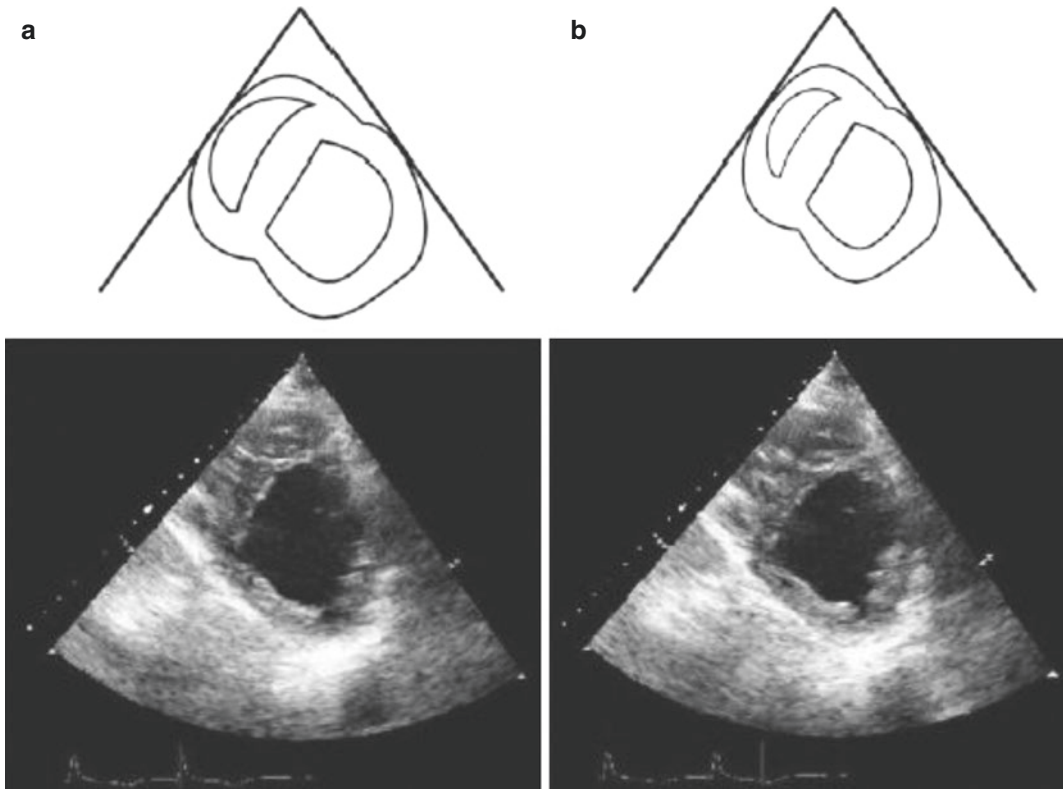

Fig. 19.7 Case 3: parasternal short-axis echo images showing pronounced flattening of the interventricular septum during diastole (**a**) which is still present during systole (**b**). This produces a "D-shaped appearance" of the left ventricle as emphasized in the cartoon above. Severe left ventricular dysfunction is suggested by the minimal change in area of the left ventricular cavity

and diastole suggests that the pressure in the right ventricle (and hence the pulmonary artery) is very high during both systole and diastole.

The patient was treated with inotropic therapy using milrinone, as well as a continuous infusion of furosemide. He was felt to have advanced heart failure, but his high pulmonary vascular resistance precluded heart transplantation because of the risk that the transplanted heart would develop acute right ventricular failure. He underwent placement of a left ventricular assist device which functions as an additional mechanical pump that reroutes blood from the left ventricle into the aorta. With this intervention, he had a dramatic improvement in symptoms and exercise tolerance as well as a marked reduction in PCWP and pulmonary artery pressure.

Pearls of Assessment

- The history and physical examination provide the majority of the hemodynamic information required to manage acute decompensated heart failure.
- No single symptom or sign is perfectly sensitive or specific for the diagnosis of acute decompensated heart failure.
- The most reliable sign of elevated right atrial pressure is elevation of the jugular venous pressure.
- Paroxysmal nocturnal dyspnea is a specific symptom for elevated PCWP.
- Transthoracic echocardiography is an important means of establishing the mechanism of newly diagnosed heart failure and of excluding new structural problems as the trigger for heart failure exacerbation.
- Echocardiography is not needed in routine heart failure exacerbations when a cause for decompensation is clear.
- Need for right heart catheterization is being obviated by noninvasive means of estimating hemodynamic parameters in most situations.
- Right heart catheterization in acute decompensated heart failure is indicated when volume status and cardiac filling pressures are unclear and clinically significant hypotension or worsening renal function during therapy occurs and for the evaluation of pulmonary vascular resistance.

Review Questions

1. A patient with known chronic systolic heart failure is admitted with acute decompensated heart failure. The patient has orthopnea and paroxysmal nocturnal dyspnea. On exam, the jugular venous pressure (JVP) is elevated and estimated to be 10 cm above the sternal angle while the patient is seated upright. Auscultation reveals an S3 gallop. Which of the following suggests an elevated pulmonary capillary wedge pressure (PCWP)?
   A. Orthopnea
   B. S3 gallop
   C. Elevated JVP
   D. All of the above
   Answer D
   Orthopnea and paroxysmal nocturnal dyspnea are the most specific symptoms for elevated PCWP. Although an S3 gallop is not sensitive, it is the most specific sign of left ventricular filling pressure. Elevated jugular venous pressure, although directly estimates right atrial pressure, is a surrogate for elevated PCWP in the vast majority of cases.
2. A patient admitted with decompensated heart failure undergoes right heart catheterization. The right atrial pressure is 5 mmHg, the pulmonary capillary wedge pressure is 10 mmHg, and the cardiac output is 4.0 L/min with cardiac index 1.9 L/min/m^2.
   This is an example of:
   A. Warm and wet heart failure
   B. Warm and dry heart failure
   C. Cold and wet heart failure
   D. Cold and dry heart failure
   Answer D
   The cardiac output of 4 L/min is close to normal. However, this patient has a large body surface area, and his calculated cardiac index is low. The PCWP and RA pressure are both in the normal range.

3. A 72-year-old male presents to the emergency department with a 2-week history of progressive shortness of breath with orthopnea and paroxysmal nocturnal dyspnea. On exam, he has peripheral edema and an elevated JVP at 12 cm above the sternal angle while seated upright. A prominent third heart sound is heard. The patient has inspiratory rales to the mid lung zones bilaterally. A chest X-ray confirms the presence of pulmonary congestion with vascular redistribution, Kerley B lines, and small bilateral pleural effusions.

   The most appropriate next study to assess this patient's etiology of heart failure and hemodynamics is:

   A. 2D echocardiogram with Doppler
   B. Right heart catheterization
   C. Computed tomography with IV contrast
   D. Magnetic resonance imaging

   Answer A

   Echocardiography is a noninvasive, readily available and relatively inexpensive tool for evaluation of left ventricular function, valvular disease, and hemodynamics. It is recommended as a first-line investigation for patients with a new diagnosis of heart failure.

4. The following are all appropriate indications for use of a pulmonary arterial catheter in heart failure except:

   A. Distinction of pulmonary edema related to heart failure from other causes of hypoxia in a critically ill patient in the intensive care unit
   B. Assessment of a patient in shock when intracardiac filling pressures cannot be adequately estimated by noninvasive means
   C. Monitoring of response to beta blocker therapy on routine annual follow-up
   D. Measurement of pulmonary pressures and calculation of pulmonary vascular resistance prior to planned heart transplantation

   Answer C

   For reasons discussed in the section on hemodynamic assessment, the use of pulmonary artery catheters in heart failure should be limited to certain scenarios such as those outlined in answers A, B, and D.

5. A patient admitted with decompensated heart failure undergoes right heart catheterization. The right atrial pressure is 10 mmHg, and the pulmonary arterial pressures are 59/32 mmHg with a mean of 40 mmHg. The pulmonary capillary wedge pressure is 34 mmHg, and the cardiac output is 4.0 L/min.

   The pulmonary pressure in this case could be described as:

   A. Normal – no evidence of pulmonary hypertension
   B. Elevated on the basis of pulmonary venous hypertension
   C. Elevated on the basis of pulmonary arterial hypertension
   D. Representing a mixture of pulmonary venous and pulmonary arterial hypertension

   Answer B

   A pulmonary pressure in this range is clearly abnormal. Determining the extent to which these pressures are elevated due to elevated left-sided pressures alone hinges on the calculation of the pulmonary vascular resistance. The pulmonary vascular resistance calculates out to be 1.5 Wood units, which is within the normal range. This suggests that if the LVEDP could be brought down to normal (with diuresis for example), the pulmonary pressures would become normal. This is the definition of pulmonary venous hypertension.

References

1. Benjamin EJ, Blaha MH, Chiuve SE, et al. Heart disease and stroke statistics – 2017 update: a report from the American Heart Association. Circulation. 2017;135(10):e146–603.
2. Kupari M, Lindroos M, Iivanainen AM, et al. Congestive heart failure in old age: prevalence, mechanisms and 4–year prognosis in the Helsinki Ageing Study. J Intern Med. 1997;241:387–94.
3. Owan TE, Hodge DO, Herges RM, et al. Trends in prevalence and outcome of heart failure with preserved ejection fraction. N Engl J Med. 2006;355:251–9.
4. Ponikowski P, Voors AA, Anker SD, et al. 2016 ESC guidelines for the diagnosis and treatment of acute and chronic heart failure: the task force for the

diagnosis and treatment of acute heart failure of the European Society of Cardiology (ESC). European Heart J. 2016;37:2129–200.
5. Fonarow GC, Adams KF, Abraham WT, et al. Risk stratification for in-hospital mortality in acutely decompensated heart failure. JAMA. 2005;293:572–80.
6. Bergethon KE, Ju C, DeVore AD, et al. Trends in 30-day readmission rates for patients hospitalized with heart failure: findings from the GWTG-HF registry. Circ Heart Fail. 2016;9(6):e002594.
7. Drazner MH, Hamilton MA, Fonarow GC, et al. Relationship between right and left-sided filling pressures in 1000 patients with advanced heart failure. J Heart Lung Transplant. 1999;18:1126–32.
8. Drazner MH, Prasad A, Ayers C, et al. The relationship of right- and left-sided filling pressures in patients with heart failure and preserved ejection fraction. Circ Heart Fail. 2010;3(2):202–6.
9. Campbell P, Drazner MH, Kato M, et al. Mismatch if right- and left-sided filling pressures in chronic heart failure. J Card Fail. 2011;17(7):561–8.
10. Drazner MH, Brown RN, Kaiser PA, et al. Relationship of right- and left-sided filling pressures in patients with advanced heart failure: a 14-year multi-institutional analysis. J Heart Lung Transplant. 2012;31(1):67–72.
11. Stevenson LW, Perloff JK. The limited reliability of physical signs for estimating hemodynamics in chronic heart failure. JAMA. 1989;261:884–8.
12. Drazner MH, Hellkamp AS, Leier CV, et al. Value of clinician assessment of hemodynamics in advanced heart failure: the ESCAPE trial. Circ Heart Fail. 2008;1:170–7.
13. From AM, Lam CS, Pitta SR, et al. Bedside assessment of cardiac hemodynamics: the impact of noninvasive testing and examiner experience. Am J Med. 2011;124(11):1051–7.
14. Yancy CW, Jessup M, Bozkurt B, et al. 2013 ACCF/AHA guideline for the management of heart failure: a report of the American College of Cardiology Foundation/American Heart Association Task Force on Practice Guidelines. JACC. 2013;62(16):e147–239.
15. Nagueh SF, Bhatt R, Vivo RP, Krim SR, Sarvari SI, Russell K, Edvardsen T, Smiseth OA, Estep JD. Echocardiographic evaluation of hemodynamics in patients with decompensated systolic heart failure. Circ Cardiovasc Imaging. 2011;4(3):220–7.
16. Rudski LG, Wyman WL, Afilalo J, Hua L, Handschumacher MD, Chandrasekaran K, Solomon SD, Louie EK, Schiller NB. Guidelines for the echocardiographic assessment of the right heart in adults: a report from the American Society of Echocardiography. J Am Soc Echocardiogr. 2010;23:685–713.
17. Ommen SR, Nishimura RA, Appleton CP, Miller FA, Oh JK, Redfield MM, Tajik AJ. Clinical utility of Doppler echocardiography and tissue Doppler imaging in the estimation of left ventricular filling pressures: a comparative simultaneous Doppler-catheterization study. Circulation. 2000;102:1788–94.
18. Andersen OS, Smiseth OA, Dokainish H, et al. Estimating left ventricular filling pressure by echocardiography. JACC. 2017;69(15):1937–48.
19. Mullens W, Borowski AG, Curtin RJ, Thomas JD, Tang WH. Tissue Doppler imaging in the estimation of intracardiac filling pressures in decompensated patients with advanced systolic heart failure. Circulation. 2009;119:62–70.
20. Armstron WF, Ryan T, editors. Feigenbaum's echocardiography. 7th ed. Philadelphia: Lippincott Williams & Wilkins; 2009.
21. Binanay C, Califf RM, Hasselblad V, O'Connor CM, Shah MR, Sopko G, et al. Evaluation study of congestive heart failure and pulmonary artery catheterization effectiveness: the ESCAPE trial. JAMA. 2005;294(13):1625–33.
22. Lindenfeld J, Albert NM, Bochmen JP, et al. HFSA 2010 comprehensive heart failure practice guideline. J Card Fail. 2010;16:e1–194.
23. Adamson PB, Abraham WT, Bourge RC, et al. Wireless pulmonary artery haemodynamic monitoring in chronic heart failure: a randomized controlled trial. Lancet. 2011;377:658–66.
24. Liang KV, Hiniker AR, Williams AW, et al. Use of a novel ultrafiltration device as a treatment strategy for diuretic resistant, refractory heart failure: initial clinical experience in a single center. J Cardiol Fail. 1996;12(9):707–14.
25. Bart BA, Goldsmith SR, Lee KL, et al. Ultrafiltration in decompensated heart failure with cardiorenal syndrome. N Engl J Med. 2012;367:2296–304.
26. Stevenson L, Belili D, Grover-McKay M, et al. Effects of afterload reduction (diuretics and vasodilators) on left ventricular volume and mitral regurgitation in severe congestive heart failure secondary to ischemic or idiopathic dilated cardiomyopathy. Am J Cardiol. 1987;60:654–8.
27. Rosario LB, Stevenson LW, Soloman SD, et al. The mechanism of decrease in dynamic mitral regurgitation during heart failure treatment: importance of reduction in the regurgitant orifice size. J Am Coll Cardiol. 1998;32:1819–24.
28. Palardy M, Stevenson LW, Tasissa G, et al. Reduction in mitral regurgitation during therapy guided by measured filling pressures in the ESCAPE trial. Circ Heart Fail. 2009;2:181–8.
29. Mullens W, Abrahams Z, Francis GS, et al. Sodium nitroprusside for advanced low-output heart failure. J Am Coll Cardiol. 2008;52(3):200–7.
30. Opasich C, Cioffi G, Gualco A. Nitroprusside in decompensated heart failure: what should a clinician really know? Curr Heart Fail Rep. 2009;6(3):182–90.
31. Mullens W, Abrahams Z, Francis GS, et al. Usefulness of isosorbide dinitrate and hydralazine as add-on therapy in patients discharged for advanced decompensated heart failure. Am J Cardiol. 2009;103:113–9.
32. Cuffe MS, Calif RM, Adams KF Jr, et al. Short-term intravenous milrinone for acute exacerbation of

chronic heart failure: a randomized controlled trial. JAMA. 2002;287:1541–7.
33. Jennings DL, Thompson ML. Use of combination therapy with a beta-blocker and milrinone in patients with advanced heart failure. Ann Pharmacother. 2009;43(11):172–1876.
34. Tsvetkova T, Feguson D, Abraham WT, et al. Comparative hemodynamic effects of milrinone and dobutamine in heart failure patients treated chronically with carvedilol. J Card Fail. 1998; 4(Suppl 1):36.
35. Stevenson LW, Tillisch JH. Maintenance of cardiac output with normal filling pressures in patients with dilated heart failure. Circulation. 1986;74: 1303–8.
36. Mullens W, Abrahams Z, Francis GS, et al. Importance of venous congestion for worsening of renal function in advanced decompensated heart failure. J Am Coll Cardiol. 2009;53:589–96.
37. Winton FR. The influence of venous pressure on the isolated mammalian kidney. J Physiol. 1931;72(1):49–61.
38. Firth JD, Raine AE, Ledingham JG. Raised venous pressure: a direct cause of renal sodium retention in oedema? Lancet. 1988;1(8593):1033–5.
39. Kendrick AH, West J, Papouchado M, et al. Direct Fick cardiac output: are assumed values of oxygen consumption acceptable? Eur Heart J. 1988;9:337–42.
40. Steimle AE, Stevenson LW, Chelimsky-Fallick C, et al. Sustained hemodynamic efficacy of therapy tailored to reduce filling pressures in survivors with advanced heart failure. Circulation. 1997;96:1165–72.
41. McHugh TJ, Forrester JS, Adler L, Zion D, Swan HJC. Pulmonary vascular congestion in acute myocardial infarction: hemodynamic and radiologic correlations. Ann Intern Med. 1972;76:29–33.
42. Bergstra A, Svilaas T, van Veldhuisen DJ, van den Heuvel AF, van der Horst IC, Zijlstra F. Haemodynamic patterns in ST-elevation myocardial infarction: incidence and correlates of elevated filling pressures. Neth Heart J. 2007;15(3):95–9.
43. Forrester JS, Diamond G, Chatterjee K, Swan HJC. Medical therapy of acute myocardial infarction by application of hemodynamic subsets. N Engl J Med. 1976;295:1361.
44. Menon V, White H, LeJemtel T, Webb JG, Sleeper LA, Hochman JS. The clinical profile of patients with suspected cardiogenic shock due to predominant left ventricular failure: a report from the SHOCK trial registry. J Am Coll Cardiol. 2000;36:1071–6.

Intracardiac Shunts

20

Olcay Aksoy, Alper Ozkan, and E. Murat Tuzcu

Introduction and Epidemiology of the Disease State

In the normal circulation, deoxygenated blood comes into the right heart and passes through the pulmonary circulation to become oxygenated. Then oxygenated blood goes through the left heart to the systemic circulation. An abnormal communication between two heart chambers resulting in an intracardiac (IC) shunt may take place from systemic to pulmonary circulation (left to right) or from pulmonary to systemic circulation (right to left) or may be bidirectional. In this chapter, we review the evaluation and treatment of intracardiac shunts.

While congenital heart diseases are the most common causes of intracardiac shunts, acquired pathologies may also result in IC shunts. Left to right (L → R) shunt in postmyocardial infarction VSD and right to left (R → L) shunt in platypnea-orthodeoxia syndrome (POS) are two examples of acquired IC shunts.

O. Aksoy (✉)
David Geffen School of Medicine, UCLA Medical Center, Los Angeles, CA, USA
e-mail: oaksoy@mednet.ucla.edu

A. Ozkan
Acibadem University, Istanbul, Turkey
e-mail: alper.ozkan@acibadem.edu.tr

E. M. Tuzcu
Heart and Vascular Institute, Cleveland Clinic, Cleveland, OH, USA
e-mail: tuzcue@ccf.org

Detection, localization, and quantification of intracardiac shunts are clinically important in the management of IC shunts and can be performed using noninvasive and invasive techniques. Noninvasive techniques include transthoracic or transesophageal echocardiography, cardiovascular magnetic resonance (CMR), and radionuclide tests. Invasive techniques apply catheter insertion and selective blood sampling of oxygen saturation to diagnose and quantify IC shunts.

Noninvasive Assessment of Intracardiac Shunts

Transthoracic echocardiography (TTE) is a safe, reproducible, and relatively inexpensive method that is widely used in the assessment of intracardiac shunts. Transesophageal echocardiography (TEE) is an excellent tool for defining the anatomy of IC shunts and provides additional information; however, its incremental value in shunt assessment is limited. Magnetic resonance imaging (MRI) allows precise measurement of cardiac volumes and flows yielding accurate IC shunt calculations.

Echocardiographic Assessment of Intracardiac Shunts

Echocardiography has been the primary diagnostic tool and plays an essential role in providing

A. T. Askari, A. W. Messerli (eds.), *Cardiovascular Hemodynamics*, Contemporary Cardiology,
https://doi.org/10.1007/978-3-030-19131-3_20

morphologic assessment and hemodynamic evaluation in congenital heart disease. TTE permits comprehensive anatomic information regarding the location and the size of the defect. TEE may be needed as a complementary imaging tool particularly in lesions located posteriorly and in patients who will undergo percutaneous or surgical intervention. Color flow Doppler plays a critical role in the detection and localization of IC shunts as well as in determining the direction of shunting—though the sensitivity of echocardiographic evaluation with color Doppler or 2D imaging only is limited. The use of contrast echocardiography with agitated saline together with Valsalva maneuver will increase right atrial pressure and may allow for increased sensitivity when diagnosing intracardiac shunting, when a patent foramen ovale is present. If microbubbles from agitated saline injected from a peripheral vein is seen to enter the left heart chambers within 3 beats; this is consistent with an intracardiac communication between right and left chambers of the heart. If there is delayed appearance of microbubbles in the left chambers (>5 beats), this is associated with intrapulmonary shunting. TEE and transcranial Dopplers with microbubble administration have also enhanced the detection of shunts not otherwise visualized by TTE techniques [1].

In addition to the detection of shunts, echocardiographic techniques can also provide quantification of the degree of shunting. Pulmonary blood flow (Q_p) to systemic blood flow (Q_s) ratio can be calculated using Doppler and 2D echocardiography.

Comprehensive evaluation of a patient with IC shunt is not limited to the detection and quantification of the shunt flow. It also involves the evaluation of the associated abnormalities and secondary findings. For example, in a patient with ASD, the evaluation of right atrial and right ventricular size and septal motion and for other associated anomalies such as anomalous pulmonary venos return is as important as the quantification of the defect.

The hemodynamic significance of intracardiac shunts can be evaluated based on volumetric flow calculations using cross-sectional area (CSA) and velocity time integral (VTI) across the outflow tracts of both ventricles. Pulmonary flow (Q_p) equals systemic flow (Q_s) in the absence of shunt. Formulas are used to calculate volumetric flow with two important assumptions. The first assumption is blood flow has a uniform pattern and constant velocity. The second assumption is that the shape of the outflow tract is circular.

Flow formula is as follows:

$$Q = \mathrm{CSA} \times \mathrm{VTI}$$

(Q = flow, CSA = cross-sectional area, VTI = velocity time integral)

CSA is calculated based on circular shape assumption:

$$\mathrm{CSA} = \pi \times r^2$$

(π = pi constant, which is 3.14; r = radius of the outflow tract)

For the pulmonary flow, the formulas are as follows:

$$Q_p = \mathrm{CSA}_{\mathrm{RVOT}} \times \mathrm{VTI}_{\mathrm{RVOT}}$$

$$Q_p = \pi \times \left(\frac{\text{RVOT Diameter}}{2} \right)^2 \times \mathrm{VTI}_{\mathrm{RVOT}}$$

$$Q_p = \pi \times \frac{\left(\text{RVOT Diameter}\right)^2}{4} \times \mathrm{VTI}_{\mathrm{RVOT}} \quad \text{with} \left(\frac{\pi}{4} = 0.785 \right)$$

$$Q_p = 0.785 \times \left(\text{RVOT Diameter}\right)^2 \times \mathrm{VTI}_{\mathrm{RVOT}}$$

For the systemic flow, the formula would be simplified as follows:

$$Q_s = 0.785 \times \left(\text{LVOT Diameter}\right)^2 \times \text{VTI}_{\text{LVOT}}$$

After simplification, the formula of Q_p/Q_s is

$$\frac{Q_p}{Q_s} = \frac{\left(\text{RVOT Diameter}\right)^2 \times \text{VTI}_{\text{RVOT}}}{\left(\text{LVOT Diameter}\right)^2 \times \text{VTI}_{\text{LVOT}}}$$

See the example in Fig. 20.1. (Q_p = pulmonary flow; Q_s = systemic flow; RVOT = right ventricle outflow tract; LVOT = left ventricle outflow tract).

Potential Source of Errors and Pitfalls

Precise measurements of LVOT and RVOT diameters require appropriate site selection. LVOT diameter should be measured at the level of the aortic annulus during systole in parasternal long axis view of the LV, whereas RVOT is measured at the level of pulmonary valve annulus in parasternal short axis view (see Fig. 20.1). It is important to note that CSA is calculated as if it is a perfect circle even though the shape of the outflow tracts change throughout the cardiac cycle as these are dynamic structures. Positioning of

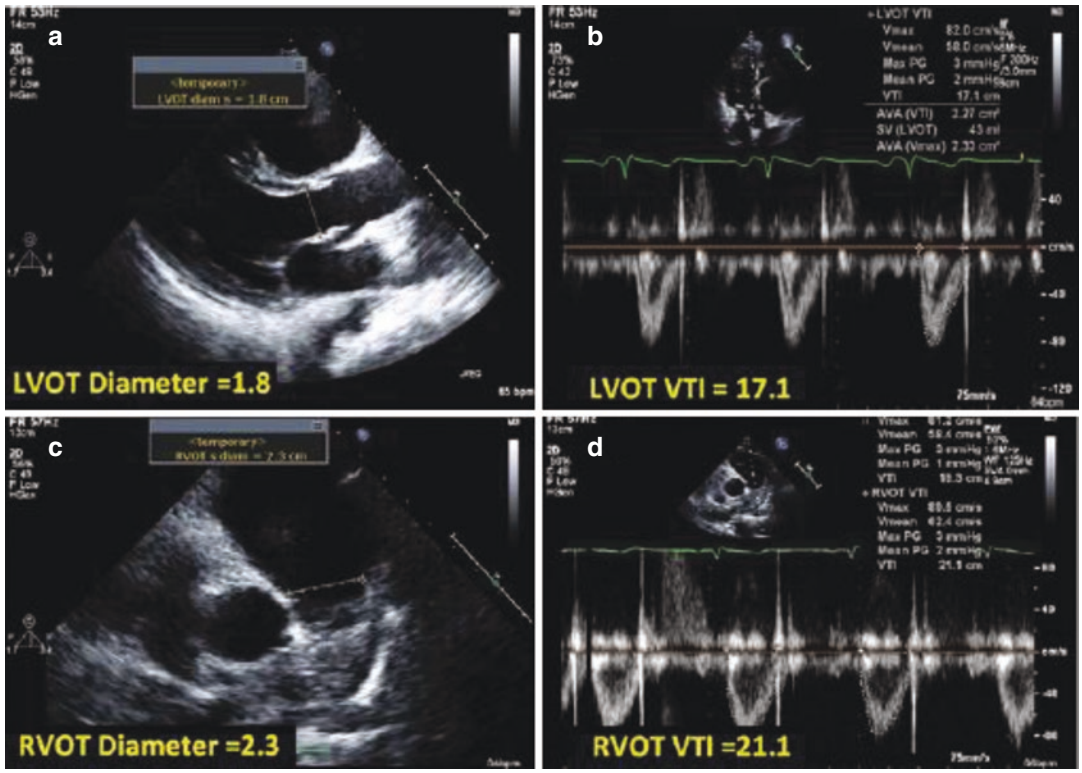

Fig. 20.1 Quantification of IC shunts using transthoracic echocardiography. Systemic stroke volume or flow (Q_s) can be calculated by using CSA of LVOT, which is derived by LVOT diameter at the end of systole (**a**), and LVOT VTI (**b**) pulmonary stroke volume or flow (Q_p) can be measured using CSA of RVOT, which is derived by RVOT diameter at the end of systole (**c**) and RVOT VTI (**d**)

$$\frac{Q_p}{Q_s} = \frac{\text{CSA RVOT} \times \text{VTI RVOT}}{\text{CSA LVOT} \times \text{VTI LVOT}}, \quad \frac{Q_p}{Q_s} = \frac{3.14 \times (2.3/2)^2 \times 21.1}{3.14 \times (1.8/2)^2 \times 17.1}, \quad \frac{Q_p}{Q_s} = \frac{87.6}{43.5} = 2.$$

CSA cross-sectional area, *LVOT* left ventricle outflow tract, *VTI* velocity time integral, and *RVOT* right ventricle outflow tract

sample volume of pulsed wave Doppler signals should be obtained at the levels where RVOT and LVOT diameters were measured. Optimal Doppler signals must be acquired for accurate velocities and VTI. Respiratory variations can affect the position of PW sample location or Doppler velocities.

Many other pitfalls such as arrhythmia, heart rate variability, and presence of valvular heart disease in particular aortic and mitral regurgitation may also complicate shunt assessment. A small error in the diameter measurement is magnified in the calculation of cross-sectional area translating into large errors in flow calculations.

Assessment of Intracardiac Shunt with Cardiovascular Magnetic Resonance

Although echocardiography provides the clinician with an initial screening tool for the assessment shunts, cardiovascular magnetic resonance (CMR) has become a complementary tool for the noninvasive evaluation of the size and morphologic features of the congenital cardiac defects. MRI provides not only the exact visualization of cardiac anatomy but also allows accurate and reproducible quantification of IC shunts. Studies have demonstrated that MRI measurements of IC shunts correlate with those obtained by invasive methods in children [2–5] as well as in adults [5] using different MRI applications [6, 7]. Volumetric MRI and phase contrast cine MRI are the commonly used protocols for the assessment of IC shunt. With these techniques, ventricular stroke volume can be calculated for each ventricle with short axis and/or four chamber views (Fig. 20.2). In the absence of significant valvular regurgitation or ventricular septal defect (VSD), the ratio of the RV to LV stroke volumes yields the Q_p/Q_s ratio. Velocity-encoded (VENC) cine MR is another application for the measurement of IC shunt [6]. Each voxel has its own velocity across the vessel in the gray scale images. Flow can be estimated using the cross-sectional area of the vessel and integrated into the velocity of the blood at the same level. Magnitude images provide an accurate measurement for the cross-sectional areas of the vessel, and phase cine MR images offer reliable quantification for mean flow velocity [3] (Fig. 20.3a, b).

MRI has many advantages when compared to other noninvasive imaging modalities. Unlike echocardiography, MR allows visualization of vascular structures in addition to cardiac chambers. It is possible to make reliable and reproducible measurements of blood flow velocities and assess stenotic and regurgitant valvular lesions by CMR. These can be accomplished with much less subjectivity compared with echocardiography. In contrast to radionuclide technique or cardiac computed tomography (CT), MR does not have any ionizing radiation. In addition to the accurate quantification of IC shunts, MRI is a promising technique for the guidance of transcatheter closure of congenital heart defects [8]. After the closure of such defects, MRI can clearly show the anatomic location of the device and can quantify its effectiveness [9–11]. However, MRI requires more patient compliance, and a comprehensive MR exam takes time and is relatively expensive. Many stents, devices, and vascular filters are MR compatible. Whereas implantable cardiac devices have previously been considered as absolute contraindications, MRI-conditional and MRI-safe pacemakers are now available.

Other Noninvasive Imaging Modalities

Radionuclide techniques can also be used for the assessment of IC shunt. Radionuclide scintigraphy can be considered as an alternative noninvasive method for the quantification of IC shunt and evaluation of LV function in patients with post-MI VSR [12].

Cardiac CT can provide comprehensive anatomic information in the assessment of congenital cardiac defects. Although cine CT makes some hemodynamic measurements possible such as cardiac output, quantification of IC shunts with CT has not been well established.

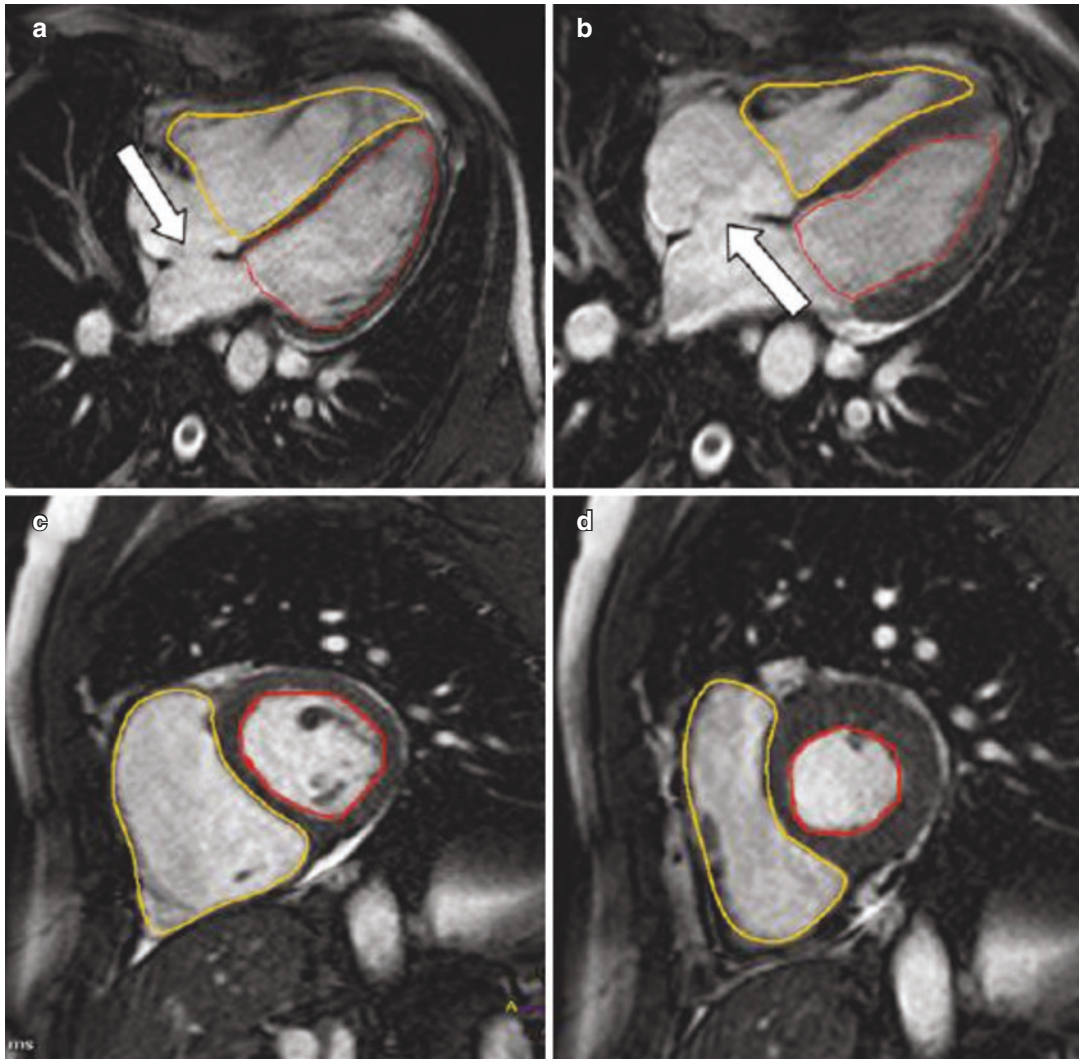

Fig. 20.2 Volumetric method for the quantification of IC shunt. Diastolic (**a**) and systolic (**b**) four chamber cine MR images of both ventricles demonstrate moderately dilated RV with normal systolic function. Diastolic (**c**) and systolic (**d**) short axis cine MR images of both ventricles. The ratio of the RV to LV stroke volumes gives shunt ratio (Q_p/Q_s). LV EDV = 194 cm^3; LV ESV = 102 cm^3; LV SV = 92 cm^3; LV EF = 48%, RV EDV = 289 cm^3; RV ESV = 124 cm^3; RV SV = 165 cm^3; and RV EF = 57%. Shunt ratio can be therefore calculated for this ASD case (*white arrows* show the defect); Q_p/Q_s = 165/92 = 1.8 (ASD atrial septal defect, EDV end diastolic volumes, ESV end systolic volumes, LV left ventricle, RV right ventricle)

Invasive Quantification of Intracardiac Shunts

IC shunts have been calculated using various invasive methods. Indocyanin dilution and/or dye curve technique have been used in the past. Contrast angiography provides qualitative evaluation and localization of the shunts but is not suitable for precise shunt quantification. The widely used invasive technique is the oxymetric study, which is based on blood sampling from different locations in the circulation.

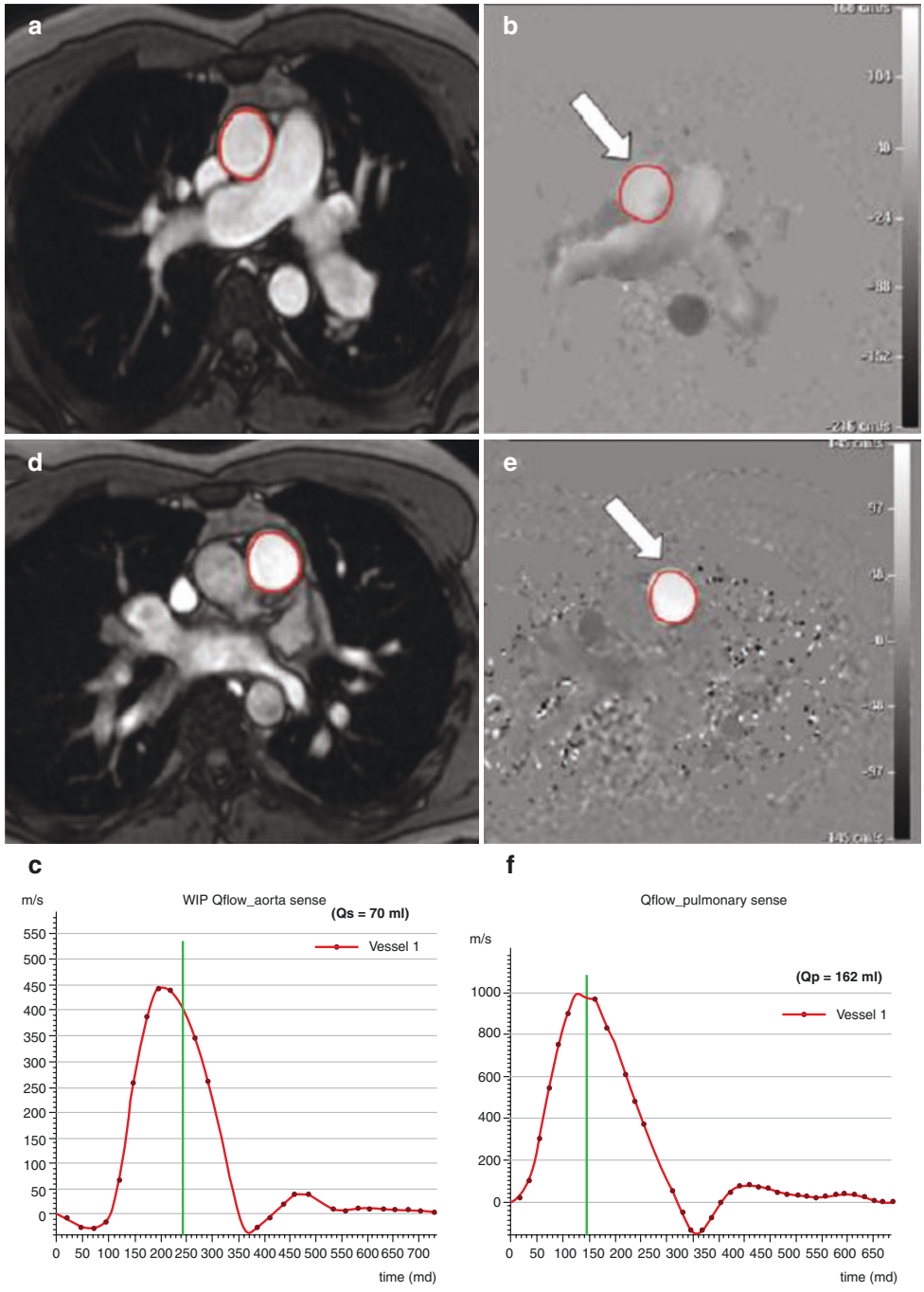

Fig. 20.3 (**a**–**c**) Velocity-encoded (phase contrast) cine MR imaging for the quantitation of systemic flow (Q_s). (**a**) Magnitude image of the ascending aorta for the measurement of cross-sectional area of the vessel. The plane is positioned at the level of the bifurcation of the main pulmonary artery. (**b**) Phase contrast image perpendicular to the ascending aorta (*white arrow*). (**c**) Through-plane velocity mapping creates flow vs. time curves. The area under the curve represents stroke volume of the ascending aorta (Q_s), which was measured 70 mL/beat for this case. (Q_s = 70 mL). (**d**–**f**) Phase contrast cine MR imaging for the quantitation of pulmonary flow(Q_p). (**a**) Magnitude image of the main pulmonary artery. (**b**) Phase contrast image perpendicular to the main pulmonary artery (*white arrow*). (**c**) Through-plane velocity mapping demonstrates flow vs. time curves across the main pulmonary artery. The area under the curve represents stroke volume of the pulmonary artery (Q_p), which was calculated 162 mL/beat for this case. The shunt ratio was therefore calculated Q_p/Q_s = 162/70 = 2.2, which indicates significant left to right shunting

Oxygen Saturation Run

Knowledge of basic principles of Fick's method is fundamental to understanding how IC shunts are calculated in catheterization laboratory.

Blood Sampling

Blood samples should be obtained after a "steady state" of heart rate, respiratory rate, and blood pressure is reached on room air if tolerated by patient. A large hole catheter should be used for easy blood draw. It should be kept in mind that very rapid aspiration or a faulty connection may allow the entry of microbubbles into the syringe, resulting in erroneously increased O_2 saturation and overestimation of Q_p [13]. Sites for blood sampling must be carefully chosen depending on the underlying pathology (Fig. 20.4) Blood sampling procedure should be completed within 5–10 min (or at the same time that oxygen consumption is calculated) in order to minimize the variability in oxygen consumption. After each sample is obtained, the catheter must be cleared with a saline flush. Obtaining blood samples from distal to proximal during catheter "pull-back" from pulmonary artery (PA) is more practical. If possible, the patient should not be receiving supplemental oxygen greater than 30%, as the increased dissolved O_2 in the right heart might cause increased pulmonary flow resulting in overestimation of the shunt ratio.

Variability of oxygen measurements and oxygen content should be taken into account during the sampling process, particularly in the right-sided heart chambers. In a study with 980 patients [14] without shunting, differences of O_2 saturation were found between SVC and RA, RA and PA, and SVC and PA, 3.9 ± 2.4%, 2.3 ± 1.7%, and 4.0 ± 2.5%, respectively. In another study [15], 102 adults without left to right shunt were assessed in order to find the limits of normality of O_2 content differences. The outcomes were from right atrium to mixed venous, right ventricle to right atrium, and pulmonary artery to right ventricle, 0.5 mL/dL, 0.6 mL/dL, and 0.9 mL/dL, respectively.

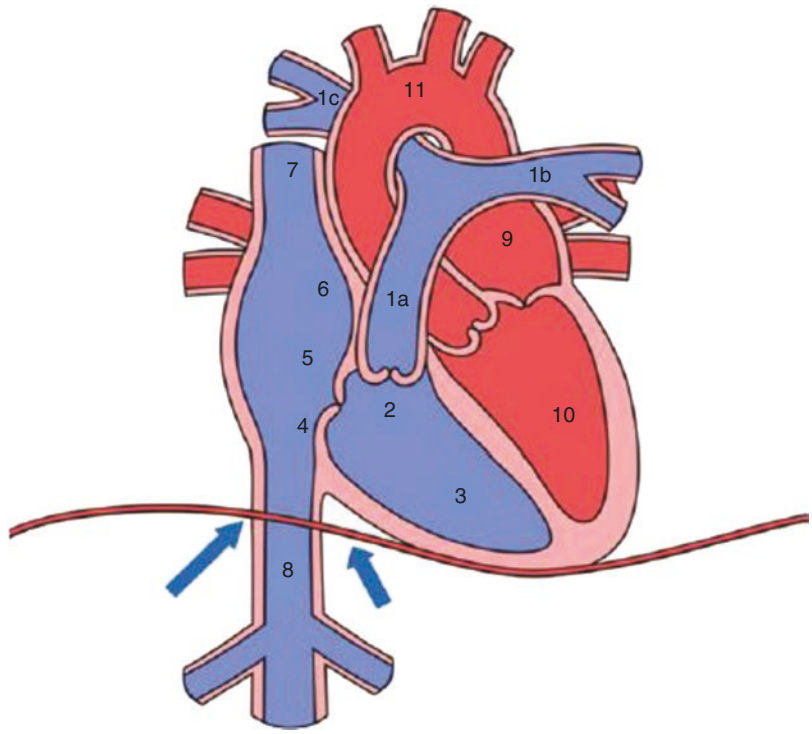

Fig. 20.4 Exact localization for the blood sampling in oxymetric run study. *1a* main pulmonary artery, *1b* left pulmonary artery, *1c* right pulmonary artery, *2* right ventricular outflow tract, *3* right ventricle, *4* low right atrium, *5* mid right atrium, *6* high right atrium, *7* superior vena cava, *8* inferior vena cava (sample should be obtained just below the diaphragm (*blue arrows*); hepatic vein must be taken into account while obtaining inferior vena cava blood), *9* left atrium, *10* left ventricle, *11* aorta or femoral artery

Mixed Venous Oxygen Saturation

In the normal circulation, deoxygenated blood is mixed in the pulmonary artery (PA). However, in the setting of left to right shunt, the site of mixed venous blood would vary according to the location of the lesion. Unfortunately, there is no practical way to measure mixed venous oxygen (MVO_2) because the various sources of MVO_2 (superior vena cava, inferior vena cava, coronary sinus) have different amounts of blood with varying saturations. As a general rule, blood samples should be obtained proximal and distal to the lesion and blood from the chamber(s) proximal to the shunt site is used for MVO_2 measurement. For instance, in the case of patent ductus arteriosus (PDA), arterial blood mixes with venous blood at the pulmonary artery at the level of the aorta. Thus, venous samples should be taken from RV, which is the proximal chamber to the shunt site. In patients with a ventricular septal defect, RAO_2 saturation can represent MVO_2 site. In the case of an atrial septal defect, the location where the arterial shunt mixes with venous blood is not constant. Different formulas are used for the calculation of MVO_2. The most commonly used formula in the estimation of MVO_2 is ((3 × SVC + 1 × IVC)/4) [16]. Other formulas may also be considered for an estimation of MVO_2 as follows:

$$\begin{bmatrix} = \dfrac{\left(\left(1\times \mathrm{SVC_{Sat}}\right)+\left(2\times \mathrm{IVC_{Sat}}\right)\right)}{3} \\ \mathrm{MVO_2} = \dfrac{\left(\left(2\times \mathrm{SVC_{Sat}}\right)+\left(3\times \mathrm{IVC_{Sat}}\right)\right)}{5} \end{bmatrix}$$

where MVO_2 = mixed venous oxygen saturation, SVC_{Sat} = superior vena cava saturation, and IVC_{Sat} = inferior vena cava saturation [15, 17].

Calculation of Shunt Size "Pulmonary to Systemic Flow Ratio (Q_p/Q_s)"

In the absence of a shunt, pulmonary blood flow (Q_p) is equal to the systemic blood flow(Q_s). Q_p/Q_s ratio is calculated based on Fick's principle as follows:

$$\text{Cardiac output} = \frac{\text{Oxygen consumption}}{\left(\text{Arterial } O_2 - \text{Venous } O_2\right)\times \text{Hemoglobin concentration}\times 1.36\times 10}$$

Since the pulmonary circulation occurs between pulmonary veins and pulmonary artery, the formula is adapted as follows:

$$Q_p = \frac{\text{Oxygen consumption}}{\left(\mathrm{PVO_2} - \mathrm{PAO_2}\right)\times \text{Hemoglobin concentration}\times 1.36\times 10}$$

where Q_p = pulmonary blood flow, PVO_2 = pulmonary vein oxygen saturation, and PAO_2 = pulmonary artery oxygen saturation.

Systemic circulation takes place between the aorta and the point where the venous blood is assumed to be fully mixed. Therefore, the formula corresponds to:

$$Q_s = \frac{\text{Oxygen consumption}}{\left(\mathrm{AoO_2} - \mathrm{MVO_2}\right)\times \text{Hemoglobin concentration}\times 1.36\times 10}$$

where Q_s = systemic blood flow, AoO_2 = aortic or systemic arterial oxygen saturation, and MVO_2 = mixed venous oxygen saturation).

These formulas can be simplified to calculate Q_p/Q_s as follows:

$$\frac{Q_p}{Q_s} = \frac{(AoO_2 - MVO_2)}{(PVO_2 - PAO_2)}$$

For right to left or bidirectional shunts:

Effective pulmonary blood flow must be calculated. The net difference of systemic flow to shunt flow should be considered as effective pulmonary flow.

Clinical Utility of the Shunt Ratio in Practice

Shunt ratio (Q_p/Q_s) can help clinicians to better understand the hemodynamic importance of the IC shunt and is clinically very important in decision-making about the requirement of possible intervention. If the ratio is less than 1.5, it generally indicates a "small lesion," a ratio of 1.5–2.0 indicates "likely to require intervention," and a ratio of 2 or more is usually considered to be "severe." Nevertheless, each case should be evaluated individually with its clinical presentation, and shunt ratio should be determined within the clinical context of the disease state. If there is inconsistency between invasive and noninvasive measurements, symptoms attributable to shunt defect, possible associated congenital abnormalities, as well as measurement pitfalls should be carefully reviewed. Secondary findings such as the quantification of chamber enlargement or ventricular function can also help in decision-making.

Review Questions

Q1—A 30-year-old woman presented with dyspnea on exertion. Echocardiographic examination revealed enlargement of right-sided heart chambers with an increased pulmonary flow. Left to right shunt was detected by color flow Doppler assessment in the interatrial septum. Which one of the following echocardiographic measurements is *not* necessary for the quantification of atrial shunt in this patient?

A. Diameter of LVOT
B. Diameter of RVOT
C. Diameter of defect
D. RVOT VTI
E. LVOT VTI

Q2—In which of the following congenital heart diseases, volumetric MRI measurement is *not* an appropriate method for the quantification of the intracardiac shunt?

A. Muscular type VSD
B. Secundum type ASD
C. Patent ductus arterious
D. Partial anomalous pulmonary venous return
E. Aorticopulmonary window

Q3—Which one of the following formulas can be used to estimate mixed venous blood (MVO_2) saturation during cardiac catheterization?

A. $MVO_2 = \frac{(3\times SVC_{sat} + 1\times IVC_{sat})}{4}$

B. $MVO_2 = \frac{(SVC_{sat} + IVC_{sat})}{2}$

C. $MVO_2 = \frac{(2\times SVC_{sat} + 3\times IVC_{sat})}{5}$

D. $MVO_2 = SVC_{sat}$

E. All of the above

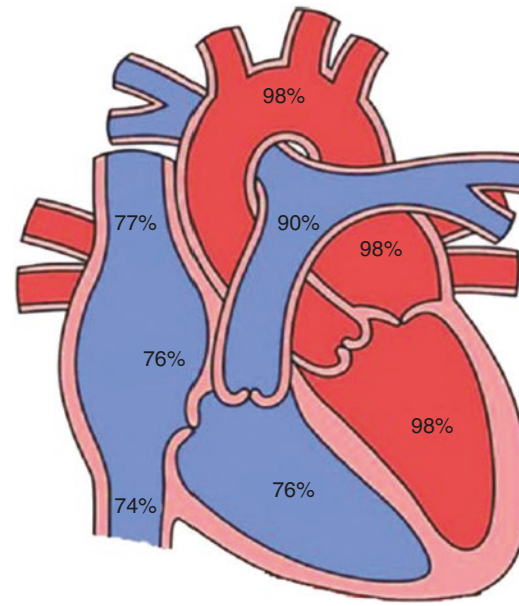

Q4—A 16-year-old patient underwent cardiac catheterization for further investigation with the suspicion of congenital heart disease. Her hemoglobin level is 13 g/dL and calculated O_2 consumption is 190 mL/min. According to the saturation run study results, shown below, which is the correct diagnosis?

A. Muscular type VSD − Q_p/Q_s = 1.5
B. Ostium primum type ASD − Q_p/Q_s = 2.8
C. Ostium secundum type ASD − Q_p/Q_s = 2.8
D. Patent ductus arteriosus − Q_p/Q_s = 2.8
E. Patent ductus arteriosus − Q_p/Q_s = 1.5

Q5—A 36-year-old man who was diagnosed secundum type ASD with left to right shunting. Calculated Q_p/Q_s ratio was reported as 2.1 with right atrial and ventricular enlargement. There was no associated significant valvular abnormality and he was still on normal sinus rhythm (68 beats/s). He was complaining of palpitations and exertional dyspnea and referred to you for further investigation and treatment. The following oxygen saturations were measured in catheterization room while the patient was breathing 21% oxygen room air O_2 cont; IVCsat: 69%, SVCsat: 73%, PAsat: 80%, femoral artery sat: 98%.

What would you do for the next step in the evaluation of this patient?

A. Invasive Q_p/Q_s ratio cannot be calculated with these data; hemoglobin and cardiac output should have been reported.
B. Echocardiographic shunt ratio indicates significant left to right shunting with an enlargement of right-sided heart chamber, which is enough for the decision on closure of this ASD.
C. Room oxygen level is not enough; oxymetric study should be repeated while the patient is breathing 80% oxygen.
D. Invasive Q_p/Q_s indicates significant left to right shunt so the defect should be closed as soon as possible.
E. Invasive Q_p/Q_s indicates nonsignificant left to right shunt; therefore, the patient should be treated medically and must be closely monitored.

Answers of the Questions

A1—The correct answer is C.

Echocardiography is the primary tool for the assessment of congenital heart disease. Although echocardiography can provide sizing of the defect, it is not required in the quantification of shunt ratio. The defect size, however, cannot give an idea about the shunt ratio. Small lesion can be associated with small shunt ratio, whereas big lesions can be complicated by Eisenmenger physiology with right to left or bidirectional shunting.

A2—The correct answer is A.

Gradient echo cine MR can provide comprehensive volumetric assessment for both ventricles. The shunt volume can be easily calculated as net difference between LV and RV stroke volumes. In the setting of VSD, however, IC shunt occurs at the ventricular level and quantification of Q_p/Q_s is impossible using this method. On the other hand, if there is severe valvular regurgitation, due to substantial back flow into the atria, stroke volumes can be underestimated.

A3—The correct answer is E.

Although the most common formula is (3 × SVC + IVC)/4, in the estimation of saturation MVO_2 blood**,** other formulas can be considered.

A4—The correct answer is D.

The diagnosis is PDA with L → R shunt. O_2 step up can be clearly seen in the main pulmonary artery. Hence, we can easily calculate Q_p/Q_s using simplified formula, which is

$$\frac{Q_p}{Q_s} = \frac{\left(AoO_2 - MVO_2\right)}{\left(PVO_2 - PAO_2\right)}$$

$$\frac{Q_p}{Q_s} = \frac{\left(98-76\right)}{\left(98-90\right)} = \frac{\left(22\right)}{\left(8\right)} = 2.75$$

Step-by-step approach for the assessment of intracardiac shunt quantification:

Step 1: Compute oxygen content for main locations

$$\text{Arterial oxygen content} = 0.98 \times 1.36 \times 13 \times 10 = 173$$
$$\text{Pulmonary vein oxygen content} = 0.98 \times 1.36 \times 13 \times 10 = 173$$
$$\text{Pulmonary artery oxygen content} = 0.90 \times 1.36 \times 13 \times 10 = 160$$
$$\text{Mixed venous oxygen content} = 0.76 \times 1.36 \times 13 \times 10 = 134$$

(As this is a PDA case, RVsat can represent MVO_2)

Step 2: Compute systemic flow (Q_s)

$$\frac{190}{173-134} = 4.87$$

Step 3: Compute pulmonary flow (Q_p)

$$\frac{190}{173-160} = 14.6$$

Step 4: Compute Q_p/Q_s

$$\frac{14.6}{4.87} = 3$$

A5—The correct answer is B.

Invasive oxymetric measurement of the Q_p/Q_s ratio is 1.5, which is inconsistent with echocardiographic shunt ratio. This is not an uncommon situation in daily practice. Although Q_p/Q_s ratio is clinically very important in decision-making, if there is strong clinical suspicion or laboratory evidence of a significant shunt (this patient is symptomatic and TTE revealed right-sided heart chamber enlargement), then the defect should be closed. On the other hand, it should be kept in mind that atrial shunts can easily be affected by ventricular filling patterns such as compliance or stiffness and might be underestimated in the setting of severe tricuspid regurgitation or atrial fibrillation.

Hemoglobin and oxygen contents are not exactly necessary for an estimation of Q_p/Q_s ratio. Because same parameters are used in the denominator and nominator of the equations, simplified method can be used practically.

References

1. Lang RM, Goldstein SA, Kronzon I, Khandheria BK, Mor-Avi V. ASE's comprehensive echocardiography, Patnet foramen ovale. 2nd ed. Elsevier; 2011. p. 840–5.
2. Brenner LD, Caputo GR, Mostbeck G, et al. Quantification of left to right atrial shunts with velocity-encoded cine nuclear magnetic resonance imaging. J Am Coll Cardiol. 1992;20:1246–50.
3. Korperich H, Gieseke J, Barth P, et al. Flow volume and shunt quantification in pediatric congenital heart disease by real-time magnetic resonance velocity mapping: a validation study. Circulation. 2004;109:1987–93.
4. Beerbaum P, Korperich H, Barth P, Esdorn H, Gieseke J, Meyer H. Noninvasive quantification of left-to-right shunt in pediatric patients: phase-contrast cine magnetic resonance imaging compared with invasive oximetry. Circulation. 2001;103:2476–82.
5. Debl K, Djavidani B, Buchner S, et al. Quantification of left-to-right shunting in adult congenital heart disease: phase-contrast cine MRI compared with invasive oximetry. Br J Radiol. 2009;82:386–91.
6. Hundley WG, Li HF, Lange RA, et al. Assessment of left-to-right intracardiac shunting by velocity-encoded, phase-difference magnetic resonance imaging. A comparison with oximetric and indicator dilution techniques. Circulation. 1995;91:2955–60.
7. Beerbaum P, Korperich H, Gieseke J, Barth P, Peuster M, Meyer H. Rapid left-to-right shunt quantification in children by phase-contrast magnetic resonance imaging combined with sensitivity encoding (SENSE). Circulation. 2003;108:1355–61.
8. Ratnayaka K, Raman VK, Faranesh AZ, et al. Antegrade percutaneous closure of membranous ventricular septal defect using X-ray fused with magnetic resonance imaging. JACC Cardiovasc Interv. 2009;2:224–30.
9. Lapierre C, Raboisson MJ, Miro J, Dahdah N, Guerin R. Evaluation of a large atrial septal occluder with cardiac MR imaging. Radiographics. 2003;23:Spec No:S51–8.
10. Weber M, Dill T, Deetjen A, et al. Left ventricular adaptation after atrial septal defect closure assessed by increased concentrations of N-terminal pro-brain natriuretic peptide and cardiac magnetic resonance imaging in adult patients. Heart. 2006;92:671–5.
11. Schoen SP, Kittner T, Bohl S, et al. Transcatheter closure of atrial septal defects improves right ventricular volume, mass, function, pulmonary pressure, and functional class: a magnetic resonance imaging study. Heart. 2006;92:821–6.
12. Wynne J, Fishbein MC, Holman BL, Alpert JS. Radionuclide scintigraphy in the evaluation of ventricular septal defect complicating acute myo-

cardial infarction. Catheter Cardiovasc Diagn. 1978;4:189–97.
13. Matta BF, Lam AM. The rate of blood withdrawal affects the accuracy of jugular venous bulb. Oxygen saturation measurements. Anesthesiology. 1997;86:806–8.
14. Hillis LD, Firth BG, Winniford MD. Variability of right-sided cardiac oxygen saturations in adults with and without left-to-right intracardiac shunting. Am J Cardiol. 1986;58:129–32.
15. Pirwitz MJ, Willard JE, Landau C, Hillis LD, Lange RA. A critical reappraisal of the oximetric assessment of intracardiac left-to-right shunting in adults. Am Heart J. 1997;133:413–7.
16. Flamm MD, Cohn KE, Hancock EW. Measurement of systemic cardiac output at rest and exercise in patients with atrial septal defect. Am J Cardiol. 1969;23:258–65.
17. French WJ, Chang P, Forsythe S, Criley JM. Estimation of mixed venous oxygen saturation. Catheter Cardiovasc Diagn. 1983;9:25–31.

Shock

21

Jose Mariano T. Tan and Michael P. Brunner

Epidemiology of Shock

Shock is a pathophysiological state characterized by inadequate tissue oxygenation. It is a life-threatening condition that may lead to cellular death and vital organ dysfunction. Common clinical manifestations of shock include tachycardia, hypotension, oliguria, and confusion. Laboratory tests often demonstrate signs of end-organ damage such as acute liver or kidney injury, metabolic acidosis, and lactic acidosis.

There are four major categories of shock: cardiogenic, hypovolemic, distributive, and obstructive shock. However, it is important to note that these major categories of shock are not mutually exclusive and combinations with other form(s) of shock may occur.

Cardiogenic shock (CS) is often depicted as shock due to pump failure. The primary disorder in CS is low cardiac output due to intrinsic cardiac dysfunction. It is often a complication of myocardial infarction, but it may also be due to arrhythmia, congestive heart failure, or a primary valvular disorder. CS is estimated to complicate 3–8% of cases of acute myocardial infarction [1–3]. The mortality rate associated with CS in patients with acute myocardial infarction historically approached 80% [1]. Due to contemporary strategies in the management of acute coronary syndrome, the adjusted mortality rate ranges from 45 to 66% [4].

Hypovolemic shock is shock due to hemorrhagic or nonhemorrhagic volume loss. It is often related to traumatic injury, gastrointestinal bleeding, vomiting, or diarrhea. The incidence of hypovolemic shock varies depending on its underlying etiology.

The most common etiology of *distributive shock* is sepsis, a dysfunctional systemic response to an infection. Every year, 1.6 million patients are diagnosed with sepsis in the United States [5]. In its severe form, septic shock may ensue. The mortality associated with severe sepsis and septic shock is estimated to be 14.7–29.9% [6]. These figures are likely underestimated as severe sepsis and septic shock often occur concomitantly with other leading causes of mortality including pneumonia, urinary tract infection, gastrointestinal tract infection, skin infection, and malignancy.

The primary disorder in *obstructive shock* is low cardiac output due to extrinsic cardiac dysfunction. The incidence of obstructive shock varies according to its etiology which includes pulmonary embolism, cardiac tamponade, and tension pneumothorax.

J. M. T. Tan (✉) · M. P. Brunner
Spectrum Health Medical Group,
Grand Rapids, MI, USA
e-mail: Jose.Tan@Spectrumhealth.org;
Michael.Brunner@Spectrumhealth.org

A. T. Askari, A. W. Messerli (eds.), *Cardiovascular Hemodynamics*, Contemporary Cardiology,
https://doi.org/10.1007/978-3-030-19131-3_21

Clinical Presentation of Shock: A Case-Based Approach

Understanding the pathophysiology associated with each category of shock is essential in performing an appropriate clinical assessment and guiding appropriate therapy. Examples of different conditions associated with each major category of shock are listed in Table 21.1. The following cases are examples from each category of shock.

Case 1: Cardiogenic Shock

A 55-year-old male with hypertension, dyslipidemia, and a family history of coronary artery disease presents to the emergency department

Table 21.1 Etiologies of shock

Cardiogenic[a]	**Distributive**
Myopathic	Sepsis; pancreatitis
Acute myocardial infarction	Pancreatitis
Left ventricular failure	Anaphylaxis
Right ventricular failure	Bacterial toxins
Acute myocarditis	Acidosis
Idiopathic cardiomyopathy	Adrenal crisis
Restrictive/constrictive cardiomyopathy	Myxedema coma
Stress-induced (Takotsubo) cardiomyopathy	Iatrogenic
Acute heart transplant rejection	Neurogenic insult
Iatrogenic (negative inotropic or vasodilatory medications)	Post-resuscitation syndrome
Post-cardiac arrest	Post-cardiopulmonary bypass
Mechanical	**Hypovolemic**
Ventricular septal rupture	Hemorrhagic
Ventricular Free Wall rupture	Trauma
Hypertrophic obstructive cardiomyopathy	Gastrointestinal bleeding
Dynamic left ventricular outflow tract obstruction	Ruptured hematoma
Atrial myxoma	Hemorrhagic pancreatitis
Traumatic	Fractures
Valvular	Ruptured aortic aneurysm
Papillary muscle/chordal rupture	Acute aortic dissection
Acute mitral regurgitation	Plasma extravasation related
Prosthetic valve obstruction	Systemic inflammatory response
Severe aortic regurgitation	Sepsis
Critical aortic stenosis	Major surgery
Severe mitral stenosis	Pancreatitis
Arrhythmic	Major surgery
Tachycardia	Fluid loss related
Sustained ventricular tachycardia	Dehydration
Ventricular fibrillation	Severe burns
Bradycardia	Emesis
High-grade AV block	Diarrhea
Complete heart block	Diaphoresis
	Insensible losses
	Inadequate fluid intake
	Obstructive
	Cardiac tamponade
	Pulmonary embolism
	Pulmonary hypertension
	Tension pneumothorax

[a]*Causes that may complicate acute myocardial infarction are italicized*

with severe substernal chest pain and shortness of breath. Initial vital signs demonstrate tachycardia and hypotension. A third heart sound (S3) is auscultated. He has inspiratory rales in both lung bases, and his internal jugular vein is appreciated above the clavicle in an upright position. His extremities are cool, mottled, and cyanotic. An electrocardiogram reveals ST segment elevation across the anterior precordial leads.

This case describes a patient with CS caused by acute myocardial infarction. CS is a clinical condition in which inadequate tissue perfusion is the consequence of intrinsic cardiac dysfunction. It is characterized by a reduction in cardiac output despite adequate filling pressures. Causes of CS include myopathic, mechanical, valvular, and arrhythmic processes (Table 21.1). The criteria typically used to define CS include systolic blood pressure less than 90 mmHg for at least 30 min or the need for a vasopressor or mechanical circulatory support to maintain a systolic blood pressure greater than 90 mmHg; pulmonary capillary wedge pressure greater than 15 mmHg; and cardiac index less than 2.2 L/min/kg/m^2 [7].

Tachycardia, hypotension, oliguria, confusion, cyanosis, and cold extremities typically characterize the clinical presentation of CS. Tachycardia occurs in an effort to maintain cardiac output when the stroke volume is reduced. Oliguria and confusion are the result of poor tissue perfusion. Cool, mottled, and cyanotic extremities are manifestations of peripheral vasoconstriction.

Peripheral pulses are often diminished in CS due to decreased pulse pressure (*pulsus parvus*). In a failing left ventricle, the strength of every other beat may alternate, a phenomenon known as *pulses alternans*. Delayed pulses (*pulsus tardus*) may be seen in cardiogenic shock in the setting of severe aortic stenosis.

CS due to left ventricular failure may present with pulmonary congestion; patients may complain of orthopnea and paroxysmal nocturnal dyspnea (PND). Examination may demonstrate bilateral inspiratory rales, S3 gallop, and laterally displaced apical impulse due to left ventricular dilatation. Chest radiography may demonstrate cardiomegaly, pulmonary vessel cephalization, Kerley B lines, and parenchymal edema. If right ventricular failure is also present, evidence of venous congestion may be observed including jugular vein distention, hepatojugular reflux, and bilateral lower extremity edema.

Of note, a significant proportion of patients in the SHOCK (SHould we emergently revascularize Occluded Coronaries in cardiogenic shocK?) trial had no pulmonary congestion [8]. Neither auscultation nor chest radiograph detected pulmonary edema in 28% of patients.

Right ventricular infarction complicates up to half of all transmural inferior-posterior myocardial infarctions [9]. Patients with hemodynamically significant right ventricular infarction classically present with hypotension, clear lung fields, and jugular venous distention. Right ventricular failure may be associated with a holosystolic tricuspid regurgitation murmur at the left lower sternal border, jugular venous distension, liver engorgement, pulsatile liver, and peripheral edema. Patients with patent foramen ovale and acute right ventricular infarction may present with profound hypoxia due to decreased compliance in the infarcted right ventricle and right-to-left shunting.

Mechanical complications of acute myocardial infarction may result in CS and can sometimes be evident on physical exam. Acute mitral regurgitation, tricuspid regurgitation, and ventricular septal rupture are associated with holosystolic murmurs. However, if there is rapid equalization of pressure in the atria and ventricles, acute regurgitant lesions may not cause a significant murmur. Prominent jugular *v*-waves suggest severe tricuspid regurgitation. Jugular cannon *a*-waves suggest complete heart block. Ventricular free wall rupture will frequently result in fulminant cardiac tamponade (see section "Case 4: Obstructive Shock").

In CS, a compensatory increase in systemic vascular resistance (SVR) typically occurs through peripheral vasoconstriction in an effort to maintain tissue perfusion. However, this classic paradigm has been challenged. Data from the SHOCK trial demonstrated that many patients with CS instead have low systemic resistance, similar to patients with septic shock [10]

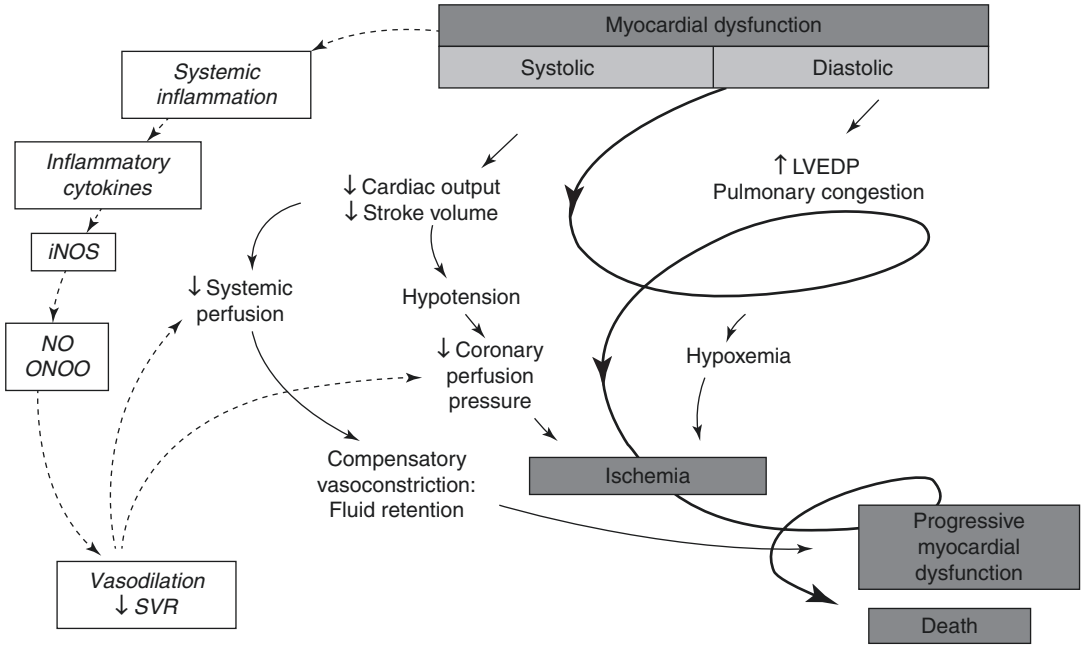

Fig. 21.1 Expansion of the pathophysiological paradigm of cardiogenic shock to include the potential contribution of inflammatory mediators. LVEDP left ventricular end-diastolic pressure; NO nitric oxide; iNOS inducible nitric oxide synthase; ONOO− peroxynitrite; SVR systemic vascular resistance. (Reprinted with permission from Hochman and Ohman [26])

(Fig. 21.1). It has been postulated that a systemic inflammatory response-like syndrome with a low SVR may be encountered in up to one-fifth of patients with acute myocardial infarction complicated by CS [11].

The clinical presentation can be utilized to risk-stratify patients with acute myocardial infarction complicated by CS. Killip described a case series of 250 patients presenting to an academic university intensive care unit with myocardial infarction [12]. He divided the patients into four classes according to the clinical presentation. Class I had no clinical signs of heart failure; class II presented with basilar rales and/or S3 gallop and/or elevated jugular venous pressure; class III had frank pulmonary edema; and class IV had cardiogenic shock. Reported mortality was 6%, 17%, 38%, and 67% for each class, respectively.

Current mortality with reperfusion therapy is dramatically lower than that observed in the original observation. However, Killip Class II, III, and IV continue to identify a high-risk subset of patients.

Therapeutic measures for CS often need to be implemented before invasive hemodynamic data are available. The clinical presentation may guide the most effective therapy. For example, patients with a clinical presentation consistent with myocardial infarction require urgent revascularization. A profile consistent with left ventricular failure may require inotropic or vasoactive agents and/or mechanical circulatory support in the form of an intra-aortic balloon pump, percutaneous left ventricular assist device, or extracorporeal membrane oxygenation. Patients with findings consistent with right ventricular infarction may require rapid fluid resuscitation and/or percutaneous right ventricular assist device placement.

Case 2: Hypovolemic Shock

A 25-year-old male patient presents shortly after a gunshot wound to the abdomen. He has experienced profound bleeding. He is tachycardic, hypotensive, and confused. Neck veins are

flat and lung fields are clear. The mucus membranes and skin are dry. Extremities are cool and clammy. He has a large drop in blood pressure and is more tachycardic when changing from supine to standing position.

The second case describes a patient with hypovolemic shock related to traumatic hemorrhage. Hypovolemic shock is characterized by inadequate intravascular volume. Etiologies are generally related to hemorrhage, plasma extravasation, or fluid loss (see Table 21.1). Hemorrhagic etiologies include trauma, gastrointestinal bleeding, ruptured hematoma, hemorrhagic pancreatitis, fracture, and ruptured abdominal aortic aneurysm. Etiologies related to plasma extravasation include systemic inflammatory response, major surgery, and severe pancreatitis. Fluid loss may be due to severe burns, emesis, diarrhea, diaphoresis, other insensible losses, and inadequate oral intake.

Hypotension, tachycardia, confusion, oliguria, and cold extremities typically characterize the clinical presentation of hypovolemic shock. Cardiac output generally falls as a result of decreased ventricular preload. Compensatory tachycardia and an increase in SVR, mediated by peripheral vasoconstriction, occur in an effort to improve tissue perfusion. Increased sympathetic activity may cause narrow pulse pressure and diaphoresis. Peripheral vasoconstriction results in cool, mottled, and cyanotic extremities.

The clinical history will generally suggest the underlying etiology. However, clinical findings may overlap with cardiogenic shock. A key difference is that the intracardiac filling pressure is adequate or elevated (PCWP greater than 15 mmHg) in CS, whereas it is generally low in hypovolemic shock due to inadequate intravascular volume. In hypovolemic shock, the lung fields are generally clear, and there is no evidence of jugular venous distension or peripheral edema.

The physical diagnosis of hypovolemia has been systematically reviewed in adults [13]. The most helpful physical findings include severe postural dizziness or a postural pulse increment of at least 30 beats/min, a systolic pressure decrement of at least 20 mmHg, or a diastolic pressure decrement of at least 10 mmHg for measurements obtained 2 min after assuming an upright posture (orthostasis). Supine hypotension and tachycardia were frequently absent, even after up to 1150 mL of blood loss [13]. In patients with vomiting, diarrhea, or decreased oral intake, the presence of a dry axilla supports the diagnosis of hypovolemia. In adults, the capillary refill time and poor skin turgor have no proven diagnostic value.

Case 3: Distributive Shock

An 80-year-old female with recurrent urinary tract infection presents with fever, tachycardia, hypotension, decreased urine output, and confusion. She is diaphoretic and has foul smelling urine. Her neck veins are flat and the lung fields are clear. The extremities are warm and hyperemic. Capillary refill is brisk. Her hypotension does not improve despite aggressive fluid resuscitation.

This third case describes a patient with distributive shock related to severe sepsis. Inappropriate vasodilation, decreased SVR, hypotension, and poor tissue oxygenation characterize distributive shock. Etiologies of distributive shock include systemic inflammatory response syndrome, severe sepsis, bacterial toxins (e.g., staphylococcal toxic shock), anaphylaxis, adrenal insufficiency, myxedema coma, neurogenic insult, post-resuscitation syndrome, and post-cardiopulmonary bypass (see Table 21.1).

Septic shock is the most common presentation of distributive shock. Septic shock is defined by sepsis-induced hypotension that persists despite adequate fluid resuscitation (20–30 mL/kg starch or 40–60 mL/kg saline or PCWP 12–20 mmHg) [14].

Clinical presentations of distributive shock vary by etiology but are generally characterized by tachycardia, hypotension, oliguria, confusion, and warm, well-perfused extremities. Compensatory tachycardia, oliguria, and confusion are manifestations of poor tissue perfusion. Warm and hyperemic extremities with brisk capillary refill time are the result of inappropriate

vasodilatation and decreased SVR. The cardiac output is typically elevated in distributive shock and may manifest as bounding pulses. The lungs are typically clear, and there is no jugular venous distension or peripheral edema.

Patients with severe sepsis and shock may have fever or hypothermia, diaphoresis, and rigors. Findings associated with an infectious process (e.g., pneumonia) may be present. Tachypnea is common and occurs in an effort to compensate for severe metabolic acidosis caused by elevated lactate. Hoarseness, stridor, wheezing, pruritus, flushing, hives, and abdominal pain may accompany anaphylactic shock. Hypothermia, hypoventilation, and somnolence are associated with myxedema coma (severe hypothyroidism). Profound orthostatic hypotension and skin hyperpigmentation may be presenting signs of adrenal insufficiency. Although most patients with distributive shock present with tachycardia, patients with neurogenic shock may have bradycardia due to sympathetic denervation.

Case 4: Obstructive Shock

A 65-year-old female patient with metastatic breast cancer presents with dyspnea and palpitations. Although she is tachycardic, her heart sounds seem distant. Her initial blood pressure is 80/50 mmHg. Her internal jugular vein is distended, but her breath sounds are clear to auscultation. Careful examination of her blood pressure demonstrates an exaggerated dissipation of Korotkoff sounds during inspiration. She has no leg edema and has not observed any recent fever, bleeding, vomiting, or diarrhea. Chest radiography revealed cardiomegaly with no significant parenchymal disease.

The fourth case is representative of obstructive shock due to cardiac tamponade. In the setting of breast cancer, pericardial metastasis is suspected. Classic findings of cardiac tamponade include distant, muffled heart sounds, jugular venous distension, and hypotension. Ventricular interdependence, manifested by an inspiratory drop in blood pressure (*pulses paradoxus*) greater than 10 mmHg, may also be observed.

Other causes of obstructive shock include tension pneumothorax and pulmonary embolism. Tension pneumothorax may be accompanied by dyspnea with tympany and decreased breath sounds in the affected hemithorax. Pulmonary embolism may be associated with cough, hemoptysis, and limb asymmetry in the context of prolonged immobilization. Both may present with desaturation.

Diagnostic Evaluation of Shock

The etiology of shock can often be determined using data acquired from the medical history, physical examination, basic laboratory evaluation, and radiographic findings. However, additional diagnostic tests may be needed in the optimal assessment and management of shock. Intra-arterial pressure monitoring, echocardiography, and pulmonary artery catheterization are frequently utilized diagnostic modalities.

Brachial cuff measurements are often inaccurate in states of shock. Intra-arterial pressure monitoring provides a continuous assessment of the blood pressure and heart rate and allows for safe and effective titration of vasoactive medications.. Additional data may also be obtained by assessing the arterial waveform. Further, the pulse pressure (systolic blood pressure − diastolic blood pressure) may be helpful in differentiating various shock states.

The 2004 American College of Cardiology/American Heart Association (ACC/AHA) guidelines for the management of patients with ST segment elevation myocardial infarction state that intra-arterial pressure monitoring should be performed (class I indication) for severe hypotension (systemic arterial pressure less than 80 mmHg), during the administration of vasopressor and/or inotropic agents, and for cardiogenic shock [15]. Although the 2016 ACC/AHA guideline does not make any reference to intra-arterial pressure monitoring, it continues to be employed frequently for the same indications. Potential complications of intra-arterial pressure monitoring include pain, infection, hematoma, arterial obstruction, and arterial embolus.

Echocardiography is an invaluable tool in the assessment of shock. It may help determine the etiology of shock and guide management. Echocardiography can be utilized to assess left and right ventricular function and can detect tamponade, restrictive/constrictive physiology, severe valvular regurgitation or valvular stenosis, ventricular septal or free wall rupture, and proximal aortic dissection. Echocardiographic findings of a clot-in-transit and right ventricular dysfunction may suggest the presence of a hemodynamically significant pulmonary embolism.

Echocardiography using agitated saline is a sensitive diagnostic modality for detecting intracardiac and pulmonary vascular shunting. Hemodynamic parameters such as central venous pressure, pulmonary artery pressure, and left ventricular end-diastolic pressure can be estimated using conventional echocardiographic methods.

The pulmonary artery catheter can be valuable in determining the etiology of shock and may help in guiding management. Data obtained from the pulmonary artery catheter includes central venous pressure, right atrial pressure, right ventricular pressure, pulmonary artery pressure, and pulmonary capillary wedge pressure. Obtaining a mixed venous oxygen saturation permits the calculation of the cardiac output, cardiac index, and systemic venous resistance. Furthermore, important diagnostic information may also be determined by analyzing the pressure waveforms.

The hemodynamic data gathered with a pulmonary artery catheter can be utilized to titrate vasopressor therapy, assess hemodynamic effects of changes in mechanical ventilation (e.g., positive end expiratory pressure), and guide fluid resuscitation. In addition, the data may help differentiate between cardiogenic and noncardiogenic pulmonary edema when a trial of diuretic and/or vasodilator therapy has failed.

Pulmonary artery catheterization may aid in determining if pericardial tamponade is present when clinical assessment is inconclusive and echocardiography is not available. Findings of cardiac tamponade include diastolic equalization of pressures and blunted y descent of the arterial waveform (see Chap. 15). Other uses of pulmonary artery catheterization include assessment of valvular heart disease severity and reversibility of pulmonary vasoconstriction in patients being considered for heart transplant. An oximetry run may also be performed using a pulmonary artery catheter. This is important in the investigation of cardiac shunts, which may occur as a complication of myocardial infarction.

Despite its potential advantages, pulmonary artery catheterization has not been shown to broadly improve patient outcomes. Its use is therefore controversial and is not favored in some centers. Whether the lack of benefit on important outcomes is a result of the severity of illness in the patients for whom the use of this tool is contemplated, or a result of incorrect interpretation and use of the data obtained, is a debated topic. It is important to note that the Evaluation Study of Congestive Heart Failure and Pulmonary Artery Catheterization Effectiveness (ESCAPE) trial showed no significant difference in endpoints of mortality and days out of hospital in the management of congestive heart failure refractory to standard medical therapy [16]. However, this trial demonstrated that the use of the pulmonary artery catheter for this group of patients was safe.

In ESCAPE, the addition of pulmonary artery catheterization to careful clinical assessment was associated with a higher frequency of adverse events but did not affect overall mortality and hospitalization. Adverse events included implantable cardioverter-defibrillator firing, cardiogenic shock, ischemia/angina, pulmonary artery catheter infection, myocardial infarction, stroke or ischemic attack, cardiac arrest, and infection. The only individual event that was statistically different (p value < 0.05) between the groups was pulmonary artery catheter infection (p value $= 0.03$).

The external validity of the findings of the ESCAPE trial has been debated [17]. Many of the registry patients did not get randomized into the trial because pulmonary artery catheterization was deemed necessary for management by a study investigator. Subsequently, only patients with clinical equipoise in whom physicians were comfortable managing heart failure decompensation with or without hemodynamic monitoring were included in the study. As such, the study is not applicable to the critically ill heart failure

patients who are often considered for pulmonary artery catheterization.

The routine use of pulmonary artery catheterization in intensive care units is also controversial. A 2005 meta-analysis of 13 randomized trials including over 5000 critically ill patients showed that the use of pulmonary artery catheters was not associated with benefit or increased mortality [18]. However, the meta-analysis included patients who were critically ill from a wide variety of causes.

There have not been any randomized studies aimed at directly evaluating the utility of pulmonary artery catheters in patients presenting with CS. There were 2968 patients with cardiogenic shock enrolled in the Global Utilization of Streptokinase and Tissue Plasminogen Activator for Occluded Coronary Arteries (GUSTO-1) trial. Mortality among patients (n = 995) managed with PA catheters (45.2%) was less than that among patients (n = 1406) not managed with PA catheters (63.4%) [19].

A potential limitation of pulmonary artery catheter hemodynamic monitoring is that many physicians do not know how to correctly interpret findings from the device [20]. A 31-question multiple-choice exam was administered to 496 medical doctors at 13 different institutions to assess their knowledge and understanding of the use of the pulmonary artery catheter and interpretation of data derived from it. The examination was given unannounced at general meetings in the departments of medicine, anesthesiology, and surgery. The mean score was 67%; almost half of the responders (47%) could not read a pulmonary capillary wedge pressure from a clear tracing.

The 2013 ACCF/AHA guidelines for the management of heart failure provide guidance for appropriate pulmonary catheter use in hemodynamic assessment [21]. It is a class I indication to use pulmonary artery catheter monitoring to guide therapy in patients with respiratory distress or clinical evidence of impaired perfusion when intracardiac filling pressures cannot be determined by clinical assessment. The guidelines also state that pulmonary artery catheters "can be" useful (class IIa indication) in acute heart failure with persistent symptoms despite seemingly appropriate adjustments of standard therapies if fluid status, perfusion, systemic vascular resistance, or pulmonary vascular resistance is uncertain. Similarly, pulmonary artery catheters can be useful in the setting of renal dysfunction, vasoactive agent use, or mechanical circulatory support. The 2017 ACC/AHA/HFSA Focused Update of the aforementioned guideline did not provide additional guidance on the use of pulmonary artery catheterization.

Routine invasive monitoring of hemodynamics is not recommended in normotensive patients with acute decompensated heart failure responding appropriately to therapy [21]. Potential complications of pulmonary artery catheter use include infection, right bundle branch block, ventricular tachycardia, pulmonary artery rupture, and pulmonary infarction. Over time, pulmonary artery catheters tend to soften and migrate distally, leading to spontaneous wedging even when the balloon tip is not inflated.

Hemodynamic Assessment of Shock

A fundamental understanding of the hemodynamics of shock is critically important. The etiology of shock may not be evident despite the data acquired from the medical history, physical examination, basic laboratory evaluation, and radiographic findings. Hemodynamic data can help diagnose the correct etiology of shock and guide appropriate management.

Systemic tissue perfusion (blood pressure) is determined by the cardiac output (CO) and SVR. Similar to Ohm's law, whereas electrical current through a circuit is directly proportional to the potential difference across the circuit and inversely proportional to the resistance, cardiac output (CO) is directly proportional to the blood pressure difference across the systemic circulation (mean arterial pressure [MAP] − mean right atrial pressure [mean RAP]) and inversely proportional to SVR. Therefore [CO = (MAP − mean RAP)/SVR].

Cardiac output can be measured with a pulmonary artery catheter by utilizing either the Fick method or thermodilution technique (see

Table 21.2 Hemodynamic patterns classically associated with different categories of shock

	RA (mmHg)	RV (mmHg)	PA (mmHg)	PCWP (mmHg)	CI (L/min/kg/m^2)	PP (mmHg)	HR (bpm)	SVR (dynes)	SVO_2 (%)
Normal values	<6	<25/0–12	<25/0–12	<6–12	>2.5	40–50	60–100	800–1600	70
Cardiogenic	↑	↑	↑	↑ (>15)[a]	↓ (<2.2)	↑↓	↑	↑[b]	↓
Distributive	↑↓	↑↓	↑↓	↑↓	↑[c]	↑	↑[d]	↓	↑↓[e]
Hypovolemic	↓	↓	↓	↓	↓	↓	↑	↑	↓

RA right atrium, *RV* right ventricle, *PA* pulmonary artery, *PCWP* pulmonary capillary wedge pressure, *CI* cardiac index, *PP* pulse pressure, *HR* heart rate, *SVR* systemic vascular resistance, *SVO_2* mixed venous oxygen saturation

[a]In the SHOCK trial, 28% of patients had no auscultatory or radiographic evidence of pulmonary edema suggestive of elevated PCWP

[b]A systemic inflammatory response-like syndrome with a low SVR may be encountered in up to one-fifth of patients with acute myocardial infarction complicated by cardiogenic shock

[c]Cardiac output can be reduced in distributive shock due to myopathic processes such as severe acidosis or when preload is decreased because of inadequate intravascular volume

[d]Patients with neurogenic shock may have bradycardia due to sympathetic denervation

[e]SVO_2 is generally increased in sepsis due to poor oxygen utilization

Chap. 4). Different categories of shock can be discriminated using the calculated cardiac output. Whereas cardiac output is low in cardiogenic shock and hypovolemic shock, it is generally elevated in distributive shock (Table 21.2). However, cardiac output can also be reduced in distributive shock due to myopathic processes such as severe acidosis or when preload is decreased because of inadequate intravascular volume.

Systemic vascular resistance (SVR) can be calculated if the blood pressure, right atrial pressure, and cardiac output are known. The drop in arterial pressure across the systemic circulation divided by cardiac output is equal to SVR. [SVR = [MAP − mean RAP]/CO]. The units for SVR are mmHg/mL/m^2 (Woods units) and are typically multiplied by 80 to convert to dynes/cm^5 (dyn). Pulmonary vascular resistance can be calculated by substituting the drop in pressure across the systemic circulation with that of the pulmonary circulation (mean pulmonary artery pressure − mean pulmonary capillary wedge pressure). SVR is reduced in distributive shock but is generally elevated in CS and hypovolemic shock [22].

Mixed venous oxygen concentration (SVO_2) may help differentiate shock from its different categories. In distributive shock related to sepsis, SVO_2 is generally elevated because the mitochondria are unable to utilize oxygen appropriately. As a result, there is a higher than expected venous oxygen saturation. In other states of shock, SVO_2 is generally low.

Elevated pulmonary capillary wedge pressure (greater than 15 mmHg) has classically been used to distinguish CS from noncardiogenic causes of shock. However, in the SHOCK trial, 28% of patients had no auscultatory or radiographic evidence of pulmonary edema to suggest elevated PCWP [8]. Severe sepsis can cause myocardial depression and may elevate left-sided pressures as well. CS related to right ventricular infarction may be associated with marked hypotension, low cardiac output, and shock despite a normal pulmonary capillary wedge pressure.

The intra-arterial pressure waveform can help differentiate various shock etiologies. Pulse pressure equals the difference between systolic and diastolic blood pressure and is normally 40–50 mmHg (Fig. 21.2). The pulse pressure is a reflection of the stroke volume and the strength of each ventricular contraction.

In patients with CS related to left ventricular failure, the pulse pressure is reduced (see Fig. 21.3). A narrow pulse pressure, defined as a pulse pressure <25% of the systolic blood pressure, has a sensitivity and specificity of 91% and 83% for a cardiac index of <2.2 L/min/m^2 [23]. Other causes of narrow pulse pressure include profound intravascular volume loss, cardiac tamponade, and aortic stenosis.

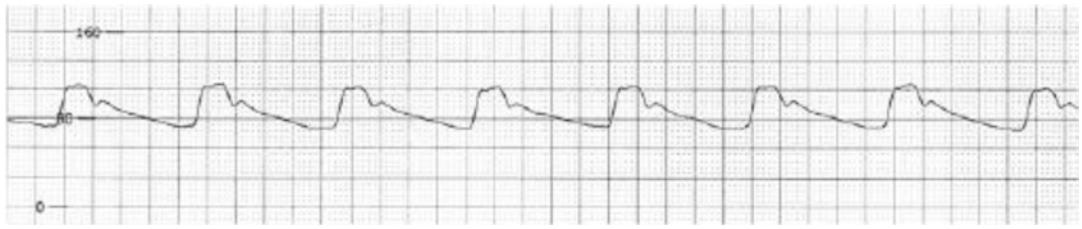

Fig. 21.2 Normal aortic waveform

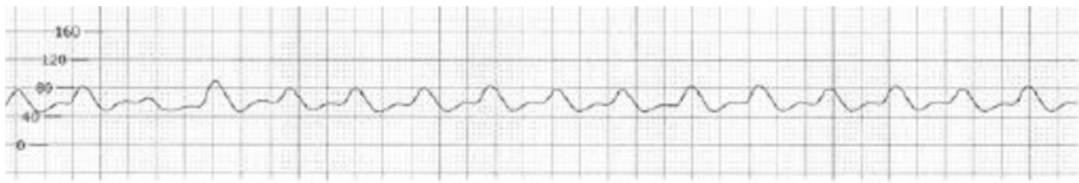

Fig. 21.3 Example of narrow pulse pressure in a patient with cardiogenic shock

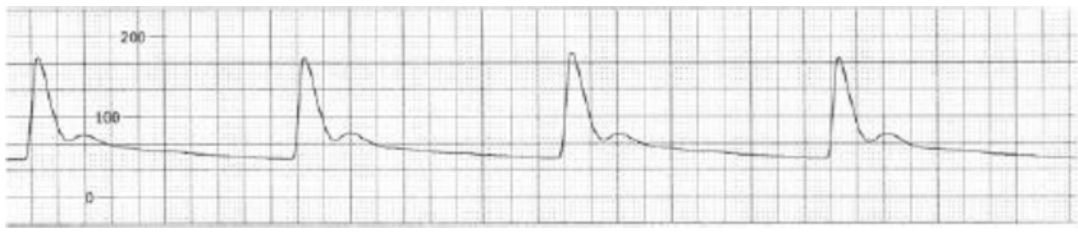

Fig. 21.4 Example of wide pulse pressure in a patient with complete heart block

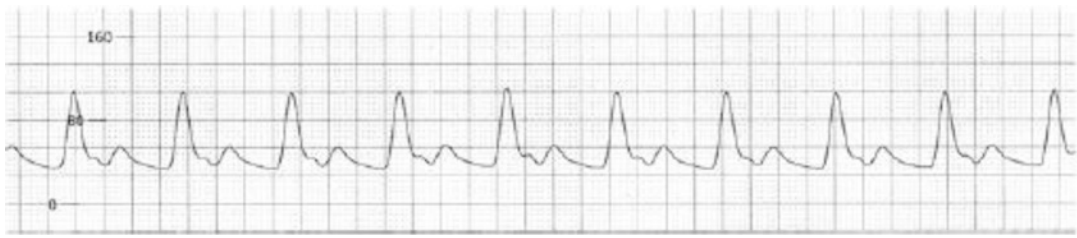

Fig. 21.5 Example of narrow pulse width in a patient with acute aortic dissection

Widened pulse pressure is a physiological response to exercise and can be seen pathologically with atherosclerosis, aortic insufficiency, complete heart block, aortic dissection, arteriovenous fistula, fever, anemia, thyrotoxicosis, pregnancy, and elevated intracranial pressure (see Fig. 21.4).

The pulse width is also a reflection of stroke volume. Patients in shock with normal or hypercontractile ventricles often have aortic waveforms with narrow pulse widths but normal pulse pressures. Both noncardiac (e.g., anaphylaxis and severe sepsis) and cardiac (e.g., tamponade, acute mitral regurgitation, post-myocardial infarction ventricular septal defect, and aortic dissection) etiologies of shock may be associated with narrow pulse widths. A narrow pulse has a spike appearance with a dicrotic notch that appears low (see Fig. 21.5).

Pulsus alternans occurs when there is an alternating rise and fall in systolic pressure

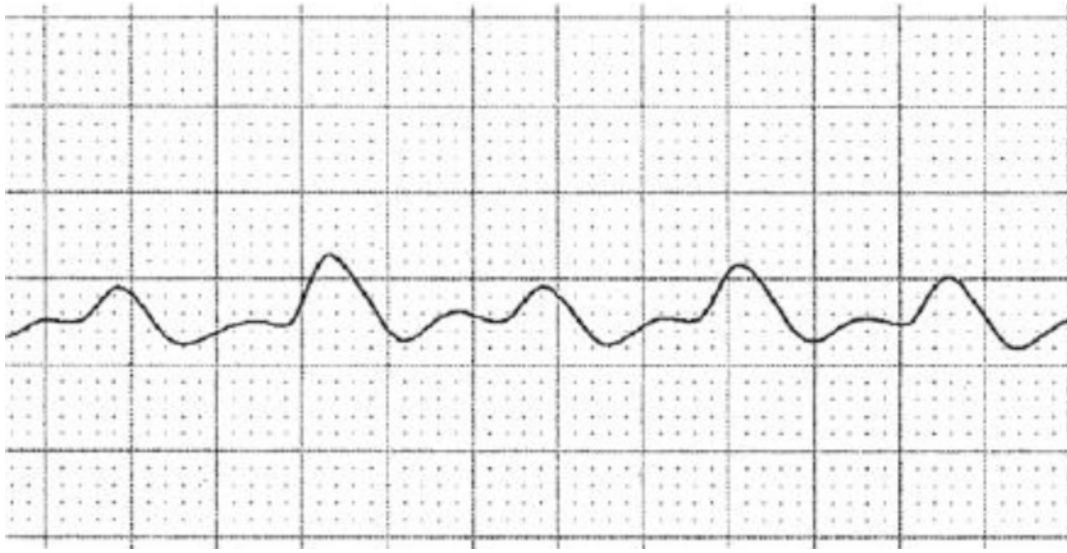

Fig. 21.6 Example of pulses alternans in a patient with advanced left ventricular failure

from beat to beat despite a regular rhythm (see Fig. 21.6). *Pulsus alternans* implies severe myocardial dysfunction and is most often seen in left ventricular failure. It may also occur in association with severe aortic stenosis and severe coronary artery disease. *Pulsus alternans* is thought to be due to variability in myocardial contractility on a beat-to-beat basis because of abnormal intracellular calcium cycling [24].

Pulmonary artery catheter intravascular waveform tracings can also help differentiate various etiologies of shock. Large *v*-waves on the pulmonary capillary wedge pressure tracing suggest shock from acute, severe mitral regurgitation. Likewise, large *v*-waves may be seen on the RAP tracing with severe tricuspid regurgitation. Cannon *a*-waves suggest complete heart block. Elevated and equalized diastolic pressures with loss of y descent suggest cardiac tamponade. Markedly elevated right atrial and right ventricular diastolic pressures and a normal pulmonary capillary wedge pressure suggest CS related to right ventricular infarction. An increase in right-sided pressures with inspiration (Kussmaul's sign) may be observed in right ventricular infarction due to decreased ventricular compliance.

Data obtained from the pulmonary artery catheter may reveal complications of acute myocardial infarction that occur in association with CS. For example, an oxygen step-up upon advancing the catheter from the right atrium to the right ventricle suggests left to right shunting related to ventricular septal rupture.

Arterial hypoxia may complicate shock. Evaluation of hypoxia begins with calculation of the alveolar-arterial (A-a) oxygen gradient. A normal A-a gradient equals 4 + (age/4) or 2.5 + (0.21 × age). Alveolar oxygen is calculated using the alveolar air equation: partial pressure alveolar oxygen (P_AO_2) = oxygen concentration (F_iO_2) × (barometric pressure at sea level (760 mmHg) − partial pressure water vapor (43 mmHg)) − (partial pressure carbon dioxide (P_ACO_2)/respiratory exchange ratio (0.8)). [$P_AO_2 = (F_iO_2 \times (760 - 43)) - (P_ACO_2/0.8)$]. Arterial partial pressure of oxygen is measured using conventional blood gas analysis.

If the A-a gradient is normal and P_aCO_2 is increased, hypoventilation is the suggested cause of hypoxia. With an elevated A-a gradient, proceed to check the mixed venous oxygen saturation. A low mixed venous oxygen saturation suggests hypermetabolism, anemia, or decreased cardiac output. If mixed venous oxygen is normal, administer 100% oxygen. If hypoxia corrects, ventilation/perfusion mismatch is suggested. Ventilation/perfusion mismatch

is caused by airway (e.g., asthma and chronic obstructive pulmonary disease), alveolar (e.g., pneumonia and congestive heart failure), and vascular (e.g., pulmonary embolism) phenomenon. Shunting is suggested if hypoxia does not correct with oxygen supplementation and may be physiological or vascular. Physiological shunting occurs with alveolar collapse (e.g., atelectasis) or decreased alveolar filling (e.g., pneumonia and congestive heart failure). Vascular shunting occurs with right-to-left intracardiac shunts (e.g., atrial or ventricular septal defect) and intrapulmonary shunts (e.g., arteriovenous malformation and hepatopulmonary syndrome).

Hemodynamic data can also be utilized to risk-stratify patients with acute myocardial infarction complicated by CS. In the SHOCK trial, cardiac power (cardiac power = MAP × CO/451) was the strongest independent correlate of in-hospital mortality in patients with CS [25].

Pearls of Assessment

There can be considerable overlap in the clinical presentation of the various categories of shock. Although classically associated with vasoconstriction and cold extremities, patients with CS can present with peripheral vasodilation and warm extremities. Indeed, in the SHOCK trial, the average SVR was not elevated, and the range of values was wide, suggesting that compensatory vasoconstriction is not universal [8].

Patients with distributive shock typically have increased cardiac output. However, in sepsis, depressed myocardial function may occur due to metabolic acidosis and other factors. Acidemia is detrimental to LV contractility and may result from decreased clearance of lactate by the liver, kidneys, and skeletal muscle, further compounded by an anaerobic metabolic state. Inadequate intravascular volume may complicate distributive shock and result in decreased cardiac preload and cardiac output.

Review Questions

1. Which of the following types of shock is typically associated with a high mixed venous oxygenation saturation?
   (a) Septic
   (b) Cardiogenic
   (c) Hypovolemic
   (d) Anaphylactic
   - Answer: (a) In severe sepsis, the mitochondrial respiratory chain does not utilize oxygen effectively. As a result there is more oxygen than expected in the venous blood.
2. Which of the following hemodynamic profiles is most consistent with cardiogenic shock?
   (a) Systolic blood pressure 120 mmHg, pulmonary capillary wedge pressure 10 mmHg, cardiac index 3.5 L/min/m^2, systemic vascular resistance (SVR) 1000 dyn, and mixed venous oxygen 75%
   (b) Systolic blood pressure 80 mmHg, pulmonary capillary wedge pressure 5 mmHg, cardiac index 1.3 L/min/m^2, SVR 1800 dyn, and mixed venous oxygen 60%
   (c) Systolic blood pressure 80 mmHg, pulmonary capillary wedge pressure 10 mmHg, cardiac index 3.5 L/min/m^2, SVR 600 dyn, and mixed venous oxygen 85%
   (d) Systolic blood pressure 80 mmHg, pulmonary capillary wedge pressure 20 mmHg, cardiac index 1.3 L/min/m^2, SVR 1800 dyn, and mixed venous oxygen 60%
   - Answer: (d) Hemodynamic criteria typically associated with cardiogenic shock include systolic blood pressure less than 90 mmHg for at least 30 min or need for vasopressor or intra-aortic balloon support to maintain systolic blood pressure greater than 90 mmHg, pulmonary capillary wedge pressure greater than 15 mmHg, and cardiac index less than 2.2 L/min/kg/m^2 [7].
3. An 85-year-old male presents with hypotension, oliguria, and confusion. An electrocardiogram reveals inferior ST segment elevation. A pulmonary artery catheter is inserted, and the hemodynamic parameters are consistent with cardiogenic shock. His lung fields are clear, and the jugular venous pulse is elevated.

A transthoracic echocardiogram reveals normal left ventricular function. What is the cause of this patient's clinical presentation?
(a) Right ventricular infarct
(b) Ventricular septal rupture
(c) Acute mitral regurgitation
(d) Tamponade
- Answer: (a) The classic findings of right ventricular infarction are hypotension, jugular venous distension, and clear lung fields.

4. An 85-year-old female presents 1 week after developing severe chest pain. She has dyspnea with minimal activity. She is hypotensive and has pulmonary rales. An electrocardiogram reveals anterior *q*-waves. Troponin is elevated but CK-MB is within normal limits. Other laboratory analysis reveals renal and liver injury. Pulmonary artery catheter hemodynamic findings are consistent with cardiogenic shock. An oxygen saturation run reveals an increased oxygen gradient upon advancing from the right atria to the right ventricle. Which complication of acute myocardial infarction is the cause of this patient's shock?
(a) Ventricular free wall rupture
(b) Ventricular septal rupture
(c) Acute mitral regurgitation
(d) Tamponade
- Answer: (b) Ventricular septal rupture may complicate myocardial infarction. An oxygen step-up upon advancing from the right atria to the right ventricle is typical.

Acknowledgments We would like to thank Venu Menon for his contribution to the previous edition of this chapter.

References

1. Goldberg RJ, Gore JM, Alpert JS, et al. Cardiogenic shock after acute myocardial infarction. Incidence and mortality from a community-wide perspective, 1975 to 1988. N Engl J Med. 1991;325:1117–22.
2. Goldberg RJ, Spencer FA, Gore JM, Lessard D, Yarzebski J. Thirty-year trends (1975 to 2005) in the magnitude of, management of, and hospital death rates associated with cardiogenic shock in patients with acute myocardial infarction: a population-based perspective. Circulation. 2009;119:1211–9.
3. Holmes DR Jr, Berger PB, Hochman JS, et al. Cardiogenic shock in patients with acute ischemic syndromes with and without ST-segment elevation. Circulation. 1999;100:2067–73.
4. De Luca L, Olivari Z, Farina A, Gonzini L, Lucci D, Di Chiara A, Casella G, Chiarella F, Boccanelli A, Di Pasquale G, De Servi S, Bovenzi FM, Gulizia MM, Savonitto S. Temporal trends in the epidemiology, management, and outcome of patients with cardiogenic shock complicating acute coronary syndromes. Eur J Heart Fail. 2015;17(11):1124–32.
5. Novosad SA, Sapiano MR, Grigg C, et al. Vital signs: epidemiology of sepsis: prevalence of health care factors and opportunities for prevention. MMWR Morb Mortal Wkly Rep. 2016;65:864–9. https://doi.org/10.15585/mmwr.mm6533e1.
6. Gaieski DF, Edwards JM, Kallan MJ, Carr BG. Benchmarking the incidence and mortality of severe sepsis in the United States. Crit Care Med. 2013;41(5):1167–74.
7. Crawford MH. Current diagnosis & treatment cardiology. 3rd ed. New York: McGraw-Hill; 2009.
8. Menon V, White H, LeJemtel T, Webb JG, Sleeper LA, Hochman JS. The clinical profile of patients with suspected cardiogenic shock due to predominant left ventricular failure: a report from the SHOCK trial registry. SHould we emergently revascularize Occluded Coronaries in cardiogenic shocK? J Am Coll Cardiol. 2000;36:1071–6.
9. Kinch JW, Ryan TJ. Right ventricular infarction. N Engl J Med. 1994;330:1211–7.
10. Hochman JS. Cardiogenic shock complicating acute myocardial infarction: expanding the paradigm. Circulation. 2003;107:2998–3002.
11. Kohsaka S, Menon V, Lowe AM, et al. Systemic inflammatory response syndrome after acute myocardial infarction complicated by cardiogenic shock. Arch Intern Med. 2005;165:1643–50.
12. Killip T III, Kimball JT. Treatment of myocardial infarction in a coronary care unit. A two year experience with 250 patients. Am J Cardiol. 1967;20:457–64.
13. McGee S, Abernethy WB III, Simel DL. The rational clinical examination. Is this patient hypovolemic? JAMA. 1999;281:1022–9.
14. Dellinger RP, Levy MM, Carlet JM, et al. Surviving sepsis campaign: international guidelines for management of severe sepsis and septic shock: 2008. Crit Care Med. 2008;36:296–327.
15. Antman EM, Anbe DT, Armstrong PW, et al. ACC/AHA guidelines for the management of patients with ST-elevation myocardial infarction—executive summary: a report of the American College of Cardiology/American Heart Association task force on practice guidelines (writing committee to revise the 1999 guidelines for the Management of Patients with Acute Myocardial Infarction). Can J Cardiol. 2004;20:977–1025.

16. Binanay C, Califf RM, Hasselblad V, et al. Evaluation study of congestive heart failure and pulmonary artery catheterization effectiveness: the ESCAPE trial. JAMA. 2005;294:1625–33.
17. Allen LA, Rogers JG, Warnica JW, et al. High mortality without ESCAPE: the registry of heart failure patients receiving pulmonary artery catheters without randomization. J Card Fail. 2008;14:661–9.
18. Shah MR, Hasselblad V, Stevenson LW, et al. Impact of the pulmonary artery catheter in critically ill patients: meta-analysis of randomized clinical trials. JAMA. 2005;294:1664–70.
19. Hasdai D, Holmes DR Jr, Califf RM, et al. Cardiogenic shock complicating acute myocardial infarction: predictors of death. GUSTO investigators global utilization of streptokinase and tissue-plasminogen activator for occluded coronary arteries. Am Heart J. 1999;138:21–31.
20. Iberti TJ, Fischer EP, Leibowitz AB, Panacek EA, Silverstein JH, Albertson TE. A multicenter study of physicians' knowledge of the pulmonary artery catheter. Pulmonary artery catheter study group. JAMA. 1990;264:2928–32.
21. Yancy CW, Jessup M, Bozkurt B, Butler J, Casey DE Jr, Drazner MH, Fonarow GC, Geraci SA, Horwich T, Januzzi JL, Johnson MR, Kasper EK, Levy WC, Masoudi FA, McBride PE, McMurray JJV, Mitchell JE, Peterson PN, Riegel B, Sam F, Stevenson LW, Tang WHW, Tsai EJ, Wilkoff BL. 2013 ACCF/AHA guideline for the management of heart failure: executive summary: a report of the American College of Cardiology Foundation/American Heart Association task force on practice guidelines. J Am Coll Cardiol. 2013;62:1495–539.
22. Hochman JS, Buller CE, Sleeper LA, et al. Cardiogenic shock complicating acute myocardial infarction—etiologies, management and outcome: a report from the SHOCK trial registry. SHould we emergently revascularize occluded coronaries for cardiogenic shocK? J Am Coll Cardiol. 2000;36:1063–70.
23. Stevenson LW, Perloff JK. The limited reliability of physical signs for estimating hemodynamics in chronic heart failure. JAMA. 1989;261:884–8.
24. Lab MJ, Lee JA. Changes in intracellular calcium during mechanical alternans in isolated ferret ventricular muscle. Circ Res. 1990;66:585–95.
25. Fincke R, Hochman JS, Lowe AM, et al. Cardiac power is the strongest hemodynamic correlate of mortality in cardiogenic shock: a report from the SHOCK trial registry. J Am Coll Cardiol. 2004;44:340–8.
26. Hochman JS, Ohman EM. Pathophysiology. In: Cardiogenic shock. Hoboken: Wiley-Blackwell; 2009.

Intracoronary Hemodynamics

22

James E. Harvey and Stephen G. Ellis

Selective coronary angiography is the gold standard for evaluating the presence and extent of epicardial coronary artery disease. Despite advances in fluoroscopic imaging and catheterization techniques, the evaluation of the intermediate coronary stenosis (luminal diameter narrowing between 40% and 70%) remains a challenge for invasive cardiologists secondary to multiple issues. Angiography provides only a two-dimensional projection of the arterial lumen along the length of the vessel. Vessel characteristics (e.g., significant angulation and tortuosity) and limitations related to image acquisition (e.g., vessel overlap, inability to obtain a true perpendicular projection of the lesion, and the visualization of a focal short stenosis) impair the accuracy of lesion severity assessment despite obtaining coronary angiograms in multiple fluoroscopic views. Studies comparing coronary angiography and postmortem histopathological analysis have demonstrated the discrepancy between angiographic and actual anatomic findings [1–3]. Significant intra- and interobserver variability is also a factor when determining the percent narrowing of a stenosis by angiography [4]. The application of quantitative coronary angiography (QCA) may minimize this discrepancy, but it does not eradicate the limitations of coronary angiography. Intravascular visualization techniques such as intravascular ultrasound (IVUS) or optical coherence tomography (OCT), augment anatomical analysis but do not necessarily provide information on the functional significance of a lesion. Thus, cardiologists have focused on physiologic assessment of a lesion to aid in management decisions. Noninvasive testing (i.e., stress testing) to determine objective evidence of ischemia is frequently conducted prior to performing coronary angiography and subsequent percutaneous coronary intervention (PCI). However, these studies are not always feasible nor are the results always reliable; therefore a physiologic method of evaluating an intermediate coronary lesion while in the catheterization suite is desirable.

Sensor-tipped 0.014″ diameter guidewires have been manufactured to accurately and safely measure flow velocities or pressure within a coronary artery. By employing this technology, three methods [coronary flow reserve (CFR), fractional flow reserve (FFR), and instantaneous wave-free ratio (iFR)] have been developed to evaluate the physiologic or functional significance of coronary lesions in the cardiac catheterization suite.

Case Vignette #1

A 58-year-old woman with history of diabetes mellitus (DM) and family history of premature CAD presents with a 7-month history of exertional chest

J. E. Harvey (✉)
York Hospital, WellSpan Health System, York, PA, USA

S. G. Ellis
Cleveland Clinic, Cleveland, OH, USA
e-mail: elliss@ccf.org

A. T. Askari, A. W. Messerli (eds.), *Cardiovascular Hemodynamics*, Contemporary Cardiology,
https://doi.org/10.1007/978-3-030-19131-3_22

discomfort. Exercise nuclear stress test revealed reversible perfusion defects in the apical anterior and anteroseptal wall and in the mid inferior wall. Coronary angiography revealed "normal coronary arteries" and intravenous infusion of ergonovine did not precipitate coronary vasospasm. Coronary flow reserve (CFR) of the left anterior descending artery was 1.2 consistent with severe microvascular dysfunction.

Coronary Flow Reserve (CFR)

CFR is defined as the ratio of mean blood velocity at maximal hyperemia to mean blood velocity at rest for a given coronary artery [5]. Developed in the 1970s, it is based on the principle that the volume of blood flow in a healthy coronary artery will increase with hyperemia to a greater extent than that of an artery with a physiologically significant stenosis (Fig. 22.1). Since blood flow as volume per time cannot be directly measured in the cardiac catheterization suite, blood velocity is measured as a surrogate because it is proportional to blood volume flow for a constant lumen area. CFR is assessed by placing a Doppler-tipped guide wire into a coronary artery distal to the epicardial stenosis in question. One then measures the flow velocities at rest and at maximal hyperemia. Hyperemia is pharmacologically induced typically by intravenous infusion of adenosine. The Doppler-derived CFR, which is inversely proportional to lesion severity [6], has been validated with good correlation to nuclear stress testing. A CFR value of ≤2.0 indicates a physiologically significant stenosis (Fig. 22.2) [7–10].

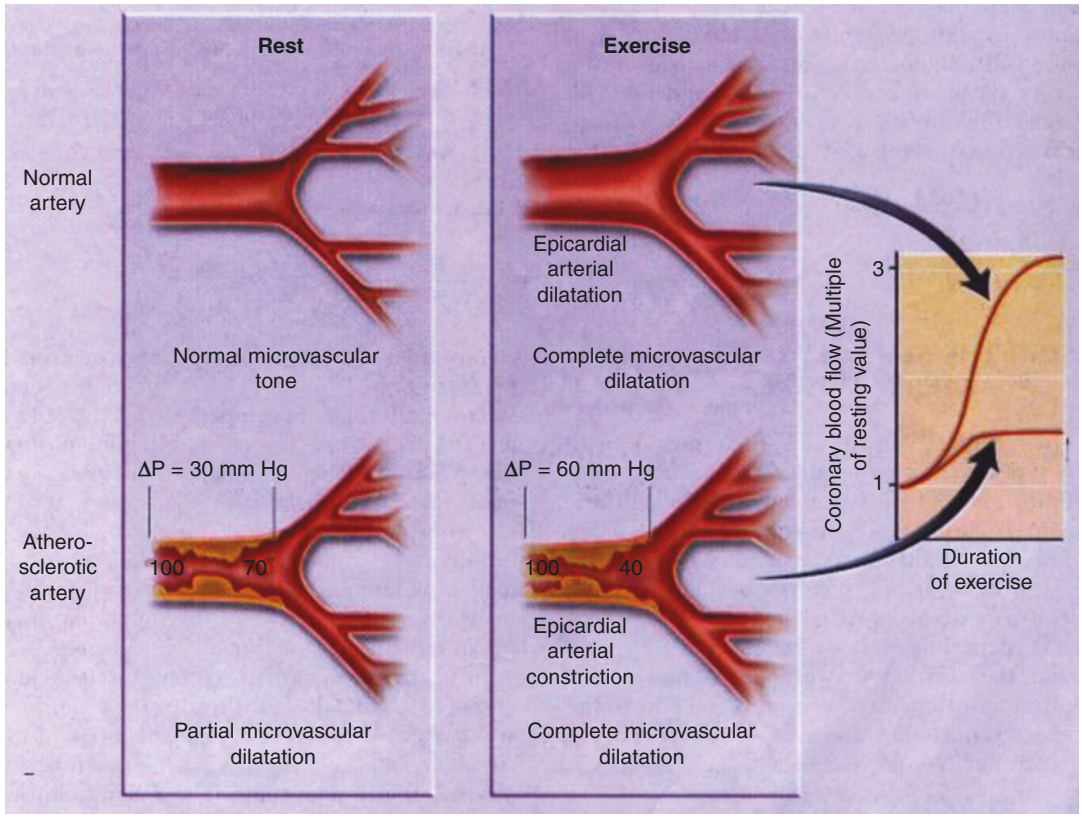

Fig. 22.1 Depiction of coronary blood flow at rest and at maximal hyperemia. A normal coronary artery will have a larger increase in blood flow than a diseased artery with a hemodynamically significant stenosis. By measuring the blood velocity or pressure proximal and distal to the stenosis, one can calculate the relative increase in blood flow or decrease in pressure caused by inducing maximal hyperemia

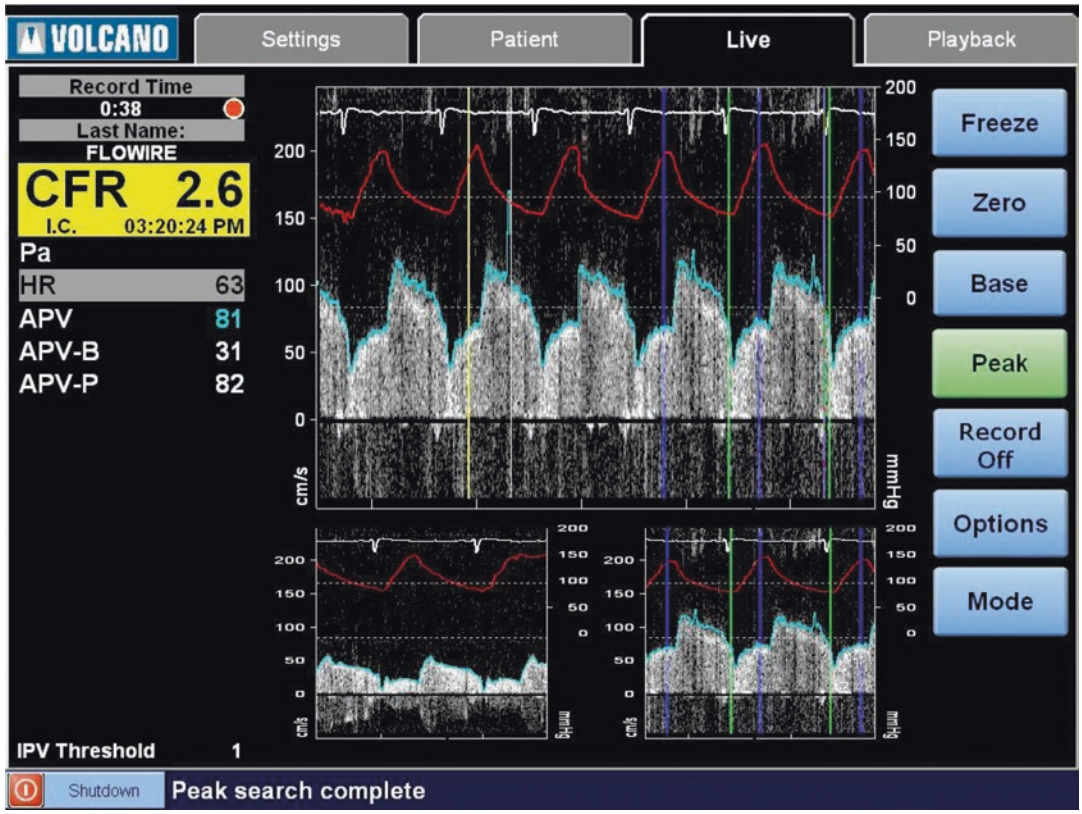

Fig. 22.2 A typical CFR display screen. Intracoronary Doppler blood flow velocity waveforms before intracoronary adenosine are shown on the small graph on the lower left portion of the display screen. Intracoronary Doppler blood flow velocity waveforms after intracoronary adenosine are shown on the small graph on the lower right portion of the display screen and on the large graph in the center of the display. CFR is the ratio of the average peak velocities before and after adenosine; here it is reported as 2.6 on the top left portion of the display. This is suggestive of normal microvascular function

Unfortunately, CFR is affected by both the severity of an epicardial stenosis and the extent of microvascular resistance. Microvascular resistance is influenced by common conditions such as diabetes mellitus, age, and ventricular hypertrophy. Each of these can significantly affect the CFR value regardless of the severity of epicardial stenosis [11–14]. In an effort to overcome this inherent limitation, the concept of relative CFR was developed. Relative CFR is determined by dividing the CFR of the diseased vessel by the CFR of another undiseased coronary vessel and accounts for the contribution of microvascular resistance to the CFR value. This improved the correlation in the detection of ischemia by stress myocardial perfusion imaging [15]. Use of this method requires increased time and risk of evaluating an additional vessel. Due to these inherent limitations of CFR and relative CFR, these modalities are now rarely used to evaluate the severity of an epicardial arterial stenosis. Instead, FFR has become the method of choice for determining the physiologic significance of an epicardial arterial stenosis.

Cardiac Syndrome X

Despite its limitations in the interrogation of epicardial stenoses, CFR is the modality of choice for evaluation of coronary artery microvascular dysfunction. Cardiac syndrome X, or angina with an abnormal cardiac stress test and angiographically normal coronary arteries, is an increasingly

recognized disorder with significant prognostic implications [16]. Diminished coronary flow velocity reserve in response to intracoronary adenosine, defined as a CFR ≤ 2.0, is suggestive of microvascular dysfunction and seen in up to 47% of patients with angina and no significant epicardial stenoses [17]. The patient described in *Clinical Vignette 1* has findings consistent with cardiac syndrome X. Patients with this condition have a rate of adverse cardiac events (myocardial infarction, congestive heart failure, stroke, and sudden cardiac death) of 2.5% per year [16].

Case Vignette 2

A 62-year-old man with past medical history of hypertension, hyperlipidemia, and cigarette smoking presents with 1 month of worsening exertional chest discomfort that radiates down his left arm. Left heart catheterization reveals a focal 70% stenosis in the proximal left circumflex artery (LCx) and a long 60% stenosis in the mid right coronary artery (RCA). A pressure sensor-tipped 0.014″ coronary wire was advanced down the LCx and FFR was performed with a value of 0.83. The pressure sensor-tipped 0.014″ coronary wire was withdrawn and then advanced down to the distal RCA. FFR was 0.72. Percutaneous coronary intervention (PCI) was performed on the mid RCA lesion. No PCI was performed on the LCx, but rather aggressive medical management was employed.

Fractional Flow Reserve (FFR)

FFR is a method to invasively assess the hemodynamic significance of an intermediate coronary stenosis while in the catheterization suite. It is defined as the ratio of the mean distal coronary artery pressure to the mean aortic pressure while at maximal hyperemia [18–20]. It is performed by advancing a 0.014″ pressure-sensor tipped coronary wire across an epicardial stenosis and simultaneously recording the pressure distal to the stenosis (via the coronary wire) and proximal to the stenosis (via the guide catheter) while at maximal hyperemia (Fig. 22.3). Adenosine is the pharmacologic agent typically used to achieve maximal hyperemia because of its safety profile and low cost; however, papaverine or dobutamine can also be used [21–23].

As opposed to CFR, FFR measurement is baseline independent of blood pressure, heart rate, prior infarction, or contribution of collateral circulation [20, 24]. A normal FFR value is 1, while a value of <0.75 is associated with provocable ischemia; this has been shown to correlate well with ischemia demonstrated on noninvasive stress testing [19, 20, 25, 26]. Mortality and adverse cardiovascular event (MACE) rates have been shown to be very low in patients with an FFR >0.75 [27, 28], and multiple studies have demonstrated that PCI can be safely deferred in such patients [19, 27, 29].

Multivessel CAD

FFR is "lesion specific" and can be used to assess intermediate lesions in patients with single-vessel or multivessel CAD. [30] This is particularly useful in clinical scenarios in which patients present with symptomatic CAD and are found to have multivessel disease with multiple intermediate stenoses. In this subset of patients, noninvasive stress testing can demonstrate "balanced ischemia," and thus interpretations of culprit lesions are often inaccurate. Because of this, it has become commonplace to perform multivessel PCI for complete revascularization in this group, although this approach is not proven to be associated with improved outcomes. It was hypothesized that utilization of FFR could aid in the better identification of culprit lesions and thus more appropriate management. To assess the utility of FFR in this group of patients, 1005 patients with multivessel coronary artery disease were randomized to PCI with drug-eluting stents of all stenoses ≥50% versus FFR-guided PCI of stenoses with a value ≤0.80. At 1 year, the rate of death, non-fatal myocardial infarction, and repeat revascularization was significantly lower in the FFR-guided group than in the angiography-guided group (13.2% versus 18.3%), and the FFR group received a significantly fewer number of stents [31]. Eighty percent of patients in both groups

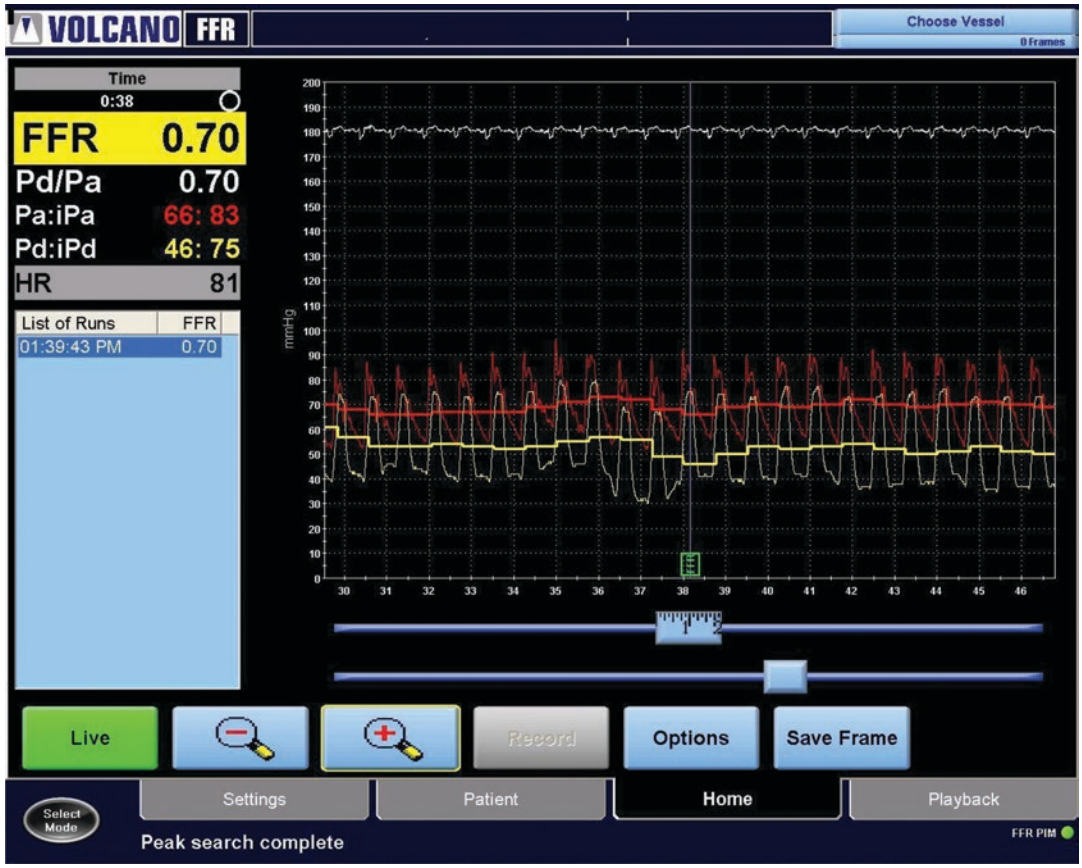

Fig. 22.3 A typical FFR measurement display screen. The aortic pressure is measured through the guiding catheter (red line). The pressure distal to the coronary lesion is measured by the 0.014″ pressure sensor-tipped wire (yellow line). In this example, the ratio of the distal coronary pressure to proximal coronary pressure is 0.70 and consistent with a hemodynamically significant stenosis

were angina-free at 1 year; however, the FFR-guided strategy was significantly less expensive than the angiography-guided group ($14,315 versus $16,700) [31].

Diffuse CAD or Long Coronary Lesions

Another subset of patients in which FFR can be helpful to guide the decision for PCI is in patients with diffuse disease or long coronary lesions. Similar to the assessment of multiple lesions in a single vessel, the pressure-sensor tipped wire can be slowly withdrawn from a vessel during maximal hyperemia and concomitant fluoroscopy can be used to precisely indicate where hemodynamically significant lesions exist. A gradual loss of pressure is consistent with diffuse disease and may suggest that PCI is technically less favorable and that possibly coronary artery bypass grafting (CABG) or medical management should be considered. However, an abrupt decrease in pressure is consistent with a focal hemodynamically significant stenosis and suggests that PCI may be more favorable [32, 33].

Left Main Coronary Disease and Bifurcation Lesions

Angiographic assessment of a left main coronary artery stenosis poses a great challenge for operators. As previously mentioned, factors such

as vessel overlap and unfavorable vessel orientation in relation to achievable camera angles often result in a suboptimal angiographic assessment of the vessel and significant intra-observer variability [34]. In this subset of patients, the use of FFR to further assess the vessel has been shown to be beneficial. One study demonstrated that patients with an intermediate left main stenosis and an FFR >0.75 had superb 3-year outcomes suggesting that PCI can safely be deferred in this subgroup [35].

Similar to left main coronary artery lesions, the evaluation of bifurcation lesions poses a significant challenge to the angiographer. By performing a separate FFR of each branch of the bifurcation, the hemodynamic significance of the lesions can be reliably determined and can assist the operator in deciding the most appropriate course of action for the patient [36].

Coronary Bypass Grafts

There is a paucity of data regarding the utility of FFR in assessing the physiologic significance of intermediate stenoses in a saphenous vein graft (SVG). A small study observed 10 veterans who had a stress myocardial perfusion imaging (MPI) study and were referred for PCI of an SVG stenosis. The sensitivity, specificity, and accuracy of FFR <0.75 for the detection of ischemia on stress MPI were 50%, 75%, and 70%, respectively. The authors concluded that the use of FFR to assess the physiologic significance of SVG lesions was feasible and provided acceptable sensitivity and specificity in comparison to stress MPI.

Acute Myocardial Infarction and Post Myocardial Infarction

While FFR does provide valuable information regarding intermediate coronary lesions in patients with stable and unstable angina, it should not be used in the acute phase of a myocardial infarction (MI). Animal studies have shown that even after reperfusion of an epicardial coronary occlusion, significant perivascular edema and capillary leukocyte plugging occur causing microvascular dysfunction and incomplete restoration of myocardial perfusion [37]. This has been shown to result in up to a 5% overestimation of FFR in humans [38]. Six days after an MI, however, FFR has been shown to be accurate and can be used to identify hemodynamically significant coronary lesions that supply areas with significant remaining ischemic but viable myocardium [39]. Myocardial perfusion SPECT imaging and FFR were performed in 57 patients who had sustained a myocardial infarction at least 6 days prior. Patients with demonstrable ischemia on SPECT imaging had a significantly lower FFR value than those who had evidence of scar without ischemia. When using a cutoff FFR value of 0.75, this demonstrated a sensitivity and specificity of 82% and 87%, respectively. However, when only truly positive and truly negative stress tests were considered, the sensitivity and specificity rose to 87% and 100%, respectively. When sensitivity and specificity were plotted against FFR, the value of FFR for which sensitivity and specificity were equal (88%) was 0.78; however, this value did not show a statistically significant difference in accuracy when compared to a cutoff value of 0.75.

FFR Post PCI

FFR has been shown to have significant prognostic value after PCI has been performed [40–42]. An FFR $\geq$ 0.90 is considered a successful result for balloon angioplasty, and an FFR $\geq$0.94 is successful post stent deployment. FFR values lower than these predict adverse outcomes.

Another area where FFR can be helpful is in the evaluation of jailed side branches after stenting. One study observing the feasibility of FFR for the assessment of jailed side branches showed that only 20% of lesions with QCA >75% had an FFR <0.75 and no lesion with QCA <75% had an FFR <0.75 [43]. These data suggest that most jailed side branches do not have hemodynamically significant stenoses and that PCI of

the daughter vessel can likely be safely deferred. This information is particularly useful given the higher rate of restenosis and stent thrombosis associated with dual stenting of bifurcation lesions [44].

Limitations of FFR

While several randomized controlled trials have demonstrated the clinical benefit of FFR-guided coronary revascularization, certain limitations do exist. FFR is not always accurate in AMI and will often show a falsely elevated value due to microvascular dysfunction. Also, animal studies have suggested that up to 16% of subjects undergoing FFR with adenosine or papaverine do not achieve maximal hyperemia [45]. This suggests that the physiologic significance of some lesions may be underestimated when using standard current vasodilator doses and that higher doses may be needed in order to achieve maximal hyperemia.

Instantaneous Wave-Free Ratio (iFR)

Recently, a new method of invasively assessing the severity of intermediate coronary stenoses has been introduced called the Instantaneous Wave-Free Ratio (iFR). Unlike FFR, coronary lesion assessment with iFR is performed during the resting, or non-hyperemic state, such that the administration of adenosine or other vasodilating agents is not necessary.

iFR is based on the finding that there are multiple distinct pressure waves that occur throughout the cardiac cycle that affect the instantaneous flow and pressure in a coronary artery. The relationship between intracoronary pressure and flow varies throughout the cardiac cycle and is different in the region proximal to a coronary stenosis than it is in the region distal to a coronary stenosis [46]. However, there is a period of time in diastole called the wave-free period (WFP) where there is an absence of new intracoronary pressure waves. During this period, the intracoronary pressure and the intracoronary flow decline in a parallel linear fashion and the microvascular resistance is significantly lower and more stable than that over the remainder of the cardiac cycle [47]. As such, this provides an ideal set of circumstances to allow for the assessment of the hemodynamic significance of a coronary stenosis in a non-hyperemic state.

Similar to FFR, iFR is performed by advancing a 0.014″ pressure-sensor tipped coronary wire across an epicardial stenosis and simultaneously recording the pressure distal to the stenosis (via the coronary wire) and proximal to the stenosis (via the guide catheter) (Fig. 22.3). However, unlike FFR, the iFR measurement is recorded during the instantaneous wave-free period of diastole. As such, this is done with the patient in the resting state without inducing hyperemia.

iFR and the Hybrid Approach

Initially, it was proposed that the use of iFR would complement that of FFR via a "hybrid approach" for the assessment of intermediate intracoronary lesions. With this strategy, iFR would be performed with the patient in the resting state. An iFR value of more than 0.93 would be considered not significant and revascularization would be deferred, while an iFR value of less than 0.86 would be considered ischemic and revascularization would be pursued. However, the values ranging between 0.86 and 0.93 would be considered in the "gray zone." In these patients, adenosine would be administered to calculate the FFR to determine whether or not the lesion should be revascularized. Utilization of this strategy was able to reduce the unnecessary use of adenosine in 60 to 70% of patients [48]. While this strategy provided a practical way to integrate the use of iFR into current clinical practice, two large randomized clinical trials have recently demonstrated the non-inferiority of iFR when compared to FFR such that utilization of the hybrid approach is no longer necessary.

iFR Versus FFR in Clinical Trials

Two large randomized clinical trials have demonstrated that the use of iFR with a single cut-off value of ≤0.89 to guide revascularization is a safe and feasible alternative to FFR. With a primary endpoint of MACE at 1 year, the Functional Lesion Assessment of Intermediate Stenosis to Guide Revascularization (DEFINE-FLAIR) trial was a double-blinded, controlled trial that randomized 2492 patients to iFR vs. FFR for guidance of coronary revascularization for intermediate lesions [49]. The primary endpoint occurred in 78 of 1148 patients (6.8%) in the iFR group and in 83 of 1182 patients (7.0%) in the FFR group ($p < 0.001$ for non-inferiority). In addition, the number of patients with adverse procedural symptoms or clinical signs was significantly lower in the iFR vs. FFR group (3.1% vs. 30.8%, respectively; $p < 0.001$) as was the median procedural time (40.5 min vs. 45.0 min; $p = 0.001$). Similarly, the Instantaneous Wave-free Ratio versus Fractional Flow Reserve in Patients with Stable Angina Pectoris or Acute Coronary Syndrome (iFR SWEDEHEART) trial was an open-label randomized trial comparing iFR to FFR guided revascularization in patients presenting with stable angina or an acute coronary syndrome. Among the 2037 patients enrolled, the primary endpoint of MACE at 1 year occurred in 68 of the 1012 patients (6.7%) in the iFR group and in 61 of the 1007 patients (6.1%) in the FFR group ($p = 0.007$ for non-inferiority) [50]. The secondary endpoint of adverse procedural symptoms was again significantly higher in the FFR group with chest pain occurring in 68.3% of these patients compared to only 3.0% in the iFR group ($p < 0.001$).

Despite the demonstration of non-inferiority of iFR to FFR, the DEFINE-FLAIR and iFR SWEDEHEART trials demonstrated that the deferral of revascularization occurred more frequently in patients undergoing iFR as compared to those undergoing FFR [51]. In a pooled analysis of the two trials, revascularization was deferred in 1119 of the 2240 patients (50.0%) in the combined iFR groups and in 1015 of the 2246 patients (45.0%) in the combined FFR groups. Most importantly, the primary outcome between the groups was similarly low despite the higher rate of deferral in the pooled iFR group. As a result, the resultant healthcare costs for the iFR group were significantly lower than that of the FFR group.

In addition to the benefits of decreased adverse procedural symptoms, procedural time, and procedural cost of iFR vs. FFR, another potential benefit exists. In the hyperemic state such as that during FFR, coronary flow distal to a stenosis begins to decrease once the stenosis is 40–50% narrowed. As such, when multiple sequential intermediate lesions are present, the hyperemic flow through the proximal stenosis is affected by that of the distal stenosis and vice versa. Thus, it is not possible to determine the severity of an individual stenosis in the hyperemic state [52]. Conversely, coronary flow in the resting state is preserved distal to a coronary lesion until a critical stenosis develops [46]. As a result, there is minimal interaction between sequential intermediate stenoses. This allows for accurate assessment of individual lesion severity in the presence of tandem stenoses with slow pullback of the 0.014″ pressure-sensor tipped coronary wire.

Conclusions

CFR and relative CFR can be used to invasively measure flow velocity in a coronary artery and thus evaluate the hemodynamic significance of epicardial stenoses or microvascular dysfunction. Due to the limitations of CFR and increased time requirements and risk of relative CFR, these methods are now rarely used to assess epicardial lesions. However, CFR is still the test of choice to evaluate for microvascular dysfunction.

FFR is the current method of choice to evaluate the physiologic significance of an intermediate epicardial stenosis. Designated as "lesion specific," it compares the ratio of distal to proximal pressure across an epicardial stenosis. This technique adds important functional information that augments the anatomic information provided by angiography and intravascular imaging modalities (i.e., IVUS and OCT). It has been validated

to improve clinical outcomes when used to guide PCI in patients with single and multivessel CAD and also has been shown to provide useful information when examining a variety of coronary lesions. Furthermore, the use of FFR to guide PCI has been shown to significantly reduce the cost of treatment when compared to PCI guided by angiography alone.

iFR is the newest method of invasively assessing the severity of intermediate coronary stenoses. There are several advantages of iFR over FFR including decreased procedural time and cost and reduced adverse procedural symptoms. With the completion of two large randomized trials, the use of iFR is supported by more than twice the outcome data of that of FFR. Although slowly being adopted by practitioners worldwide, it is believed that iFR will become the method of choice for the evaluation of intermediate coronary stenoses in the years to come.

Review Questions

Questions 1–2

A 62-year-old patient undergoing left heart catheterization for chest pain has a 65% stenosis in a large first diagonal branch. While performing an FFR measurement, the aortic pressure is 102/77 mmHg and the distal diagonal branch mean pressure is 60 mmHg.

1. What is the FFR of the diagonal branch?
   A. 0.779
   B. 0.588
   C. 0.703
   D. Cannot be determined with the information provided.
2. Is PCI of the diagonal branch indicated?
   A. Yes. The FFR was >0.75
   B. No. The FFR was <0.75
   C. Yes. The FFR was <0.75
   D. It depends on the severity of the stenosis in the artery.

Questions 3–4

A 63-year-old hypertensive patient presents with 12 months of intermittent exertional chest pain. An exercise nuclear stress test performed at an outside hospital reported a reversible perfusion defect involving the anteroseptal and lateral walls; however, left heart catheterization revealed angiographically normal coronary arteries. You perform CFR of the LAD which gives a result of 1.6.

3. What is the diagnosis does this patient have?
   A. Non-cardiac chest pain.
   B. Cardiac chest pain due to missed coronary stenosis.
   C. False-positive nuclear stress test.
   D. Cardiac syndrome X.
4. What is the risk of this patient having an adverse cardiovascular event in the next year?
   A. 2.5%
   B. 1%
   C. 10%
   D. 15%
5. You perform a left heart catheterization on a 59-year-old man with worsening exertional angina. Coronary angiography of the RCA reveals a mid 60% stenosis followed by a distal 60% stenosis; the left main trunk, LAD, and LCx have mild disease. You perform iFR of the RCA with slow pullback of the pressure sensor-tipped 0.014″ coronary wire. You obtain the following results:

   - iFR of the right posterior descending artery: 0.76
   - iFR of the RCA between the mid and distal lesions: 0.81
   - iFR of the proximal RCA: 1.00

   What is the most appropriate management decision at this time?

   A. Perform PCI on both the mid and distal RCA lesions.
   B. Perform PCI on the mid RCA lesion.
   C. Perform PCI on the distal RCA lesion.
   D. None of the above.

Answers

1. The Answer is **C**. In order to calculate the FFR you first need to calculate the mean pressure (MP) in the aorta. This can be calculated by the following equation: MP = Diastolic

pressure + (Systolic pressure − diastolic pressure)/3. Plugging the numbers into the equation, the MP = 85.3 mmHg. FFR = MP_{distal}/MP_{aorta} = 60/85.3 = 0.703.

2. The Answer is **C**. PCI is indicated based on the DEFER (FFR <0.75) and FAME (FFR <0.80) studies.
3. The Answer is **D**. Cardiac syndrome X, or angina with an abnormal cardiac stress test and angiographically normal coronary arteries. A CFR ≤2 is suggestive of microvascular disease, the underlying pathophysiology of this syndrome.
4. The Answer is **A**. This patient has a 2.5% chance of having a myocardial infarction, stroke, sudden cardiac death, or developing congestive heart failure over the next year.
5. The Answer is **B**. Performing a slow pullback across multiple serial stenoses in a single vessel during iFR allows the operator to determine the hemodynamic significance of each individual stenosis. In this example, the hemodynamic contribution of the distal RCA stenosis was 0.95 ((1 − (0.81 – 0.76) = (1 – 0.05) = 0.95). The hemodynamic significance of the mid RCA stenosis was 0.81. Thus, the most appropriate management decision is to perform PCI on the mid RCA lesion only.

References

1. Grondin CM, Dyrda I, Pasternac A, Campeau L, Bourassa MG, Lesperance J. Discrepancies between cineangiographic and postmortem findings in patients with coronary artery disease and recent myocardial revascularization. Circulation. 1974;49:703–8.
2. Hutchins GM, Bulkley BH, Ridolfi RL, Griffith LS, Lohr FT, Piasio MA. Correlation of coronary arteriograms and left ventriculograms with postmortem studies. Circulation. 1977;56:32–7.
3. Arnett EN, Isner JM, Redwood DR, et al. Coronary artery narrowing in coronary heart disease: comparison of cineangiographic and necropsy findings. Ann Intern Med. 1979;91:350–6.
4. Fisher LD, Judkins MP, Lesperance J, et al. Reproducibility of coronary arteriographic reading in the coronary artery surgery study (CASS). Catheter Cardiovasc Diagn. 1982;8:565–75.
5. Gould KL, Lipscomb K, Hamilton GW. Physiologic basis for assessing critical coronary stenosis. Instantaneous flow response and regional distribution during coronary hyperemia as measures of coronary flow reserve. Am J Cardiol. 1974;33:87–94.
6. Gould KL, Kirkeeide RL, Buchi M. Coronary flow reserve as a physiologic measure of stenosis severity. J Am Coll Cardiol. 1990;15:459–74.
7. Doucette JW, Corl PD, Payne HM, et al. Validation of a Doppler guide wire for intravascular measurement of coronary artery flow velocity. Circulation. 1992;85:1899–911.
8. Labovitz AJ, Anthonis DM, Cravens TL, Kern MJ. Validation of volumetric flow measurements by means of a Doppler-tipped coronary angioplasty guide wire. Am Heart J. 1993;126:1456–61.
9. Miller DD, Donohue TJ, Younis LT, et al. Correlation of pharmacological 99mTc-sestamibi myocardial perfusion imaging with poststenotic coronary flow reserve in patients with angiographically intermediate coronary artery stenoses. Circulation. 1994;89:2150–60.
10. Heller LI, Cates C, Popma J, et al. Intracoronary Doppler assessment of moderate coronary artery disease: comparison with 201Tl imaging and coronary angiography. FACTS study group. Circulation. 1997;96:484–90.
11. Akasaka T, Yoshida K, Hozumi T, et al. Retinopathy identifies marked restriction of coronary flow reserve in patients with diabetes mellitus. J Am Coll Cardiol. 1997;30:935–41.
12. Lorenzoni R, Gistri R, Cecchi F, et al. Coronary vasodilator reserve is impaired in patients with hypertrophic cardiomyopathy and left ventricular dysfunction. Am Heart J. 1998;136:972–81.
13. Czernin J, Muller P, Chan S, et al. Influence of age and hemodynamics on myocardial blood flow and flow reserve. Circulation. 1993;88:62–9.
14. Schafer S, Kelm M, Mingers S, Strauer BE. Left ventricular remodeling impairs coronary flow reserve in hypertensive patients. J Hypertens. 2002;20:1431–7.
15. Voudris V, Avramides D, Koutelou M, et al. Relative coronary flow velocity reserve improves correlation with stress myocardial perfusion imaging in assessment of coronary artery stenoses. Chest. 2003;124:1266–74.
16. Bugiardini R, Bairey Merz CN. Angina with "normal" coronary arteries: a changing philosophy. JAMA. 2005;293:477–84.
17. Reis SE, Holubkov R, Conrad Smith AJ, et al. Coronary microvascular dysfunction is highly prevalent in women with chest pain in the absence of coronary artery disease: results from the NHLBI WISE study. Am Heart J. 2001;141:735–41.
18. Pijls NH, van Son JA, Kirkeeide RL, De Bruyne B, Gould KL. Experimental basis of determining maximum coronary, myocardial, and collateral blood flow by pressure measurements for assessing functional stenosis severity before and after percutaneous transluminal coronary angioplasty. Circulation. 1993;87:1354–67.
19. Pijls NH, De Bruyne B, Peels K, et al. Measurement of fractional flow reserve to assess the functional

severity of coronary-artery stenoses. N Engl J Med. 1996;334:1703–8.
20. Kern MJ, de Bruyne B, Pijls NH. From research to clinical practice: current role of intracoronary physiologically based decision making in the cardiac catheterization laboratory. J Am Coll Cardiol. 1997;30:613–20.
21. Di Segni E, Higano ST, Rihal CS, Holmes DR Jr, Lennon R, Lerman A. Incremental doses of intracoronary adenosine for the assessment of coronary velocity reserve for clinical decision making. Catheter Cardiovasc Interv. 2001;54:34–40.
22. Wilson RF, White CW. Intracoronary papaverine: an ideal coronary vasodilator for studies of the coronary circulation in conscious humans. Circulation. 1986;73:444–51.
23. Bartunek J, Wijns W, Heyndrickx GR, de Bruyne B. Effects of dobutamine on coronary stenosis physiology and morphology: comparison with intracoronary adenosine. Circulation. 1999;100:243–9.
24. de Bruyne B, Bartunek J, Sys SU, Pijls NH, Heyndrickx GR, Wijns W. Simultaneous coronary pressure and flow velocity measurements in humans. Feasibility, reproducibility, and hemodynamic dependence of coronary flow velocity reserve, hyperemic flow versus pressure slope index, and fractional flow reserve. Circulation. 1996;94:1842–9.
25. Caymaz O, Fak AS, Tezcan H, et al. Correlation of myocardial fractional flow reserve with thallium-201 SPECT imaging in intermediate-severity coronary artery lesions. J Invasive Cardiol. 2000;12:345–50.
26. Leesar MA, Abdul-Baki T, Akkus NI, Sharma A, Kannan T, Bolli R. Use of fractional flow reserve versus stress perfusion scintigraphy after unstable angina. Effect on duration of hospitalization, cost, procedural characteristics, and clinical outcome. J Am Coll Cardiol. 2003;41:1115–21.
27. Bech GJ, De Bruyne B, Bonnier HJ, et al. Long-term follow-up after deferral of percutaneous transluminal coronary angioplasty of intermediate stenosis on the basis of coronary pressure measurement. J Am Coll Cardiol. 1998;31:841–7.
28. Bech GJ, De Bruyne B, Pijls NH, et al. Fractional flow reserve to determine the appropriateness of angioplasty in moderate coronary stenosis: a randomized trial. Circulation. 2001;103:2928–34.
29. Kern MJ, Donohue TJ, Aguirre FV, et al. Clinical outcome of deferring angioplasty in patients with normal translesional pressure-flow velocity measurements. J Am Coll Cardiol. 1995;25:178–87.
30. Chamuleau SA, Meuwissen M, Koch KT, et al. Usefulness of fractional flow reserve for risk stratification of patients with multivessel coronary artery disease and an intermediate stenosis. Am J Cardiol. 2002;89:377–80.
31. Tonino PA, De Bruyne B, Pijls NH, et al. Fractional flow reserve versus angiography for guiding percutaneous coronary intervention. N Engl J Med. 2009;360:213–24.
32. Pijls NH, De Bruyne B, Bech GJ, et al. Coronary pressure measurement to assess the hemodynamic significance of serial stenoses within one coronary artery: validation in humans. Circulation. 2000;102:2371–7.
33. De Bruyne B, Pijls NH, Heyndrickx GR, Hodeige D, Kirkeeide R, Gould KL. Pressure-derived fractional flow reserve to assess serial epicardial stenoses: theoretical basis and animal validation. Circulation. 2000;101:1840–7.
34. Mintz GS, Kent KM, Pichard AD, Satler LF, Popma JJ, Leon MB. Contribution of inadequate arterial remodeling to the development of focal coronary artery stenoses. An intravascular ultrasound study. Circulation. 1997;95:1791–8.
35. Bech GJ, Droste H, Pijls NH, et al. Value of fractional flow reserve in making decisions about bypass surgery for equivocal left main coronary artery disease. Heart. 2001;86:547–52.
36. Ziaee A, Parham WA, Herrmann SC, Stewart RE, Lim MJ, Kern MJ. Lack of relation between imaging and physiology in ostial coronary artery narrowings. Am J Cardiol. 2004;93:1404–7, A9.
37. Engler RL, Schmid-Schonbein GW, Pavelec RS. Leukocyte capillary plugging in myocardial ischemia and reperfusion in the dog. Am J Pathol. 1983;111:98–111.
38. Claeys MJ, Bosmans JM, Hendrix J, Vrints CJ. Reliability of fractional flow reserve measurements in patients with associated microvascular dysfunction: importance of flow on translesional pressure gradient. Catheter Cardiovasc Interv. 2001;54:427–34.
39. De Bruyne B, Pijls NH, Bartunek J, et al. Fractional flow reserve in patients with prior myocardial infarction. Circulation. 2001;104:157–62.
40. Hanekamp CE, Koolen JJ, Pijls NH, Michels HR, Bonnier HJ. Comparison of quantitative coronary angiography, intravascular ultrasound, and coronary pressure measurement to assess optimum stent deployment. Circulation. 1999;99:1015–21.
41. Pijls NH, Klauss V, Siebert U, et al. Coronary pressure measurement after stenting predicts adverse events at follow-up: a multicenter registry. Circulation. 2002;105:2950–4.
42. Rieber J, Schiele TM, Erdin P, et al. Fractional flow reserve predicts major adverse cardiac events after coronary stent implantation. Z Kardiol. 2002;91(Suppl 3):132–6.
43. Koo BK, Kang HJ, Youn TJ, et al. Physiologic assessment of jailed side branch lesions using fractional flow reserve. J Am Coll Cardiol. 2005;46:633–7.
44. Colombo A, Moses JW, Morice MC, et al. Randomized study to evaluate sirolimus-eluting stents implanted at coronary bifurcation lesions. Circulation. 2004;109:1244–9.
45. Jeremias A, Filardo SD, Whitbourn RJ, et al. Effects of intravenous and intracoronary adenosine 5′-triphosphate as compared with adenosine on coronary flow and pressure dynamics. Circulation. 2000;101:318–23.

46. Nijjer SS, de Waard GA, Sen S, et al. Coronary pressure and flow relationships in humans: phasic analysis of normal and pathological vessels and the implications for stenosis assessment: a report from the Iberian-Dutch-English (IDEAL) collaborators. Eur Heart J. 2016;37:2069–80.
47. Sen S, Escaned J, Malik IS, et al. Development and validation of a new adenosine-independent index of stenosis severity from coronary wave-intensity analysis: results of the ADVISE (ADenosine Vasodilator Independent Stenosis Evaluation) study. J Am Coll Cardiol. 2012;59:1392–402.
48. Escaned J, Echavarria-Pinto M, Garcia-Garcia HM, et al. Prospective assessment of the diagnostic accuracy of instantaneous wave-free ratio to assess coronary stenosis relevance: results of ADVISE II international, multicenter study (ADenosine Vasodilator Independent Stenosis Evaluation II). JACC Cardiovasc Interv. 2015;8:824–33.
49. Davies JE, Sen S, Dehbi HM, et al. Use of the instantaneous wave-free ratio or fractional flow reserve in PCI. N Engl J Med. 2017;376:1824–34.
50. Gotberg M, Christiansen EH, Gudmundsdottir IJ, et al. Instantaneous wave-free ratio versus fractional flow reserve to guide PCI. N Engl J Med. 2017;376:1813–23.
51. Escaned J, Ryan N, Mejia-Renteria H, et al. Safety of the deferral of coronary revascularization on the basis of instantaneous wave-free ratio and fractional flow reserve measurements in stable coronary artery disease and acute coronary syndromes. JACC Cardiovasc Interv. 2018;11:1437–49.
52. Kim HL, Koo BK, Nam CW, et al. Clinical and physiological outcomes of fractional flow reserve-guided percutaneous coronary intervention in patients with serial stenoses within one coronary artery. JACC Cardiovasc Interv. 2012;5:1013–8.

Index

A. T. Askari, A. W. Messerli (eds.), *Cardiovascular Hemodynamics*, Contemporary Cardiology,
https://doi.org/10.1007/978-3-030-19131-3